TRANSACTIONS
American Society for Metals
VOL. XXXIII 1944

QUENCHING AND HARDENABILITY OF HOLLOW CYLINDERS

By J. H. Hollomon and C. Zener

Abstract

The purpose of this paper is to determine by calculation the diameter of a solid steel cylinder, which, when quenched in a given medium, will have the same hardness in the center as the minimum hardness in the wall of a hollow cylinder when quenched in the same medium. In performing these calculations, it was found expedient to use a new criterion for equal hardnesses other than the half-temperature time suggested by Grossmann and Asimow. This new criterion is essentially one of equal cooling rates. In comparing hardnesses at the centers of flat plates and round bars, or in the mid-walls of cylinders, it is suggested that this criterion of equal cooling rates is not only simpler to use, but has more physical significance than the criterion used by Grossmann and Asimow. Calculations based on this new criterion have been made to determine the size of rounds equivalent to hollow cylinders and flat plates for various conditions of quenching. In a comparison of the theoretical results with experiments, it is concluded that quenching of the inside of hollow cylinders is more efficacious than the quenching of the outside under the usual quenching procedure.

THE method of Grossmann for calculating the effect of alloying elements on the hardenability of rounds has been described in detail in the literature (1) to (8)*. After calculating the multi-

*The figures appearing in parentheses pertain to the references appended to this paper.

The statements or opinions expressed in this paper are to be considered those of the authors and do not necessarily express the views of the Ordnance Department.

A paper presented before the Twenty-fifth Annual Convention of the Society, held in Chicago, October 18 to 22, 1943. Of the authors, Lt. J. H. Hollomon is stationed at Watertown Arsenal, Watertown, Mass., and C. Zener is physicist at this Arsenal. Manuscript received April 28, 1943.

plicative effects of the alloying elements, a series of curves can be determined for the effect of carbon content and grain size (2) on the diameter which would just harden throughout in an ideal quenching medium. In an ideal quenching medium the surface of the round is maintained at the temperature of the medium. This is approximated in practice by agitated or sprayed brine. In an actual quench, the diameter of the round which will just harden throughout is the smallest one having no "unhardened core" visible in either the fracture or the etch test. The center of such a hardened round is approximately 50 per cent martensitic. After estimating the ideal diameter for some composition, the actual size of round which would just harden throughout may be determined from a series of curves for different quenching media which relate the actual size of round to this ideal diameter.

The primary purpose of this paper is to extend the general method of Grossmann to the case of hollow cylinders. In this extension it was found expedient to use a new criterion for complete hardenability rather than the half-temperature time. This new criterion is not only simpler to use, but has more physical significance.

Discussion and Results

In order to calculate the diameter of the solid steel cylinder which when quenched in a given medium will have the same hardness at its center as the minimum hardness in the wall of the hollow cylinder quenched in the same medium, it is first necessary to determine the conditions of time and temperature during cooling for which the hardness at the two positions of the two steel shapes will be the same. Grossmann, in comparing the hardness distribution from the center to outside of solid cylinders, found that the time required to reach half the difference between the quenching and final temperature during cooling determined the hardness; that is, if the outside of one solid cylinder of a given steel composition required the same time to cool half way from the quenching temperature to room temperature as the inside of some other cylinder of the same composition, the hardnesses at the specified positions would be very nearly the same. It was noted that the shapes of the cooling curves at different positions in solid rounds are quite dissimilar. If the cooling rate at the center of one bar is the same as that of the outside of another, the "half-temperature times" will

be widely different. Since the time spent below the critical temperature before transformation is of importance in determining the precise products of transformation, in comparisons where the initial parts of the cooling curves are of different shapes the time to reach half temperature is probably a better criterion than that of cooling rate. Grossmann and his collaborators (2) presented some experimental evidence that cooling time is the more applicable criterion of hardenability when positions other than the centers of round sections are compared and assumed that this condition is also the more applicable in comparing the cooling at the centers of different round bars.

In certain important cases, the rate of cooling in the appropriate temperature range may be specified by a single parameter, c, in the manner indicated below:

$$\frac{dT}{dt} = -cT, \qquad (1)$$

where T is the temperature of the element referred to that of the quenching medium. Throughout the temperature range in which Eq. (1) is obeyed a plot of T vs. t on semi-log paper will yield a straight line. Such a plot is presented as Fig. 1 for the centers of solid cylinders from calculations of Russell (10). As the quenching proceeds the curves approach straight lines. The less severe the quench or rather the smaller the product of H (severity of quench) times D (diameter of the round) the more rapidly is the asymptote approached. For each different product, HD, in this graph the diameter (D) of the bar has been chosen which renders the various asymptotes parallel. Thus if a bar diameter D_1 just hardens through when quenched in a medium of severity H_1, in order to find the diameter of D_2 (of the same steel) that would just harden through in some other medium of severity H_2, it is necessary to find the corresponding line which is parallel (the cooling curve having the same "c"). The centers of the bars represented in Fig. 1 quenched in different media have the same "c" while their half-temperature times are quite different, having the ratio 2.4 : 3.0 : 4.0 for HD equal to 0, 1, and ∞ respectively. Since most of the difference in half-temperature times occurs before the critical temperature is reached, it is not significant. For this example the quenching temperature was assumed to be 1700 degrees Fahr. (925 degrees Cent.), the critical temperature 1600 degrees Fahr. (870 degrees Cent.), and the temperature of the nose of the "S" curve 1050

degrees Fahr. (565 degrees Cent.). The half-temperature time starting from the critical rather than the initial temperature are in the ratio of 2.1 : 2.1 : 2.4 which is not far from the ratio 1 : 1 : 1. Since the difference between the initial and critical temperatures is

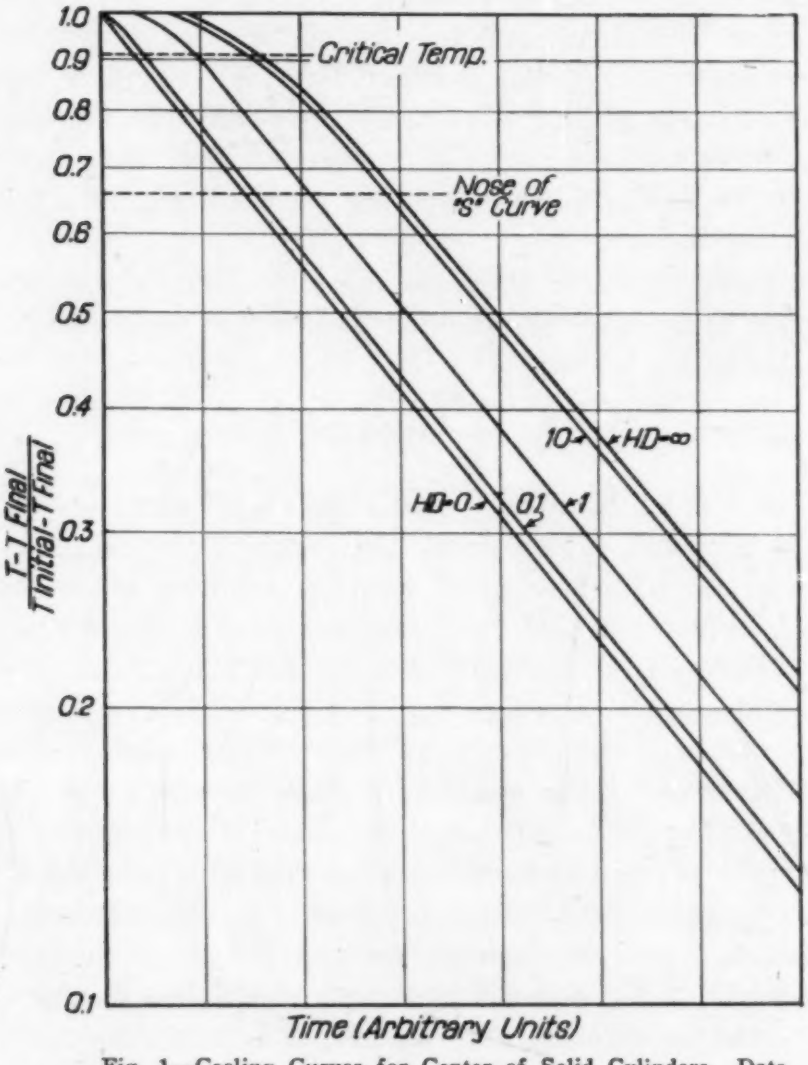

Fig. 1—Cooling Curves for Center of Solid Cylinders. Data from Russell (10).

variable and very difficult to fix in actual quenching practice it may be concluded that when center hardnesses are to be compared the slopes of the linear portion of the curves of Fig. 1 are a better measure of the hardenability than the half-temperature times. The criterion of hardenability used throughout this paper is applicable only when the centers of hollow cylinders, round bars and flat plates are compared. The cooling curves for the outside are very different from those shown in Fig. 1, approaching asymptotes only at very

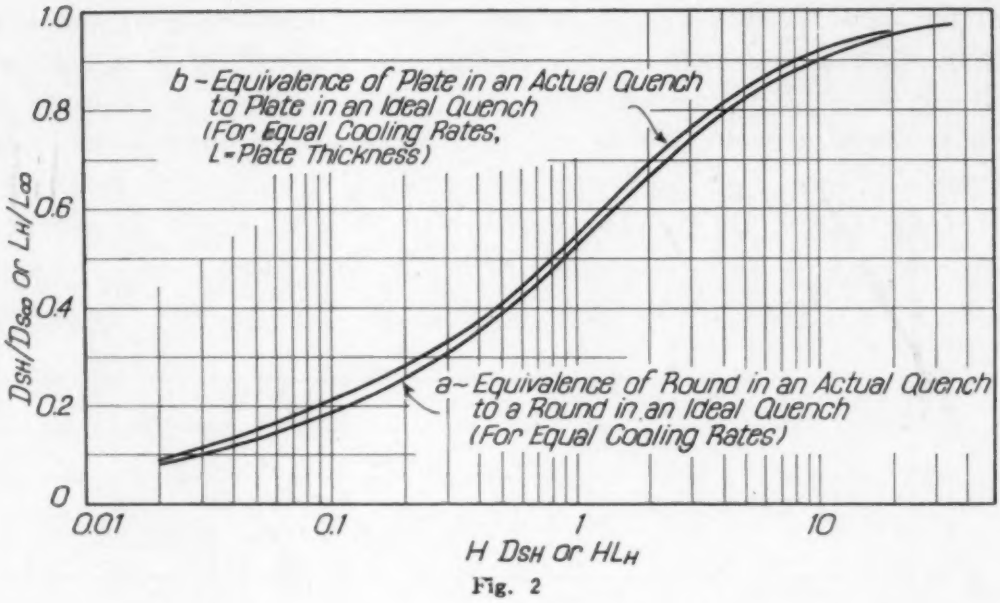
1.0
0.8
0.6
0.4
0.2
0
DSH/Dsoo or LH/Loo
b - Equivalence of Plate in an Actual Quench to Plate in an Ideal Quench (For Equal Cooling Rates, L = Plate Thickness)
a - Equivalence of Round in an Actual Quench to a Round in an Ideal Quench (For Equal Cooling Rates)
0.01
0.1
1
10
H DSH or HLH

Fig. 2

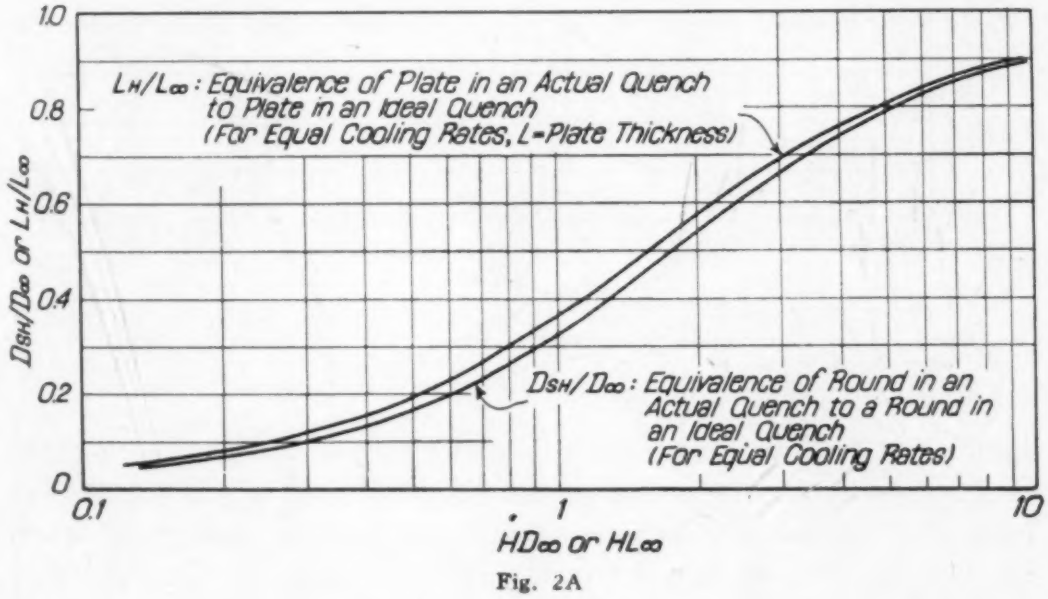
1.0
0.8
0.6
0.4
0.2
0
DSH/Doo or LH/Loo
LH/Loo : Equivalence of Plate in an Actual Quench to Plate in an Ideal Quench (For Equal Cooling Rates, L = Plate Thickness)
DSH/Doo : Equivalence of Round in an Actual Quench to a Round in an Ideal Quench (For Equal Cooling Rates)
0.1
1
10
HDoo or HLoo

Fig. 2A

low temperatures. Therefore, if the center and outside of hardnesses are to be compared, then the criterion of half-temperature time is probably more nearly correct.

A comparison has been made, using this new measure of hardenability, of the hardenability of rounds in an actual quench to that of rounds in an ideal quench. A similar comparison has been made for plates. The results are given as Figs. 2 and 2A. The first figure is to be used when the hardenability in the actual quench (D_{SH}) is known, the second figure when the hardenability

in the ideal quench ($D_{S\infty}$) is known. As an example of the first case, suppose a 2-inch round just hardens throughout in a medium whose severity of quench (H) is 1.5 inch^{-1}, and it is required to know the size round which will just harden throughout in an ideal quench. From Fig. 2 one sees that when H D_{SH} is 2×1.5, namely 3, $D_{SH}/D_{S\infty}$ is 0.74. Therefore $D_{S\infty}$ is 2/0.74, or 2.7 inches. In order that a comparison may be made with Grossmann's method, Fig. 3 has been constructed. It may be readily seen from this

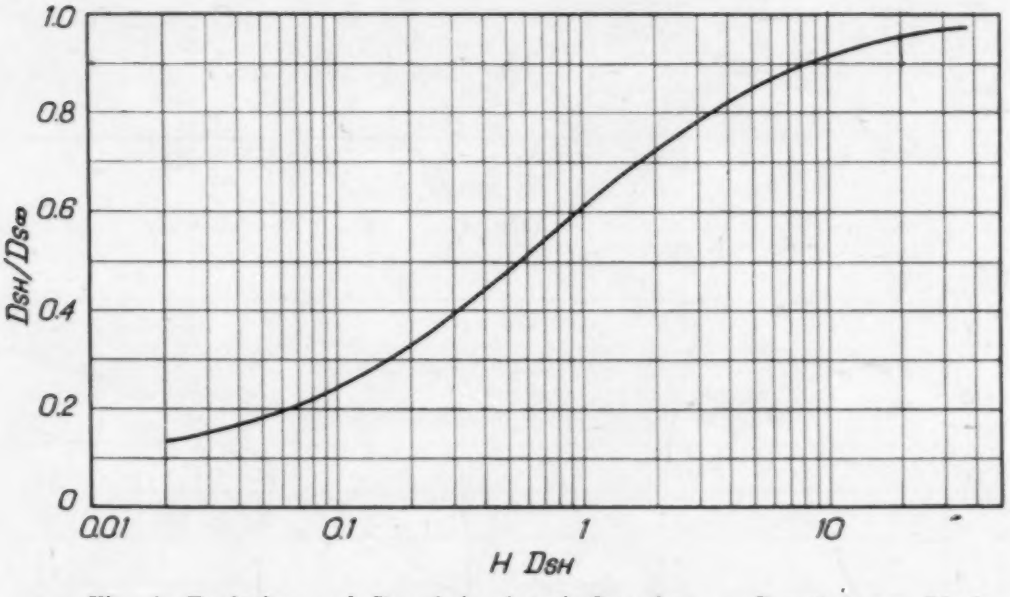

Fig. 3—Equivalence of Round in Actual Quench to a Round in an Ideal Quench. (For Equal Half Temperature Times). Taken from Calculations by Grossmann, et al.

figure that Grossmann's method would lead to an answer of 2/0.78, or 2.56 inches for the above problem. As an example of the second case, suppose that a 2-inch round will just harden throughout when the severity of quench is 1.5 inch^{-1} and it is required to know what size round of the same steel will just quench when the severity of quench is 3 inch^{-1}. As before, one finds from Fig. 2 that for this steel $D_{S\infty} = 2.7$ inches. From Fig. 2A one now finds that when H $D_{S\infty} = 3\times2.7$, or 8.1, the ratio $D_{S_3}/D_{S\infty}$ is 0.94. Therefore for this steel $D_{S_3} = 0.94\times2.7 = 2.54$ inches.

The relation between the size round which will just harden throughout in a given quench and the thickness of plate (L_H) of the same steel which will just harden throughout in any other specified quench may be obtained from Figs. 2, 2A and from the following relation:

$$D_{S\infty} = 1.53\ L_{\infty}$$

The observed values (9) of D_S/L lie between the values $D_{S\infty}/L_{\infty}$ and D_{SO}/L_O calculated by the new criterion of hardenability, namely between 1.53 and 2. See equations (9) and (10). The value (3) for a particular quench as calculated by Grossmann's method is 1.37.

The calculation of the ideal round diameter equivalent to a hollow cylinder is more complicated, for the outside and inside diameters can be varied independently. In this paper the equivalent

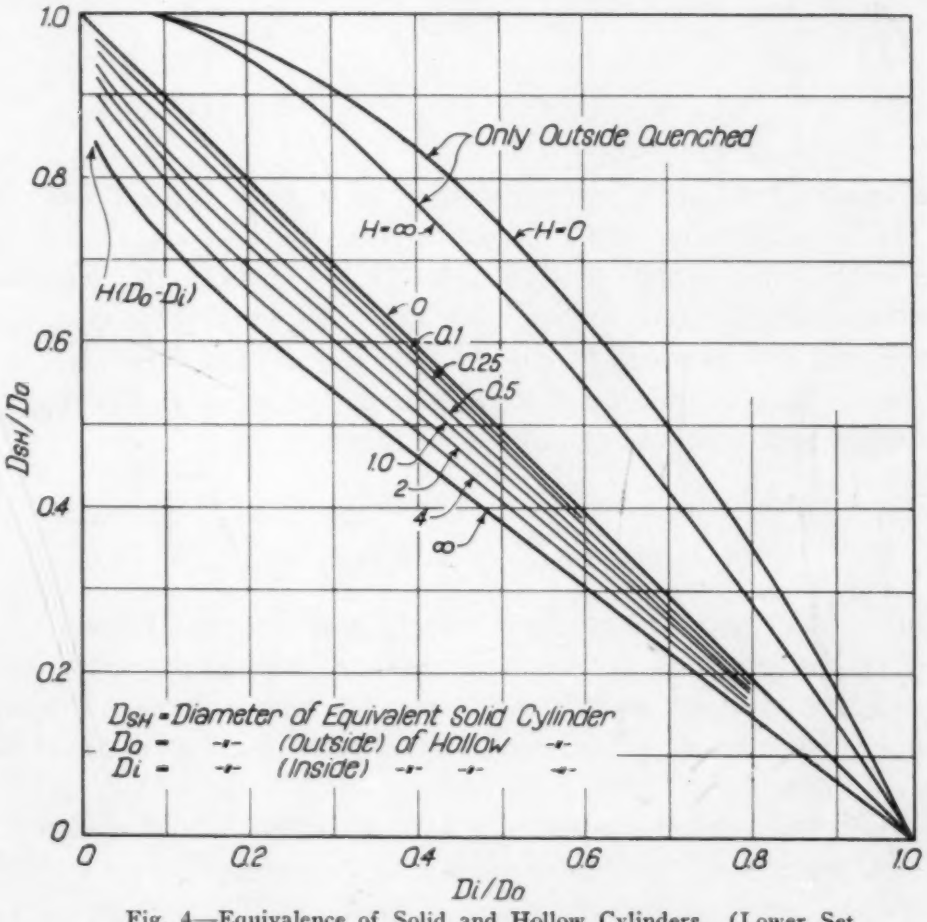

Fig. 4—Equivalence of Solid and Hollow Cylinders. (Lower Set of Curves Refers to Both Inside and Outside Quenching.)

round diameter is determined for a given wall ratio for a severity of quench measured by the product of H times the difference between the inside and outside diameters.

The results of calculations (Appendix) based on the new criterion of equal cooling rates are presented as Fig. 4 in which the ratio of equivalent round diameter (D_{SH}) to outside diameter (D_o) is plotted as a function of D_i/D_o for different values of H times (D_o—D_i)

where D_i is the inside diameter. D_{SH} is the diameter of the round which has the same cooling rate at its center as the minimum cooling rate in the wall of the hollow cylinder when quenched in a medium of severity H. The use of curve *a* of Fig. 2 and Fig. 4 can be best understood through an example; let us assume that the equivalent ideal diameter of a round is to be determined for the following situation:

Severity of quench (H) = $1''^{-1}$
Outside diameter (D_o) = 4"
Inside diameter (D_i) = 2"

$D_i / D_o = 0.5$
$D_o - D_i = 2''$
$H(D_o - D_i) = 2$

The value of D_{SH}/D_o corresponding to a wall ratio of 0.5 and an $H(D_o—D_i)$ value of 2 is read from Fig. 4. D_{SH}/D_o in this case is 0.43 and when multiplied by D_o (4 inches), an equivalent round diameter of 1.72 inches is obtained. By employing graph *a* of Fig. 2 and the product of $D_{SH}(1.72)$ and H(1), $D_{SH}/D_{S\infty}(0.63)$ is found. D_{SH} divided by this ratio fixes the ideal round diameter equivalent to the hollow cylinder (2.7 inches).

Experimental

In order to determine how closely the theoretical results outlined in the previous section approximate the actual relationships between the sizes of hollow cylinders and rounds having the same minimum hardness, experiments described in this section have been performed.

The ideal critical diameter of a steel of the following composition was calculated by the method of Grossmann.

C	Mn	Si	S	P	Cr	Cu	Mo	Al
0.40	0.79	0.43	0.070	0.018	0.14	0.105	0.16	0.004

The critical diameter in mildly agitated water was measured by quenching from 1575 degrees Fahr. (855 degrees Cent.) (neutral atmosphere) rounds of various diameters from 1¼ to 2½ inches all machined from a 2¾-inch round bar. In all cases the length of the solid cylinder was 4 times the diameter. The water in the quenching tank was agitated by a stream of water entering from the bottom through a ½-inch diameter aperture at about 25 gal. per minute.

The diameters of the unhardened cores were determined after sectioning by etching with a hot sulphuric-hydrochloric acid mixture. The critical diameter of the steel and the H value of the medium were then determined by the method of Grossmann and were found to be 1.5 inches and 1.4 inches^{-1} respectively. The ideal diameter calculated from the composition was 2.2 inches while the measured diameter was equal to 2.1 inches. The ratio D_i/D_o of the hollow cylinder with outside diameter of 2½ inches and for both inside and

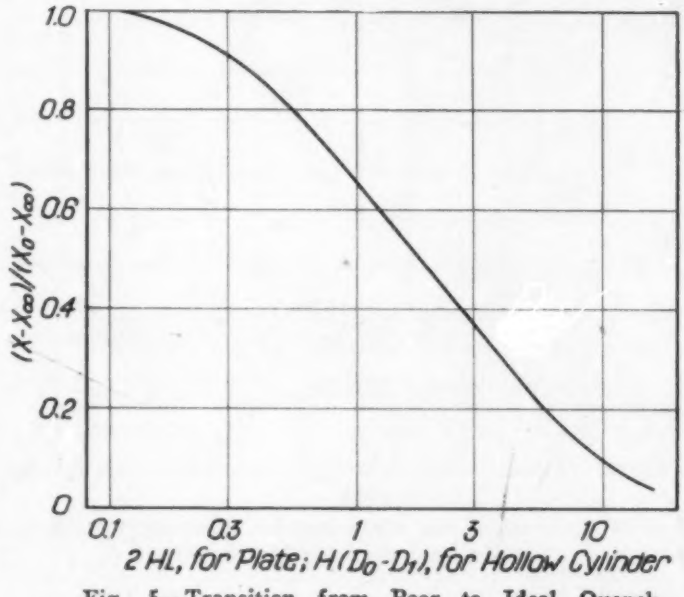

Fig. 5—Transition from Poor to Ideal Quench, $X = D_s/L$, For Plate $X = D_s/(D_o-D_i)$, For Hollow Cylinder.

outside quenched which would be equivalent to this solid round (1.5 inch) was read from Fig. 4 and D_i/D_o is equal to 0.3. The wall ratio (D_i/D_o) for the equivalent hollow cylinder for the case in which only the outside is quenched was found from Fig. 4 to be 0.6. Five hollow cylinders with wall ratios (D_o=2.5 inches) less than each of these two critical values were machined from the 2¾-inch round stock. One set of five hollow cylinders was quenched from 1575 degrees Fahr. (855 degrees Cent.) into the water and supported directly over the aperture. Thin plates were welded over the ends of the second set of hollow cylinders and these were quenched as nearly like the solid cylinders as possible.

The Rockwell "C" hardness distribution for each of the hollow and solid cylinders was measured and the minimum hardnesses are plotted in Fig. 6. A typical hardness survey for both inside and outside quenching is presented in Fig. 7. The size of the round

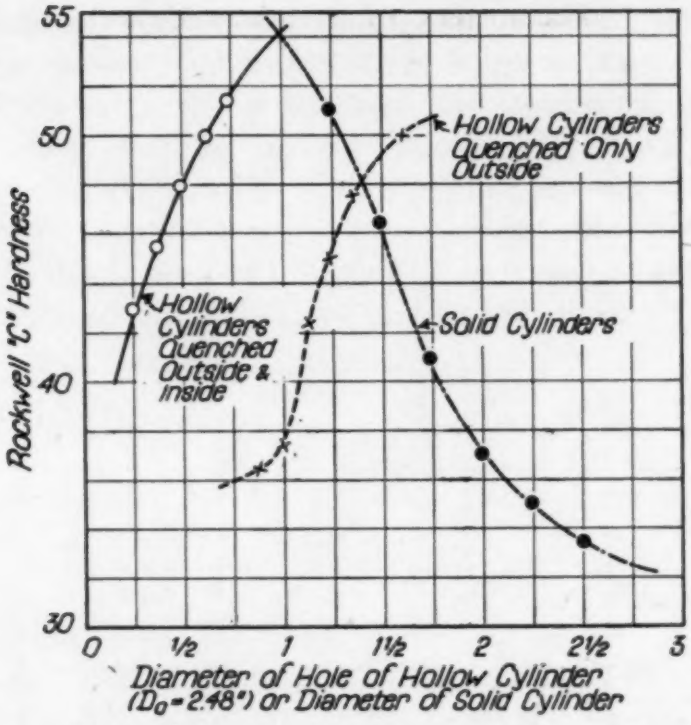

Fig. 6—Minimum Hardness of Solid and Hollow Cylinders as a Function of Dimension (Experimental).

Table I
Comparison of Theoretical and Experimental Equivalent Solid Cylinders (For Same Minimum Hardness)

Hollow Cylinder Only Outside Quenched D_i (Inches)	D_o (Inches)	Diameter of Equivalent Solid Cylinder (Inches) Exp.	Theo.
1.00	2.48	1.94	1.93
1.13	2.48	1.70	1.81
1.25	2.48	1.57	1.66
1.38	2.48	1.44	1.53
1.50	2.48	1.38	1.38
Both Inside and Outside Quenched			
0.38	2.48	1.55	1.75
0.50	2.48	1.44	1.69
0.63	2.48	1.31	1.54
0.75	2.48	1.20	1.45
0.88	2.48	1.10	1.35

which would have the same minimum hardness as each of the hollow cylinders was determined from Fig. 6. The experimental determinations and the corresponding theoretical values read from Fig. 4 are tabulated in Table I. The difference between theory and experiment for the hollow cylinders with only the outside quenched is less than 6 per cent. For the case of both inside and outside quenching the difference is about 15 per cent, the theory predicting a larger equivalent round size. For these small size cylinders, the

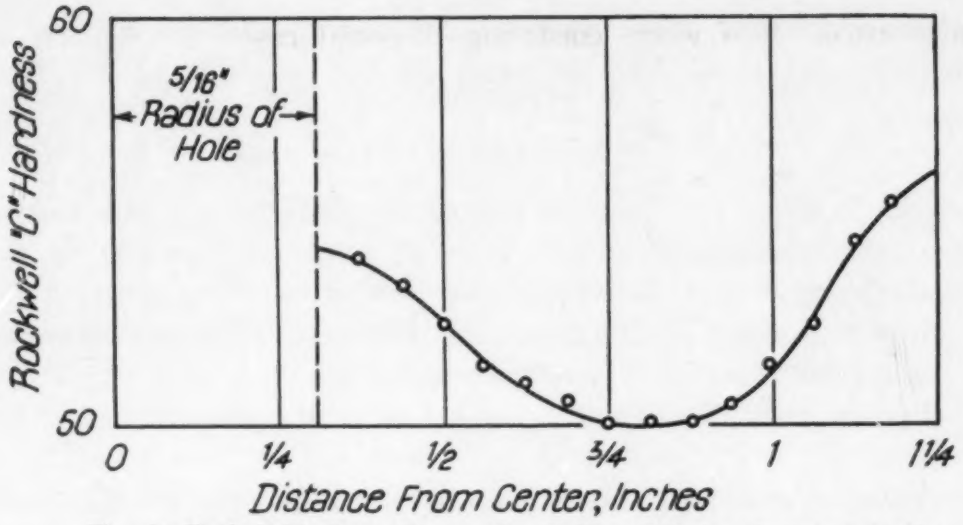

Fig. 7—Typical Hardness Survey for Hollow Cylinder Quenched Inside and Outside.

inside quenching is more efficacious than the outside for the particular conditions of our experiment. In these experiments, it appears that the severity of quench is larger on the inside than the outside and the equivalent solid cylinder is necessarily smaller than that predicted assuming that the inside and outside of the hollow cylinder were quenched identically.

Appendix A—Calculations

General Theory

The purpose of this section is to find the relation between the equivalent ideal critical diameter ($D_{S\infty}$) of a solid cylinder and of a hollow cylinder of inside diameter D_i and outside diameter D_o, when quenched in some medium. This relation will contain as parameters the severity of the quench in the actual medium, H, and the wall ratio (a) of the inside diameter over the outside diameter. Thus

$$D_s = F(a, H, D_o).$$

The mathematical problem to be solved is the determination of the constant c (Eq. 1) for hollow and for solid cylinders, for various severities of quench.

The differential equation for heat flow is

$$\partial T/\partial t = k\Delta^2 T. \qquad (2)$$

In this equation, k is the thermal diffusion coefficient, $\triangle^2$ is the

LaPlacian operator. Since we are considering the special case in which Eq. (1) is satisfied, we shall set

$$T = T_o \{\exp(-ct)\} U(r). \quad (3)$$

Here, as in Eq. (1), T is the temperature of element referred to that of the quenching medium, U is an unknown function of coordinates, and c is a constant to be determined.

Substitution of Eq. (3) into Eq. (2) gives Eq. (5) below as the differential equation for U(r); with

$$m^2 = c/k. \quad (4)$$

Only those solutions of this differential equation are desired which satisfy the appropriate boundary condition. The boundary condition which has been found to be fairly accurate is given by Newton's law of cooling. This law states that the flow of heat across a boundary is proportional to the temperature drop across that boundary. Since the flow of heat is proportional to the temperature gradient, the appropriate boundary condition is that the temperature gradient at the boundary is proportional to the difference in temperature between the solid and the quenching medium. The constant of proportionality is taken as —h, the gradient being taken in the direction from the solid to the quenching medium. The constant h is equal to twice the H used by Grossmann. This boundary condition may be written as in Eq. (6). Eqs. (5) and (6) below form the complete mathematical formulation of the problem.

Differential equation for U:

$$\Delta^2 U = -m^2 U. \quad (5)$$

Boundary condition for U:

$$\text{gradient}_n U = -hU \text{ at surface.} \quad (6)$$

Plates and Solid Cylinders

The solution of these equations has previously been given for the cases of a plate and of a solid cylinder. In the case of the plate, of thickness L,

$$U = \cos mx,$$

where m is the lowest root of the equation

$$\tan \tfrac{1}{2} mL = h/m. \quad (7)$$

In the case of a solid cylinder of radius r_s

$$U = J_o(mr),$$

where m is the lowest root of the equation

$$J_1(mr_s)/J_o(mr_s) = h/m. \tag{8}$$

Equations (7) and (8) have no solution for arbitrary values of m, but only for a discrete set of values. In the present case one is interested only in the lowest value of m. The higher values are important only when the transient effects are being studied.

Limit h=o. In the case of a very poor quenching medium, $h \to o$ and also $m \to o$. The left members of Equations (7) and (8) may therefore be replaced by the first term in a Taylor expansion. We obtain

$$\tfrac{1}{2}mL = h/m, \tag{7a}$$

$$\tfrac{1}{2}mr_s = h/m. \tag{8a}$$

The ratio of the diameter of the solid cylinder to the thickness of equivalent plate is therefore given by the equation

$$r_s/L = 1, \quad D_s/L = 2 \tag{9}$$

Limit $h = \infty$. The case of an ideal quench is obtained by setting $h = \infty$. Equations (7) and (8) now become, with $r_{s\infty}$ written for r_s,

$$mr_\infty = \pi, \tag{7b}$$

$$mr_{s\infty} = 2.404. \tag{8b}$$

In this case we obtain the ratio

$$r_{s\infty}/L_\infty = 0.765, \quad D_{s\infty}/L_\infty = 1.53 \tag{10}$$

Intermediate Quenches. The relation between the hardenability in an actual quench to the hardenability in an ideal quench may be obtained by substituting the values of *m,* as given by Equations (7b) and (8b), into Equations (7) and (8), respectively. Upon replacing *h* by 2H, one obtains

$$\tan(\tfrac{1}{2}L_H/L_\infty) = (2/\pi)\, HL_\infty \tag{7c}$$

and

$$\frac{J_1(2.404\, D_{SH}/D_{S\infty})}{J_0(2.404\, D_{SH}/D_{S\infty})} = \frac{H\, D_{S\infty}}{2.404} \qquad (8c)$$

These equations are plotted in Fig. 2A, from which the ratio L_H/L_∞ may be obtained when HL_∞ is given and the ratio $D_{SH}/D_{S\infty}$ may be obtained when $HD_{S\infty}$ is given. Since in certain cases one wishes to know these ratios in terms of $H\,L_H$ and $H\,D_{SH}$, respectively, Fig. 2A has been replotted in Fig. 2 in which the latter quantities are taken as the independent variables. This was done by multiplying the abscissas of the appropriate graphs in Fig. 2A by L_H/L_∞ and by $D_{SH}/D_{S\infty}$.

It is of considerable interest to know how the ratio of round diameter to equivalent plate thickness changes from 1.53 for the case of an ideal quench to 2.0 for the case of a very poor quench. This transition is most vividly represented by a plot of the quantity $(X_H - X_\infty)/(X_0 - X_\infty)$, where $X_H = D_{SH}/L_H$, etc. against one of the dimensionless quantities HL_H, HL_∞. Such a plot is given as Fig. 5. This plot was constructed by the simultaneous use of Fig. 2A and of the relation $D_{S\infty}/L_\infty = 1.53$.

Hollow Cylinder, Inside and Outside Quenched

In a hollow cylinder the general solution of Eq. (5) must be used, namely

$$U(r) = C_0\, J_0(mr) + C_1 N_0(mr), \qquad (11)$$

where J_0 and N_0 are Bessel functions of the first and second type, respectively (11). The two constants must be so chosen as to satisfy the boundary condition Eq. (6) at both the inner and the outer surfaces.

The boundary condition Eq. (6), applied to both the inner and outer surfaces, gives two simultaneous linear homogeneous equations in the two unknowns C_0 and C_1. These equations are soluble only if the determinant of the coefficients is zero. This condition gives the following equation, which corresponds to Eq. (8) for a solid cylinder.

$$\frac{m\,J_o'(mr_o)+h\,J_o(mr_o)}{m\,N_o'(mr_o)+h\,N_o(mr_o)} = \frac{m\,J_o'(amr_o)-h\,J_o(amr_o)}{m\,N_o'(amr_o)-h\,N_o(amr_o)} . \qquad (12)$$

Limit h=o. One obtains the extreme case of a poor quench by letting h, and hence also m, approach zero. In this case each Bessel function may be replaced by the first term in the Taylor expansion. Using the expansion given in reference (11), one reduces Equation (12) to

$$\tfrac{1}{2}\, mr_o(1-a) = h/m. \qquad (12a)$$

Upon dividing Equation (8a) by Equation (12a) one obtains

$$r_s/r_o = 1-a \qquad (13)$$

as the ratio of the radius of the round to that of an equivalent hollow cylinder.

Limit h=∞. The extreme case of an ideal quench is obtained by letting h approach ∞ in Eq. (12). In this case Eq. (12) reduces to

$$\frac{J_o(mr_o)}{N_o(mr_o)} = \frac{J_o(amr_o)}{N_o(amr_o)} . \qquad (12b)$$

Since m may be replaced by $2.404/r_{s\infty}$ from Eq. (8b), the ratio $r_{s\infty}/r_o$ may be determined as a function of *a*. This function has been determined by a graphical method, and is given in Fig. 4.

Intermediate Quenching. The variation of the ratio $x=r_s/r_o$ with severity of quench may best be studied through the ratio $(x-x_\infty)/(x_o-x_\infty)$. At least in the case of a thin hollow cylinder, a = 1, the dependence of this ratio upon h (r_o-r_i) will be given by the graph in Fig. 5 which was derived originally from a comparison of rounds with plates (pages 13 and 14). A numerical calculation for r_s/r_o was carried out for the cases a=0.1 and a=0.5. The results showed that Fig. 5 was applicable to values of *a* at least as low as 0.1. The intermediate lines in Fig. 4 have been based upon Fig. 5.

Hollow Cylinder, Only Outside Quenched

In the case of a hollow cylinder quenched only on the outside, we must again use the general solution given in Eq. (11). The constants C_o and C_1 are to be so chosen that the boundary condition Eq. (6) is satisfied with *h* set equal to zero at the inner boundary. The two conditions corresponding to the two boundaries lead to two linear homogeneous equations in C_o and C_1. These equations are soluble only when the determinant of the coefficients is zero. Upon equating this determinant to zero, one obtains the equation

$$\frac{m\,J_o'(mr_o)+h\,J_o(mr_o)}{m\,N_o'(mr_o)+h\,N_o(mr_o)}=\frac{J_o'(a\,mr_o)}{N_o'(a\,mr_o)} \qquad (14)$$

Limit h=o. Proceeding as on page 15, we retain only the first terms in the Taylor expansion of the functions in Equation (14). In this case Equation (14) reduces to

$$\tfrac{1}{2}mr_o(1-a^2)=h/m. \qquad (14a)$$

Upon comparing this equation with Equation (8a), we obtain

$$r_s/r_o=(1-a^2).$$

This relation is given in Fig. 4.

Limit h=∞. In the case of an ideal quench, h=∞, Equation (14) reduces to

$$\frac{J_o(mr_o)}{N_o(mr_o)}=\frac{N_o(amr_o)}{J_o(amr_o)} \qquad (14b)$$

This equation has been solved graphically in the same manner as was Equation (12b). The result is given in Fig. 4.

Intermediate Quenching Rates. When a=1, the distribution of temperature in the hollow cylinder becomes identical to the temperature distribution throughout one-half of a plate quenched on both sides, whose thickness is double the real thickness of the hollow cylinder. The transition from h→0 to h→∞ is therefore obtained from Fig. 5 provided the abscissa is now $2H\cdot(D_o-D_i)$ in place of $H(D_o-D_i)$.

References

1. M. Asimow and M. A. Grossmann, "Hardening Characteristics of Various Shapes," TRANSACTIONS, American Society for Metals, Vol. 28, 1940, p. 949.
2. M. A. Grossmann, T. P. 1437, American Institute of Mining and Metallurgical Engineers, February, 1942.
3. M. A. Grossmann, M. Asimow, and S. E. Urban, "Hardenability of Alloy Steels," published by American Society for Metals, 1939.
4. W. E. Jominy, METAL PROGRESS, December, 1941.
5. M. Asimow and M. A. Grossmann, *Journal,* Society of Automotive Engineers, Vol. 49, No. 1, p. 266.
6. M. A. Grossmann and M. Asimow, *The Iron Age,* April 25 - May 2, 1940.
7. A. E. Focke, *The Iron Age,* Vol. 150, No 9, p. 43.
8. M. Asimow, A. Craig, and M. A. Grossmann, *Journal,* Society of Automotive Engineers, 1941, p. 283.
9. C. Post, O. V. Greene, and W. H. Fenstermacher, "Hardenability of Shallow Hardening Steels," TRANSACTIONS, American Society for Metals, Vol. 30, 1942, p. 1202.
10. T. F. Russell, First Report of the Alloy Steels Research Committee, Iron and Steel Institute, 1936, p. 149.
11. E. Jahnke and F. Emde, *Funktionentafeln,* Berlin, 1928.

DISCUSSION

Written Discussion: By Morse Hill, assistant metallurgist, Materials Laboratory, Engineering Division, Materiel Command, Army Air Forces, Wright Field, Dayton, Ohio.

The authors have studied and developed Russell's data in a most interesting manner. They have emerged with a new measure of quenching power and have extended the previous calculations to still another shape. It is unfortunate that the relationships involved are so complicated that prolonged study is necessary to understand them. However the resulting figures are clear enough to make their application easy.

Their proposed experimental method for evaluation of quenching severity or hardenability seems to be to determine the diameter which will just harden through with a steel of known hardenability or a quench of known severity. Since this criterion seems difficult to use in practice, involving as it does numerous samples and the determination of an unclear borderline of through hardening, can the authors elaborate on the procedures to be used in determining the severity of quench or the hardenability?

This and any other procedure based on heat flow calculations makes certain assumptions which cannot be too often noted. First, modifications in the cooling curve on passing through the critical are ignored. Second, it is assumed that the severity of quench remains constant through the cooling. Third, it is assumed that the quench is equally severe for all shapes and sizes of specimens. Fourth, it is assumed that the thermal diffusivity of the steel remains constant through cooling. Elementary reasoning from the mechanics of quenching makes it seem doubtful that these assumptions are fully justified. Before we can have full faith in the quantitative values of the calculation there must exist a considerable body of experimental data showing agreement of calculations and determinations.

Oral Discussion

M. A. GROSSMANN:[1] It seems to me that the criterion selected by the authors is a most excellent one because of its validity when applied to the rate of cooling during the temperature range where the changes are actually taking place; and although, as they say, the criterion has only been developed when applied to the center positions up to now, nevertheless its validity seems to be indicated by the relationship which they have developed between round bars and flat plates. Where some of our own earlier work indicated a relationship of 1 to 1.37 with ideal quenches, they show a relationship of 1.53, I believe, and that as it turns out is closer to the experimental relationship developed by Greene and the authors of the paper appearing on page 19 of this volume.

Another interesting item was the fact which they developed experimentally that the severity of quench on the inside of the hollow cylinder seemed to be a little greater than it "ought to be," so to speak. You will recall that in the paper under discussion the flow of the cooling liquid is along the axis of the bars. So far as I remember, the specimens are vertical and water flows in from the bottom. In some quenches of round bars under similar conditions of quenching we found this curious situation: that as the diameter of the bar was increased the severity of the quench increased for ostensibly similar quenching conditions.

I suppose this has something to do with turbulence in the flow along surfaces of that kind. At any rate, if one imagines the diameter increased indefinitely and the severity of quench increasing slightly up to the point where the surface is flat and then begins to be turned inside out, one has a condition then of the inside of a hollow cylinder, and, as a matter of fact, the authors did find here that the severity of the quench was greater.

Authors' Reply

We should like to thank both Messrs. Hill and Grossmann for their comments. In reply to Mr. Hill: The method of determining the severity of quench by measuring the depth of hardening of rounds of different diameter was proposed by Dr. Grossmann and his collaborators and not by the present authors. There are a number of ways in which the depth of hardening may be measured: by hardness surveys, by fracture tests, and by etch tests.

As to the advisability of applying heat-flow calculations to the problem of quenching, there are assumptions involved in applying any theory to physical fact. The question which must be asked is whether or not the results derived from such theory with the use of the best assumptions possible, are in sufficient agreement with actual experiment to warrant their practical use.

The authors believe that the calculations based on the assumptions which Mr. Hill questions permit the determination of relations which are sufficiently accurate to be applied to practical quenching problems.

The authors should particularly like to thank Dr. Grossmann for his kind remarks and for the confirmation of the authors' conclusion that severity of quench is greater on the inside than on the outside of a hollow cylinder.

---

[1]Director of research, Carnegie-Illinois Steel Corp., Chicago.

RATES OF COOLING IN BLOCKS AND CYLINDERS

By C. B. Post and W. H. Fenstermacher

Abstract

Experimental center cooling rates (degrees Fahr. per second at 1300 degrees Fahr.) are determined for the oil quenching of cylinders, bars and slabs of various length and thickness. These data show that the effect of length on the center rate of cooling past 1300 degrees Fahr. (705 degrees Cent.) of cylinders and bars is negligible until the length becomes almost equal to the radius or the smallest of the cross section dimensions.

A method is outlined for computing the rates of cooling (degrees Fahr. per second at 1300 degrees Fahr.) throughout finite sections such as cylinders, bars and blocks. This method utilizes simple combinations of the temperature functions for the quenching of cylinders of infinite length and slabs for which tables are available.

These calculated rates of cooling in finite sections are compared with the data obtained from several standard methods of testing hardenability (Rockwell hardness as a function of rate of cooling past 1300 degrees Fahr.) to obtain computed Rockwell contours throughout the section. Several finite sections are considered in detail and experimental and computed Rockwell contours compared.

THE prediction of hardness contours in steel blocks and cylinders of finite length, based upon Rockwell hardness as a function of rate of cooling through the critical temperature range, necessitates methods for calculating cooling rates in these finite sections. Comprehensive tables of temperature functions for the quenching of slabs and cylinders of infinite length have been given by H. Scott[1] and T. F. Russell[2]. It is the purpose of this report to discuss methods of combining temperature functions for slabs and cylinders of infinite length when rates of cooling during quench-

[1]H. Scott, Transactions, American Society for Metals, Vol. 22, 1934, p. 68-94.

[2]T. F. Russell, First Report of Alloy Steels Research Committee, British Iron and Steel Institute, 1936, p. 149-187.

A paper presented before the Twenty-fifth Annual Convention of the Society, held in Chicago, October 18 to 22, 1943. The authors, C. B. Post and W. H. Fenstermacher, are associated with the Metallurgical Department, Carpenter Steel Co., Reading, Pa. Manuscript received May 31, 1943.

ing are desired throughout finite sections such as blocks, bars, etc.

The data obtained from the Jominy hardenability test[3] determines the hardness developed by a given steel as a function of the rate of cooling (degrees Fahr. per second) past 1300 degrees Fahr. (750 degrees Cent.). Grossmann and Asimow[4, 5] considered the calculation of hardness contours in finite sections from Jominy hardenability test data. In order to do this, it was necessary that Grossmann and Asimow evaluate the Jominy hardenability test in terms of the so-called "half-temperature time" and "ideal critical bar diameter" instead of the rate of cooling past 1300 degrees Fahr. (705 degrees Cent.). A direct method will be discussed here for calculating rates of cooling (degrees Fahr. per second) past 1300 degrees Fahr. (705 degrees Cent.) throughout blocks, bars and other finite sections. Thus the Rockwell hardnesses obtained from the Jominy test bar can be used to predict hardness contours in various finite sections when the rate of cooling past 1300 degrees Fahr. (705 degrees Cent.) is assumed to be the criterion of hardenability.

Experimental Determination of Rates of Cooling

The effect of length of cylinder, length of bar, and edges of slabs on the variation of the center cooling rates (degrees Fahr. per second at 1300 degrees Fahr.) during oil quenching was determined for various finite sections. These data are useful in estimating the degree of agreement to be expected between rates of cooling computed by the proposed theoretical methods with experimentally determined rates in finite sections.

32 per cent nickel steel was used in these experiments because it has been shown by Scott[1] that the thermal diffusivity of this steel is approximately the same as that of austenite. A thermocouple was inserted at the center of a 1.5-inch round by 8-inch long cylinder as shown in Fig. 1. The thermocouple was directly connected to a sensitive milliammeter. A stop-watch was laid near the face of the meter, and the milliammeter and stop-watch were simultaneously photographed by means of a movie camera during the course of cooling. The quenching temperature was 1490 degrees Fahr. (810

[3]W. E. Jominy and A. L. Boegehold, Transactions, American Society for Metals, Vol. 26, 1938, p. 574-599.

[4]M. Grossmann and M. Asimow, Transactions, American Society for Metals, Vol. 28, 1940, p. 949-978.

[5]M. Asimow, W. F. Craig and M. Grossmann, *S.A.E. Journal (Transactions)*, Vol. 49, 1941, p. 283-292.

degrees Cent.) and the temperature of the large oil bath was room temperature (25 degrees Cent.) in all of the experiments discussed below.

The center cooling curve of the 1.5-inch round by 8-inch long bar during oil quenching was determined. Subsequent experiments consisted in decreasing the length of the bar and studying the effect of length on the resulting center cooling rates.

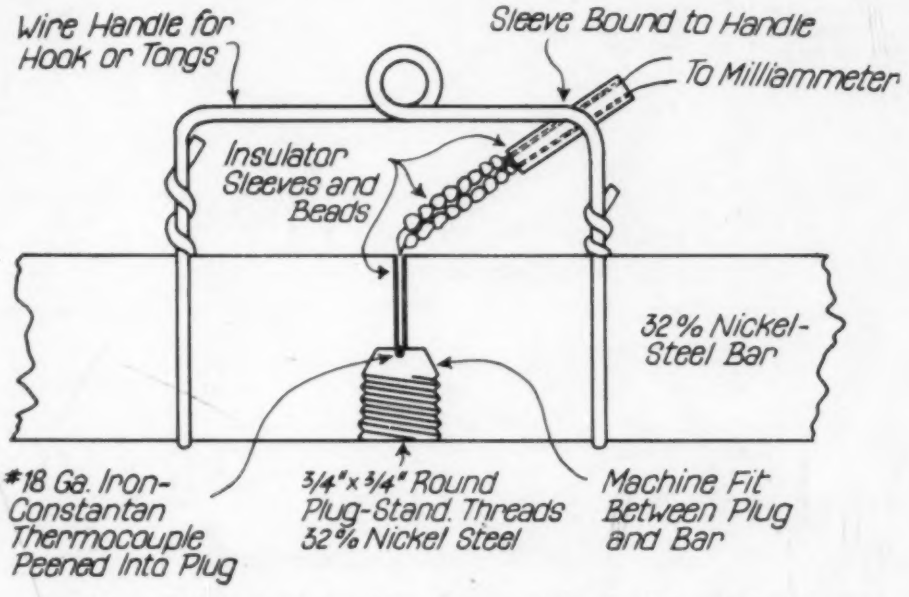
Wire Handle for Hook or Tongs
Sleeve Bound to Handle
To Milliammeter
Insulator Sleeves and Beads
32% Nickel-Steel Bar
#18 Ga. Iron-Constantan Thermocouple Peened Into Plug
3/4" x 3/4" Round Plug-Stand. Threads 32% Nickel Steel
Machine Fit Between Plug and Bar

Fig. 1—Method of Attaching Thermocouple for Determining Center Cooling Rates During Oil Quenching.

The center cooling rates during oil quenching were determined for a slab 1.5 inches thick by 5 inches square. A similar method of attaching the thermocouple, as shown in Fig. 1, was used in these experiments. Subsequent experiments determined the center cooling rate when the sides of the slab were gradually decreased to eventually yield a bar 1.5 by 1.5 by 5 inches.

The center cooling rates of a bar originally 1.5 by 1.5 by 6 inches long were determined as the length of the bar was decreased to 1.125 inches. All of the above data are given in Table I.

The time-temperature curves for the center cooling of the 1.5-inch round by 8-inch long cylinder and the 1.5-inch by 5-inch square slab during oil quenching are shown in Figs. 2 (a) and 2 (b). Also shown in these figures are the calculated center time-temperature curves for the cylinder and slab using the tables of Russell[2] and a value of thermal diffusivity (α) of 0.040 centimeter square

Table I

Center Cooling Rates (Degrees Fahr. Per Second) at 1300 Degrees Fahr. (705 Degrees Cent.) Oil Quenching, Quenching Temperature = 1490 Degrees Fahr. (810 Degrees Cent.), Oil Bath Temperature = 77 Degrees Fahr. (25 Degrees Cent.)

Rounds	Degrees Fahr. Per Second At 1300 Degrees Fahr.	Slabs	Degrees Fahr. Per Second At 1300 Degrees Fahr.
1.5 inch round by 8 inch long	25.7	5 by 5 by 1.5 inch	12.6
1.5 inch round by 5 inch long	25.8	5 by 2.5 by 1.5 inch	16.9
1.5 inch round by 3.5 inch long	25.7	5 by 1.75 by 1.5 inch	20.7
1.5 inch round by 2.5 inch long	25.9	5 by 1.5 by 1.5 inch	25.0
1.5 inch round by 1.75 inch long	30.2		
1.5 inch round by 1.5 inch long	33.3		
1.5 inch round by 1.125 inch long	41.4		

Bars	Degrees Fahr. Per Second At 1300 Degrees Fahr.
1.5 by 1.5 by 6 inch	23.8
1.5 by 1.5 by 3 inch	24.2
1.5 by 1.5 by 1.75 inch	29.5
1.5 by 1.5 by 1.5 inch	31.0
1.5 by 1.5 by 1.125 inch	37.2

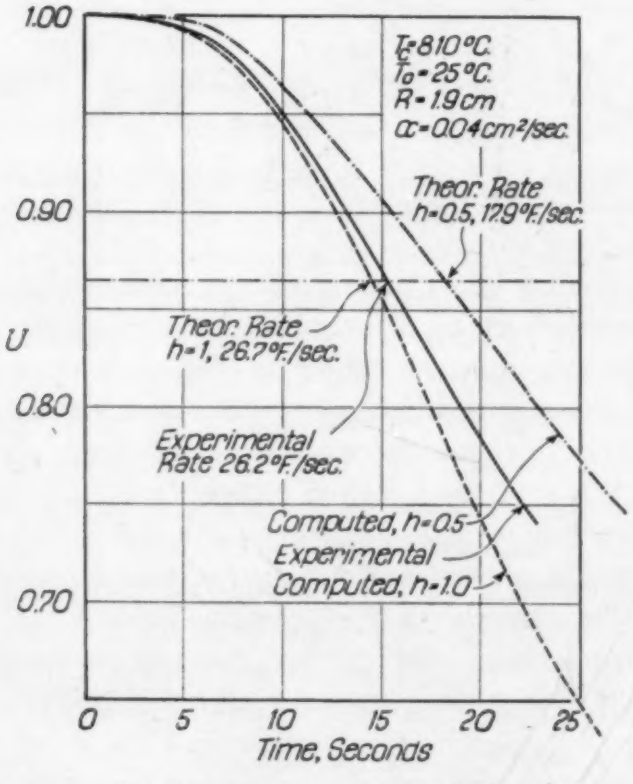

Fig. 2a—Comparison of Calculated and Experimental Center Cooling Rates in 32 Per Cent Nickel Steel Cylinder, 1.5 Inch Diameter by 8 Inches Long; Oil Quench.

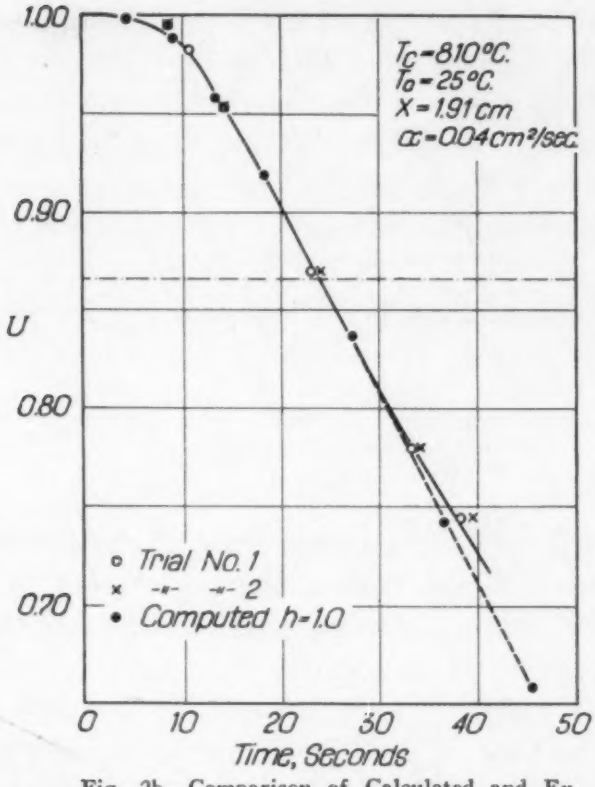

Fig. 2b—Comparison of Calculated and Experimental Center Cooling Rates in 32 Per Cent Nickel Steel Slab, 1.5 Inch Thick; Oil Quench.

per second, T_c (the quenching temperature) equal to 1490 degrees Fahr. (810 degrees Cent.), and T_o (the temperature of the quenching medium) equal to 76 degrees Fahr. (25 degrees Cent.). This value of thermal diffusivity has been determined by Scott[1] and has been independently redetermined in these Laboratories. An inspection of Figs. 2 (a) and 2 (b) shows that the severity of quench (h) is equal to unity for the oil quenching used in these experiments.[6]

Qualitatively, the results of these experiments show that the end or edge effect of cylinders on center rates of cooling during quenching are negligible until the length of the cylinder becomes almost equal to the diameter; similarly, the end effect of a bar on center cooling rates is negligible except when the length of the bar becomes almost equal to the smallest of the side dimensions.

Calculation of Cooling Rate Contours in Finite Sections

Appendix I considers the solution of the heat-conduction equation for the quenching of bars, blocks and cylinders of finite lengths.

[6]Note that Grossmann's parameter expressing severity of quench is one-half the parameter used in this work, i.e., H = ½ h.

Table I

Center Cooling Rates (Degrees Fahr. Per Second) at 1300 Degrees Fahr. (705 Degrees Cent.) Oil Quenching, Quenching Temperature = 1490 Degrees Fahr. (810 Degrees Cent.), Oil Bath Temperature = 77 Degrees Fahr. (25 Degrees Cent.)

Rounds	Degrees Fahr. Per Second At 1300 Degrees Fahr.	Slabs	Degrees Fahr. Per Second At 1300 Degrees Fahr.
1.5 inch round by 8 inch long	25.7	5 by 5 by 1.5 inch	12.6
1.5 inch round by 5 inch long	25.8	5 by 2.5 by 1.5 inch	16.9
1.5 inch round by 3.5 inch long	25.7	5 by 1.75 by 1.5 inch	20.7
1.5 inch round by 2.5 inch long	25.9	5 by 1.5 by 1.5 inch	25.0
1.5 inch round by 1.75 inch long	30.2		
1.5 inch round by 1.5 inch long	33.3		
1.5 inch round by 1.125 inch long	41.4		

Bars	Degrees Fahr. Per Second At 1300 Degrees Fahr.
1.5 by 1.5 by 6 inch	23.8
1.5 by 1.5 by 3 inch	24.2
1.5 by 1.5 by 1.75 inch	29.5
1.5 by 1.5 by 1.5 inch	31.0
1.5 by 1.5 by 1.125 inch	37.2

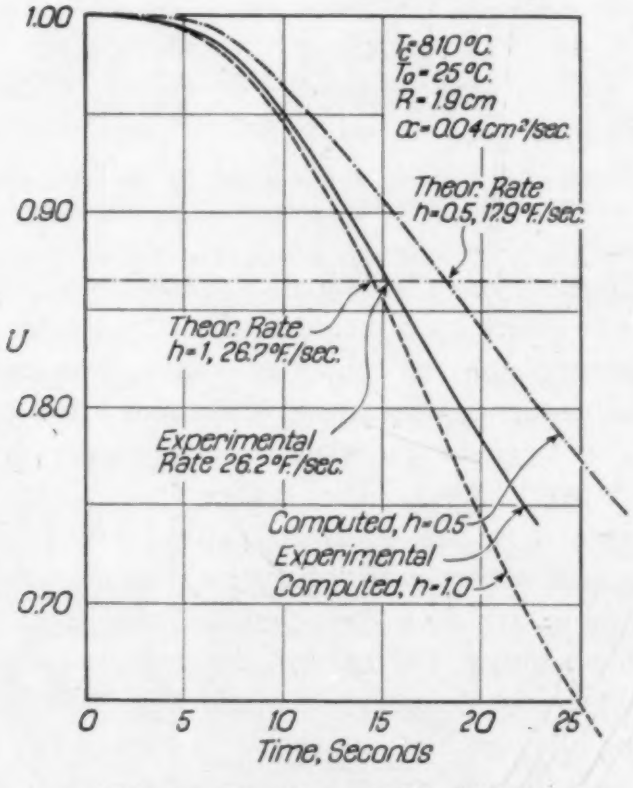

Fig. 2a—Comparison of Calculated and Experimental Center Cooling Rates in 32 Per Cent Nickel Steel Cylinder, 1.5 Inch Diameter by 8 Inches Long; Oil Quench.

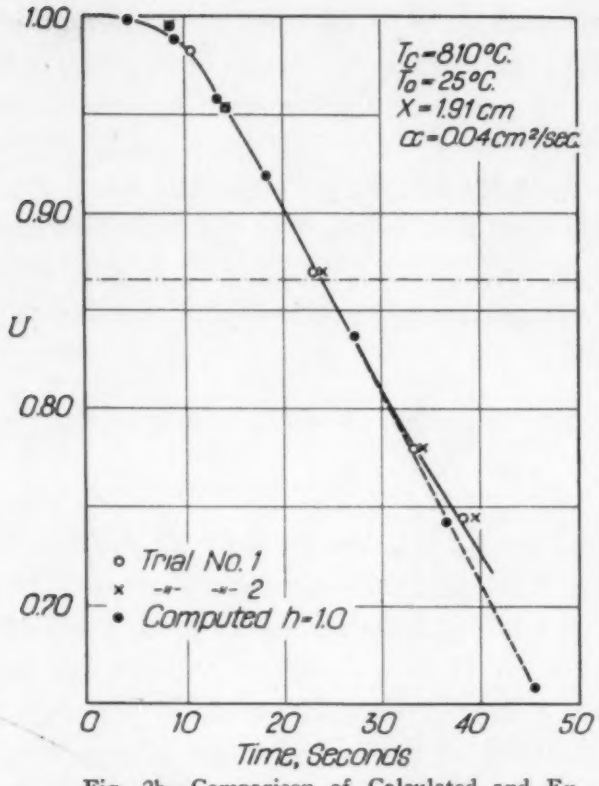

Fig. 2b—Comparison of Calculated and Experimental Center Cooling Rates in 32 Per Cent Nickel Steel Slab, 1.5 Inch Thick; Oil Quench.

per second, T_c (the quenching temperature) equal to 1490 degrees Fahr. (810 degrees Cent.), and T_o (the temperature of the quenching medium) equal to 76 degrees Fahr. (25 degrees Cent.). This value of thermal diffusivity has been determined by Scott[1] and has been independently redetermined in these Laboratories. An inspection of Figs. 2 (a) and 2 (b) shows that the severity of quench (h) is equal to unity for the oil quenching used in these experiments.[6]

Qualitatively, the results of these experiments show that the end or edge effect of cylinders on center rates of cooling during quenching are negligible until the length of the cylinder becomes almost equal to the diameter; similarly, the end effect of a bar on center cooling rates is negligible except when the length of the bar becomes almost equal to the smallest of the side dimensions.

Calculation of Cooling Rate Contours in Finite Sections

Appendix I considers the solution of the heat-conduction equation for the quenching of bars, blocks and cylinders of finite lengths.

[6]Note that Grossmann's parameter expressing severity of quench is one-half the parameter used in this work, i.e., H = ½ h.

Briefly, these solutions are based upon the assumption that the heat flow through the surface of the body during quenching is normal to the surface at all points and proportional to the difference between the temperature of the surface and the temperature of the coolant. In other words, no edge effects are considered except those naturally arising from the heat flow normal to the two surfaces forming the edge.

Using the customary reduced temperature for problems of this sort, i. e.,

$$U = \frac{T - T_o}{T_c - T_o}, \text{ where}$$

T_c is the original quenching temperature, T_o is the temperature of the coolant, and T is the temperature of a point in the body for which the rate of cooling is to be determined, the tables of Russell[2] can be used to obtain U as a function of time for any point along the radius of an infinitely long cylinder, or for any point between the center and surface of a slab, when an appropriate value for the thermal diffusivity (a) is known in addition to the severity of quench (h).

Referring to the cylinder of radius R and length 2Z shown in Fig. 3, the rate of cooling of the point P due to quenching from a temperature T_c into a coolant at temperature T_o may be considered to be controlled by two different factors,

(1), The heat flow due to the quenching of a slab of thickness 2Z, and

(2), the heat flow due to the quenching of a cylinder of radius R.

The results of Appendix I show that if the position of the point P is defined in terms of r/R and z/Z where r and z are the distances of the point from the center of the cylinder and slab respectively, then the reduced temperature of the point P at time (t) is given by

$$U = U_R \cdot U_z \cdot$$

In this equation U_R is the reduced temperature of the point P (r/R) at time (t) due to the quenching of the infinitely long cylinder of radius R, and U_Z is the reduced temperature of the point P (z/Z), at time (t) due to the quenching of the slab of thickness 2Z.

In the same manner, the rate of cooling of a point in a bar of cross sectional dimensions 2X and 2Y may be considered to be controlled by

(1), the heat flow due to the quenching of a slab of thickness 2X, and

(2), the heat flow due to the quenching of a slab of thickness 2Y. Appendix I shows that if the position of the point P is defined by x/X and y/Y where x and y are the distances of the point

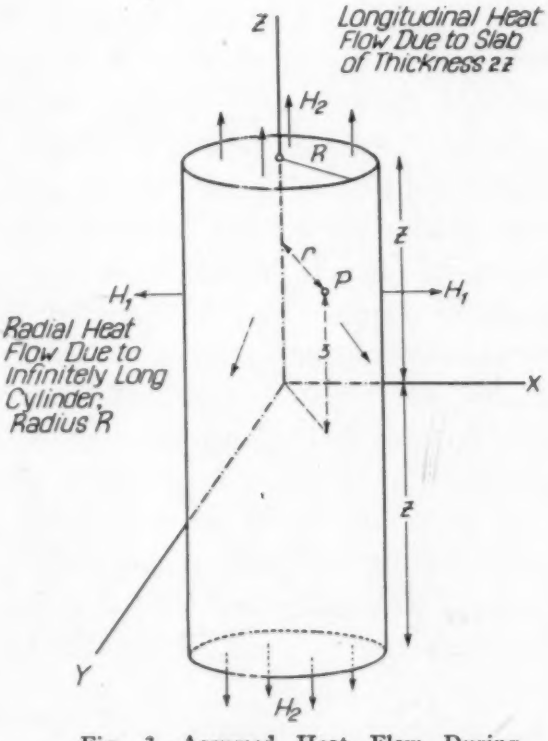

Fig. 3—Assumed Heat Flow During Quenching in a Cylinder of Length 2Z and Radius R.

from the center of the two slabs of thickness 2X and 2Y respectively, then the reduced temperature of the point P at time (t) is

$$U = U_x \cdot U_Y \cdot$$

Here U_X is the reduced temperature of the point P(x/X) at time (t) due to the quenching of the slab of thickness 2X, and U_y is the reduced temperature of the point P (y/Y) at time (t) due to the quenching of the slab of thickness 2Y.

Extending these considerations to the case of a block of side dimensions 2X, 2Y and 2Z, the reduced temperature of a point P

(x/X, y/Y, z/Z) at time (t) is

$$U = U_x \cdot U_Y \cdot U_z, \text{ where}$$

U_X, U_Y and U_Z are the reduced temperatures of the point P at time (t) arising from the quenching of the three mutually perpendicular slabs.

To facilitate computations, Figs. 4 and 5 show the reduced temperature as a function of time in seconds in slabs and cylinders of infinite length for water and oil quenching. The diameter of the rounds and thickness of the slabs vary from 0.5 to 3 inches. The reduced temperatures of a point at the center, 6/10, and 8/10 the distance from the center to the surface ($r/R = 0$, $r/R = 0.6$, $r/R = 0.8$) are shown for the cylinder and also for the slab ($x/X = 0$, $x/X = 0.6$, $x/X = 0.8$). Figs. 4 and 5 were constructed with the help of the tables of Russell[2] using a thermal diffusivity (α) of 0.040 centimeter square per second for austenite, $h = 10$ and $h = 1$ for the severity of quench during brine and oil quenching[7].

The oil quenching charts (Fig. 5) may be compared directly with the experimental data on the variation of center cooling velocity in cylinders and bars of variable length, and in slabs as one side is decreased to form a bar. As an example, let $T_c = 810$ degrees Cent. (1490 degrees Fahr.), $T_o = 76$ degrees Fahr. (25 degrees Cent.) $h = 1$ (oil quenching) and let the center cooling rate be desired at the temperature of 1300 degrees Fahr. (705 degrees Cent.) for a cylinder 1.5 inches round by 1.5 inches long. The reduced temperatures shown below were obtained directly from Fig. 5.

Time in Seconds	U_R ($r/R = 0$)	U_Z ($z/Z = 0$)	U	Rate (Degrees Fahr. Per Sec.) $= (T_c - T_o) \times \frac{9}{5} \times \frac{\Delta U}{\Delta t}$
8	0.970	0.990	0.96	
10	0.945	0.98	0.925	>24.7
12	0.912	0.968	0.873	>36.7
15	0.855	0.945	0.807	>31.0
18	0.80	0.92	0.735	>33.8

If these reduced temperatures (U) are plotted as a function of time, it will be found that the cooling rate at 1300 degrees Fahr. (705 degrees Cent.), which corresponds to $U = 0.865$, is 34 degrees Fahr. per second. This cooling rate is to be compared with the experimentally determined rate of 33.3 degrees Fahr. per second (see Table I).

[7]See Appendix II for a convenient method of determining severity of quench.

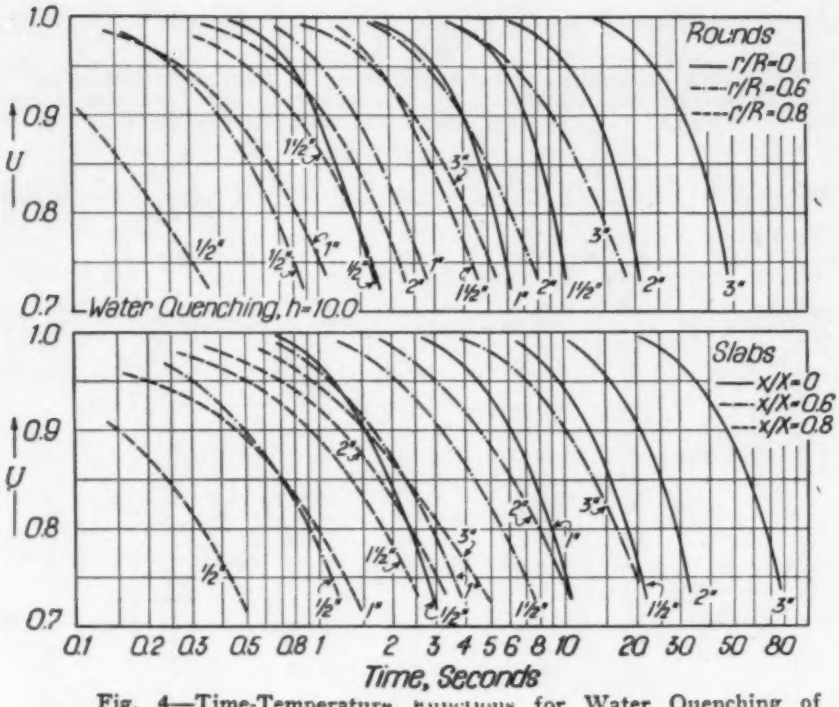

Fig. 4—Time-Temperature Functions for Water Quenching of Cylinders and Slabs.

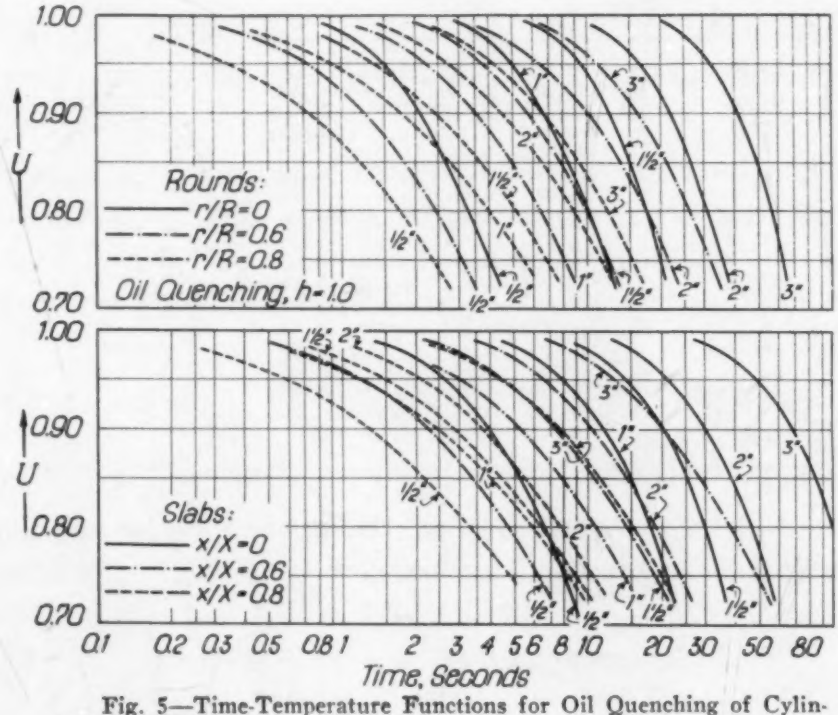

Fig. 5—Time-Temperature Functions for Oil Quenching of Cylinders and Slabs.

Table II lists some computations for a few of the cylinders and bars previously considered. The agreement between the experimental and calculated center cooling rates in the oil quenching of

Table II

Calculation of Center Cooling Rates (Degrees Fahr. Per Second) at 1300 Degrees Fahr. (705 Degrees Cent.) Oil Quenching, h = 1, T_e = 1490 Degrees Fahr. (810 Degrees Cent.), T_o = 77 Degrees Fahr. (25 Degrees Cent.), See Fig. 5.

Rounds	Time (Seconds)	U_R	U_Z	U	Rate (Degrees Fahr. per Second) $= 1410 \times \frac{\Delta U}{\Delta t}$	Experimental Rate at 1300 Degrees Fahr.
1.5 inch round by 8 inch long	6	0.99	.....	0.99		
	8	0.97	.....	0.97	>14.1	
	10	0.945	.....	0.945	>17.6	
	12	0.915	.....	0.915	>21.1	
	15	0.86	.....	0.86	>25.9	25.7
	18	0.80	.....	0.80	>28.2	
1.5 inch round by 1.5 inch long	6	0.99	0.998	0.99		
	8	0.97	0.99	0.96	>21.1	
	10	0.945	0.98	0.925	>24.6	
	12	0.915	0.968	0.885	>28.2	33.3
	15	0.86	0.945	0.812	>34.3	
	18	0.80	0.92	0.735	>36.0	
1.5 inch round by 1.125 inch long	6	0.99	0.99	0.98		
	8	0.97	0.97	0.945	>24.7	
	10	0.945	0.945	0.898	>33.1	
	12	0.915	0.925	0.845	>37.4	41.4
	15	0.86	0.895	0.77	>38.0	
	18	0.80	0.85	0.68	>42.2	

Bars	Time (Seconds)	U_X	U_Y	U_Z	U	Rate (Degrees Fahr. per Second) $= 1410 \times \frac{\Delta U}{\Delta t}$	Experimental Rate at 1300 Degrees Fahr.
1.5 by 1.5 by 6 inch	8	0.99	0.99	1.00	0.98		
	10	0.98	0.98	.....	0.96	>14.1	
	12	0.968	0.968	.....	0.935	>17.6	
	15	0.945	0.945	.....	0.895	>18.8	
	18	0.922	0.922	.....	0.85	>21.1	23.8
	20	0.905	0.905	.....	0.82	>21.1	
	25	0.86	0.86	.....	0.74	>22.4	
1.5 by 1.5 by 1.5 inch	8	0.99	0.99	0.99	0.97		
	10	0.98	0.98	0.98	0.94	>21.1	
	12	0.968	0.968	0.968	0.902	>26.7	
	15	0.945	0.945	0.945	0.845	>26.7	
	18	0.922	0.922	0.922	0.782	>29.4	31.0
	20	0.905	0.905	0.905	0.74	>29.6	
1.5 by 1.5 by 1.25 inch	8	0.99	0.99	0.980	0.96		
	10	0.98	0.98	0.945	0.91	>35.2	
	12	0.968	0.968	0.925	0.865	>32.0	
	15	0.945	0.945	0.885	0.792	>34.2	37.2
	18	0.922	0.922	0.85	0.72	>50.8	

32 per cent nickel cylinders and bars is satisfactory for the purpose of extending these proposed methods of hardenability calculations.

Hardenability in Finite Sections

Fig. 6 shows the calculated rates of cooling (degrees Fahr. per second at 1300 degrees Fahr.) during oil quenching along the center section of a block measuring 1.5 inches by 2 inches by 3 inches. The quenching temperature was considered to be 1490 degrees Fahr.

(810 degrees Cent.) while the temperature of the coolant was set at 76 degrees Fahr. (25 degrees Cent.). These rates were calculated by means of Fig. 5 and the methods outlined previously and below.

In Fig. 6, the rate of cooling of the point A is considered to be due to the heat flow at the point $x/X = 0$ in a 3-inch slab, the heat flow at the point $y/Y = 0$ in a 1.5-inch slab, and the heat flow at the point $z/Z = 0$ in a 2-inch slab. Similarly, the rate of cooling

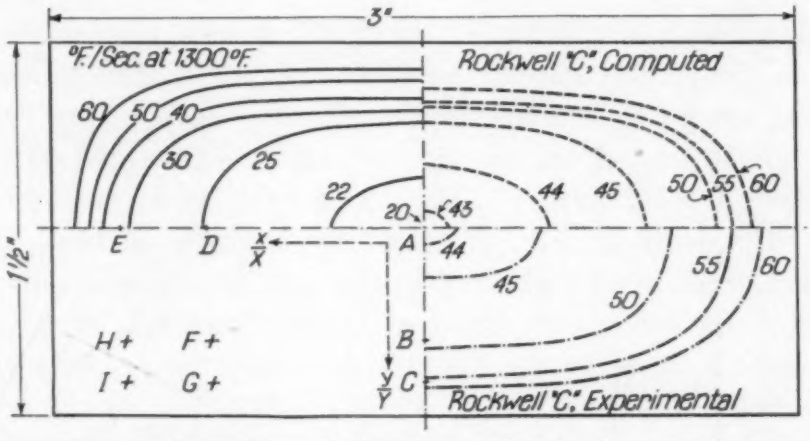

Fig. 6—Comparison of Computed and Experimental Hardness Contours in a 1.5 by 2 by 3 Inch Block.

of the point I is considered to be due to the heat flow at the points $x/X = 0.8$ in a 3-inch slab, $y/Y = 0.8$ in a 1.5-inch slab, and $z/Z = 0$ in a 2-inch slab. The use of Fig. 5 yields the following reduced temperature of the point A as a function of time:

Point A

t (sec.)	3-Inch $x/X = 0$ U_x	1.5-Inch $y/Y = 0$ U_y	2-Inch $z/Z = 0$ U_z	U	Rate (Degrees Fahr. Per Sec.) at 1300 Degrees Fahr. $= 1410 \times \frac{\Delta U}{\Delta t}$
6	1.00	0.998	1.00	0.998	
8	1.00	0.99	1.00	0.99	> 5.6
10	1.00	0.98	1.00	0.98	> 7.1
12.5	1.00	0.963	0.99	0.953	>15.2
15	1.00	0.945	0.98	0.925	>15.8
18	1.00	0.92	0.968	0.89	>16.5
20	1.00	0.905	0.958	0.865	>17.6
25	0.995	0.86	0.93	0.795	>19.8
30	0.988	0.81	0.90	0.718	>21.7

A plot of U against time (t) yields 18.8 degrees Fahr. per second as the calculated rate of cooling of the point A past 1300 degrees Fahr. (705 degrees Cent.). The calculated rates of cooling

of the other points shown in Fig. 6 are B — 23.8, C — 44, D — 24.7, E — 30.0, F — 31.0, G — 50.8, H — 49.5, and I — 63.5 degrees Fahr. per second past 1300 degrees Fahr. (705 degrees Cent.).

A 3½-inch bar sample of steel analyzing

Per Cent						
C	Mn	Si	P	S	Cr	Ni
0.93	1.66	0.31	0.015	0.006	0.15	0.04

was machined into a block 1.5 by 2 x 3 inches, and also tested by means of the Jominy flat-end hardenability test[3]. The Jominy specimen was heated to a temperature of 1490 degrees Fahr. (810 degrees Cent.), soaked ten minutes at heat and then end-quenched in a standard Jominy fixture. The block was heated to 1490 degrees Fahr. (810 degrees Cent.), soaked ten minutes at heat, and then quenched into the oil bath used in the previous experiments. After hardening, the block was sectioned so that Rockwell hardness readings could be taken on the longitudinal midplane of dimensions 1.5 by 3 inches.

Using the rates of cooling (degrees Fahr. per second at 1300 degrees Fahr.) on the Jominy specimen as recommended by the Society of Automotive Engineers, the following are the Rockwell hardnesses to be associated with the various rates of cooling for the steel in question:

Degrees Fahr. Per Second at 1300 Degrees Fahr.	"C" Rockwell Hardness
70	62.5
50	61.5
40	58.5
35	55.0
30	49.0
25	45.0
20	42.5
10	38.0

The rates of cooling shown in Fig. 6 were combined with the results of the Jominy hardenability test to obtain the Rockwell contours in the upper right quadrant of Fig. 6. The experimental Rockwell hardnesses are shown in the lower right quadrant of Fig. 6.

In order to compare predicted rates of cooling obtained from Fig. 4, for water quenching with experimental data, a series of cylinders, 0.75 inch round by 1.5 inches, 0.75 inch round by 0.75 inch,

and 0.75 inch round by 0.625 inch were made from a 1-inch round bar of 1.10 per cent carbon tool steel of the following analysis:

Per Cent						
C	Mn	Si	P	S	Cr	Ni
1.08	0.26	0.35	0.018	0.013	0.09	0.04

The hardenability (Rockwell hardness as a function of rate of cooling at 1300 degrees Fahr.) of this steel was determined by oil quenching a cone-test hardenability specimen[8] from 1600 degrees Fahr. (865 degrees Cent.), reheated to 1450 degrees Fahr. (788 degrees Cent.), soaking ten minutes at heat and then brine quenching. The hardenability of the steel was as follows:

Degrees Fahr. Per Second at 1300 Degrees Fahr.	"C" Rockwell Hardness
145	41
175	42
198	45
213	50
222	55
232	60
248	64
260	65

The rates of cooling at 1300 degrees Fahr. (705 degrees Cent.) during water quenching were computed for the cylinders listed above using Fig. 4 and the methods outlined previously. These computed rates of cooling were then used in conjunction with the hardenability data above to obtain a predicted Rockwell contour at the center plane in these cylinders.

The cylinders listed above were oil-treated at 1600 degrees Fahr. (865 degrees Cent.), followed by heating to 1450 degrees Fahr. (790 degrees Cent.), soaking ten minutes at heat and then brine-quenching. The cylinders were packed in a 1-inch diameter pipe during the latter treatment to reproduce approximately the rate of heating of the cone-test specimen through the critical temperature range, since it has been shown[8] that the rate of heating of 1.10 per cent carbon tool steel through the critical temperature range influences the resulting hardenability. After the pipe and cylinders reached 1450 degrees Fahr. (790 degrees Cent.), the cylinders were placed on the hearth of the furnace and soaked ten minutes at heat, followed by brine-quenching. The cylinders were then split at the center and Rockwell hardness contours obtained to compare with the computed contours. Fig. 7 shows the predicted and experimental Rockwell

[8] C. B. Post, O. V. Greene, W. H. Fenstermacher, TRANSACTIONS, American Society for Metals, Vol. 30, 1942, p. 1202.

contours in these cylinders. Considering the fact that the 0.75-inch round bar is close to the critical section for this steel, i.e., the size round which would just harden through to a Rockwell hardness of R_c 55, the agreement between experimental and computed Rockwell contours in this size of cylinder is satisfactory for hardenability studies.

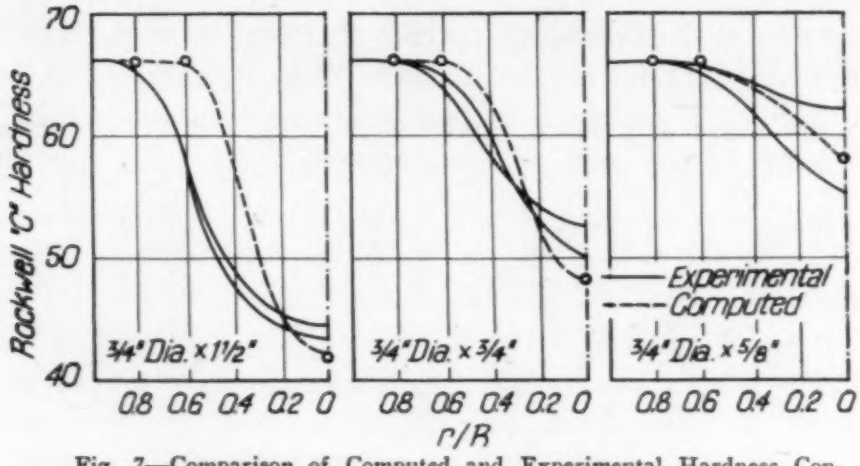

Fig. 7—Comparison of Computed and Experimental Hardness Contours, 0.75-Inch Round Cylinders.

Conclusions

1. Experimental center cooling rates (degrees Fahr. per second at 1300 degrees Fahr.) were determined for the oil quenching of cylinders and bars of variable length, and slabs when one side of the slab is steadily decreased until a bar is formed. These data show that the effect of the length of cylinders and bars on the center cooling rates at 1300 degrees Fahr. is negligible until the length becomes almost equal to the radius or one of the cross section dimensions.

2. Methods are outlined for computing the rates of cooling throughout finite sections such as cylinders, bars and blocks. These methods are based upon the assumption that heat flow during quenching is normal to the surface at all points and proportional to the difference in temperature between the surface and coolant. By these methods, the temperature functions for finite sections can be obtained by simple combinations of the temperature function for cylinders of infinite length and slabs, for which excellent tables are available.

3. Finally, the data obtained from the Jominy flat-end test[3] and cone-test specimen[8] for measuring the hardenability of steel in terms

of degrees Fahr. per second at 1300 degrees Fahr. (705 degrees Cent.) are combined with the computed rates of cooling (degrees Fahr. per second at 1300 degrees Fahr.) to predict Rockwell hardness contours in various finite sections. These methods have been applied to several specific shapes and found to yield satisfactory estimates of hardenability in finite sections.

4. An indirect conclusion of this work is that the rate of cooling past 1300 degrees Fahr. (705 degrees Cent.) is a workable criterion of the hardenability of steel.

Acknowledgment

The generous co-operation of the Staff of the Metallurgical and Chemical Laboratories of The Carpenter Steel Company in carrying out this investigation is gratefully acknowledged. The authors wish to thank Mr. J. H. Parker, President, and Mr. B. H. DeLong, Chief Metallurgist, of The Carpenter Steel Company, for permission to publish these results.

Appendix I
Mathematical Analysis

Referring to Fig. 3 consider a finite cylinder of radius R and length 2Z. Assume that the temperature gradient at the surface is normal at all points to the surface and proportional to the difference in temperature between the surface and coolant. The complete boundary value problem for this case is as follows:

$$\frac{\partial U}{\partial t} = \alpha\left[\frac{\partial^2 U}{\partial r^2} + \frac{1}{r}\frac{\partial U}{\partial r} + \frac{\partial U^2}{\partial z^2}\right] \quad \text{.....(1)}$$

$$\left(\frac{\partial U}{\partial r}\right)_{r=R} = -hU \quad \text{.....(2)}$$

$$\left(\frac{\partial U}{\partial z}\right)_{z=+Z} = -hU\,; -\left(\frac{\partial U}{\partial z}\right)_{z=-Z} = -hU \quad \text{.....(3)}$$

$$U_{t=0} = F(r, z) \quad \text{.....(4)}$$

where α equals the thermal diffusivity, $U = \dfrac{T - T_o}{T_c - T_o}$ and h is

the so-called "severity of quench". Letting the initial temperature of the cylinder be constant throughout at time t = O, i. e., $U_{t=o} = U_c$, then the solution of the differential Eq. (1) and the boundary conditions (2) and (3) is

$$U = \sum_{i=1}^{\infty} \sum_{k=1}^{\infty} D_{ik} J_o(\lambda_k r) \cos(\mu_i z) \exp(-\lambda_k^2 \alpha t) \exp(-\mu^2 \alpha t) \quad \ldots (5)$$

where $J_o(\lambda_k r)$ are Bessel functions of the first kind and zero order, and λ_k and μ_i must be chosen to satisfy the following equations expressing the boundary conditions (2) and (3):

$$\frac{\lambda_k R}{hR} = \frac{J_o(\lambda_k R)}{J_1(\lambda_k r)} \quad \ldots (6)$$

$$\frac{\mu_i Z}{hZ} = \cot(\mu_i Z) \quad \ldots (7)$$

Solutions of (6) and (7) are given in standard treatises on heat conduction.[9]

At time t = O, Eq. (5) reduces to

$$U_c = \sum_{k=1}^{\infty} \left[\sum_{i=1}^{\infty} D_{ik} \cos(\mu_i Z) \right] J_o(\lambda_k r) \quad \ldots (8)$$

For each fixed z-value between O and Z, this series is the Fourier-Bessel series of the function $J_o(\lambda_k R)$ of the variable r, $(O \leqslant r \leqslant R)$, provided the coefficients satisfy certain orthogonal relationships. Then, by well known methods,

$$\sum_{i=1}^{\infty} D_{ik} \cos(\mu_i z) = 2 \frac{U_c \int_o^R r \cdot J_o(\lambda_k r)\, dr}{J_1^2(\lambda_k r)} =$$

$$\left(\frac{2}{\lambda_k R}\right) \frac{J_1(\lambda_k R)}{J_o^2(\lambda_k R) + J_1^2(\lambda_k R)} \quad \ldots (9)$$

and finally,

$$D_{ik} = \left[\left(\frac{2}{\lambda_k R}\right) \frac{J_1(\lambda_k R)}{J_o^2(\lambda_k R) + J_1^2(\lambda_k R)}\right]\left[\frac{2 \sin(\mu_i Z)}{(\mu_i Z) + \sin(\mu_i Z) \cos(\mu_i Z)}\right] =$$

$$A_k B_i \quad \ldots (10)$$

[9] Gröber-Eck, "Die Grundgesetze der Wärmübertragung," Berlin, J. Springer, 1933, p. 51.

which yields the following approximate equation for the temperature of a point (r, z) inside a finite cylinder at time (t),

$$U = \sum_{k=1}^{\infty} \sum_{i=1} A_k B_i J_o(\lambda_k r) \exp(-\lambda_k^2 \alpha t) \cos(\mu_i Z)$$

$$\exp(-\mu_i^2 \alpha t) \quad \ldots\ldots (11)$$

The temperature function for a point distant r from the axis of an infinitely long cylinder is,

$$U_R = \sum_{k=1}^{\infty} A_k J_o(\lambda_k r) \exp(-\lambda_k^2 \alpha t) \quad \ldots\ldots (12)$$

while the temperature function for a point distant z from the center of a slab of thickness 2Z is given by

$$U_z = \sum_{i=1}^{\infty} B_i \cos(\mu_i z) \exp.(-\mu_i^2 \alpha t) \quad \ldots\ldots (13)$$

so that the approximate equation giving the temperature function U for a point (r, z) in a finite cylinder of radius R and length 2Z at the time t, is

$$U = U_R U_z \quad \ldots\ldots (14)$$

where U_R and U_Z are the temperature functions for the points r/R in an infinitely long cylinder and z/Z in a slab of thickness 2Z.

Similarly, the boundary value problem of heat conduction for the quenching of an infinitely long bar of side dimensions 2X and 2Y from a temperature T_c into a coolant at temperature T_o is given by:

$$\frac{\partial U}{\partial t} = \frac{\partial^2 U}{\partial x^2} + \frac{\partial^2 U}{\partial y^2} \quad \ldots\ldots (15)$$

$$-\left(\frac{\partial U}{\partial x}\right)_{x=-X} = -hU; \quad \left(\frac{\partial U}{\partial x}\right)_{x=+X} = -hU \quad \ldots (16)$$

$$-\left(\frac{\partial U}{\partial y}\right)_{y=-Y} = -hU; \quad \left(\frac{\partial U}{\partial y}\right)_{y=+Y} = -hU \quad \ldots (17)$$

$$U_{\substack{(xy)\\ t=o}} = F(xy) \quad \ldots\ldots (18)$$

The solution of the differential Eq. (15) and the two boundary conditions (16) and (17) is

$$U = \sum_{i=1}^{\infty}\sum_{k=1}^{\infty} C_{ik} \sin(m_i x) \sin(n_k y) \exp\{-\alpha (m_i^2 + n_k^2) t\}$$

$$+ \sum_{i=1}^{\infty}\sum_{k=1}^{\infty} D_{ik} \cos(m_i x) \cos(n_k y) \exp\{-\alpha (m_i^2 + n_k^2) t\} \quad (19)$$

where m_i and n_k must be chosen to satisfy the boundary conditions (16) and (17) or

$$\frac{hX}{m_i X} = -\tan(m_i X) \quad (20)$$

and

$$\frac{n_k Y}{hY} = -\tan(n_k Y) \quad (21)$$

By a straightforward analysis similar to the previous discussion for the finite cylinder, it can be shown that the temperature function of the point (xy) at time (t) in an infinitely long bar of side dimensions 2A and 2B can be obtained to a first approximation by

$$U = U_x U_y \quad (22)$$

In Eq. (22) U_x and U_y are defined to be the reduced temperatures at time (t) due to the quenching of two slabs of thickness 2X and 2Y respectively.

Generalizing Eq. (22) to include the case of a three-dimensional solid block, we may write

$$U = U_x U_y U_z. \quad (23)$$

All of the above solutions make explicit use of the temperature functions for a cylinder of radius R, and infinite length (U_R) and slabs of thickness 2X, (U_x, U_y and U_z). Figs. 4 and 5 show the temperature functions for infinitely long cylinders and slabs for two quenches, i.e., brine (h = 10) and oil (h = 1).

Appendix II

Determination of "Severity of Quench" by Rates of Cooling and Rockwell Hardness

Fig. 8 shows the center cooling velocities (degrees Fahr. per second at 1300 degrees Fahr.) for cylinders and slabs of various

sizes when the quenching temperature is taken to be 1500 degrees Fahr. (810 degrees Cent.) and the temperature of the quenching medium is 77 degrees Fahr. (25 degrees Cent.). Fig. 8 was constructed by means of the tables of Russell.[2]

To apply Fig. 8 to the determination of severity of quench, it is convenient to select a given lot of steel and determine its hardenability by means of the Jominy flat-end test[3] for the deeper hardening grades of steel, or the cone hardenability test[8] for shallow hardening steels. Either of these tests will evaluate the Rockwell hardness

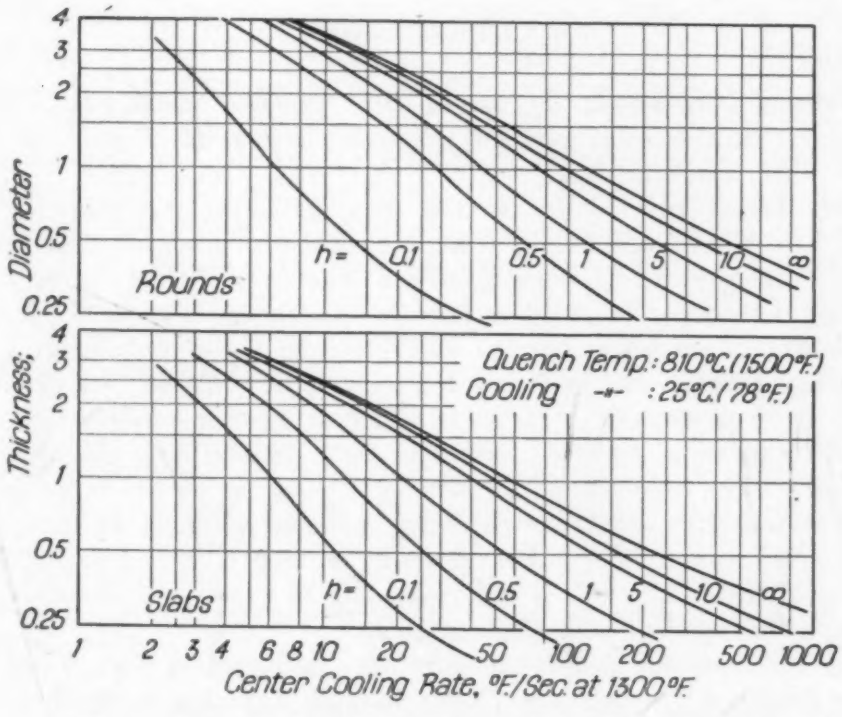

Fig. 8—Center Cooling Rates (Degrees Fahr. Per Second at 1300 Degrees Fahr.) in Cylinders and Slabs as a Function of Severity of Quench.

of the steel as a function of the rate of cooling (degrees Fahr. per second) past 1300 degrees Fahr. (705 degrees Cent.).

If one or more cylinders or slabs of the steel are hardened from the same temperature as the hardenability test, sectioned, and the center Rockwell hardness determined, a comparison of the center hardness with the hardenability test data will enable the center cooling rate (degrees Fahr. per second) past 1300 degrees Fahr. (705 degrees Cent.) to be determined for these cylinders or slabs. It is assumed that the length of the cylinder is about three times

the diameter and the breadth and length of the slab is about four times the thickness.

If the hardenability test and the cylinders or slabs have all been hardened from 1500 degrees Fahr. (810 degrees Cent.), using identical heating cycles, soaking at temperature the same length of time, then Fig. 8 may be used to determine the severity of quench used in these experiments. This is done by comparing the center rates of cooling obtained for the various sized round bars with the data shown in Fig. 8.[10]

DISCUSSION

Written Discussion: By Morse Hill, assistant metallurgist, Materials Laboratory, Engineering Division, Materiel Command, Army Air Forces, Wright Field, Dayton, Ohio.

The authors have shown a most able derivation and interpretation of cooling in combined shapes. It is most profitable to compare their derivation with that of Newman (Reference 275 of McAdams' "Heat Transmission").

Their verification of the derivation by experiment is good to have. It is possible that if we knew how to allow for the probable inaccuracy of the assumptions made in cooling derivations the results would be even closer. The quantity h of the authors' equation 16 is a heat transfer coefficient of the sort with which chemical engineers have long been dealing, even though it varies with time. Since it is affected by changes in liquid properties at the interface, and these properties must change during cooling, it cannot be expected that h will be a constant in practice. Further, since h is also a function of the diameter of the specimen it is not reasonable to expect the identical severity of quench for all sizes in a single medium.

The information which the authors have presented in Figs. 4 and 5 may also be presented in other ways. For instance by using a logarithmic scale for U and a linear scale for time, cooling curves are obtained which are easy to interpolate for intermediate severities of quench. Likewise for other sorts of interpolation plots other than time temperature are useful.

Oral Discussion

M. A. GROSSMANN:[11] It seems to me that there might well be some question about the criterion of the cooling rate at 1300 degrees Fahr. (705 degrees Cent.) because, as Mr. Post remarked, there have been numerous controversies and discussions about a good criterion. It seems to me, too, that the criterion of cooling rate at 1300 degrees Fahr. (705 degrees Cent.) has

[10]It is to be noted that Fig. 8 is strictly valid only when the quenching temperature of the rounds or slabs is 1500 degrees Fahr. (810 degrees Cent.). For any other quenching temperature, a new chart can be drawn up similar to Fig. 8.

[11]Director of research, Carnegie-Illinois Steel Corp., Chicago.

something to be said in its favor even though we ourselves did use a different criterion. Most of the argument as to whether a cooling rate at 1300 degrees Fahr. (705 degrees Cent.) is a good criterion revolves around the fact, that the most rapid rate of pearlite formation is around 1100 to 1000 degrees Fahr. (595 to 540 degrees Cent.) and not 1300 degrees Fahr. (705 degrees Cent.). But one must take into account the fact that the 1300 degrees Fahr. (705 degrees Cent.) cooling criterion does correlate rather well with actual data.

Possibly that is not as much of a discrepancy as might appear on the surface because if one quenches from say 1500 degrees Fahr. (815 degrees Cent.), into a medium at low temperature and takes the cooling rate at 1300 degrees Fahr. (705 degrees Cent.), that cooling rate does pretty well represent the cooling rate over the range 1300 to 1100 degrees Fahr. (705 to 595 degrees Cent.). It is well known that in addition to the time for actual formation of pearlite at 1100 degrees Fahr. (595 degrees Cent.), there is also in isothermal transformation certainly, and presumably in quenching, a necessary incubation period, and perhaps the necessary explanation as to why the 1300 degrees Fahr. (705 degrees Cent.) cooling rate is good even though pearlite forms at 1100 degrees Fahr. (595 degrees Cent.) is that the cooling rate over this range includes both incubation and pearlite formation, that that cooling rate does cover the total period that we are interested in, which would be 1300 to 1100 degrees Fahr. (705 to 595 degrees Cent.) and not merely 1300 degrees Fahr. (705 degrees Cent.) alone or 1100 degrees Fahr. (595 degrees Cent.) alone.

I. S. Reid:[12] I was greatly interested in quenching and hardenability. Ordinarily when quenching in oil the part or parts are quenched in oil circulated by a pump through a cooling system. Now you have certain cooling curves using this method. I used to do this with an aeroplane cylinder. We obtained physical properties much lower than when we put this same quench under pressure of 50 pounds with a pump capacity of 200 gallons per minute. Will the cooling curve be the same?

	Before Pressure Quench		After Pressure Quench	
	Steel No. 1*	Steel No. 2†	Steel No. 1*	Steel No. 2†
Elastic Limit, psi.	101,000	105,000	135,000	136,000
Max. Stress, psi.	109,600	117,700	151,000	151,500
Elongation in 2 inches, per cent	3.1	5.5	10.2	8.6
Reduction of Area, per cent	5.5	7.8	15.2	15.2
Brinell at 2000 Kg.	296	296	296	296

*S.A.E. 4140 with the following composition: carbon 0.42, manganese 0.73, chromium 0.97, molybdenum 0.23.

†S.A.E. 4140 with the following composition: carbon 0.42, manganese 0.75, chromium 0.96, molybdenum 0.23.

Authors' Reply

The comments by Mr. Hill are appreciated. There is not much that we can add to Mr. Hill's remarks except to state that we have tried to give as clear a derivation of these equations as is possible in this limited space without

[12]Superintendent of Heat Treat, Ford Motor Co., Windsor, Canada.

becoming involved in highly technical mathematical details which might have the questionable advantage of making the derivations shorter.

Grossmann's discussion of the various criteria of hardenability is much valued because of the work which he has done in this particular field. It is the authors' viewpoint, however, that all the parameters specifying hardenability which have been proposed are artificial and the only justification for preferring one over the other is according to the agreement shown between predicted cooling rates and that actually determined in steel sections. By this we mean to say that in the case of round bars it is obvious that the rate of cooling past 1300 degrees Fahr. (705 degrees Cent.) is related in some manner to the rate at 1000 degrees Fahr. (540 degrees Cent.), or, if one prefers, even at 800 degrees Fahr. (425 degrees Cent.). When heat equations are set up for expressing the heat transfer during the quenching of round bars, it will be found that if the necessary parameters such as the thermal diffusivity and severity of quench are chosen to make a cooling curve at the center of the bar agree with experimental determinations, then the parameters must be readjusted in order to make theoretical cooling curves agree exactly with the experimentally determined rates near the surface for any one of these temperatures. The less the readjustment necessary to bring theoretical and calculated cooling rates into agreement throughout the section, the better the selected criterion of hardenability.

Our principal tool used at the present time for studying hardenability is a measure of the hardness developed, and by and large the Rockwell machine is not too accurate for making a fine choice between these various criteria of hardenability. In the absence of critically designed experiments to indicate the correct criteria to be used in studying hardenability, we prefer to treat the methods developed by Howard Scott, H. J. French, Grossmann and ourselves, as workable tools for the extrapolation and prediction of hardness contours in round bars, slabs and various finite sections from limited data. Essentially Grossmann and we are adjusting certain parameters in the classical heat conduction equations so that reasonable agreement is reached between theoretical and actually determined Rockwell contours in various sections. Grossmann has consistently used the one-half temperature time as his criteria, whereas we have just shown that the rate of cooling past 1300 degrees Fahr. (705 degrees Cent.) yields the same order of agreement. Grossmann's and our first thought in all of this work has been to provide methods whereby if the hardenability of the steel is known in terms of an assumed parameter or criterion of hardenability, then the classical heat equations (together with adjusted values of thermal diffusivity, severity of quench, etc.) can be used to extrapolate limited data to predict the so-called hardenability of steel in various sections. To read into these hardenability studies anything else is an error.

As to Mr. Reid's question concerning the high-pressure quenching of parts in oil, we feel that he is working with a phenomena which is very incompletely understood at the present time. When the question was put to us orally at the convention we did not have time to give it the proper consideration. It appears that in oil quenching a film forms next to the piece which for all intents and purposes determines all of the characteristics of the oil quench, i.e., a milder severity of quench, small distortion, etc. If the specimen is now agitated so

that turbulent areas are set up in the neighborhood of the corners, etc., it will be found that the severity of quench will be impeded and that the oil is not exercising its full quenching powers because of the formation of these turbulent areas. This leads at once to the common practice of limiting agitation in oil to a slow figure-of-eight motion. If, however, submerged oil sprays are used such that the oil stream is impinged almost normally on specimen surfaces, and if high enough pressures are used, the facts from several sources seem to indicate that this film is broken and higher severity of quenches are obtained. This is nicely illustrated by the physical properties shown by Mr. Reid in his discussion. Unfortunately Mr. Reid did not give too much information on this data but if the aircraft cylinders are drawn down to a hardness of 296 Brinell as shown in the two cases, then the physical properties shown are understandable because this illustrates the fact that higher physical properties can be obtained with a completely quenched structure than with a mixed structure when both are drawn back to the same Brinell hardness. We do not believe the charts shown in Fig. 5 would apply to this type of submerged high-pressure oil-quenching.

AN EVALUATION OF QUENCHING OILS

By E. K. Spring, P. T. Lansdale and C. W. Alexander

Abstract

A study was made of the quenching rates and physical properties of various commercial quenching oils.

The data here presented indicate: (a) There are negligible differences in the quenching rates of new and used oils. (b) There is an optimum oil temperature to produce the maximum cooling rates at the nose of the "S-curve." Oil temperatures above or below this optimum temperature retard the cooling rate in this important temperature range. Warm oil has the desirable effect of giving slower cooling rates in the region of the martensitic transformation. (c) Similar quenching rates are exhibited by oils of mineral and animal origin. (d) The slight differences in the quenching rates of "light" and "heavy" oils can be compensated for by adjusting the oil temperature. (e) The greatest variation in quenching rates developed by the oils tested is but a minor factor in terms of steel hardenability.

Since it has been shown that all oils are metallurgically equal the selection of a quenching oil should be primarily controlled by the consideration of two factors: (A) a "flash and fire point" sufficiently high to prevent undue danger from fires and (B) the cost per pound of steel quenched under normal operating conditions.

IN considering the use of oils, or other liquids, for the quenching of steel it is necessary that certain basic facts be considered. We have attempted to establish these facts experimentally and provide a sound basis for the evaluation of quenching oils. With this information it is expected a more intelligent selection of oils for the quenching of steels can be made.

The oils were chosen for examination to represent those most commonly used for the quenching of steel. Among these oils are represented some based on animal oils, some based on mineral oils without special preparation for the purpose, others are mineral oils

A paper presented before the Twenty-fifth Annual Convention of the Society, held in Chicago, October 18 to 22, 1943. Of the authors, E. K. Spring is chief metallurgist, P. T. Lansdale is assistant metallurgist and C. W. Alexander is chief metallurgical inspector, Henry Disston & Sons, Inc., Tacony, Philadelphia. Manuscript received May 20, 1943.

specially prepared for use in quenching. It is felt the choice made covers the field and provides a sufficiently wide representation to include all types to be met with in practice.

As a first step in distinguishing between the oils, the physical data commonly used in grouping oils was taken. In addition, evaporation losses at different temperatures were determined. These data are recorded in Table I.

The oils were tested both as received and after considerable quenching had been carried out in them; to determine what and how much change in quenching capacity had taken place with use.

Flash and fire characteristics are important mainly from a safety standpoint. Specific gravity and viscosity are relatively unimportant in themselves. However, certain quenching characteristics can be connected with viscosity since the more viscous oils have a higher drag-out loss than the more fluid oils. Experience has shown that evaporation characteritsics of quenching oils have some bearing on their life if not on their performance.

The various oils were evaluated by plotting time vs. temperature curves for the quenching of a standard block of 18-8 stainless steel into the oils being studied. It was chosen to avoid the heat effects of critical transformations. The block was $\frac{13}{16}$ inch round by 1½ inch long with a $\frac{3}{16}$-inch hole drilled in from one end to a depth of ¾ inch to contain a 20-gage chromel-alumel thermocouple. An 8-inch long, ¼-inch I.D. pipe was threaded into the end of the block to prevent direct contact between the thermocouple and the quenching medium. A yoke was arranged to hold the couple in intimate contact with the bottom of the hole. The temperature of the specimen was indicated by a Leeds & Northrup mirror galvanometer and was recorded by projecting a pencil of light from the galvanometer mirror to a piece of photographic paper mounted on a drum revolving at a constant speed of one revolution per minute. A typical photographic record produced with this apparatus is shown in Fig. 1. The sensitivity and response of the galvanometer is such that the apparatus is capable of following temperature changes of the order of 500 degrees Fahr. per second. The size of the specimen was chosen to give quenching rates under 100 degrees Fahr. per second maximum to assure being within the limits of the galvanometer. The volume of oil used in each experiment was approximately four gallons. This was sufficient to prevent any great change in oil temperature resulting from the introduction of the hot specimen.

Table I

Physical Properties of Oils Studied

Symbol	Type	Condition	Flash Point °F.	Fire Point °F.	Spec. Grav. 130° F.	Viscosity 130° F. *	% Evaporation Loss after 6 Hrs. at Temp. 150° F.	200° F.	250° F.
A	Mixture of 100% Animal Oils	New	522	639	.903	55⅛	.21	.27	.29
A′	The same mixture of 100% Animal Oils after use	Used	475	604	.909	69	Nil	.15	.82
B	A Proprietary blended oil with intermediate rate	New	360	409	.869	49¼	.38	1.84	12.11
B′	Same Proprietary blended oil after use	Used	357	380	.859	49	.14	1.29	20.46
C	A Proprietary blended oil with low rate of cool	New	501	522	.875	531¾	.05	.14	.44
C′	Same Proprietary blended oil after use	Used	510	585	.880	739	.03	.19	.85
D	Straight Light Mineral Oil	New	360	398	.859	48	.11	1.70	19.10
D′	Same light Mineral Oil after use	Used	343	362	.862	47½	.11	2.96	27.59
E	Straight Heavy Mineral Oil	New	522	568	.891	445	.03	.06	.14
F	Straight Medium Mineral Oil	Used	431	469	.868	151	.03	.11	4.64
G	Proprietary Mineral Oil with high rate of cool	New	361	400	.848	51	.07	2.04	10.30
H	Fuel Oil	New	193	212	.838	36	19.48	....	.....

*Viscosity figures were obtained with the use of the Dudley Pipette and are expressed as the number of seconds required for a standard quantity of oil to run through a standard size orifice at a given temperature.

The information obtained with this apparatus was analyzed and replotted to give time versus temperature curves for the several oils under various conditions. This was done to make them more understandable and directly comparable with other curves obtained in the same manner. All oils were tested at a series of initial temperatures. It was decided in advance that these would be 80, 130, 220, 300, and 450 degrees Fahr. as nearly as possible. In some cases all five tem-

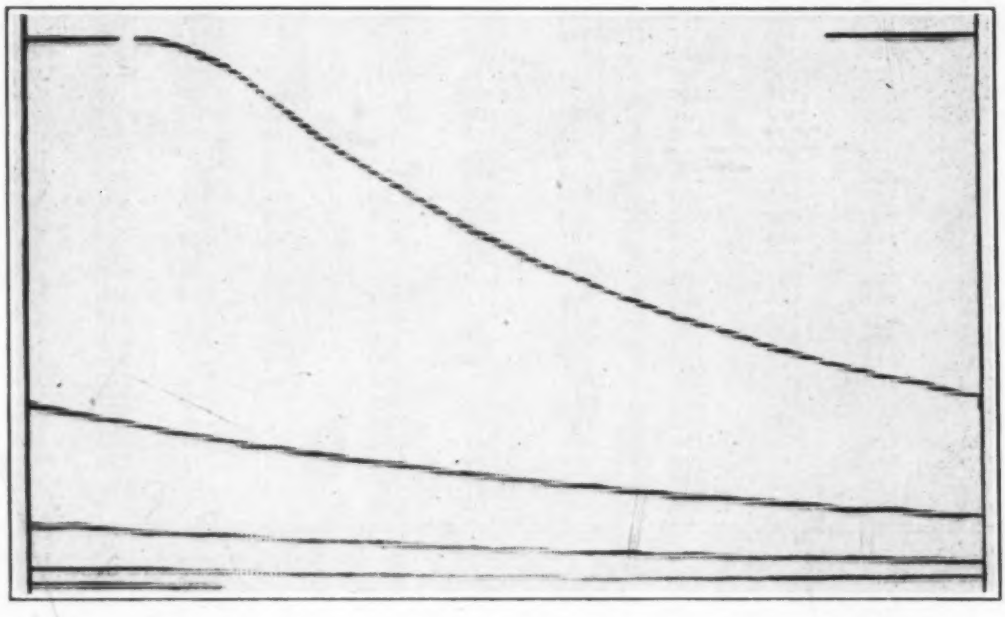

Fig. 1—A Typical Photographic Record Produced with this Apparatus.

peratures were employed, in others the low temperatures only were used. The limits were determined by the flash and fire characteristics of the oils in question. From the information on time versus temperature, data on quenching rates were calculated and temperature versus rate curves were plotted.

Since all of the curves are not reproduced, the basic information from which they were plotted is given in tabular form. Table II is the time versus temperature data and Table III is the temperature versus rate data. In these tabulations the actual oil temperature at which a test was conducted is given at the head of its appropriate column. A typical illustration of time versus temperature curves for an oil shown in Table II appears in Fig. 2. A similar illustration of temperature versus rate curve based on an oil in Table III appears in Fig. 3.

Fig. 3 is a plot of instantaneous cooling rate versus temperature

Table II
Time Versus Temperature Data

Time Sec.	Oil A — New 80 °F.	130 °F.	216 °F.	Oil A — Used 79 °F.	132 °F.	220 °F.	Oil B — New 82 °F.	132 °F.	220 °F.	295 °F.
0	1550	1550	1550	1550	1550	1550	1550	1550	1550	1550
1	1550	1550	1550	1550	1550	1550	1550	1550	1550	1550
2	1533	1550	1550	1533	1550	1550	1546	1550	1540	1541
3	1525	1533	1533	1525	1539	1514	1537	1550	1532	1532
4	1499	1506	1516	1499	1527	1496	1519	1534	1523	1513
5	1466	1480	1483	1483	1511	1470	1502	1517	1514	1495
6	1432	1445	1449	1466	1488	1442	1466	1501	1487	1477
7	1398	1410	1415	1449	1465	1405	1413	1485	1470	1440
8	1364	1384	1364	1415	1441	1397	1368	1452	1442	1422
9	1330	1349	1297	1381	1409	1351	1306	1420	1405	1367
10	1297	1322	1230	1348	1371	1315	1243	1403	1369	1331
12	1195	1252	1162	1297	1309	1260	1163	1338	1296	1257
14	1128	1190	1095	1230	1254	1206	1110	1289	1242	1202
16	1076	1129	1010	1178	1207	1152	1039	1240	1170	1166
18	1025	1077	976	1128	1100	1097	975	1192	1115	1093
20	993	1032	930	1076	1113	1041	938	1130	1080	1065
25	889	927	840	970	1020	947	842	1030	970	946
30	800	840	768	896	935	860	767	951	880	873
35	723	761	705	824	865	788	698	878	807	800
40	660	699	653	763	802	735	638	816	771	745
45	612	638	608	711	748	673	588	758	717	681
50	571	577	565	663	702	635	541	710	664	635
60	505	507	495	597	620	555	465	625	590	553
70	451	445	448	508	553	493	402	558	530	490
80	407	393	408	452	507	445	349	507	465	443
90	368	358	375	408	463	410	307	460	420	418
100	333	322	350	366	430	390	278	422	375	380
120	272	262	309	301	373	335	240	361	320	343
140	227	227	274	248	320	300		320	285	307
160	202	200	253	218	288	286		291	275	289
180	179	174	238	195	245	280		264	250	280
200	155	155	220	177	226	257		248	230	270
220	133	142	155		214	250		225		270
240	110	130	138		210	230				

Time Sec.	Oil B — Used 80 °F.	130 °F.	220 °F.	Oil C — New 88 °F.	128 °F.	221 °F.	300 °F.	450 °F.
0	1550	1550	1550	1550	1550	1550	1550	1550
1	1550	1550	1550	1550	1550	1550	1550	1543
2	1550	1550	1550	1542	1535	1534	1525	1535
4	1533	1541	1533	1534	1511	1511	1499	1520
3	1517	1524	1515	1509	1472	1459	1465	1481
5	1483	1515	1468	1484	1433	1409	1379	1443
6	1449	1480	1429	1459	1393	1360	1319	1405
7	1398	1463	1394	1421	1338	1318	1285	1359
8	1364	1428	1360	1384	1291	1277	1242	1313
9	1314	1393	1325	1342	1236	1235	1207	1275
10	1297	1358	1290	1300	1189	1186	1165	1229
12	1212	1306	1204	1209	1110	1102	1105	1160
14	1128	1244	1152	1142	1047	1053	1045	1100
16	1076	1182	1100	1084	985	1003	1002	1038
18	1025	1130	1035	1026	945	970	960	992
20	975	1088	985	976	898	937	925	954
25	893	995	890	884	828	870	865	870
30	812	908	800	800	765	805	797	793
35	752	831	732	734	710	747	762	747
40	708	763	682	685	662	697	710	702
45	662	708	640	634	616	655	667	680
50	620	660	603	584	585	615	642	650
60	540	572	538	510	515	558	600	602
70	468	508	490	453	460	508	530	565
80	410	453	449	403	420	465	496	542
90	369	409	413	361	375	425	470	512
100	333	369	381	320	340	400	438	495
120	277	308	333	270	287	360	402	475
140	235	263	295	228	250	315	370	450
160	192	232	270	195	215	290	350	436
180	160	209	255	170	177	275	335	420
200	140	188	240	145	170	260	318	
220	122	171	228	130		240	300	
240	100	155		120		225	300	

Table II (Continued)
Time Versus Temperature Data

Time	Oil C — Used					Oil D — New			
Sec.	83 °F.	132 °F.	221 °F.	300 °F.	450 °F.	84 °F.	132 °F.	218 °F.	300 °F.
0	1550	1550	1550	1550	1550	1550	1550	1550	1550
1	1550	1542	1550	1550	1550	1550	1550	1550	1541
2	1550	1533	1550	1542	1550	1550	1541	1532	1532
3	1542	1525	1533	1510	1510	1540	1532	1505	1523
4	1533	1517	1499	1462	1470	1531	1523	1479	1514
5	1499	1491	1483	1406	1413	1511	1514	1443	1506
6	1482	1466	1449	1358	1365	1491	1497	1407	1488
7	1445	1433	1415	1310	1317	1482	1479	1399	1470
8	1396	1399	1381	1261	1261	1462	1461	1353	1452
9	1345	1366	1364	1205	1213	1442	1443	1318	1434
10	1297	1332	1330	1157	1164	1423	1416	1282	1407
12	1208	1282	1264	1092	1100	1374	1363	1210	1363
14	1140	1231	1229	1037	1035	1315	1302	1120	1310
16	1100	1181	1178	988	987	1266	1220	1030	1247
18	1030	1139	1128	940	955	1217	1166	960	1194
20	970	1097	1076	908	923	1158	1113	905	1140
25	885	980	993	844	842	1050	997	825	1015
30	808	904	925	788	793	952	908	780	926
35	745	828	856	740	746	863	818	710	838
40	710	762	805	700	713	785	748	655	766
45	660	703	700	667	682	727	675	620	704
50	628	652	695	635	657	667	622	585	650
60	560	560	637	588	617	570	520	510	570
70	500	500	603	540	577	492	443	475	510
80	458	442	547	510	553	423	380	430	447
90	415	400	501	477	530	355	336	405	420
100	377	357	451	450	515	305	300	375	392
120	312	290	391	410	490	237	246	328	349
140	263	248	350	380	467	187	212	292	322
160	230	206	310	365	458	169	185	270	304
180	208	186	281	350	450	130	166	252	300
200	190	165	268	332	440	100	157	240	295
220	172	147	259	315	433	100	150	222	291
240	150	140	250	300	425	100	140	208	288

Time	Oil D — Used			Oil E — New				
Sec.	82 °F.	131 °F.	225 °F.	82 °F.	132 °F.	220 °F.	296 °F.	440 °F.
0	1550	1550	1550	1550	1550	1550	1550	1550
1	1550	1550	1550	1550	1550	1542	1550	1526
2	1550	1541	1550	1550	1542	1519	1535	1502
3	1533	1533	1550	1533	1531	1479	1511	1470
4	1524	1515	1532	1516	1510	1440	1472	1430
5	1498	1498	1523	1499	1486	1385	1425	1390
6	1481	1490	1505	1482	1423	1330	1378	1334
7	1447	1446	1477	1456	1375	1290	1292	1286
8	1412	1411	1459	1430	1327	1250	1253	1246
9	1377	1376	1423	1396	1287	1211	1206	1206
10	1325	1346	1368	1353	1239	1171	1175	1166
12	1222	1289	1295	1250	1160	1118	1105	1102
14	1152	1237	1204	1130	1097	1045	1050	1030
16	1083	1167	1131	1062	1057	1000	1003	974
18	1048	1100	1076	993	992	958	972	942
20	995	1070	1022	950	953	920	937	910
25	891	980	912	838	865	857	858	854
30	815	892	828	770	793	785	800	798
35	755	815	752	702	738	745	753	758
40	685	753	694	660	682	690	707	718
45	625	702	643	617	635	650	667	686
50	580	655	600	574	595	612	628	662
60	510	572	528	505	525	550	573	614
70	445	512	475	452	460	492	520	582
80	400	452	433	400	414	450	488	542
90	360	410	390	368	375	425	456	518
100	320	370	360	352	340	382	425	502
120	250	313	330	282	295	335	378	470
140	200	263	305	250	254	304	347	455
160	168	230	280	230	222	270	330	438
180	135	212	260	196	200	257	315	430
200	115	195	246	180	175	245		
220	105	174	228	162	163	232		
240	100	145		145	150	225		

Table II (Continued)
Time Versus Temperature Data

Time Sec.	Oil F — Used			Oil G — New			Oil H — New	
	81 °F.	128 °F.	220 °F.	78 °F.	132 °F.	220 °F.	80 °F.	132 °F.
0	1550	1550	1550	1550	1550	1550	1550	1550
1	1550	1550	1550	1550	1550	1550	1550	1550
2	1550	1550	1550	1550	1550	1550	1550	1532
3	1541	1550	1533	1533	1516	1533	1541	1523
4	1532	1533	1517	1515	1499	1516	1528	1497
5	1514	1517	1484	1498	1466	1483	1515	1479
6	1497	1483	1467	1468	1415	1450	1497	1443
7	1479	1477	1434	1429	1364	1400	1479	1417
8	1443	1433	1401	1394	1330	1350	1462	1390
9	1408	1400	1368	1360	1297	1283	1444	1354
10	1372	1370	1334	1325	1263	1250	1426	1337
12	1301	1300	1268	1274	1195	1182	1382	1249
14	1212	1250	1201	1204	1145	1133	1338	1194
16	1140	1199	1150	1152	1110	1083	1276	1070
18	1070	1130	1090	1100	1035	1033	1213	926
20	1015	1085	1065	1052	1001	990	1143	785
25	910	987	980	949	911	900	1010	605
30	820	907	900	858	833	832	905	555
35	748	833	828	771	766	769	807	520
40	690	772	767	705	707	715	718	480
45	647	719	711	649	652	669	647	465
50	609	669	662	600	606	627	585	450
60	544	580	578	517	518	550	483	395
70	490	505	510	446	454	490	418	360
80	441	447	460	392	407	431	346	340
90	402	404	422	349	366	387	301	290
100	368	366	391	313	328	350	267	270
120	310	314	340	250	268	305	204	225
140	263	270	308	208	212	271	169	198
160	230	239	280	184	190	250	142	180
180	202	212	257	157	160	239	116	160
200	181	192	232	130	144	227	98	155
220	162	170	220	107	133	215	90	150
240	145	148		100	130		80	145

and is typical of all oils examined. The curves on Fig. 3 show cooling rates of an oil when the initial temperature of the quenching bath is varied. It is evident that as the initial temperature of the oil bath is increased the rate at which heat is removed from the steel at the nose of the S-curve first increases, then decreases with further elevation of the initial oil temperature. The rates of heat removal at lower points on the several cooling curves approach one another though they are never identical. In the neighborhood of the martensite change the rates of heat removal are inversely proportional to the initial oil temperature.

Consideration of the mechanical behavior of oil will explain this seeming anomaly, i.e. that as an oil is warmed up it will remove heat from a hot body immersed in it faster than when it is cold. As the oil is warmed up it becomes more fluid and is capable of flowing more readily. The oil immediately adjacent to the steel being quenched is heated and tends to rise through the oil bath and can do so more readily when the entire body of oil is warm and of low viscosity.

The greater fluidity of the warm oil permits thermal currents to form and flow more readily. A large part of the heat removed from the body being quenched results from these thermal currents. Conduction of heat is dependent on the difference in temperature between the body being cooled and the coolant. When the steel passes the nose of the S-curve, temperature differences, steel to oil, are great

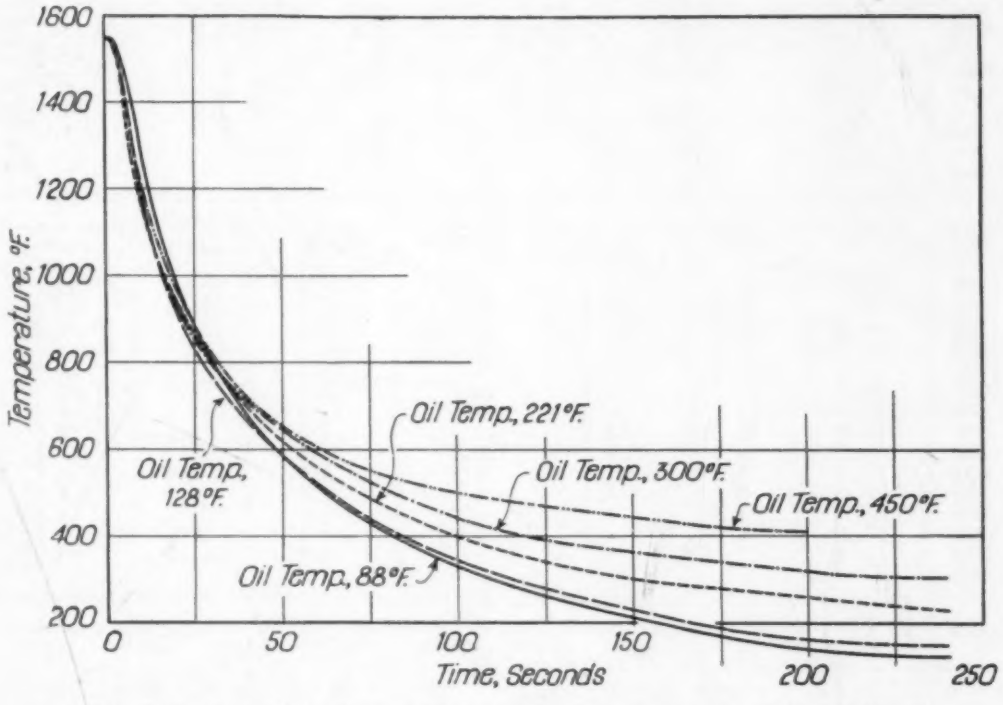

Fig. 2—Typical Time Versus Temperature Curves for an Oil in Table II.

and increases in oil temperature of as much as 100 degrees Fahr. retard the flow of heat but slightly. Hence we can conclude that the higher rate of heat removal accomplished by warm oil at the nose of the S-curve is attributable to greater ease of forming convection currents. With further increase in temperature of the coolant a reversal takes place and the rate of heat removal decreases with further warming up of the oil. At some stage the oil temperature is sufficiently high so that conversion of the oil to vapor gives sufficient blanketing effect to offset the further flow of heat into the warmed oil. In other words, there is a critical temperature where the behavior of the oil changes.

The above conditions do not apply when cooling through the martensite forming region. Here the cool oil is slightly faster than the warm oil. However, it is necessary to miss the nose of the S-

Table III
Temperature Versus Rate Data

Temp. °F.	Oil A — New			Oil A — Used		
	80 °F.	130 °F.	216 °F.	79 °F.	132 °F.	220 °F.
1500	28.3	40.0	29.0	22.0	18.7	31.9
1400	45.5	35.2	48.5	27.6	26.9	31.7
1300	41.8	32.4	53.2	28.7	29.6	30.3
1200	32.8	29.5	43.3	28.1	26.7	27.7
1100	26.3	26.2	32.2	25.4	20.2	24.2
1000	22.2	22.6	24.8	20.5	15.5	20.8
900	17.8	18.9	19.3	15.3	12.6	17.1
800	15.4	15.4	14.8	11.8	10.2	13.5
700	12.2	12.5	11.3	9.4	8.3	10.3
600	9.0	10.0	8.3	7.5	6.4	7.8
500	6.3	7.8	5.7	5.9	4.6	5.5
400	4.3	5.8	3.6	4.4	2.8	3.3
300	2.6	3.7	1.8	3.1	1.0	1.0
200	1.3	1.7		1.9		
100						

Temp. °F.	Oil B — New				Oil B — Used		
	82 °F.	132 °F.	220 °F.	295 °F.	80 °F.	130 °F.	220 °F.
1500	23.8	19.4	18.6	23.8	38.2	25.8	33.5
1400	59.2	29.0	28.6	36.3	41.0	31.3	43.2
1300	50.0	26.6	37.2	37.2	38.3	30.1	38.3
1200	40.0	23.4	31.8	32.1	31.5	25.3	31.3
1100	31.9	20.2	23.8	25.1	26.8	21.2	26.8
1000	24.0	16.9	19.4	19.7	21.7	17.9	22.7
900	19.0	14.1	15.3	15.8	17.0	15.2	18.6
800	15.6	11.5	12.0	12.9	13.2	12.8	14.0
700	12.8	9.1	9.2	10.5	10.2	10.7	10.2
600	10.3	7.1	7.1	8.3	8,1	8.6	7.1
500	8.0	5.2	5.2	6.0	6.3	6.5	4.8
400	5.7	3.3	3.6	3.6	4.7	4.7	3.1
300	3.3	1.5	2.1	1.2	3.1	3.1	1.7
200					1.7	1.7	
100							

Temp. °F.	Oil C — New					Oil C — Used				
	88 °F.	128 °F.	221 °F.	300 °F.	450 °F.	83 °F.	132 °F.	221 °F.	300 °F.	450 °F.
1500	27.9	38.1	39.4	38.0	39.2	29.0	20.7	29.0	35.5	35.5
1400	41.0	55.0	66.8	53.0	51.3	53.4	32.0	30.4	51.4	55.0
1300	43.2	61.3	53.5	58.8	45.0	45.5	26.4	27.4	50.4	57.2
1200	39.3	49.0	37.5	46.0	33.6	33.1	22.9	23.5	43.5	40.0
1100	27.9	34.4	27.2	28.0	25.5	27.4	20.5	20.1	28.0	28.8
1000	22.2	24.3	19.8	19.4	20.0	22.8	18.1	16.7	20.5	20.5
900	17.8	17.5	14.5	13.8	15.3	17.5	15.7	13.3	14.8	14.7
800	14.5	13.2	10.7	10.2	11.0	12.1	13.3	10.2	10.0	9.8
700	11.4	10.0	8.0	7.2	7.1	8.8	10.9	7.6	7.0	6.0
600	8.8	7.5	5.9	5.2	4.2	6.3	8.4	5.6	4.8	3.4
500	6.6	5.4	4.2	3.5	1.8	4.3	6.2	3.9	3.1	1.8
400	4.6	4.0	2.7	2.1		2.7	4.3	2.6	2.0	1.3
300	2.9	2.3	1.3	1.0		1.2	2.8	1.5	1.2	
200	2.0	1.6					1.6			
100										

curve before hardening can be accomplished. Having accomplished this we can afford a slowing up in the neighborhood of the martensite change. Actually this condition is desirable since the reactions taking place within the steel will be less violent. This is illustrated by performance with certain intricate dies, which must many times be quenched in warm oil to avoid the danger of cracking.

In spite of the fact that warm oil is used, the same high

Table III (Continued)
Temperature Versus Rate Data

Temp. °F.	Oil D — New				Oil D — Used		
	84 °F.	132 °F.	218 °F.	300 °F.	82 °F.	131 °F.	225 °F.
1500	18.8	16.4	27.7	14.6	20.5	20.5	17.0
1400	23.9	27.7	31.8	24.6	35.5	30.5	42.6
1300	27.4	32.6	35.9	30.0	55.2	32.0	42.1
1200	26.8	27.7	40.1	30.0	40.0	30.2	33.8
1100	21.9	22.4	43.2	26.7	29.0	19.0	29.5
1000	18.4	20.0	32.6	20.7	22.5	16.8	25.1
900	16.3	17.9	17.5	16.5	17.5	15.5	19.4
800	14.2	15.3	13.7	13.4	14.3	13.3	15.0
700	11.9	12.6	10.4	10.1	11.4	10.5	11.3
600	10.0	10.1	7.5	8.3	8.9	8.0	8.0
500	8.0	7.8	5.0	5.8	6.7	6.0	5.3
400	6.2	5.7	3.1	3.2	4.9	4.2	3.2
300	4.2	3.6	1.6	0.7	3.5	2.6	1.6
200	2.3	1.4			2.5	0.9	
100	0.3						

Temp. °F.	Oil E — New					Oil F — Used		
	82 °F.	132 °F.	220 °F.	296 °F.	440 °F.	81 °F.	128 °F.	220 °F.
1500	16.0	30.7	40.0	32.0	36.0	31.8	33.7	30.5
1400	45.0	53.5	51.6	55.1	57.1	33.7	33.9	33.7
1300	53.4	48.5	48.5	55.1	45.5	34.0	32.0	32.3
1200	55.4	37.6	38.2	36.7	36.3	33.0	28.0	27.0
1100	43.5	29.7	30.7	31.0	31.5	30.2	24.2	21.5
1000	29.3	23.3	22.8	20.5	24.1	24.5	21.3	17.7
900	19.5	16.5	15.7	14.0	13.0	18.9	18.7	15.0
800	13.9	12.6	12.0	11.1	8.9	14.0	16.2	12.5
700	10.5	10.0	9.5	8.7	6.1	10.3	13.6	10.2
600	8.0	7.8	7.3	6.4	3.9	7.6	11.0	8.0
500	6.0	5.9	5.3	4.1	1.9	5.7	8.8	5.8
400	4.2	4.2	3.5	2.0	2.6	4.0	6.8	3.5
300	2.6		1.6	0.4	1.3		5.0	1.3
200	1.0						3.0	
100							1.1	

Temp. °F.	Oil G — New			Oil H — New	
	78 °F.	132 °F.	220 °F.	83 °F.	132 °F.
1500	34.7	58.3	37.7	16.5	22.5
1400	32.1	39.4	43.3	24.1	34.4
1300	29.3	32.3	43.3	30.5	45.9
1200	26.5	27.8	30.5	34.8	53.0
1100	23.8	24.1	23.3	27.2	61.5
1000	21.0	19.9	19.4	23.2	58.2
900	18.1	16.2	16.2	20.3	58.1
800	15.4	13.4	13.3	17.8	53.5
700	12.6	11.2	10.5	15.2	33.2
600	9.8	9.2	8.2	12.2	15.7
500	7.3	7.3	6.0	9.2	7.1
400	5.2	5.5	4.1	6.5	3.8
300	3.2	3.6	2.4	4.2	2.5
200	1.5	1.7	0.8	2.3	1.7
100				0.4	

hardness is obtained as on pieces quenched in cooler oil.

Fig. 4 is a selection of temperature versus rate data taken on the oils under consideration at temperatures such as appeared to give the most nearly uniform performance throughout the entire group.

Consideration of Fig. 4 indicates that while instantaneous rates for various oils, in the neighborhood of the S-curve nose, vary to some extent, rates in the area of the martensitic transformation are ex-

tremely close. Since the rates of cool, at the higher temperature, of all of the oils are sufficient to miss the S-curve nose of those steels normally hardened in oil, variations in rate in this region are not important. Since rates of cool, at the martensite transformation range, are for all purposes identical we can again conclude there are no significant differences in the oils examined.

Fig. 5 compares the cooling rates of several oils at the same initial oil temperature. Here we find a condition parallel to that found in Fig. 4. A difference in rate of cooling in the temperature

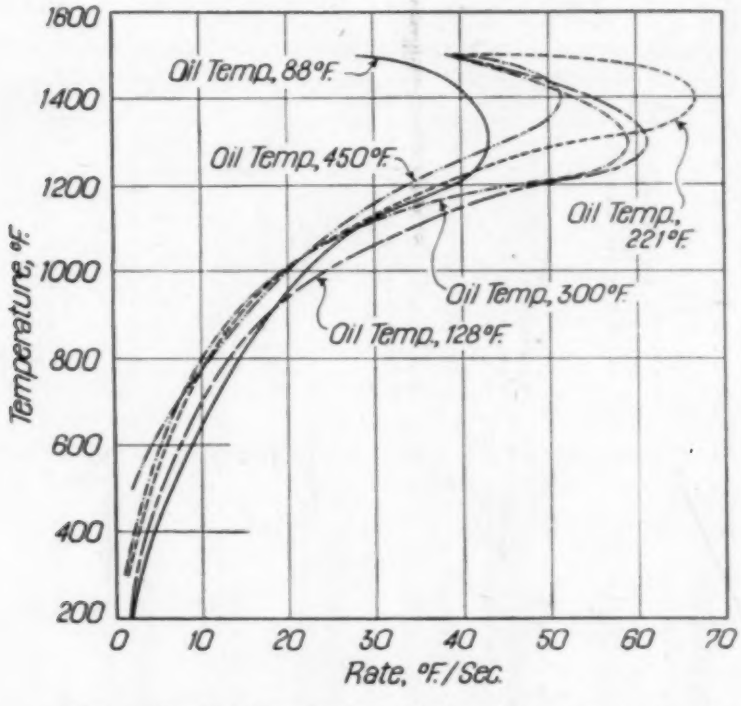

Fig. 3—Typical Temperature Versus Rate Curves for an Oil in Table III.

range of the "nose" of the S-curve is to be observed for the different oils. Note high rate of heat removal in the temperature range of the "nose" of most S-curves. At lower temperatures, below 1050 degrees Fahr. (565 degrees Cent.), the rate of heat removal has become practically the same for all oils regardless of type or source.

All oils are derived from one of three sources, animal, vegetable and mineral. Since no vegetable oils were considered in this present work we have only three possible classifications, namely, straight animal oils, blended animal and mineral oils, and straight mineral oils. The curves studied were grouped according to this

scheme to see if any behavior pattern would evolve. The diversities noted are as follows: The straight animal oils exhibit the greatest change in quenching rate with continued use. This change is in the order of 33 per cent decrease in speed of quench after considerable use. The straight mineral oils showed some tendency to maintain their maximum quenching rates to somewhat lower temperatures than did the other groups. Expressed differently, the mineral oils maintain a high rate of heat removal over a considerably wider tempera-

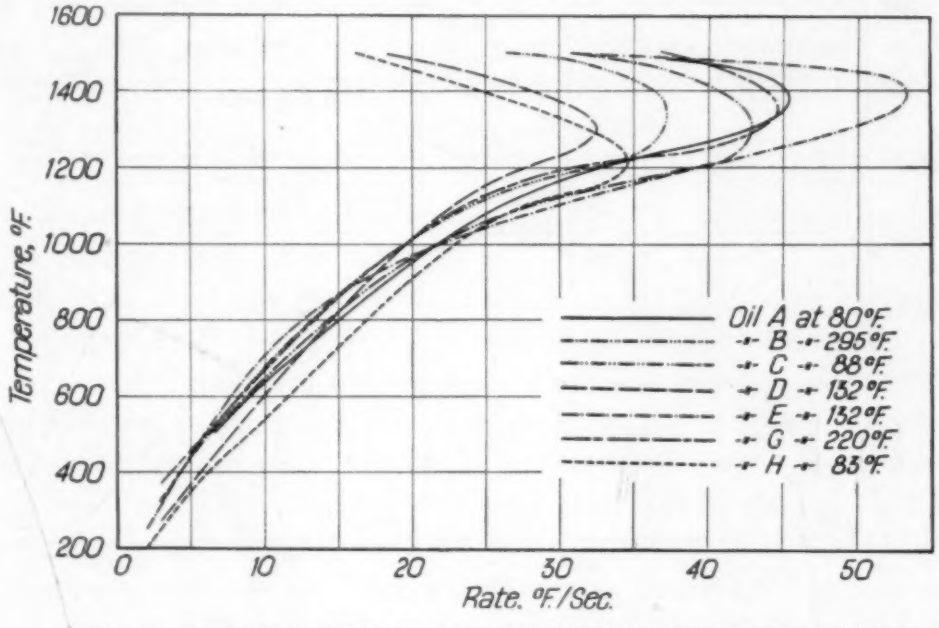

Fig. 4—Comparison of Various New Oils Used at Temperatures Indicated to Produce Similar Operating Results.

ture range than the other oils. The high rate of heat removal for the animal and the blended oils covers about 200 degrees on the Fahr. scale, while with the mineral oils it varies up to as much as 400 degrees Fahr.

Other differences between the three groups were negligible and in no case were the differences of such a nature or magnitude as to direct the choice of one group over the others as a preferred quenching medium.

The various oils examined rather naturally divide themselves into four general classes when considered in the light of their physical properties. This is only a rough division for the purposes of comparison but is generally accurate with some exceptions. These classes are heavy oils, including A, C and E; medium oils with F

as the single representative; light oils of which B, D and G are members; and the very light oil H. The one notable exception to this grouping is A whose viscosity figures align it with the light oils while the remainder of its physical properties correspond with those of the heavy oils. Since physical properties are the criteria by which oils are designated and selected, let us see if the quenching characteristics follow this rough general grouping.

It might be expected that the lighter the oil the faster the quench

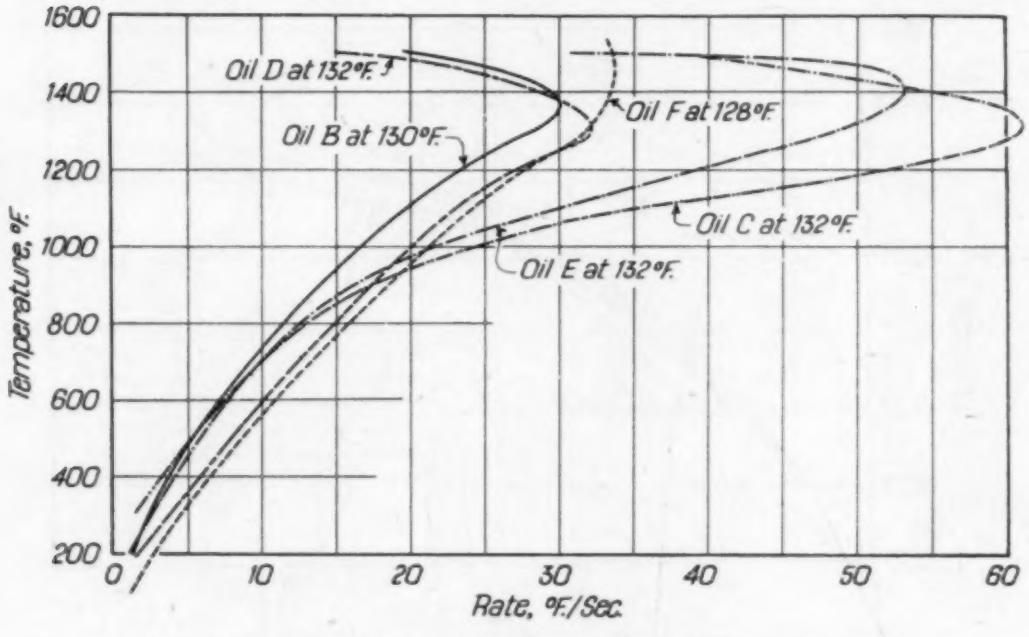

Fig. 5—Comparison of Various New Oils at Same Temperature.

would hold as a general rule. A careful consideration of the rate curves obtained reveals that is far from true. The three lighter classes are practically indistinguishable and the heavy oils in the used condition also follow the same general pattern. The heavy oils, when new, give some of the highest quenching rates encountered which is directly opposite to our expectations. It is true that the very light oil H does give a higher quenching rate over a longer temperature interval when tested at 132 degrees Fahr. initial temperature than any other oil considered, but this is so close to its flash point as to make it unusable. When tested at a safe temperature it is much like the others.

It might be well to note here that the highest maximum rate achieved by any oil was 66.8 degrees Fahr. per second, developed by

oil "C" at an initial temperature of 221 degrees Fahr. and the slowest maximum rate was 27.4 degrees Fahr. per second developed by oil "D" at an initial temperature of 84 degrees Fahr. In terms of hardenability this represents the difference between $\frac{5}{16}$ and $\frac{9}{16}$ inch on the standard Jominy test bar. It is also interesting to observe that with the oil having the lowest maximum quenching rate it is possible to approach the highest rate obtained by suitably adjusting conditions and in a similar manner with the oil having the highest maximum quenching rate it is possible to approach the lowest rate obtained, again by adjusting conditions.

From the foregoing it is apparent that quenching oils cannot be chosen on the basis of their physical properties, that other factors must influence the choice. These determinants will vary. Some are: suitability to present equipment, availability, safety and others. After due allowance has been made for these things the final consideration will be economics.

In considering the purchase of oil for new quenching systems, it is the opinion of the writers that too much consideration need not be given to high sounding sales talk. Actually, similar results can be expected from most of the oils now used for the purpose. As has been pointed out, differences in capacity to quench are negligible with proper handling. Where confidence has been established in an oil by long-time use, the maintenance of that confidence in the mind of the employees may be the main consideration in repeated orders for oil. This may only be justified for a maintenance of morale in the men. Actually, there is no reason for not going to a more economic oil.

Bibliography

1. Davenport and Bain, "Transformation of Austenite at Constant Subcritical Temperatures," Technical Publication No. 348, American Institute of Mining and Metallurgical Engineers.
2. "Molybdenum in Steel," Section 2, Chromium-Molybdenum, Climax Molybdenum Company.
3. Post, Greene and Fenstermacher, "Hardenability of Shallow Hardening Steels," TRANSACTIONS, American Society for Metals, Vol. 30, 1942, p. 1202.
4. H. J. French, "The Quenching of Steels," published by American Society for Metals, 1930.
5. A. Rose, "Cooling Power of Quenching Agents for Steel," *Archiv für das Eisenhüttenwesen*, Vol. 13, 1940, p. 345.

DISCUSSION

Written Discussion: By H. Gershinowitz, director of research, and G. W. Waters, senior research chemist, Shell Oil Company, Inc., New York.

We have read Messrs. Spring, Lansdale and Alexander's paper with both interest and pleasure. Their conclusion that all quenching oils are metallurgically equal is not unattractive, for it would free us, as producers of oil, from the necessity of probing the science of metals, a field in which we are generally inadequately equipped with either facilities or background. On the basis of limited tests in which we have cooperated, however, we are surprised by these conclusions and the discussion of this paper from the metallurgical standpoint by those much better qualified than we is accordingly anticipated with great interest.

The indications obtained by the authors that the quality of quenching oils is not determined by their physical properties focus attention on chemistry in its proper relation to the economics of quenching oils. A brief consideration of this paper from the chemical standpoint may be instructive. Straight animal oil is reported to exhibit the greatest change in quenching rate with continued use. Since this oil showed relatively low evaporation tendencies, it seems logical to assume that the thermal and oxidation stabilities are the determining factors of change during use. That thermal and oxidation stabilities of oils are functions of chemical composition has been amply demonstrated by studies of thermal decomposition and oxidation of oils. Further than simple resistance to deterioration, it has been shown that chemical composition influences the course of oxidation. The problems may be complex since, for example, those hydrocarbons which would be expected to be most resistant to thermal decomposition may, on the other hand, produce undesirable products of oxidation, e.g., sludge. However, the knowledge of the role chemical composition plays should lead to the formulation of quenching oils fortified against the various specific factors which interfere with quenching efficiency. The authors draw attention to the fact that heavy oils, contrary to expectation, give some of the highest quenching rates. This observation which is at variance with their analysis of the mechanical behavior of oils may well have its explanation in the chemistry of the components. It appears possible therefore that through chemical variation quenching oils can be improved metallurgically.

We do not wish to miss this opportunity to stress an important conclusion which can be drawn from the authors' work, namely, the inadequacy of arbitrary specifications as basis for the selection of petroleum oils. Quality on the basis of performance is a much more logical and substantial standard and cannot fail to emphasize the authors' fundamental recommendation that selection of quenching oils be controlled by "the cost per pound of steel quenched."

Written Discussion: By Arthur E. Focke, research metallurgist, Diamond Chain and Manufacturing Co., Indianapolis, Ind.

We are indebted to the authors for taking the time during this busy period to correlate and publish their data on quenching oils.

Over ten years ago, our metallurgical staff carried out a comprehensive study of quenching oils based principally on laboratory tests for viscosity, flash, fire, etc. From these tests it was concluded that for our parts, a straight min-

eral quenching oil with a viscosity of about 100 Saybolt Universal Seconds at 100 degrees Fahr. was satisfactory and this conclusion has been confirmed by our continued satisfactory use of this type of quenching oil in production.

However, in 1941, as soon as it became obvious that during this emergency we could not continue to obtain the high alloy steels around which our designs and practices had been developed, we reopened this investigation to study some of the new proprietary quenching oils which contain special compounds.

Since we were concerned principally with the ability of the quenching medium to harden our parts, we limited our preliminary study to hardenability tests only. For this purpose we used a combination of the Post and Greene Conical sample,[1] the Jominy End-Quench,[2] and interpreted our results by means of the Grossmann charts.

Briefly, we cut conical samples 5 inches long, 0.25 inch in diameter at the small end tapering out uniformly to 1.25 inch at the large and standard Jominy End-Quench samples from the same 1.25-inch diameter bar of S.A.E. 1040 steel. The Jominy samples and the cones were heated in charcoal at 1600 degrees Fahr. (870 degrees Cent.) for 2 hours after which the Jominy samples were end-quenched in the standard manner while the cones were quenched (without agitation) into 25 gallons of the medium to be tested at 75 degrees Fahr. (24 degrees Cent.).

The end-quench samples on this steel showed a "critical hardness" of 40 Rockwell "C" at 0.15 inch from the water-quenched end. From the standard Jominy-Cooling Rate curve[3] this would correspond to a cooling rate of about 150 degrees Fahr. per second. From one of Grossmann's curves[4] this hardness at this point would correspond to a D_1 value of 1.5.

The cones were ground to a flat wedge and hardness readings taken along the axis. The results of several of these tests in which the hardness is plotted against the diameter of the cone at the distance from the small end corresponding to that at which the hardness reading was made are shown in Fig. A. The diameter of the cone at that point at which the "critical hardness" is found on the axis corresponds to the Grossmann D_c value and since D_1 has been established by the End-Quench test, the intersection of lines from these values on another Grossmann curve[5] provides the quench rate H.

In Table A are shown the H values calculated by this method from the data in Fig. A.

Table A

Test	Quenching Medium	H	Dc
OA	New Mineral Oil	0.36	0.30
OB	New Mineral Oil Plus 10 Per Cent Proprietary Compound B	0.36	0.30
OC	Used Mineral Oil	0.40	0.34
OD	Proprietary Quenching Oil D	0.44	0.40
W	Water	0.76	0.90

[1]Fig. 1, *S.A.E. Journal*, Vol. 49, No. 1, July 1941, p. 278.

[2]S.A.E. Standard Procedure Recommended for Testing Hardenability of Steel, *S.A.E. Journal*, Vol. 50, No. 1, January 1942, p. 15.

[3]Fig. 2, *S.A.E. Journal*, Vol. 49, No. 1, July 1941, p. 268.

[4]Fig. 11, *S.A.E. Journal*, Vol. 49, No. 1, July 1941, p. 291.

[5]Fig. 63, "Principles of Heat Treatment," M. A. Grossmann, published by American Society for Metals, 1940.

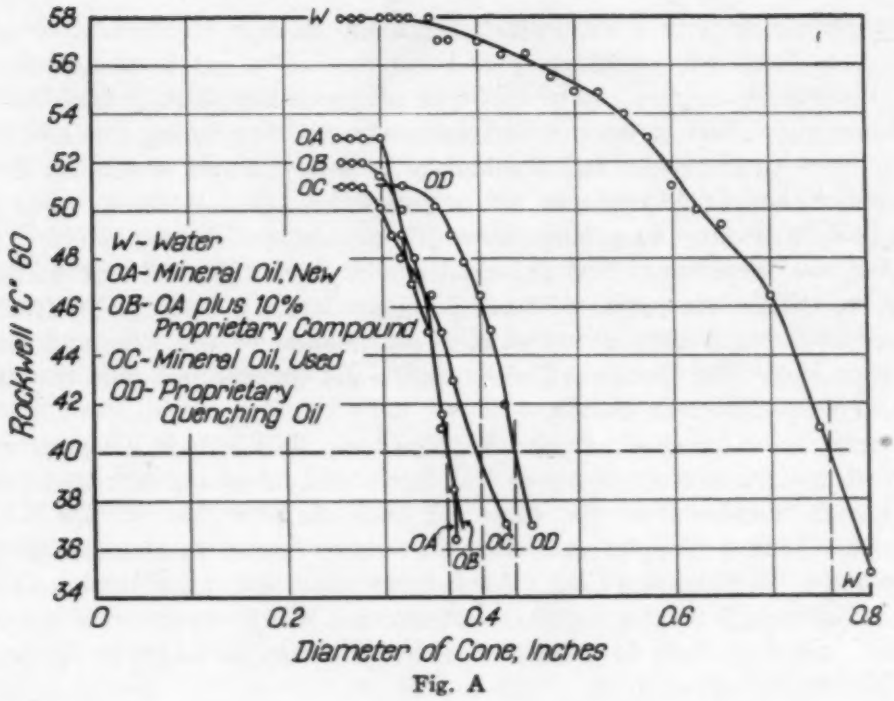

Fig. A

These values for H are in agreement with those reported by Grossmann for similar quenching media[6] and since the difference between the H value of the standard mineral quenching oil and that of the better compounded proprietary quenching oil is less than that which Grossmann found could be obtained by increased agitation, we decided that these new oils did not have sufficient value to justify their use on our production.

However, we continued to learn of special cases in which the change from a straight mineral oil to one of these special oils made the difference between success and failure and we have continued our investigation. Briefly, these latest tests seem to show that:

(1) The new compounded oils do not result in increased depth of hardening under the same quenching conditions if the D_1 value of the steel is greater than about 1.4.

(2) On tool steel with D_1 values close to 1.0, these new compounded oils are effective and this effect is greater than can be produced by increased agitation alone.

From all this, then, we are forced to conclude that, while in general, we agree with the conclusions presented by the authors of this paper, we recognize that in certain special cases, the new compounded quenching oils are very useful.

Written Discussion: By Arnold P. Seasholtz, metallurgist, E. F. Houghton & Co., Philadelphia.

This paper is of considerable interest and brings out many factors to be considered in the evaluation of quenching media. The author points out that physical properties of the oils are not a proper criterion to be used when prejudging either results or costs. Viscosity, he states, is mainly important because

[6]Technical Publication No. 1437, American Institute of Mining and Metallurgical Engineers, February 1942.

experience has shown that evaporation of quenching oil has a bearing on its life and its performance.

Our own experience has checked with this, in that stability of the oil to resist fractional distillation will result in longer life, less tendency to sludge, and a constant viscosity which will not be materially altered by long usage. Oils with high viscosity have a higher drag-off loss than the more fluid oils. Further, these higher viscosity oils will not wet out as fast as a more fluid oil.

Another important factor is the variation in quenching speed obtained by adjusting the oil temperature; however we question the advisability of heating an oil in order to obtain maximum quenching speed. The safety factor would preclude temperatures of conventional quenching oils above, perhaps, 180 or 190 degrees Fahr.

It will be noted that this paper is based on tests made on thorough hardening oil quenching steel. With this type of high alloy steel it should be pointed out that any of the oils tested will have a sufficiently rapid quenching rate to exceed the critical cooling rate of the steel. This grade of steel, however, is in the minority today as compared to the oil quenching steels now in production. The N.E. (National Emergency) steels and others with lean alloy content are of such analysis that the cooling rate throughout the section does not exceed the critical cooling rate. With such steels it has been proven necessary to determine what oil possesses a fast quenching rate, and choose the oil quite largely on the basis of speed. Of course, stability is also an important factor.

A difference in rate of cooling in the temperature range at the nose of the S-curve is observed for the different oils described in this paper. When using the semi-thorough hardening steels, it has been found necessary to use an oil which possesses a fast cooling rate through the temperature range at the nose of the S-curve, thus providing optimum results, such as maximum hardness, greater penetration of hardness and better physical properties in the hardened steel.

It may be of interest here to describe a procedure for testing the cooling speed of quenching oils which has been worked in conjunction with a large government institution. The specification states:

"The oil shall have a high initial quenching speed. It shall remove not less than 38 per cent of contained heat from 1-inch diameter by 2.5-inch long steel test pieces when quenched from 1500 degrees Fahr. (815 degrees Cent.) for five seconds in oil, the temperature of the oil being less than 200 degrees Fahr. (95 degrees Cent.). The test pieces may be heated in an open fire in which a reasonably nonscaling atmosphere is maintained.

"To determine the percentage of the contained heat removed from the test piece, two identical sample test pieces shall be used. The samples shall be heated and quenched under identical conditions, except that one shall be quenched cold and the other for five seconds as specified. The comparative rise in temperatures of the quenching baths is a rough measure of quenching speed."

As a result of tests run by the foregoing procedure, it has been determined that in the five-second test the following percentage of heat may be expected to be removed from these different types of oils:

100 Viscosity Mineral Oil	15 to 23 per cent
Compounded Quenching Oil	20 to 30 per cent
Compounded High Speed Quenching Oil treated for fast wetting speed	38 to 45 per cent

We would make one other point which the authors for their purposes did not attempt to consider: The question as to whether the measuring of the cooling rate at the center of the bar would present as true a picture as could be determined by hardness testing methods. The latter procedure would reveal uniformity of surface hardness, maximum surface hardness and depth of penetration. The lower thermal conductivity of stainless steel here tested would in our opinion not make it desirable as a basis for obtaining actual cooling rates at the center of the bar.

These alternatives are presented to show the many factors which must be considered in attempting to evaluate quenching of oils, it being realized that the authors did in no way attempt to tackle the whole problem for the many types of oil quenching steels. The work which was undertaken does, however, reveal some important factors of quenching oils. Further work to determine results obtained by agitating the oil instead of using a still oil bath, and by testing semi-thorough hardening steels, would be of added interest.

Written Discussion: By Morse Hill, assistant metallurgist, Materials Laboratory, Engineering Division, Materiel Command, Army Air Forces, Wright Field, Dayton, Ohio.

The authors have presented more of the data which is necessary if any general picture of the quenching operation is to be gained. We can make numerous speculations on the time-temperature relationships but unless there is experimental evidence with which to compare them the speculative results can not be fully trusted.

It would be very interesting to compare the authors' curves with the predictions from the formulae J. H. Awbery develops in the Journal of the Iron and Steel Institute (1941, p. 144). Can they therefore describe the oils more fully so that it would be possible to estimate the following quantities: viscosity, specific heat, density, heat conductivity and average molecular weight?

It is unfortunate that the authors chose to work with 18-8 steel for its thermal diffusivity is so poor that some of the differences between quenching oils may have been masked. Thermal effects at the critical are generally well suppressed in steels such as 4340.

I have had occasion to determine some cooling curves under similar conditions by using ordinary steels and have found it extremely difficult to reproduce closely any cooling curve. What reproducibility do the authors consider satisfactory?

Written Discussion: By H. M. Fearon and Maurice Reswick, Engineering Division, Sales Department, Standard Oil Company of New Jersey, New York.

This paper is an excellent presentation of a subject of interest to not only the metallurgists of the industry, but also to the suppliers of the media used in the quenching of steel. Considerable work was no doubt entailed by the authors in assembling and preparing the data for publication, only a portion of which is included.

The problem of quenching oils has many phases, and the authors have wisely limited themselves to but one phase, namely, the rate of heat absorption from an 18-8 stainless steel specimen, which material eliminates the heat of transformation effect, and enables us to view the cooling rate phenomenon clearly. The authors are to be commended for this direct approach, and our

comments are limited to this particular phase of the quenching problem.

It is gratifying to know that the equipment used is such that can be duplicated, and the work initiated by the authors continued in other laboratories, and the results thus correlated.

The physical properties table is a necessary adjunct to the curves shown, as a means of better understanding the types of oils tested. For practical consideration the authors have used specific gravity temperature determination approximating operating conditions, rather than the conventional 60 degrees Fahr. used in the petroleum industry. The viscosity determination itself varies from the Saybolt Universal method common to the industry.

These departures from the orthodox are somewhat confusing to the oil engineer seeking correlation, and furthermore, do not tie in with purchase specifications covering the oils in general use. However, the values are relative, and as far as the evaluation is concerned, are considered as such. As an approximation, we estimate that the viscosities of the listed oils at 210 degrees Fahr., in terms of Saybolt Universal Seconds, are roughly the same as the values obtained by the authors with the Dudley Pipette at 130 degrees Fahr.

The tests have included both new and used oils in the three most important categories, namely, animal oils, proprietary blended oils, and straight mineral oils. This idea is to be commended as emphasis has been placed, in some cases, on the difference in cooling performance of used oils versus new oils. Such differences in performance may be due to a number of factors, such as evaporation of any minute quantity of moisture contained in the oil, boiling off the extra light fractions, increase in relative viscosity due to oxidation, sludging, etc. We should like to ask the authors over what period of time the oils were in service. This may explain the variation in the physical properties shown for the several types listed.

For the sake of simplicity, the effect of mechanically produced convection currents on the rate of cooling was not considered by omitting a test with mechanical circulation in the four (4) gallon quenching oil bath. Nevertheless, it would be interesting to know how the experimenters immersed the steel specimen, that is, whether it was simply dropped in the bath, suspended in some manner, or moved about in a figure eight pattern, etc.

The work of the authors represents one more attempt to remove the mystery from quenching oils. In fact this may be regarded as the last bulwark to be attacked by the metallurgists who have made such rapid progress in all other directions. It is significant that all investigations along these lines made in recent years at plant laboratories and in heat treating departments have resulted in the same conclusions at which the authors have arrived. Namely, that the quenching of steel is nothing else but heat removal as a function of time. Practical consideration limits the quenching medium to petroleum oil on account of its ready availability and suitable physical characteristics. It is conceivable that minor apparent improvements may be shown by blending straight petroleum oil with animal oil but it is equally true that the same effects can be produced more effectively mechanically by improving circulation and agitation of the oil, and close temperature control of the quenching medium.

It is of interest to note that metallurgical laboratories which have done considerable experimenting with different types of proprietary blends of quench-

ing oils have not succeeded in confirming the claims made for them and the best they can say is that by paying a higher price for the proprietary quenching oil they hope to obtain an oil which is more resistant to oxidation, sludging and breakdown than if they were to purchase just an oil at the lowest market price. It is obvious that if an oil of a high degree of stability is justified such an oil may be purchased under general specifications as to quality.

Written Discussion: By Blaine B. Wescott, chief metallurgist, and L. W. Vollmer, section chief, Materials Section, Gulf Research & Development Co., Pittsburgh.

The authors have elected to base their evaluation of quenching oils solely on cooling rates experimentally determined by the general technique used by many other investigators, but the results presented and some of the conclusions drawn from these results do not parallel those of other investigators, including the commentators. It is particularly significant that none of the typical cooling

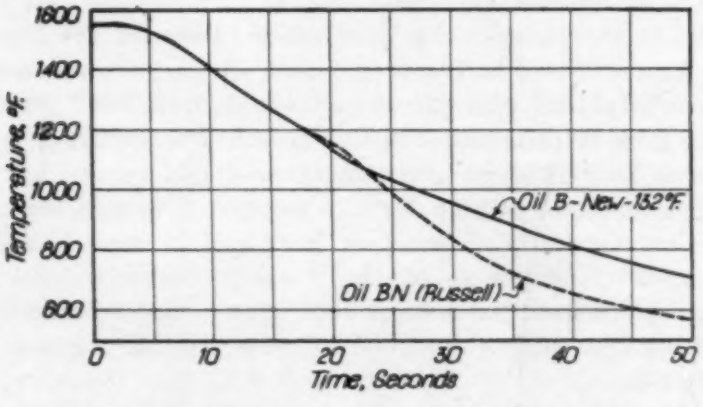

Fig. B—Comparison of the Center Cooling Curves Obtained by Russell[8] on 25-20 Stainless Steel Ball, 1 Inch Diameter, Quenched in Oil BN, and the Authors' Curve on 18-8 Stainless Steel Specimen, $\frac{11}{16}$ Inch Diameter by 1½ Inch, Quenched in Oil B—New—132 Degrees Fahr.

curves or the temperature : cooling rate curves shows all of the three distinct stages in the cooling cycle first demonstrated by Pilling and Lynch.[7] To avoid the complications of transformation, Pilling and Lynch used cylinders of nickel containing 5 per cent silicon that were 0.25 inch in diameter and 2 inches long and a "string" or Einthoven galvanometer having a very short period (about 0.01 second) in their temperature recording apparatus. The so-called A (vapor blanket), B (vapor transport), and C (liquid cooling) stages of cooling were plainly evidenced by the three mineral oils tested by them.

More recently Russell[8] studied the cooling characteristics of oils using in some experiments a 1-inch diameter sphere of 25 per cent chromium-20 per cent nickel stainless steel and a galvanometer having a period of 0.2 second. Since the surface : volume ratio of Russell's sphere (6) approaches that of the

[7]N. B. Pilling and T. D. Lynch, "Cooling Properties of Technical Quenching Liquids." *Transactions*, American Institute of Mining and Metallurgical Engineers, Vol. 62, 1920, p. 665.

[8]T. F. Russell, Second Report of the Alloys Steel Research Committee, Iron and Steel Institute, Special Report No. 24, 1939, p. 283.

authors' cylinder (4.92 if end effects are ignored) the cooling curve obtained by Russell for his Oil BN (the properties of which are listed in Table B) is shown replotted with different coordinates in Fig. B in comparison with the curve obtained by the authors for Oil B—new—at 132 degrees Fahr. Russell's curve shows definite termination of the A or vapor blanket stage of cooling at about 1100 degrees Fahr. (595 degrees Cent.), and the beginning of faster B-stage cooling. The authors' curve appears to show only continuous A-stage cooling down to the zone where C-stage cooling begins.

The commentators have also made a comprehensive study of quenching oils during which cooling curves of various sizes of 18-8 stainless steel cylinders

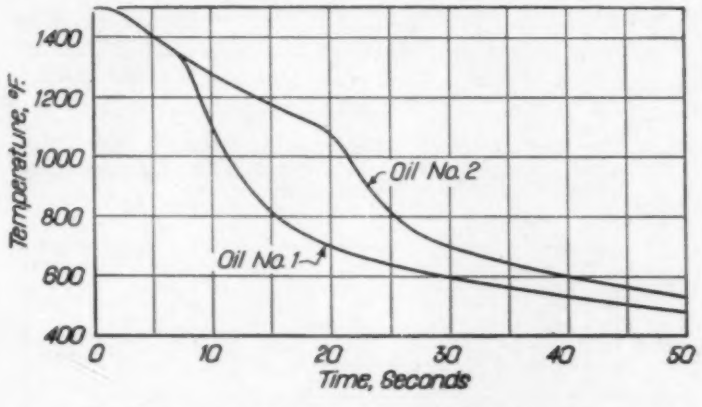

Fig. C—Center Cooling Curves Obtained with a Slow (No. 2) and a Fast (No. 1) Quenching Oil and a Short Period (0.019 Sec.) Oscillograph. ¾ Inch Diameter by 3 Inch, 18-8 Stainless Steel Specimen Quenched in Fast Mineral Oil No. 1 and Slow Mineral Oil No. 2. Bath Temperature 120 Degrees Fahr. No Agitation.

were determined using a temperature recorder equipped with an oscillograph having a period of 0.0192 second and a damping ratio of about 0.5. The center cooling curves for a 0.75-inch diameter by 3-inch specimen quenched in a fast mineral quenching oil and a slow mineral quenching oil are shown in Fig. C. The three stages of cooling are very evident and are even more sharply indicated than in Russell's curve (Fig. B).

It is the opinion of the commentators that the differences in sharpness of definition of the three cooling stages shown by the curves in Figs. B and C are due to the characteristics of the galvanometers used in each case. The authors employed a Leeds and Northrup galvanometer described only as having a sensitivity and response "such that the apparatus is capable of following temperature changes of the order of 500 degrees Fahr. (260 degrees Cent.) per second." Leeds and Northrup mirror galvanometers ordinarily are not made with periods less than 1.5 seconds; the period of the usual laboratory mirror galvanometer is at least 2 seconds. Such instruments will institute large dynamic errors in high speed measurements involving changes in rate. French and Klopsch[9] have stated that "ordinary galvanometers or potentiometers are

[9]H. J. French and O. Z. Klopsch, "Quenching Diagrams for Carbon Steels in Relation to Some Quenching Media for Heat Treatment," TRANSACTIONS, A.S.S.T., Vol. 6, 1924, p. 251.

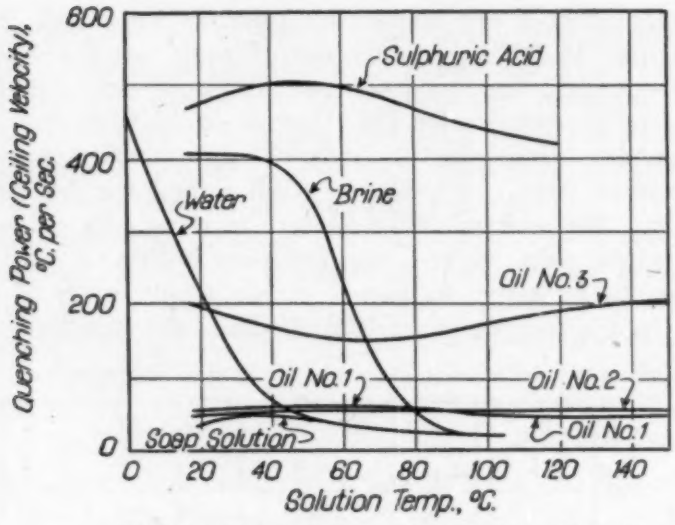

Fig. D—The Influence of Quenching Bath Temperature on Cooling Velocity at 700 Degrees Cent. Taken from Pilling and Lynch.[7]

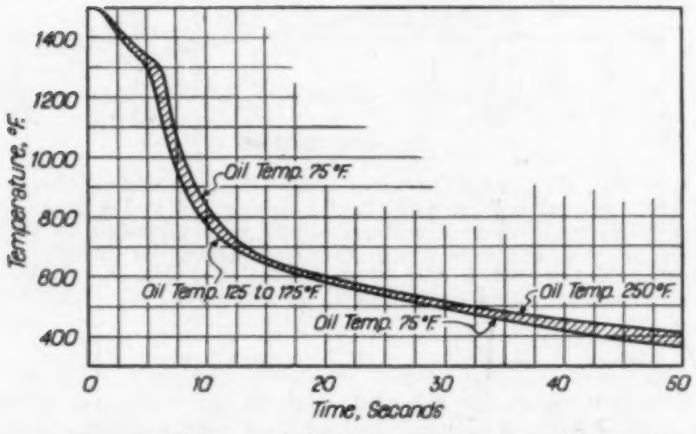

Fig. E—Effect of Bath Temperature on the Center Cooling Curve for Fast Quenching Oil No. 1. ½ Inch Diameter by 2½ Inch, 18-8 Stainless Steel Specimen Quenched in Fast Quenching Oil No. 1. Bath Temperature Range 75 to 250 Degrees Fahr. No Agitation.

entirely unsuited for detecting the thermal transformations and even following the time-temperature relations in quenching, on account of the rapid rates of temperature change encountered." It is believed that the authors' temperature recording apparatus is not sufficiently responsive to indicate accurately the changes in rate of cooling in a specimen of the size used. A sluggish galvanometer will fail to indicate true peak rates of cooling and therefore will not develop the real differences in quenching rates of the oils tested.

The highest maximum rate given by the authors, 66.8 degrees Fahr. per second for oil C—new—at an initial temperature of 221 degrees Fahr., does not seem to be justified by the time-temperature data in Table II; the time : temperature relationship for this oil at 1400 degrees Fahr. (760 degrees Cent.) is practically a straight line indicating a cooling rate of 49.5 degrees Fahr. per second. The maximum cooling rates obtained from the center cooling curves

of the 0.75-inch diameter cylinders in Fig. C of this discussion are 55 degrees Fahr./seconds for the slow oil and 95 degrees Fahr./seconds for the fast oil.

The observation that quenching power of oils can be equalized by adjusting bath temperatures is not in accordance with the conclusions of Pilling and Lynch,[7] Russell,[8] and many others. It is generally agreed that aside from the initial improvement resulting from the decrease in viscosity of oil, an increase in bath temperature within workable, safe limits has little or no influence on

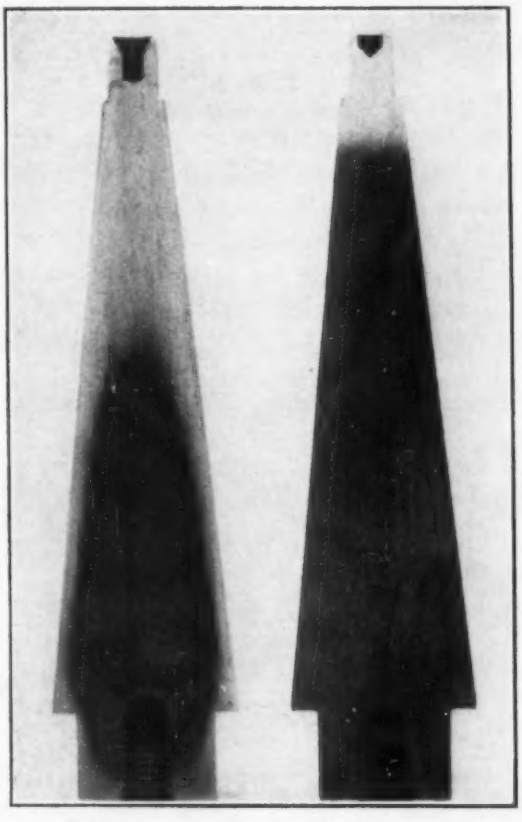

Fig. F—S.A.E. 1095 Cones Quenched in Fast Oil No. 1 (Cone at Left) and Slow Oil No. 2 (Cone at Right) at 125 Degrees Fahr. and Violently Agitated.

the quenching power of oils suitable for quenching. Fig. D taken from Pilling and Lynch[7] shows the negligible effect of bath temperatures up to 300 degrees Fahr. (150 degrees Cent.) on the cooling velocity (at 700 degrees Cent.) of the three mineral oils tested by them. Fig. E, obtained in the course of our investigations, similarly shows the minor effect of bath temperature on the cooling curve for a 0.5-inch diameter by 2.5-inch 18-8 specimen quenched in fast quenching oil No. 1. With bath temperatures from 125 to 250 degrees Fahr., cooling rates remain practically unchanged in the A and B cooling stages.

It is believed that the authors are unjustifiably optimistic in their statement to the effect that the critical cooling rates of steels normally quenched in oil can be attained by all of the oils tested by them. This does not take into account the mass of the steel to be quenched or the wide variation in harden-

ability that may and does obtain in different heats of the same steel. In fact the N.E. steels and the wider usage of plain carbon steels for alloy conservation purposes increase the importance of the differences in quenching rates of oils in the vicinity of the S-curve nose because of the relatively high critical cooling rates involved.

Cooling curves are of unquestioned value for investigating quenching oils. Experience gained from an identical investigation extending over a period of several years, however, has convinced the commentators that it is unwise to

Table B
Properties of Oils

Property	Oil		
	BN (Russell[8])	No. 1	No. 2
Specific gravity at 60 degrees Fahr.	0.891	0.8686	0.8708
Viscosity, S.U.S. 100 degrees Fahr.	120	88.9	101.0
210 degrees Fahr.	.....	38.6	39.5
Viscosity index	.....	106	99
Pour point, degrees Fahr.	.....	+25	+15
Flash point, O.C., degrees Fahr.	385	350	360
Fire point, O.C., degrees Fahr.	.....	400	410
Neutralization No.	0.62	0.13	0.05
Saponification No.	7.21	0.20	0.50

rely wholly on data obtained in this manner to predict the results obtainable from the heat treatment of hardenable steels. Usually we are lacking in accurate knowledge of the cooling rates at different points in the pieces to be hardened and of the critical cooling rate of the steel.

Proof that the differences between a fast and a slow quenching oil are real and useful is shown in Fig. F. These cones (0.5 inch diameter by 2.75 inches by 0.75 inch diameter) were machined from adjoining lengths of the same bar of S.A.E. 1095 steel. Cone A was quenched in fast oil No. 1 (Fig. C), Cone B in slow oil No. 2. The quenching temperature was 1450 degrees Fahr. (790 degrees Cent.); bath temperature 125 degrees Fahr.; agitation violent mechanical. The H value for fast oil No. 1 under these quenching conditions was determined to be 1.41 (Grossmann[10] and Post, Greene and Fenstermacher[11]). From Grossmann's relation between D_1 and D_e the H value for slow oil No. 2 was found to be not greater than 0.55. It will be noted that violent agitation of the baths did not overcome the difference in quenching power of the two oils indicated by the cooling curves. This difference has been demonstrated repeatedly both by laboratory experiments and in commercial heat treating operations.

The commentators would like to know if there is any relation between the viscosity determined by the Dudley pipette and that determined by the Saybolt viscosimeter as specified by the American Society for Testing Materials.

Written Discussion: By F. E. Rosenstiehl, assistant manager, Technical and Research Division, The Texas Co., New York.

I believe the authors should be complimented on the thoroughness in which

[10] M. A. Grossmann, "Principles of Heat Treatment," published by the American Society for Metals.

[11] C. B. Post, O. V. Greene, and W. H. Fenstermacher, "Hardenability of Shallow Hardening Steels," TRANSACTIONS, American Society for Metals, Vol. 30, 1942, p. 1202.

they have studied this subject. The tests we have made indicate that differences of hardness are obtained by the use of different quenching oils; however, all of our tests were conducted with the different oils at the same initial temperature. In connection with hardness, it would be very interesting to compare the method of the authors, which predicts hardenability from quenching rates, with the method of Asimow and Grossmann, which predicts quenching rate from actual hardness data. In connection with the cooling rate study, it is noted that the authors draw conclusions regarding obtainable hardenability results. I am wondering if these conclusions would hold true in actual practice where shallow hardening steels are being quenched.

We are not in complete agreement with the authors' assertion that a quenching oil should be selected on the basis of its flash and fire, and its cost per pound of steel quenched, since we feel this assertion is too general and therefore apt to be misleading. It has been our experience that certain quenching oils are more prone to chemical deterioration or oxidation than others through use. The more unstable oils are liable to cause formation of troublesome sludge or carbonaceous deposits. These may not be serious enough in themselves to necessitate replacement, though they may lead to trouble in oil cooling systems; adversely affect the ease of future operation such as descaling, or even change the quenching characteristics of the quenching medium. Further, through use, certain of the more unstable quenching oils may show appreciable changes in their physical characteristics, such as viscosity increase or decrease, or decrease in flash or fire points. While again these changes may not be serious enough to cause replacement of the oil, they may cause a change in the quenching characteristics enough to necessitate a change of the quenching bath temperature to insure optimum hardness or safe working conditions.

We also feel that adjusting the quenching bath temperature to the results desired, as suggested by the authors, while possible, is not always practical. To hold certain oils at a low temperature range, such as 80 to 90 degrees Fahr., might be expensive and difficult to maintain. Likewise, holding other oils at high temperatures, such as 220 degrees Fahr. or higher, might also prove difficult.

Written Discussion: By H. P. Langston, metallurgist, and G. R. Pease, associate chemist, Laboratory, Springfield Armory, Springfield, Mass.

The authors are to be commended for their sincere attempt to remove the veil of mystery that has persistently surrounded the selection of quenching oils. On the other hand, the impression should not remain that all oils are essentially alike or that "differences in capacity to quench are negligible with proper handling." This quoted statement may be true when heat treating the high hardenability tool steels. However, our experience has indicated that the differences in cooling capacity of various oils assumes considerable significance when engineering steels are involved. Reference is made to a number of heats of steel which it was possible to fully harden only by using an oil with a high initial quenching speed.

In one case, a 1.25-inch section of S.A.E. 4150 steel failed to harden when quenched into a straight paraffin base mineral oil with a low initial quenching speed, whereas, this same heat hardened uniformly and throughout the full section when quenched into an oil having a high initial quenching speed. In

another instance a similar improvement in hardening various lots of S.A.E. X1045 strip steel (0.033 inch maximum thickness) was accomplished with a change in the quench oil.

It has been our experience that it cannot be predicted with certainty that a given oil will fulfill the necessary quenching speed requirements when evaluated on the basis of the time-temperature curve at the center of a 1-inch diameter test plug quenched into that oil. This condition was especially true in the case of the thin section mentioned previously.

A method of measuring the initial quenching speed which appears to be much more reliable for thin sections of steel, at least, is a test which measures that percentage of contained heat above room temperature which is removed from a 1-inch round by 3-inch long test plug in the first five seconds of quench. In this test, oils which showed a low percentage of heat removed during the first five seconds invariably failed to produce a full quench while those oils which showed a high percentage of heat removed quenched satisfactorily.

It has also been found by experience that finely dispersed water to the extent of only 0.4 per cent suspended in a normally "fast" oil will reduce its initial quenching speed to a point where frequently the oil is no longer satisfactory. In this case, again, the results of the five-second test correlated better with quenching performance on S.A.E. X1045 strip steel than did time-temperature characteristics.

Temperatures at which a quenching oil may be used are limited in practice not only by the flash and fire points, but by their resistance to oxidation and sludging. It is probable that no commercial product will be usable for more than a few weeks at the reported test temperatures of 220, 300, and 450 degrees Fahr. One oil of mineral origin under test in this laboratory showed 9 per cent of sludge formation in 18 days at 210 to 220 degrees Fahr. Although this rate of deterioration is not typical of the best commercial oils, most oils do undergo a similar breakdown at these high temperatures over a period of time.

It is suggested that the following factors be considered in addition to those recommended by the authors in choosing the proper quenching oil:

1. The initial quenching speed under specified test conditions.
2. Resistance of the oil to oxidation and sludging.
3. Limitation of the water content to not more than traces.

The five-second test, mentioned before, has been found to be a simple yet reliable method for determining the initial quenching speed. A simple laboratory oven test on a small volume of oil at 210 to 220 degrees Fahr. with or without air agitation will give a comparative measure of oxidation and sludging characteristics which is sufficiently accurate for quenching oil tests. Water is usually determined by distillation with water-immiscible solvent.

Written Discussion: By Malcolm F. Hawkes, instructor, Department of Metallurgical Engineering, Carnegie Institute of Technology, Pittsburgh.

Metallurgists should welcome this paper for it supplies a great deal of data on a subject which, surprisingly enough, has received scant attention in the last few years. It is interesting and important to note that oils should be compared not at one fixed quenching bath temperature but rather at their optimum temperature for fastest cooling rate. One must agree with the authors that a surprising degree of control can be exerted by varying the quenching bath

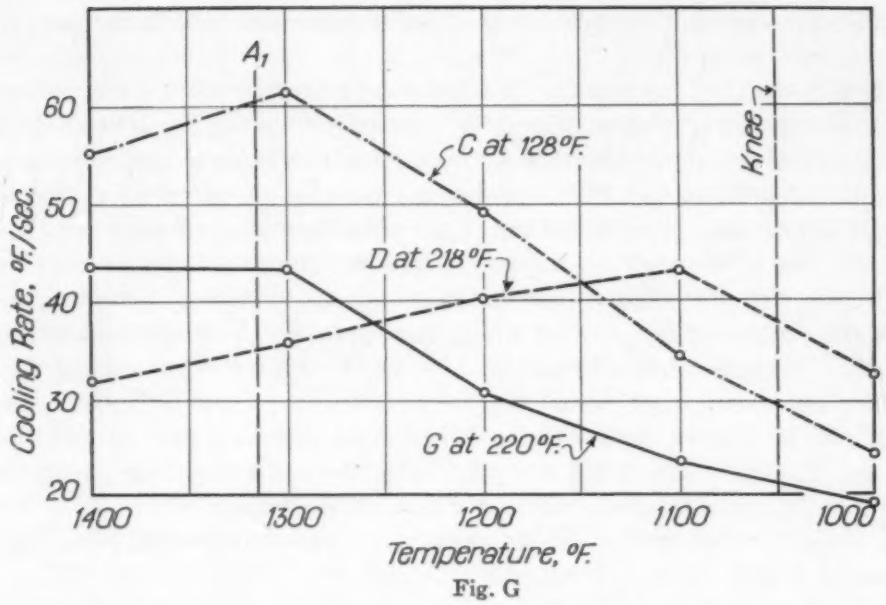

Fig. G

temperature for various oils, but many, I feel, would hesitate to agree that the evidence shows a variation in oils produces no important effect on depth of hardening.

However, rather than argue over what constitutes an important effect, I wish to suggest that consideration of this type of data alone may not be an easy way to compare the hardening power of various oils. The shape of the cooling curves obtained differs considerably, hence so does the relation between cooling rate and specimen temperature at which that cooling rate is measured. Fig. G, plotted from the authors' data, shows some interesting features about this relation. Curves are shown for three oils each used at its optimum quenching bath temperature for fast cooling. Oil D, which has a relatively low cooling rate at temperatures slightly below the critical, gives steadily increasing cooling rates almost down to the knee of the S-curve; here the rate is appreciably higher than that obtained using oil G which gives steadily decreasing cooling rates over the same temperature range. Consider also oil C. At 1300 degrees Fahr. (705 degrees Cent.), where cooling rates are frequently recorded, it affords a rate considerably greater than oil D, but the latter affords a greater rate at temperatures near the knee. With rates varying in this manner it is not a simple matter to estimate the effect on depth of hardening and I should like to make this suggestion. When comparing quenching oils would it not be advisable to make direct measurements on this important factor? Results from a simple but precise hardenability test, using each of the oils under consideration, would not entail much effort and would greatly strengthen the inferences to be drawn from cooling rate data.

Oral Discussion

G. W. WATERS:[12] If I am permitted I would like to append a question. We would be very interested in hearing a few more specific details on the manner in which these oils were aged so that they became used oils. We

[12]Senior research chemist, Shell Oil Co., Inc., New York.

would like if possible for the authors to give us some idea of the temperature at which the oils were aged.

HOWARD SCOTT:[13] In discussing oils we should keep in mind their ultimate function. Why do we quench in oil? It is primarily to avoid distortion; otherwise, we would use water. On that account a relatively long cooling rate is essential. Perhaps there has been too much emphasis on speed of quenching and too little on avoidance of distortion in the selection of quenching oils.

It is also clear from the way this discussion has gone that oils are used for several different purposes. The major one is to avoid distortion. But sometimes you get in the embarrassing position of having to harden a steel of inadequate hardenability. That requires one specific type of oil different from the general purpose oil that you might prefer to use.

It is an oil of high cooling velocity in the early stages of the quench, such as "C" and "E" of the paper, but not necessarily fast at low surface temperatures. In this case avoidance of scale on the work is imperative.

There is still another type of oil that may be used to considerable advantage; namely, one of high flash and fire point.

Most of you have heard Mr. B. F. Shepherd tell of the remarkable results he gets by quenching in molten salts at 400 to 500 degrees Fahr. (205 to 260 degrees Cent.). The same results can be obtained in oils, simply by raising their temperature, but then you get into the difficulty that Mr. Seasholtz men-

Table C

Comparison of Quenching Oils on Basis of Cooling Rate at 700 Degrees Fahr. Oil Temperature 130 Degrees Fahr.

Oil No.	Flash Point (Degrees Fahr.)	Viscosity	Cooling Rate—Degrees Fahr./Sec. 1100 Degrees Fahr.	700 Degrees Fahr.	Ratio of Rates
C	501	531	34.4	8.0	0.23
E	522	445	29.7	10.0	0.30
A	522	55	26.2	12.5	0.43
B	360	49	20.2	9.1	0.45
G	361	51	24.1	11.2	0.46
H	193	36	61.5	33.2	0.54
D	360	48	22.4	12.6	0.56

tioned. However, there are many furnaces in operation now which quench from and in a protective atmosphere so that there is no longer a serious fire hazard. An oil of high stability and therefore high flash point is then required.

Use of the latter oil at 400 degrees Fahr. (205 degrees Cent.) or higher is indicated particularly for 40 to 50 carbon S.A.E. or N.E. alloy steels, which steels present quite a problem in cracking. The hardening transformation occurs in them at such a high temperature that work cannot be withdrawn from the bath and cooled in air to avoid cracking with retention of full hardening. The next best thing then is to use the quenching medium in which the rate of cooling changes rapidly between the nose of the "S" curve and the temperature at which transformation starts, which is about 700 degrees Fahr. (370 degrees Cent.).

On that basis, I have calculated the ratio of the cooling rate at 700 degrees Fahr. (370 degrees Cent.) to that at 1100 degrees Fahr. (595 degrees Cent.) for the different oils at 130 degrees Fahr. Dr. Grossmann pointed out it does

[13]Section engineer, metallurgical section, Westinghouse Electric & Manufacturing Co., East Pittsburgh.

not make too much difference whether the nose temperature is taken as 1100 or 1300 degrees Fahr. (595 or 705 degrees Cent.). Now one can see how the several oils tested compare on the basis of this criterion, Table C. With a low ratio—that is, a high cooling rate at the nose of the "S" curve and a low cooling rate when transformation starts—minimum residual stress is developed. We have every reason to believe that the residual stresses which cause cracking develop as the transformation proceeds, that is, after, not before it starts, which is in the neighborhood of 700 degrees Fahr. for medium carbon steels.

From the foregoing viewpoint, one should choose oil "A" or "E" for use in a bath at say 400 degrees Fahr. (205 degrees Cent.) because of their high flash point. Both have adequate cooling power at 1100 degrees Fahr. (595 degrees Cent.) which, in the case of "E," at least is not lost when the bath temperature is raised to 440 degrees Fahr. "E," however, is preferable to "A" because of its low cooling rate at 700 degrees Fahr. (370 degrees Cent.) relative to that at 1100 degrees Fahr. (595 degrees Cent.). The use of such an oil might well extend the range of applications for "martempering."

Whether or not the preceding illustration is an apt one, it is a tribute to the authors' presentation of their data which permits convenient study of the effects of all the factors varied by them.

Authors' Reply

The authors are quite gratified by the volume of comment which this paper has evoked and wish to thank those who took part. Apparently this is a subject which is of considerable interest to many people and on which a wide divergence of opinion exists. On some points there was considerable repetition among the commentators; consequently we will consider the comments as a group rather than each one individually.

Four different discussions suggested that the lean N.E. steels need more severe quenching than the heretofore standard steels. Virtually all lists of the N.E. steels show the N.E. steels and the S.A.E. steels with which they are comparable. In other words, it is perfectly feasible to pick an N.E. steel capable of direct substitution for each of the S.A.E. steels. Existent data point to physical properties and hardnesses in the N.E. steels quite on a par with S.A.E. steels and nowhere is the use of special quenching oils indicated.

Two commentators suggest a special "five-second test" basically similar to a specific heat test. The authors hold no brief for any specific test. Our effort was to establish that but little if any difference existed in the capacities of the various oils to remove heat and that those differences could be adjusted by control of the oil bath temperature. In this connection the equipment used has been both commended and decried. We believe that it was sufficient for the purpose intended since we were able to answer the questions brought up in our shops which were the basis for the investigation. Hardness tests were suggested as another means by which this investigation might have been conducted. This is, of course, a valuable testing procedure and much useful information has been gained thereby.

The point made as regards chemical stability is well taken. Mixed oils will give high evaporation losses. It is the duty of the oil industry to provide the metals industry with stable oils. In the face of chemical instability, as evinced by evaporation, essentially identical cooling capacities were found.

The adjustment of oil bath temperatures has been said to be "not always practical." To hold temperatures to extremely low levels is difficult, requiring the handling of very large volumes of cooling water. As pointed out by the authors these low temperatures are not necessary. If and when high oil temperatures are carried, a much smaller volume of cooling water need be handled to control the bath temperature.

It is perhaps unfortunate that some of the standards used in measuring the physical properties of oils are not those common to the Petroleum Industry. However, they are comparable among oils investigated and are the units in which a great mass of data on quenching oils has been gathered over a period of years. Both the authors and some commentators concluded that physical properties of oils are unimportant except inasmuch as they affect cost per pound of steel quenched. The only true basis for evaluating the performance of quenching oils is quality of the quenched product as was brought out by one of our commentators.

We were surprised to hear that some investigations have indicated that variations in bath temperature do not affect quenching rates since this is at variance with the results of our tests and with some others.

It was stated that our curves do not show the three stages of quenching generally found in all time-temperature curves of quenching. While these three stages may not be apparent on casual examination they are none the less present. This was demonstrated in considerable work we did in deriving mathematical expressions for the various curves obtained experimentally. This work was not published.

We were very interested in hearing from one party, whose interests in the subject have been of long standing, that "all investigations along these lines made in recent years at plant laboratories and in heat treating departments have resulted in the same conclusions at which the authors have arrived."

We have been queried as to the actual identity of the oils discussed in our paper. For obvious reasons the disclosure of this information had best be withheld. We will emphasize that all of the oils examined are commercial and obtainable in the open market. It is admitted all brands of quenching oil were not represented.

In so much as all oils examined were not in regular use in our plant it was considered advisable to "age" each oil used. Scrap metal was repeatedly quenched in a fixed quantity of each oil until each quantity had been subjected to a like amount of abusive treatment.

We pointed out that we standardized the size of specimen, temperature, and quantity of oil used. Likewise the handling of the specimen from the furnace to the oil and in the bath was after a prescribed manner. The container of oil was placed at the mouth of the furnace. The specimen containing the thermocouple as described was withdrawn from the furnace and at once immersed in the oil to a depth of 9 inches, which placed it at least 5 inches from any container surface. The specimen was held in a fixed position in the oil, being neither moved around nor subjected to agitation of the oil.

Reproducibility of the apparatus was determined by taking a group of curves run on the same oil under the same conditions and calculating therefrom the average deviation within the group. This deviation was 4.65.

AN X-RAY STUDY OF BRASSES FORMED BY THE INTERDIFFUSION OF COPPER AND ZINC DEPOSITED ON GLASS BY VAPORIZATION

By Arthur A. Burr, H. S. Coleman and W. P. Davey

Abstract

By using the technique developed by Coleman and Yeagley, alloys were made by the interdiffusion of films of copper and zinc deposited on glass microscope slides by vaporization methods and X-ray investigations carried out. Data were obtained by means of the standard photographic powder method and by means of an Automatic X-ray Spectrometer. Metal films used were of the order of 6 x 10^{-5} centimeters in thickness. (A) It is shown that the metal films formed on glass by vaporization and the resulting alloys formed by diffusion have the same crystal structure as the bulk metal. (B) A series of samples in the beta brass range were subjected to heat treatment at 198 degrees Cent. (390 degrees Fahr.) for varying lengths of time. Their diffraction patterns show that formation of any higher phase by diffusion involves temporary existence of all the other copper-zinc phases as intermediate states. (C) Diffraction patterns recorded by the Automatic Spectrometer show orientation in the films. This gives experimental support to a proposed picture of the nature of phase changes during diffusion based on calculations from the lattice parameters. Techniques and procedure developed in this work suggest a method of determination of constitution diagrams and diffusion rates at low temperatures.

Introduction

USING the method of Coleman and Yeagley (1)[1], thin superimposed films were made of copper and zinc on the surface of glass microscope slides, each about 6 x 10^{-5} centimeters thick which

[1]The figures appearing in parentheses refer to the bibliography appended to this paper.

Of the authors, Arthur A. Burr is research physicist, Armstrong Cork Co., Lancaster, Pa., formerly, graduate assistant in physics, The Pennsylvania State College, State College, Pa.; H. S. Coleman is instructor, and W. P. Davey is research professor, in the Department of Physics, The Pennsylvania State College, State College, Pa. Manuscript received June 9, 1943.

were interdiffused at 198 degrees Cent. (390 degrees Fahr.). X-ray diffraction studies show (A) that the thin films have the same crystallographic constants as the bulk metal, so that conclusions based on work with thin films can be carried over safely to the bulk materials; (B) that the crystals of the thin films had a definite preferred orientation on the glass surface, and that a centered rectangle of atoms is always substantially parallel to the glass surface. This leads at once to a simple and reasonable picture of the mechanism of the phase changes in the copper-zinc system.

The Apparatus—The apparatus consists of:

1. A vaporization and diffusion apparatus.
2. An X-ray apparatus used for obtaining powder photographs.
3. An Automatic X-ray Spectrometer.

1. The vaporizing and diffusion apparatus is the same as that used by Coleman and Yeagley (1).

2. The X-ray apparatus used in the obtaining of powder photographs is a General Electric unit, Code ABNRY, Cat. No. A4904A.

3. The Automatic X-ray Spectrometer is a new instrument developed by S. W. Harding, F. R. Smith, and W. P. Davey (2). The Automatic Spectrometer is so designed as to make it possible to impose geometrical limitations on the diffracting planes, thus making possible a study of orientation of crystal phases in respect to the surface of the glass on which they are deposited.

Procedure

The Powder Method—The metal films used in this work were deposited on microscope slides by the Coleman and Yeagley method. Bimetallic samples of copper and zinc were prepared having approximately the same thicknesses for each metal; the total thickness was approximately 6×10^{-5} centimeters. These specimens were then heated to 198 degrees Cent. (390 degrees Fahr.) in order that diffusion might occur at a convenient rate. The diffusion was stopped at predetermined time intervals by removing the specimen from the diffusion apparatus and quenching it in either air or water. The partially diffused specimen was then removed from the glass slide by scraping with a razor blade and mounted in a cellophane specimen holder (3). X-ray powder photographs were then obtained. Relatively long exposure times (90 minutes) were neces-

sary because of the small quantity of specimen available (about two milligrams).

The Automatic Spectrometer Method—A bimetallic film of zinc and copper, containing as nearly as possible equal thickness of copper and zinc, was prepared as outlined above and was subjected to similar heat treatments. After each heat treatment, a diffraction pattern was taken of the film in situ on the glass slide. The purpose of the spectrometer was to examine the relative intensities of the diffraction maxima. (Because of the high background, this could not have been done densitometrically by using powder photographs.) Films of pure zinc and of pure copper were also examined by means of the automatic spectrometer.

Data—The diffusion series of powder photographs is shown in Figs. 1 and 2. Fig. 3 is a chart showing the position to scale and a rough approximation of the relative intensities of the lines shown in Figs. 1 and 2. Figs. 4 and 5 show the automatic X-ray spectrometer recordings for the diffusion which occurred during the time the specimen was heated before quenching. Fig. 6 is a spectrometer recording showing the relative intensities of zinc deposited on glass as compared with the relative intensities of zinc filings. Fig. 7 shows a comparison of the relative intensities of the first four lines of copper deposited on glass and the relative intensities of the copper filings.

Discussion of the Data—It is evident from the powder photographs and the chart which represents them (Figs. 1, 2, 3) that:

1. Films of zinc and copper deposited by vaporization methods have the same crystal structure as do the bulk metals. If this had not been so, our conclusions could certainly not be applied to the case of the metals in bulk. Indeed, it is doubtful whether they could have been completely justified even in the case of thin films.

2. During the first 30 seconds of the interdiffusion of copper and zinc, the copper, alpha, beta, gamma, epsilon and zinc phases are present simultaneously.

3. A homogenized specimen of equal portions of zinc and copper at 198 degrees Cent. exhibits the body-centered cubic characteristics of beta brass.[2]

4. The interplanar distances between the zinc (10.1) family of planes, the copper (111) family of planes, the alpha brass (111)

[2]This phase may be either Beta or Beta'. The A.S.M. Handbook lists the Beta phase in its tabular data and the Beta' phases in its constitution diagram.

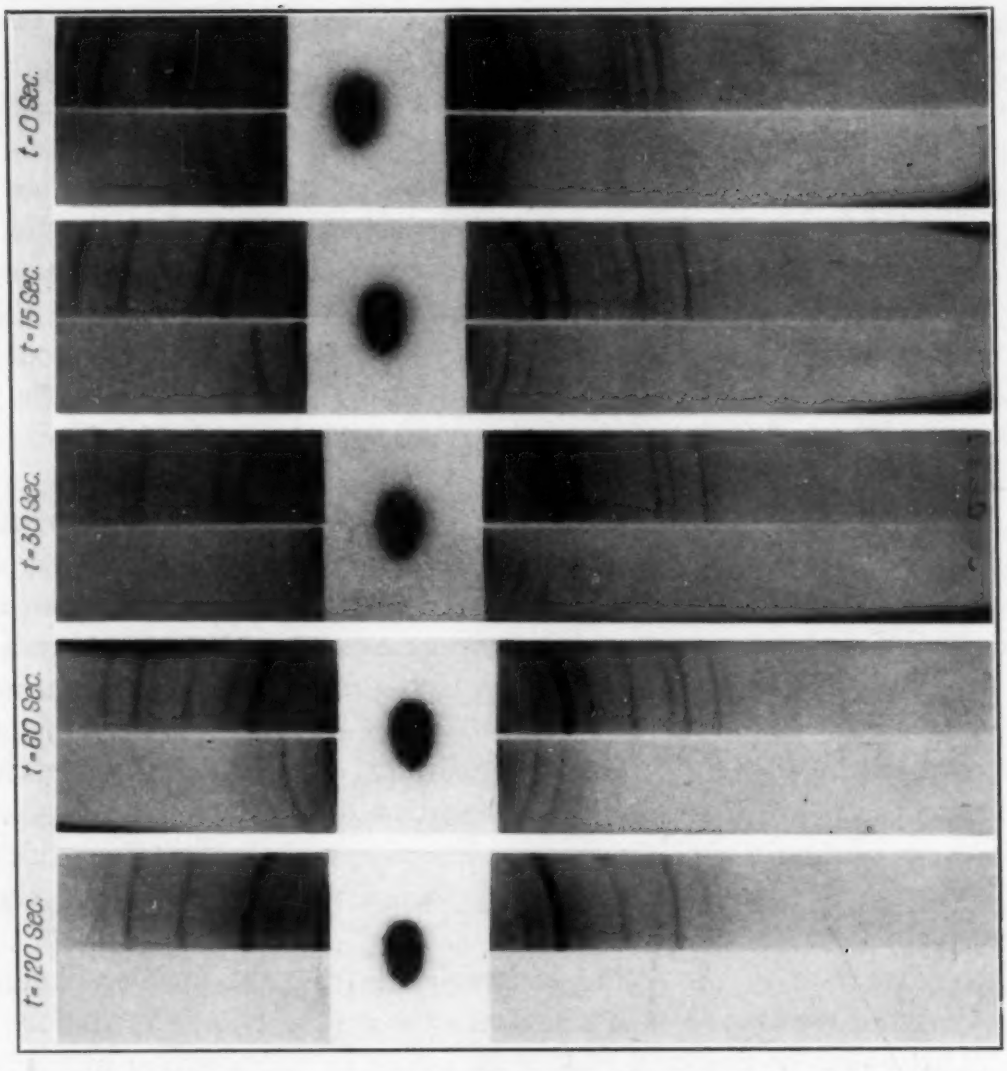

Fig. 1—Powder Photograph Showing Formation of Beta Brass by Diffusion of Thin Films of Copper and Zinc at 198 Degrees Cent. (0 to 120 Seconds).

family of planes, and the beta brass (110) family of planes are very nearly the same. It follows that the distances between the centers of adjacent atoms in these planes are nearly the same.

It is evident from Figs. 4 and 5 that:

1. The combined intensities of the zinc (10.1) line and the copper (111) line remain practically constant during the diffusion of zinc and copper, whereas the zinc (00.1) line practically disappears two minutes after the diffusion has been in progress at 198 degrees Cent. (390 degrees Fahr.). This indicates a very rapid disorganization of the zinc.

2. The specimen that was permitted to diffuse for two hours (almost completely homogenized) shows anomalous relative in-

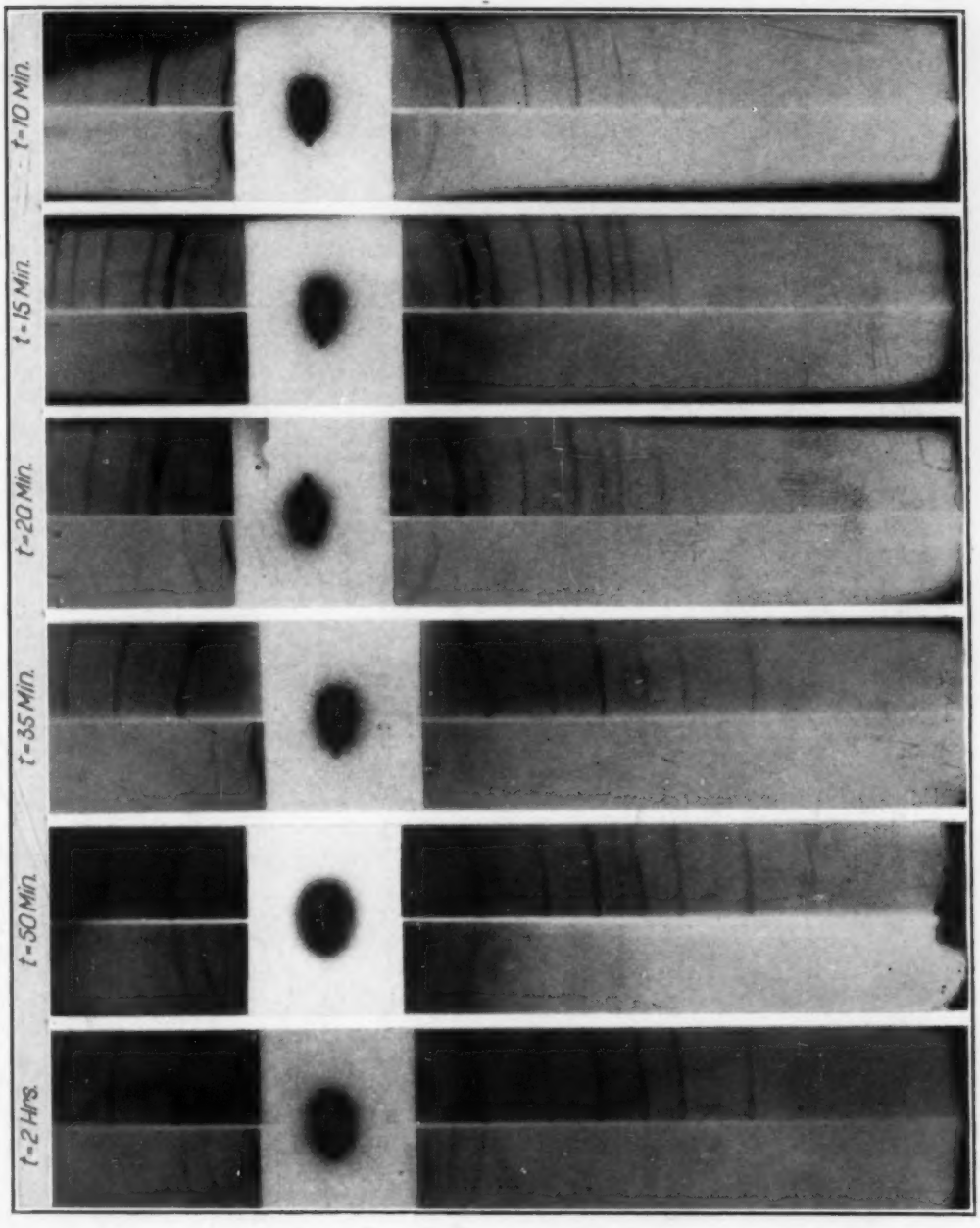

Fig. 2—Powder Photograph Showing Formation of Beta Brass by Diffusion at 198 Degrees Cent. (10 to 120 Minutes).

tensities for beta brass; the only strong line being the (110) line for beta brass, the other lines being nearly absent. This anomaly suggests that the (110) crystal planes have a preferred orientation and that they are parallel to the glass slide.

Fig. 6 shows that there is a different intensity distribution for the various lines of copper in the form of filings than there is for copper which has been condensed on a glass surface. Fig. 7 shows

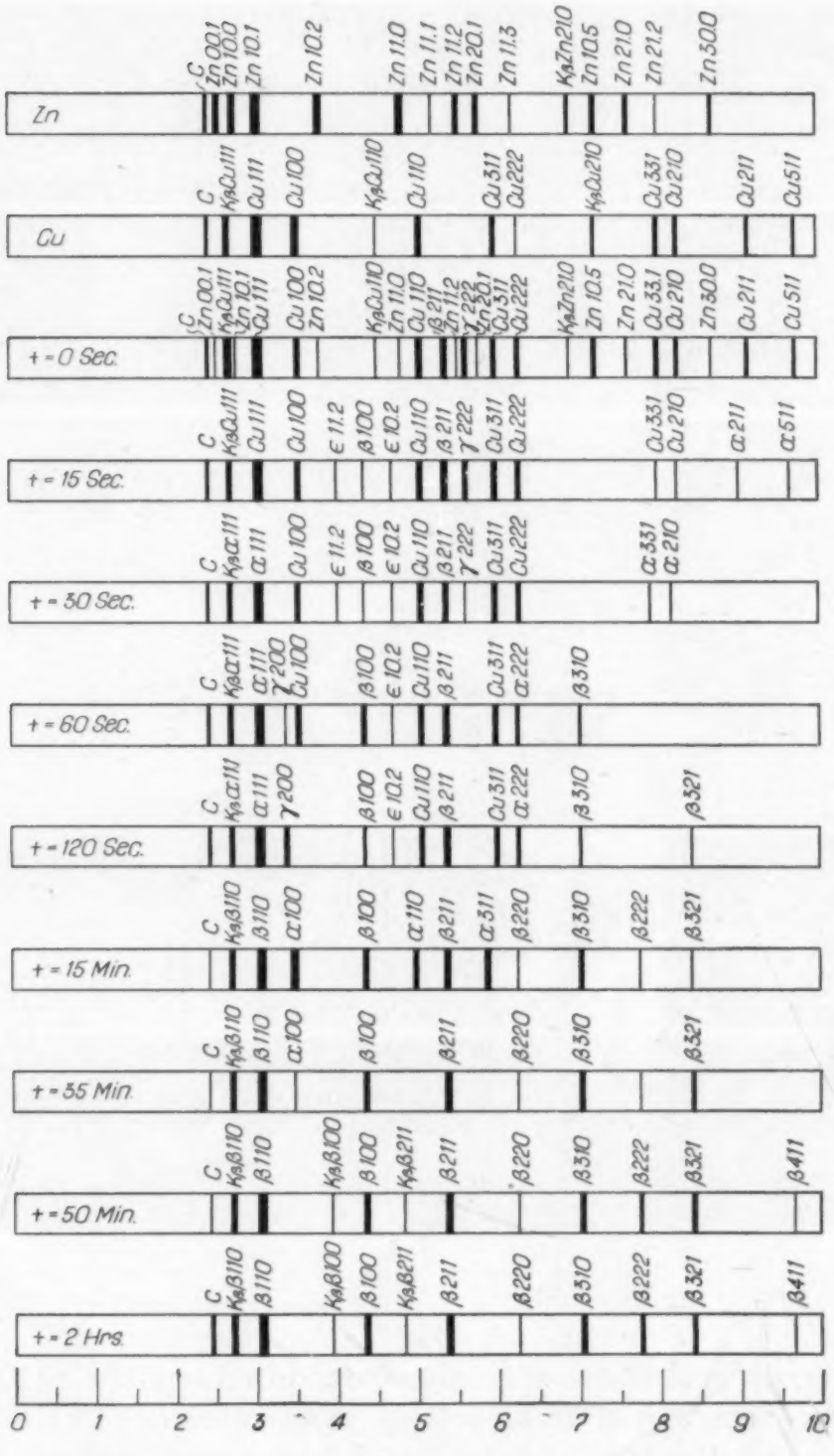

Fig. 3—Chart Showing Positions and Relative Intensities of Lines Shown in Figs. 1 and 2.

that there is a different intensity distribution of the lines of zinc in the form of filings as compared to zinc which has been condensed on

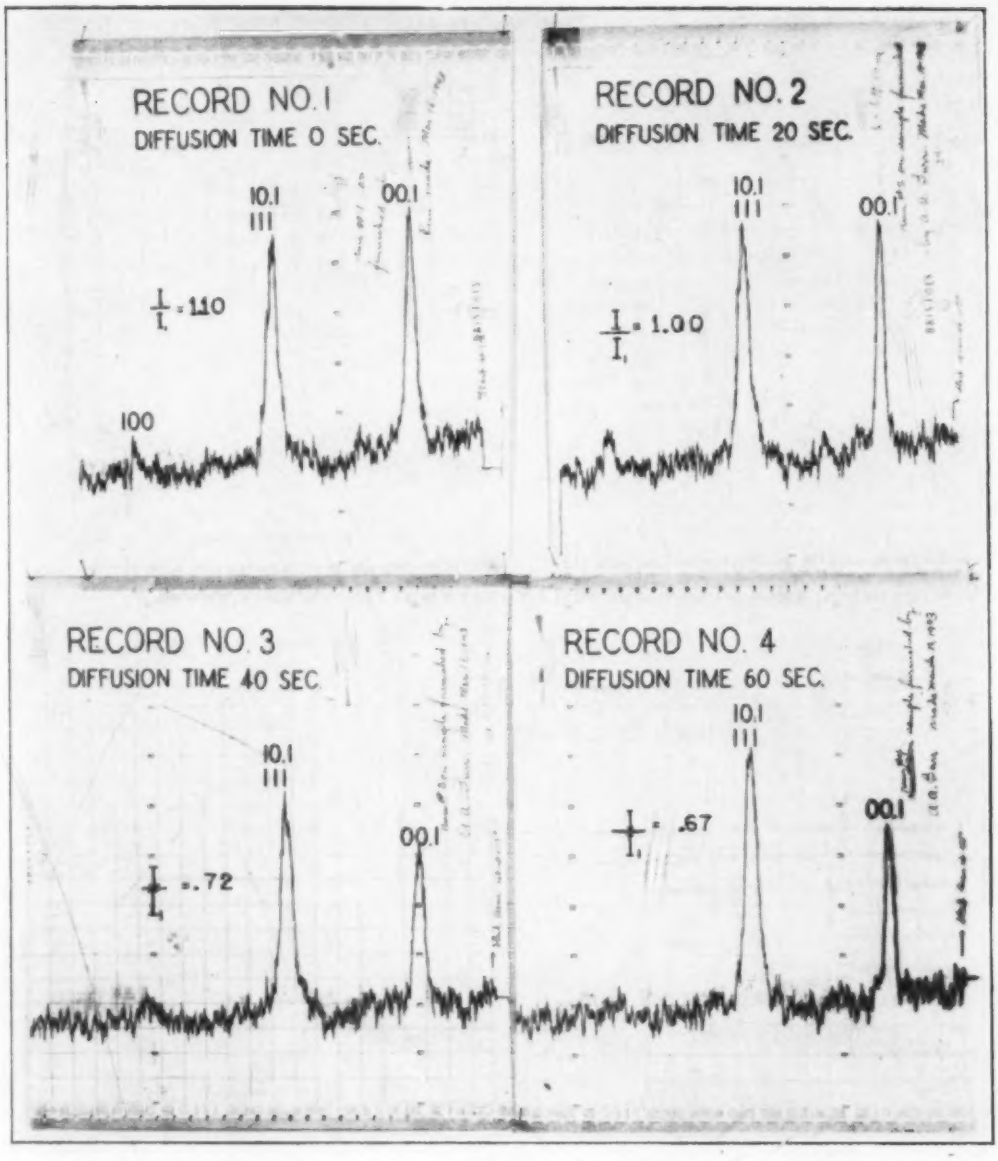

Fig. 4—Recordings from Automatic X-Ray Spectrometer for Diffusion at 198 Degrees Cent. (0 to 60 Seconds). (Note that the Spectrometer Only Shows Peaks for Planes Parallel to the Surface of the Glass Microscope Slide. Note Also the High Background Caused by Scattering of X-Rays by Glass).

glass. A study of the fundamental reasons for the apparent anomalies in intensities of Figs. 5, 6, and 7 indicates that the condensed films have a tendency to be oriented with respect to the glass plate. Although this orientation in itself is not surprising, the deductions that may be made from the fact of orientation are of particular importance. It is apparent that there is a strong tendency for the zinc (00.1) and (10.1) planes to be oriented parallel to the glass, and to a lesser extent for the copper (111) and (100) planes to be oriented such that they are parallel to the glass surface. Further,

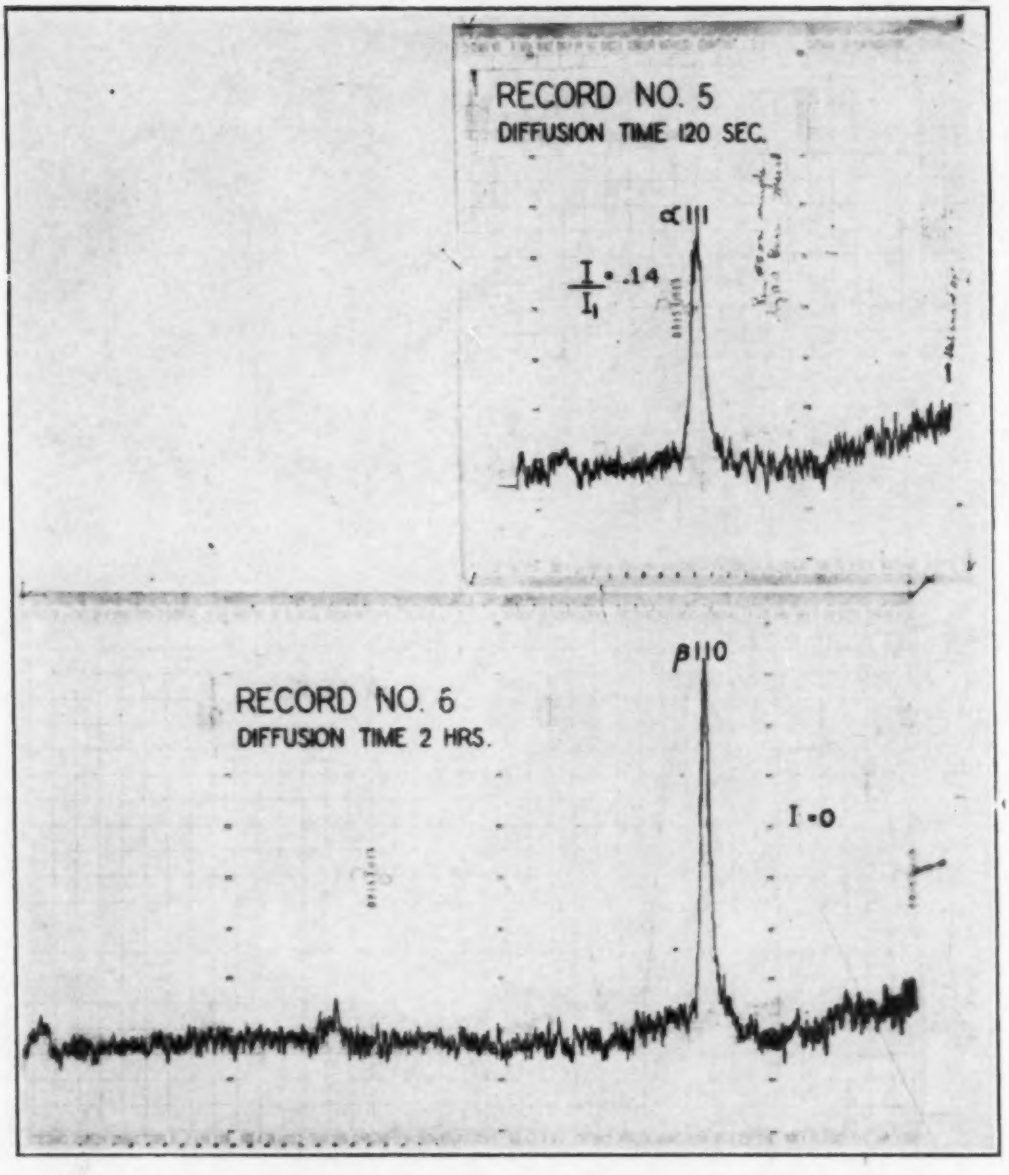

Fig. 5—Recordings from Automatic X-Ray Spectrometer for Diffusion at 198 Degrees Cent. (2 Minutes to 2 Hours). (Note that the Spectrometer Only Shows Peaks for Planes Parallel to the Glass).

it is evident that the final beta brass formed as a result of interdiffusion of "50-50" zinc and copper films show that the (110) family of planes of beta brass is also parallel to the glass surface. These facts suggest a mechanism of phase changes which are presented systematically in Fig. 8.[3]

It is easy to see that when a metal vapor (e.g., copper or zinc) is condensed on the amorphous surface of a microscope slide, the

[3]A similar transformation was worked out for the alpha to gamma and gamma to alpha transformation of iron, by Mehl and Smith (4). They used a one component system, while here two components are involved (zinc and copper).

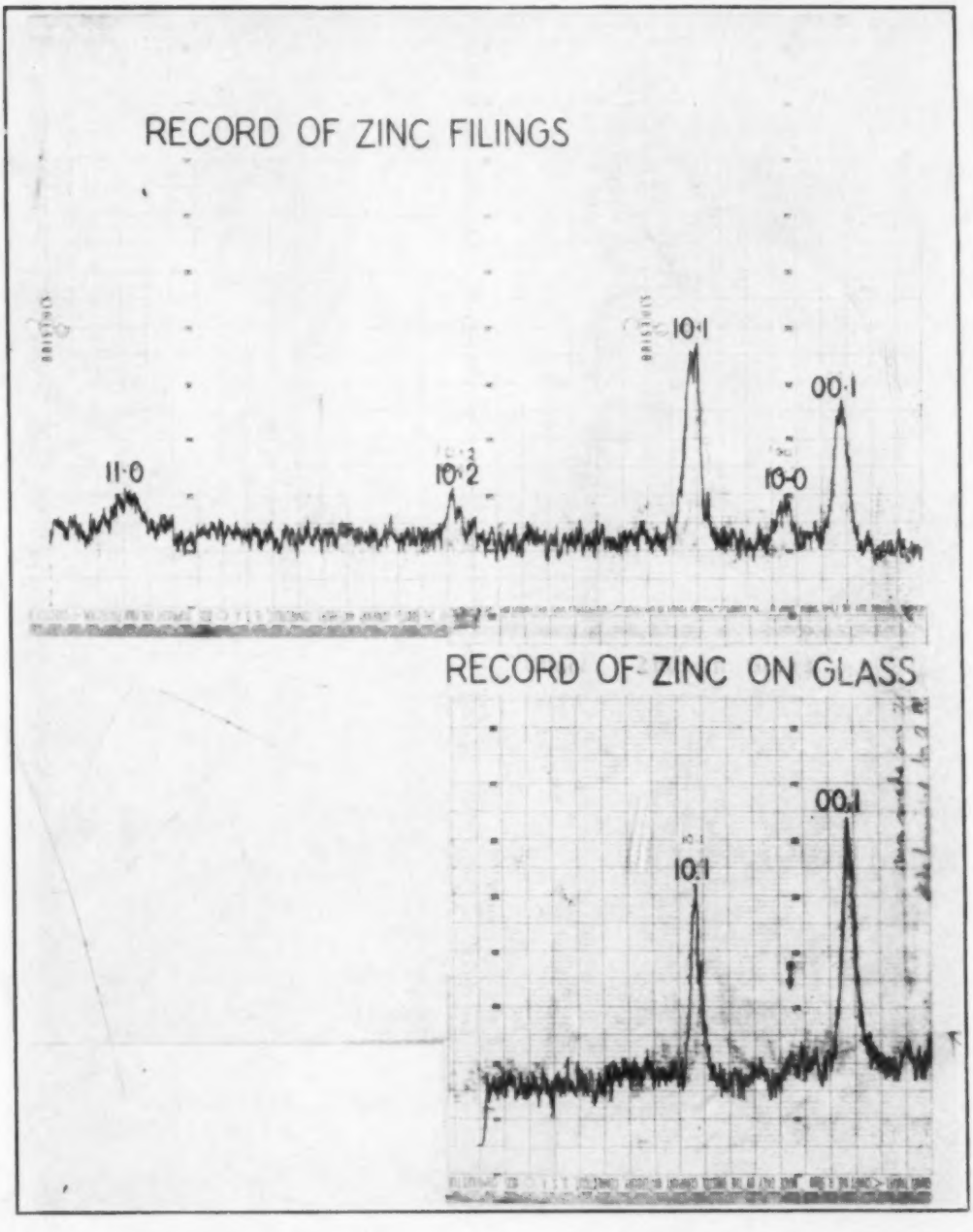

Fig. 6—Recordings from Automatic X-Ray Spectrometer Comparing a Thin Film of Zinc on Glass with Zinc Filings. (Note that the Spectrometer Only Shows Peaks for Planes Parallel to the Glass).

first step toward crystallization must be the formation of triangles by the chance collision of three atoms of metal. These triangles must be either equilateral or isosceles, and their planes must be substantially parallel to the glass surface. The addition of still other metal atoms to these triangles must produce two-dimensional and finally three-dimensional seed-crystals.

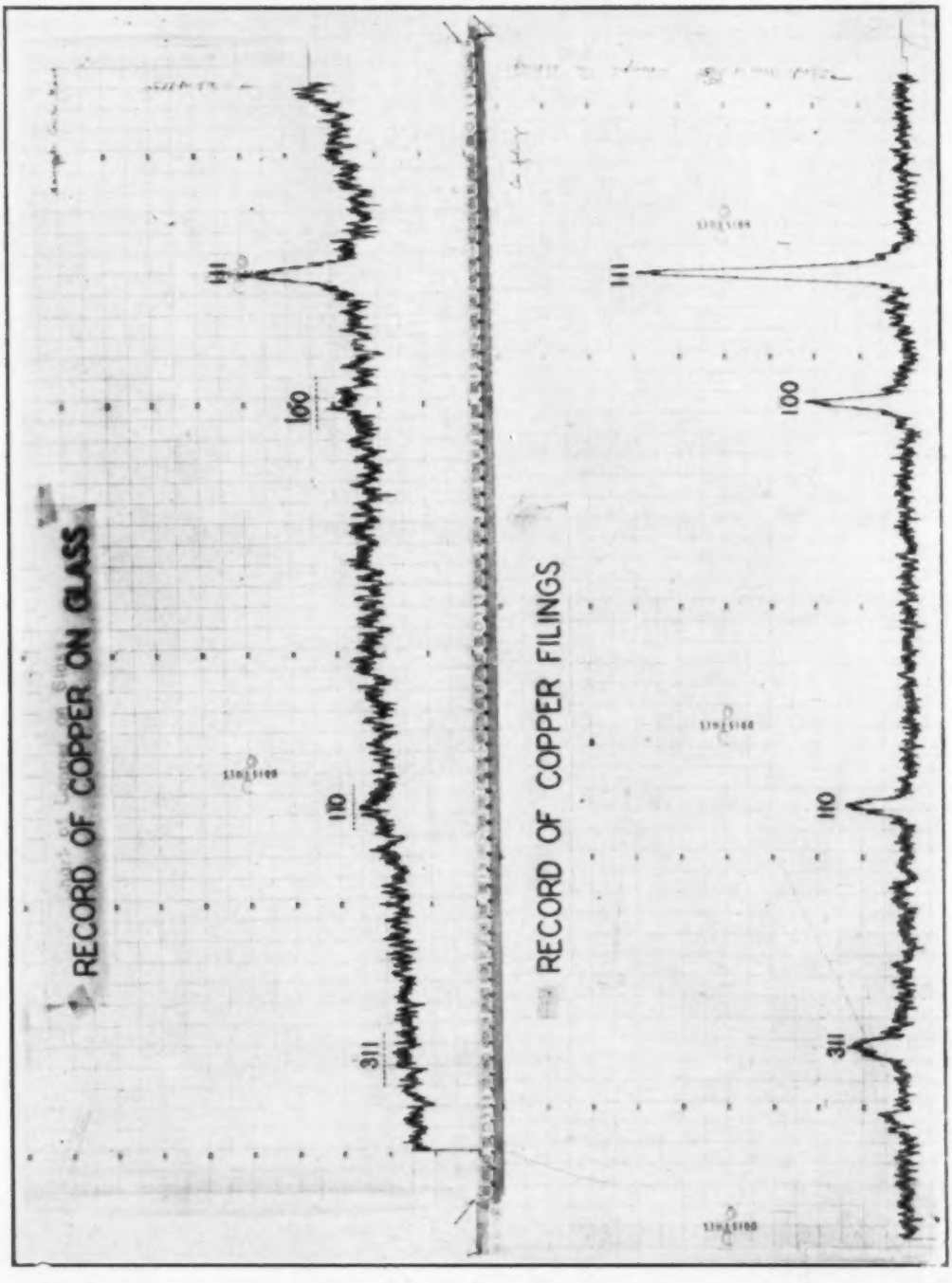

Fig. 7—Recordings from Automatic X-Ray Spectrometer Comparing a Thin Film of Copper on Glass with Copper Filings. (Note that the Spectrometer Only Shows Peaks for Planes Parallel to the Glass).

This picture of equilateral or isosceles triangles as the fundamental unit for crystal growth leads at once to a possible systematic sequence of steps, consistent with the data of Figs. 4, 5, 6, and 7, by which zinc can be added bit by bit to pure copper to form, in

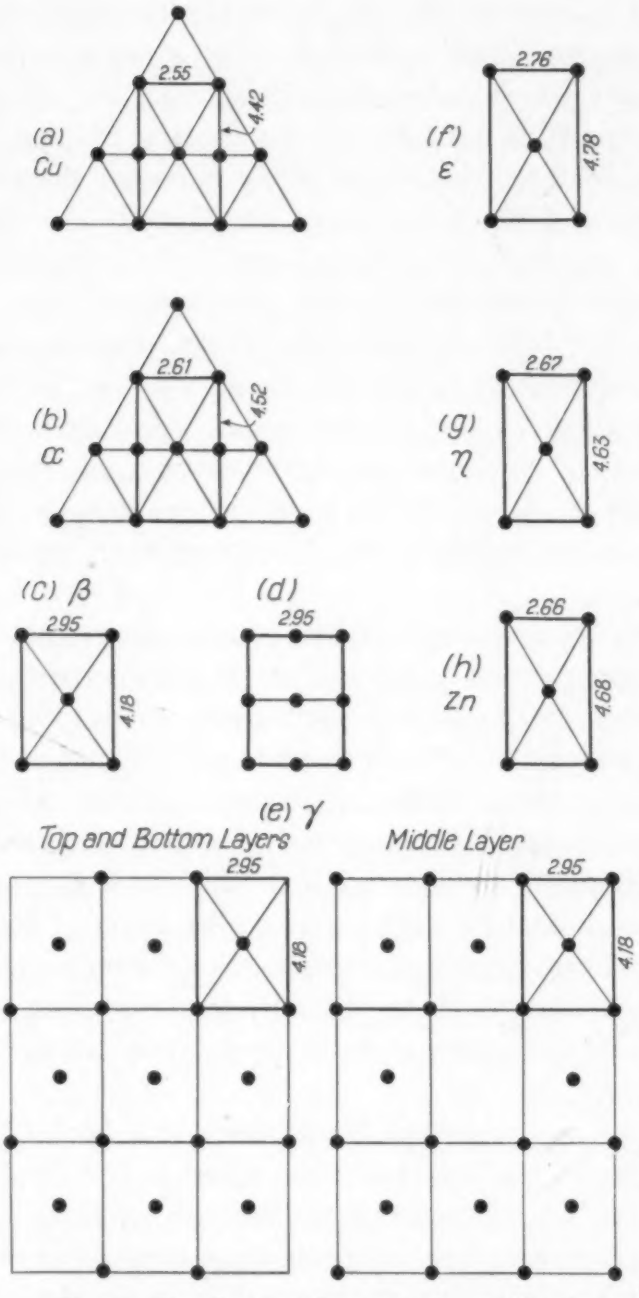

Fig. 8—The Centered Rectangle in all Members of the Copper-Zinc System Which is the Basis of the Phase-Changes; (a) Pure Copper; (b) Alpha Phase; (c) Beta Phase; (d) the Beta Phase as Seen in a Direction Perpendicular to the Plane of (c); (e) Gamma Phase (omitting Certain Negligible Distortions); (f) Epsilon Phase; (g) Eta Phase; (h) Pure Zinc.

succession, alpha, beta, gamma, epsilon, and eta brass. Of course, the sequence can be pictured equally well in reverse order, adding copper bit by bit to pure zinc. It has already been pointed out that Fig. 4 shows a rather high degree of orientation of copper such

that the (111) planes of the copper tend to lie parallel to the surface of the microscope slide. Obviously this gives a network of equilateral triangles whose sides are 2.55Å long. Fig. 8 (a), drawn to scale, shows that this network can be considered just as truly to be a network of centered rectangles whose sides are respectively 2.55Å, and 4.41Å long. The progressive addition of zinc to the copper lattice (thus making the solid solution called "alpha brass") will progressively lengthen the lattice parameter of the face-centered cube of copper. (For instance (5), in the case of a solid solution of 37.5 parts of zinc in 62.5 parts of copper, Fig. 8 (b) shows that the rectangle becomes 2.61Å wide and 4.52Å long.) Finally, when the proportions of zinc and copper are about equal, the face-centered cube has been stretched to the point where a body-centered cubic structure[4] is more stable. This body-centered cubic structure is "beta brass".

Fig. 5 shows that the beta brass has a strong tendency to have its (110) planes parallel to the surface of the microscope slide. This means that the (110) planes of beta brass are parallel to the (111) planes of copper and of alpha brass and suggests that the (111) planes of alpha brass, saturated with zinc, changed themselves into the (110) planes of beta brass. Such a transformation, shown to scale in Fig. 8 (c), requires motions of less than 0.3Å or about one-tenth of the packing diameter of a copper or zinc atom. Fig. 8 (d) shows that the mechanism proposed for the transformation from alpha to beta brass in planes which are parallel to the surface of the microscope slide is also consistent with the location of the other atomic planes.[5]

It is to be assumed that the addition, bit by bit, of still more zinc will progressively lower the symmetry of the fundamental cube of beta brass. This could not produce any sudden change either in inter-atomic spacings or in the general type of crystallization up to the point where some other structure is more stable than that of beta brass. Before such a point is reached, however, the interdiffusion of copper and zinc is able to attain a low type of cubic symmetry which can only be expressed in terms of a larger crystal-

[4]Copper at the corners of the cube, and zinc at the body-center. In the face-centered cube, the lengths of the edges of the rectangles in the (111) planes stand in the ratio $1:\sqrt{3}$. In the body-centered cube the lengths of the edges of the rectangles in the (110) planes stand in the ratio $1:\sqrt{2}$.

[5]Figs. 4 and 7 indicate that a few of the crystals of copper have oriented themselves so that their (100) planes are parallel to the surface of the microscope slide. Trial shows that the transformation from the (100) planes of alpha brass to (110) planes of beta brass is about as easy as in the case outlined above.

lographic unit, whose lattice parameter should be some simple multiple of the original unit. It is not surprising, then, that the unit-cube of gamma brass has a lattice parameter somewhere between 8.84 and 8.87Å (5), since 3 times the parameter of beta brass (2.95Å) is 8.85Å. Such a cubic array would be expected to contain $2 \times (3)^3 = 54$ atoms, but the Hume-Rothery Rule for the gamma phase permits only 52 atoms, i.e., Cu_5Zn_8. Bradley and Thewis (6) have shown that this is done by omitting from the combined unit array of 27 body-centered cubes (a) the zinc (or copper) atom at the body-center of the cubic unit array, and the eight copper (or zinc) atoms at the corners of the cubic unit array (each of which, of course, only belongs $\frac{1}{8}$ to the unit cubic array). The resulting distortions are negligible so far as the present discussion is concerned. Portions of the gamma structure are shown in Fig. 8 (e). The orientation and dimensions of the rectangles in the (110) planes must therefore be unaltered in the transformation from beta to gamma brass. The transition from beta to gamma brass is therefore particularly easy in terms of the rectangles in the (110) planes.

We have now followed the mechanism of the successive transformation of the copper lattice to that of the alpha, beta, and gamma brasses. The further bit by bit addition of zinc introduces such distortions that the crystals can no longer show cubic symmetry. From this point on, the symmetry must be described in terms of the hexagonal close-packed structure of zinc. The basal plane (00.1) of the hexagonal close-packed structure may be considered to be made up of rectangles whose sides stand in the ratio of $1:\sqrt{3}$. Fig. 8 (f) shows such a rectangle drawn to scale for epsilon brass. The rectangle of the gamma phase becomes the rectangle of the epsilon phase by changing its dimensions from 2.95 x 4.18Å to 2.76 x 4.78Å, a maximum atomic movement of less than a fourth of an atomic diameter. This transformation should, therefore, if our reasoning is correct, produce for the epsilon phase a hexagonal close-packed structure whose (00.1) planes would be parallel to the surface of the microscope slide. The further bit by bit addition of zinc to the epsilon phase will shorten the sides of the rectangle (thus giving the eta phase), without altering its orientation. This is shown to scale in Fig. 8 (g). Finally, we approximate pure zinc, whose rectangle is shown in Fig. 8 (h). We have, therefore, in effect, predicted that zinc, deposited on the surface of a glass

microscope slide, should be so oriented that its basal planes (00.1) will lie parallel to the surface of the slide. Fig. 6 shows that this is one of the two preferred orientations found experimentally in zinc deposited on a microscope slide. Fig. 6 shows that zinc also tends to deposit with its (10.1) planes parallel to the surface of the microscope slide. These (10.1) planes are of very nearly the same orientation as the (30.2) planes which contain isosceles triangles of substantially the same size as the triangles shown in Fig. 8 (h) for the (00.1) planes and which, when taken in pairs, form slightly puckered rectangles which simulate the centered rectangles which have been employed above. The mechanism of transformation between eta brass and pure zinc is therefore assumed to be essentially the same no matter whether we start with the (00.1) or the (10.1) planes.

We have now completely described a mechanism for all the low temperature transitions of the copper-zinc system. The outstanding feature of this mechanism is that it requires the existence of a centered rectangle whose orientation remains substantially unchanged in all the phases from 100 per cent copper to 100 per cent zinc, and whose dimensions do not change by more than a fourth of an atomic diameter in any single transition. Using the Automatic X-ray Diffraction apparatus, this constancy of orientation has been shown for thin films of pure copper, alpha brass, beta brass and pure zinc. It is, therefore, easy to assume it for the other phases (gamma, epsilon, and eta), which lie between beta brass and pure zinc. This mechanism is doubly convincing when we remember that (see Figs. 1 and 3) in the first 30 seconds of the diffusion process at 198 degrees Cent., six of the total of seven phases[6] were found to be present. It is hardly conceivable that these various phases should have changed over so quickly and so easily as to give an almost perfectly oriented set of beta crystals unless there had been some configuration of atoms (e.g., the centered rectangle) which was common to all the phases. We feel that our conclusions may be safely applied to the case of metals in bulk, since Figs. 1, 2, and 3 show that our thin films when scraped off their glass mountings have crystal properties identical to those of the bulk metals.

[6]Within the precision of our data we could not distinguish with certainty between the eta phase and pure zinc. The interplanar spacings of some of the families of planes in the beta, epsilon, and gamma structures are so nearly the same that their strongest lines fall at the same place in the "powder" photographs. This accounts for some of the apparent lack of data on epsilon and gamma in Figs. 3 and 8.

Bibliography

1. H. S. Coleman and H. L. Yeagley, "The Method of Thin Films for the Study of Intermetallic Diffusion and Chemical Reactions at Metallic Surfaces", TRANSACTIONS, American Society for Metals, Vol. 31, 1943, p. 105.
2. Harding, Smith, and Davey, *Physical Review*, Vol. 62, 1942, p. 296.
3. A. A. Burr, *Review of Scientific Instruments*, Vol. 13, 1942, p. 127.
4. R. F. Mehl and D. W. Smith, Technical Publication 521, Iron and Steel Division, American Institute of Mining and Metallurgical Engineers, 1934.
5. A.S.M. METALS HANDBOOK, 1939, p. 1368.
6. Bradley and Thewis, *Proceedings*, Royal Society, Vol. 112A, 1926, p. 678.

DIMENSIONAL CHANGES ENCOUNTERED IN TUBE SINKING

By William Marsh Baldwin, Jr., and Thomas S. Howald

Abstract

The wall thickness changes occurring during tube sinking were investigated for copper and a number of copper alloys. It was determined that wall thickness changes were affected by the magnitude of the reduction per pass, the relative thickness of the tube, and the temper of the metal, but were unaffected by the absolute dimensions of the tube, the metal itself, the die contour or finish, and the lubrication. Siebel and Weber's theoretical treatment was applied to the experimental data and gave qualitative agreement. A straight line relation was found to exist between the relative thickness ratio (wall thickness/outside diameter) and the reduction in outside diameter up to 30-40 per cent reductions, which relation is followed not only by the data reported in the present paper, but by all the data on dimensional changes during tube sinking that are reported in the literature on lead, steel, 17S aluminum, and brass.

Introduction

THE principle of tube sinking consists essentially in drawing a tube or hollow cylindrical shape through a die without supporting the internal surface of the tube by means of a mandrel or plug. As a consequence of this lack of internal support, the tube wall is free to increase or decrease in thickness—increasing in the case of relatively thin-walled tube, decreasing in the case of relatively thick-walled tube.

Experimental quantitative measurements of wall thickness changes have been made on hot sunk steel (1)*, lead, (2) 17S aluminum (3) and brass (3), (4), (5). Siebel and Weber (2) have attempted to develop a theoretical method by which the experimental

*The figures appearing in parentheses refer to the bibliography appended to this paper.

A paper presented before the Twenty-fifth Annual Convention of the Society, held in Chicago, October 18 to 22, 1943. Of the authors, W. M. Baldwin, Jr., is chief metallurgist, Euclid Case Plant, and T. S. Howald is research assistant, Midwestern Division, Chase Brass & Copper Co., Inc., Cleveland. Manuscript received May 21, 1943.

data may be reproduced. The method is based on the observation by Roš and Eichinger (6) and by Lode (7) that the rates of strain in the three principal directions are proportional to the differences between the individual stresses in those directions and the average of the three principal stresses. Their procedure is accomplished in four steps:

1. Equations for the three principal stresses are assumed. The longitudinal stress, S_1 (the stress lying parallel to the drawing direction) is expressed as:

$$S_1 = \frac{K_{ave.}}{E} \epsilon.$$

where K_{ave} is the average yield strength of the metal; E is the efficiency of the process, i.e., the ratio of the stress for a frictionless, loss-free drawing process, to the actual stress; and ε is the principal deformation. The tangential stress, S_t, by virtue of the constant flow stress principle, is

$$S_t = K - S_1$$

where K is the yield strength of the metal. The radial stress, S_r, is obtained as the product of the tangential stress and a function of the starting relative thickness ratio (i.e. the ratio of the wall thickness to outside diameter) which ratio, Siebel and Weber assumed constant throughout the sinking operation.

$$S_r = \left(1 - \frac{ID}{D_m} \right). S_t$$

where ID is the inside diameter of the tube, and D_m is the mean diameter of the tube. The stresses are plotted graphically as a function of the principal deformation, ε prin.

2. The three stresses are averaged and the differences between the individual stresses and the average stress are determined and plotted, as before, as a function of the principal deformation, ε prin.
3. The largest stress difference existing at any given deformation is divided into the other two stress differences. By the

Roš-Eichinger-Lode principle, the resulting quotient is the rate of the deformation occurring in a given direction with respect to the principal deformation, i.e., $d\varepsilon_{min.}/d\varepsilon_{prin.}$ These rates are again plotted as a function of the principal deformation $\varepsilon_{prin.}$.

4. The areas under the rate curves are determined planimetrically, giving the minor deformations as a function of the principal deformation according to the equation:

$$\int \frac{d\epsilon_{min.}}{d\epsilon_{prin.}} d\epsilon_{prin.} = \epsilon_{min.}$$

Application of this method to their own experimental data on lead tube and to Pomp and Schylla's experimental data on hot sunk steel seamless tube resulted in a family of curves passing near or through an incoherent set of experimental points (see inset to Fig. 4) thus failing to demonstrate as clearly as was possible the validity of their theory.

The present paper attempts to determine whether wall thickness changes during sinking can be represented in a congruous manner, so that the general mechanism underlying dimensional changes can be discerned; further, it attempts to determine the effect of certain factors on wall-thickness behavior, and to develop graphical methods for the rational prediction of wall-thickness changes.

Procedure

There are many variables that conceivably could affect the change in wall thickness on sinking. These variables include: the nature of the metal being sunk, i.e., the alloy and its temper; the dimensions of the tube; the contour of the die; the surface conditions, i.e., the surface finish of the die and tube, the type and degree of lubrication; the speed at which the tube is sunk; the temperature at which the tube is sunk; and the reduction in outside diameter effected by the operation.

Variables were studied singly in one or more series of tests in which all other variables were held constant. For example, brass tubes (66.5 per cent copper, 0.5 per cent lead, balance zinc) identically prepared, were sunk to the same outside diameter, at the same drawing speed, at room temperature, with the same lubricant, on

chrome-plated dies of varying contours: 14, 30, 55 degrees, total included angle conical dies, and different trumpet-shaped dies; a second series was carried out in the same manner as above except that no lubricant was used; a third series was conducted with the same set of conditions as the first series, except that the tubes were sunk to a different outside diameter, etc.

The tubes were measured before and after sinking. At least eight readings were made and averaged to give the values reported here. In those cases where the tube was too small or too thick to permit micrometer measurement of the wall thickness, this dimension was determined on a metallograph.

Results and Discussion

The following variables were found to have a very slight or negligible effect on the change in wall thickness occurring during sinking; the alloy, the die contour, the die finish and the lubrication.

For this phase of the work, copper, red brass (85 per cent copper, balance zinc) leaded tube brass (66.5 per cent copper, 0.5 per cent lead, balance zinc) and antimonial Admiralty brass (71 per cent copper, 1.05 per cent tin, 0.035 per cent antimony, balance zinc) were investigated. The wall thickness changes of all four alloys were practically the same. As will be brought out in a later section, the data for steel, lead, cartridge brass and 17S aluminum given in the literature follow almost the same curves as those obtained from the above copper alloys, so that it may be concluded that the effect of variation of alloy itself is small.

The die contours used in the present investigation have already been listed. The conical dies were both plain steel (polished), and chrome-plated; the trumpet-shaped dies were plain steel, chrome-plated, and tungsten carbide. These contours and finishes, both with and without lubricant, were without effect on the wall thickness changes. Further, Siebel and Weber's data on lead tube sunk without lubricant through both polished and rough steel dies will be shown to fit the same curves as those obtained in the present investigation.

Tubes drawn with and without a commercial drawing lubricant (soap base with high free fat content) gave identical results. This is consistent with Remmers' report (8) that two copper wires drawn with and without lubricant yielded "no measurable difference"

between the two contours of the butt ends of the respective wires . . .

The factors that do influence the change in wall thickness are the temper or physical condition of the metal, the reduction in outside diameter effected in a pass, and the ratio of the wall thickness to the outside diameter, (G/OD).

The effect of the temper of the metal is shown in Fig. 1 where

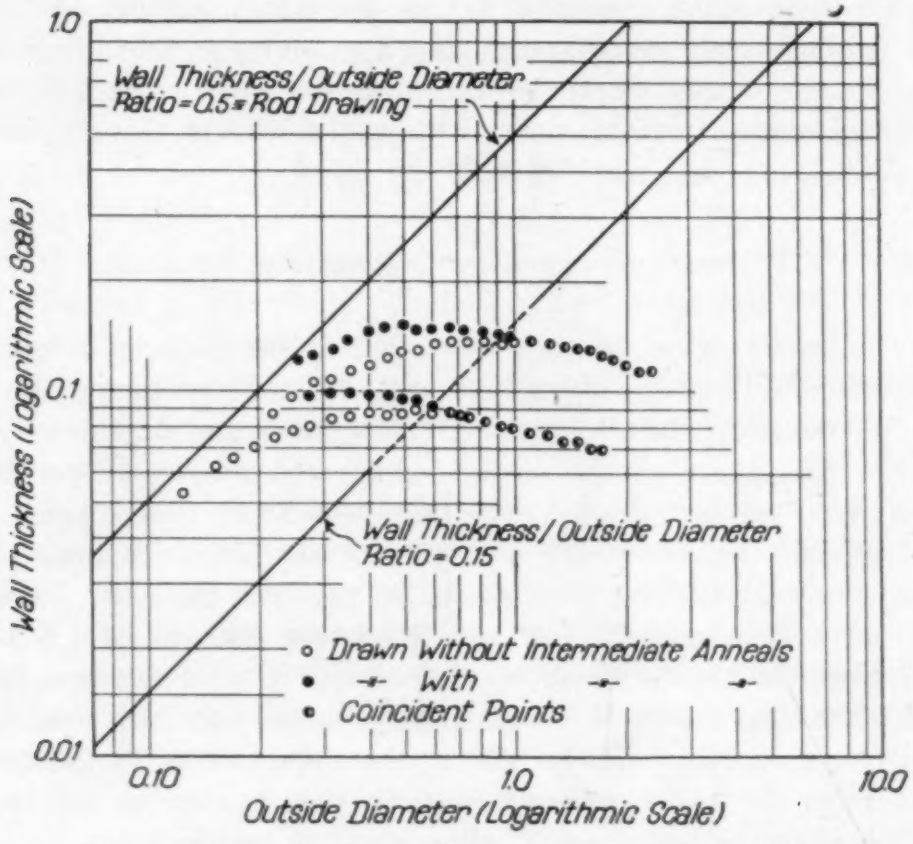

Fig. 1—Effect of Temper on Dimensional Changes During Tube Sinking. (Copper).

the dimensions of two pairs of tubes are plotted. One tube of each pair was soft in the original condition and was annealed before each pass, the other tube of each pair was hard and was not annealed between passes. The behavior of the hard and soft tubes is essentially the same up to the point where the relative thickness ratio of the tubes is 0.15 but beyond this point the wall of the hard tubes is reduced at a faster rate than that of the annealed ones.

The effect of the second factor is seen in Fig. 2 where the dimensions of four pairs of tubes are plotted. One tube of each pair was sunk from one inch outside diameter to 0.500 inch in one pass while the other tube of each pair was sunk in several small

passes, without intermediate annealing. The tubes sunk in several small passes have a greater wall thickness in every instance than those sunk directly.

The effect of the G/OD ratio is illustrated in Fig. 3 where the dimensions of several tubes which have been given successive ten per

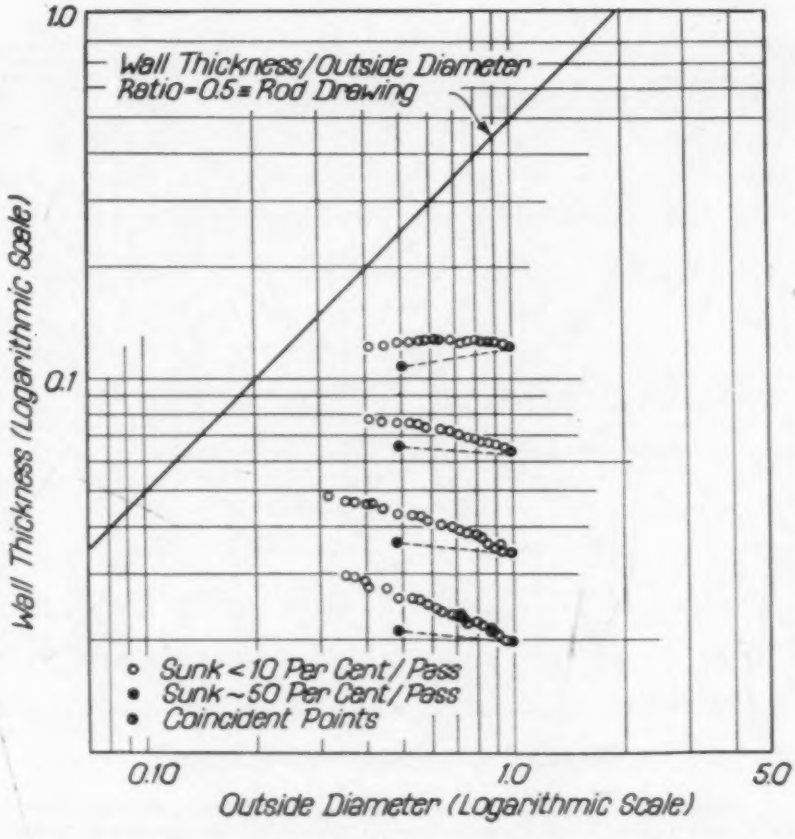

Fig. 2—Effect of Reduction per Pass on Dimensional Changes During Tube Sinking. (Tube Brass).

cent reductions in outside diameter with intermediate anneals are plotted. There are several interesting points about this graph. It will be noticed that all the curves, if transposed along constant wall thickness/outside diameter ratio lines, can be superimposed to form a common curve. In other words, the absolute dimensions of the tube are of no consequence other than fixing the G/OD ratio. Further, it is seen that the data fit one master curve, whether they are for copper or for leaded tube brass.

It is to be mentioned at this point that the accuracy of the experimental data as presented in Fig. 3 is no greater than that reported by previous authors: the coherence of the master curve is a

result of the properties plotted, the quantity $\Delta G/G_o$ employed by Siebel and Weber (see inset to Fig. 4) being overly sensitive. For example, a 1 inch by 0.040 inch tube on being given a 10 per cent reduction in outside diameter may possess a wall thickness of 0.0405 inches to 0.0415 inches. Such variations consistently occurred despite all efforts to maintain sinking conditions as constant as possible.

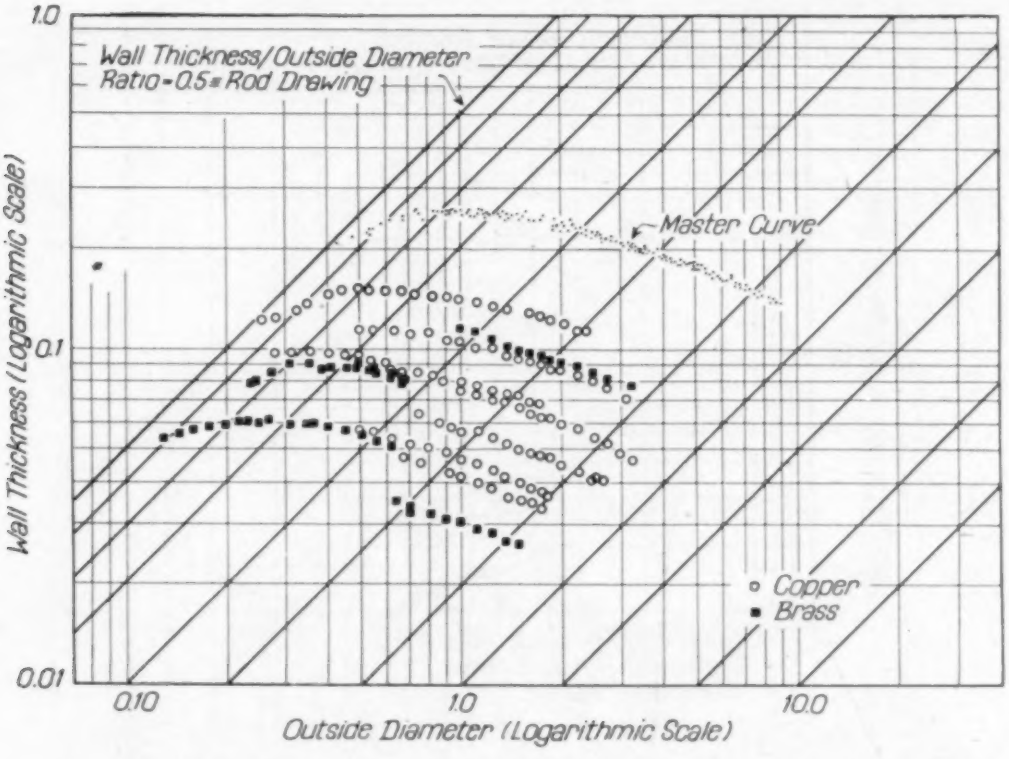

Fig. 3—Effect of Dimensions on Wall-Thickness Changes During Tube Sinking. (Tube Brass and Copper). The experimental points when transposed along constant wall thickness/outside diameter ratio lines form one constant master curve.

These dimensions will give values of 1.25 per cent to 3.33 per cent respectively for the quantity $\Delta G/G_o$—a variation comparable to that shown by the graphical representation made by Siebel and Weber.

Since, as was just seen, the reduction per pass has a definite effect on the wall-thickness change, the master curve given in Fig. 3 is valid only for 10 per cent reductions per pass. Master curves for 25 and 50 per cent reductions per pass are given in Fig. 4.

The application of Siebel and Weber's theory (2) to these curves is of interest. To this end, it is advantageous to transfer their curves from $(\Delta G/G_o)$ — $(\Delta OD/OD_o)$ co-ordinates to those employed in this paper, i.e., log wall thickness — log outside diameter co-ordinates. A simple method is one suggested by the constant de-

rivative method, described by von Kármán and Biot (9) and is illustrated in Fig. 4. For example, Siebel and Weber predict a 4.3 per cent wall-thickness change for a 10 per cent outside diameter change at 50 per cent drawing efficiency for a tube whose G/OD ratio is 0.05 (see inset to Fig. 4). A number of straight lines representing these two simultaneous changes are constructed from the lines G/OD

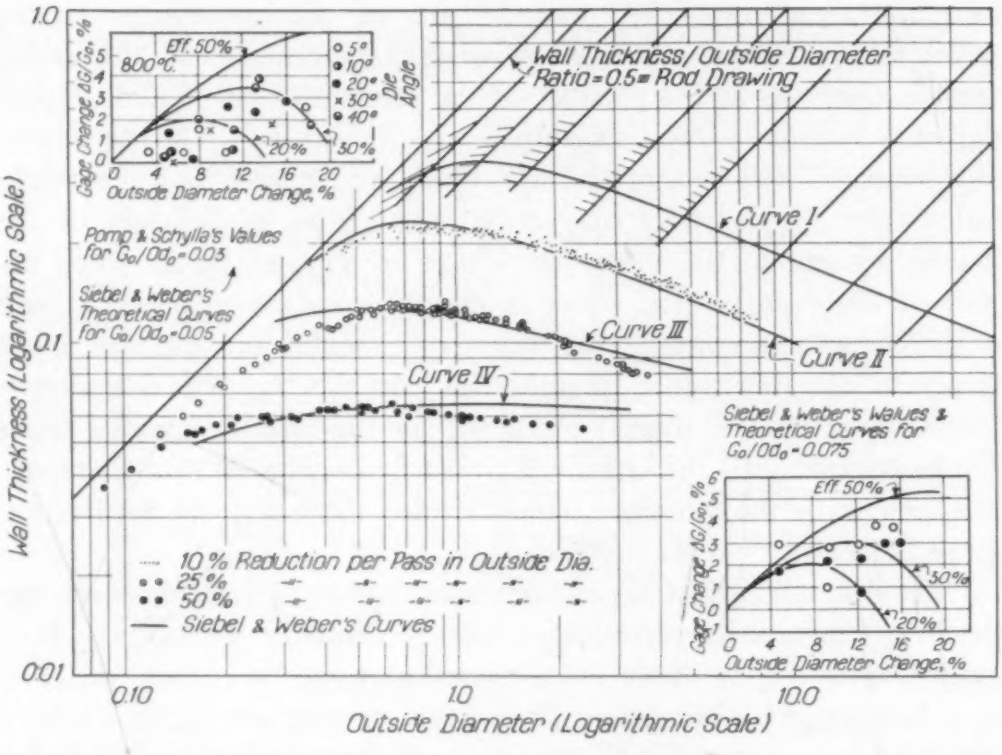

Fig. 4—Experimental Master Curves for Dimensions of a Sunk Tube. The solid lines were obtained by Siebel and Weber's method as described in the text.

=0.05 (Curve 1, Fig. 4.) Similar construction, always for a 10 per cent outside diameter change, are made for other G/OD ratios and a line is drawn through these slopes.

Direct application of Siebel and Weber's method to 25 per cent and 50 per cent reductions per pass leads to an anomaly, however, since for the efficiencies obtained at such reductions, their theory predicts that the tubes would break in tension. Accordingly, the actual stress-strain curves obtained during the sinking experiments were adopted and Siebel and Weber's method was applied from this point on. Curves II, III and IV in Fig. 4 are for 10 per cent, 25 per cent and 50 per cent reductions in outside diameter per pass respectively. In the case of the 10 per cent reduction, the experimental

results are duplicated with good accuracy, but in the case of the two higher reductions considerable discrepancies appear.

One difficulty in the application of Siebel and Weber's method to heavier reductions in outside diameter is that, during such reductions, the relative thinness ratio is affected considerably. For example, a 1 by 0.100-inch tube when sunk to one-half inch outside diameter will assume a 0.100-inch wall thickness—thus the G/OD ratio increases from 0.100 to 0.200 during the operation. In the Siebel and Weber method, however, the magnitude of the radial stress is obtained as the product of the tangential stress and a function of a *constant*—(the starting)—G_o/OD_o ratio. The deviations thus incurred will be greatest for heavy reductions and for thick-walled tube. This effect may contribute to the explanation of the shallow descent of the theoretical curve as opposed to the steep descent of the experimental curve in the thick-walled regions. It will be noticed, furthermore, that the experimental curves rise more steeply in the thin-walled regions than do the theoretical curves—more steeply, indeed, than is predicted for the limiting case of tubes of infinitesimal wall thickness. It must be concluded that there are complexities to the problem which hinder the universal application of the Siebel and Weber method.

The discussion thus far has been confined to operations involving a series of consecutive constant percentage diameter reductions. It is possible, however, to apply the experimental master curves to determine the change in dimensions of a given starting size of tube where single sinking passes of varying degree are contemplated. Thus, the ready-to-finish dimensions of a tube may be assumed to be OD_o and G_o. The 10 per cent master curve is transposed along constant G/OD_o lines until it is superimposed upon the point, (OD_o, G_o). A point is taken from this curve at a distance of 10 per cent to the left of (OD_o, G_o), i.e., at $OD_p = 0.90\ OD_o$. Next, the 25 per cent per pass master curve is similarly superimposed on (OD_o, G_o) and a point is taken from this curve at $OD_q = 0.75\ OD_o$. An identical construction is carried out with the 50 per cent pass master curve. Lastly, these points are connected by a suitable line.

In Fig. 5, data obtained some ten years ago in our laboratories are plotted, showing the actual variations in dimensions for several starting sizes, using single sinking passes of varying amount. The smooth curves with arrows were constructed by the method described in the preceding paragraph applied to these same starting sizes. The

agreement between the actual and computed curves is very good throughout.

To obtain the ready-to-finish dimensions of a tube, given the final tube dimensions, a reverse construction is carried out, points being laid off on the appropriate master curves at $OD_p = OD_o/0.9$,

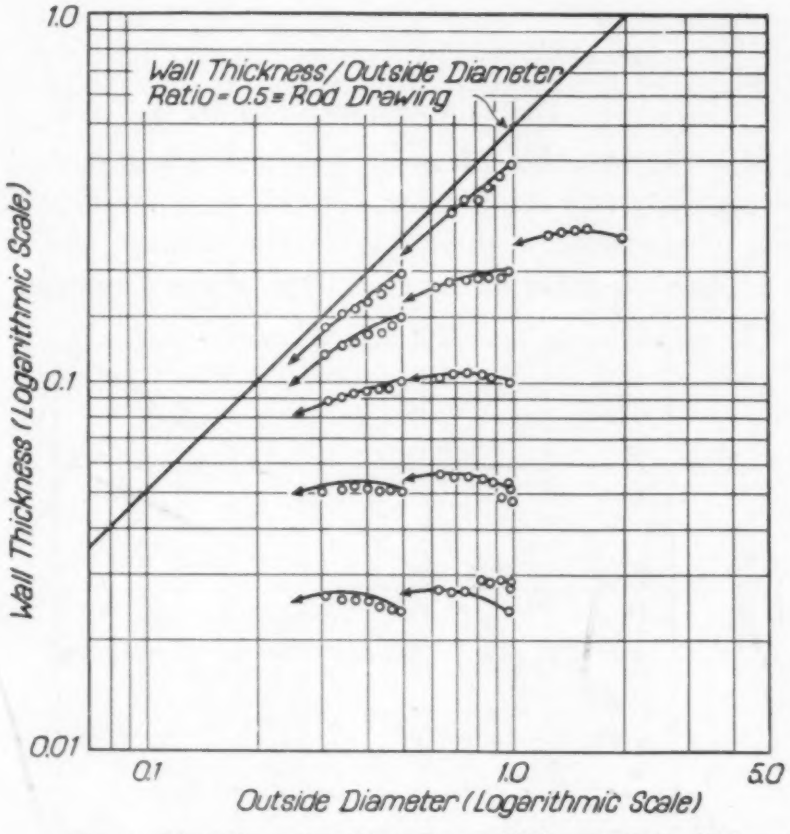

Fig. 5—Dimensions Resulting From Sinking a Tube Different Amounts from a Given Size. Tubes of the dimensions given by the original point in each series were sunk *directly* to the outside diameter given by subsequent points. Solid line curves were constructed by manipulating the master curves given in Fig. 4, in the manner described in the text.

$OD_q = OD_o/0.75$, and $OD_r = OD_o/0.5$, where OD_o is the final outside diameter.

The above methods of representation give coherent data and produce curves that are universally applicable, but they require manipulation. A simpler method of representing the data was developed for more practical use.

It will be noticed that the curves contained in Fig. 5 can be approximated within a segment representing a 40 per cent reduction of outside diameter by a straight line. The slopes of these straight line approximations vary with the G/OD ratio, or the log G/OD

ratio. Such approximations may be written in the form of an equation for a straight line, viz.,

$$\text{Log } G_o - \text{Log } G = m\ (\log OD_o - \log OD), \quad \ldots\ldots\ldots\ldots\ldots\ldots (1)$$
$$m = f\ (\log G_o/OD_o).$$

Equation (1) can be reduced to

$$\text{Log}\frac{G}{OD} = -\ (m-1)\log\frac{OD_o}{OD} + \log\frac{G_o}{OD_o} \quad \ldots\ldots\ldots\ldots\ldots\ldots (2)$$
$$(m-1) = f'\ (\log G_o/OD_o),$$

which is also the equation of a straight line when plotted on log G/OD — log OD_o/OD coordinates. In this case, log G_o/OD_o is the intersection of the line and the log G/OD coordinate, and the slope, —(m — 1), is a function of log G_o/OD_o. From a number of con-

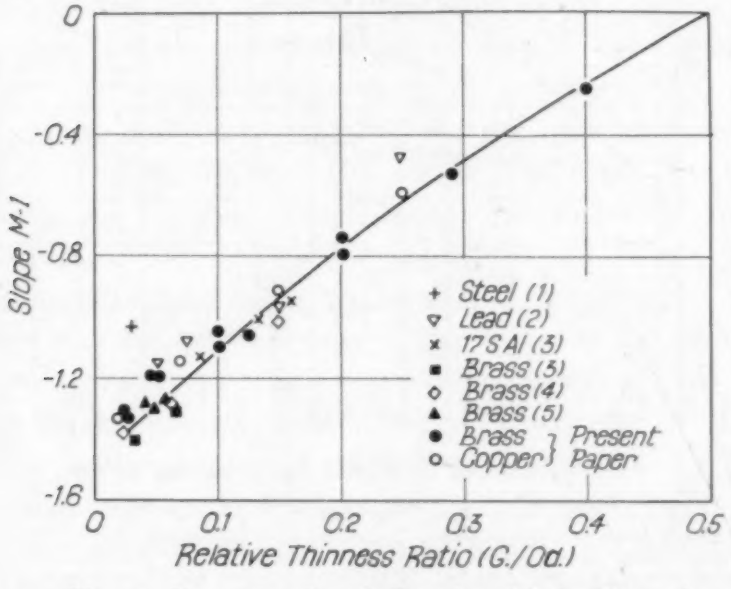

Fig. 6—Slope, (m—l), of Equation (2) in Text as a Function of the Starting Relative Thinness Ratio (G_o/OD_o). The solid line has been drawn from constructions made by manipulation of the experimental master curves given in Fig. 4. The individual symbols have been taken from the experimental curves given in Fig. 7.

structions such as were carried out in Fig. 5, the values of m as a function of log G_o/OD_o were determined, and these were converted to values of (m — 1) as a function of log G_o/OD_o. The latter were plotted graphically as a solid line in Fig. 6. In Fig. 7, a number of straight lines have been constructed for different G_o/OD_o ratios with appropriate (m — 1) values. Also plotted in Fig. 7 are the experimental data for hot sunk steel (1), lead (2), 17S aluminum (3) and brass (3), (4), (5), tube as reported in the literature as well

as data for copper and brass developed in the present investigation. The data not only form straight lines, but these straight lines possess slopes consistent with those predicted.

Attention is drawn to the data for lead where it is seen that the points for such tubes sunk without lubrication whether through polished or rough dies give coincident lines.

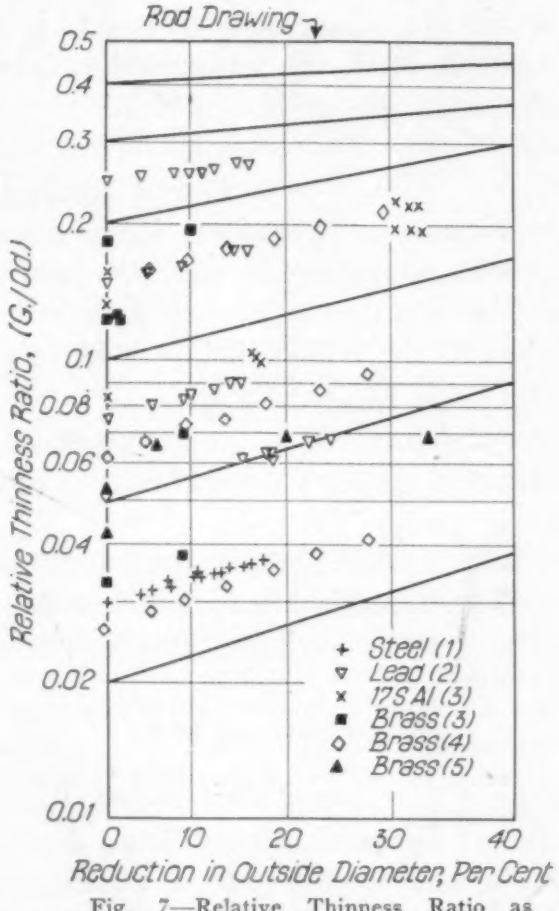

Fig. 7—Relative Thinness Ratio as a Function of Reduction in Outside Diameter for Sunk Tube. The solid lines have been drawn in from the curve shown in Fig. 6. Experimental data from the literature for hot sunk steel (1), lead (2), 17-S aluminum (3), brass (3), (4), (5), are given by the individual symbols. Data for hot sunk steel is for 700, 800, 900 degrees Cent. with a 10-degree die angle. Data for lead is for both rough and polished dies.

The exact slopes of the experimental straight lines have been determined and have been entered as individual points in Fig. 6. It is seen that brass, copper and aluminum fall closest to, lead deviates slightly from, and hot sunk steel falls farthest from the solid line originally constructed.

Summary and Conclusions

1. The wall-thickness changes occurring during tube sinking were investigated for copper and a number of copper alloys.

2. The wall-thickness changes on sinking were found to depend upon (a) the temper of the metal, (b) the magnitude of the reduction per pass, and (c) the relative thickness of the tube.

3. The wall-thickness change was shown to be substantially independent of the metal itself, the absolute dimensions of the tube, the die contour, the die finish and the lubrication.

4. Siebel and Weber's theoretical treatment was applied to the experimental results. While this treatment predicts in general the type of curve experimentally determined, it has limited applicability for reasonably accurate prediction of wall thickness changes.

5. A straight line function was found to exist between the relative thickness ratio and the reduction in outside diameter for sunk tubes for reductions up to 30-40 per cent.

6. Experimental data given in the literature for lead, hot sunk steel, 17S aluminum, and brass were found to conform to this straight line relationship.

7. From the latter relationship, it was found that copper, brass and aluminum are almost identical in dimensional behavior, while hot sunk steel gives the greatest variance, and lead is of intermediate value.

Acknowledgment

The authors wish to express their appreciation to Dr. D. K. Crampton, Director of Research, Chase Brass & Copper Company, Inc., for his active interest in the present work and for the use of the data presented in Fig. 5.

Bibliography

1. Pomp and Schylla, *Mitt. a.d. KWI. f. Eisenf. z. Düss.,* Vol. 16, 1934, p. 31.
2. Siebel and Weber, *Mitt. a.d. KWI. f. Eisenf. z. Düss.,* Vol. 16, 1934, p. 217.
3. Jung-König, Linicus, and Sachs, *Metallwirtschaft,* Vol. 11, 1932, p. 395.
4. Crampton, D. K. *Transactions,* American Institute of Mining and Metallurgical Engineers, Institute of Metals Division, 1930, p. 233.
5. Sachs and Espey, *Transactions,* American Institute of Mining and Metallurgical Engineers, Vol. 147, 1942, p. 74.
6. Roš and Eichinger, *Mitt. eidg. Mat. Prüf. Amt.,* Tech. Hoch., Zürich, 1926.
7. Lode, *Z. angew., Math. u. Mech.,* Vol. 5, 1926, p. 142.
8. Remmers, *Transactions,* American Institute of Mining and Metallurgical Engineers, Institute of Metals Division, 1930, p. 107.
9. Von Kármán and Biot, "Mathematical Methods in Engineering," 1940, McGraw-Hill.

DISCUSSION

GEORGE SACHS:[1] I would like to congratulate the authors for this interesting paper. I think it is quite a step forward that methods are being developed and experimentations are being carried on which will replace the purely empirical practices which are predominant at the present time.

The authors have demonstrated that for a given reduction in outside diameter a thin-walled tube will suffer an increase in wall thickness while a thick-walled tube will suffer a decrease in wall thickness. They have similarly demonstrated that the reduction of outside diameter effected in a single pass is a decisive factor.

I should like to inquire into the effect obtained when other factors are varied, namely, die contours, die materials and other factors which affect the frictional conditions of sinking. According to theory, I would assume that a die with low friction should yield thicker walls than a die with high friction. I do not know exactly how the die contour would affect final wall thickness but it would be normal to expect that dies with acute angles would produce more friction than dies with a wide or open angle. One would expect slightly different conditions to exist, furthermore, between a carbide die and a steel die. These factors are of interest to people who are sinking tube to very close tolerances.

Could the authors tell me whether there is any experimental material which would give some indication of the extent to which these variables affect wall thickness?

Authors' Reply

We wish to thank Dr. Sachs for his remarks. We believe that his questions can be best answered by referring to Fig. 7 in the paper where Pomp and Schylla's experimental data for lead tube sinking are plotted. The points shown in Fig. 7 have been taken indiscriminantly from Pomp and Schylla's graphs for tubes sunk through a polished die and tubes sunk through a rough die. It is seen from Fig. 7, that all points adhere to the same straight line. Similarly, the data for hot sunk steel given in Fig. 7 were taken from Siebel and Weber's graphs for steel sunk through a 10-degree die at 700, 800 and 900 degrees Cent. (1290, 1470 and 1650 degrees Fahr.). These points likewise adhere to one straight line. As mentioned in the paper, our experiments included tube sinking carried out with conical dies with 7, 15 and 35-degree half-angles, trumpet-shaped dies as well as tungsten carbide and chrome plated steel dies. We also sunk tubes with and without lubricant. The wall thickness obtained under these widely varying conditions were always duplicated within given limits of accuracy. For example, a 1-inch by 0.040-inch tube when sunk to 0.900-inch outside diameter under a given set of conditions would yield a wall thickness of 0.0405 to 0.0415 inches. The same tube sunk to the same outside diameter under a different set of conditions would yield a wall thickness lying between these same two limits.

We agree with Dr. Sachs that on the basis of theoretical considerations one would expect differences in the resulting wall thickness when such factors as die contour, lubrication, etc., are varied, and we must admit that we were quite surprised to find these variables had such little effect. In this respect, it should

[1]Professor of physical metallurgy, Case School of Applied Science, Cleveland.

be pointed out that Siebel and Weber's theoretical treatment predicts that such factors would effect wall thickness changes.

There are a few abnormal conditions which have prevented effect upon dimensional changes in tube sinking which were discovered by chance by the authors after the present report had been completed. Two examples will be cited. A copper tube when sunk in successive 10 per cent reduction in outside diameter gave wall thickness values considerably below those shown by the master curve given in Fig. 3. Subsequent examination showed the copper to have been severely attacked by hydrogen embrittlement. A second copper tube when sunk under similar conditions gave irregular results with regard to wall thickness changes. Subsequent investigation showed this tube to be composed of abnormally large grains of such dimensions as to fill the entire wall thickness.

A METALLOGRAPHIC STUDY OF THE DECOMPOSITION OF AUSTENITE IN MANGANESE STEELS*

By John V. Russell and Francis T. McGuire

Abstract

The beginning of the martensite transformation, Ar", has been determined for steels between 1 and 11 per cent manganese in three carbon sections: 0.50, 0.80 and 1.0 per cent. End quenched hardenability data are presented as well as the "S-curves" of three steels in the 0.5 per cent carbon section. The effect of manganese on the "S-curve" has been shown to move both the beginning and ending curves to the right, but the influence is greater on the ending. No rapid intermediate transformation has been detected. The carbides formed by isothermal transformation have the crystal structure of Fe_3C.

MANGANESE as an alloy addition to steel was systematically studied as early as 1888 by Hadfield (1)†. At that time low carbon ferromanganese was not available and as a consequence the higher manganese steels also contained high percentages of carbon. A direct outcome of this research was Hadfield's austenitic manganese steel.

In recent years the influence of alloy additions to steel has come to the fore. The work of Davenport and Bain (2) demonstrated that the decomposition curves of austenite in a eutectoid steel at sub-critical temperatures follow the general shape of an "S" with the "knee" of the "S" around 500 to 550 degrees Cent. (930 to 1022 degrees Fahr.). The further the beginning curve is moved to the right on the time axis by alloy addition or other factors, the longer is the time for beginning of isothermal transformation or, as shown by Grange and Kiefer (3), the slower can be continuous cooling without formation of primary troostite.

†The figures appearing in parentheses pertain to the references appended to this paper.

*Much of the material in this paper is from a thesis submitted by Mr. Russell in partial fulfillment of the requirements for the degree of Master of Science, University of Kentucky, June, 1943.

A paper presented before the Twenty-fifth Annual Convention of the Society, held in Chicago, October 18 to 22, 1943. Of the authors, John V. Russell is metallurgist, South Chicago Plant, Republic Steel Corp., South Chicago, Ill., and Francis T. McGuire is associate professor of physical metallurgy, University of Kentucky, Lexington, Ky. Manuscript received June 21, 1943.

Davenport (4) in the Howe Lecture emphasized that alloy additions may not only displace the curves, but also open bays and distort their shape. Alloys which retard reaction at Ar′ may not do so at lower temperatures and combinations of alloy additions do not have a simple additive effect on the decomposition characteristics of austenite at sub-critical temperatures.

One of the prime functions of alloy additions to constructional steels is to decrease the critical cooling velocity which is that velocity just sufficient to suppress the formation of primary troostite on continuous cooling. If the austenite phase does not form troostite on quenching and no fast intermediate reactions are encountered the martensite formation will begin at a temperature known as Ar″. Greninger (5) proved that with cooling velocities as high as 4000 degrees Cent./sec. the temperature at which this transformation begins is independent of the rate of cooling. Greninger and Troiano (6) among others have shown that Ar″ is a function of carbon content. They likewise noted that martensite forms very rapidly but only while the temperature is lowered. It is not a time, but a temperature dependent reaction and for this reason does not properly belong on the "S-curve" unless some schematic representation of the conditions such as suggested by Cohen (7) is employed.

In most hardening heat treatments it is desirable to obtain a fully martensitic structure prior to tempering. The advantages have been summarized by Bain (8). To obtain a fully martensitic structure a steel must be quenched at such a rate that the slowest cooling section avoids transformation to some primary troostite or intermediate product. The temperature at which Ar″ occurs is important since if this is near room temperature a mixture of retained austenite and martensite will result. Lowering the specimen temperature by refrigeration or other means is the only practical way to cause the austenite → martensite transformation to proceed. This transformation can also be accomplished by plastic deformation. This has application only in entirely austenitic steels such as the 18-8 variety of stainless steel or the Hadfield type. In some steels as reported by Gulyaev (9), Gordon and Cohen (10) and Troiano (11) aging at room temperature has a stabilizing effect on austenite and lowers Ar″ in steels which begin to form martensite below room temperature. It is important therefore in practical heat treatment to recognize this effect if refrigeration is to be employed to further the transformation.

Little data are available on the influence of manganese on the

"S-curves". Wever and Mathieu (12) have reported an intermediate region of rapid transformation velocity in a low carbon and a low manganese series. These investigators used magnetometric determinations and were mainly concerned with the maximum transformation velocity. This is the slope of the tangent to the reaction rate curve at its steepest portion. The beginning and ending "S-curves" may not necessarily give an indication that this intermediate transformation occurs. In the region of fast maximum velocity some of the

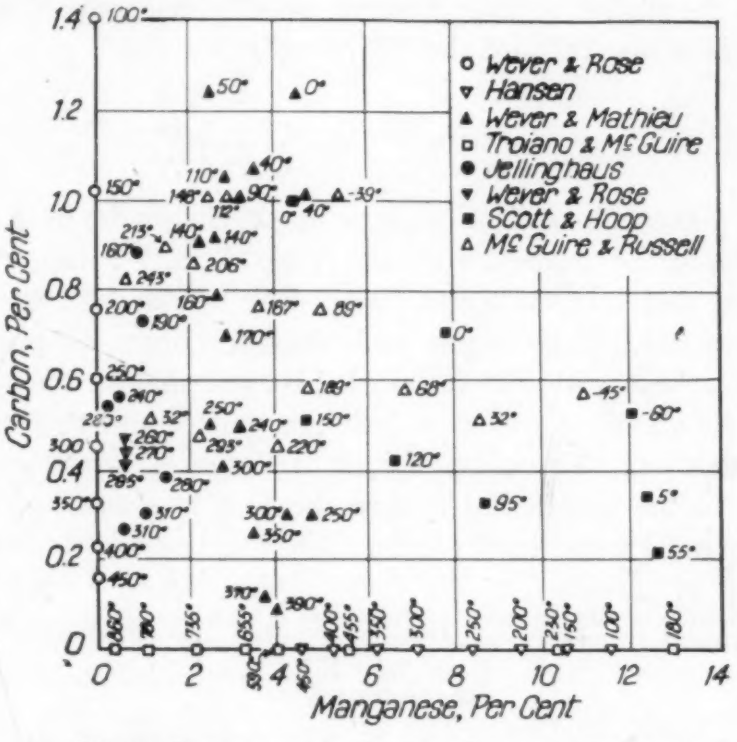

Fig. 1—Temperature in Degrees Cent. of Previous Ar" Determinations.

"S-curves" of equal increments of transformation will converge. Magnetometric methods for determining reaction rate curves are open to important criticism. The shape and distribution of the product formed as well as its amount affects the observed magnetic quantity, thus while the beginning and ending points obtained with sensitive equipment might agree with data from other methods the general shape of the reaction rate curve would not.

European metallurgists prefer to report some average or maximum of the transformation velocity of the austenite → ferrite + carbide reaction at various sub-critical temperatures. One cannot derive

an "S-curve" from this information since neither average nor maximum velocity supplies the necessary data.

The Ar″ temperatures of some manganese steels have been reported by Wever and Mathieu (12), Scott and Hoop (13), and Jellinghaus (14). Fig. 1 is a compilation of reported Ar″ values prepared by Wever and Mathieu (12) with supplementary data from the work of Troiano and McGuire (15) on the iron-manganese system together with present determinations. Microscopic data over a wide range of compositions in definite carbon sections are not available, and the object of this research was to determine the influence of manganese on Ar″ and the "S-curve".

Experimental Methods

The present investigation was on steels made in a size "U" Moore Rapid Lectromelt furnace from Armco scrap, electrolytic manganese, and ferromanganese according to standard basic electric furnace practice. Four ingots each weighing about 60 pounds were cast from a heat with the carbon held constant and the manganese increased by additions of electrolytic manganese and ferromanganese prior to each tap. The compositions of the steels made are listed in Table I. In the numbering system the first two numbers show the amount of manganese in per cent while the last two indicate tenths of per cent of carbon.

Table I
Chemical Analyses

Steel	C	Mn	P	S	Cr	Ni	Cu	Al**	Si
0105	0.51	1.56	0.04	0.04	0.03	0.04	0.06	0.018	0.04
0205	0.47	2.10	0.04	0.04	0.06	0.04	....	0.016	0.01
0405	0.53	4.05	0.03	0.03	0.04	0.04	....	0.012	0.05
0506	0.58	4.83	0.04	0.03	....	....	....	.....	0.01
0706	0.58	6.89	....	....	....	....	....	.....	....
0905	0.51	8.60	0.04	0.02	....	....	....	.....	0.01
1105	0.57	10.98	0.04	0.02	....	....	....	.....	0.02
0108	0.75	0.72	0.01	0.03	*	0.03	0.06	0.011	0.02
0208	0.77	2.12	0.02	0.03	*	0.03	0.08	0.011	0.01
0408	0.74	3.52	0.02	0.02	*	0.03	0.04	0.020	0.02
0508	0.75	5.00	....	....	....	....	....	.....	....
0608	0.84	6.54	....	....	....	....	....	.....	....
1008	0.82	10.20	0.05	0.20	....	....	....	.....	0.13
0109	0.87	1.40	0.01	0.05	....	....	....	.....	0.12
0210	1.05	2.44	0.06	0.17	....	....	0.07	.....	0.05
0310	1.05	2.82	0.02	0.04	....	....	....	.....	0.16
0510	1.07	5.51	0.06	0.13	....	....	0.06	.....	0.05
0610	1.07	6.25	0.06	0.07	....	....	0.07	.....	0.19
1010	1.05	10.60	0.04	0.02	....	....	....	.....	0.16

*Trace.
**Total aluminum.

The ingots, 12 inches high by 4 inches square, were cast big end up with a hot top. All were forged at 2000 degrees Fahr. (1095 degrees Cent.) with a 1500-pound steam hammer to 1¾-inch square bars which were subsequently softened by austempering according to the schedules given in Table II. No difficulty was encountered in forging these steels.

Table II
Softening Treatments

Steel	Tempering Temp., ° F.	Time Hours	Hardness Re
0105	1100	72	10
0205	1100	48	13
0405	1100	72	16
0506	1100	112	22
0706	1100	72	39
0905	1100	212	32
1105	1100	212	35
0108	1200	8	13
0208	1200	8	20
0408	1100	20	21
0508	1100	20	21
1008	1100	48	38
0109	1100	72	20
0210	1000	48	26
0310	1100	72	20
0510	1000	48	32
0610	1000	48	38
1010	1100	120	40

Center sections of the bars were used for the study and were machined to 0.4-inch square rods for Ar″ determination. These were homogenized and the treatments are listed in Table III.

Table III
Homogenization Treatment Prior to Ar″ Determination

Steel	Temperature ° F.	Time Hours
0105	2000	4
0205	2100	5
0405	2000	8
0506	2200	9
0706	2200	8
0905	2200	15
1105	2200	12
0108	1650	4
0208	1650	4
0408	2000	5
0504	2000	5
1008	2200	15
0109	2000	5
0210	2000	5
0310	2000	6
0510	2000	6
0610	2200	6
1010	2200	16

Determination of Ar″

The metallographic technique developed by Greninger and Troiano (6) was used for determining Ar″. This method, though tedious, was selected because of the ease of unambiguous interpretation and the relatively simple apparatus required.

Furnaces were placed close together and controlled to ± 2 degrees Fahr. Martensite formed between Ar″ and any particular bath temperature was tempered for 10 seconds in a second furnace at 600 degrees Fahr. (315 degrees Cent.). Low temperatures were obtained with dry ice and acetone mixtures or liquid nitrogen. Microscopic examination for tempered martensite was made after removal of 0.030 inch from the surface of $\frac{3}{16}$ x $\frac{3}{16}$ x $\frac{5}{16}$ inch specimens.

Determination of Hardenability

Separate sections of the bars of 0105, 0205, 0405, 0108, 0208 and 0408 were homogenized at 2250 degrees Fahr. (1230 degrees Cent.) for 3 hours and air-cooled. Softening treatments were followed as stated in Table II. Bars one inch in diameter were turned for standard end-quench hardenability determination. Quenching was from 1550 degrees Fahr. (845 degrees Cent.) for all these steels and Rockwell "C" hardness was measured at sixteenth-inch intervals with a special indexing jig.

Determination of "S-curves"

Specimens $\frac{3}{16}$ x $\frac{3}{16}$ x $\frac{5}{16}$ inch with the longitudinal surface prepared for polishing were machined from hardenability bars and the spare 1-inch diameter stock. All specimens were austenitized at 1650 degrees Fahr. (900 degrees Cent.) for one-half hour in a dry nitrogen atmosphere and were quenched into lead baths at temperatures from 660 to 1200 degrees Fahr. (350 to 650 degrees Cent.) and Wood's metal at 500 degrees Fahr. (260 degrees Cent.). The molten metal baths were controlled to ± 5 degrees Fahr. and surface oxidation was minimized by a bath covering of charcoal. The time at various temperatures was recorded from immersion and the actual time at temperature was from 1 to 2 seconds less than plotted. The beginning curves represent about 1 per cent and the ending curves 99 per

cent decomposition. The A_1 and A_3 transformation temperatures were determined microscopically after treating specimens for 3 hours at various temperatures.

X-Ray Diffraction

Small slivers $\frac{1}{32}$ inch in diameter and $\frac{5}{8}$ inch long were used for carbide study. They were etched in a 2 per cent aqueous solution of HCl to dissolve ferrite preferentially. This technique developed by Troiano (16) increases carbide concentration on the surface. This process must be closely controlled in order to avoid anodic

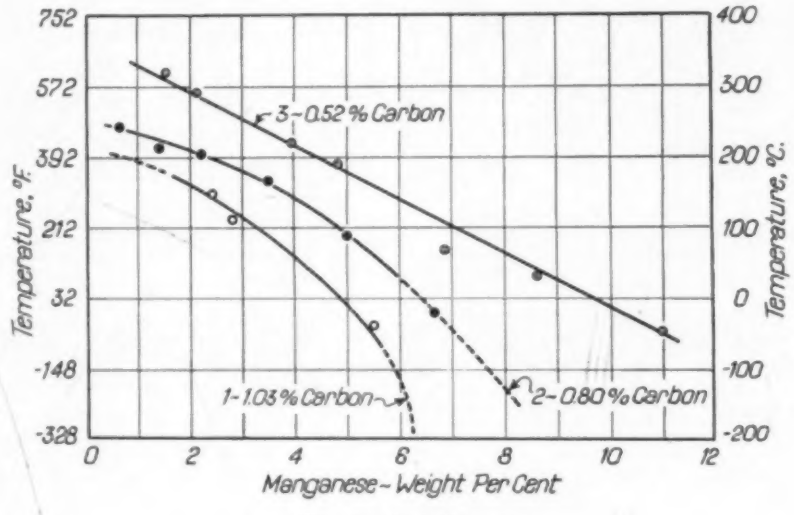

Fig. 2—Ar″ Curves.

oxidation of the specimen. Diffraction patterns were made with filtered chromium radiation from a Baird gas type X-ray tube. Debye cameras of 11.4 cm diameter were used.

Results

Ar″

The potent effect of manganese in lowering Ar″ is clearly shown by Fig. 2. The dip downward in the 0.80 and 1.00 per cent carbon sections is real and not the result of aging. Extrapolation of the curves to zero manganese gives values for iron-carbon alloys in good agreement with the data of Greninger. The results are summarized in Table IV.

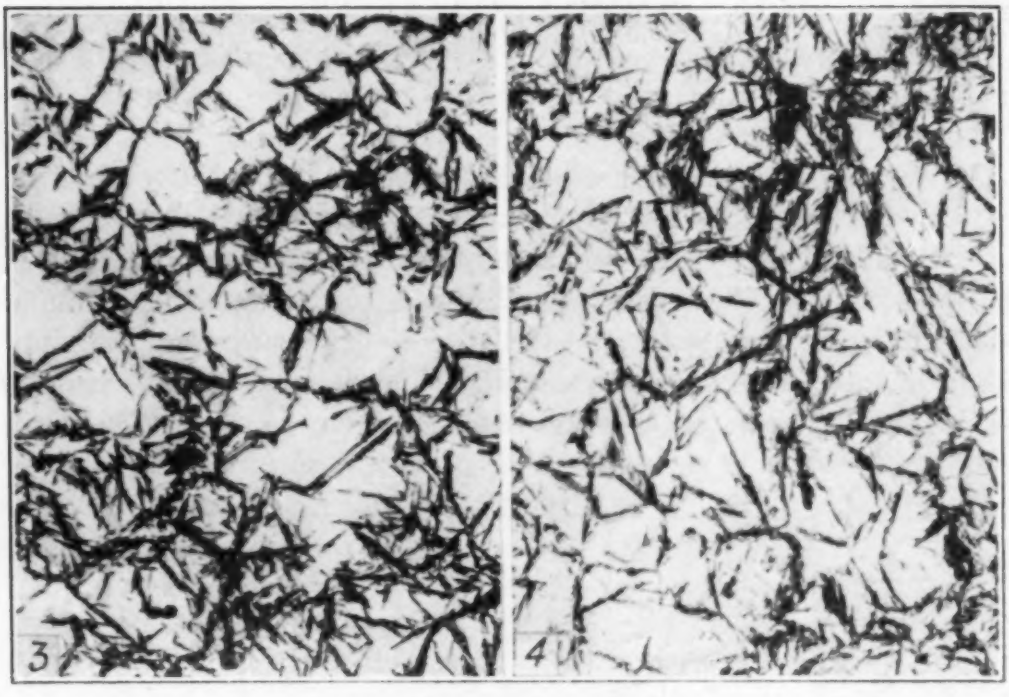

Fig. 3—Photomicrograph of Steel 0510. 1150 Degrees Cent. for 1 Hour → Water Quenched. 120 Days at Room Temperature Then Cooled to —80 Degrees Cent. Tempered at 300 Degrees Cent. for 5 Minutes and Water-Quenched. Nital Etched. × 100.

Fig. 4—Photomicrograph of Steel 0510. 1150 Degrees Cent. for 1 Hour → Water Quenched and Quickly Transferred to a Bath at —80 Degrees Cent. Tempered at 300 Degrees Cent. for 5 Minutes and Water-Quenched. Nital Etched. × 100.

Table IV
Ar″ for Manganese Steel

Steel	Austenitizing Temp., ° F.	Quenching Media	Ar″ ° F.
0105	1650	Tin	608
0205	1650	Tin	560
0405	1650	WM*	428
0506	1650	WM	372
0706	1650	H_2O + NaOH	154
0905	1650	H_2O + NaOH	90
1105	1830	Acetone	—49
0108	1650	WM	469
0208	1650	WM	403
0408	1650	WM	333
0508	1650	WM	192
0608	1830	H_2O + $CaCl_2$	—4
1008	1830	LN**	< —320
0109	1650	WM	415
0210	1650	WM	298
0310	1650	WM	234
0510	1830	Acetone	—38
0610	1830	LN	< —320
1010	1830	LN	< —320

*Wood's metal.
**Liquid nitrogen.

Austenite Stabilization Study

The influence of time at room temperature on Ar″ was studied in steel 0510 which begins to form martensite at —38 degrees Fahr. (—36 degrees Cent.). The temperature of Ar″ was found to be the same in a steel quenched into a solution of 10 per cent NaOH in water and rapidly transferred to a refrigerated acetone bath as one aged 120 days at room temperature prior to refrigeration. The

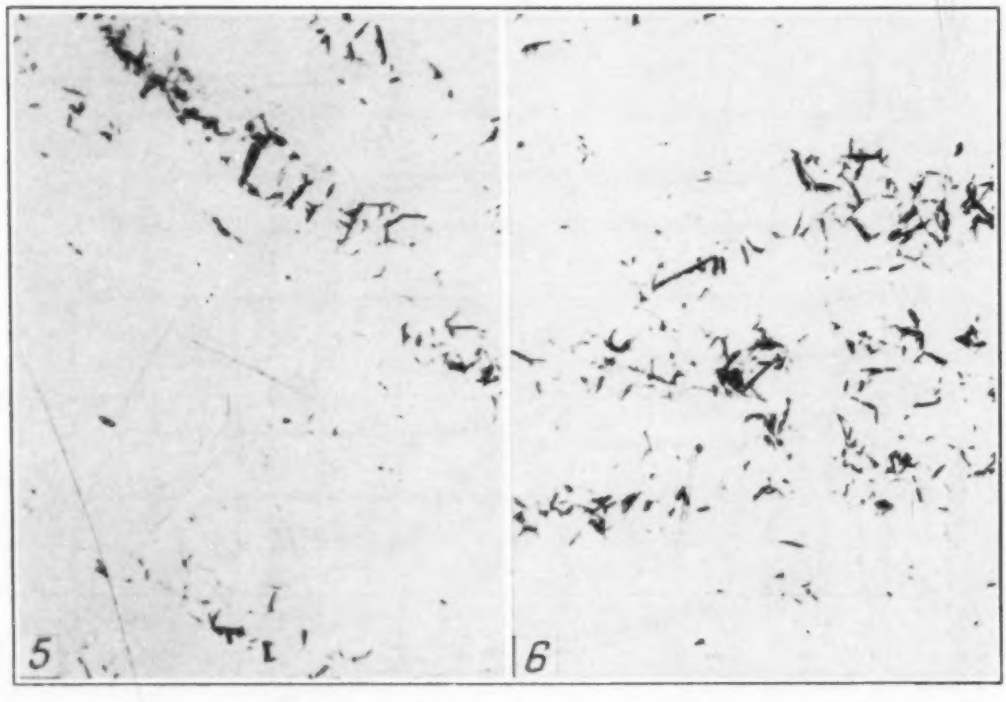

Fig. 5—Photomicrograph of Steel 0405. 900 Degrees Cent. for 30 Minutes → 400 Degrees Cent. for 5 Minutes → 210 Degrees Cent. for 5 Minutes → 400 Degrees Cent. for 1 Minute → Water-Quenched. Nital Etched. × 75.

Fig. 6—Photomicrograph of Steel 0405. 900 Degrees Cent. for 30 Minutes → 210 Degrees Cent. for 5 Minutes → 400 Degrees Cent. for 1 Minute → Water-Quenched. Nital Etched. × 75.

amount of martensite between Ar″ and —110 degrees Fahr. (—79 degrees Cent.) was about the same in both as illustrated in Figs. 3 and 4.

Aging at 750 degrees Fahr. (400 degrees Cent.) for 5 minutes did not influence Ar″ in steel 0405. Photomicrographs of the aged and directly quenched specimens are shown in Figs. 5 and 6. These indicate that the amount of martensite formed is likewise unaffected by aging.

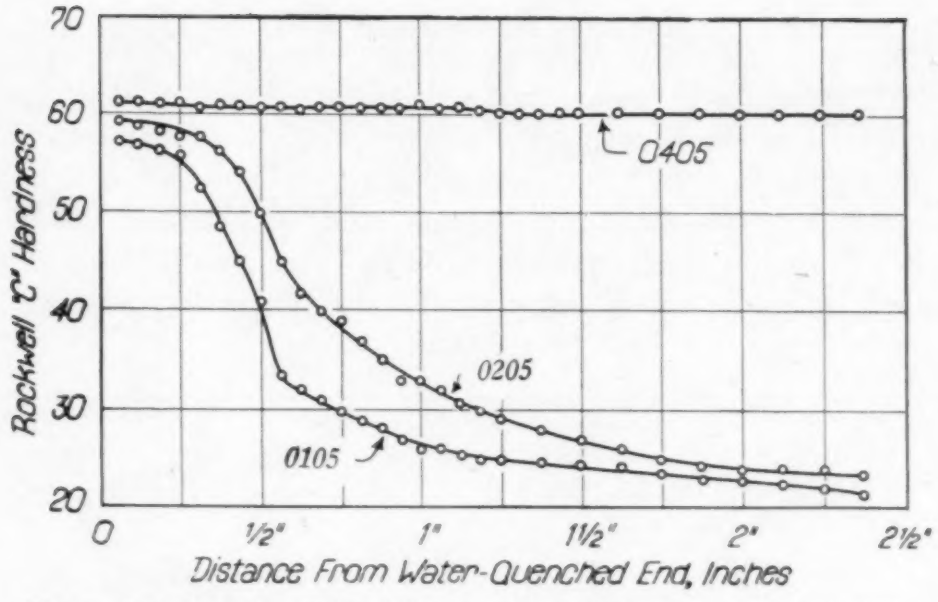

Fig. 7—End-Quenched Hardenability Curves of Steels 0105, 0205, and 0405.

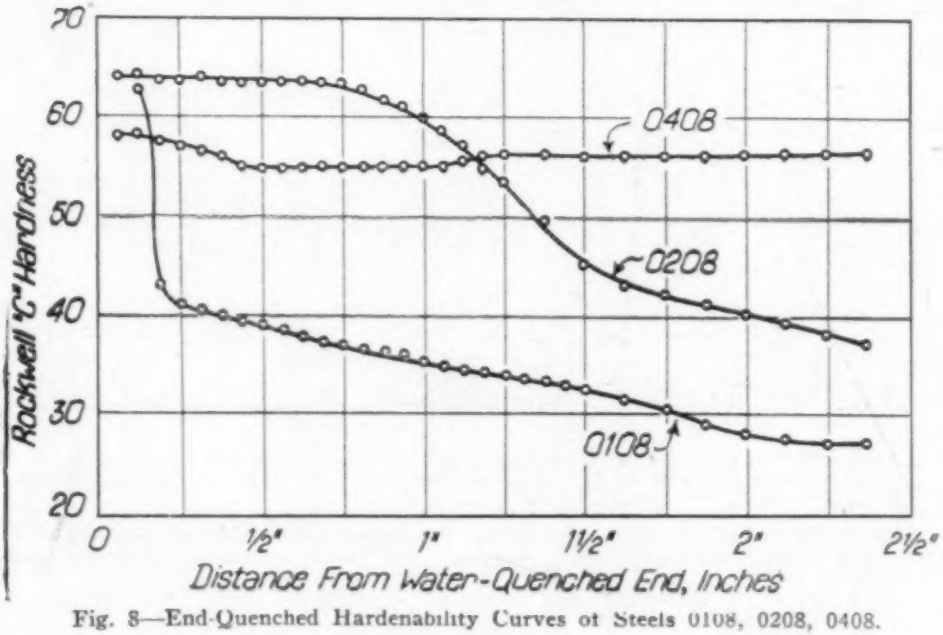

Fig. 8—End-Quenched Hardenability Curves of Steels 0108, 0208, 0408.

Hardenability

The end quench hardenability curves of 0105, 0205, 0405, 0108, 0208 and 0408 are illustrated in Figs. 7 and 8. Calculated ideal critical diameters from the chemical analyses using Grossmann's factors (17) agree within limits of the method with observed values. The summary of these calculations is shown in Table V.

Table V
Observed and Calculated Ideal Critical Diameters

Steel	Grain Size	D_1 (calc.)	D_1 (obs.)
0105	2	2.7	2.6
0205	2	3.6	3.4
0108	4	1.3	1.5
0208	2	3.8	5.0

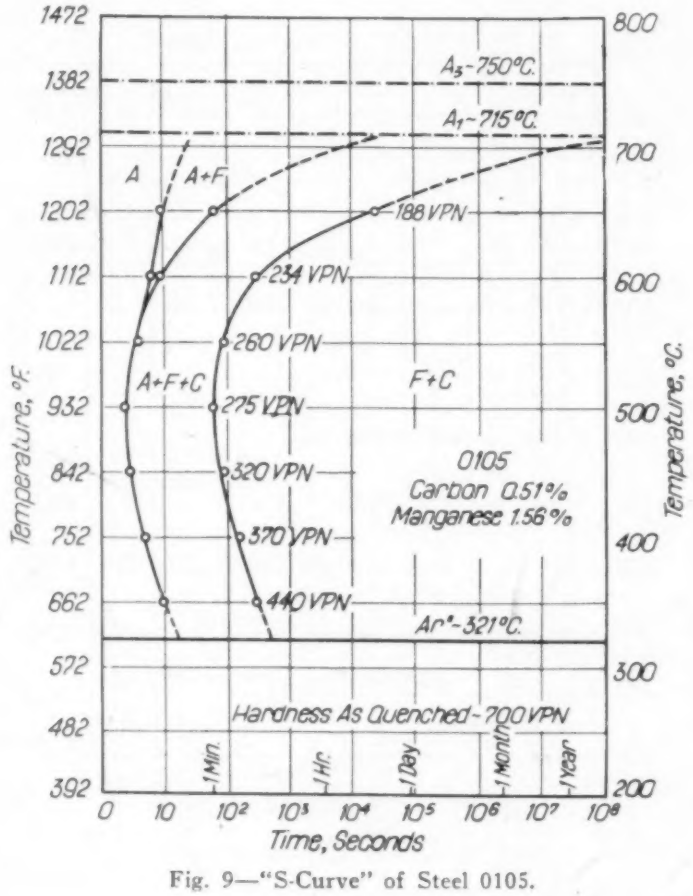

Fig. 9—"S-Curve" of Steel 0105.

"S-Curves"

The effect of manganese on the "S-curve" is to move both the beginning and ending curves to the right as shown in Figs. 9, 10 and 11. The effect is much greater on the ending curve than on the beginning. With 4 per cent manganese the curves become severely distorted from the general "S" shape. In 0405 isothermal decomposition begins at about the same time at 707 degrees Fahr. (375 degrees Cent.) as at 1020 degrees Fahr. (550 degrees Cent.) but the time for completion at the lower temperature is much longer than at

1020 degrees Fahr. The products formed at various isothermal temperatures in steels 0105 and 0205 follow the general structures noticed in plain carbon steels. The microstructures resulting from isothermal transformation of 0405 differ in many respects. In Figs. 12 to 16 are shown some of the products.

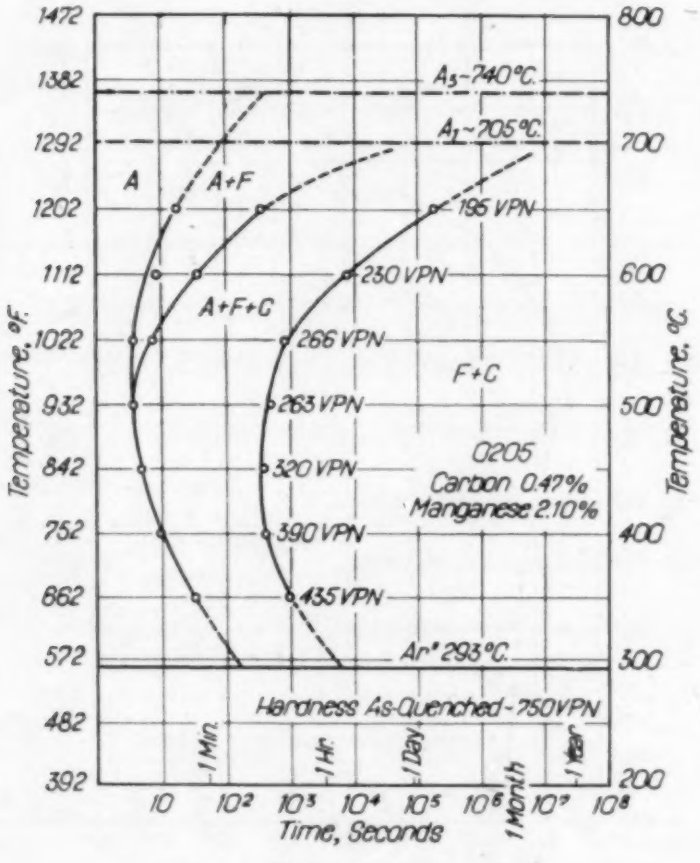

Fig. 10—"S-Curve" of Steel 0205.

Carbides

Carbides analogous to those in chromium steels have been reported in the manganese-carbon system by Westgren (18, 19). He stated that manganese carbides decompose rapidly on exposure to water and atmosphere. The technique employed in the present study might not be satisfactory for preserving any manganese carbide for a time long enough to obtain a diffraction pattern. As shown in Table VI only carbides of the Fe_3C type have been noted and it is emphasized that the manganese content could not be determined. The position of lines near back reflection was about the same in all

patterns but their quality did not allow for precise parameter determination.

Table VI
Carbide Study

Steel	Treatment	Carbide Type
0408	1650° F.—½ Hr. → 575° F.— 60 Hrs.	Fe_3C
0408	1650° F.—½ Hr. → 750° F.— 40 Hrs.	Fe_3C
0408	1650° F.—½ Hr. → 930° F.— 44 Hrs.	Fe_3C
0610	1650° F.—½ Hr. → 1000° F.— 48 Hrs.	Fe_3C
1010	1850° F.—½ Hr. → 1100° F.—120 Hrs.	Fe_3C

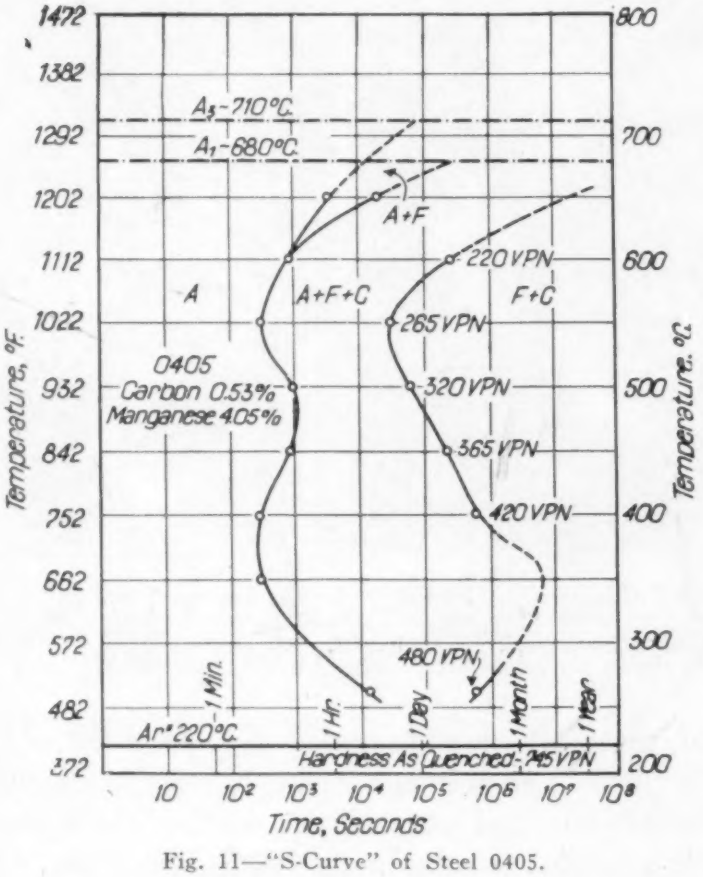

Fig. 11—"S-Curve" of Steel 0405.

Discussion

"S-Curves"

In the Howe Lecture of 1932 Bain (20) discussed the influence of manganese on isothermal reaction at two different temperatures. The products formed at temperatures above Ar′ were similar in all the manganese series. This observation has been confirmed. Below

the Ar′ range the microstructure of the products formed is affected by manganese. Often as many as three different microconstituents are evident in one specimen. This is clearly shown in Fig. 14 of a 4 per cent manganese steel reacted at 750 degrees Fahr. (400 degrees Cent.) for 40 minutes. The nodular product is absent in the micro-

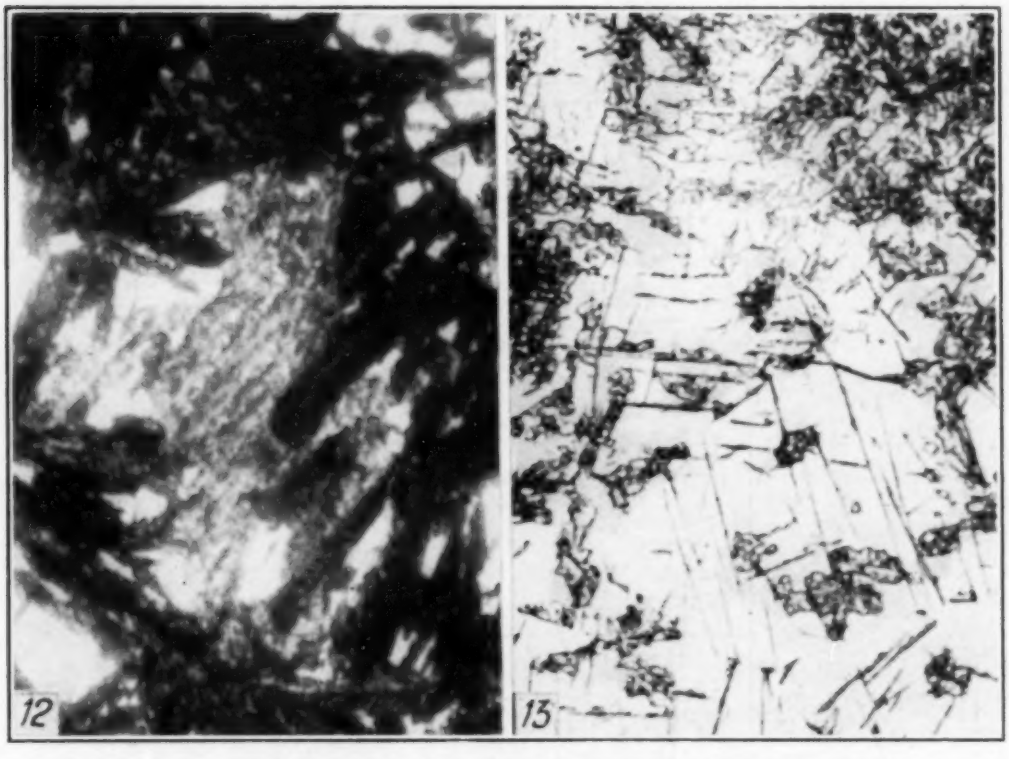

Fig. 12—Photomicrograph of Steel 0405. 900 Degrees Cent. for ½ Hour → 260 Degrees Cent. for 11 Hours and Water-Quenched. Nital Etched. × 1000.

Fig. 13—Photomicrograph of Steel 0405. 900 Degrees Cent. for ½ Hour → 350 Degrees Cent. for 14 Days and Water-Quenched. Nital Etched. × 1000.

structure of the steel reacted at 650 degrees Fahr. (350 degrees Cent.) (Fig. 13). The acicular ferrite in Fig. 13 precipitates after the granular product and concentrates in the last region to go to completion in a banded structure. At 500 degrees Fahr. (260 degrees Cent.) the product is entirely different and is similar to "Lower Bainite" of plain carbon steels. The product formed throughout the period of reaction has this same microstructure.

Ar″

It is clear that austenitic steels can be made with many combinations of manganese and carbon. With 1.0 per cent carbon a 6 per cent manganese steel would be austenitic at all normally encountered

sub-atmospheric temperatures. To obtain Ar″ of about 32 degrees Fahr. (0 degrees Cent.) the manganese content must be doubled when the carbon content is halved. The unit lowering of Ar″ by manganese is greater when added in amounts over 6 per cent on the 0.8 and 1.0 per cent carbon steels.

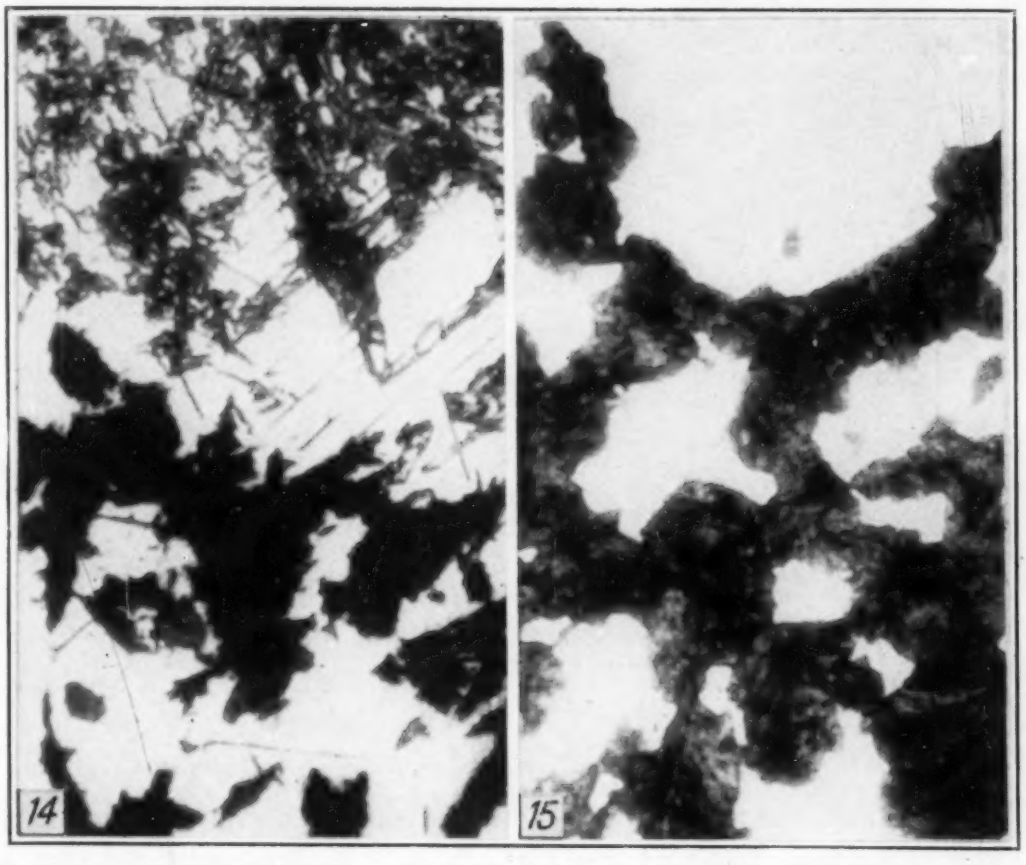

Fig. 14—Photomicrograph of Steel 0405. 900 Degrees Cent. for ½ Hour → 400 Degrees Cent. for 40 Minutes and Water-Quenched. Nital Etched. × 1000.

Fig. 15—Photomicrograph of Steel 0405. 900 Degrees Cent. for ½ Hour → 500 Degrees Cent. for 1 Hour and Water-Quenched. Nital Etched. × 1000.

Austenite Stabilization

The absence of a noticeable aging effect in the manganese steels precludes any explanation for this phenomenon based on relief of quenching stresses. To date no satisfactory reasons have been published as to the cause of stabilization. It is not known if this effect is present in the austenitic nickel steels. It is hoped that investigators of other systems will look for this effect since it is of importance in certain practical heat treatment.

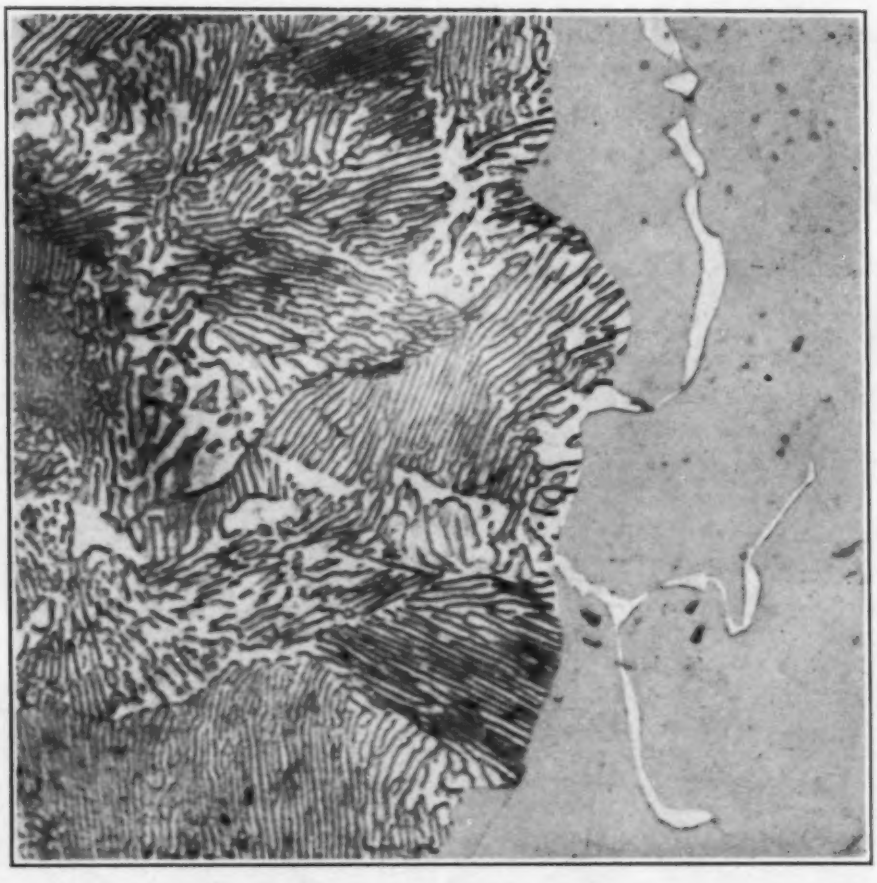

Fig. 16—Photomicrograph of Steel 0405. 900 Degrees Cent. for ½ Hour → 650 Degrees Cent. for 80 Hours and Water-Quenched. Nital Etched. × 1000.

Carbides

Although the authors in this limited survey study report no carbides other than those of the Fe_3C type, it is acknowledged that a small amount of carbides of another structure might be unnoticed by X-ray diffraction methods. The possibility of decomposition of carbides in water or the atmosphere must likewise be taken into account.

Hardenability

The agreement with Grossmann's data is satisfactory. However, the present data indicates that the manganese factor curve is not a straight line but rather curves upward as was noted for nickel by Edson (21). Additional experimental work would be necessary to extend the manganese factor curves of Grossmann. This is not meant as a criticism of Grossmann's data since he did not intend his factor to be used above about 1.5 per cent manganese.

Summary

The effect of manganese on Ar″ has been determined.

No noticeable stabilizing effect by room temperature aging has been noticed on the austenite → martensite transformation.

The carbides present in the steels studied have the crystal structure of iron carbide (Fe_3C).

Grossmann's factors have been found to give calculated ideal critical diameters, for steels up to 1.55 per cent manganese, which agree well with those determined from end-quench hardenability data.

The "S-curve" is markedly affected by manganese. Its influence is far greater on delaying the ending of transformation. The structures formed above 900 degrees Fahr. (480 degrees Cent.) are either primary troostite or an aggregate of ferrite and pearlite. Below 900 degrees Fahr. in the higher manganese steel as many as three distinct microstructures are formed at one temperature.

Acknowledgment

The authors wish to thank Dr. R. S. Dean of the Bureau of Mines and Mr. K. M. Leute of Electro-Manganese Corporation for donating electrolytic manganese.

Dean James H. Graham, Professor C. S. Crouse and Professor M. W. Beebe were a constant source of encouragement.

Mr. T. A. Kendall, Mr. W. D. Danks, Mr. J. P. Sheehan, Mr. H. B. Dyer, Mr. B. Duncan, Mr. S. Saunier, Mr. F. Mangelsen aided in many phases of the experimental work.

References

1. R. A. Hadfield, "On Manganese Steel," *Journal,* Iron and Steel Institute, 1888 (II), p. 41-82.
2. E. S. Davenport and E. C. Bain, "The Transformation of Austenite at Constant Sub-critical Temperatures," *Transactions,* American Institute of Mining and Metallurgical Engineers, 1930, Vol. 90, p. 117-144.
3. R. A. Grange and J. M. Kiefer, "Transformation of Austenite on Continuous Cooling and Its Relation to Transformation at Constant Temperature," TRANSACTIONS, American Society for Metals, 1941, Vol. 29, p. 85-116.
4. E. S. Davenport, "Isothermal Transformation in Steels," TRANSACTIONS, American Society for Metals, 1939, Vol. 27, p. 837-886.
5. A. B. Greninger, "The Martensite Thermal Arrest in Iron-carbon Alloys and Plain Carbon Steels," TRANSACTIONS, American Society for Metals.
6. A. B. Greninger and A. R. Troiano, "Kinetics of the Austenite to Martensite Transformation in Steel," TRANSACTIONS, American Society for Metals, 1940, Vol. 28, p. 537-574.
7. M. Cohen, Discussion of (6).

8. E. C. Bain, "The Alloying Elements in Steel," American Society for Metals, 1940.
9. A. Gulyaev, "Transformation of Retained Austenite in High Speed Steel at Sub-zero Temperatures," *Metallurg,* 1937, Vol. 12, p. 65-77.
10. M. P. Gordon and M. Cohen, "The Transformation of Retained Austenite in High Speed Steel at Sub-atmospheric Temperatures," TRANSACTIONS, American Society for Metals, Vol. 30, 1942, p. 569.
11. A. R. Troiano, Discussion (10), TRANSACTIONS, American Society for Metals, Vol. 30, 1942, p. 590.
12. Wever and Mathieu, "On the Transformation in Manganese Steels," *Mitteilungen,* Kaiser Wilhelm Institut für Eisenforschung, 1940, Vol. 22, p. 9-18.
13. H. Scott and J. G. Hoop, "The Hardening Transformation in Manganese Steels," TRANSACTIONS, American Society for Metals, 1933, Vol. 21, p. 233-259.
14. W. Jellinghaus, *Mitteilungen,* Kaiser Wilhelm Institut für Eisenforschung, 1933 (15), p. 15-20.
15. A. R. Troiano and F. T. McGuire, "A Study of the Iron-Rich, Iron-Manganese Alloys," TRANSACTIONS, American Society for Metals, Vol. 31, 1943, p. 340.
16. A. R. Troiano, Private Communication.
17. M. A. Grossmann, "Hardenability Calculated from Chemical Composition," *Transactions,* American Institute of Mining and Metallurgical Engineers, 1942, Vol. 150, p. 227-259.
18. A. Westgren, *Jernk. Ann.,* 1933, Vol. 117, p. 501-512.
19. A. Westgren, *Jernk. Ann.,* 1935, Vol. 119, p. 231-240.
20. E. C. Bain, "On the Rates of Reaction in Solid Steel," *Transactions,* American Institute of Mining and Metallurgical Engineers, 1932, Vol. 100, p. 13-46.
21. A. P. Edson, Discussion of (17).

DISCUSSION

Written Discussion: By Charles Nagler, metallography instructor, University of Minnesota, Minneapolis, Minn.

The authors are to be complimented for the nice piece of work which they did in their study of austenite decomposition in manganese steels. In reading the paper a statement on page 105 is "Magnetometric methods for determining reaction rate curves are open to important criticism. The shape and distribution of the product formed as well as its amount affects the observed magnetic quantity, thus while the beginning and end points obtained with sensitive equipment might agree with data from other methods the general shape of the reaction curve would not." It is the opinion of the writer on the basis of many hundreds of austenite transformation curves determined by a magnetometric method, and checked by microscopic examination, that good correlation between the two methods can be had for all points along the isothermal transformation curve determined for any subcritical temperature. The writer, in a publication which appeared in the TRANSACTIONS of the A.S.M. for June 1942, described a magnetometric device which was used for transformation studies. The studies were made on cast irons as the writer was interested in studying isothermal transformation rates in cast iron rather than in steel. As far as the actual transformations are concerned they are the same; the austenite being quenched to some subcritical temperature is held at that temperature until transformation is completed.

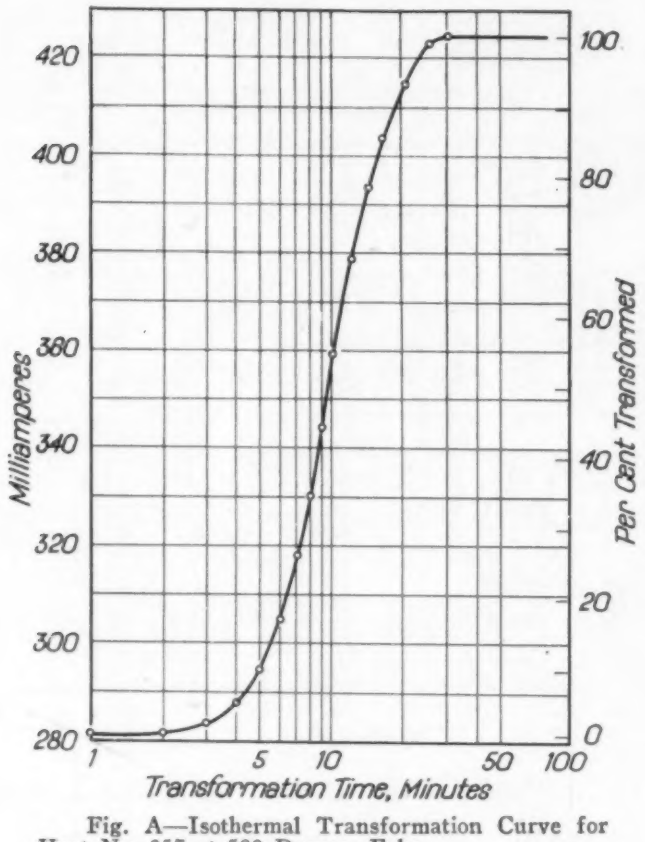

Fig. A—Isothermal Transformation Curve for Heat No. 357 at 500 Degrees Fahr.

In Fig. A is illustrated a typical transformation curve for a cast iron of the following analysis: Carbon 3.04, silicon 1.83, manganese 0.72, phosphorus 0.212, sulphur 0.072, and molybdenum 0.149 referred to on the figure as Heat No. 357. After this curve had been determined by the magnetometric method samples of the same cast irons were transformed for times indicated by different positions taken along the curve, and the amount of acicular troostite formed for each time interval estimated microscopically and this amount checked against that determined from the curve determined by the magnetometric method. Fig. A is taken from a paper which the writer is preparing covering additional studies which he carried out to prove the validity of the magnetometric method for determining austenite transformation rates.

Written Discussion: By Eugene P. Klier, assistant instructor, University of Notre Dame, Notre Dame, Ind.

The authors indicate that the work of Wever and Mathieu[1] was confined to low carbon, low manganese steels. This, however, is erroneous. Wever and Mathieu studied 19 steels concentrated between 1.81 and 4.80 per cent manganese, 13 of which ranged between 0.30 and 1.38 per cent carbon, only 6 contained less than 0.30 per cent carbon. Examination of Fig. B will indicate how thoroughly the manganese steels were covered. It can be seen that numerous steels of hypereutectoid as well as hypoeutectoid composition were investigated.

[1]Wever and Mathieu, *Mitteilungen aus dem Kaiser Wilhelm Institut für Eisenforschung*, Vol. 22, 1940, p. 9-18.

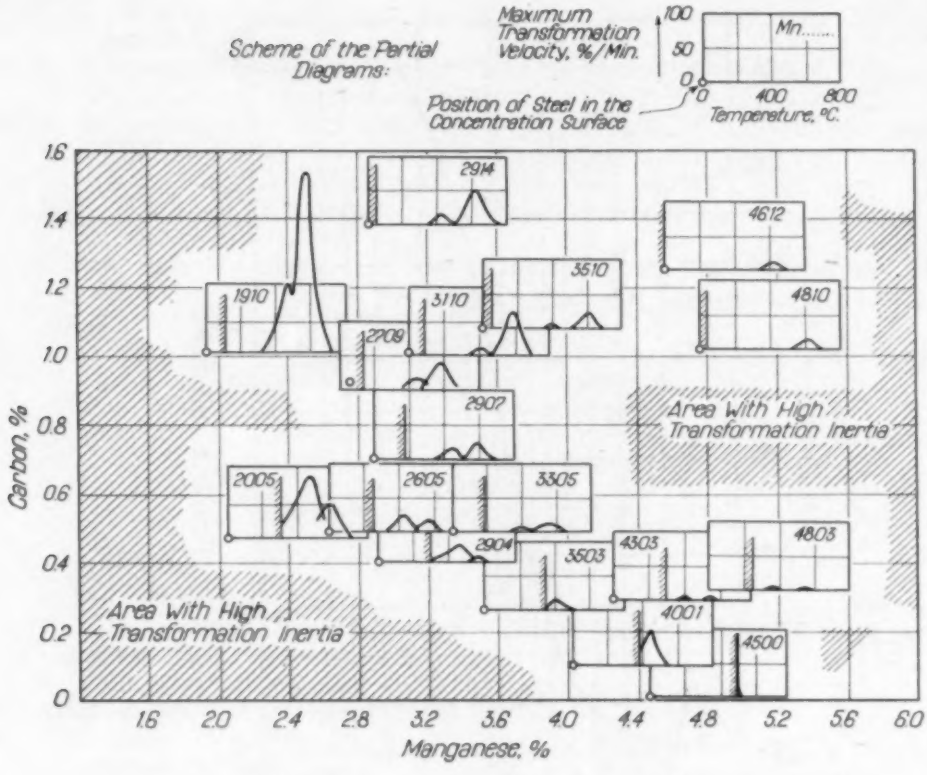

Fig. B—Transformation Curves for the Manganese Steels.

The curves plotted in Fig. B are reaction rate curves and indicate the maximum reaction rate at temperature. Such representation is one of convenience and does not include the course of the isothermal transformation; however, neither does it include certain errors of representation as is common for S-curves.

The divergent views of the authors and Wever and Mathieu with respect to a second region of fast reaction can only in part be attributed to a difference in experimental technique. Thus the authors' Fig. 10 indicates a region of maximum average reaction rate at 400 degrees Cent. (750 degrees Fahr.), which is in quite good agreement with the results of Wever and Mathieu for an almost identical steel. The S-curve presented in Fig. 11 indicates an average reaction rate at 260 degrees Cent. (500 degrees Fahr.) greater than any average rate between 260 and 400 degrees Cent. (500 and 750 degrees Fahr.).

The authors indicate that the magnetometric method for the determination of S-curves is open to serious question. The results presented in Fig. C indicate that this objection is invalid, while the work of Wever et al.[2, 3, 4] indicates good agreement with this method of dilatometric and electrical resistance measurements.

---

[2]Wever and Lange, ibid, Vol. 14, 1932, p. 72-83.
[3]Wever and Jellinghaus, ibid, Vol. 14, 1932, p. 85-89.
[4]Wever and Jellinghaus, ibid, Vol. 15, 1933, p. 167-177.

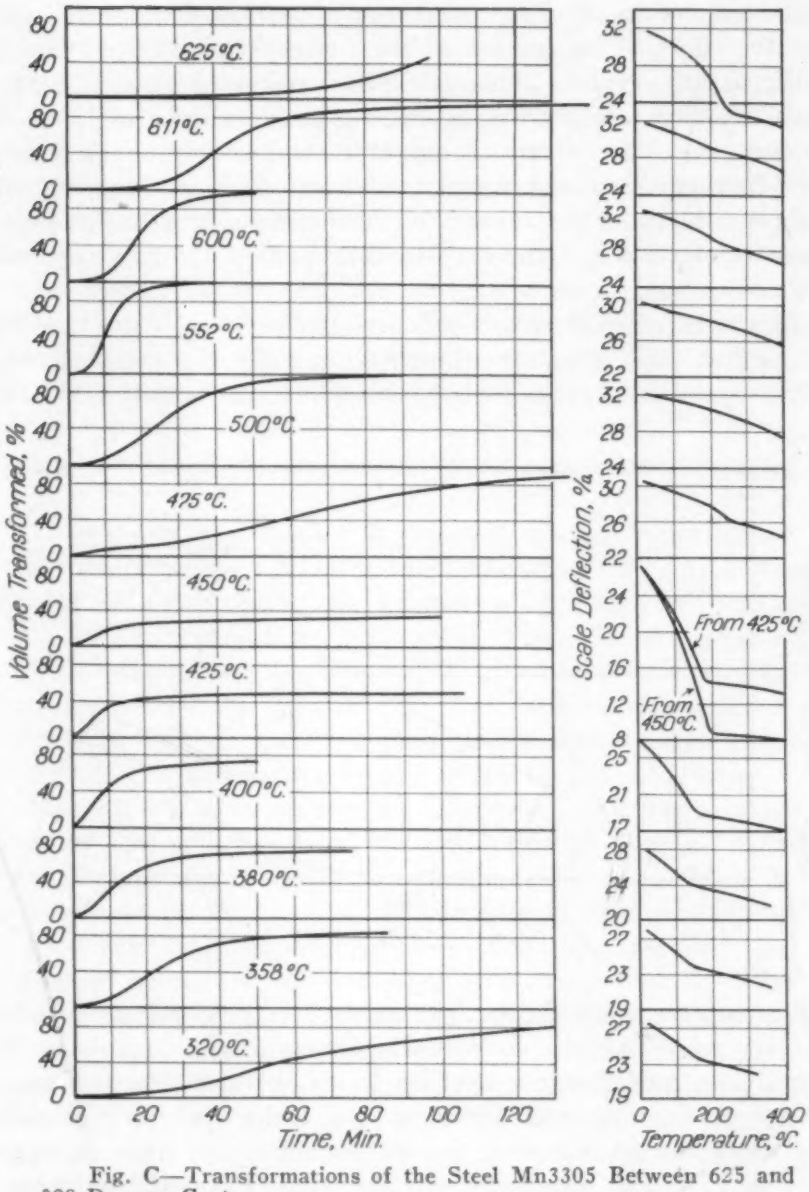

Fig. C—Transformations of the Steel Mn3305 Between 625 and 320 Degrees Cent.

Oral Discussion

H. H. CHISWIK:[5] I would like to ask the authors whether increased amounts of manganese (above 4.00 per cent), and possibly wider variations in the carbon content, could be expected to produce an "intermediate" transformation in the S-curve? I think the German investigators referred to by the authors did find an "intermediate" rapid transformation zone at certain manganese and carbon contents.

Authors' Reply

In reply to Mr. Chiswik, the authors wish to state that they do not dispute the data of Wever and Mathieu. The German investigators reported the effect

[5]Research metallurgist, Battelle Memorial Institute, Columbus, Ohio.

of manganese and carbon on the maximum transformation velocity whereas in this paper the effect of manganese on the conventional S-curves has been presented. Fig. 2 may serve to illustrate the two points of view. The graph is a hypothetical reaction rate curve in which one phase transforms to two different microconstituents. The curve starting at A and ending at E represents the amount of decomposition as a function of time. It is obvious from the shape that there are two products forming. Each of the products has its own reaction rate curve and it is important to note that reaction 1 does not cease when reaction 2 commences.

The data most often reported in American literature is the time for beginning and ending. European metallurgists generally study transformation velocity. Wever and Mathieu reported maximum transformation velocity which

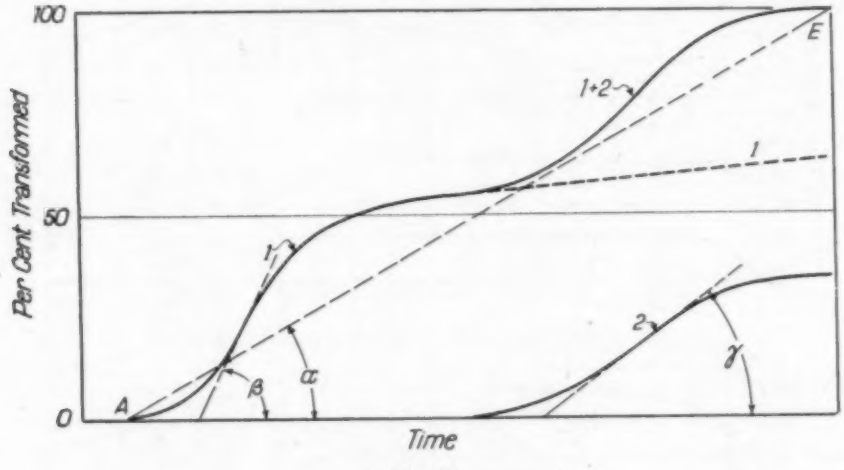

Fig. D

is the tangent of the angle Beta. The average transformation velocity is the tangent of the angle Alpha. From a theoretical viewpoint neither beginning and ending points, maximum nor average transformation velocities supply sufficient data for study of reaction kinetics. The entire curve is essential. From a practical viewpoint the beginning and ending time is of most significance. It can be seen in Fig. 10 of the paper that the temperature of maximum average velocity is about 842 degrees Fahr. (450 degrees Cent.). This is the temperature for which Wever and Mathieu report the highest value of maximum transformation velocity. Since the decomposition of austenite results in one microconstituent at this temperature, the temperature of both maxima should agree.

Professor Nagler writes in defense of the magnetic method and the authors do not wish to imply that his technique is not valid in most instances. It certainly has the advantage of minimum work since a single specimen suffices for one curve while as many as thirty are often necessary with the microscopic method. It is felt, however, that the observed magnetic quantity can be made to vary by simply changing the size, shape, and distribution of the precipitated phase—not to mention mechanical strain. Magnetic or any other technique should be checked with microscopic data. If the magnetic apparatus is sufficiently sensitive the beginning and ending points should agree but in some

instances the curve such as AE in Fig. D of the discussion might have a slightly different shape.

Klier's discussion was received late and is answered in part by the above treatment of reaction rate curves. The authors meant to imply that the data of Wever and Mathieu indicate that the general trend toward low manganese and low carbon gives a strong intermediate reaction and not that they used only a low carbon-low manganese series. It can be seen from Fig. B that in a low manganese section or a low carbon section one gets a strong intermediate. The combination of high carbon and high manganese does not show it.

The authors selected a steel similar to the Wever and Mathieu 2005 in order to see if the region of rapid transformation velocity in the intermediate range would show up as a shelf projecting toward zero time on the S-curve. This is important since it affects the products formed in a "slack quench." One cannot at all predict from the data of Wever and Mathieu whether this is the case.

It can be seen in Fig. C that the maximum transformation velocity in Fig. 5 (500 degrees Cent.) is about equal to that in Fig. 7 (450 degrees Cent.). However, at 500 degrees Cent. the reaction is completed in 90 minutes whereas at 450 degrees Cent. (840 degrees Fahr.) it is only 35 per cent complete in that time. This example from the Wever and Mathieu work shows the limitation of the maximum transformation data. It gives no indication of the time required for beginning or ending at all temperatures. The above comparison is between the troostite and intermediate reactions. The case is even more complicated if more than one transformation product is formed. The present paper has clearly demonstrated that one can have the rapid maximum transformation velocity without a displacement of the S-curve to the left.

The question of accuracy of various experimental methods cannot be answered by simply referring to Fig. C. Actually the quantity observed by any of the present methods is not weight or volume per cent but some fraction of another measured quantity which requires deductive reasoning to relate it to the amount of decomposition. The objection to magnetometric technique is a finely drawn one and it is hoped that readers will accept it in that light. For a certainty the microscopic method is poor for judging amounts first because only a small area of one plane is studied and second because of the difficulty of measurement. Because of this great limitation, no attempt was made to plot reaction rate curves.

The authors are well aware of the limitations of the S-curve method of presenting austenite transformation data. However, one can obtain from the S-curve the beginning and ending time (of very practical importance), the average transformation velocity, as well as a prediction of the products formed on cooling at rates less than the critical cooling velocity. Actually the best method of presenting data would be to plot the complete reaction curve at each isothermal temperature.

THE MICROHARDNESS TESTER AS A METALLURGICAL TOOL

By Constance B. Brodie

Abstract

The microhardness tester has been developed as a useful metallurgical tool. The procedure for using the instrument and its applications are described. Small samples, e.g., 0.20 millimeter wire, and minute areas in alloys, e.g., a few hundredths of a millimeter wide, can be tested. A table comparing the Knoop hardness with Rockwell and diamond pyramid hardnesses is given. The recommended minimum spacings for indentations are also tabulated. Photomicrographs are used to illustrate various applications.

HARDNESS determination is one of the oldest of metallurgical tests; recently a new instrument for measuring microhardness has made its appearance[1] and is rapidly assuming considerable importance in metallographic investigations. The hardness of individual phases in an alloy, the hardness of thin sheets or wires, a microscopic survey of the hardness variations in a weld are representative of the types of determinations of hardness that can now be made with a microhardness tester. A report on the uses of such an instrument is made herein for the benefit of those who may not be familiar with this new metallurgical tool.

Procedure

The instrument used for this work was the Tukon Tester, described by the Wilson Company in their publications, and by Knoop, Peters, and Emerson.[1] A picture of the equipment is shown in Fig. 1. The mechanical operation of the machine is simple and has been adequately described elsewhere,[1] and therefore, the details will not be given here. The load is applied for twenty seconds through a diamond indenter shown schematically in Fig. 2. The

[1]A Sensitive Pyramidal-Diamond Tool for Indentation Measurements, F. Knoop, C. G. Peters, and W. B. Emerson; *Journal of Research* of the National Bureau of Standards, Vol. 23, July 1939.

[2]Chauncy G. Peters and Frederick Knoop; "Metals in Thin Layers--Their Microhardness", *Metals and Alloys*, Vol. 13, 1940, p. 292.

A paper presented before the Twenty-fifth Annual Convention of the Society, held in Chicago, October 18 to 22, 1943. The author, Constance B. Brodie, is associated with the Research Laboratory, General Electric Co., Schenectady, N. Y. Manuscript received June 24, 1943.

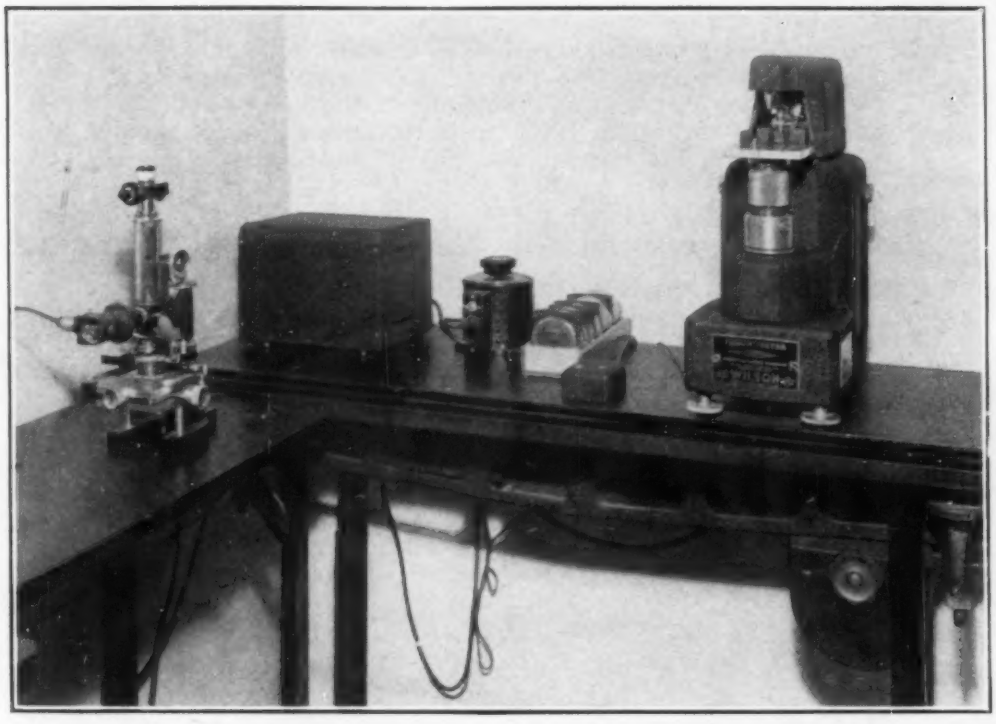

Fig. 1—Equipment Used for Microhardness Determinations.

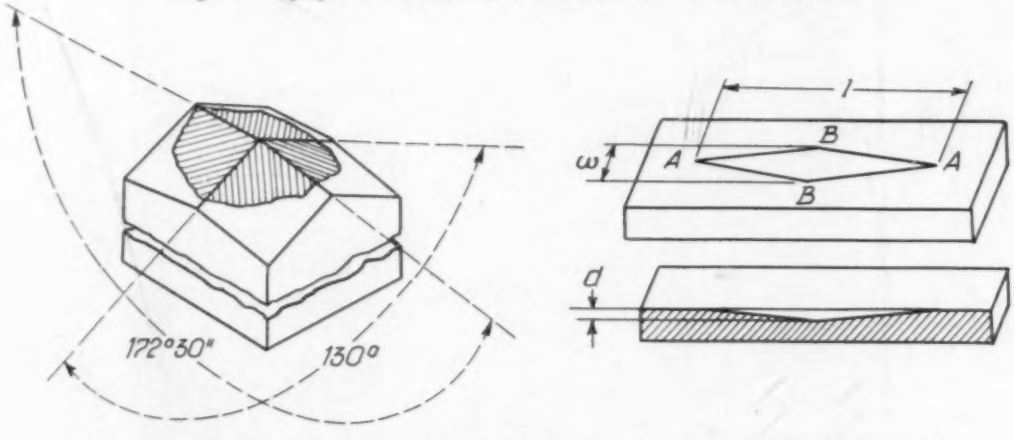

Fig. 2—The Design of the Indenter and Shape of the Indentation. (Knoop, Peters and Emerson.)

diagonals of the resulting indentation can be measured with a micrometer microscope. The long diagonal does not change dimension[1] when the load is removed, but the short diagonal becomes shorter because of the elastic recovery of the material. Thus the "unrecovered" and "recovered" areas in the plane of the surface can be calculated. The microhardness, called the Knoop Hardness, is obtained by dividing the load in kilograms by the *unrecovered* area in the following manner:

$$I = \frac{L}{Ap} = \frac{L}{l^2 Cp}$$

I = Knoop hardness number
L = Load (in kilograms) applied to indenter
Ap = Unrecovered projected area of indentation (in sq. mm.)
1 = Measured length of long diagonal of the indentation (in mm.)
Cp = Constant relating 1 to the projected area. For an indenter of 172° 30′ longitudinal angle and 130° 0′ transverse angle, Cp equals 7.028×10^{-2}

For general use a table is available showing the hardness corresponding to various lengths of the impression.

The relative elastic recoveries of various materials can be judged from the recovered projected areas, determined by measuring both

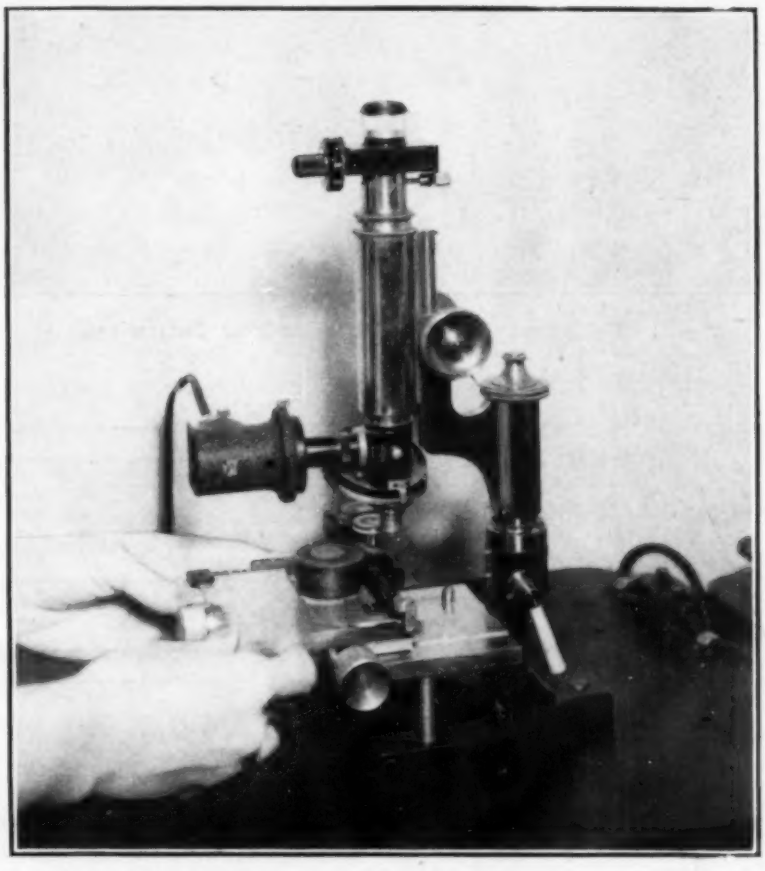

Fig. 3a—Transferable Stage Being Mounted on Microscope.

long and short diagonals. The hardness determined from the *recovered* area is given by

$$I_r = \frac{2L}{1w}$$

where
I_r = Knoop number based on the recovered projected area.
L = Applied load in kilograms.
1 = Measured length of long diagonal in mm.
w = Measured length of short diagonal in mm.

The relative elastic recoveries of materials can be compared by comparing $I_r - I$ for such materials. Such a study is of interest in special cases, but generally the Knoop Hardness, I, is of primary interest.

The length, l, of the indentation is about seven times the width, w, and thirty times the depth, d. An indentation having a length of approximately 0.1 millimeter has been found to be most suitable.

Fig. 3b—Transferable Stage Being Mounted on Microhardness Tester.

The machine as received was found to be unsuitable for making indentations in small areas which had to be located precisely, e.g., within 1/50 millimeter; therefore, a special stage was designed and constructed for this work. This stage, shown in Fig. 3, could be transferred from the hardness tester to the microscope. An area of even a few thousandths of a square millimeter could be accurately located under the microscope, the stage transferred to the hardness tester, and the impression made within a few hundreths of a millimeter of the desired location. In order to obtain this accuracy of

location of the indentation, the stage was built with a flat projection on one edge of the bottom and a V-shaped projection on the other (see Fig. 3). The space between the flat and the V does not come in contact with the platform of the tester or microscope. The V slide rests in a V groove on the fixed platforms. The stage is thus located accurately in one direction in the horizontal plane. Accurate

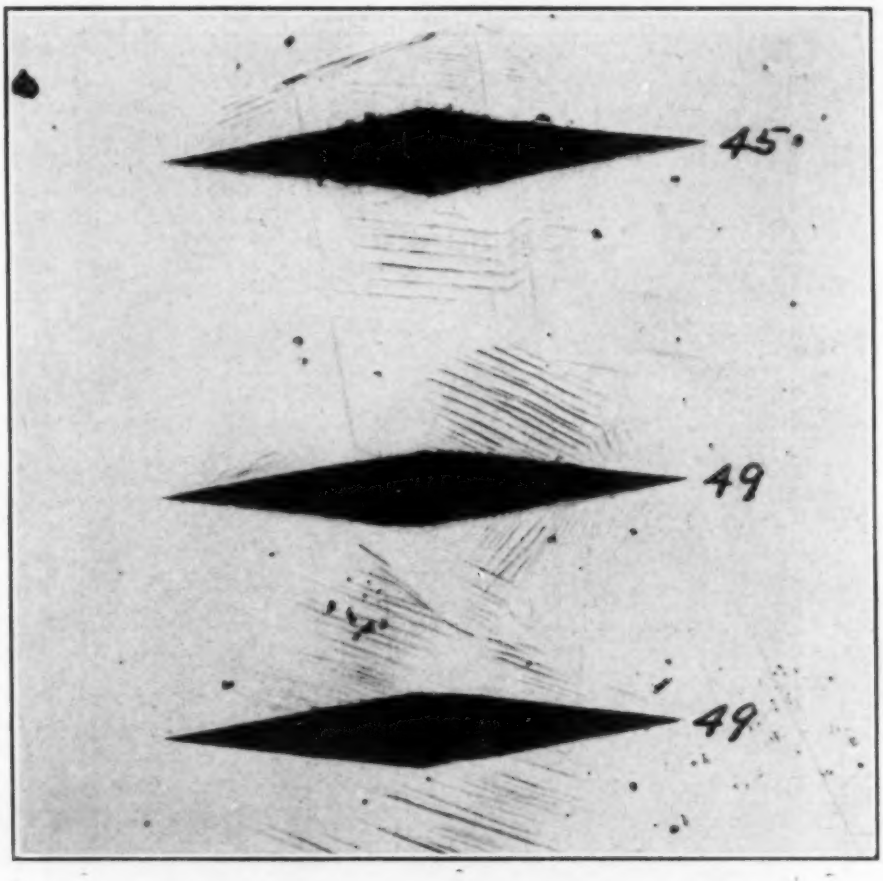

Fig. 4—Deformed Metal Around Microhardness Indentations. Impressions Spaced Too Closely Are Likely To Give Erroneous Hardness Readings. × 100.

location in the other direction was obtained by adjustable stops on the platforms of the tester and microscope. The transferable stage was built in three parts, a bottom which was stationary, a center part which had an adjustable screw to move it in one direction, and a top part which had an adjustable screw to move it in a direction 90 degrees from the direction of motion of the center part. The screws were accurately machined so that an area on the sample could be located within one-hundredth of a millimeter. For holding the sample and locating it approximately under the indenter, a Bausch

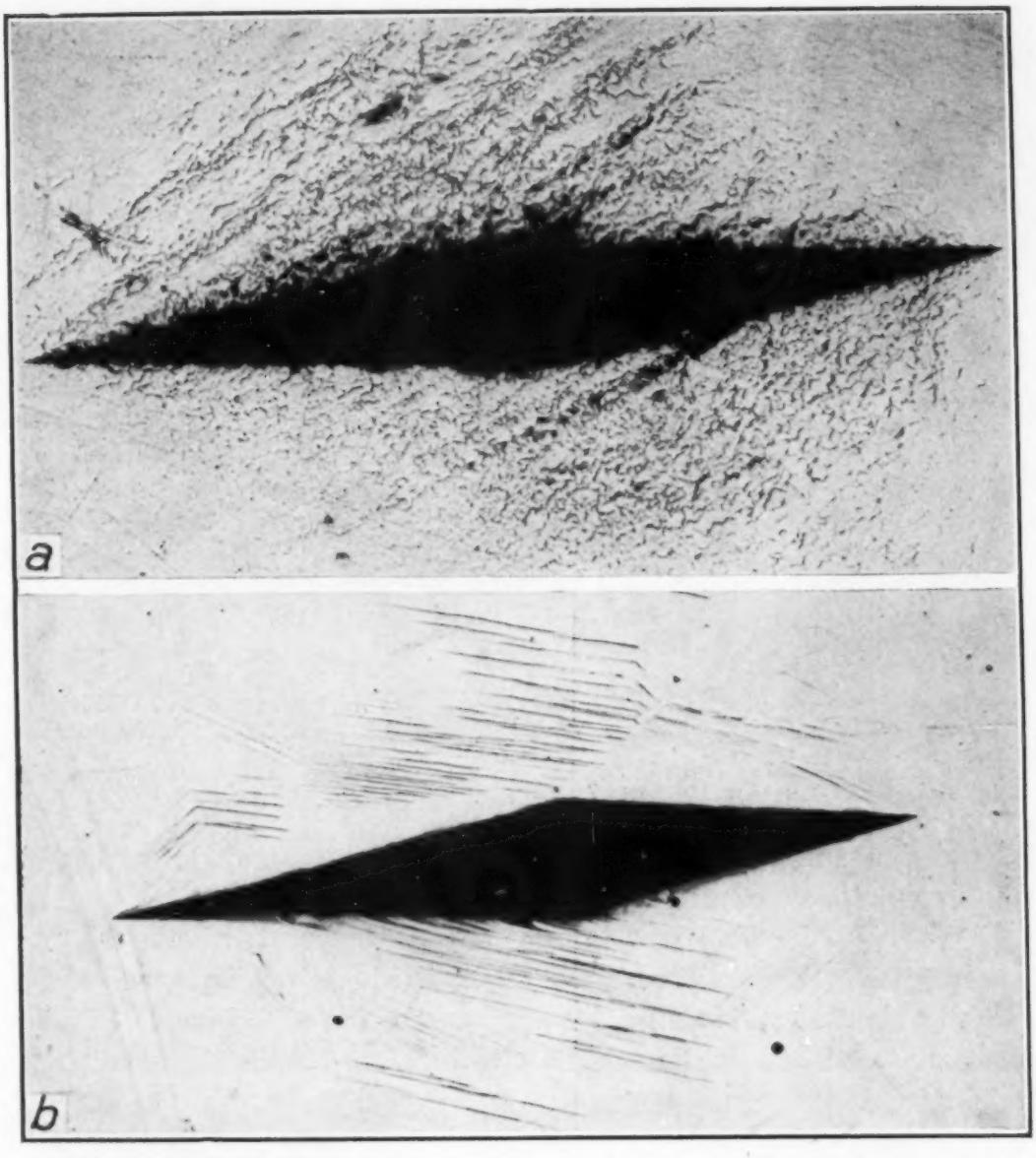

Fig. 5a and b—Deformation Patterns Around Indentations in Different Materials: (a) Zinc, (b) Silver. × 100.

and Lomb mechanical stage was mounted on the top part of the special stage.

The preparation of the sample for microhardness testing is important. A brightly polished surface is necessary for accurate measurement of the indentation. The polished sample is mounted in plasticene on a glass slide, care being taken to keep the sample flat and horizontal. The sample is then placed on the special stage and under the microscope the desired area is located. The stage is transferred to the hardness tester and the indentation made.

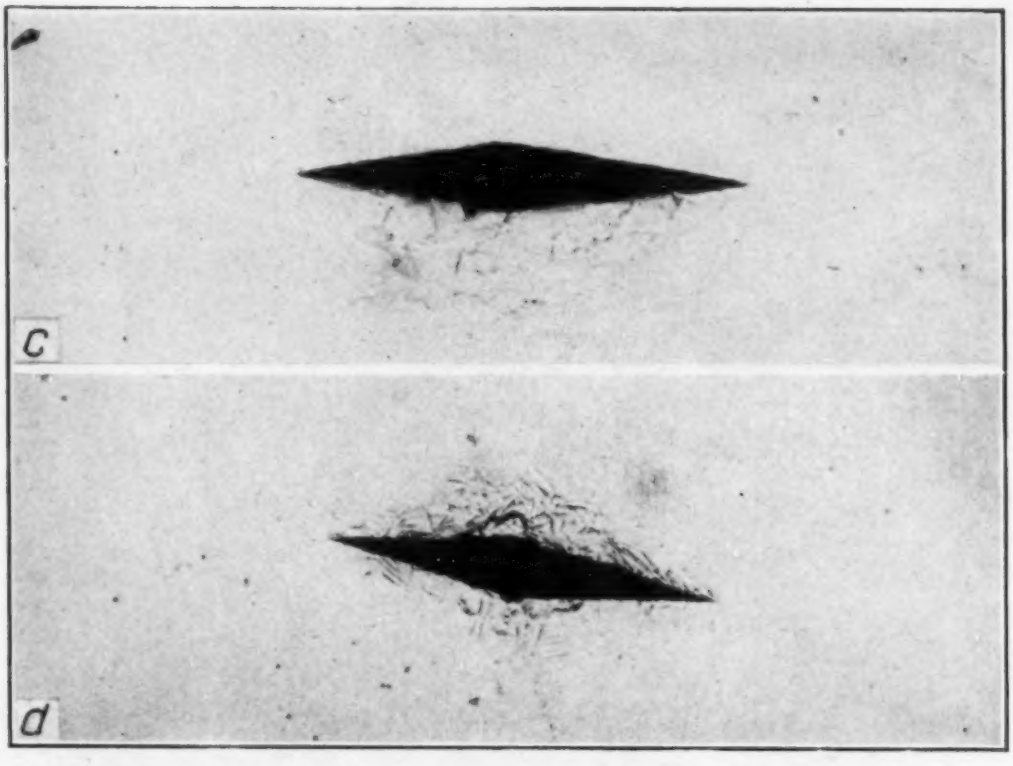

Fig. 5c and d—Deformation Patterns Around Indentations in Different Materials: (c) Nickel, (d) Beryllium-Copper. × 100.

Again the sample is placed under the microscope and the length of the indentation measured.

Varying the load causes little change in the hardness reading except, perhaps, at low loads where the hardness readings tend to be slightly high. Loads above 200 grams were found to give essentially constant hardness readings. This is in accord with the results of others.[1]

Applications

The uses for the microhardness tester are manifold. Thus far the instrument has been used successfully in the study of the following:

1. Welds—for exploring the hardness across a weld. Hard regions only a few hundredths of a millimeter thick can be located.

2. Small wires—samples having very small cross sections, e.g., wires 0.25 millimeter in diameter, can be tested.

3. Thin strips—having a thickness of a few hundredths of a millimeter can be tested.

4. Surface layers—e.g., carburized, nitrided, or calorized surfaces can be measured.

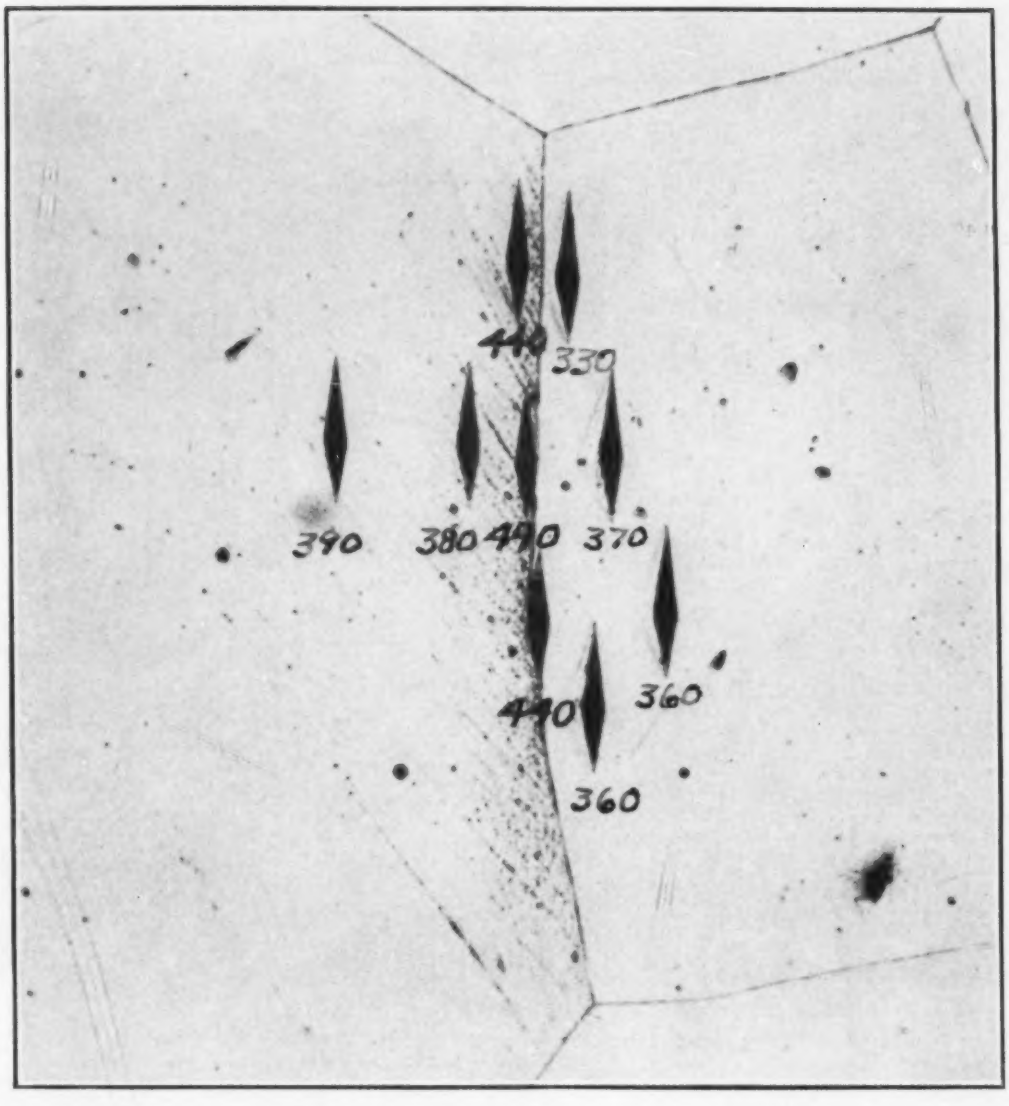

Fig. 6—Variations in Hardness Readings Near a Grain Boundary of an Iron-Molybdenum Alloy. Precipitation of the Iron-Molybdenum Compound Had Started in One Grain But Not in the Other. × 250.

5. The hardness of different phases in metallographic samples can be determined if the areas are more than a few hundredths of a millimeter wide.

6. Tool steels—tips of cutting tools can be measured to indicate hardness and check the effect of decarburization, or the presence of retained austenite.

7. Extremely soft materials, such as lead, can be tested.

8. Extremely hard or brittle materials, such as diamonds, carbides, glass, and silicon, can be tested.

Table I gives the Knoop hardness for a number of materials.

Table I

Material	Condition	Knoop Hardness Number	Rockwell Hardness	Diamond Pyramid Hardness 25Kg Load
1.1 C Steel	1 hr. 775 °C., W.Q. 1 hr. 150 °C., A.C.	700–800	R_c 65	843
0.40 C Steel	1 hr. 800 °C., W.Q. 1 hr. 150 °C., A.C.	600–700	R_c 55	690
1.1 C Steel	1 hr. 775 °C., W.Q. 1 hr. 350 °C., A.C.	550–580	R_c 50	580
1.1 C Steel	1 hr. 775 °C., W.Q. 1 hr. 450 °C., A.C.	400–500	R_c 42	455
Beryllium Copper, 2.25% Be	2 hrs. 850 °C., W.Q. 16 hrs. 300 °C., A.C.	406	R_c 42	400
1.1 C Steel	1 hr. 775 °C., W.Q. 1 hr. 550 °C., A.C.	300–400	R_c 35	360
1.1 C Steel	1 hr. 850 °C., F.C.	280	R_b 95	240
0.20 C Steel	Cold rolled	260	R_b 95	240
1.1 C Steel	1 hr. 775 °C., W.Q. 1 hr. 650 °C., A.C.	225	R_b 92	210
0.40 C Steel	1 hr. 800 °C., A.C.	194	R_b 87	205
0.20 C Steel	1 hr. 850 °C., F.C.	188	R_b 83	185
Beryllium Copper, 2.25% Be	Solution quenched and cold worked	175	R_b 81	180
65:35 Brass	Cold drawn	145	R_b 76	140
Commercial Nickel	Annealed	125	R_b 60	125
Dural 17 ST	Hardened	120	R_b 65	125
OFHC Copper	Cold drawn	118	R_b 45	100
Electrolytic Iron	Annealed	100–120	R_h 95	92
65:35 Brass	Annealed	80	R_b 34	80
OFHC Copper	Annealed, 1 hr. 400 °C.	52	R_h 76	50
Fine Silver	Annealed, 1 hr. 425 °C.	51	R_h 55	33
Aluminum—2S	Cold Worked	35	R_h 57	30
Horse Head Special Zinc	As cast	34	R_h 45	28
Aluminum—2S	Annealed, 1 hr. 400 °C.	24	....	19
Alton Lead	Annealed	5	....	..

Table II

Load	Knoop Hardness	Recommended Minimum Spacing	
100g	50–100	5 mils	0.125 mm
	100–200	2	0.050
	200–500	2	0.050
	500–750	1	0.025
	750 up	½	0.012
200g	50–100	5 mils	0.125 mm
	100–200	2–5	0.050–0.125
	200–500	2	0.050
	500–750	1	0.025
	750 up	½	0.012
500g	50–100	10 mils	0.250 mm
	100–200	5	0.125
	200–500	2	0.050
	500–750	2	0.050
	750 up	1	0.025
1000g	50–100	20 mils	0.500 mm
	100–200	10	0.250
	200–500	5	0.150
	500–750	2	0.050
	750 up	2	0.050
2000g	50–100	20 mils	0.500 mm
	100–200	10	0.250
	200–500	5	0.150
	500–750	5	0.150
	750 up	2	0.050

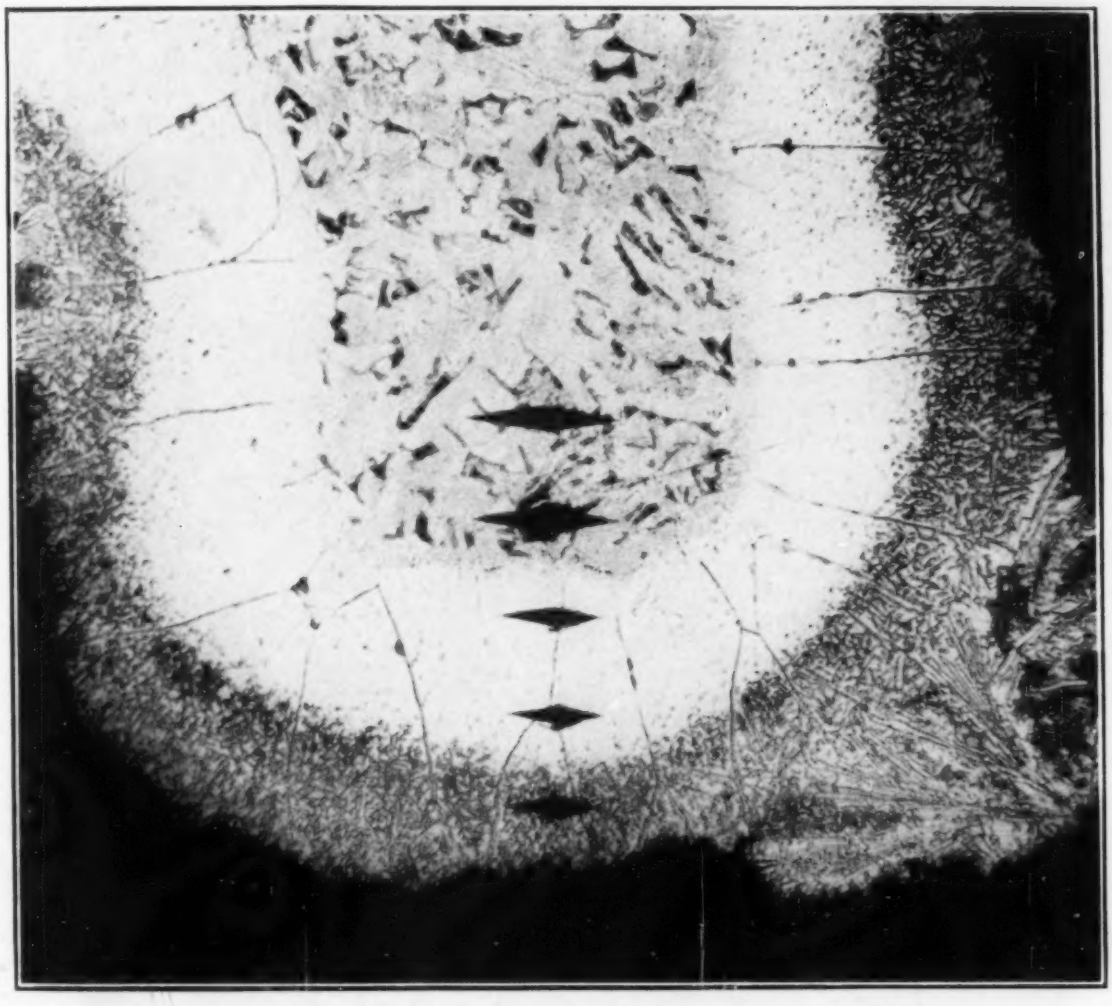

Fig. 7—A Low Carbon Steel with a Hard Alloy Case. × 100.

Rockwell and diamond pyramid hardness numbers were also determined on the same samples and these results are listed in the table. The Knoop hardness is very nearly the same as the diamond pyramid hardness. Knoop, Peters, and Emerson[1] found a similar correlation, and they showed that Brinell hardness was only slightly lower (approximately 25 points).

By the use of the special stage previously described, it was possible to make indentations at small regular intervals. This was done for a number of materials and the minimum spacing determined so that the deformation due to the indentation would not affect the readings of the adjacent impressions. These results are summarized in Table II.

Some of the interesting results obtained with the microhardness tester are illustrated in Fig. 4 through 8. The effect of placing the

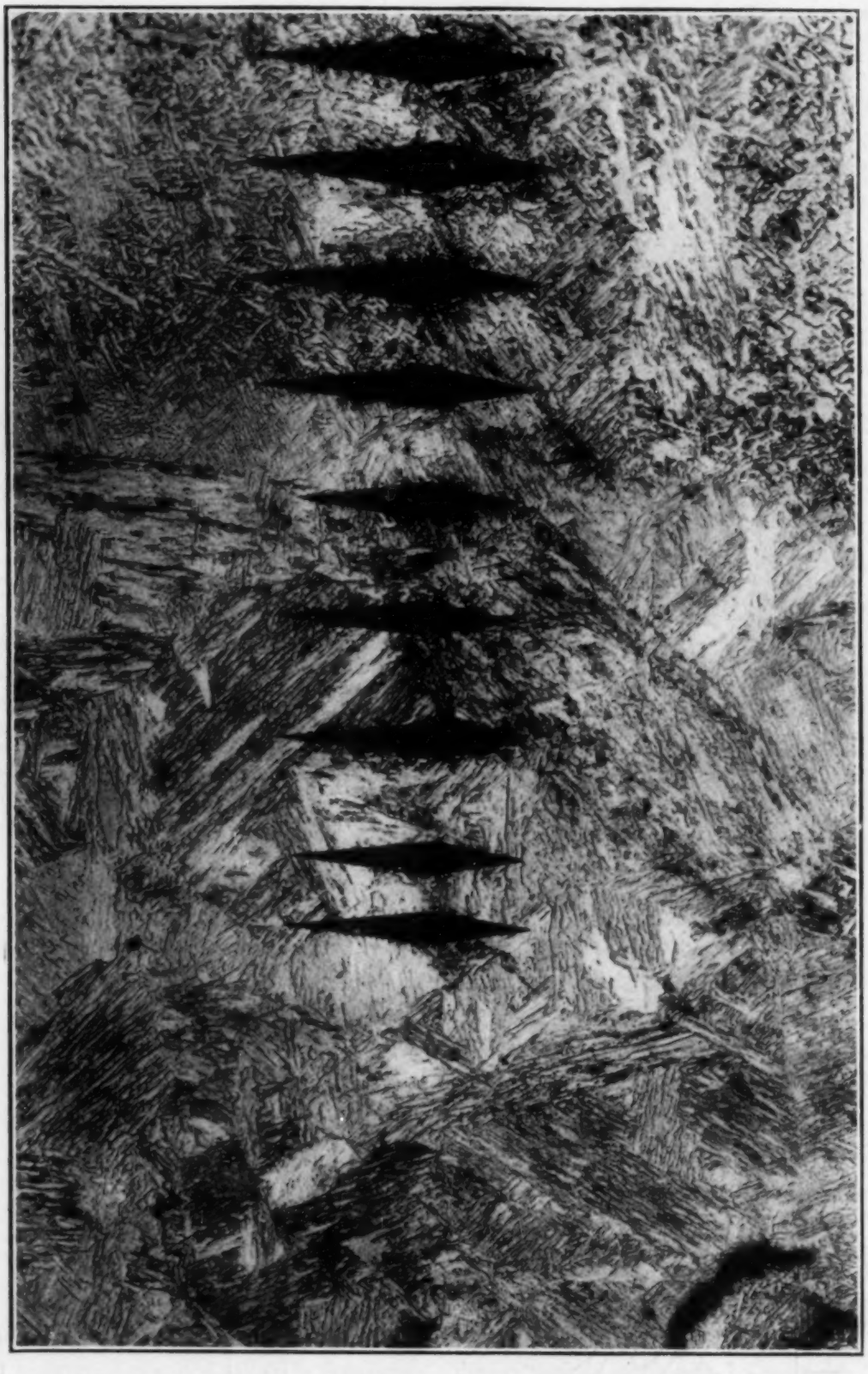

Fig. 8—Microhardness Indentations in a Weld. The Crack is in the Weld Metal. Hardness Values Reading from Top to Bottom are 197, 185, 218, 245, 366, 340, 340, 340, 317. × 100.

Fig. 9—Microhardness Indentations in a Constituent of a Meteorite. × 100.

indentations too closely is shown in Fig. 4. The metal is deformed around the indentation for a distance greater than the spacing. Consequently, every reading except the first one is high.

The deformation in the surrounding metal produced by the indenter yields different patterns for different materials. Some of the interesting patterns are shown in Fig. 5.

Some precipitation hardening alloys show precipitation in or near the grain boundaries before general precipitation occurs. Fig. 6 shows microhardness indentations in such a region in an iron-molybdenum alloy. The effect of the precipitation is local and variations can be readily detected.

Fig. 7 is a photomicrograph of an alloy case on a low carbon steel, showing a series of indentations. That the case is much harder than the steel is evident from a comparison of the indentations.

Fig. 8 shows hardness readings taken in the weld zone of a nickel-chromium steel. The highest hardness is just inside the weld metal. Note the crack in the weld. The indentations in this sample are asymmetrical because the sample was not mounted horizontally.

Fig. 9 shows microhardness indentations in a constituent of a meteorite which is about 0.06 millimeter in width. The accuracy with which the indentation can be located by the use of the transferable stage is thus demonstrated.

There are numerous other items of interest, such as the determination of directional properties. For example, a tungsten wire was found to have a hardness of 520 when the long axis of the indenter was parallel to the axis of the wire, but when the long diagonal was across the wire, the hardness was 630.

Of practical interest is the hardness of a thin nitrided case on steel (approximately 0.0001 inch thick). The hardness of this case seemed to be about 1200 when the indentations were made on the nitrided surface.

Carbides vary a great deal in hardness. Tungsten and tantalum carbides were tested and found to have hardnesses greater than 2200, while iron carbide was found to be around 900.

From the foregoing brief description of the microhardness tester as a metallurgical tool, the reasons for its growing popularity are evident. As the uses for this important instrument are extended, the appreciation of its utility will grow.

ACKNOWLEDGMENTS

For assistance in making the hardness readings, the author wishes to express her gratitude to Margaret Wheeler, Eileen Meals, and Catharine Ferguson.

DISCUSSION

Written Discussion: By Erle J. Hubbard, assistant to chief metallurgist, Research Laboratory, Koppers Co., American Hammered Piston Ring Division, Baltimore, Md.

I would like to congratulate the author on bringing into the limelight a relatively new metallurgical tool for hardness testing. A need for such an instrument has been known for some time. Its development and use in industrial and research laboratories will help considerably to eliminate another question mark in physical metallurgy.

We have had a Tukon tester in our Research Laboratory for more than six months and have made repeated tests on other Tukon testers for a similar period before that time. Our primary use has been in determining the hardness of plated materials, essentially chromium plate. We have found that chromium plate, which was plated at different plating conditions, gave plate hardness results entirely different. The Tukon tester has enabled us to determine the proper chromium plate hardness best suited for satisfactory service. We have also found that the chromium plate hardness will vary from below 700 to as high as 1200 Knoop hardness, using a 100-gram load on the Tukon tester, when plated under these varying conditions and treated differently after plating. We hope to be able to publish information covering our investigations in the near future.

The author has treated this subject very well and confirms a number of our investigations we have undertaken to date.

We notice that in Table I the Knoop hardness of a number of different materials is given. We believe that in order to make the table complete, a statement should accompany the table giving the load used in making the indentations as there are some varying results obtained when going from a 100-gram load to 2000-gram or 3600-gram on the same specimen. We have made a number of experiments and tests on polished standard Rockwell test blocks and have found that with increasing load there is a slight decrease in Knoop hardness. Undoubtedly, that is probably taken into consideration by the author in Table I where a Knoop hardness number is given as 700 to 800 for hardened 1.1 per cent carbon steel.

The author mentioned that varying loads cause little change in hardness except at low loads where the hardness tends to be high. That is essentially true, which again brings up the point that in order for complete clarification of hardness results by everybody in the field the load used in making the indentations must be specified along with the Knoop hardness number of the material tested. We have had to standardize our measurements to one definite load for

chromium plate because it is brittle and too great a load will cause cracking of the plate around the area of the impression, giving low and erratic results. We use a load on the Tukon tester of 100 grams and specify every hardness test reported, as taken at that load. Experience has shown us that loads greater than this give a large percentage of cracked impressions resulting in erratic readings.

To help eliminate the variance encountered when measuring the hardness of normal materials especially at lower loads the makers of this instrument have developed a solenoid which is attached to the beam of the Tukon tester. This is done to eliminate any additional loading force due to inertia effect of applying the load, and also to eliminate any small loading effect due to vibration from the elevating screw motor on the Tukon tester. In this way, only part of the total load is applied by forcing the indenter into the specimen by the upward motion of the elevating screw. The remainder of the load is supported by the solenoid located over the beam, and this load is applied at a relatively slow rate by cutting off the current in the solenoid after the upward motion of the elevating screw has stopped. The smaller part of the load is again removed before the beam lift motor raises the indenter from the impression. The current for the loading solenoid is obtained from a rectifier tube and is controlled by cams on the outer plate attached to the timing motor shaft.

We have recently had one case where the solenoid was not working properly and we obtained erratic and low readings. Immediately, we investigated and corrected the trouble and we are now firmly convinced that the solenoid's operation is essential for consistent accurate readings.

I might also state that we have had no trouble determining the hardness of chromium plate which was only 0.001 inch thick, the depth of the diamond impression, as made with the Knoop indenter, as far as we have determined on our material was in the neighborhood of 0.0002 inch.

As the author stated, hardness of inclusions, carbides, martensitic areas, and retained austenite may be measured, and it may easily be realized the enormous field of metallurgical research which is opening through the development of this microhardness tester.

Written Discussion: By Morse Hill, assistant metallurgist, John Casey, 1st Lt. A.C., and J. C. McGee, Materials Laboratory, Engineering Division, Wright Field, Dayton, Ohio.

The author is to be congratulated on pointing out some of the many phases of the application of micro-hardness instruments. As such instruments come to be more frequently used, a better understanding of the sometimes confusing things we see under the microscope must result. In particular, we shall not have to be content with giving a micro-constituent a name to disguise our ignorance of its properties. We will at least be able to describe one of its most significant properties—hardness.

There is another micro-hardness instrument than that the author used which deserves attention. It is the device of Eberbach & Sons Co. which uses a miniature Vickers indenter. As shown in Fig. A it mounts in the objective holder on the inverted as well as the upright microscope, and the indentation is made and measured without disturbing the specimen.

The indenter is supported on a plunger within the body of the instrument

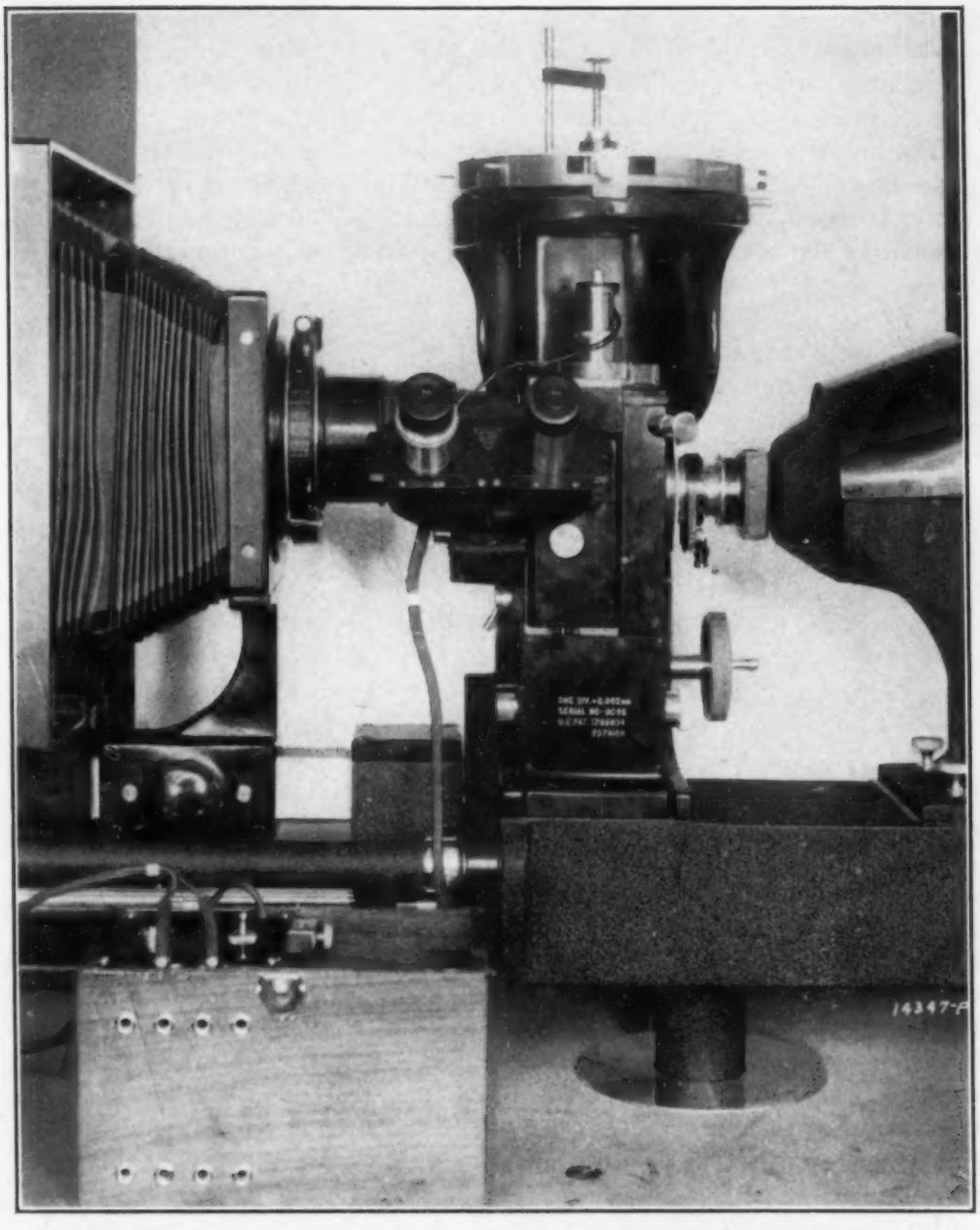

Fig. A—Micro-Hardness Instrument in Position on Microscope. Box Contains Indicator and Relay.

against a contact ring through which the indenter protrudes to bear against the specimen. The indenter is forced against the contact by a spring. When the pressure of the specimen against the indenter exceeds that of the spring the indenter moves from the contact and a circuit is opened which flashes a light. If the load is increased slowly by raising the instrument with the fine adjustment, the load at which the light flashes is very constant. Suitable means are provided for adjusting and measuring the spring pressure from 25 to 500 grams.

As shown in the accompanying pictures the light load makes possible the

use of very small impressions which may be very accurately located, since the indentation may be placed in any desired part of the field within 0.0001 inch. The indentation may occupy as little as $\frac{1}{16}$ of a field at × 2000. Of course a group of indentations can be made and measured later.

The instrument has two marked disadvantages: repeated use tends to wear out the fine adjustment of the microscope, and the weighing of the load on the indenter is less accurate than is desirable. The first difficulty may be overcome by mounting the instrument external to the microscope and using a transferal

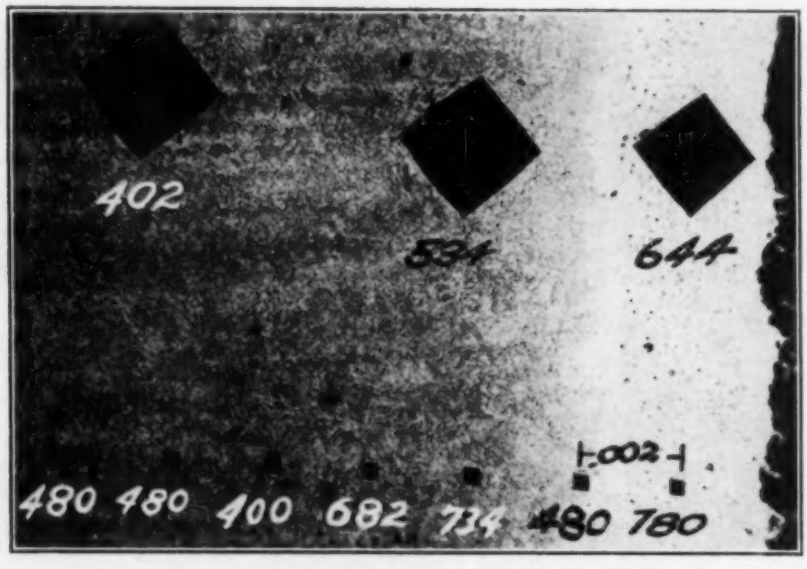

Fig. B—Vickers and Microhardness Indentations Compared. × 100.

stage of the type suggested by Mrs. Brodie. The second difficulty has been overcome by correlating the instrument readings with the Vickers instrument by use of specimens with an exceedingly fine sorbitic structure. Such a correlation is shown in Fig. B. Two specimens suffice to permit calculation of the load using the Vickers formula in reverse and readings may then be calculated using this load over the whole scale of hardness. 100 grams is the load usually used but 25 grams may be used. In the latter case a 0.85 NA objective is used with a filar micrometer to measure indentation size.

Measurements have been of two sorts: comparative, in which case the loads are constant but not carefully determined, and precise to serve as an extension of the Vickers to small areas and specimens. In the field of comparative results surveys have been made through spot welds, coring of cast alloys has been studied, analysis of the structure of heat treated steels for micro-constituents has been made. Precision measurements have been made on the hardness of chromium and nickel platings two thousandths of an inch thick; traverses of nitrided cases have been made and materials in the microscopic field which are different from the ground-mass have been identified. The photographs show some of the cases of applications.

The indentations with the Vickers type indenter are deeper for a given load than the Knoop type indenter, but if a shallow indentation is desired the load

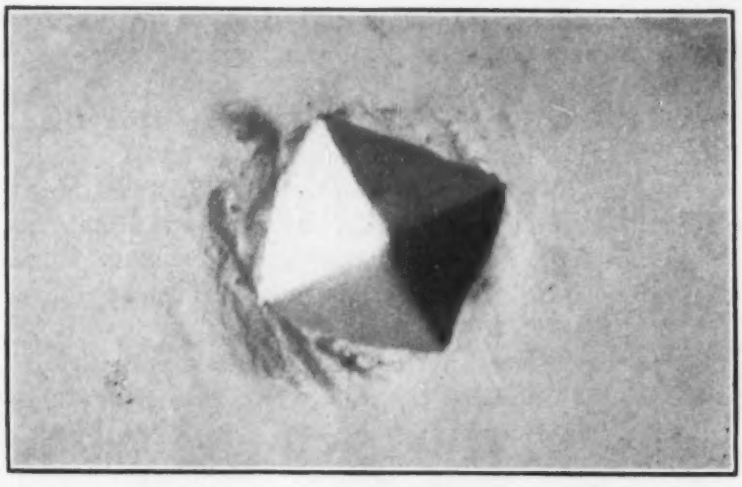

Fig. C—Indentation in Nickel Plate at × 1000.

may be reduced, even to 10 grams with extreme care. This instrument and the "Tukon tester" eventually will probably each be found to have their own special field of application, although it is unfortunate that it is necessary to introduce still another hardness scale into the already complicated situation.

Written Discussion: By C. G. Peters and H. K. Herschman, National Bureau of Standards, U. S. Department of Commerce, Washington, D. C.

Mrs. Brodie's paper was read with interest and we believe that it should add materially to the appreciation of the technique required in making microhardness determinations.

We have provided most of our microhardness machines with cross slides similar to that shown by Mrs. Brodie in Fig. 3b, which facilitate the spotting of selected areas of metallurgical specimens. The microhardness machines developed at the National Bureau of Standards have the beams supported on pivots, knife-edges or flexure plates and apply the load by lowering the weight beam.[3, 4] With these machines we have found tests made with loads of 100 grams or less give hardness numbers which are appreciably higher than those obtained with higher loads. This appears to be in accord with the findings of the author. This result is attributed to work hardening of the surface layer by grinding and polishing during the preparation of the specimen.[5, 6]

However, results obtained at this Bureau on the conventionally operated Tukon tester, which applies the load by raising the pillar which supports the specimen, showed that the hardness numbers obtained with 25, 50 and 100-gram loads were appreciably lower than those obtained with the higher loads. This was attributed to side sway of the pillar which tended to cut the surface laterally simultaneously with the indenting or vertical action of the indenting tool.

To test such machines for this effect, the beam should be brought into balance with the weight pan removed. A 5 or 10-gram weight should be placed

[3] *Journal of Research*, National Bureau of Standards, Vol. 23, July 1939, p. 39.

[4] National Bureau of Standards Circular C433, February 1943, p. 56.

[5] *Journal of Research*, National Bureau of Standards, Vol. 26, March 1941, p. 261.

[6] H. K. Herschman, "The Effect of Moderate Cold Rolling on the Hardness of the Surface Layer of 0.34 Per Cent Carbon Steel Plates," TRANSACTIONS, American Society for Metals, Vol. 31, 1943, p. 501.

on the end of the beam just above the indenter and the machine operated in the usual manner. If an excessively low hardness number is obtained, side motion of the pillar is indicated.

All of the applications listed by Mrs. Brodie on pages 132 and 133 have been successfully made at this Bureau. To this list might be added, small metal pivots and sapphire or glass jewels used in watches and instruments, thin metal sheets and plated layers, and the large list of crystals and materials classed as glasses. For these latter brittle substances the resistance to fracture can also be determined by increasing the load until fractures appear around the indentation.

As an illustration, ordinary pyrex glass fractures with the 100-gram load while the more recently developed alumina glasses may withstand loads up to 4000 grams before fracture occurs.

While the diamond will withstand exceedingly high static pressure it may fracture under relatively light shock. Therefore, in testing hard carbides suggested by the author, application 8, page 133, great care should be exercised to avoid damage to the indenter. For testing diamonds the rate of descent of the indenter should be only about one three hundredths the normal rate of descent and the instrument should be free from vibration while the indenter is in contact with the test surface. It is inadvisable to attempt to test the hardness of diamonds unless the means for resharpening the indenter are available.

Does the author's reference to Diamond Pyramid Hardness, Table I, page 134, refer to tests made on the Vickers machine?

Written Discussion: By Douglas R. Tate, National Bureau of Standards, Washington, D. C.

This paper is of interest to metallurgists as it offers one solution to the problem of accurately locating microhardness indentations on the specimen and of finding the indentation after it has been made. Probably such a transfer stage, a plate which rigidly holds the specimen while it is transferred back and forth between the microscope and tester, offers the best and most practical solution to this problem.

Several types of transfer stage have been developed for transferring hardness specimens from the microscope to the Tukon tester and back. In general it is desirable that once a definite location on the specimen is centered under the cross hairs of the microscope, the stage and specimen can be transferred to the Tukon tester, and an indentation made on the selected location without further adjustment. The stage should be so constructed that the center of the indentation will be within five or ten microns of the selected spot. The stage may then be returned to the microscope and the indentation should appear fairly well centered under the cross hairs, even with magnifications around × 800.

A stage of this type, designed by Dr. L. B. Tuckerman and D. R. Tate, and constructed in the National Bureau of Standards instrument shop, is shown in Figs. D, E and F. The stage has a point-line-plane type of support consisting of three hardened 10-millimeter steel balls set in countersunk holes in both the microscope stage and the Tukon stage, and a countersunk hole, a milled vee groove and a milled plane located on the bottom of the transfer plate.

This transfer stage has the disadvantage that it is necessary to lower the Tukon stage somewhat more for its insertion and removal than in the case of

sliding types of transfer stage, but it has the advantage of very precise positioning of the indentation. The transfer stage is equipped with a micrometer screw such that rows of indentations can be made with any desired interval between indentations. The micrometer screw has proved a very useful feature of the stage. Very likely the manufacturers of the Tukon tester will in time provide a microscope and transfer stage as a part of the tester.

The author has pointed out in her paper the likelihood of errors due to spacing indentations too close together. Experiments at the Bureau have indicated that spacing of indentations closer than about one and one-half times the

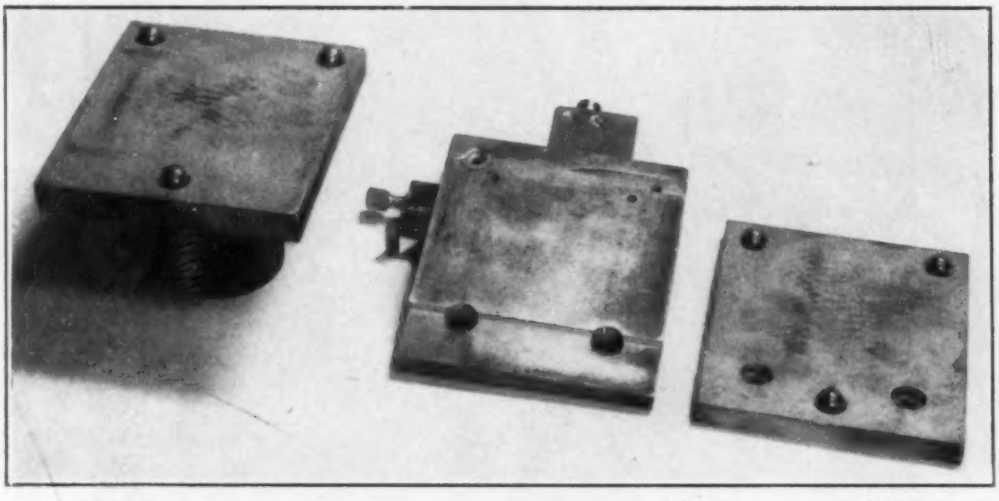

Fig. D

length of the indentation between indentation centers may introduce errors greater than 1 per cent, probably due to cold working in metal specimens. This may be shown very easily by making a row of indentations and then sandwiching indentations in the spaces between the indentations of the first row.

In dealing with small forces, small disturbances which are negligible in comparison with larger forces may become of importance. In our first experiments with the Tukon tester under light loads (less than 200 grams) we obtained results which were inconsistent by a few per cent. These were traced to three causes: vibration transmitted through the frame of the machine, added inertial load caused by lifting the beam and load from its rest, and finally, rocking of the indenter caused by lateral motion of the column which supports the specimen. These produced no appreciable errors with loads of 300 grams and higher, but caused increasing irregularity with smaller loads.

The largest part of the trouble came from vibration transmitted from the control box through the supporting table to the frame of the tester. These were eliminated by placing the control box upon an independent support separated from the table.

The added inertial load was eliminated by a solenoid device designed by D. R. Tate which prevents the application of the full load to the indenter until the lifting mechanism has ceased to operate. This is housed in the cylindrical case shown at the top in Fig. F.

The rocking of the indenter was reduced to a negligible value by a spring

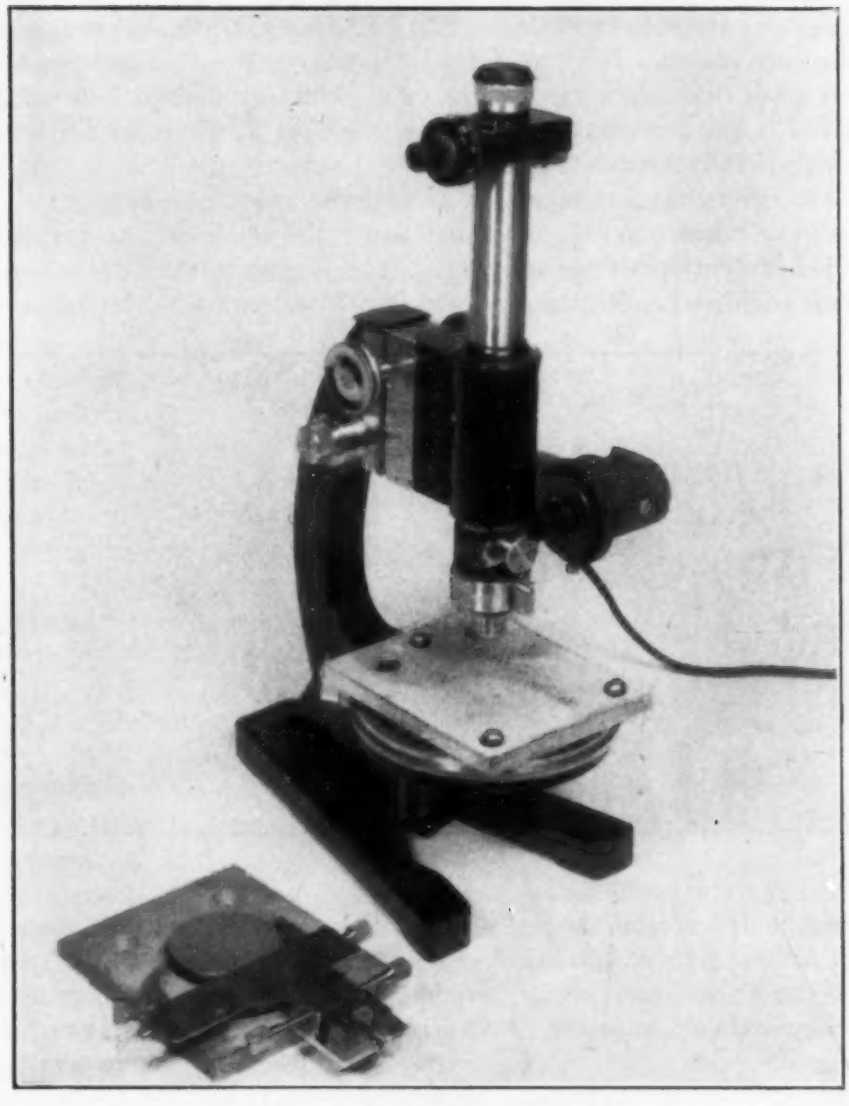

Fig. E

attached to a torque arm on the elevating screw, which prevents play of the screw in its bearing during the raising of the specimen. A careful check with these devices and precautions has shown no appreciable effects of vibration, inertial overload or lateral play under loads as low as 25 grams.

It may of course be expected that very large errors will be present in tests made in machines not properly maintained. Experience has shown that machines such as the Tukon tester and the standard and superficial Rockwell hardness testing machines should be frequently lubricated with particular attention paid to the elevating screw.

It is of interest to compare indentations made with Knoop and Vickers diamond pyramid indenters under equal loads. Fig. G shows Knoop and Vickers indentations made under loads of 100, 500, 1000 and 3000 grams for each indenter. The indentations were made on a polished block of stainless steel having a Knoop number of about 550 for a 1000-gram load. For a given load

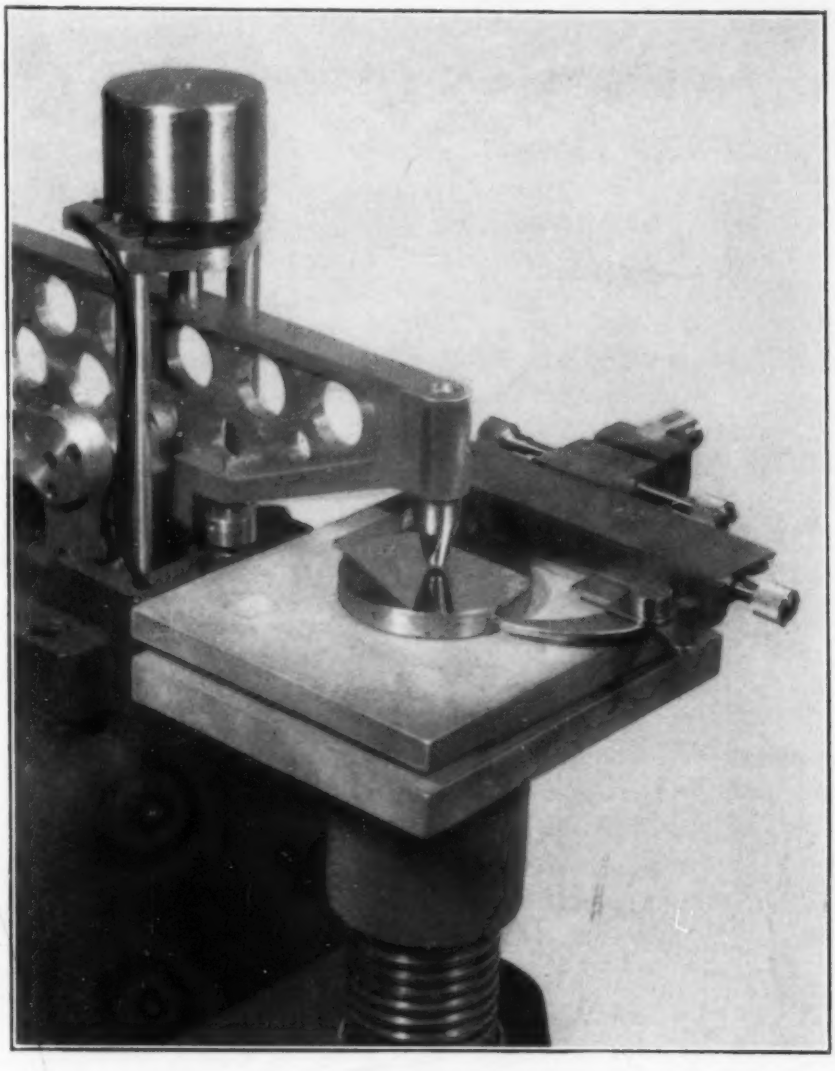

Fig. F

on a uniform material, the Vickers indenter penetrates almost twice as far into the specimen as the Knoop indenter and the diagonal of the Vickers indentation will be on the order of one-third the length of the Knoop indentation. This means that the Vickers test is less sensitive to surface conditions than the Knoop test and that for equal loads the Vickers indentation, because of its shorter length, is more affected by the experimental errors in measuring the indentation.

Since the length of the indentation appears as a second power term in the formulae for the hardness number for both these tests, the percentage error in determining the hardness number is about twice the percentage error in measuring the indentation. The Knoop test offers, therefore, a considerable advantage in microhardness work under very low loads.

The author has mentioned the fact that Knoop hardness readings tend to be slightly high at low loads. Experiments on this effect have also been made at the National Bureau of Standards under loads as low as 25 grams in a Tukon tester equipped with the solenoid device to eliminate errors due to inertia. The

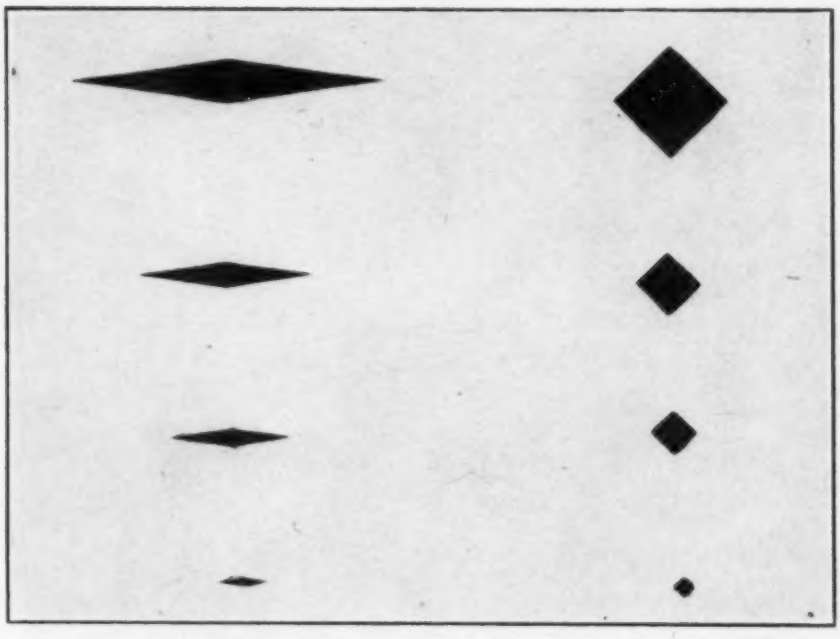

Fig. G

following results were obtained from measurements of a set of fifty indentations made in a polished block of stainless steel with Knoop and Vickers indenters both used in the same Tukon tester.

Load Grams	Length of Indentation — Knoop Microns	Length of Indentation — Vickers Microns	Hardness Number — Knoop	Hardness Number — Vickers
3200	291.1	105.4	537	534
800	141.0	52.0	573	549
200	67.4	25.7	626	562
50	32.1	12.9	690	557
25	21.5	9.3	770	536

The data above represent the average of five indentations for each indenter with each load. The Vickers number appears to be almost independent of the load while the Knoop number increases with decreasing loads.

Under loads of 3200 grams the Knoop and Vickers indenters gave approximately the same number, about 535; under loads of 25 grams the Knoop number was 770, while the Vickers number was 536. The Knoop number increased steadily with decreasing load, while the Vickers number varied from about 535 to 560.

Oral Discussion

C. B. SADTLER:[7] I would like to call attention to the part of the paper that relates to the unrecovered areas. For my part, I am very much in the dark about how unrecovered areas are determined, and what proof there is of their existence. I wonder if Mrs. Brodie can throw a little light on that?

[7]Metallurgist, Barber-Colman Co., Rockford, Ill.

Author's Reply

The author wishes to thank the discussers for their interest and contributions which add considerably to the value of the paper.

In reply to Mr. Hill, Lieut. Casey and Mr. McGee, I have had no personal experience in the operation of the Eberbach tester.

Mr. Hubbard's remarks about the different hardness values obtained on chrome plates explains the variation in hardness which we have observed on similar samples. In our case the range of hardness varied from 900 to 1200.

The Knoop hardness numbers in Table I cover the range of hardness obtained with loads varying from 100 to 2000 grams. Hardness readings were

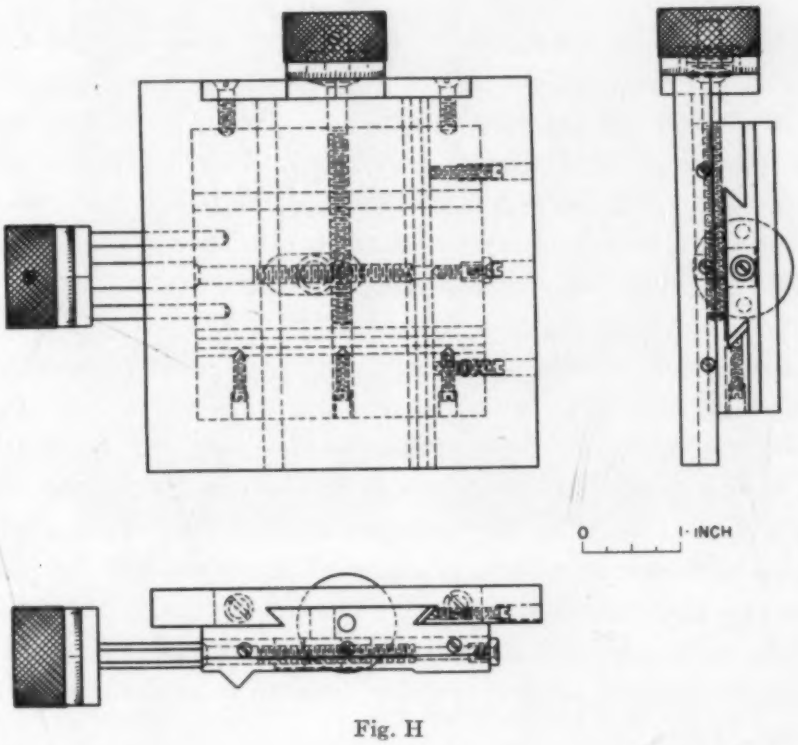

Fig. H

essentially constant for loads greater than 200 grams. Whenever a range is given in the table, the spread takes into account the difference in hardness obtained with the 100-gram load and other loads.

In reply to Mr. Peters and Mr. Herschman, the diamond pyramid indenter was used in the Rockwell machine with a 25-kilogram load.

In answer to Mr. Sadtler, Knoop, Emerson and Peters in National Bureau of Standards Research Paper RP1220 from *Journal of Research* of National Bureau of Standards, Volume 23, July 1939, reported observations which led them to the conclusion that there was little or no difference in the length of the long diagonal while the load is on or when it was taken off. I have not investigated this personally.

Since there has been considerable interest in the transferable stage mentioned in the paper, the drawing for it is shown in Fig. H.

INTERCRYSTALLINE COHESION OF METALS

By E. R. Parker

Abstract

The investigations and theories concerning high temperature intercrystalline failures are reviewed. New data are given which illustrate the various types of high temperature fractures. The theories of the structure of crystal boundaries are discussed and their limitations cited. A new suggestion is made concerning the mechanism of intercrystalline failures.

ROSENHAIN (1)[1] and others found that when a metal fractures in a rather slow tensile test at high temperatures the path of the fracture is around the crystals rather than through them as normally occurs in metals fractured at low temperatures. Fig. 1a shows a low temperature transcrystalline fracture and Fig. 1b shows an intercrystalline fracture characteristically obtained at high temperatures. Rosenhain's view was that at ordinary temperatures the boundaries are much stronger than the crystals so that deformation and fracture occur within the crystals. As the temperature of deformation is increased, a temperature is reached where this relationship is reversed and the boundaries yield more readily than the mass of the crystal. He concluded that the crystals are held together by a film of metal in the amorphous condition. This amorphous material he considered as being softened more rapidly by temperature than the crystalline material. The amorphous cement theory conveniently explained the fact that at temperatures near the melting point, metals broken under tension fracture around rather than through the crystals.

Jeffries (2) extended this work and developed the concept of "equi-cohesive temperature", the temperature above which failure occurs through the boundary material rather than through the crystals.

Low temperature fractures of metals are transcrystalline (except in special cases such as an alloy having a brittle network surrounding the crystal), while high temperature failures may be either

[1]The figures appearing in parentheses pertain to the references appended to this paper.

A paper presented before the Twenty-fifth Annual Convention of the Society, held in Chicago, October 18 to 22, 1943. The author, E. R. Parker, is associated with the Research Laboratory, General Electric Co., Schenectady, N. Y. Manuscript received June 24, 1943.

transcrystalline or intercrystalline, depending upon the rate of straining. Transcrystalline fractures may be produced at temperatures near the melting point by very rapid straining, while slower strain rates (produced by lower loads) will cause intercrystalline fractures. It thus becomes apparent that time is a factor in high temperature intercrystalline failures, and, as Jeffries (2) points out, the equicohesive temperature represents only one rate of straining or duration of loading. Thus it is not a definite temperature unless assigned

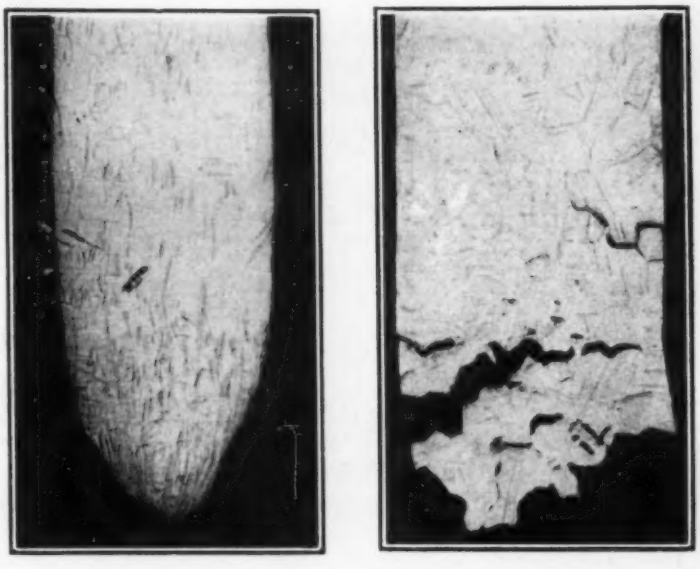

Fig. 1a (left)—A Low Temperature Transcrystalline Fracture of a Copper Bar. × 7.
Fig. 1b (right)—A High Temperature Intercrystalline Fracture of a Copper Bar. × 7.

a definite time for fracture. At temperatures near the melting point, intercrystalline fractures can occur in stressed metal in a relatively short time. As the temperature is lowered, longer times of stressing are necessary to cause such failures. Fig. 2 shows the log-log plot of stress versus time to fracture of a steel at three temperatures. The short time fractures are transcrystalline while the long time fractures are intercrystalline. The time under stress required to cause intercrystalline failures is greater as the temperature is lowered. The change in the *slope* of the lines where intercrystalline failures begin is due to the life shortening effect of intercrystalline oxidation (3), which occurs coincidently with the intercrystalline cracking in an oxidizing atmosphere such as air. In the absence of oxidation, the rupture curve does not change slope, but intercrystalline failures begin to occur at the same stress and life. There is no

theoretical reason for the existence of a minimum temperature at which intercrystalline failures may occur. All failures involve the thermal movement of atoms and are influenced by the stress. At any temperature, a minimum time characteristic of the temperature is necessary to allow intercrystalline failures to occur. The mobility of atoms decreases gradually with temperature so that progressively longer times are necessary for intercrystalline failures to occur as the temperature is lowered. As shown in Fig. 2, the minimum time required for intercrystalline failure increases rapidly as the tempera-

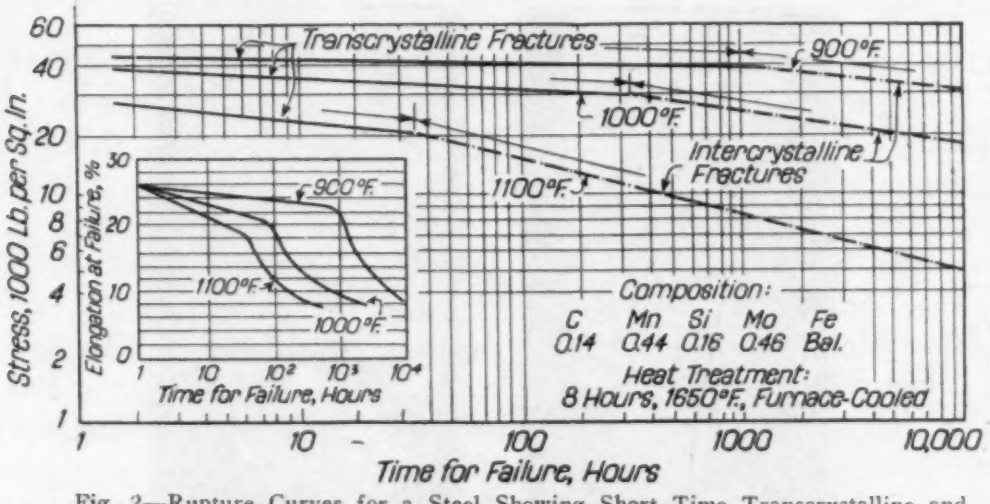

Fig. 2—Rupture Curves for a Steel Showing Short Time Transcrystalline and Long Time Intercrystalline Fractures.

ture is lowered, so that for all practical purposes there is a temperature below which intercrystalline failure will not occur (at least within a normal lifetime!).

The total elongation at failure is also shown in Fig. 2 as a function of time. The elongation drops slowly at first, and then more rapidly when intercrystalline failures begin to occur. Intercrystalline failures generally occur with less ductility than transcrystalline failures. In extreme cases, intercrystalline failures may occur without appreciable deformation of the crystals, and thus appear to be "brittle" fractures. Generally, however, the crystals do deform considerably while under load and the final elongation may be fairly high. This is evident in Fig. 2 which shows elongations between 10 and 20 per cent for many of the test bars showing intercrystalline failures.

The grain boundaries are a source of weakness at high temperatures, and a source of strength at low temperatures. Consequently, at ordinary temperatures a small crystal size will be characterized

by high strength, while at high temperatures large crystals are desirable. With rising temperature a point is reached where small and large crystal structures have equal strength (for a fixed time under stress). This temperature Jeffries and Archer (2) consider to be the equi-cohesive temperature.

The recrystallization temperature has sometimes been assumed to be the same as the equi-cohesive temperature. This assumption seemed justified because experimentally determined recrystallization and equi-cohesive temperatures were very nearly the same. However, more recent work has shown that this is a coincidence, common to most metals and alloys. Fig. 3 shows rupture curves at three temperatures for a 13 per cent chrome-iron, one of the exceptions. This material will recrystallize at 1100 degrees Fahr. (595 degrees Cent.), yet all failures were transcrystalline within the time limit of the test (17,000 hours). A similar case was observed with 2S aluminum which required prolonged loading above 750 degrees Fahr. to cause intercrystalline failures; this material recrystallizes below 400 degrees Fahr. (205 degrees Cent.).

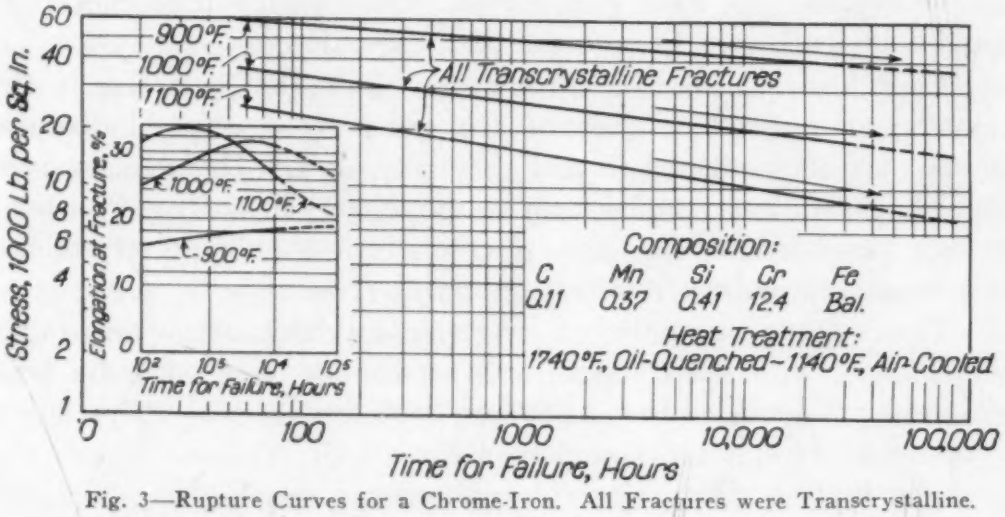

Fig. 3—Rupture Curves for a Chrome-Iron. All Fractures were Transcrystalline.

At high temperatures, it seems that two processes are occurring simultaneously in a material under stress. Creep is occurring within the crystals, and intercrystalline deformation is forming minute imperfections which may eventually grow to such magnitude that intercrystalline failure occurs. The crystals of some materials such as the 13 per cent chrome-iron and the 2S aluminum seem to creep at a faster rate than intercrystalline imperfections can form and grow. In such cases, failure occurs by creep within the crystals before intercrystalline failure has time to occur.

The volume of the boundary material is minute compared with the volume of the crystalline material, and the independent flow of the boundary material is greatly limited by the irregularly shaped crystals. Hence it seems unlikely that creep within the crystal boundaries can contribute measurably to the total creep. It is thought, however, that crystal boundaries have a profound influence on the creep of the crystals, because such boundaries appear to be sources of dislocations which travel through the crystals causing creep. Thus the boundaries may contribute indirectly to the creep of the crystals but extension within the boundary transition zone could contribute very little to the total extension.

In a material like the chrome-iron that fails by creep of the crystals, intercrystalline failures can occur if by some means the crystals are strengthened so that they creep less. This can be done by adding sufficient molybdenum to the alloy. In chrome-iron containing molybdenum, the rate of creep is less and intercrystalline failure may occur before failure occurs by creep.

The relative strengths of crystals and boundaries vary with temperature, with the composition of the alloy, and with the heat treatment. The elongation at failure is determined by the relative strengths of crystal and boundary materials.

The study of high temperature fractures was begun before the turn of the century. It was Beilby's (4) theory of the amorphous state of solid metals that started Rosenhain on his classic studies of the structure of the grain boundaries. As a result of his studies, Rosenhain concluded that the crystals in metal are held together by a film of metal in the amorphous condition. This film acted as a cement, holding the crystals together. According to Rosenhain (5) "the amorphous condition is one in which the crystalline arrangement of the molecules is completely broken up, so that the molecules remain in a state of irregular arrangement similar to that which is supposed to exist in the liquid state." As Rosenhain (5) pointed out, the theory of an amorphous cement between crystals has not received general acceptance. However, the amorphous cement theory did provide a simple means of explaining many phenomena associated with the deformation of metals. Beilby conceived the idea that deformation on slip planes produced local disturbances of arrangement thus forming a thin layer of amorphous metal which was mobile during the time slip was occurring, but afterwards would set and become a hard non-plastic layer which would prevent further slip from taking place on that plane. The crystals would then slip on

other planes and become progressively harder until all the planes were used up, then fracture would occur.

Since the early work of Beilby and Rosenhain, a number of experimental facts have been presented which are not in accordance with the amorphous metal theory. The most important of these are summarized below:

1. Experiments of Taylor and Elam (6) on the deformation of single crystals have shown that slip planes not participating in the deformation are often strengthened *more* than the planes on which slip occurred—an impossible condition if the amorphous cement theory were correct.

In this work, tensile tests were made on single crystals of various materials. Some crystals were so oriented that slip first occurred on one plane then, after some deformation, slip started on a second plane. The stress required to cause slip to start on the second plane was often found to be *greater* than that required to cause slip to *continue* on the already strained first plane. According to the amorphous theory of strain hardening, the second plane should not have been strengthened by slip on the first plane.

2. In a precipitation hardened copper alloy containing iron, the iron (solid solution) first precipitates as a nonmagnetic phase (7), presumably as face-centered gamma iron, instead of the magnetic body-centered alpha iron as the phase diagram would indicate. Probably the face-centered structure of copper influences the lattice of the precipitating iron so that it remains nonmagnetic even when the particles are large enough to be seen microscopically. If an amorphous material existed at the crystal boundaries (in this case, phase boundaries) no such continuity of structure could exist.

3. Certain conclusions can be drawn from the work on thin films (8, 9). Studies of thin films of platinum condensed on glass have shown that crystals from as small as ten to twenty atoms across (instead of forming an amorphous film.) The work of Suhrmann & Barth (9) indicates that some metal vapors condensed into thin films become crystalline at temperatures as low as 100 degrees K. Thin films, however, often show anomalous structures, sometimes differing considerably from the normal crystal structure. The environment of atoms in thin films is much different from that in crystal boundaries, so conclusions from work on thin films should be drawn with caution.

Electron diffraction studies of polished metal surfaces may eventually lead to an understanding of the structure of the Beilby

layer. At the present time, however, the interpretation of the electron diffraction patterns obtained from polished metal surfaces seems to be questionable (10). Some investigators interpret the patterns as showing an amorphous layer, others as showing a crystalline layer, and still others believe that the pattern is not due to the metal at all, but to occluded gas or an oxide film.

For a more comprehensive discussion of the published work on crystal boundaries, the reader is referred to the critical survey of this subject by Bucknall (11).

Fig. 4—An Electron Micrograph of a Crystal Boundary in Copper. × 10,000. (1mm = 1000Å)

Very little is actually known about the structure of intercrystalline boundaries. No direct methods are available for the study of them, and conclusions concerning their structure must be deduced from indirect measurements, such as the effect of grain size on low and high temperature strength and on damping capacity (12). The modern concept of the crystal boundary structure is that there is a gradual transition across the boundary from one orientation to the other. Thus the positions of crystal boundary atoms form a pattern determined by the neighboring crystals. The width of the crystal boundary is determined by the relative orientation of adjacent grains, being narrow for those having similar orientations, and wide for those differing the most. The actual width of grain boundaries is, of course, not known. Seitz and Read (12) have stated that grain boundaries are probably narrow, i.e., of the order of five atoms wide. Work with the electron microscope may help to establish an upper limit for the width of grain boundaries. Fig. 4 shows an electron micrograph of a grain

boundary in copper which is perpendicular to the polished surface. The effect of the boundary on the etching of the adjacent grain seems to extend less than 75 atoms into the grains.

The crystal boundary atoms are arranged in a less symmetrical way than atoms within the crystals; consequently, they are less densely packed, less tightly bound. Because of the unsymmetrical atomic arrangement, crystal boundaries have no "slip planes" and

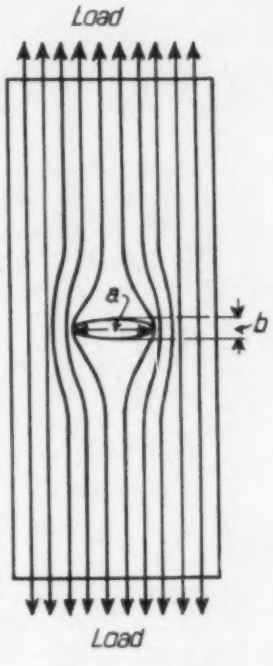

Fig. 5 — The Stress Concentrating Effect of an Elliptical Hole in a Flat Plate Subjected to a Tensile Load. The Stress Concentration is $(1 + 2\frac{a}{b})$

are difficult to deform at low temperatures. However, the transition zone between crystals is continuous from one grain to the next, and can transmit deformation whenever sufficiently stressed.

The atoms of the transition zone between crystals are influenced by temperature more than the atoms of the crystals because they are less strongly bound. At high temperatures, they may become active enough to be moved by low stresses, provided, of course, that sufficient time is allowed for the thermal movement of the atoms to act in the direction of the stress. Less energy is required for the atoms to move in the direction of the stress than

against it (13); so movement of atoms is more probable in the direction of the maximum shear stress (45 degrees to the tensile stress). Fig. 6 indicates a condition in a hypothetical crystal boundary which might be the origin of intercrystalline failures. This schematic picture postulates the existence of imperfections in the boundary material. These imperfections may be voids where a few atoms are missing from the structure. Presumably, such imperfections could result from a concentration of dislocations in the crystal boundaries. Foreign material, such as minute nonmetallic impurities, or any type of atomic discontinuity would act as imperfections.

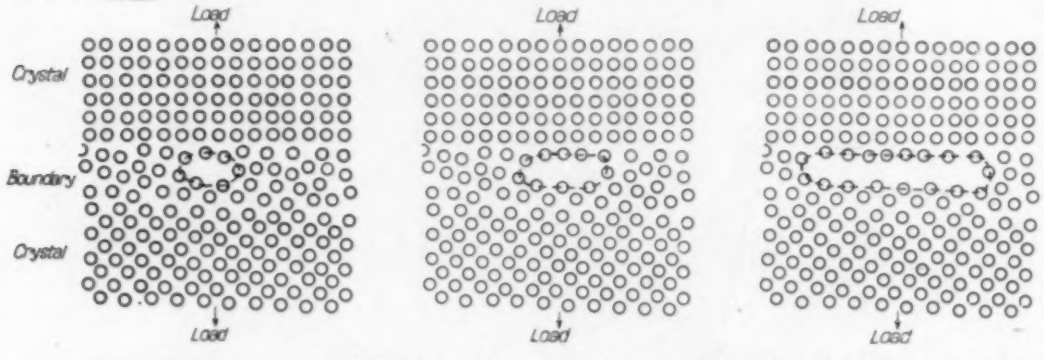

Fig. 6—Suggested Mechanism of the Growth of a Discontinuity in a Crystal Boundary Due to a Tensile Load.

The stress concentrating effect of an elliptical hole in a flat plate subjected to a tensile load is shown schematically in Fig. 5. Even in ductile materials such a stress raiser causes the material to fail along the long axis of the elipse. Similarly, intercrystalline cracks generally form in the plane of maximum tensile stress (see Fig. 1b).

A similar stress concentration would exist around imperfections in the crystal boundaries of metals. Fig. 6 shows the progress of the growth of a hypothetical imperfection in a crystal boundary into an intercrystalline crack. When loaded, the atoms at the sides of the imperfection are under higher than average stress. Local fluctuations of thermal motion of atoms occasionally cause the highly stressed atoms to move in the direction of the maximum shear stress (the easiest direction of motion). These atoms find it more difficult to move back against the stress. This atomic movement shifts the high load to the next neighboring atom which undergoes, after a time, a similar movement, and thus the imperfection grows along the crystal boundary, eventually becoming a

crack. Other cracks form and meet, finally causing intercrystalline failure. Whenever the crystals are strong and resist creep, the stress is higher at the edges of the imperfections, thus increasing the probability that intercrystalline cracks will grow. If the crystals deform rapidly, high local stresses cannot form near the flaws and the cracks would grow slowly (e.g. 13 per cent chrome iron, the crystals of which creep a great deal before fracture).

The foregoing discussion is offered as a simplified explanation (perhaps too simplified!) of the mechanism of intercrystalline fractures. A more comprehensive theory seems unwarranted at the present time since we know so little about the actual structure of crystal boundaries.

Acknowledgments

The author wishes to express his appreciation to the Turbine Engineering Department of the General Electric Company for the use of the rupture curves and to Mrs. C. B. Brodie for the photomicrographs.

References

1. W. Rosenhain, Discussion of paper by Bengough, *Journal,* Institute of Metals, No. 1, 1912, p. 123-190.
   W. Rosenhain and D. Ewen, "Intercrystalline Cohesion in Metals," *Journal,* Institute of Metals, No. 2, 1912, p. 149-185.
2. Zay Jeffries, "The Amorphous Metal Hypothesis and Equi-cohesive Temperatures," *Transactions,* American Institute of Metals, 1917, p. 300.
   Zay Jeffries and R. S. Archer, *"The Science of Metals,"* McGraw-Hill.
3. R. H. Thielemann and E. R. Parker, "Fracture of Steels at Elevated Temperatures After Prolonged Loading," *Transactions,* American Institute of Mining and Metallurgical Engineers, Vol. 135, 1939, p. 559.
4. G. T. Beilby, "The Hard and Soft States in Metals," *Journal,* Institute of Metals, No. 2, 1911, p. 5-43.
5. W. Rosenhain and J. L. Haughton, "An Introduction to the Study of Physical Metallurgy," 1935.
6. G. I. Taylor and C. F. Elam, "The Plastic Extension and Fracture of Aluminum Crystals," *Proceedings,* Royal Society, Vol. A108, 1925.
   C. F. Elam, "Deformation of Metal Crystals," Oxford University Press.
7. R. B. Gordon and M. Cohen, "Age Hardening of a Copper-Cobalt and a Copper-Iron Alloy," *Age Hardening of Metals,* American Society for Metals, 1940, p. 161.
8. G. P. Thompson, N. Stewart and C. A. Murison, "The Crystalline State of Thin Sputtered Films of Platinum," *Proceedings,* Physical Society, Vol. 45, 1933, p. 381.
9. R. Suhrmann and G. Barth, "Über die Änderung des Elektrischen Widerstandes und des Reflexionsvermögens von bei tiefer Temperatur Kondensierten Metallspiegeln," *Zeit. f. Physik,* Vol. 103, 1936, p. 133.
10. M. L. Fuller, "Electron Diffraction Effects from Polished Zinc Surfaces," *Transactions,* American Institute of Mining and Metallurgical Engineers, Vol. 133, 1939, p. 253.

11. E. H. Bucknall, "The Boundaries of Metal Crystals—A Critical Review," *Metal Industry*, Vol. 49, July-Dec. 1936, p. 311, 369, 396.
12. F. Seitz and T. A. Read, "The Theory of the Plastic Properties of Solids —Part IV," *Journal*, Applied Physics, Vol. 12, No. 7, p. 538.
13. G. I. Taylor, "The Mechanism of Plastic Deformation of Crystals," *Proceedings*, Royal Society, Vol. 145, 1934, p. 388.

DISCUSSION

Written Discussion: By S. L. Hoyt, technical adviser, Battelle Memorial Institute, Columbus, Ohio.

The problem of grain boundaries and intercrystalline cohesion remains very much of a mystery though it is over thirty years since Rosenhain proposed his amorphous cement hypothesis. Even today it seems as though his picture is at least partially consistent with the behavior of grain boundaries. Its function was to account for the grain boundary as a source of strength at low temperatures and as a source of weakness at high temperatures, when slowly loaded. For rapid loading, the high resistance of amorphous bodies was brought into play though, if we are to use that analogy, some modification is needed to explain why the metal is ductile, since an amorphous material is known to be brittle under the same circumstances. Thus, while agreeing that Rosenhain's hypothesis "explained" high temperature strength, we can complain that it is not as successful with ductility. On the other hand, his assumption of a film of truly amorphous metal of the order of a hundred atoms thick (to account for the higher rate of evaporation of fine-grained metal) is no longer accepted. Furthermore, I have heard it asserted by a good authority that the so-called "strong grain boundary" effect is apparent rather than real and is to be accounted for on the basis of the slip process of polycrystal metal.

The information presented by the author I believe to be well chosen to present the problem of high temperature behavior, but I feel the argumentation can be improved upon by some modification. First of all, the concept of "equicohesive" temperature has lacked precision because it was incorrectly stated. When the stress is increased, the alternatives are intercrystalline rupture and *slip*, not transcrystalline failure. When slip occurs, as in rapid loading, the grains stretch out and, while ultimately the fracture is transcrystalline, the conditions of strain hardening and grain geometry are so drastically modified that this cannot be an alternate to intercrystalline failure with little or no deformation. It seems to me it would be more profitable to focus attention on the strength or properties of the metal in its initial condition, before it has undergone the amount of deformation represented by ductile extension and fracture. Viewed in this light, the grains can either (1) pull apart, (2) fracture, or (3) deform by slip. With the common FCC metals and fast loading, we have only Case 3 at all temperatures; for slow loading, Case 1 enters at elevated temperatures. With common steel, the situation is different in one particular, because, at some low temperature, failure is by fracture through the grains, Case 2. The latter is the only case known in which the grain can be said to show evidence of being weaker than the grain boundary. I think it is clear that for Case 3 we can know nothing about the relative strength of the grain and the grain boundary. What the situation is after deformation starts must be a second problem.

Turning to the evidence cited against the amorphous metal theory, I have advanced the author's first point myself,[2] but to show that Beilby's picture of strain hardening was wrong, not Rosenhain's amorphous cement theory. It may be recalled here that this line of reasoning applies to single crystals, in which there is no grain boundary or amorphous cement. In other words, while Point 1 refutes Beilby's hypothesis of amorphous metal forming along slip planes, it has no bearing, that I can see, on Rosenhain's.

By and large, as the author points out, little is known about grain boundaries, and I wonder if that is not the proper way to leave the matter—at least until we do know something about them. The proposal advanced seems to be an adaptation of Taylor's "dislocation" hypothesis; both may be right and both may be wrong. Until plausibility of these assumptions is demonstrated, or until they are given truly adequate indirect support (like Dalton's atomic hypothesis) and are shown not to conflict with direct evidence, they must remain assumptions of very dubious validity.

Since the above was written, Dr. Barrett has stated in oral discussion that the author's Point 1 is not convincing. If amorphous metal forms along primary slip planes, it must also form on the secondary slip planes at the intersections. Thus, primary slip would strengthen the secondary planes too. It seems to me this overlooks the point made originally (1) that the secondary planes are actually *stronger* than the first. Dr. Barrett's idea could explain, it seems to me, an increase for the secondary planes over the initial condition, but not the amount actually observed. As long as slip is pictured as block movement along slip planes—as Beilby did—the amount of amorphous metal which forms on the inactive or secondary slip planes must, by geometry, be less than that produced on the active slip planes. However, if more evidence against Beilby's hypothesis (not Rosenhain's) is required, I would cite the rotation of the slip planes of zinc single crystals which simply cannot be transmitted from one block to its neighbor through amorphous metal.[3]

Oral Discussion

C. S. BARRETT:[4] I should like to ask what etchant was used in preparing Fig. 4. The etchants that have been tried on polycrystalline copper at Carnegie Tech[5] have produced interesting mosaic-type patterns when viewed in the electron microscope using the polystyrene-silica technique. Fig. 4 shows no structure of this type, and I wonder whether the difference lies in the etchant, the sample, or the technique of replica preparation.

The grain boundary in Fig. 4 is perhaps the narrowest in any photomicrograph that has been published, so it is important to know just how certain the author is in his identification of this marking as being an actual grain boundary,

[2]S. L. Hoyt, "Metallic Single Crystals and Plastic Deformation," TRANSACTIONS, American Society for Metals, Vol. 24, 1936, p. 789.

[3]*Transactions*, American Institute of Mining and Metallurgical Engineers, 1927, *Proceedings*, Institute of Metals Division, p. 116.

[4]Associate professor, Department of Metallurgy, Carnegie Institute of Technology, Pittsburgh.

[5]C. S. Barrett, "Metallography with the Electron Microscope," American Institute of Mining and Metallurgical Engineers Technical Publication 1637, *Metals Technology*, September, 1943.

rather than, say, a twin boundary, or even an edge of a torn and folded formvar replica.

The author's Point 1, page 155, has never been a convincing argument. If any amorphous metal is produced at a slip plane by the movement of one block over another, it would be expected to lie as a thin layer along the slip plane. Since the parallel slip planes of a set are separated from each other by distances of several hundreds or thousands of angstroms, it would be possible for new slip planes, parallel to the first ones, to form between the first ones. The new slip planes would not encounter any of the hypothetical amorphous metal left by the first slip planes of the same crystallographic set. On the other hand, if new slip planes of another set that lies at an angle to the first set become active, these planes will cut through the first set and would encounter any amorphous layers produced along the first set, hence should have higher slip resistance than continued slip on the first set. Now I do not maintain that this higher slip resistance that is observed on the second planes proves that amorphous layers must exist along the first planes; I merely contend that it does not *disprove* the theory. Another point of view—more attractive to me—is that a thin layer of cold-worked metal is left along the plane where slip occurs, this layer containing centers of high (microscopic) residual stresses which oppose further deformation along any slip plane that encounters the stresses.

C. ZENER:[6] I wish to point out a type of stress concentration[7] which Mr. Parker has not spoken of. If one assumes that the grain boundaries are perfectly homogeneous but that their resistance to slip is less than the resistance of the interior of the grain, then one will get a situation where automatically the stress becomes concentrated on the grain boundaries. How this occurs one may best see by imagining a checkerboard arrangement of grains. The slip along grain boundaries will occur only where the shearing stress is large, that is, along those boundaries making an angle of nearly 45 degrees with the axis of tension. This inhomogeneity of shearing strain will automatically give rise to a concentration of normal stress at the grain boundaries, particularly at the corners where the grain boundaries are restricted.

Authors' Reply

I should like to take this opportunity to thank Dr. Hoyt, Dr. Barrett and Dr. Zener for their interesting discussions of this paper. These discussions add materially to the value of the paper.

The reagent used for etching the copper sample shown in Fig. 4 was the potassium bichromate etch listed on p. 1472 of the A.S.M. Metals Handbook. This reagent develops an etched surface on copper that is apparently smooth; no structure is visible in the formvar replica except grain boundaries, twin boundaries and similar regions where differences in elevation exist. The marking shown in Fig. 4 is, we believe, a grain boundary. The irregularity of the line, which can easily be seen in the electron micrograph, indicates that it is not a twin boundary. We were able to follow the line on the original formvar replica until in joined another grain boundary.

[6] Senior physicist, Watertown Arsenal, Watertown, Mass.

[7] C. Zener, "Theory of Elasticity of Polycrystals with Viscous Grain Boundaries," *Physical Review*, Vol. 60, 1941, p. 906.

PLASTIC FLOW AND RUPTURE OF METALS

By C. Zener and J. H. Hollomon

Abstract

This paper constitutes an attempt to co-ordinate and interpret the present knowledge of the plastic flow and rupture of metals. Certain of the data found in the literature required the introduction of new concepts for their explanation. New models have been suggested which appear to co-ordinate better the existing knowledge in this broad field.

Two systems have been in common use for specifying (a) the conditions for the initiation of plastic flow, (b) the precise nature of flow under a given stress pattern, (c) the relation between the strain hardening occurring in different types of flow. In this paper these two systems are discussed in detail, and a comparison is made between their predictions and the experimental observations. A new theoretical treatment is given of the application of these systems to the problem of strain hardening.

Almost insuperable difficulties prevent the direct determination of the relation between stress and strain at high rates of strain. An indirect method is proposed whereby this information may be easily obtained.

Inexplicable phenomena in metals have frequently been disposed of by the assumption of imperfections. In this paper many phenomena not previously understood are shown to be explicable in a qualitative manner by a single type of imperfection which may be quite precisely defined, namely by the concept of microscopic cracks. These phenomena include: the decrease in the rate of strain hardening in torsion at large strains compared with the strain hardening in tension, the elongation which accompanies large angles of twist, the effect of a prior twist upon the type of tensile fracture. A quantitative analysis, first suggested by Griffiths, is applied to these cracks. This analysis attempts a correlation of the fracture stress with the size of these micro cracks which are correlated with certain elements of the microstructure.

The statements or opinions expressed in this article are to be considered those of the authors and do not necessarily express the views of the Ordnance Department.

A paper presented before the Twenty-fifth Annual Convention of the Society, held in Chicago, October 18 to 22, 1943. Of the authors, C. Zener is senior physicist, Watertown Arsenal, and J. H. Hollomon is 1st Lt., Ordnance Department, Watertown Arsenal, Watertown, Mass. Manuscript received May 13, 1943.

A KNOWLEDGE of the plastic and rupture properties of metals are of utmost importance in many engineering applications, yet these properties have apparently not received their fullest fundamental consideration by metallurgists and physicists.

The object of this paper is therefore to review and correlate the existing information concerning the plastic and rupture properties of metals. In many instances it was found necessary to fill certain of the gaps in the knowledge with data from simple experiments and with new interpretations of older experiments. Certain of these additions have been made and reported in the appropriate positions in the treatise. It is hoped that this paper will be of use not only as a source of information to metallurgical engineers, but will be a stimulant to further investigation.

The terms elasticity and plasticity are used by physicists and metallurgists to denote rather vaguely defined properties of solids. This vagueness is not due to any lack of mental astuteness on the part of those who have written upon the subject, but rather to the versatile behavior of the solids, particularly of metals. Precise definitions of elasticity and plasticity would automatically exclude all real metals, for no metals accurately obey precise laws. It is therefore considered wiser not to attempt to state how a given metal behaves in states of elasticity or plasticity, but to describe the properties of an idealized metal. A metal will then be said to be more or less elastic, or plastic, according to how closely its properties correspond to those of the idealized material. The idealized material will be so defined as to have the gross characteristics of real materials.

The first part of the stress-strain curve (A-B, Fig. 1) of the idealized material is associated with the elastic state. It is considered to have the attributes of linearity and of reversibility. These attributes are not revealed completely by any actual metal. The first part of an actual stress-strain curve may appear to be linear if determined in the usual manner, but more sensitive measurements reveal an observable, though often small, departure from a straight line. Likewise, the first part of the stress-strain curve may appear to be reversible if examined with the usual instruments. Strict reversibility, however, implies the absence of any hysteresis, yet metals have hysteresis as is manifested by their property of damping elastic vibrations. For the idealized material, the slope of the initial part of the stress-strain curve is considered to be independent of rate of deformation. In actual solids this slope varies with rate of

strain, the slope associated with rapid adiabatic deformation being about 0.3 per cent steeper than that associated with slow isothermal deformation.

Considering the idealized metal, in the part of the stress-strain curve associated with the plastic state (beyond B in Fig. 1), the relation between stress and strain is given by a curve which may be,

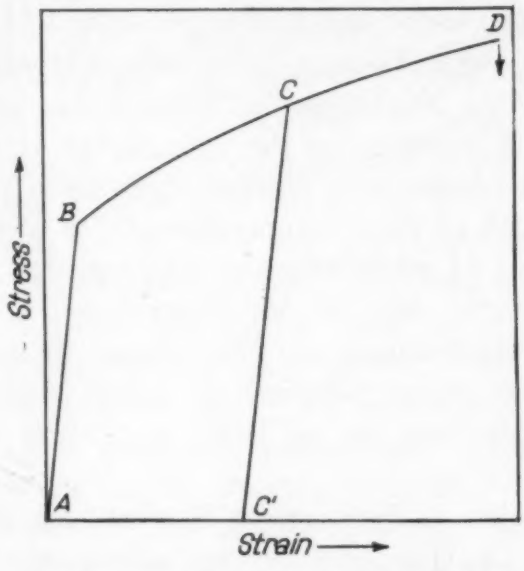

Fig. 1—Stress-Strain Curve for Idealized Material.

though infrequently is, linear and whose slope is everywhere much less than that associated with the elastic state. The essential attribute of this part of the stress-strain curve is its irreversibility. This characteristic property of the plastic state is not evident when the metal deforms upon application of an increasing stress, but is apparent only when the applied stress is decreased. If the stress is increased up to the value associated with C in Fig. 1, and then reduced to zero, the idealized metal will describe the path C-C′, which is parallel to A-B. Upon reapplication of the stress, the stress-strain relation now retraces elastically the path C′-C, joining the path associated with the plastic state of C. In the idealized metal, the stress-strain relation in the plastic, as well as in the elastic, state, is considered to be independent of rate of deformation.

In actual metals, the transition from the initial part of the stress-strain curve, A-B, or C′-C, to the part associated with the plastic state is rarely ever abrupt or sharp. The extent of the transition region may often be narrowed considerably, though, by a special treat-

ment called "pre-straining". In this treatment the metal is given a permanent set, then either allowed to rest at room temperature for extended periods, as for example, several days, or it is subjected for a short time (1 hour) to a relatively low temperature (perhaps 200 degrees Fahr.). This resting period, or thermal treatment, lowers the hysteresis which is associated in actual metals with the line C′-C.

In actual metals the stress-strain relation associated with the plastic state is even more dependent upon rate of deformation than that of the elastic state. There is, apparently, a true speed effect (1)* which influences the height of the stress-strain curve, quite apart from the effect of speed upon the adiabaticity of the deformation. This speed effect is especially marked at elevated temperatures and comparatively small at room temperature. (In steels, for example, an increase in rate of strain at room temperature by a factor of 10 raises the tensile strength by at most 5 per cent). The thermal effects of high rates of deformation are also greater in the plastic than in the elastic state, for the temperature rise which occurs in an adiabatic plastic deformation may be as large as a few hundred degrees Fahr.

The elastic state of the isotropic idealized material is completely specified by Hooke's law and by two elastic constants, but actual metals which have been subjected to deformation exhibit some anisotropy. If the material is anisotropic, more than two elastic constants are necessary to specify the elastic behavior. Further, because of the highly anisotropic nature of the individual crystals and because of their partially or completely random orientations, the elastic deformation is not uniform if viewed on too small a scale. These difficulties, which are always present, in no wise detract from the usefulness of the standard elasticity theory for media which are homogeneous and isotropic on a macroscopic scale.

The behavior of metals in the plastic state has not been successfully systematized into a set of laws corresponding to Hooke's law for the elastic state. However, two fairly successful systems for plastic behavior have been proposed. The first system, introduced by Mohr (2)**, focusses attention upon the planes of maximum shearing stress. In the second system, proposed by von Mises (3), attention is directed to certain quadratic invariants of stress and of

*The figures appearing in parentheses refer to the bibliography appended to this paper.

**In this paper the authors have associated the names of Mohr and von Mises with these viewpoints even though they realize other workers have contributed much to their development and application.

strain. These two systems may be regarded as complementary. In the first, deformation is regarded as highly anisotropic, simple shear strain occurring only across the planes of maximum shear stress. In the other, deformation is regarded as being perfectly isotropic, as in a viscous fluid. The plastic behavior of metals seems to be intermediate between that predicted by these two complementary systems.

The authors believe that little progress is to be made in attempts to modify either the Mohr or von Mises systems to obtain better agreement with the few standard types of experiments. Rather it is believed that fruitful progress is possible only by a careful study of those experiments in which the plastic behavior is radically different from that predicted by either system. By such inquiries new concepts may be reached regarding the fundamental nature of plastic deformation. In the following sections, emphasis has been placed on those phases of plastic deformation requiring new physical concepts for their explanation.

The stress-strain curve is terminated by rupture, and this is usually thought of as occurring suddenly, as represented by D in Fig. 1. In stress-strain curves actually recorded, however, the effect of rupture may be evident even before complete fracture occurs. In tensile tests on ductile materials, a macroscopic crack usually first starts in the interior of the specimen and considerable reduction in area will occur between the initiation of this macroscopic crack and complete rupture.

The primary factor which determines the initiation of rupture is thought generally to be the maximum tensile stress without regard to transverse stresses. However, no thorough investigation has apparently been reported of the effects of transverse stresses, the amount and type of prior plastic deformation, and the microstructure. In the following sections on rupture, these factors are considered in connection with a rather detailed model of the mechanism of rupture. In addition to correlating the available published data with this model, the authors present some new experimental data in corroboration.

Initiation of Plastic Flow

Homogeneity of Initial Plastic Flow

A strengthening of the material is usually associated with plastic deformation. The strengthening is revealed by a positive slope of

that part of the stress-strain curve pertaining to the plastic state, as in Fig. 1, and is necessarily associated with a homogeneous deformation of the material, since a region will not continue to flow unless the surrounding regions have been equally strengthened.

Some metals (4), particularly mild steel, require less stress for the continuance of plastic flow than for its initiation. This results in a sudden drop in the tensile stress-strain curve at the incidence of plastic deformation (Fig. 2), and also a heterogeneity of deforma-

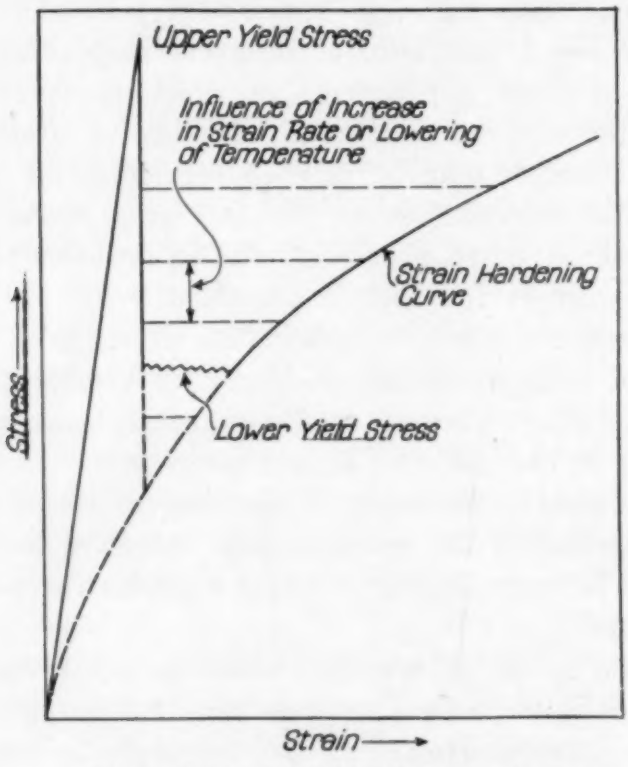

Fig. 2—Initial Portion of Stress-Strain Curve for Inhomogeneous Deformation.

tion. The region which first yields is weakened, yielding an observable amount before the surrounding region begins deformation. The magnitude of the maximum stress in the elastic state, called the upper yield point, is very sensitive to the shape of the specimen, to the axiality of loading, and to the surface finish (5). It appears that the metal behaves elastically until the shear stress or shear strain energy density reaches a critical value in some region of the bar. Once this region has yielded, its resistance to further deformation is lowered. The redistribution of stress, occasioned by this local yielding, raises the stress in neighboring regions (6), so that the neighboring regions yield under a lower net load. Any local stress

concentration will thus lower the maximum average stress, and hence the maximum load, before yielding. (Surface imperfections and the fillets are the usual sources of high stress concentrations.)

In the tensile bar the initial heterogeneous deformation occurs along planes inclined at nearly 45 degrees to the axis of the specimen, as shown in illustration *a* of Fig. 3. The measured stress during

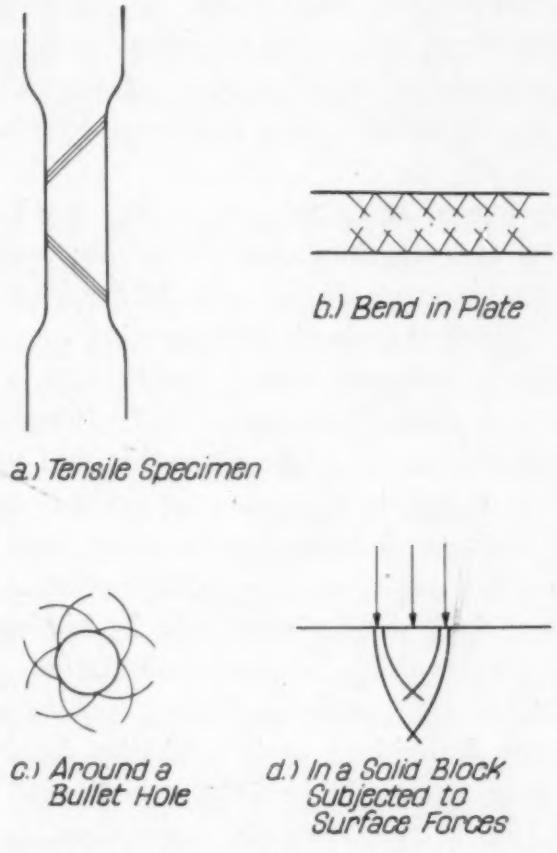

Fig. 3—Examples of Heterogeneous Deformation.

this heterogeneous flow fluctuates rapidly about a constant value until all the material in the gage length has been traversed by deformation bands (commonly called "Lüders' bands"). The mean stress during the heterogeneous deformation is called the lower yield stress. The value of this lower yield stress is believed to be much more sensitive to rate of deformation and to temperature than is the strain-hardening curve. Hence the stress-strain curves at various rates of strain may be represented, to a fair approximation, as in Fig. 2, by the elastic portion and the strain-hardening portion joined by horizontal lines. The height of each horizontal line is a function of temperature and of rate of deformation. The dependence of the

upper yield point upon temperature has, apparently, not been reported in the literature.

In stress systems where distribution of stresses is not uniform, as in bending and in twisting, the deformation bands associated with initial yielding must spread gradually from the more highly stressed surface to the less stressed interior. In such cases the load does not drop abruptly at the upper yield point, but fades off in a gradual manner calculable from theory (7). Many excellent examples of the deformation bands at the initiation of plastic deformation in various shaped specimens have been illustrated by Nadai (8). Some are reproduced in Fig. 3.

The phenomenon of an initial drop in stress, with its accompanying heterogeneous deformation, may be readily understood by considering the general features of plastic deformation in polycrystalline aggregates. Since the plastic deformation of the grains occurs by slip along crystallographic planes, aside from possible twinning the strain is uniform throughout the grain.* Because of differences in orientation, the strains of adjacent grains will not be the same. This discontinuous change in strain across grain boundaries makes it necessary that for plastic deformation to occur, the material on one side of a boundary be displaced tangentially relative to the material on the other side. Such displacement will be hindered by the presence of hard precipitates along the grain boundaries. Plastic deformation of polycrystalline aggregates must therefore involve both plastic deformation of the individual grain and the displacement of the material on one side of a grain boundary relative to the material on the opposite side (9), (10). The yield stress depends either upon the resistance of the grain to plastic deformation or upon the resistance of the grains to relative movement, which ever is the smaller. In the former case the strain-hardening curve will be rather similar to that of single crystals. In the latter case the stress necessary to overcome the resistance to relative motion may be very much higher than that which an isolated crystal will support without yielding. The resistance will be overcome first in a localized region where the stress has been concentrated. This localized yielding will result in a redistribution of stress. The shearing stress will be raised on those planes which pass through the localized region on which the shearing stress is already a maximum, as has been shown by Nadai (6). This increase of stress will cause further failure at other boundaries, with a still

*The words grain and crystallite may be used interchangeably.

further increase of shearing stress along a common plane of maximum shear stress. Yielding will thus be catastrophic along planes of maximum shear stress.

The above explanation of the initial yielding in mild steel, with the attendant heterogeneous deformation, seems to explain all the observations known to the authors regarding this phenomenon. These observations are:

1. The lower yield is raised by a decrease in grain size (11), and disappears in large grained specimens (12). The larger the total area of the grain boundary, the greater will be the restraint which it imposes.

2. The heterogeneous deformation is found only in steels with a comparatively low tensile strength. A large increase in the resistance of the interior to slip prevents it, since heterogeneous deformation can occur only when the initial deformation is hindered by resistance to relative motion at the grain boundaries, rather than to the resistance to slip of the grains themselves.

3. Heterogeneous deformation does not occur in very pure iron. Removal of the last traces of insoluble impurities will remove the marked resistance to relative movement at the grain boundaries.

4. The sharp yield phenomenon, removed by a prior cold working, returns slowly upon aging, and may even be accentuated by such treatment (10). "Killing" (thorough deoxidation) prolongs the time required for aging. The precipitation of impurities in steel is probably never complete at room temperature. It is well known, however, that the precipitation is hastened by cold deformation. Therefore the relative movement at the grain boundaries accelerates further precipitation, which, in time, restores the ability of the grain boundaries to resist further slip. If the steel has been thoroughly deoxidized at molten temperatures it can be assumed that most of the gases have already been removed from solution. Therefore they cannot form further precipitates after deformation. This observation on the difference between killed and unkilled steels suggests that the effective precipitate at the grain boundaries may be oxides, or nitrides, which are thought to be associated with aging phenomena (13).

5. With strain aging the restoration of the discontinuous yielding is much more rapid than is the raising of the tensile stress. This is in agreement with the commonly accepted view that in many cases precipitation occurs more rapidly along grain boundaries than in the interior of the grains.

Conditions for Initiation of Plastic Flow

The stress at which a particular metal passes from the elastic to the plastic state can be determined by experiment, within limits, for any particular type of stress. It would be of considerable practical value if a test under one combination of stress could suffice to predict the boundary between the elastic and the plastic state under all stress combinations.

In single crystals with well defined planes of easy slip the criterion for plastic flow has been well established (14). The shearing force across at least one slip plane, resolved along a slip direction, must equal a critical value. The criterion for polycrystalline metals has been more difficult to establish, partly because the transition between elastic and plastic state is often ill defined, and partly because of the difficulty of obtaining isotropic specimens.

Numerous criteria have been proposed for polycrystalline metals. The two which have been most successful are Mohr's (2) hypothesis of maximum shear stress (also sometimes called Guest's law), and von Mises' (3) hypothesis of maximum shear energy (also sometimes called the Hencky-von Mises-Haigh theory). According to the first criterion, plastic deformation begins when the maximum shear stress in the material exceeds a critical value; according to the second criterion, it begins when the elastic shear energy exceeds a certain critical value. The elastic energy of deformation is a quadratic function of the stress components. This quadratic function may be written as the sum of two terms. The first term, called the elastic dilatation energy, depends only upon the bulk modulus, and the second term, the elastic shear energy,* only upon the shear modulus (15). According to the von Mises hypothesis, as stated above, the metal remains elastic until the elastic shear energy exceeds a certain critical value.

The two criteria for yielding may therefore be written as

maximum shearing stress = critical value (Mohr)
elastic shear energy = critical value.* (von Mises).

The Mohr and the von Mises hypotheses may be compared with experiment by determining the yield conditions under two types of stress patterns (16). Two convenient types of stress patterns are

*Elastic shear energy is proportional to the function S_I^2 defined by Eq. (a-3) in Appendix A.

associated with pure tension and pure torsion. In pure tension, the maximum shearing stress is equal to one-half the tensile stress. Hence, the Mohr hypothesis gives

$$S_o = 0.50T_o, \qquad \text{(Mohr)} \quad (1)$$

where S_o is the shearing yield stress in pure torsion and T_o the tensile yield stress in pure tension. Since according to Eq. (a-3) the shear strain energy is proportional to $(2/9)\ T_o^2$ at the inception of plastic flow in tension, to $(2/3)\ S_o^2$ at the inception of plastic flow in torsion, the von Mises hypothesis gives

$$S_o = 0.577T_o. \qquad \text{(von Mises)} \quad (2)$$

The Mohr and von Mises hypotheses may be better compared with experiment by observing the yield conditions under many different types of stress patterns. Experiments have been performed in which tension and torsion were applied to hollow cylinders in various combinations simultaneously. When a solid is subjected to a tensile stress T and at the same time to a shear stress S across planes transverse to the axis of tension, the maximum shearing stress is given by $\{S^2 + (T/2)^2\}^{1/2}$. Thus, yielding begins according to the Mohr hypothesis when

$$\{S^2 + (T/2)^2\} = (To/2)^2.$$

or

$$4(S/To)^2 + (T/To)^2 = 1, \qquad \text{(Mohr)}$$

where T and S refer to the tensile and shearing stress at plastic yielding under combined stresses and To refers to the particular tensile stress at the yielding in pure tension in which S is zero. For yielding under these combined stresses, the von Mises hypothesis requires that

$$3\,(S/To)^2 + (T/To)^2 = 1. \qquad \text{(von Mises)}$$

The results of typical experiments are presented as Fig. 4 from which it is seen that copper and aluminum obey the von Mises hypothesis almost precisely. In the opinion of Taylor and Quinney (17), the divergence in the case of mild steel is due to the anisotropy of the thin walled tubes, which condition could not be entirely eliminated.

At first sight it is surprising that yielding in single crystals is determined by the maximum shear stress, while in most polycrystalline metals it is determined by the maximum shear strain energy. This apparent discrepancy may be resolved by considering the effects

either of the random orientation of the individual crystallites, or of the restraints imposed upon each crystallite by its neighbors. Sachs (18) has shown that for a single crystal the relation between the tensile stress necessary for yielding, averaged over all orientations of the crystal, and the corresponding averaged shear stress, is very nearly the same as that given by the von Mises hypothesis, Eq. (2). Taylor (19) has shown that the restraints imposed by a crystal's neighbors prohibit simple shear on only one set of crystallographic

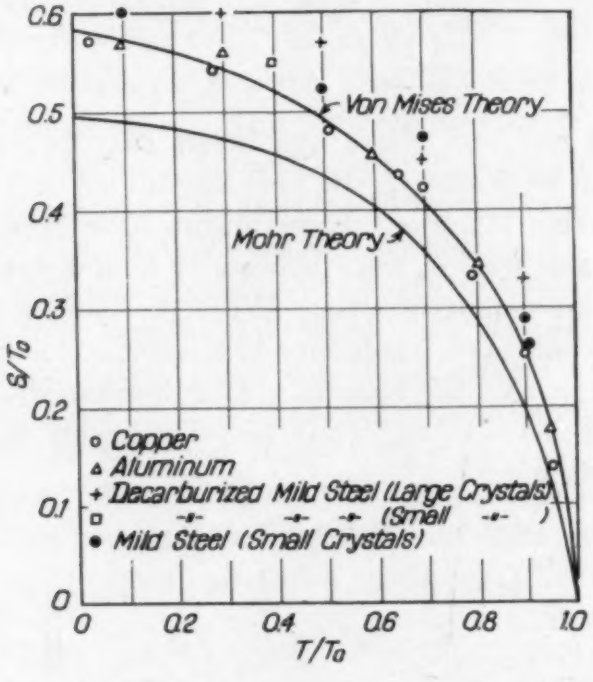

Fig. 4—Yielding Under Combined Stresses (17).

planes, but require the simultaneous operation of five sets of planes. This restraint requires that planes other than the one across which the shearing stress is a maximum operate to aid plastic deformation. Since only the von Mises hypothesis takes account of all the shearing stresses, it is to be expected that this hypothesis is the more appropriate criterion for yielding. In some metals the resistance to slip of the grain boundaries is greater than that of the crystallographic planes, and yielding is catastrophic along planes of maximum shearing stress. Since only one set of planes is operative in yielding, the Mohr hypothesis should be the more applicable. In the experiments of Taylor and Quinney (17) in Fig. 4, the mild steel had been given a prior strain and so did not have an initial drop in stress. The experimental determination of the condition for the initiation of yield

in annealed mild steel is particularly difficult because of the sensitivity of the maximum stress to surface finish and to the sharpness of the fillets.

Plastic Flow

Relation Between Stress Pattern and Plastic Flow

In a few simple stress patterns the nature of the plastic deformation may be predicted from considerations of symmetry. In a uniaxial stress system, for example, the material will extend along the stress axis and contract half this amount along the transverse direction. However, the nature of the plastic deformation cannot be so predicted in the complex stress patterns found in engineering structures without making some new assumption as to the behavior of the material.

Two alternative systems have been proposed relating to the laws governing plastic deformation in metals. In the first (Mohr), deformation is considered to take place by simple shear across the planes of maximum shearing stress. Since the orientation of these planes, as well as the shearing stress across these planes, is determined solely by the maximum and minimum principal stresses, the intermediate principal stress will have no effect upon the plastic flow. In the second (von Mises), the plastic deformation of metals is governed by the same laws as is the plastic deformation of isotropic amorphous solids. These laws have been completely described in Appendix A, and are there specified by Eq. (a-2).

A comparison of the two theories is best made by a diagram first used by Lode (16). In this diagram the ordinate is a measure of the deviation of the intermediate principal strain from the mean of the maximum and the minimum principal strain. The ordinate is defined explicitly as

$$\lambda = \frac{2\,e_2 - (e_1 + e_3)}{e_1 - e_3}, \qquad \text{(strain)}$$

e_1, e_2, e_3 being the principal strains in descending order of magnitude. The abscissa in the diagram is the corresponding function of the principal stresses;

$$\mu = \frac{2\,S_2 - (S_1 + S_3)}{S_1 - S_3}, \qquad \text{(stress)}$$

where S_1, S_2, S_3 are the principal stresses in descending order of magnitude. The relationships between λ and μ given by these two

theories of plastic flow are presented as Fig. 5, together with the careful experimental observations of Taylor and Quinney (17).

According to the Mohr theory, the intermediate principal strain, and hence also λ, is zero except in singular cases, for example when two principal stresses are equal. In these singular cases the plastic deformation is somewhat indeterminate. This indeterminacy is elim-

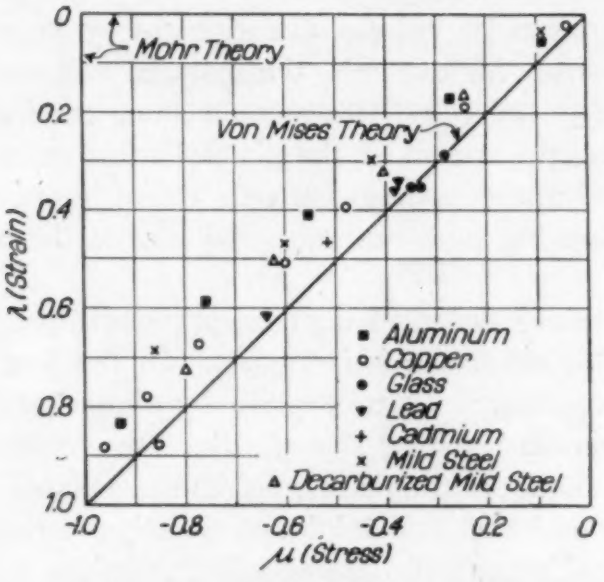

Fig. 5—Lode's Diagram for Relation Between Stress and Strain During Plastic Flow (17).

inated only by the additional assumption that when the stress has axial symmetry the strain also has axial symmetry. According to the von Mises theory, λ and μ are equal, as may be verified directly from Eq. (a-2). The experimental observations for metals lie between the curves associated with the two theories, but much nearer the von Mises curve. The observations for the amorphous solid, glass, indicate that it deforms plastically very closely in accord with the von Mises theory. The anisotropy introduced during plastic flow should render these relations of Mohr and von Mises less applicable. However, experiments at large strains have not been performed to observe the manner of the divergence.

Strain Hardening

A complete solution of the problem of plastic deformation will not only define the conditions for the initiation of plastic deforma-

tion, and the relation between stress and plastic flow, but it will also predict the strength properties in terms of microstructure and also the changes in the strength properties with plastic strain. The dependence of tensile strength upon microstructure of steels has been discussed by Gensamer (20) and collaborators. It appears to depend primarily upon the mean ferritic path. Since a metal is usually strengthened by plastic strain, the change in strength with deformation is customarily referred to as "strain-hardening".

The strain-hardening properties of single crystals are fairly well understood. The crystals shear across certain crystallographic planes (usually the planes of closest packing) along certain crystallographic directions (usually directions of closest packing). The strain-hardening curve is independent of the type of deformation if the shear stress resolved across the slip planes in the slip direction is plotted against the corresponding shear strain. Further, the strain-hardening is isotropic. Slipping across one set of planes strengthens the crystal with respect to slip across all sets of slip planes, irrespective of their orientation. A basis for a quantitative theory of the atomistic mechanism of strain-hardening has been proposed by Taylor (19). A review of the literature on this subject has been presented recently by Read and Seitz (21).

In contrast to single crystals, comparatively little is known concerning the strain-hardening properties of polycrystals. The anisotropy in strength properties introduced by plastic deformation has been investigated only in the very special case of rolling of sheet. The relation between the strain-hardening introduced by different types of deformation has been studied only for very small strains. Isolated observations have been made on the effect of reversed strains upon strength. Except for small deformations strain-hardening has apparently been investigated thoroughly only for tension and for torsion. Usually these investigations have been conducted with the specimens at a constant temperature, and the stress-strain curves so obtained are said to be isothermal. On the other hand, in many engineering applications of metals the deformation is so rapid that no appreciable amount of heat is conducted away during the deformation. The relation between stress and strain under these conditions is said to be adiabatic. It is well known that strain-hardening is, to some extent, a function of rate of deformation, but the rate must change by a large factor to have an appreciable effect upon the stress-strain curve. Stress-strain curves, as usually ob-

tained, therefore may be regarded as pertaining to a constant rate of deformation.

Constant Temperature and Rate of Deformation

In Tension—The true stress-strain curve associated with uniaxial tension becomes linear after a small initial distortion, provided the natural, rather than the conventional, strain is used. Many such linear stress-strain curves have been recorded by MacGregor (22), Gensamer (23), and Hollomon (24) and a typical actual example for an S.A.E. 1020 steel is presented as Fig. 6. In the following

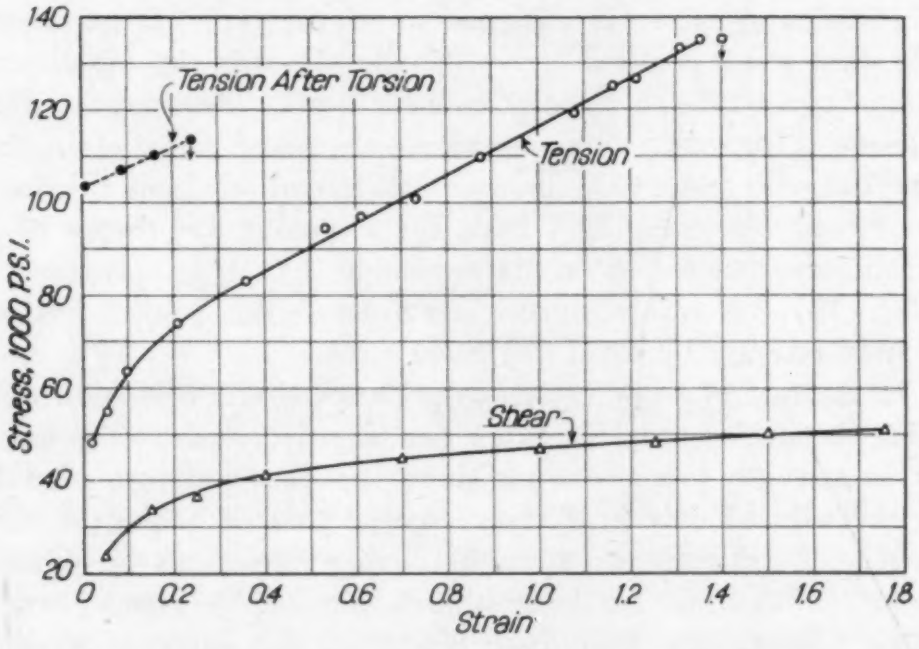

Fig. 6—Tension and Torsion Curves for Annealed S.A.E. 1020 Steel.

discussion of tensile deformation, the non-linear part of the plastic portion of the stress-strain curve will not be considered.* The relation between the natural strain, e, and the conventional strain $\Delta l/l_o$ is shown by the following equation:

$$e = \ln (1 + \Delta l/l_o).$$

The natural strain is determined experimentally by observing changes in the cross section. From the above equation, it is seen that e will be given also by the relation

*It is recognized that the linear part of the stress-strain curve represents only an average, since the stresses are not strictly constant across a necked region.

$$e = \ln (A_o/A),$$

where A_o and A are the original and final cross sectional areas, respectively. In plotting a true stress-strain curve, e is the natural abscissa, since the area under such a curve represents the work done per unit volume of the material. No simple physical significance can be attached to the usual curve in which true stress and $\Delta l/l_o$ are the co-ordinates.

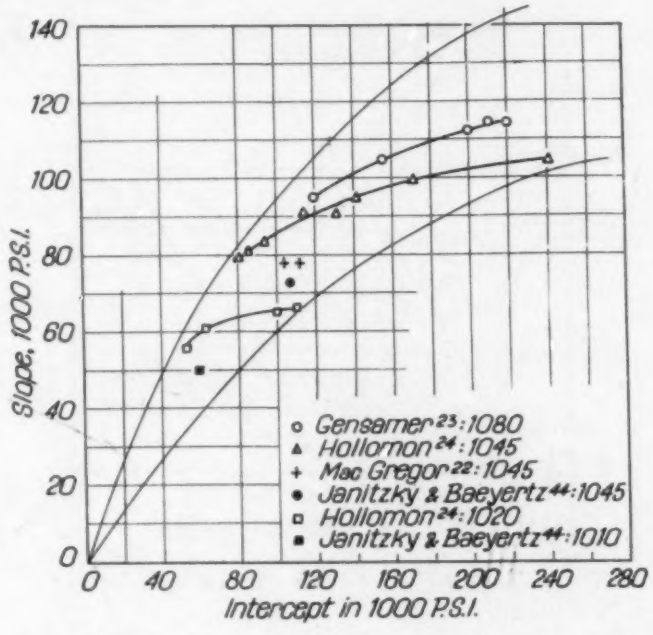

Fig. 7—Slope Versus Intercept for Tensile Strain Hardening Curves.

The linearity of the stress-strain curves extends to the highest strains which have been measured, namely to strains of 3.5. The range of the observed strain has been greatly extended by Bridgman (25), who has placed his specimens under exceedingly high hydrostatic pressure during the extension, thereby obtaining reductions of area approaching 100 per cent.

The linearity of the tensile stress-strain curves enables them to be specified by only two parameters, and hence represented by a single point in a plane in which these parmaeters are co-ordinates. All the stress-strain curves for plain carbon steels available to the authors are thus represented in Fig. 7. In this figure the abscissa is the intercept on the stress axis of the extrapolated linear part of the stress-strain curve in the plastic region.

Fig. 7 includes four sets of data in each of which the same steel

has been subjected to different heat treatments. In each set, the higher the intercept, the larger the slope—i.e. the stronger the steel, the larger its increase in strength due to a given strain. This correlation of slope and intercept for a given steel is in agreement with the well known decrease with drawing temperature of Meyer's work hardening index (26). The effect of carbon content upon the strain

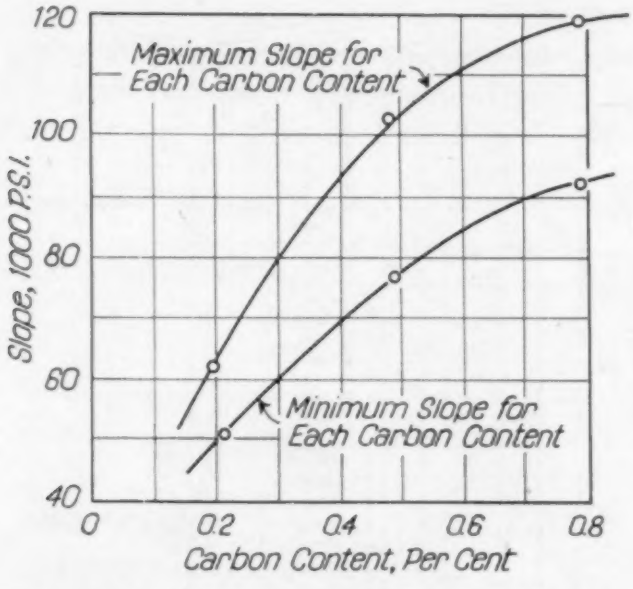

Fig. 8—Effect of Carbon Content on Slope of Strain Hardening Curve.

hardening of plain carbon steels is illustrated in Fig. 8, derived (24) from some of the data shown in Fig. 7. The general increase in rate of strain hardening with carbon content has also been observed in the rolling of sheet (27).

In Torsion—Since comparatively few results of torsion experiments have been reported, no standard convention has been adopted for the representation of the data. The most significant method is to plot the shearing stress at the surface against the shearing strain at the surface. There is a standard formula by which the shear stress at the surface of a solid cylinder may be calculated from the measured torque (28). The surface shear strain is given by $\frac{1}{2}\phi D/L$, where D and L are the diameter and length of the gauge and ϕ the total angle of twist in radians.

A typical surface shear stress versus surface shear strain curve is presented in Fig. 6. The area beneath this curve represents the work done per unit volume, just as in the case of the tensile stress-

strain curve. However the shapes of the shear and tensile curves are very different. The tensile curve soon becomes a straight line, representing a constant rate of strain hardening, but the shear curve becomes less and less steep, representing a decreasing rate of strain hardening with increasing strain. The difference in the qualitative nature of the two curves may be understood by considering the details of strain hardening. In a later section, it is shown that the phenomenon of fracture can be best understood by the assumption of microscopic cracks.* Such cracks necessitate that the strain hard-

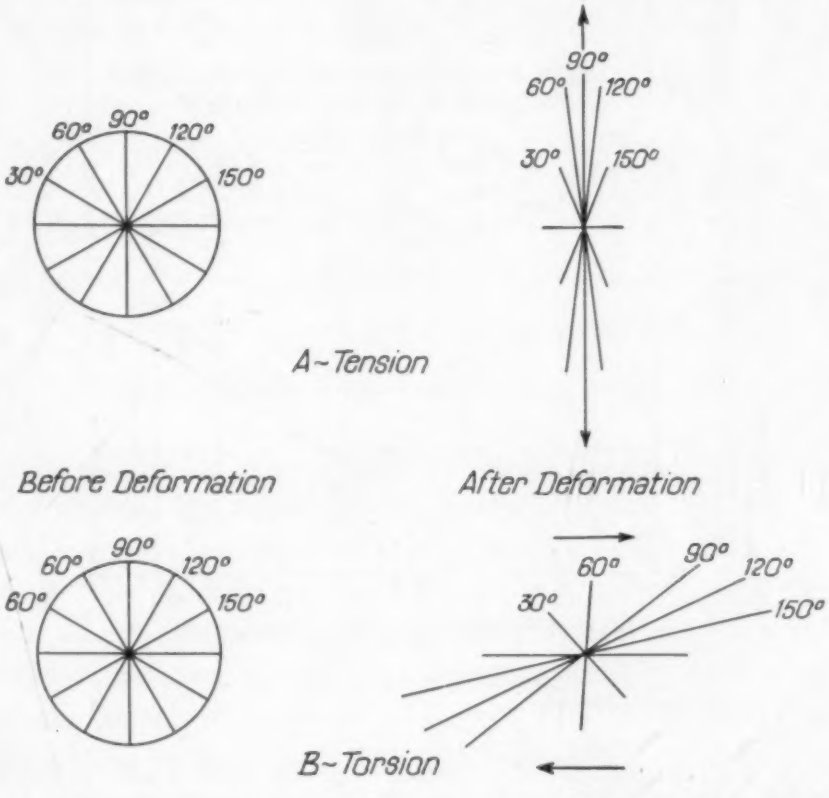

Fig. 9—Change in Orientation of Cracks During Plastic Deformation. Strain = 1.

ening of the matrix be at least partially counteracted by the propagation of cracks. The weakening effect of the cracks can be expected to be much more drastic in the case of torsion than in tension. In tension the reorientation of the cracks would tend to make them less

*In this report the term "crack" is used to refer to an internal surface or plane of weakness across which the binding forces are negligible. As is pointed out in more detail in the section Rupture, such "cracks" might be, but are not necessarily present in the virgin material. In the latter case the virgin material might contain internal surfaces across which the binding is weak, and which finally result in cracks sometimes prior to or at the point of rupture. Such internal cracks could also arise if the virgin material contained brittle constituents whose nondeformability would lead to high stress concentrations and hence to their eventual fracture.

harmful, but the reorientation accompanying shear strain would render them more effective in reducing the resistance of the material to shearing stresses. This difference in reorientation effects is illustrated schematically in Fig. 9.

Illustration B of Fig. 9 suggests that the strength properties of a specimen are rendered anisotropic by an initial twist. In the vicinity of a crack, the specimen will tend to relieve shearing stresses by a simple shear along planes parallel to the crack. When the

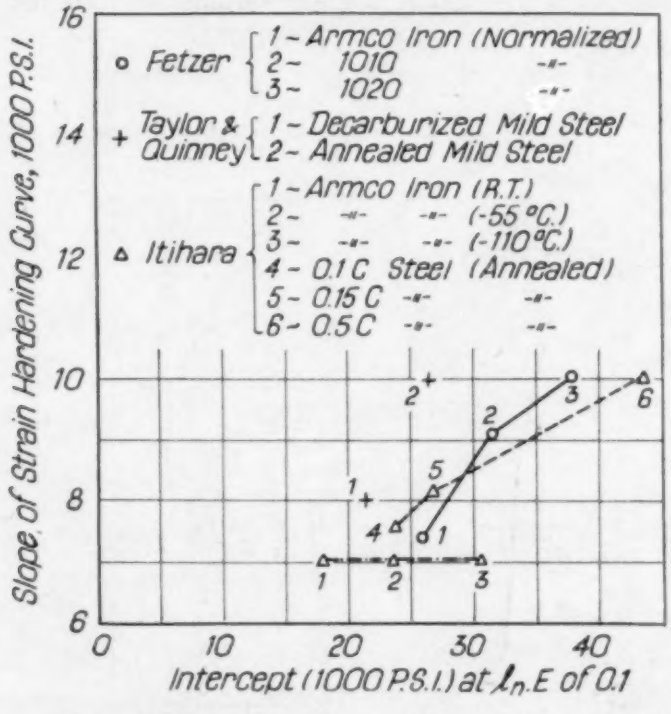

Fig. 10—Parametric Representation of Stress-Strain Curves in Torsion.

cracks are not randomly oriented, as is the case after a substantial twist, the flow properties can no longer be isotropic. The anisotropy in distribution of the cracks caused by twisting is in such a sense that slipping across the cracks will cause further twisting to be accompanied by an elongation, and this effect has been observed by Fetzer (29). Further, if a tensile stress is applied after an initial twist, the distribution of the cracks is such as to cause the specimen to continue to twist in the original sense as it elongates. The authors are unaware of any reference to this phenomenon in the literature.

For torsion, plots of stress against log of strain are essentially linear beyond a log strain of 0.1, at least for iron and steels. All

except the first part of the stress-strain curve in torsion may be specified by two parameters, and hence represented by a point on a plane. All the torsion stress-strain curves for plain carbon steels available to the authors are thus represented in Fig. 10. In this figure the abscissa is the value of the linear part of the stress versus log strain curve extrapolated to a log strain of 0.1. Two sets of data are included in which steels of increasing carbon content were given the same heat treatment. In both sets, the higher the carbon content the higher the intercept and also the higher the slope.

General Case—The term strain hardening has thus far been used only in reference to specific stress-strain curves. This term

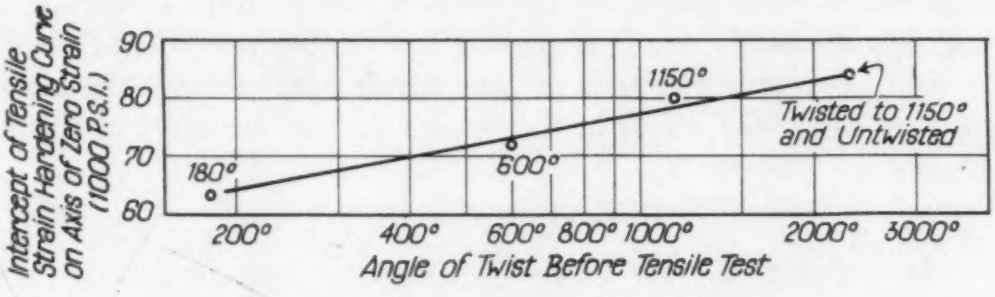

Fig. 11—Effect of Torsion on Strength in Tension (31).

may be given a more general significance if the hardening associated with deformation is essentially isotropic. If an initially isotropic specimen remains isotropic after deformation, then the term "strain hardening" can refer to the material without reference to the particular type of deformation to which the specimen has been subjected. The meager evidence in the literature indicates that strain hardening is, in fact, essentially isotropic. Copper and brass sheets hardened by rolling have practically the same tensile strength measured transverse to the axis of rolling as measured along this axis (30). The rise in the stress-strain curve in tension occasioned by prior twisting (31) is consistent with the rise in torsional strength associated with this twist (Fig. 11). Similarly, the torsional stress-strain curve is raised by a prior elongation by an amount consistent with the increase in tensile stress (31).

If strain hardening is essentially isotropic, then the possibility exists of correlating the strain hardening associated with one type of deformation with that of other types, for example, the strain hardening curve for tension with that for torsion. This correlation cannot be made without some new assumption. Two alternatives

are possible depending upon whether the Mohr or the von Mises viewpoint is adopted.

According to the Mohr viewpoint, deformation proceeds by simple shear across the planes of maximum shearing stress. The strain hardening will therefore be a function only of the total shear strain, s, across these planes. Hence all strain hardening curves should be identical if the maximum shear stress, S, is plotted against total shear strain s. As an example, the method of correlating tensile and torsion stress-strain curves is presented in the following: If T is the tensile stress, then ½ T is the maximum shear stress, across planes inclined 45 degrees to tensile axis. The total shear strain across these planes, equivalent to a tensile strain (natural) of e, is 2e. Hence if ½ T is plotted against 2e, one should obtain the same curves for tension as one obtains by plotting the shear stress against shear strain in torsion. This may be expressed symbolically as follows:

$$(\tfrac{1}{2}T,\ 2e) = (S,\ s), \qquad \text{(Mohr)}$$

According to the von Mises viewpoint, the only invariant which may be associated with an increment of strain is a certain invariant quadratic function de_I^2 of the components of strain increments, defined by Eq. (a-4) of Appendix A. The amount of strain associated with a finite deformation must therefore be defined by the integral

$$e_I = \int de_I .*$$

The stress, S_I, associated with this strain is defined by Eq. (a-3) of Appendix A. According to the von Mises viewpoint, a plot of

*The present authors' application of the von Mises viewpoint to the problem of correlating different stress-strain curves is quite different from that recently presented by Nadai and Davis (32). In their treatment of simple shear, in effect, the latter authors considered the strain e_1 to be determined solely by the end configuration. In evaluating the integral

$$e_1 = \int de_1,$$

they implicitly assumed the final configuration to be reached by a deformation in which the principal axes of the strain remain fixed in the material, which is certainly not the case in simple shear. This assumption was made perhaps unwittingly, for their definition of de_1 in terms of principal strain increments rather than in terms of an invariant expression of all the strain components. With such a definition of de_1, it would not be obvious how to calculate e_1 in those cases where the principal strain axes rotate in the body during the deformation.

The difference between the two interpretations of the von Mises theory may perhaps best be clarified by an example. If a specimen is first twisted and then untwisted to its initial position, the Nadai-Davis method of considering only the initial and final configuration, carried to its logical conclusion, would give a zero final hardening. On the other hand, the hardening as calculated by the method of the present authors would be the same as if the bar were twisted twice the initial amount in one direction, none in the other. The experiments of Swift (Fig. 11) on twisting and untwisting substantiate the interpretation of the von Mises viewpoint adopted in this paper.

S_I versus e_I should be the same for all types of deformation. As an example, tensile and torsion stress-strain curves are compared in the following. According to Eqs. (a-3) and (a-4), S_I and de_I are related to the tensile stress T and tensile strain increment de by

$$S_I = (\sqrt{2/3})\ T$$

$$de_I = (3/\sqrt{2})\ de$$

and to the shear stress S and shear strain increment ds in simple shear by

$$S_I = (\sqrt{2/3})\ S$$

$$de_I = (\sqrt{3/2})\ ds.$$

The stress-strain curves in tension and in simple shear are therefore to be correlated as follows:

$$(T/\sqrt{3},\ \sqrt{3}\,e) = (S, e) \qquad \text{(von Mises)}$$

A test of the correlation of strain hardening according to the von Mises viewpoint has been made by Schmidt (32). He found, for small strains, the stress-strain curves in which S_I is plotted against e_I to be identical in the case of a thin walled tube subjected to various combinations of axial tension and internal pressure.

The strain hardening curves for tension and for simple shear are not identical, either according to the Mohr or to the von Mises viewpoint. A comparison is given in Fig. 12 from data obtained by the authors. The strain hardening for simple shear agrees fairly well with that for tension for very small values of strain, but soon becomes much less than that for tension. This disagreement after small deformations has two obvious possible interpretations. One interpretation blames the disagreement upon the Bauschinger* and related effects which prevent strain hardening from being represented strictly by a simple scalar quantity. Since the Bauschinger effect is eliminated by a low temperature anneal, if it were responsible for the relatively slow rate of work hardening in torsion, the discrepancy between tensile and torsion stress-strain curves would largely disappear in experiments made at slightly elevated temperatures. The discrepancy however does not disappear at elevated temperatures (29).

An alternative explanation of this discrepancy may be found

*It is generally assumed that plastic strain lowers the yield point with respect to strains of an opposite sign, i.e., a tensional plastic strain lowers the yield point in compression. This phenomenon is called the Bauschinger effect.

in the concept of microscopic cracks. As has already been mentioned, the reorientation and elongation of these cracks in simple shear counteracts the strain hardening of the matrix. This interpretation suggests that the torsion stress-strain curves are much more sensitive to variations in the size and distribution of these cracks

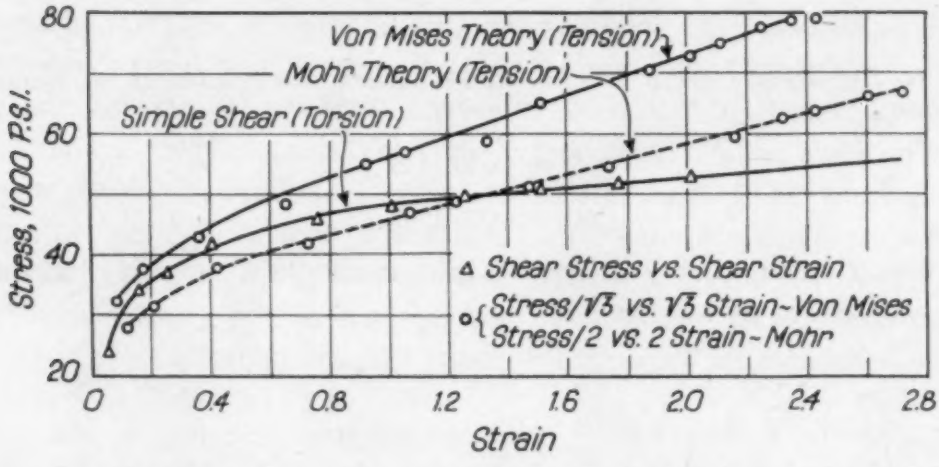

Fig. 12—Comparison of Stress-Strain Curves in Tension and in Simple Shear (Torsion).

than the tensile stress-strain curves. This new interpretation also suggests that the stress-strain curve in simple shear will depend markedly upon the orientation of the shearing plane if the cracks have been previously given a preferred orientation by processing (rolling for example).

Effect of Temperature and Rate of Deformation

The qualitative equivalence of an increase of temperature to a decrease in rate of deformation upon the effect of the mechanical properties of metals is well known. The property most thoroughly studied is the tensile strength, and for steels it varies with temperature as shown schematically in Fig. 13. The variation with rate of deformation may be expressed in either of two ways. A set of curves similar to the curve in Fig. 13 may be drawn with horizontal displacements, to the right for higher rates of deformation and to the left for lower rates. On the other hand, as has been pointed out, the effect of rate of deformation can be represented by the same curve as Fig. 13, by letting the abscissa be some measure of this rate.* The initial decrease in tensile strength, from A to B,

*Carpenter and Robertson, loc. cit., p. 164.

with either increasing temperature or decreasing rate of strain is associated with the persistence of a small plastic flow for a short time after a constant load is applied. The hump (C of Fig. 13) in the curve is associated with strain aging, which is thought to be due to the precipitation of carbides, nitrides, oxides, etc. (13). Both the precipitation and the growth of the large precipitate particles at the expense of small particles are accelerated by an increase in

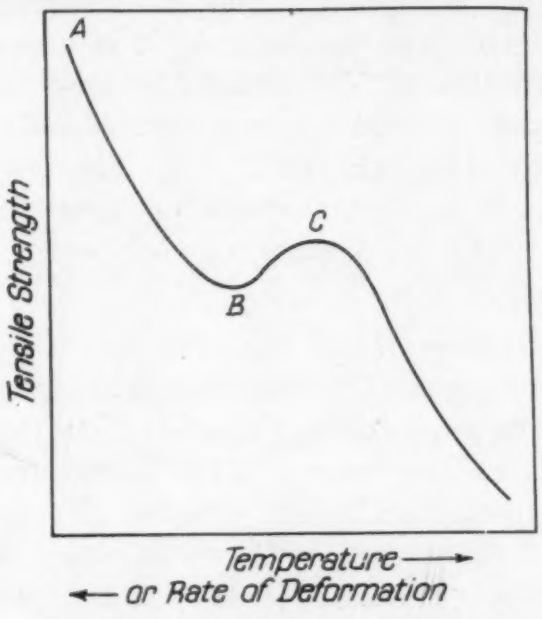

Fig. 13—Tensile Strength of Plain Carbon Steels as a Function of Temperature and Rate of Deformation.

temperature. As in all precipitation phenomena, these two conflicting tendencies result in a maximum hardness at some optimum temperature. Since precipitation induced by deformation cannot, of course, affect the yield stress, it therefore decreases steadily with an increase in temperature as well as with a decrease in the rate of deformation—to strain rates at least as low as one inch per inch per week (33)—through the region in which the tensile strength rises.* An interesting example of the qualitative equivalence of changes in temperature and in rate of strain upon the direct measurements of hardness is given by Cleaves and Thompson (34). The minimum in the hardness is shifted from 100 degrees Cent. as measured in static tests to 300 degrees Cent. in dynamic tests.

The effect of very high rates of deformation upon the stress-strain curve is very important to certain engineering applications,

*Sisco, loc. cit., p. 174.

but the direct determination of this curve at high rates of deformation is attended by almost insuperable difficulties. It is possible that these difficulties may be circumvented by making use of an equivalence of a decrease in temperature to a definite increase in the rate of deformation. The desired stress-strain relations could then be obtained by making the observations at sufficiently low temperatures using convenient rates of deformation.

In order that a given high rate of deformation may be correlated with a given low temperature, it is necessary to obtain a quantitative equivalence. The authors propose that a quantitative equivalence may be derived for temperatures and rates of strain in the region indicated by AB in Fig. 13. The formal expression is given by the following equations relating stress (S) to strain (e).

$$S = S_p(e),$$
$$p = p(\dot{e}, T).$$

The general form of the function $p(\dot{e}, T)$ may be obtained from theoretical arguments. Since the parameter p must be dimensionless, it must be expressible as a ratio of the rate of deformation and of some other time rate. This second time rate must be connected with the material itself. Nearly all time rates associated with materials are governed by heats of activation, that is, their dependence upon temperature is given by an equation of the form

$$\text{time rate} = f_o e^{-Q/RT}, \qquad (3)$$

where T is in absolute degrees, Q is the heat of activation, which if expressed in calories per gram atom, makes the constant R equal to 1.96, and the constant f_o has dimensions of time^{-1}. For the purpose of the present discussion the precise value assigned to the constant f_o is immaterial. If, as is desirable, the parameter p is to have a physical interpretation, then f_o must have some theoretical significance. The value usually assigned to this constant in diffusion problems is that first given by Dushman and Langmuir (35), namely

$$f_o = JQ/Nh,$$

where J is the mechanical equivalent of heat, N is Avogadro's number, and h is Planck's constant. If Q is in calories per gram mol, then (J/Nh) is 1.06×10^{10}. When f_o is so interpreted the time rate of Eq. (3) is essentially the number of times per second any given atom acquires the heat of activation, Q. It is therefore expected that the parameter, p, will be of the form

$$p = \dot{e}e^{Q/RT}/f_o. \qquad (4)$$

An example of the relation between the effects of rate of deformation and of temperature, as given by Eq. (4), is shown in Fig. 14. In this figure the observations of Nadai and Manjoine (36) concerning the influence of speed and temperature upon the true stress at the maximum load for copper are given as a function of the parameter p. If the heat of activation is chosen as 27,000 calories/gram mol. all the observations below 600 degrees Cent. (1110

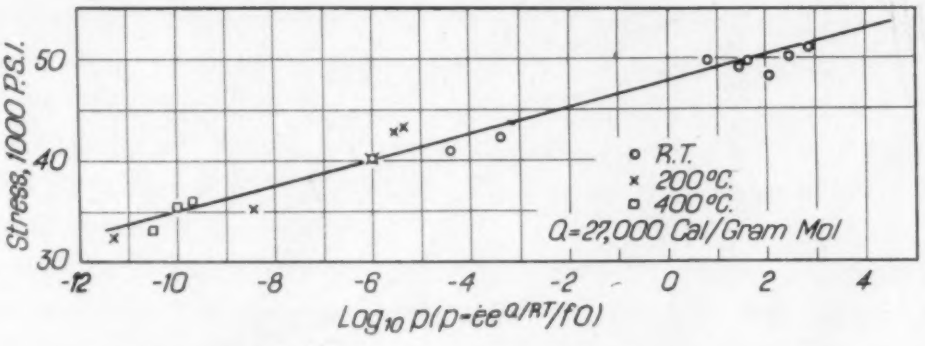

Fig. 14—Suggested Dependence of Tensile Strength of Copper Upon Temperature and Rate of Strain (36).

degrees Fahr.) lie nearly on a single curve. The measurements at 600 degrees Cent. and over were found not to lie upon this curve. The meager data (36) available for steel indicate that the parameter p is unchanged by the simultaneous increase of strain rate by a factor of 10^6 and of the temperature from —100 to 200 degrees Cent. Substitution of this information into Eq. (4) gives the heat of activation for steel, below the blue brittle range (below B in Fig. 13), equal to about 9000 calories/gram mol.

The equivalence of a decrease of temperature to an increase of rate of deformation determined by Eq. (4) is illustrated vividly in Fig. 15. In this figure the ordinate gives the effective increase in rate of strain associated with a decrease in temperature.

When the rate of deformation is sufficiently high, no appreciable amount of heat is conducted away from the region of deformation until straining has ceased, and the deformation is said to be adiabatic. Two conflicting tendencies are present when the deformation changes by an increase in speed of deformation from isothermal to adiabatic. The increase in speed is equivalent to a decrease in temperature but the actual temperature is varied by the adiabaticity of the deformation. The first effect will dominate in the early part of the deforma-

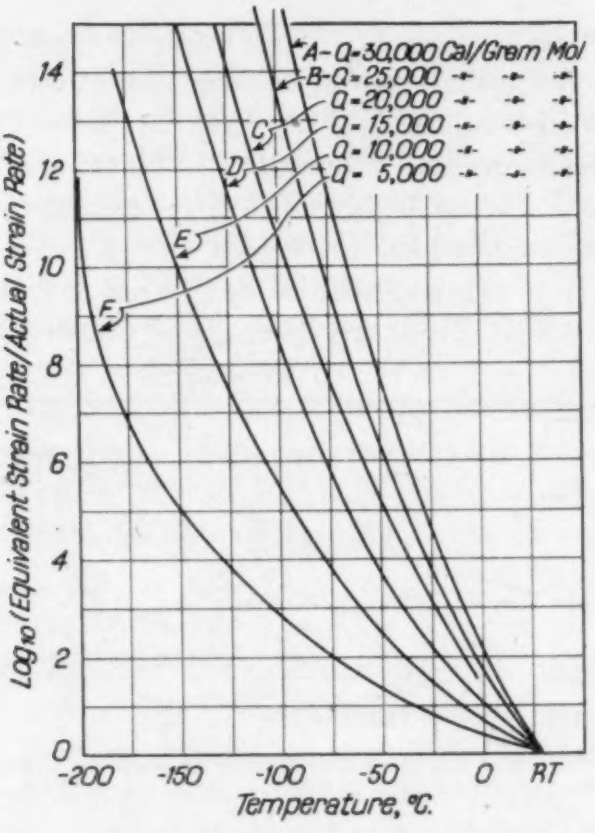

Fig. 15—Equivalence of a Decrease of Temperature to a Rise in Rate of Strain.

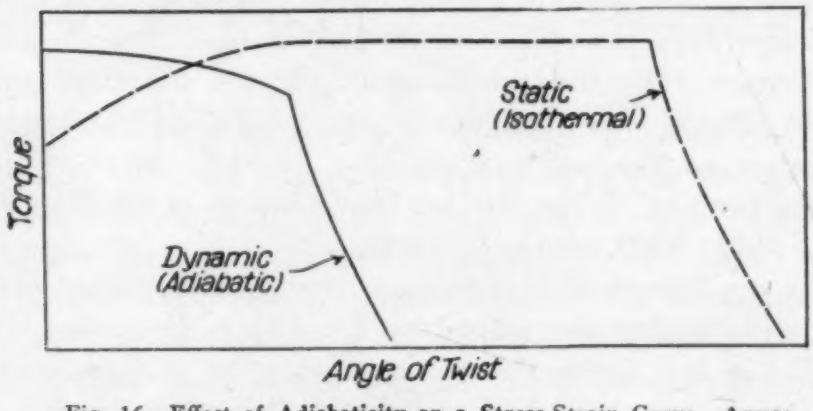

Fig. 16—Effect of Adiabaticity on a Stress-Strain Curve. Armco Iron at —160 Degrees Cent. (38).

tion, before the temperature has been raised appreciably. As the rise in temperature increases with increasing deformation, its effect may finally dominate. At least outside of the blue brittle region, the stress-strain curve will therefore be raised relatively more in the first part than in the last part, resulting in a flatter stress-strain curve. An example for the case of tension has been given by Clark and Datwyler (37). This flattening will be especially marked for

torsion stress-strain curves, which are already very flat compared with the tensile stress-strain curves. The torsion stress-strain curves at various rates of strain have been studied in detail by Itihara (38). A typical example is given in Fig. 16.

Rupture

Quasi-Static

General Theory—Finally as the stress is increased during plastic deformation, rupture occurs. The commonly accepted criteria of rupture requires that it occur when the maximum extension, the maximum tensile stress, or the maximum shearing stress (Appendix B) reaches a critical value. The validity of these criteria has been questioned by Bridgman (39), since 1912, on the basis of several observations of the anomalous behavior of some materials when subjected to various combinations of stresses and hydrostatic pressure.

The theoretical strength of a metal or other material is calculated by physicists from the maximum possible attractive force between atoms or molecules and the postulate that failure will occur when this force is exceeded. This method of calculation results in a value for the rupture strength which is far greater than that which is actually measured. The divergence between the actual and predicted strength is attributed to imperfections in the structure about which there has been considerable speculation as to their nature, size, and origin (21). A natural outgrowth of this speculation is to attribute much of the lack of understanding to these nebulous nuclei of weakness and to divert curiosity to other problems.

Even though the currently accepted criterion of failure, that of maximum tensile stress (See Appendix B), suffices for most engineering purposes, on the basis of this criterion alone the variation of the strength cannot be correlated with variations in structural characteristics of materials. It is therefore necessary to look further for a more fundamental and fruitful theory which will serve to predict the variation of maximum tensile stress necessary for fracture with structural characteristics of materials subjected to the usual engineering stress systems.

In 1921 Griffith (40), (41) postulated that in all materials there are minute cracks. He pointed out that these cracks cannot

propagate under a given stress pattern unless such propagation results in a continuously decreasing net potential energy. The propagation of a crack will result in an increase in potential energy due to the formation of the new surfaces and a decrease in energy due to the release of the elastic stress in the material surrounding the separation. The energy may also be decreased by a change in the external constraints which may arise from the separation of the material. Failure will occur only when these counteracting effects result in a continuous net decrease of the potential energy with the spreading of the crack. This is fundamentally a stability condition; that is, a material containing cracks of a given size becomes unstable and fails when the maximum principal stress approaches a critical value determined by the size and orientation of the cracks, and by the other two transverse stresses. The larger the size of the imperfection the less stress is necessary for its extension. A quantitative relation between the size of the crack and the fracture stress may be obtained by the following consideration: A homogeneous specimen is assumed to deform by such external constraints as to produce a uniform tensile stress T. The strain energy per unit volume is then $\frac{1}{2}\ T^2/E$, where E is Young's modulus. Now suppose a disk-like crack is formed, of radius r, in a plane normal to the axis of the tensile stress. The increase in potential energy due to the formation of a new surface is the surface energy per unit area multiplied by the area of new surface; or

$$\text{Surface Energy} = 2\pi r^2 S, \tag{5}$$

where S is the surface energy per unit area. On the other hand, the strain energy density will be reduced on both sides of the crack to a distance comparable with the radius of the crack. The decrease in strain energy will be approximately equal to the original strain energy density multiplied by the volume of a sphere of radius r; or

$$\text{Strain Energy} = -C(4\pi r^3/3)\ \tfrac{1}{2}T^2/E, \tag{6}$$

where C is a constant of the order of magnitude of unity. The crack will spread if in so doing the strain energy will decrease faster than the surface energy increases. From Eqs. (5) and (6), the critical value for the tensile stress which makes

$$d\ (\text{surface energy})/dr + d\ (\text{strain energy})/dr = 0$$

is given by

$$T = \sqrt{\frac{2SE.}{Cr}} \qquad (7)$$

In Griffith's theory it was implicitly assumed that the cracks were present in the original material. In extending Griffith's work, it is believed not necessary to assume that cracks are initially in the material before deformation. Cracks may be opened by the fracture of brittle components, such as cementite plates in pearlitic steels, during plastic deformation. Cracks may also be opened by exceeding the tensile strength of interphases or by the spreading of a crack in this weak interphase. These interphases may exist between the matrix and nonmetallic inclusions or between the ferrite and the cementite in steel. However the crack is formed, and whatever its shape, the criterion for its stability under pure tension will be given by Eq. (7), where 2r is some average of its plane dimensions. Under combined stresses the decrease in energy due to the relief of strain will depend upon the magnitude of all three principal stresses. The maximum decrease in energy will occur when all possible stresses are relieved by the extension of the crack; the course of the fracture being such as to accomplish this relief.

Maier (42) performed experiments on cylinders combining internal pressure and longitudinal tension and found that they fractured when either the longitudinal or transverse tension in the wall of the cylinder exceeded a value characteristic of the material. Results contrary to those of Maier have been obtained by the authors and will be the subject of a later report. In the authors' experiments, flat strips and round bars from the same bar of mild steel, heat treated in exactly the same manner, were pulled in tension and the fracture stresses determined. The flat strips were approximately 1 inch wide and $\frac{1}{8}$ inch thick. Necking of the strip along its largest transverse dimension was very nearly prevented and effectively the bar was subjected to a tensile stress parallel to this dimension. The fracture stress was decreased by about 25% by this additional stress. Kenyon and Burns (43) in an investigation of the tensile properties of low carbon steels reported that the fracture stress of Armco iron in the form of flat strips ($\frac{1}{16}$ inch thick) was about

75,000 psi. while that of a round specimen of similar composition and treatment was 125,000 psi. From this it might be inferred that the energy change due to the relief of stress associated with the opening of cracks is increased by the transverse tensile stress.

Bridgman (39) has described experiments with brittle substances like glass which fail in the absence of any tensile stress. A sketch of the apparatus is presented in Fig. 17. A small bar is subjected to a radial hydrostatic pressure in molasses by means of a hardened steel piston. Glass rods will break in this apparatus with a frac-

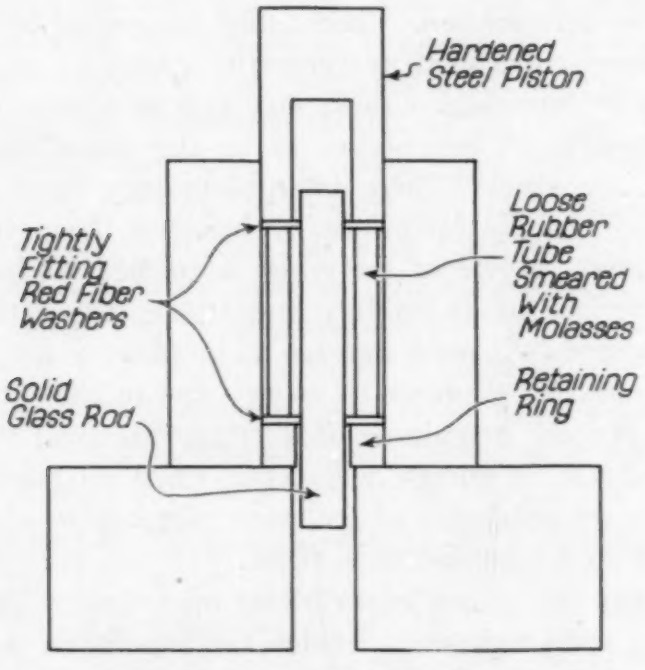

Fig. 17—Bridgman (39) Apparatus for Producing the "Pinching Off" Effect.

ture perpendicular to the axis of the specimen. This failure has been described as a "tensile type" of fracture. Griffith (40), however, in considering the concentration of stresses at notches predicted failure could occur in specimens loaded in this manner even though they were subjected to no net tensile stress. According to the instability theory of rupture outlined above it is only necessary that in the propagation of a crack the potential energy of the whole system be decreased. A crack will start at the surface of the specimen with the entrance of the fluid into this crack and the release of shearing stresses will result in a net energy decrease. In this case, as in the case of the normal tensile failure of brittle materials with no

plastic deformation, such as quenched steel, the fracture probably starts at the surface and extends inward.*

In Tension—The surface energy, S, of solid metal may be determined approximately from the heat of vaporization, and in turn the heat of vaporization may be determined from the variation of the vapor pressure of the liquid metal with temperature. The surface energy for iron has been calculated (see Appendix C) in

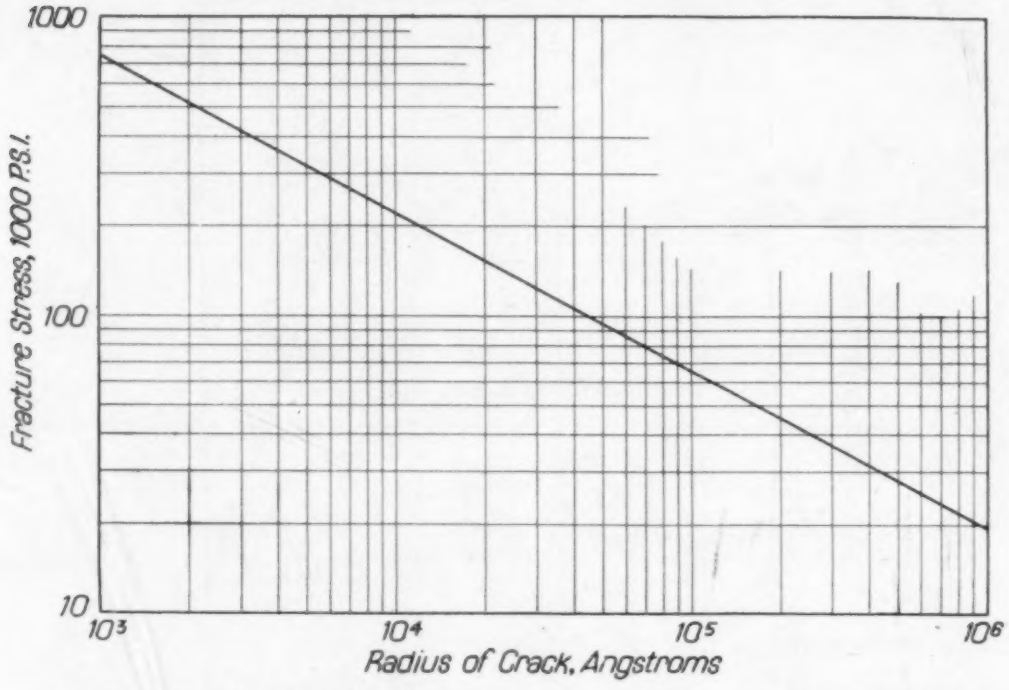

Fig. 18—Theoretical Relation Between Fracture Stress and Size of Crack (Eq. 7 with C = 1).

this manner and is equal to about 8800 ergs/cm.^{2} Using this value and Eq. (7), with C=1, Fig. 18 has been drawn relating the radius of the crack to the elastic stress necessary for fracture of iron or steel for a simple tension perpendicular to the circular cross section of radius r. The determination of the limiting fracture stress from the radii of the cracks in a tensile specimen is difficult. Not only do the shape, size and orientation of the cracks arising from the inhomogeneities or particles of dispersed phase in any real metal or alloy vary greatly from point to point in the metal, but also there is a lack of uniformity of tensile stress on the microscopic scale. Local failure may begin in a real metal in the early stages of the plastic

*Since the first draft of this paper was written, Bridgman ("private communication") has found that the tensile type of fracture is not obtained if the glass rod is protected from the molasses by a copper foil. In the opinion of the authors, this new experiment is a confirmation of their viewpoint.

flow but the cracks may be prevented from spreading by obstacles of one kind or another. At the present status it may be said that rupture of a tensile specimen will probably occur when the average maximum tensile stress in the specimen exceeds the critical value determined by the average size of the regions of weakness.

In order to obtain a check on the validity of this criterion for rupture it is necessary to know both the variation of the rupture

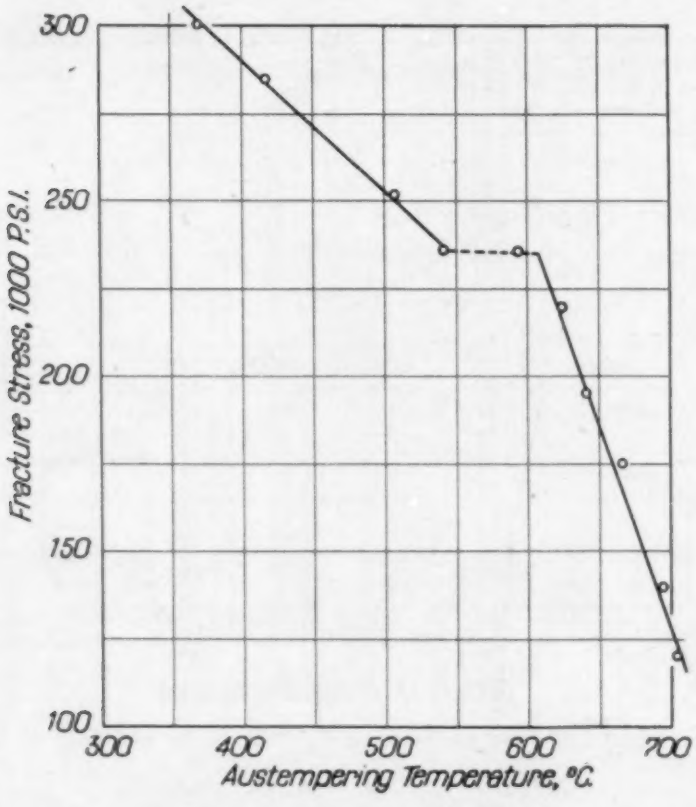

Fig. 19—Fracture Stress of 0.79 Per Cent Carbon Steel Austempered at Various Temperatures (20).

stress of some material and the average size of the cracks present in that material. There are very few complete series of data in which the fracture stress is recorded as a function of the dimensions of the microstructure. Gensamer and his collaborators (23) have determined the fracture stresses and the mean pearlite spacings of 0.78 per cent carbon steel austempered (corrected for recalescence). The fracture stress versus the austempering temperature is plotted in Fig. 19. It is to be noted that the variation of this stress with the temperature of formation is best represented by two straight lines of different slopes with a transition region at about 560 degrees Cent. (1040 degrees Fahr.). At this temperature the

structure of the decomposition product changes from pearlite to bainite. From the data on the fracture stresses of the pearlitic specimens and Fig. 18 the approximate radii of the regions of weakness may be determined. The variation of this radius with temperature is plotted as a function of the temperature of formation of the reaction products as curve A in Fig. 20. Gensamer determined the mean pearlite spacings by microscopic measurement and statistical analysis. This spacing is plotted as curve B in Fig. 20. The

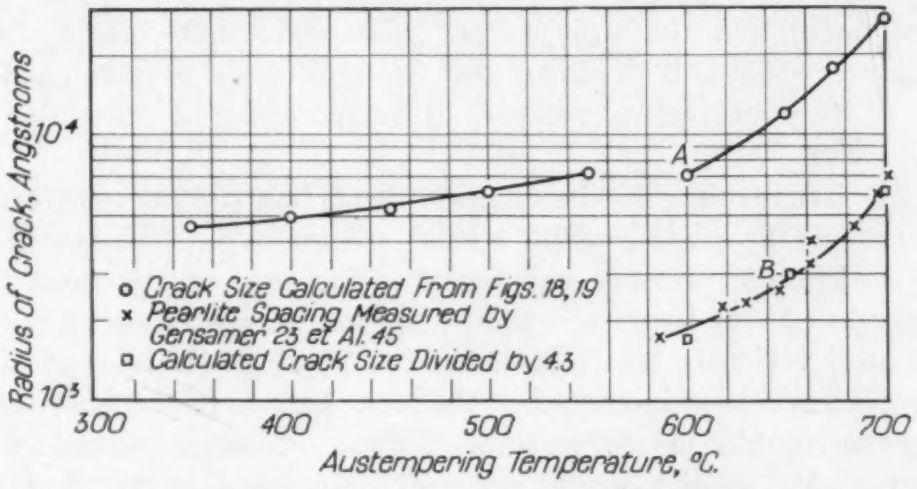

Fig. 20—Calculated Crack Size and Measured Pearlite Spacing Versus Austempering Temperature (0.79 Per Cent Carbon Steel). Temperature Corrected for Recalescence.

two curves are identical throughout the entire temperature range except for a constant factor (4.3).

Since, in the calculation of the radii, the value for the surface energy can only be approximated and the exact value of the constant C is not known, an absolute correspondence between theory and experiment cannot be expected. Furthermore, it is not known what microscopic dimension to consider as the crack in pearlitic steel. The pertinent dimension may be either the radius or the width of the cementite plate or it may be the width of the ferrite. It has been suggested that as deformation proceeds in pearlitic steels the brittle cementite plates break and the resulting transverse cracks spread through the matrix. This is probably the case and the width of the cementite plate is likely to be the pertinent dimension. The thickness of the cementite plate may be determined from the pearlite spacing and will have the same dependence upon temperature of formation as the pearlite spacing.

Further corroboration of the theoretical relation between pearl-

ite spacing and fracture stress may be obtained by comparing steels of different carbon content austempered at the same temperature. It has been reported that for such a series of steels the pearlite spacing is nearly independent of carbon content (45) and from a survey of the literature (23), (24) it is concluded that the fracture stress is likewise nearly independent of carbon content.

The variation of the theoretical initial crack radius in bainite is also plotted in Fig. 20. In this case the binding between surfaces of the cementite particles and the matrix may be very weak. It is to be noted that the size of the crack varies only slightly with temperature and it is predicted that the size of the carbide particles will be very nearly independent of temperature of formation of the bainite.

As discussed in a previous section, Bridgman (25) has performed experiments by placing small tensile specimens in a liquid under high hydrostatic pressure and by removing part of the axial load has produced very large reductions of area. For specimens of S.A.E. 1045 steel variously heat treated, he has obtained strain hardening-intercept curves by interrupting the tests before failure and measuring the resulting areas. In some of these specimens the reductions of area were as high as 90 per cent. Since the stress along the axis of the specimen is usually compressive or at least when there is net tensile stress it is very small, the extension of a crack would not result in a decrease of potential energy due to the relief of elastic tensile stress. In a sense the cracks are prevented from propagating by the hydrostatic pressure. Fracture finally occurs at a very great reduction in area, because at such large strains the specimen is actually under a large net tension. If the pressure is removed before the test bar is broken and the bar repulled at atmospheric pressure the fracture occurs usually at a much higher stress and with an additional reduction of area, as great as would be observed on a virgin specimen. This increase in fracture stress cannot be explained by any of the current theories of rupture. (See Appendix B.) However, this rather anomalous behavior finds an explanation in the theory outlined above. The dimension of the cracks perpendicular to the tension direction determines the critical fracture stress. During the extremely large deformations forced upon the sample by hydrostatic pressure these regions of weakness are elongated in the tension direction. Their dimension perpendicular to this direction becomes smaller and consequently the fracture

stress is raised. Cracks could also be prevented from spreading when the sample is under pressure. This type of explanation appears sufficient to explain in at least a qualitative way many of Bridgman's observations which are not consistent with the simple criterion for rupture, of maximum tensile stress.

In Shear—The same general type of consideration as delineated in the previous section can be employed to explain the conditions for rupture under the action of shearing stresses. Failure in shear should occur in a material containing cracks of a given size when the shearing stress reaches a value such that the spreading of a crack will relieve sufficient shear strain energy to decrease the net potential energy. This critical shear stress, X, can be expressed as a function of the radius of the inhomogeneity, r, the shearing modulus, G, and the surface energy, S, in the following manner:

$$X = \sqrt{\frac{2SG.}{C'r}} \qquad (8)$$

It is more difficult in the case of shear than in the case of tension to estimate the exact value of the constant C′. Since in torsion the tensile stress at 45 degrees to the shearing plane is exactly equal to the shearing stress it is impossible to decide, unless the constants in Eqs. (7) and (8) are known, whether or not the failure will occur at 45 or 90 degrees, or at some intermediate angle to the axis of the specimen. It has been determined experimentally that in brittle materials the fracture occurs at 45 degrees to the axis of the specimen, indicating that the failure results from the tensile stress (46). In ductile materials in torsion the failure is associated with the shear stresses since the fracture is usually perpendicular to the specimen axis. As deformation proceeds, in materials of some ductility, the projection of the cracks will extend upon the shearing plane but will remain relatively unaffected on the plane perpendicular to the maximum tensile stress. As the effective size of the imperfection increases the type of failure changes from the tensile type at 45 degrees to the axis to a shearing type perpendicular to the axis.

If steel specimens are first twisted, unloaded, and then broken in tension, the tensile fracture stress is relatively unaffected by small torsional strains, but decreases if the specimen is twisted to large angles—see Curve A, Fig. 21, from Swift (31). Concomitant

with the decrease in fracture stress the type of failure changes from the ordinary cup-cone to a helical, or "Wolf-ear", type.

Gensamer (47) attributes this decrease in fracture stress and the change in the type of failure to the reduction, by torsion, of the stress required to produce a normal failure on the 45-degree planes. He postulates that in twisting minute normal failures are developed along this plane and failure occurs in tension on this plane even though it is not the plane of maximum normal stress

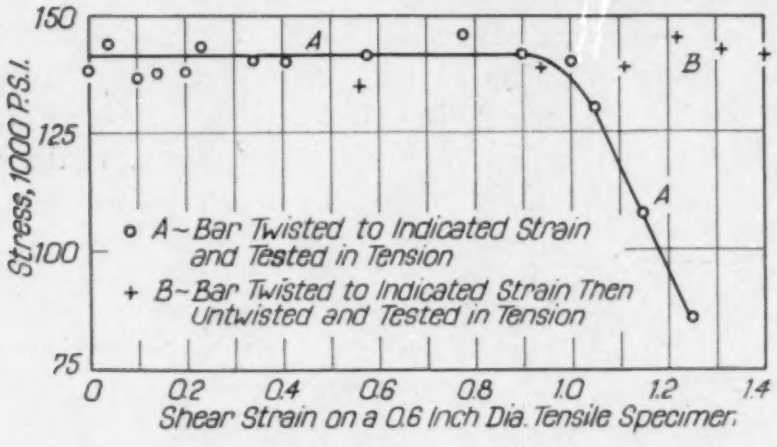

Fig. 21—Facture Stress in Tension Following Twisting (31).

in tension. Swift (31), however, untwisted samples similar to those which exhibited the "Wolf-ear" fracture in tension and found that the failure reverted to the normal cup-cone type and the fracture stress was unaffected by the torsion (Curve B, Fig. 21). It is difficult by Gensamer's postulation to account for this phenomenon for it is difficult to understand how untwisting could heal minute failures in the material, and completely restore the original fracture stress. These anomalous results may be explained if the behavior of the cracks under the torsion type of deformation is considered.

Fig. 9 is a schematic diagram of the crack distribution in a cylinder being twisted. As the cylinder is twisted the cracks tend to be oriented near the helical plane of compression. After twisting has proceeded a sufficient amount and the bar is then pulled in tension, it will break on some plane which was under compression during the torsion. This failure in tension on planes which were under compression is contradictory to Gensamer's postulation. An experiment was designed to demonstrate the validity of the conclusion deduced from the concept of cracks. The results are presented in Fig. 22. The specimen therein illustrated fractured across planes

which were under compression during twisting. Retwisting will restore the more or less random distribution of the imperfections and the failure will revert to the normal "cup-cone".

Consistent with the condition for rupture outlined in this paper it would be expected that any type of deformation which served to decrease the average size of the cracks with respect to the tensile axis of some other type of deformation would raise the fracture stress with regard to the second deformation. For in-

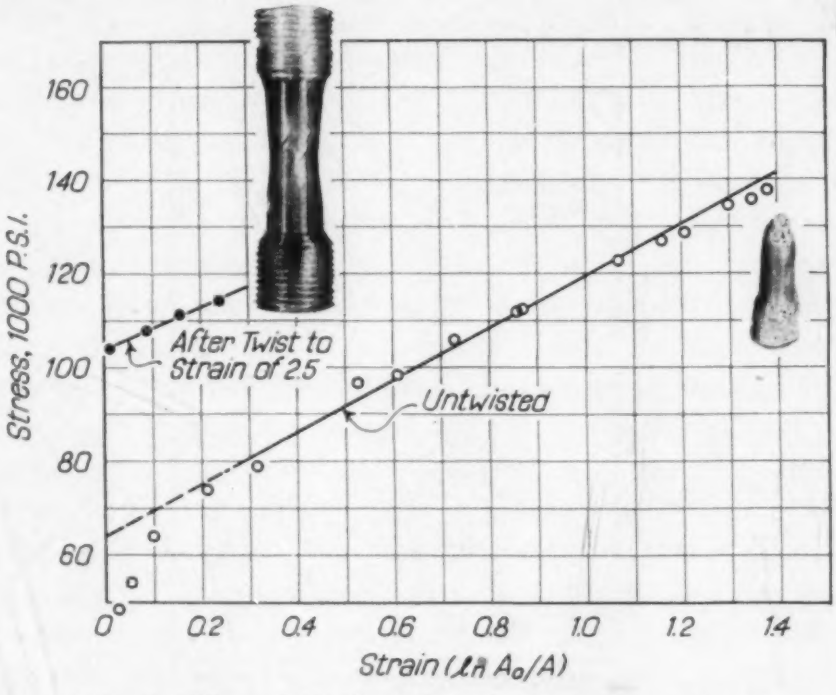

Fig. 22—Effect of Torsion on Strain Hardening and Fracture Stress in Tension.

stance, Swift (31) has reported results of tests in which samples have been pulled in tension and then twisted. The shear stress necessary for rupture in torsion increases with the amount of deformation during tension. This can be accounted for by the extension and reorientation of the cracks parallel to the tension direction. In planes parallel to the maximum shearing stress in torsion the average size of the imperfections has been decreased and as a consequence the fracture stress increased.

Dynamic Rupture

Metals, particularly steels, sometimes rupture under rapid dynamic loading with much less energy absorption than when loaded

quasi-statically. Low absorption of energy necessarily implies a small amount of deformation.* There are two fundamentally distinct mechanisms by which the deformation may be small. The plastic deformation may be small over the entire specimen. In this case, the material must separate by the method of crack propagation and the fracture will be of the so-called "brittle" type. On the other hand, the deformation may be confined to a small volume in which the deformation may be large. In this case, the material fractures by shearing across a surface and the plastic deformation is confined to the immediate vicinity of this surface.

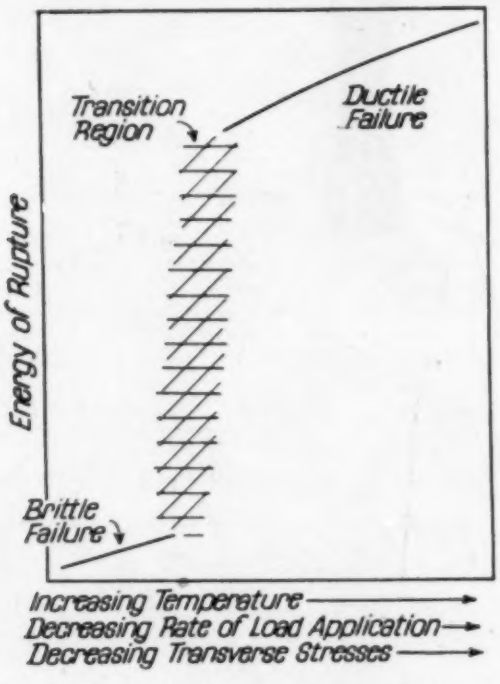

Fig. 23—Effect of Temperature, Rate of Loading and Transverse Stresses on the Type of Failure.

Brittle Type—Brittle fracture must occur whenever the pertinent stress-strain curve of the plastic state lies above the critical stress for fracture. As a load is applied under these conditions the material reaches the fracture stress with little or no plastic deformation and the specimen breaks with small absorption of energy. This brittle type of failure is favored by an increase in the rate of loading, by a decrease in the temperature, and by a multiaxial stress pattern. The general way in which the energy of rupture varies with these

*Reports of experiments (48) in which tensile bars were broken at high speed with little absorption of energy in spite of extensive deformation cannot be reconciled in light of more recent concepts. It is believed these earlier observations are uncertain because of inherent difficulties in the apparatus.

parameters is illustrated in Fig. 23; the position of the transition region being some function of the three parameters. The determination of this function is one of the outstanding problems in the study of the mechanical properties of metals.

Both an increase in the rate of deformation and a decrease in temperature raise the stress-strain curve as has been discussed under plastic flow. In materials which do not exhibit a drop in load at the yield the entire curve is raised, probably, by a constant factor. There are three effects of the multiaxial stress-pattern. Firstly, the addition of transverse tensile stresses will increase the tensile stress necessary for yielding. Both the Mohr and von Mises viewpoints predict this effect but to slightly different magnitudes for different stress-systems. As an example, if one transverse tensile stress is equal to one-half the longitudinal stress the longitudinal stress necessary for yielding will be increased by 15 per cent according to the von Mises theory. Secondly, most engineering impact tests are accomplished by bending a notched bar. In such cases, there will be a sharp gradient in the maximum shearing stress, or shearing strain energy, across the sample behind the notch, thereby raising the longitudinal stress necessary for yielding, since the stress necessary for yielding is higher when a gradient exists than when the stress is uniform (7). This rise in yield stress is due to the fact that yielding in regions of high stress concentration must necessarily extend somewhat into adjacent regions where the stress is less. Thirdly, the addition of transverse tensile stresses may lower the longitudinal stress necessary for fracture. This has been discussed in a preceding section, but to repeat an example, the addition of a transverse tensile stress equal to one-half the longitudinal stress may decrease the longitudinal stress necessary for fracture by as much as 30 per cent. The mere fact that the amount of deformation prior to fracture decreases during impact may also affect the fracture stress, for the material just prior to fracture has been changed. The magnitude or sign of this effect of deformation on the fracture stress cannot be predicted from the available data.

Gensamer (47) has discussed the qualitative effect of lowering the temperature and changing the stress system and his conclusions are summarized in Fig. 24. His explanation of the variation of the transition region with temperature and state of stress is based entirely on the effect of the increase in yield stress, on the effect of the stress system on the shearing stress (or shearing strain

energy) necessary for flow, and on the assumption that the fracture occurs when the maximum tensile stress reaches a certain value independent of the state of stress. This concept cannot explain the fact that the critical impact temperature in the notch bar impact test is on the average very near 0 degree Fahr. for steel. Since the difference between the fracture stress and yield strength in a tensile test at room temperature is usually of the order of magnitude of 100,000 psi. the effects mentioned by Gensamer are not sufficient

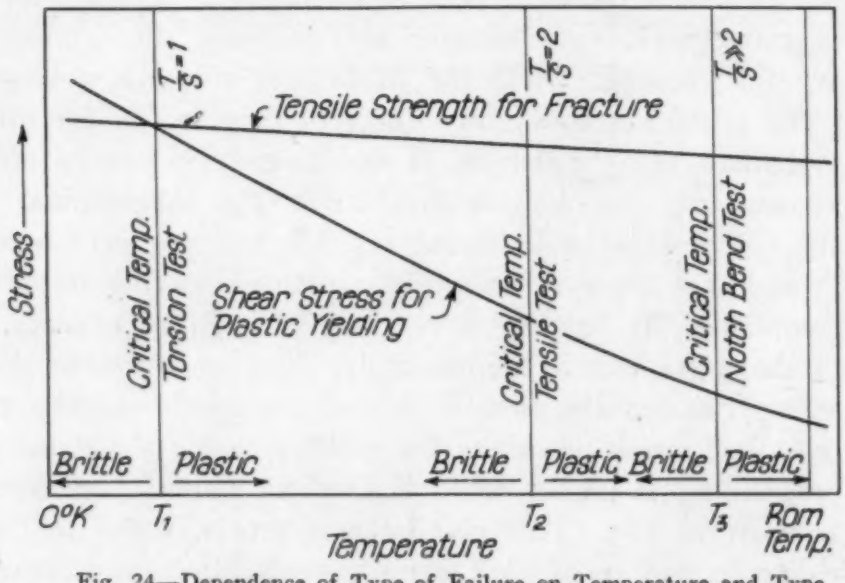

Fig. 24—Dependence of Type of Failure on Temperature and Type of Test (47).

to raise the yield stress to the fracture tensile stress with such a small temperature change. The effect of a multiaxial stress pattern in lowering the fracture stress and in raising the longitudinal yield stress by means of the stress gradient and the effects of strain rate must be of prime importance.

In the notched bar impact test at room temperature, where the tensile yield stress is very nearly equal to the tensile fracture stress, a small decrease in temperature raises the longitudinal yield stress relative to the fracture stress, and brittle rupture occurs with little energy absorption.

One of the most puzzling phenomena observed in the testing of steel is the variation in critical temperature in notched bar bend impact tests with heat treatment and processing of the specimen. For instance, the impact energy of pearlitic specimens is very much lower than that of spheroidal (quenched and tempered) specimens of the same yield and tensile strengths, as illustrated in Table I,

taken from Carpenter and Robertson.* It is recognized that the reduction of area in pearlitic steels is less than in quenched and tempered specimens of the same yield strength (49). As illustrated in Fig. 25, however, small differences in reduction of area mean

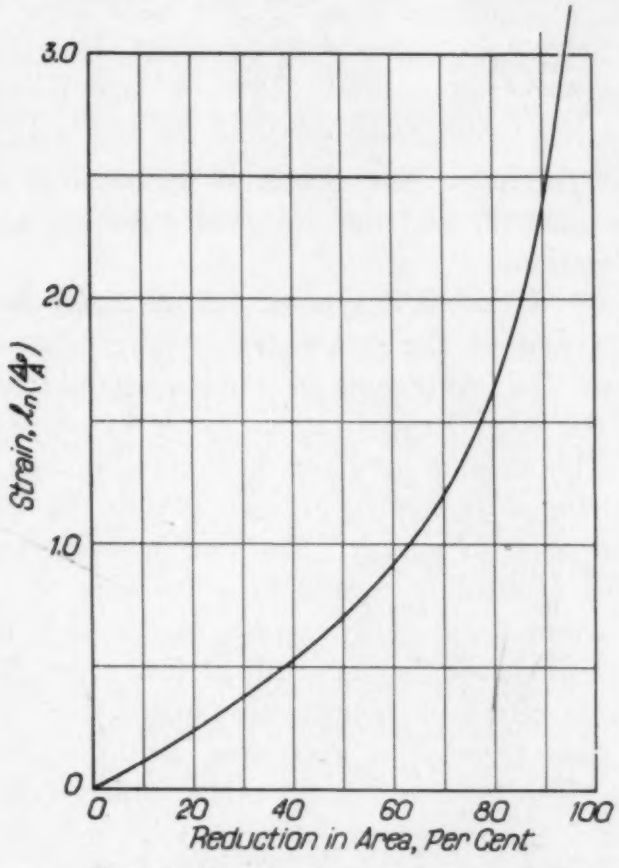

Fig. 25—Relation Between Strain and Per Cent Reduction in Area.

large differences between the true strains at fracture and therefore between the fracture stresses. For the 0.45 per cent carbon steel of Table I and Fig. 25 the difference in the strains is seen to be 0.26 and assuming a rate of strain hardening of 100,000 psi., the difference in fracture stress between the two steels is 26,000 psi. Assuming a reasonable fracture stress of steel of about 200,000 psi., the fracture stress of the pearlitic steel is 10 per cent lower than that of the spheroidized material. This effect is very large when the difference between the longitudinal stress necessary for yielding and for fracture is already reduced by the configuration of the test itself.

The whole problem of correlating microstructure with the properties of steels under a multiaxial stress system imposed by an impact,

*Loc. cit., p. 1095.

Table I
(Carpenter and Robertson, p. 1095)
Effect of Structure on Impact Energy

Steel % C	Heat Treatment (1.125" Diameter)	Ultimate Stress (psi.)	Elongation (per cent)	Reduction in Area (per cent)	Izod
0.45	Normalized	94,000	28	55	29
0.45	Tempered	94,000	27	66	57
0.28	Normalized	81,000	27	57	43
0.28	Tempered	90,000	29	54	93

requires thorough study. The effects of temperature, rate of deformation, stress pattern, and metallurgical structure are phases that justify investigation.

Shear Type—The brittle type of failure under impact is associated with a raising of the stress-strain curve with respect to the fracture stress. The shear type of failure peculiar to impact loading arises on the other hand from a change in shape of the stress-strain curve. This change in shape does not eliminate plastic deformation, but changes its nature in such a way that rupture ensues with little absorption of energy. The rise in temperature associated with high rates of loading results in a lowering of the latter part of the stress-strain curve with respect to the first part. In those cases where strain hardening is small at low rates of deformation, as in shear, this effect of temperature makes the dynamic stress-strain curve pass through a maximum and thereafter acquire a negative slope. Furthermore in materials which exhibit a drop in load at the yield, the yield strength rises with respect to the tensile strength with decreasing temperature and increasing rate of loading and consequently the load-elongation curve at low temperature and high rates of strain may exhibit a negative slope.

A negative slope is necessarily associated with an instability, for the more the material has deformed, the weaker it becomes. Deformation thus tends to become localized. In the case of shear, this localization is about a surface of shear.

Appendix A

Most physical theories may be presented from many viewpoints. In particular the von Mises theory of plastic deformation has been discussed in different ways. Since this theory is so fundamental to an understanding of plastic deformation, and since this theory has not been presented from the viewpoint consistently

adopted by the authors in this paper, it seems profitable to give such a presentation in this appendix.

In the text, stress and strain have always been so defined that the area beneath a stress-strain curve represents work done upon a unit volume of the material. In this appendix the work per unit volume, dW, associated with a small increment in deformation is carefully analyzed. In this analysis the assumption of von Mises plays an essential role. The increments in deformation is completely specified by the six strain increments de_{xx}, de_{yy}, de_{zz}, de_{yz}, de_{zx}, de_{xy}. The work dW is then equal to the sum of the products of each of these strain increments with the corresponding stress. Thus

$$dW = X_x \cdot de_{xx} + Y_y \cdot de_{yy} + Z_z \cdot de_{zz} + Y_z \cdot de_{yz} + Z_x \cdot de_{zx} + X_y \cdot de_{xy}. \tag{a-1}$$

As in the text, each strain increment refers to the material just before the increment, not before any deformation. Thus de_{xx} refers to the change in length, resolved along the X axis, of a unit length lying along the X axis just before the strain de_{xx} has occurred.

The above equation for dW can be simplified only if some relation is assumed between the stresses and the strain increments. The relation assumed in the von Mises theory is the only possible relation which satisfies simultaneously the conditions of isotropy and of constancy of volume. Expressed in mathematical terms, isotropy implies that the relation between stresses and strain increments remains unchanged upon an arbitrary rotation of the co-ordinate axes, while constancy of volume implies that $de_{xx}+de_{yy}+de_{zz}$ be equal to zero. The relation of von Mises is

$$de_{xx} = dQ \ \{X_x - \tfrac{1}{2}(Y_y + Z_z)\} \tag{a-2}$$

with two similar equations for de_{yy} and de_{zz}, and

$$de_{yz} = 3dQ \ Y_z \tag{a-2}$$

with two similar equations for de_{zx} and de_{xy}. The quantity dQ is some unspecified invariant function of the stresses. Eq. (a-2) follows formally from Hooke's law for an isotropic medium if the strains are replaced by strain increments, if the reciprocal of Young's modulus is replaced by dQ and if Poisson's ratio is given the value ½.

The expression for the element of work in Eq. (a-1) may now be simplified by substituting the von Mises relations of Eq. (a-2). The result may be expressed most concisely in terms of the following two invariant functions:

$$S_I^2=(1/9)\{(Y_y-Z_z)^2+(Z_z-X_x)^2+(X_x-Y_y)^2\}+(2/3)(Y_z^2+Z_x^2+X_y^2), \qquad \text{(a-3)}$$

and

$$(de_I)^2=(de_{yy}-de_{zz})^2+(de_{zz}-de_{xx})^2+(de_{xx}-de_{yy})^2+(3/2)(de_{yz}^2+de_{zx}^2+de_{xy}^2) \qquad \text{(a-4)}$$

The right hand member of Eq. (a-3) is the only invariant quadratic function of the stresses, aside from a constant factor, which is independent of the hydrostatic pressure, $(X_x+Y_y+Z_z)/3$. The constant factor has been so chosen that S_I is equal to the shearing stress across the octahedral planes referred to the principal stress axes. Similarly, the right hand member of Eq. (a-4) is the only invariant quadratic function of the strain increments, aside from a constant factor, which is independent of the dilatation $de_{xx}+de_{yy}+de_{zz}$. In view of Eq. (a-2), these two invariant functions are related by the following equation:

$$de_I=(9/2)\,dQ\,S_I \qquad \text{(a-5)}$$

When use is now made of Eqs. (a-3)—(a-5), substitution of Eq. (a-2) into Eq. (a-1) gives the following equation:

$$dW=S_I\,de_I. \qquad \text{(a-6)}$$

The arbitrary constant factor in the right hand member of Eq. (a-4) has been so chosen as to make the numerical factor in the right member of Eq. (a-6) equal to unity. The element of work may therefore be expressed as the product of two invariant functions. The function S_I will be called the invariant stress, de_I will be called the invariant strain increment.

The work done upon a unit volume of material during a finite deformation is obtained by integrating Eq. (a-6),

$$W=\int S_I\,de_I. \qquad \text{(a-7)}$$

It should be noted that the invariant strain, defined by the equation

$$e_I = \int de_I, \qquad \text{(a-8)}$$

is not a single valued function of the final deformation. Rather this invariant strain depends upon how the final configuration is obtained. The interpretation of e_I may be clarified by reference to the heat Q absorbed by a body defined by

$$Q = \int dQ.$$

As is well known, this heat is not a single valued function of the end state, but of the path along which the end state is reached.

The stress invariant S_I and the strain increment invariant de_I may be given simple physical interpretations. In view of Eq. (a-2), the principal axes of the strain increment coincide with the principal axes of the stresses. The shearing stresses across each of the four octahedral planes, referred to these axes, are equal, and are given precisely by S_I, as has already been mentioned. Likewise the shearing strains across each of these four octahedral planes are all equal. It may be shown that these shearing strains associated with an element of deformation are equal to $de_I/3$. Some authors, in particular Nadai, have referred to S_I and to $e_I/3$ as the octahedral shear stress and the octahedral shear strain, respectively. The present authors regard the invariancy of these functions as of more fundamental significance than their interpretation with reference to the octahedral planes, and therefore refer to S_I and de_I as the invariant stress and the invariant strain increment, respectively.

Appendix B

Current Theories of Fracture

There are certain inherent difficulties in obtaining the conditions under which fracture occurs in metals. Generally the stress necessary for plastic flow is less than that necessary for rupture and the metal deforms before fracture. In such cases the conditions of fracture have been obtained for the fracture of the metal altered by deformation rather than of the virgin material.

The original theory of Mohr did not specify whether the condition of maximum shearing stress should be applied to yielding or to

fracture. With the publication of more information, particularly by Griffith (40) it became more or less certain that for most purposes the maximum tensile stress determined fracture and that Mohr's theory was applicable only to yielding. Kuntze (50) concurred in this view, by stating that fracture occurs when the maximum principal stress reaches a value determined solely by the state of the metal at the instant of fracture, implying that the fracture stress is independent of the other principal stresses. According to Kuntze, the tensile stress necessary for fracture varies with the amount of previous deformation and he called this stress the technical cohesive strength. The technical cohesive strength as determined by the fracture stress is not that of the original metal but of material which has been altered by the deformation.

In order to obtain a measure of the true technical cohesive strength, characteristic of an undeformed metal, Kuntze measured the tensile strengths in specimens notched at various angles and depths. He found that as the depth and sharpness of the notch increased the tensile strength increased and concluded, in part, that in a bar containing a notch of infinite sharpness, and extending nearly across the bar, the stress distribution would approach the condition of equal tensile stresses in all directions. If this state of stress could be obtained, no plastic flow could occur according to any accepted theory (shearing stresses are equal to zero) and the fracture stress must be that of the virgin metal. Kuntze states that the ratio of the average radial and average longitudinal tensile stresses depends upon the depth and sharpness of the notch in the following manner

$$S_3/S_1 = \left(1 - \frac{d^2}{D^2}\right) \cdot (180 - W)/180$$

where D and d are the diameters before and after notching, respectively, and W is the angle of the notch in degrees. He found that the ultimate tensile stress was a linear function of this ratio and by extrapolating S_3/S_1 to unity he obtained a value which he believed was the true technical cohesive strength of the material. On the basis of his experiments Kuntze asserted that the cohesive strength first increased and then rapidly decreased with plastic deformation. Fig. 26 is an illustration of the variation of the co-

hesive strength and the strain hardening curve with deformation. Fracture occurs when the cohesive strength has been lowered by cold work till it intersects the rising strain hardening curve.

This concept of technical cohesive strength is based almost entirely upon tensile results obtained from notched specimens. There are several objections to such experiments. A rigorous

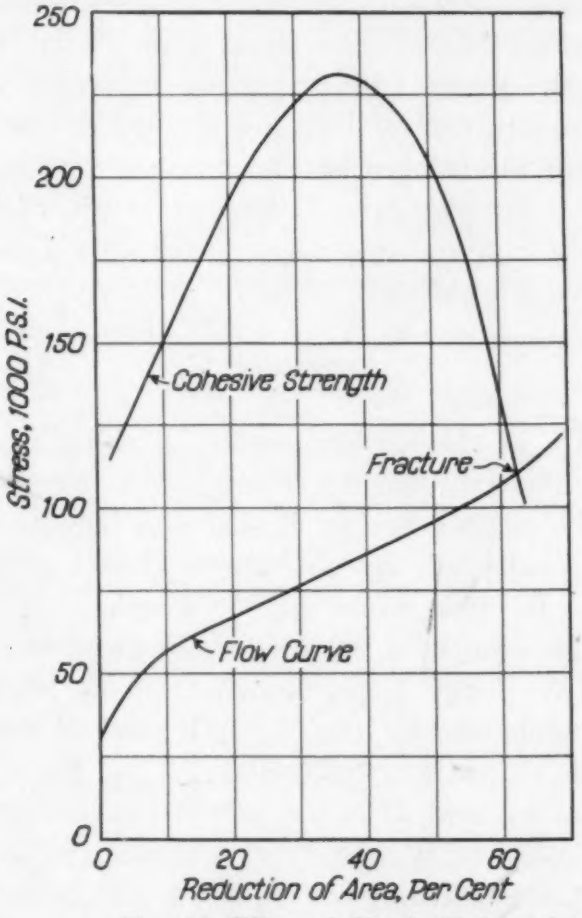

Fig. 26—Effect of Plastic Deformation on Cohesive Strength and Flow Resistance (50).

analysis of the stress distribution at the base of a given notch is extremely difficult, and Sachs (51), in particular, has questioned the validity of Eq. (b-1). The notch itself is almost impossible to reproduce in different samples. Furthermore as the unnotched area is decreased the effect of grain size may become more and more important and the size effect noted first by Griffith (40) may appear.

McAdam (52) has recently reviewed Kuntze's data and theory and concludes that the technical cohesive strength increases with

plastic deformation but not so rapidly as the strength rises due to strain hardening. He also concludes that the fracture stress does not depend upon a single stress value such as the maximum tensile stress but upon the combination of all the principal stresses. As the radial tensile stress increases the fracture stress rises after an initial small drop. However, any deductions regarding fracture stress must be regarded with suspicion if based upon notched bars.

The variation of fracture stress with radial stress was first presented by Bridgman (4th paper of reference 39). Bridgman used radial pressure exclusively, and studied brittle materials only. In such materials the fracture stress decreases with increasing hydrostatic pressure. However, the failure of brittle materials probably begins at the surface, and may be of an entirely different type from that which occurs in ductile metals.

Appendix C

An estimate of the work necessary to form a surface of unit area in iron, called the surface energy S in the text, is obtained as follows. The surface energy is taken to be equal to the energy required to evaporate one layer of atoms from a unit surface. This energy in turn is taken to be $qN^{2/3}$, where N is the number of atoms in a unit volume, q is the energy required to evaporate a single atom. The energy q is obtained from the variation of vapor pressure with temperature. Thus $(Nq/R) = d \ln P/d(1/T)$, where N is Avogadro's number, 6.06×10^{23}, R is the gas constant, 2 calories/gram atom, and T is the absolute temperature in degrees Cent. Upon substituting into this equation the known variation of P with T (Metals Handbook (53), p. 435), one obtains

$$Nq = 66{,}000 \text{ calories/gram atom.}$$

Finally, from the value $n = 8.5 \times 10^{22}$, one obtains S=8,800 ergs/cm^2.

Bibliography

1. J. H. Hollomon and C. Zener, "High Speed Testing of Mild Steel," Transactions, American Society for Metals, Vol. 32, 1944, p. 111.
2. O. Mohr, "Welche Umstande bedingen Elastizitatsgrenze und der Bruch eines Materiales," *Zeit. des Vereines Deutsches Ingenieur,* Vol. 44, 1900, p. 1525 and 1572.
3. R. von Mises, "Mechanik der Festen Korper in Plastisch-deformablen Zustand," *Machr. d. Gesellsch. d. Wissensch.* Zur Gottingen, Math-Phys. Klasse, 1913.

4. C. F. Elam, "The Influence of Rate of Deformation in the Tensile Test with Special Reference to the Yield Point in Iron and Steel," *Proceedings* of the Royal Society, Vol. 165, 1938, p. 568.
5. C. W. MacGregor, "The Yield Point of Mild Steel," American Society of Mechanical Engineers, Vol. 53, A. P. M. 1931, p. 187.
6. A. Nadai, *Ztsch. tech. Physik,* Vol. 5, 1924, p. 369, and G. I. Taylor, "Faults in a Material which Yields to Shear Stress while Retaining its Volume Elasticity", *Proceedings,* Royal Society, Vol. 145, 1934, p. 1.
7. G. Cook, "The Yield Point and Initial States of Plastic Strain in Mild Steel Subjected to Uniform and Non-uniform Stress Distribution," *Phil. Trans.,* Royal Society, Vol. 230, 1931-32, p. 103.
8. A. Nadai, "Plasticity," McGraw-Hill, 1931.
9. H. Carpenter and J. M. Robertson, "Metals," Oxford University Press, New York, p. 119.
10. C. A. Edwards, H. N. Jones and B. Walters, "A Study of Strain-Age-Hardening of Mild Steel," *Journal,* Iron and Steel Institute, Vol. 139, No. 1, 1939, p. 341.
11. J. Winlock and R. Leiter, "Some Factors Affecting the Plastic Deformation of Sheet and Strip Steel and Their Relation to the Deep Drawing Properties," TRANSACTIONS, American Society for Metals, Vol. 25, 1937, p. 163, and "Some Observations on the Yield Point of Low Carbon Steel," American Society of Mechanical Engineers, Vol. 61, 1939, p. 581.
12. C. A. Edwards and L. B. Pfeil, "The Tensile Properties of Single Iron Crystals and the Influence of Crystal Size Upon the Tensile Properties of Iron," *Journal,* Iron and Steel Institute.
13. T. B. Yensen and N. A. Ziegler, "Magnetic Aging of Iron Due to Oxygen," *Transactions,* American Institute of Mining and Metallurgical Engineers, Vol. 116, 1935, p. 397.
14. E. Schmid and W. Boas, "Kristallplastizitat," Springer, 1935, p. 119.
15. H. Hencky, "Zur Theorie Plastischer Deformation," *Ang. Math. v. Mech.,* Vol. 4, 1924, p. 323.
16. W. Lode, "Versuch Uber den Einfluss den Mittleren Hauptspannung auf das Fliessen der Metalle Eisen, Kupfer and Nickel," *Zeit. f. Physik,* Vol. 36, 1926, p. 913.
17. G. I. Taylor and Quinney, "The Plastic Distortion of Metals," *Phil. Trans.,* Royal Society, Vol. 230, 1931, p. 131.
18. G. Sachs, "The Derivations of the Conditions of Plasticity," *Z. Ver. deut. Ing.,* Vol. 72, 1928, p. 734.
19. G. I. Taylor, "Plastic Strain in Metals," *Journal,* Institute of Metals, Vol. 62, 1938, p. 307. and "The Mechanism of Plastic Deformation of Crystals," *Proceedings,* Royal Society, Vol. 145, 1934, p. 362, 388.
20. M. Gensamer, E. B. Pearsall, W. S. Pellini and J. R. Low, "The Tensile Properties of Pearlite, Bainite, and Spheroidite," TRANSACTIONS, American Society for Metals, Vol. 30, 1942, p. 983.
21. F. Seitz and T. A. Read, "Theory of the Plastic Properties of Solids," *Journal of Applied Physics,* Vol. 12, 1941, p. 100, 170, 470, 538.
22. C. W. MacGregor, "Relations Between Stress and Reduction in Area for Tensile Tests in Metals," *Transactions,* American Institute of Mining and Metallurgical Engineers, Vol. 124, 1937, p. 208.
23. M. Gensamer, E. B. Pearsall and G. V. Smith, "The Mechanical Properties of the Isothermal Decomposition Products of Austenite," TRANSACTIONS, American Society for Metals, Vol. 28, 1940, p. 380.
24. J. H. Hollomon, "Effect of Heat Treatment and Carbon Content on the Work Hardening Characteristics of Several Steels," TRANSACTIONS, American Society for Metals, Vol. 32, 1944, p. 123.
25. P. W. Bridgman, "Report on Tension Tests Under Pressure," Report to Watertown Arsenal, Jan. 15, 1943.
26. H. O'Neill, "The Hardness of Metals and Its Measurement," Sherwood Press, 1934, p. 203.

27. F. T. Sisco, "The Alloys of Iron and Carbon," Vol. II Properties, McGraw-Hill, 1937, p. 113.
28. A. Nadai, Ibid, p. 128.
29. M. C. Fetzer, "Torsional Testing and Torsional Creep Testing," Harvard Thesis, 1934.
30. A. Phillips and E. S. Bunn, "Directional Properties in Cold Rolled and Annealed Copper," *Transactions,* American Institute of Mining and Metallurgical Engineers, Vol. 93, 1931, p. 353.
31. Swift, "Tensional Effects of Torsional Overstrain in Mild Steel," *Journal,* Iron and Steel Institute, Vol. 140, 1939, p. 181.
32. A. Nadai and E. Davis, "Plastic Behavior of Metals in the Strain Hardening Range," *Journal Applied Physics,* Vol. 8, 1937, p. 205.
33. H. Quinney, "Time Effects in Testing Metals," *The Engineer,* March 30, 1931, p. 332.
34. H. E. Cleaves and J. G. Thompson, "The Metal Iron," McGraw-Hill, 1935, p. 375.
35. S. Dushman and I. Langmuir, "Diffusion Coefficient in Solids and Its Temperature Coefficient," *Physical Review,* Vol. 20, 1922, p. 113.
36. A. Nadai and M. J. Manjoine, "High-Speed Tension Tests at Elevated Temperatures, Parts II and III," *Transactions,* American Society of Mechanical Engineers, Vol. 63, 1941, A-77.
37. D. S. Clark and G. Datwyler "Stress-Strain Relations Under Tension Impact Loading," *Proceedings,* American Society for Testing Materials, Vol. 38, 1938, p. 98.
38. M. Itihara, "Impact Torsion Test," Technology Reports of the Tohoku Imperial University, Vol. 11, 16, 1933, p. 512; Vol. 12, 1936, p. 63.
39. P. W. Bridgman, 1. "Reflections on Rupture," *Journal Applied Physics,* Vol. 9, 1938, p. 517. 2. "Considerations on Rupture Under Triaxial Stress," *Mechanical Engineering,* Vol. 61, 1939, p. 477. 3. "Theoretically Interesting Aspects of High Pressure Phenomena," *Review of Modern Physics,* Vol. 7, 1935, p. 1. 4. "Breaking Tests Under Hydrostatic Pressure and Conditions of Rupture," *Philosophical Magazine,* Vol. 24, July 1912, p. 63.
40. A. A. Griffith, "The Phenomena of Rupture and Flow in Solids," *Physical Transactions,* Royal Society of London, Vol. 221, 1920, p. 163.
41. A. A. Griffith, "Theory of Rupture," *Proceedings,* First International Congress for Applied Mechanics, Vol. 55, Delft 1924.
42. Maier, "Einfluss des Spannungzustandes auf das Formanderungsvermogen der metallischen Werkstoffe," *V. D. I.,* Berlin, 1935.
43. R. Kenyon and R. Burns, "Autographic Stress-Strain Curves of Deep Drawing Sheets," TRANSACTIONS, American Society for Steel Treating, Vol. 21, 1933, p. 577.
44. E. Janitzky and M. Baeyertz, "The Interrelation Between Stress and Strain in the Tensile Test," TRANSACTIONS, American Society for Metals, Vol. 28, 1940, p. 714.
45. G. Pellissier, M. F. Hawkes, W. A. Johnson, and R. F. Mehl, "Interlamellar Spacing of Pearlite," TRANSACTIONS, American Society for Metals, Vol. 30, 1942, p. 1049.
46. R. W. E. Leiter, "An Investigation of Some Properties of Iron and Steel at Low and at Elevated Temperature by Torsion Testing," Harvard Thesis, 1930.
47. M. Gensamer, "Strength of Metals Under Combined Stresses," published by American Society for Metals, 1940.
48. H. C. Mann, "High Velocity Tension Impact Tests," *Proceedings,* American Society for Testing Materials, Vol. 36, Part II, 1936, p. 85.
49. E. C. Bain, "The Alloying Elements in Steel," published by American Society for Metals, 1939, p. 39.
50. W. Kuntze. For survey and bibliography see D. J. McAdam, *Transactions,* American Society of Mechanical Engineers, Vol. 63, 1941, p. 155, and

Transactions, American Institute of Mining and Metallurgical Engineers, Vol. 150, 1942, p. 311.
51. G. Sachs, "Report on Embrittlement of Steel Under Multiaxial Stresses," Engineering Foundation Welding Research Committee, New York.
52. D. J. McAdam, "The Technical Cohesive Strength of Metals," *Transactions,* American Society of Mechanical Engineers, Vol. 63, 1941, A-155; "The Technical Cohesive Strength and Yield Strength of Metals," Vol. 150, 1942, p. 311.
53. A.S.M. METALS HANDBOOK, Cleveland, 1939, p. 435.

DISCUSSION

Written Discussion: By A. Nadai, consulting mechanical engineer, Westinghouse Electric & Manufacturing Co., Research Laboratories, E. Pittsburgh, Pa.

The authors state in the abstract of their paper that certain data found in the literature on plastic flow and rupture of the metals required the introduction of new concepts for their explanation. With this aim in mind they devote a major portion of their paper to a review of the mechanical developments which have been proposed for expressing mathematically the plastic behavior of metals. A generous portion of this latter material has already been surveyed by others at various recent occasions so that references to these former general surveys would have been in order while a few recent mechanical investigations shared less favorably in the review which would have deserved to be brought to the attention of readers.

The authors state that they were primarily concerned with a review of the conditions of first yielding, the precise nature of flow under a given state of stress and with the extension of the theory of plastic flow into the strain hardening range of the permanent strains. This discussion will essentially be limited to these three subjects, but a few brief remarks will be included also about the rates of strain and other questions mentioned in the paper.

The authors write: "The behavior of metals in the plastic state *has not been successfully systematized into a set of laws corresponding to Hooke's law for the elastic state.*" (Italics by the present writer.) The following sentence: "However, two fairly successful systems for plastic behavior have been proposed," seems to weaken what was stated in the preceding sentence. They write: "The first system, introduced by *Mohr,* focusses attention upon *the planes of maximum shearing stress.* In the second system, proposed by *von Mises,* attention is directed to certain quadratic invariants of stress and of strain." Also: "The authors believe that little progress is to be made in attempts to modify either the Mohr or von Mises systems *to obtain better agreement with the few standard types of experiments.*"

These and other statements of a similar nature appearing in the paper may reflect the personal viewpoints of the authors. The writer must, however, express the opinion that some of these statements can hardly be substantiated through weighing the facts and that the validity of the remaining ones must be questioned.

The last sentence which was quoted is particularly misleading. It creates the impression as if one or the other or both of the quoted theories would not be in agreement with the experiments. It leaves also the impression as if both of these theories had been advanced for the same purpose; namely, for describing the plastic flow of a ductile metal. What the authors have stated about the "Mohr theory" is not correct. First of all, Otto Mohr, to the knowledge of this writer, did not propose a "theory of plastic flow." He attempted to define the conditions under which materials fail either in *rupture* or by *starting* to yield. The essence of his failure theory was the contrary of what Messrs. Zener and Hollomon claim and attributed to him. According to Mohr failures start in certain planes *which do not coincide with the planes of maximum shear.*[1] O. Mohr, L. Prandtl, von Karman, the writer and others have described numerous examples of stressed bodies in which the first macroscopically visible surfaces of slip deviated considerably from the directions of the planes of maximum shearing stress. Mohr assumed that slip in general does not occur along the planes of maximum shearing stress. His condition of failure:

$$\sigma_1 - \sigma_3 = f\ (\sigma_1 + \sigma_3)$$

in which $\sigma_1 > \sigma_2 > \sigma_3$ designate the principal stresses and in which the intermediate principal stress does not appear coincides with the maximum shearing stress theory only if the function on the right side of the equation is equal to a constant. Mohr, to the knowledge of the writer, has never investigated the plastic stress-strain relations which are a fundamental part in a theory of plastic flow. He published, however, a theory of earth pressures and discussed equilibria in loose materials (sand). In all of these investigations he made extensive use of his graphical method for representing the general states of stress, a method which is here mentioned because this method is particularly suitable for discussing, for studying and for *predicting the orientation of the surfaces of slip in stressed bodies* and because it is still so little appreciated by physicists.

These curved surfaces in plastic or loose materials have not only a practical significance but they open also from the viewpoint of the mathematician the horizon. In the theory of the propagation of sound or of the waves in supersonic flow of a compressible fluid analogous phenomena are known: The solutions of certain types of differential equations become discontinuous along certain surfaces. In plastic or loose materials (sand) something similar occurs. Solutions can be found and constructed by using these special surfaces along which discontinuities are propagated. The Mohr surfaces of slip are identical with these surfaces. From a practical viewpoint they are important because certain types of fractures possibly coincide with them. This all has not escaped men like Mohr and mathematically minded engineers who have recently studied

[1]Although the authors of the paper in a footnote (p. 166) state that they have associated the two names of "Mohr" and of "von Mises" with the viewpoints expressed in their text even though they realize other workers have contributed much to the development, it is arbitrary to associate one name with a deed not characteristic to the person in question and to connect another name with developments which chronologically were much older than his work and were carried out beyond his intentions later by others. It would have been clearer if the authors would have stated the remarkable and very fruitful contribution which von Mises made to the mechanics of plastic bodies by suggesting for the condition of plasticity the new form: $(\sigma_1 - \sigma_2)^2 + (\sigma_2 - \sigma_3)^2 + (\sigma_3 - \sigma_1)^2 = \text{const.}$

the geometric properties of these surfaces of slip and all this must be mentioned here to prove to the less informed reader that such statements as the ones quoted from the authors' paper are not justified also from *the theoretical viewpoint.* The authors throw out a healthy child with the water of the tub. Several groups of the equations including various modified forms of them are intimately related to those surfaces and have their own characteristic surfaces of slip.

The mathematical theories which have been proposed for dealing with plastic states in solids are based on idealizing assumptions. For example the theory of the steady flow of a plastic substance assumes that the stresses during the flow do not change their magnitude. On this assumption were based the theories of flow of von Mises (1913) and of St. Venant (1870). Everyone who has had a little experience with the flow of ductile metals knows how differently a metal can behave in the plastic range depending on the conditions under which it is tested (heat treatment, state of stress, previous cold work, etc.). One should, therefore, not expect that a theory which postulates *strain independent yielding* (von Mises, St. Venant) shall be applicable to the ordinary flow of any metal *known to strain harden.* Remarkably enough despite these facts this theory proved to be an excellent tool when it was applied in the strain hardening range of a metal. The authors quoted some of the first experiments by *W. Lode* (p. 176 of their paper) described in his doctor thesis and initiated by this writer which supported three of the basic assumptions of flow. By cautiously interpreting the theory, Lode could show that it could be applied to express the "instantaneous" conditions of flow in a strain hardening metal under biaxial stressing. One should expect after these remarks that the theory of the steady flow of a perfectly plastic substance is particularly suitable to express plastic states of stress in those metals which have a sharply defined yield point in a tension test. Mild steel would be a representative metal, assuming also small strains, but a soft copper would not be a good case.

The authors refer first to Hooke's law. They express themselves satisfied as follows: "The elastic state of the *isotropic* material is completely specified by Hooke's law," (notwithstanding the fact that every grain of a metal is anisotropic. Apparently they are not thinking to include in their statement for example coarse-grained or oriented structures with a marked elastic anisotropy known to exist in many cold-worked metals). But when they open their discussion on the plastic behavior of metals (p. 166) they note that this "has not been successfully systematized." The writer believes that just the contrary is the truth. Today several important cases of the plastic behavior have mechanically been defined. The question which should have been asked is this: are the simple basic assumptions which have been proposed for expressing stress-strain relations, or stress-rate of strain relations, or the state of flow while a metal is permanently deformed sufficient to predict quantitatively some of the observable facts of flow? Can these equations be utilized in important engineering applications or must they be rejected because they do not express essential facts correctly? Can and how must they be *modified* for expressing such heterogeneous cases as for example creep at high temperatures or strain hardening at low temperatures?

As far as the writer is able to see the authors have not offered anything from which would follow that for example the theory of a perfectly plastic substance does not satisfy all the requirements of a good mechanical theory. The writer advances the opinion that the simplest of the theories of flow in solids is as perfect, self-contained and complete as the theory of the isotropic elastic substance (Hooke's "law"). It is based on few assumptions and as long as it is not applied to practical cases in which one or the other of these assumptions is not valid it has been a very valuable tool. It has also proved to be extremely fruitful. During the last two decades many exact solutions have been discovered by engineers and mathematicians satisfying the plastic differential equations. These were used in the applications, of which none have been referred to in the present paper.

The plastic flow of the metals unfortunately has not a unique character like the elasticity of materials. Several important cases or types of flow have been recognized. Contrary to the opinions expressed in the paper (p. 167, second paragraph) it is the belief of those investigators who have had an occasion to study several of these types of flow, that good progress will be made (and has already been made) by *modifying* the assumptions and by attempting to generalize them more and more. To this should be added, that in a few cases with these modified theories quite good agreements were obtained with the experiments.

Metal (steel) structures in the elastic state are usually considered to behave as isotropic bodies and the strains in them can be assumed to be small. There are, however, other engineering materials in which stress is not proportional to strain. Attention has been called to a number of materials or conditions in which the above mentioned postulates of the elastic substance are not valid. (Examples: *large* elastic strains in rubber, theory of bending of anisotropic elastic plates of reinforced concrete, design of large wooden frame structures, etc. G. Tammann has shown that the elastic sound vibrations of cold-rolled copper plates are distinctly anisotropic.) The well-known Chladni sound figures produced by vibrating such plates (markedly differed from the ones observed in isotropic disks). When the necessity arose to apply the theory of elasticity to similar cases use has been made of the methods which were developed in related fields, for example in crystalelasticity. At any rate it seems that nobody raised remarks against the theory of the isotropic elastic material or the assumption of small strains because also important cases existed in which the former assumptions would not apply or in which the elastic strains became large. If an analogous attitude could be assumed by investigators when the flow of the ductile metals and the permanent plastic strains must be considered, the present differences in opinions would at once disappear. The authors have failed to bring out the important practical aspects, the limitations and even the principal aims in these mechanical theories which have been proposed since the times of St. Venant (1870), M. Levy, Duquet, and which have been improved and further developed by recent investigators.

It should be emphasized that for example the assumption of small plastic strains (which are many times larger than the elastic portions of the total strains) is frequently justified in many practical applications. To these belong the cases of flow in tubes, heavy walled cylinders, in rotating disks or under

concentrated pressures occurring in rolling, drawing, etc., at elevated temperatures. There are comparatively few cases in which a need exists to consider large permanent strains (larger than say 20 per cent in tension or compression). Ingenious new definitions have been proposed by *Ludwik* and *Leon* for dealing with them and these have been generalized by *Hencky* and others for handling large permanent strains whenever a need should develop for quantitatively considering them.

The plastic behavior of solids under high constraining hydrostatic pressures has also been thoroughly investigated in engineering laboratories since 1910 in connection with the conditions of yielding of brittle as well as of ductile materials.

Instructive experiments of the kind described by the authors "in which the plastic behavior is radically different" have been made, some of them quite a long time ago. The writer recalls that at the International Congresses for Applied Mechanics in Delft (1924) and Zurich (1926) *A. Griffith* and *L. Prandtl* brought up questions which have been touched by the authors in relation to unusual fractures. *Prandtl* pointed out that test cylinders of brittle materials under a lateral high hydrostatic pressure fail through cracking. The fluid penetrates in the small cracks of the test cylinder. Von Karman found this to be the case around 1910. After covering the specimens of a brittle material (marble) with a brass foil he prevented the penetration of the pressure fluid and could deform such "brittle" materials *plastically*.

Poulter made similar observations and found that frequently the failure occurs upon rapid release of the pressure. Formation of cracks may be influenced, however, by several concurring causes. In some previous conversations with one of the authors these details may have been called to his attention by the writer, because they were known to the latter.

At any rate, if this would have not been the case, they could have been found in several old published notes. The sentence in the footnote on page 195 in which the authors claim that the above described explanation (of the cracking of test pieces through hydrostatic pressure) is a confirmation of their *own* viewpoints should be taken with a grain of salt.

The authors believe that strain hardening has "apparently been investigated thoroughly only for tension and for torsion" (page 177). Tubular specimens have a number of times been investigated by subjecting them to the combined effects of an internal hydrostatic pressure and an axial load and the plastic deformation has been recorded until the final fracture occurred. A series of such tests was made and described by E. A. Davis using soft fully annealed copper in a recent paper which was presented at the A.S.M.E. Applied Mechanics Meeting in Pittsburgh in June 1943. The flow of copper (and of other metals) has been recorded under biaxial stressing and strain hardening studied under these conditions until fracture occurred.

These remarks may revert partially to the authors applications "of the von Mises viewpoint to the problem of correlating different stress-strain curves." They emphasize that their approach "is quite different" from that by E. A. Davis and the writer (in two papers published in 1937). The authors regard the "invariancy" of certain expressions containing the components of stress or

of strain "as of more fundamental significance" than the interpretation by the writer, who noted that they express the components of the shearing stress and shear in the octahedral planes with respect to the principal directions. Which of these two interpretations will appeal more to engineers who probably are the ones who may use them in the future may be patiently awaited.

Granting the authors the privilege claimed by them to present physical theories from many viewpoints the writer would like to ask them in which new viewpoint their own presentation of their equations (in the appendix A) differed from the ideas which guided the writer when he tried to formulate expressions for strain hardening in 1937. The writer made use of the natural strains, he confined the equations to infinitesimal increments of these strains and he postulated a functional relation between the octahedral variables for expressing strain hardening. Notwithstanding that in each of these three assumptions they followed the footsteps of the writer, they let the reader believe that their application of "the von Mises viewpoint is quite different" from the just mentioned one. The writer confined his derivation to cases in which the principal directions do not rotate. An exception was the case of simple finite shear. However, the reader will note that in this latter case the increments of the principal stresses or strains were not referred to fixed axes as the authors believed.

The imaginary twisting and untwisting experiment (footnote, page 184) with which the authors meant to argue ad absurdum can be dealt with briefly by

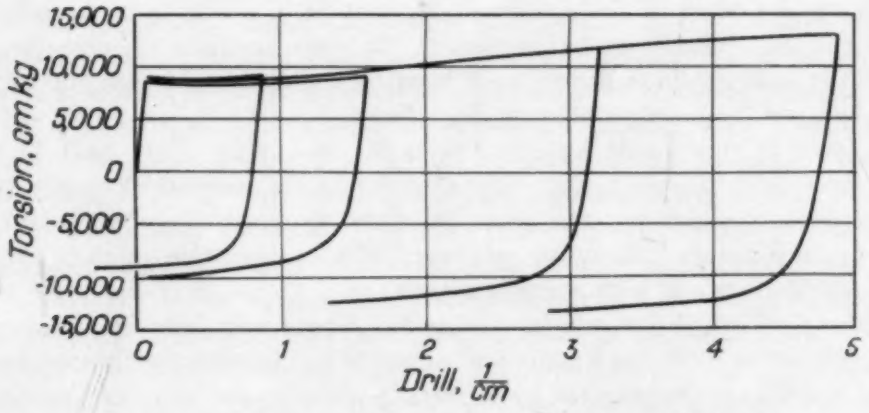

Fig. A—Twisting Tests on Hollow Cylinders.

referring them to tests of this very nature, which were made on the writer's suggestion by his former collaborator *W. Bader*. They were published in a dissertation in 1927 in Goettingen. Since this latter is not easily accessible in this country a figure of it is here reproduced (Fig. A). It shows the stress-strain curves for shear in twisting and untwisting tests made with a thick-walled cylinder of a soft grade of steel. No "theory" was needed or used for plotting these curves, only direct observation. The writer hopes they will convince the authors that *their own interpretation* of "the Nadai-Davis method of considering only the initial and final configuration carried to its logical conclusion" and their conclusion, according to which "this would give zero hardening" was

wrong. Zero hardening cannot result—independently of which theory is used —unless the curve for untwisting (as it seems it was assumed in this paper) is erroneously taken to coincide with the one for twisting.

Written Discussion: By D. Morkovin, associate in theoretical and applied mechanics, University of Illinois, Urbana, Ill.

The authors of the paper are to be congratulated for an important contribution, especially in finding a quantitative relation of equivalence (as far as the mechanical properties of metals are concerned) of an increase of straining rate to a decrease in temperature. The writer is glad to be able to report that the proposed relation seems to be substantiated also by tests of an entirely different kind than those performed by the authors.

As the authors' presentation of the theory underlying the proposed relation of equivalence is rather abbreviated, the writer begs to be excused if he starts by a recapitulation of the reasoning which the authors apparently used.

The authors proposed the relationship of equivalence of the effects of temperature and strain rate on the mechanical properties of metals at low temperature. The formal expression is given by the following equations relating the stress S at any stage of the test (i.e., some measure of the strength of the materials) to the corresponding unit strain ε

$$S = S_p(\varepsilon) \qquad (1)$$

in which the parameter p is defined by:

$$p = \frac{\dot{\varepsilon} e^{Q/RT}}{f_o} \qquad (2)$$

where $\dot{\varepsilon}$ is the strain rate, Q the heat of activation of the material, expressed in calories per gram mol, R the molal gas constant in deg./cal; and T the absolute temperature in degrees Kelvin.

They reasoned that, since the parameter p must be a dimensionless function $p(\dot{\varepsilon}, T)$, it must be expressible as a ratio of the rate of deformation and of some other time rate connected with the material. Nearly all times rates associated with materials are governed by heats of activation and their dependence on temperature is given by an equation of the form

$$\text{time rate} = f_o\, e^{-Q/RT} \qquad (3)$$

where the constant f_o has dimensions of time^{-1}.

From diffusion problems, the authors took the value usually assigned to this constant, viz.

$$f_o = \frac{JQ}{Nh} \qquad (4)$$

where J is the mechanical equivalent of heat, N is Avogadro's number and h is Planck's constant. Where f_o is so interpreted, according to the authors, the

time rate of equation (3) is essentially the number of times per second any given atom acquires the heat of activation Q. Parameter p is therefore expected to be of the form

$$p = \frac{\dot{\varepsilon}}{f_o\, e^{-Q/RT}} = \frac{\dot{\varepsilon} e^{Q/RT}}{f_o} \quad \ldots\ldots\ldots\ldots\ldots\ldots\ldots\ldots\ldots\ldots\ldots\ldots\ldots\ldots (5)$$

To show that a certain change of the rate of straining $\dot{\varepsilon}$ is, in its effects upon some mechanical properties of materials, equivalent to a certain change in the temperature T, Eq. (2) can be written as

$$\dot{\varepsilon} = p\, f_o\, e^{-Q/RT}$$

If we use $\varepsilon = v$, and $Q/R = B$ (material constant), Eq. (6) becomes

$$v = p\, f_o\, e^{-B/T} \quad \ldots\ldots\ldots\ldots\ldots\ldots\ldots\ldots\ldots\ldots\ldots\ldots\ldots\ldots\ldots\ldots (7)$$

$$\text{or} \quad \ln v = \ln A - B/T \quad \ldots\ldots\ldots\ldots\ldots\ldots\ldots\ldots\ldots\ldots\ldots\ldots\ldots\ldots\ldots\ldots (8)$$

where $A = (p\, f_o)$.

Equation (8) gives a straight line on a plot of ln v as ordinate against 1/T as abscissa. Using logarithms to base 10, equation (7) can be written

$$\log_{10} v = \log_{10} A - B_1/T \quad \ldots\ldots\ldots\ldots\ldots\ldots\ldots\ldots\ldots\ldots\ldots\ldots\ldots\ldots\ldots\ldots (9)$$

$$\text{where} \quad B_1 = Q/R \log_{10} e = B \log_{10} e \quad \ldots\ldots\ldots\ldots\ldots\ldots\ldots\ldots\ldots\ldots\ldots\ldots\ldots\ldots (10)$$

This relation plots as a straight line, if $\log_{10} v$ is plotted on the axis of ordinates and 1/T on the axis of abscissas.

Suppose a series of tensile tests with varying rates of strain v are performed. Suppose that at each rate of strain v, the temperature T_c is determined at which brittle breaks begin. Then e.g. the combination of a strain rate v^1 and a temperature T_c^1 which causes brittleness is equivalent to another combination of strain rate v^{11} and a temperature T_c^{11}, which also causes brittleness. These actual combinations of v^1 with T_c^1 and v^{11} with T_c^{11} are also equivalent to an exceedingly high strain rate v_{T_0} which would be necessary to cause brittleness at the room temperature T_o.

If a set of such strain rates v, which, in combination with their associated temperatures (critical temperatures) are all equivalent, was plotted and if the curve fitting the results had an equation of the type proposed by Hollomon and Zener, it would be an evidence of the validity of their proposition. Such a set of data would give information on the increment in strain rate $(v_{T_0} - v^1)$ which is equivalent to a given decrement of temperature $(T_o - T_c^1)$ for that particular material.

Witman and Stepanov (1) used unnotched cylindrical specimens of 0.2 per cent carbon steel annealed for 2 hours at 1832 degrees Fahr. (1000 degrees Cent.), with a mean grain diameter of 53 microns. This steel exhibited brittle statical breaks at the temperature of liquid air. The specimens were tested in bending at various temperatures and various speeds of head (ranging from 0.024 inches per second to 3270 inches per second). Table A shows a portion of their results.

Table A

Variation of the Upper Critical Temperature of Brittleness of Coarse-Grained 0.2 Per Cent C Steel with the Rate of Straining (After Witman and Stepanov)

Speed of head, inches per sec.		0.024	0.165	197	327	3270
Rate of strain v in the most stressed region, in. per in. per sec.		0.0095	0.0643	76.5	127	1275
Upper critical temperature of brittleness in bending, of unnotched specimens	t deg. Cent.	−165	−155	−110	−105	−75
	T_K deg. Kelvin	108	118	163	168	198
$\log_{10}\left(\frac{\text{equivalent strain rate at room temp.}}{\text{actual strain rate at low temp.}}\right)$		7	6.2	3.1	2.9	1.9

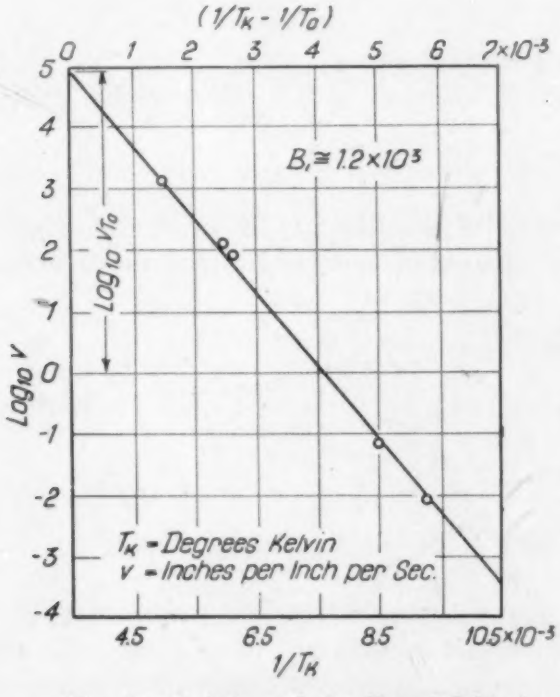

Fig. B—Variation of the Upper Critical Temperature of Brittleness with the Rate of Straining (Witman and Stepanov).

Fig. B is the graph of these results using coordinates $\log_{10} v$ and $1/T_K$. The axis of ordinates is drawn at a value of abscissa equal to $1/T_o$, where T_o is room temperature (corresponding to 20 degrees Cent.). If the scale of abscissas is expressed in terms of $(1/T_K - 1/T_o)$, the experimental data are fitted by the equation

$$\log_{10} v_{T_c} = \log_{10} v_{T_0} - B_1 \, (1/T_c - 1/T_o) \quad \ldots\ldots\ldots\ldots\ldots\ldots (4c)$$

where $\log_{10} v_{T_c}$ and $1/T_c$ are the coordinates of a point on the straight line of brittle failures.

In this expression, the values ($\log_{10} v_{T_0}$) and B_1 are constants characteristic of the material. Equation (4c) can be rewritten in the following form:

$$v_{T_c} = v_{T_0}\ e^{-B\,(1/T_c - 1/T_0)} \qquad \text{.....(5c)}$$

The constant B in equation (5c) has the following relation to constant B_1 in equation (4c):

$$B_1 = B \log_{10} e \qquad \text{.....(6c)}$$

The constant v_{T_0} in equation (5c) now acquires a meaning: it is the minimum rate of strain at which the material breaks in a brittle manner even at room temperature T_0.

Equation (5c) can be rewritten as

$$\dot{v}_{T_c} = (v_{T_0}\ e^{B/T_0})\ e^{-B/T_c} \qquad \text{.....(5.1c)}$$

or $$v_{T_c} = A\ e^{-B/T_c} \qquad \text{.....(5.2c)}$$

Thus the constant A has the value $v_{T_0}\ e^{B/T_0}$
Accordingly, from Eqs. (7) and (5.1c), the following relation appears:

$$pf_0 = v_{T_0}\ e^{Q/RT_0} \qquad \text{.....(5.3)}$$

which agrees with that of equation (5) if written for room temperature T_0. In other words, the equation of Witman and Stepanov's curve (Eq. 5.1c), and Fig. B is

$$v_{T_c} = (v_{T_0}\ e^{Q/RT_0})\ e^{-Q/RT_c} \qquad \text{.....(5.4)}$$

or $$v_{T_c}/v_{T_0} = e^{-Q/R\,(1/T_c - 1/T_0)} \qquad \text{.....(5.5)}$$

or $$v_{T_0}/v_{T_c} = e^{-Q/R\,(1/T_c - 1/T_0)} \qquad \text{.....(5.6)}$$

and $$\log_{10} v_{T_0}/v_{T_c} = Q/R\ (1/T_c - 1/T_0) \log_{10} e \qquad \text{.....(5.7)}$$

Hollomon and Zener define the equivalent strain rate as "that strain rate at room temperature which is necessary to give the same physical properties as does the actual strain rate at the low temperature of test, on the assumption that the deformation remains essentially isothermal." Witman and Stepanov's[2] tests may be considered isothermal, because when a completely brittle fracture occurs, there is no plastic flow with consequent heating up, even at high rates of strain. The above definition shows that, in Eq. (5.7), v_{T_0} corresponds to the "equivalent strain rate" for brittle fracture, and v_{T_c} to the actual strain rate for brittle fracture at the low temperature T_c. Therefore, equation (5.7) should give a curve of the type shown in the authors' Fig. 15. However, Eq.

[2]F. F. Witman and V. A. Stepanov, "Influence of Rate of Strain Upon Brittleness of Steel," *Journal of Technical Physics*, Russian, Vol. 9, No. 12, 1939, p. 1070.

(5.7) and Eq. (4c) are identical, as $B_1 = Q/R \log_{10} e$ by Eq. (10). As Eq. (4c) is the equation of the straight line on Fig. B, it appears that the authors' curves in Fig. 15 would be straight lines when plotted with similar coordinates as on Fig. B.

The value of slope on Fig. B is 1.2×10^3. Therefore, from Eq. (10) the value of Q can be calculated as Q = 5400 cal/gm mol.

From Fig. B can be seen that the equivalent strain rate v_{T_0} is practically 10^5 inches per inch per second for the high phosphorus iron shown. Dividing this equivalent strain rate v_{T_0} by the actual strain rates v_{T_c} of Table A and taking the logarithms of these ratios, the values in the last line of Table A were obtained by the writer. These values when plotted in the authors' Fig. 15

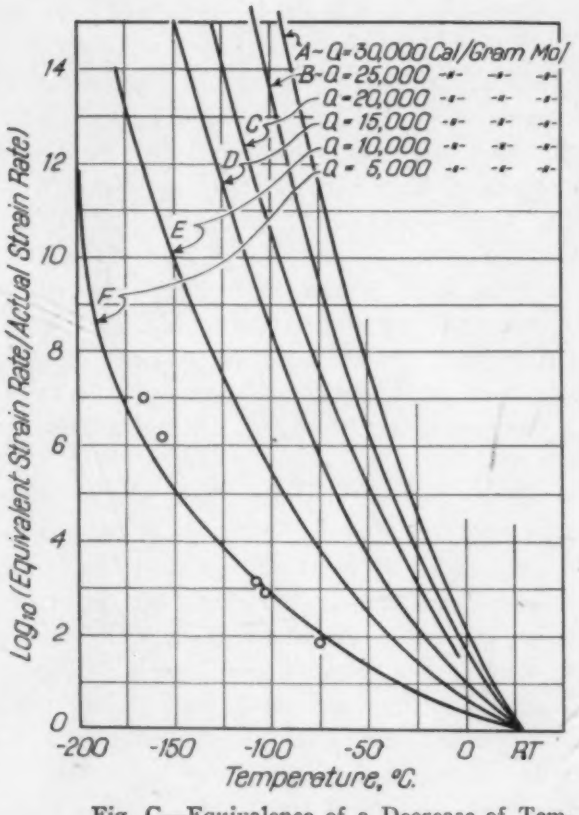

Fig. C—Equivalence of a Decrease of Temperature to a Rise in Rate of Strain.

appear as the full circles on the accompanying Fig. C. They are seen to fall near the authors' curve for Q = 5000 cal/gm mol.

Thus, the relation proposed by the authors is seen to agree with the experimental results of Witman and Stepanov[2] shown in Fig. 8. The significant thing is that these tests are of entirely different nature than those performed by the authors. The values of heat of activation determining the coefficient of diffusion in solids are usually considerably higher than the value of Q found here. However, it is to be expected that the potential barrier determining the speed of the process of relaxation should be lower than the barrier in diffusion. In diffusion, atom goes from one knot of the lattice to the next,

whereas in relaxation it just returns from between the knots to the nearest knot.

Written Discussion: By Ralph Leiter, metallurgist, and Joseph Winlock, chief metallurgist, Edward G. Budd Manufacturing Co., Philadelphia.

This paper represents an immense amount of hard work and careful study. The authors are to be congratulated on a good job well done.

We are in substantial agreement with the authors' concept of the initiation of plastic flow in annealed low carbon steel with the single exception of the cause of the upper yield point. Messrs. Zener and Hollomon believe that this high resistance to initial yielding is due to a hard precipitate on the grain boundaries. However, precipitation with and without appreciable hardening occurs in a great number of metals and alloys but heterogeneous yielding is reported on very few. We do feel that heterogeneous flow at the yield point may possibly be more common than realized. It would therefore seem to us that we need autographic load deformation curves covering a moderately wide temperature range under various conditions of heat treatment and on a large number of the metals and alloys that are susceptible to precipitation. With more knowledge of this sort we may indeed find that heterogeneous flow at the yield point is due to precipitation of particles at the grain boundaries in appropriate size, number and hardness.

Heterogeneous flow sometimes occurs throughout the plastic range. The best known example is mild steel in the "blue heat" range corresponding to hump C in the tensile strength-temperature curve of Fig. 13. The same type of plastic deformation has been observed by the writers in room temperature tests on Hadfield manganese steel, stainless steel of seventeen per cent (17 per cent) chromium, seven per cent (7 per cent) nickel analysis and 52SO aluminum alloys.

Applying Messrs. Zener and Hollomon's line of reasoning to the case of mild steel in the blue heat range we would expect heterogeneous flow and almost immediate age hardening at the yield point. The material originally deformed having developed a new and high upper yield point so that we have a second band of Lüder's lines traversing the test piece, this process continuing through the plastic range to a point where there is no additional age hardening.

In the case of Hadfield manganese steel and 17-7 chrome-nickel steel, heterogeneous flow is pronounced only after substantial plastic deformation has occurred. The formation of alpha iron resulting from the cold work may have an effect similar to precipitation of hard particles. In fact there may be a precipitation of carbides from the transformed alpha iron.

We are at a loss to explain the heterogeneous flow in 52SO aluminum alloy. It is considered as a non-aging alloy although enough precipitation may occur to be a possible cause of heterogeneous flow.

Written Discussion: By P. W. Bridgman, Physics Laboratory, Harvard University, Cambridge, Mass.

Messrs. Zener and Hollomon refer to certain recent unpublished experiments of mine on the tensile fracture produced in glass by lateral hydrostatic pressure (the "pinching-off" effect). I take this occasion to describe these experiments in more detail, and also to describe other experiments made ten years ago and not hitherto published.

The object of the recent experiments was to find whether the liquid medium

in contact with the glass specimen plays an important role in the phenomena of fracture. The apparatus was similar to that of Fig. 17 of Zener and Hollomon. The glass rod was protected from contact with the Karo corn syrup with which the outer rubber tube was smeared (corn syrup was used instead of the molasses indicated in Fig. 17) by a wrapping of 0.001-inch copper foil extending well beyond the retaining rings at either end. Tests were made in which the glass rod inside the sheath was respectively: (1) moistened with acidulated water; (2) lightly smeared with corn syrup; (3) lightly smeared with vaseline, and (4) left dry. Pressure on the rubber was in each case raised to fracture of the glass rod. A first striking difference compared with experiments made without the sheath was that in no case were the severed pieces violently expelled through the retaining rings, but in all cases the fractured rod remained in the apparatus externally geometrically intact. In the first three cases the fractures were clean tensile breaks on planes perpendicular to the axis. The break might be complete on some of the planes, so that the specimen fell apart on removal from the sheath, or on other planes the specimen might hang together, the fracture being distinctly visible in the proper lighting by internal reflection and refraction across most of the section. The whole length of the specimen between the retaining rings was divided in this way into lamellae from $\frac{1}{32}$ to $\frac{1}{16}$ inch thick. Fracture occurred at the following pressures in the rubber: (1) 10,600; (2) 29,500; and (3) 35,500 pounds per square inch. In the fourth case, the one run dry, the fracture was quite different in character; there were none of the internal fractures and lamellae in the body of the specimen, but the fracture was confined to the two regions of stress release where the specimen passes out through the retaining rings, and the fracture here was on curved surfaces, not on planes. The pressure at which fracture occurred was 59,000 pounds per square inch.

It would appear, therefore, that there can be no question that the "pinching-off" effect in glass is connected with conditions starting at the surface, as Messrs. Zener and Hollomon suggest, and is not a simple specific effect of the stress only at interior points. In view, however, of the very great effect shown above played by the nature of the liquid in contact with the glass, I think the effect cannot be characterized in terms only of a stress distribution at the bottom of surface cracks, but the effect is more complicated and involves a specific effect of the liquid on the glass. The specific effect of the liquid is also brought out by experiments which I made ten years ago, not hitherto published. Poulter had been able to apply pressures of 150,000 pounds per square inch and more to glass windows, whereas my windows of similar construction had failed below 100,000 pounds per square inch. In seeking for the reason for the discrepancy it finally appeared that the effect is due to the transmitting liquid. If pressure is transmitted by water, fracture is invariable at pressures below 100,000 pounds per square inch, but if pressure is transmitted by kerosene, pressures above 150,000 pounds per square inch may be supported. It is known that under ordinary conditions there is a strong surface action between water and glass, a glass surface exposed to the atmosphere becoming coated with a layer of water 100 to 200 molecules deep, which is exceedingly difficult to remove, as any experimenter with vacuum tubes knows. Under the action of pressure, water appears to be driven by a combination of pres-

sure and adsorption deeper into the glass. A solid sphere of glass which has been exposed to hydrostatic pressure under water will fracture if pressure is rapidly released, but if pressure is released very slowly, so that the water has time to diffuse back out of the glass, no fracture occurs.

Fracture is affected not only by the chemical nature of the liquid in contact with the glass, but also by its viscosity. Glass windows are fractured if pressure is transmitted by petroleum ether, although they are not affected by kerosene, and they are not fractured by commercial glycerine up to 180,000 pounds per square inch, although the glycerine contains considerable water. As might be expected, the situation is further complicated by time effects, which are different for different liquids.

Any water which is forced into glass by pressure is exceedingly small in amount. I made experiments with heavy walled cylinders, sealed at the ends, exposed to high pressure exerted by water over the external surface, but was never able to drive any perceptible amount of water into the internal cavity. These experiments also showed great specific differences between different sorts of glass; lead glass was always crushed into fine powder after such an exposure, pyrex was unaffected, and Scotch combustion tubing separated into concentric cylindrical shells, like an onion.

It is evident that a further quantitative experimental investigation is needed of the entire subject of the fracture of brittle substances under symmetric two-dimensional stress.

Written Discussion: By D. J. McAdam, Jr., metallurgist, U. S. Department of Commerce, National Bureau of Standards, Washington, D. C.

Although this paper presents much information of value, its usefulness is marred by the tendency of the authors to adopt various assumptions on the basis of a superficial survey of the evidence, and then proceed to a mathematical analysis. An instance of this tendency is found in the presentation of their view with regard to the influence of a transverse tensile stress on the longitudinal stress required for fracture (page 193). They refer to their experiments (not yet in print) with flat strips and round bars. They make the untenable assertion that transverse tensile stress in the direction of the breadth of the strip was induced because the specimen failed to contract in this dimension, and that the breaking stress was thus reduced 25 per cent. The notch effect of the local contraction of a flat specimen causes transverse tension perpendicular to the breadth, whereas the local contraction of a cylindrical specimen causes transverse radial stress. The experiments by Kenyon and Burns with round and flat specimens of Armco iron, cited by the authors, would give flow stress curves (on a natural strain basis) that differ greatly in slope. The round specimen that fractured at 120,000 pounds per square inch gives a much steeper slope than the flat specimen that fractured at 75,000 pounds per square inch. If these values are taken as correct, the evidence would indicate that transverse stress increased more rapidly during local contraction in the round than in the flat specimen. Do the authors imply that transverse stress in one direction lowers the breaking stress, while transverse radial stress raises the breaking stress? The evidence cited appears to be of no value in determining a criterion for failure under combined longitudinal and transverse tension. It is not impossible that one reported stress value is too low and the other too

high. Moreover, the effect of combined stresses at fracture cannot be evaluated without considering variable ductility.

In Appendix B, the authors again adopt the greatest principal stress as criterion for fracture. They mention two papers by the writer in which opposing views are presented, but dismiss them with an innuendo regarding conclusions based on notched specimens. However, the evidence presented in the papers mentioned, and in two later papers by McAdam and Mebs,[3,4] cannot be dismissed by innuendo. Comparison of mean stresses at fracture of notched and unnotched specimens shows that the technical cohesion limit tends to increase with increase in the ratio of radial to longitudinal tensile stress in the manner illustrated. These conclusions must be considered as proved, unless one wishes to assert that the actual stress at fracture of a notched specimen may be much less than the mean stress at fracture, and even much less than the mean stress at yield.

Oral Discussion

ROLLAND G. STURM:[5] I think that the authors have done a real service in stimulating interest in theories of flow of metals. While some of the points seem to be controversial, perhaps more interest has been aroused than if they had not been so.

I would like to raise a question along the line that Dr. Nadai has mentioned, that is "Where does the work of G. I. Taylor fit into the authors' analysis?" Would not his concept of avalanches and molecular discontinuities or disarrangements within the crystals take care of the situation rather than the assumption of the presence of cracks? It is difficult for me to place confidence enough in materials to risk my life to them if they are considered to be full of cracks. There might be some other explanation that would be a little easier on one's conscience and perhaps nearer the truth.

The author mentioned strain rates and said that a strain rate which is relative to time could not be integrated over a section unless it was divided by a rate also involving time. It appeared to me that the authors divided by a quantity which did not involve time. Therefore, it is not clear that they actually complied with their requirements.

There is one other thought mentioned by the last speaker that raises a question. How about the state of combined stress for strains which greatly exceed the elastic limit? We know that as you twist a specimen appreciably beyond the elastic limit the strains are not absolutely uniformly distributed according to some law. We may assume absolute homogeneity but we cannot get it. In the simple tension test there are set up within the metal complex states of strain and stress. This is especially significant when a specimen begins to neck down. Dr. Bridgman has a paper on the combined stresses for such cases. Certainly, the combined stresses affecting the technical cohesive strength

---

[3]D. J. McAdam, Jr., and R. W. Mebs, "An Investigation of the Technical Cohesive Strength of Metals," American Institute of Mining and Metallurgical Engineers, Technical Publication No. 1615, *Metals Technology*, Aug. 1943.

[4]D. J. McAdam, Jr. and R. W. Mebs, "The Technical Cohesive Strength of Metals at Low Temperatures," American Society for Testing Materials, Preprint No. 40, 1943.

[5]Research engineer physicist, Aluminum Company of America, New Kensington, Pa.

are very vital. Dr. McAdams also in one of the later sessions has a paper on that problem. There is a probability that the geometry of the piece itself enters into the distribution of strain rates.

One other question, how much attention did the authors give to the possibility of initial orientation of the crystallographic structure? When a bar is rolled or drawn the grains are oriented and the slip planes within the grains are oriented more or less in the same directions. If these slip planes are oriented in certain parallel planes the resistance to slip on those planes is less than on other planes. The well known test of a single crystal of magnesium in tension is the example of that phenomena. In this test a round bar consisting of a single crystal became elliptical in cross section when stretched because the slip occurred in only one direction. A bar of many crystals tends to deform by slip on many minute surfaces in many directions, but the statistical predominance of slip occurs in directions corresponding to planes of maximum shearing stress.

If a specimen is twisted, drawn, stretched or extruded, the orientations of the various slip planes are changed, depending upon the type and amount of deformation to which it has been subjected. Each of these deformations may cause orientations which have an effect on the amount and character of elongation as well as the strength of the final piece. The effects of such variations in orientation do not contradict existing theories of flow but may explain some of the anomalies noted by the authors.

L. R. JACKSON:[6] I would like to congratulate the authors on presenting a very stimulating paper. There are two questions, however, which I would like to ask. In finding a reason for these weaknesses that are supposed to exist in steel, two of the more or less critical tests that led to their formulation were, first, the discrepancy between the strain hardening in tension and torsion and, second, the behavior of the tension test piece which had been twisted in torsion prior to tension testing. I would like to ask the authors if their curves for strain hardening were corrected for the necking of the tensile test pieces, that is, necking will introduce additional stresses which may affect the results. As there is generally a difference in tensile properties between the transverse and rolling directions, the twisting of a torsion test piece that has been cut along the direction of rolling, the fibers are twisted so that later in tension the stress would actually be in the transverse direction. Has this factor been taken into account in interpreting results?

Authors' Reply

The writers regret that Dr. Nadai is in disagreement both with the spirit and the details of this paper, especially so, since for many years Dr. Nadai has been recognized in this country as the outstanding authority upon the plasticity of metals. The difference in spirit with which Dr. Nadai and the writers approach this subject may be due to a difference in interest. As an engineer, Dr. Nadai has been interested primarily in a self-consistent scheme within which lie the problems usually encountered in industrial processing. On the other hand, the writers, as students of metals per se, are interested primarily

[6]Research engineer, Battelle Memorial Institute, Columbus, Ohio.

in the laws which govern the behavior of metals under all possible conditions.

The influence of this difference in interest is most strikingly brought out by a comparison of the two approaches to the subject of strain hardening. Dr. Nadai was apparently content with a theory limited to the case where the principal axes remain fixed in the body, presumably because such a theory was sufficient for most industrial purposes. On the other hand, the writers have taken particular care so as to formulate the theory of strain hardening, that it may readily be applied to the most general types of strain hardening. At Dr. Nadai's request, a detailed comparison is given at the end of this closure of the two methods of formulation, together with an analysis of the fundamental error which the authors believe Dr. Nadai made in attempting to apply his own formulation to a case where the principal axes rotate.

As to a detail, Dr. Nadai criticizes the nearly complete absence of reference to the contribution of the various workers in this field. It was the authors' purpose to present clearly what they considered as the present status of the theory of the plastic state. They had felt that the clarity would be obscured by a detailed description of the opinions and contributions of all the many investigators in the field. It is regretted if this method of presentation has led to any disparagement or misunderstanding of the contributions of individuals, as it may have done in the case of Mohr.

The writers wish to thank Dr. Morkovin for his very interesting presentation of the confirmation of their ideas upon equivalence of strain rate and temperature by the Russian work. It is regretted that such excellent work which the Russians are apparently doing in this field has remained so inaccessible.

The writers are fascinated with Messrs. Leiter and Winlock's interpretation of the cause of the inhomogeneous deformation in "blue heat" range of mild steel. The writers have in the past been deeply indebted to the ideas of Messrs. Leiter and Winlock upon heterogeneous flow in steel, and so take double pleasure in thanking them for the new contributions presented in their discussion.

The experiments described by Professor Bridgman in his discussion are believed to be of fundamental importance to any attempt at constructing a unified theory of the fracture of brittle materials. It is hoped that Professor Bridgman will later find occasion to describe these experiments in more detail.

The writers find themselves in disagreement with most of Dr. McAdam's remarks. (1) According to the von Mises system, which describes the plastic behavior of metals very well, plastic deformation in a transverse direction can be prevented only by the presence of a transverse stress equal to one-half of the longitudinal stress. Therefore, if the specimen in a flat strip is not contracting across its width, one may safely assume the specimen has a transverse stress across its width equal to nearly one-half of the tensile stress. (2) Upon re-examining the experiments of Kenyon and Burns to which Dr. McAdam refers, the writers find that the slopes of the true stress vs. natural strains for the round and flat specimens differ by not more than 15 per cent. It is assumed that Dr. McAdam compared the slopes of the true stress vs. reduction of area curves of Kenyon and Burns. (3) The writers maintain the viewpoint that extreme caution must be used in the interpretation of experi-

ments based upon notched bars. With regard to the particular point raised by Dr. McAdam, Sachs and Lubahn[7] have shown that an increase in notch depth is in certain cases accompanied by a more uniform stress distribution across the neck at rupture, and therefore by an increase in observed fracture stress.

The writers agree with Mr. Sturm that Taylor's dislocations, the microscopic stress inhomogeneities and crystallographic reorientations may all influence the plastic behavior, as well as the fracture stress of metals. They have not, however, been able to find by means of these phenomena a logical explanation of those observations described in the text which follow so readily from the concept of microscopic cracks. The instinct of Mr. Sturm not to risk his life on a metal which contains any type of crack however small is unrealiable.

	Tension	Simple Shear
Original Configuration	l_1	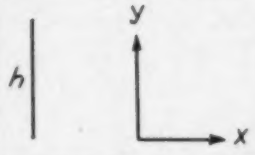
Intermediate Configurations	$\frac{l}{l+\Delta l}$	
Δ Conv. Strain	$\Delta l/l_1$	$\Delta x/h$
Δ Nat. Strain	$\Delta l/l$	$\Delta x/h$
Final Configuration	l_2	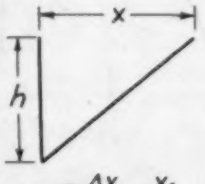
Conv. Strain	$\Sigma \frac{\Delta l}{\Delta l_1} = \frac{l_2 - l_1}{l_1}$	$\Sigma \frac{\Delta x}{h} = \frac{x_1}{h}$
Nat. Strain	$\Sigma \frac{\Delta l}{l} = l_n \frac{l_2}{l_1}$	$\Sigma \frac{\Delta x}{h} = \frac{x_1}{h}$

Fig. D—Examples of Difference Between Conventional and Natural Strains.

The analysis of Griffiths assures us that the cracks become dangerous only when they become sufficiently large. In fact, the behavior of a crack is more predictable than that of an "avalanche". Mr. Sturm has pointed out an error in the oral presentation of the paper, namely the omission of the factor f_o, with dimensions of 1/time, from Equation 3 of text.

Mr. Jackson has suggested that the discrepancy between strain-hardening in tension and in shear might be reduced if proper account is taken of the

[7]G. Sachs and J. D. Lubahn, "Notched-Bar Tensile Tests on Heat-Treated Low Alloy Steels," TRANSACTIONS, American Society for Metals, Vol. 31, 1943, p. 125.

effect of transverse stresses in the neck. At the time the paper was written no analysis had been given which took into account these transverse stresses. Fortunately such an analysis is being presented at this meeting by Professor Bridgman. In Fig. F is presented the observations on tension and shear previously presented as Fig. 12, but corrected in the manner of Bridgman. It is seen that the observations for tension and for simple shear now agree up to a strain of unity if compared by the von Mises method. Beyond a strain of unity the slope of the strain hardening curve in shear still becomes considerably less than that expected either according to the von Mises or to the Mohr

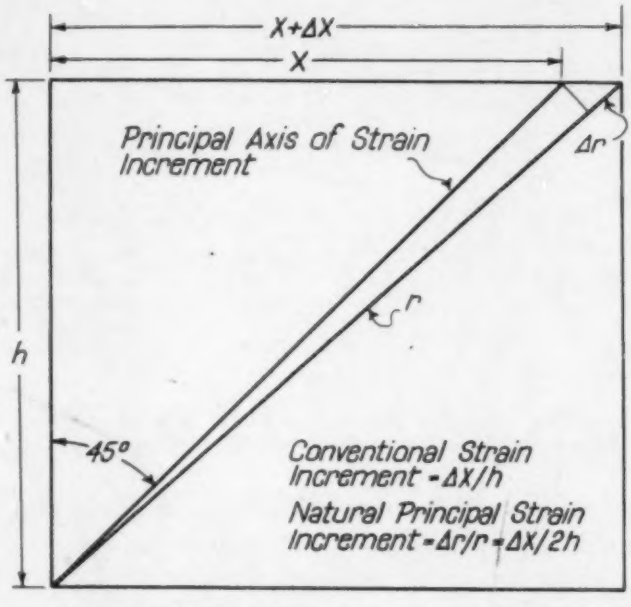

Fig. E—Method of Computation of Principal Strain Increment for Case of Simple Shear.

viewpoint. Mr. Jackson likewise has suggested that the initial anisotropy of a test specimen may affect the behavior in tension of a specimen subjected to shear. In the experiments described in the text the specimens were cut from forged bars. In such specimens the initial orientation of the microscopic cracks is very likely not isotropic, as Mr. Jackson suggests, but has a preferred distribution about the axis of the specimen. Such an initial distribution would, however, have no effect upon the qualitative behavior of a specimen in tension which had been subjected to a prior shear. The reorientation of the microscopic cracks by twisting will still be such as to cause fracture across planes which were under compression during twisting.

As requested by Dr. Nadai, the authors present below in detail the difference between their formulation of strain hardening and that presented by him in 1937.

Every worker in the subject of plasticity since Ludwik[8] has recognized the paramount importance of his concept of natural strain as contrasted with the conventional strain. When a strain is computed in the conventional manner, each increment of distortion is always referred to the original configuration

[8]P. Ludwik, *Zeitschrift für Metallkunde*, Vol. 16, 1924, p. 207.

before any distortion whatever. According to the Ludwik method, each small increment of strain is referred to the configuration of the system before that particular strain increment. The difference in the two methods of calculating strain may be most vividly presented by a diagram, as in Fig. D. It is seen that while the two types of strain are different in the case of tension, they are identical in the case of simple shear such as occurs in torsion. The reason is of course that the base line to which increments are referred is continually changing in the case of tension, but remains unaltered in the case of simple shear.

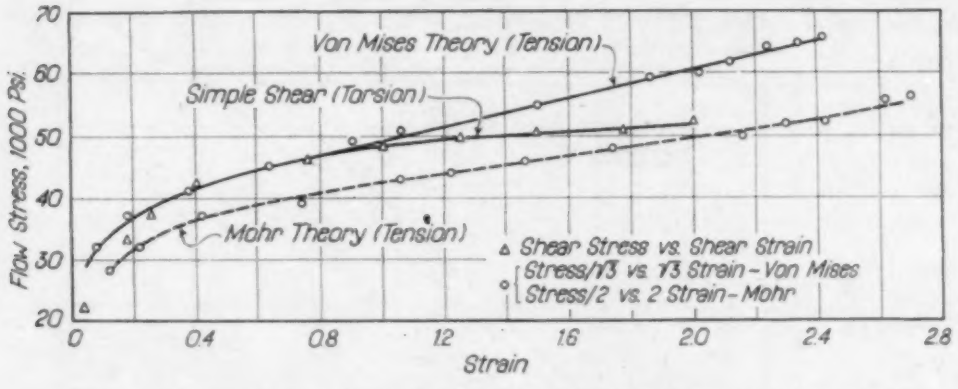

Fig. F—Comparison of Stress-Strain Curves in Tension and in Simple Shear (Corrected for Transverse Stresses in Neck, After Bridgman).

The concept of a generalized stress and of a generalized strain is necessary to any attempt to obtain a unified theory of strain hardening. In such a unified theory, strain hardening under all types of deformation is given by a single relation, namely that which relates the generalized stress to the generalized strain. In the Nadai formulation of the theory, the generalized stress and generalized strain increments are called the octahedral stress and octahedral strain increments, respectively. They are defined in terms of axes pertaining to the specimen itself and may vary both in time and in position. Thus the octahedral stress is defined in terms of the principal stresses, and the octahedral strain increment is defined in terms of the principal strain increments. It is to be noted that the axes of principal strain increments are not necessarily parallel to the axes of principal stresses. In the writers' formulation of the theory, the generalized stress and generalized strain increments are called stress invariant and strain increment invariant, respectively. They are defined in terms of a set of cartesian axes fixed in space. In both formulations of the theory, the strain increments refer to the configuration before the particular strain increment occurred. The generalized strains are thus natural in Ludwik's sense.

The two ways of formulating the theory correspond closely to the two ways of formulating the general equations of hydrodynamics, the Eulerian and Lagrangian methods. In the first, attention is focussed upon co-ordinates in the body, in the second upon co-ordinates in space. In working a particular problem, one should choose that formulation which is the simpler for that particular problem. If the principal axes of strain in the body are rotating, special

care must be taken if the Nadai formulation is used. As an example of the use of the two formulations of general strain, the case of simple shear will be worked out completely by each method.

The method introduced by the writers will first be used. The plane of shear will be taken to be the x, y plane. Then according to Eq. (a-4) of Appendix A, the invariant strain increment de_i is given by:

$$de_i = (3/2)^{1/2}\, de_{xy},$$

and therefore the generalized strain e_i given by:

$$e_i = (3/2)^{1/2}\, e_{xy}.$$

The generalized strain is therefore proportional to the conventional shear strain, in agreement with the analysis presented in Fig. D.

The octahedral strain increment $d\gamma_n$ is given in terms of the natural principal strain increments de_1, de_2, de_3 by:

$$d\gamma_n = 2(2/3)^{1/2}\,(de_1^2 + de_1\, de_2 + de_2^2)^{1/2},$$

which is Nadai's Equation (24) of ref. 32. In the particular case of simple shear, the principal strain increments de_1 and de_2 will be taken to be in the x, y plane. Then, as Nadai points out, $de_2 = -de_1$, so:

$$d\gamma_n = 2(2/3)^{1/2}\, de_1.$$

In the interpretation of the resulting integral:

$$\gamma_n = 2(2/3)^{1/2}\, e_i \qquad \text{(Nadai's Eq. 46)},$$

extreme caution must be used in the interpretation of the symbol e_i. The strain increment de_i has been defined in Ludwik's sense, that is, for each element of distortion, the corresponding de_i is computed with respect to the configuration before that particular distortion occurred. Following Nadai the conventional shear strain will be denoted by γ. Then from Fig. E one sees that:

$$de_i = d\gamma/2,$$

and hence

$$e_i = \gamma/2.$$

At this point, Dr. Nadai presumably went astray in his interpretation of his own symbol e_i. His value for e_i is given by the following equation:

$$e_i = (1/2)\ln \quad [1 + (\gamma^2/2) + \gamma(1 + \gamma^2/4)^{1/2}\ ] \quad , \qquad \text{(Nadai)}$$

(Equations (43) and (44) of Nadai).

This is precisely the value one would obtain if each element of volume had acquired its final configuration not by a simple shear, but by a pure shear combined with a rotation. This mistake probably arose from the fact that Dr. Nadai used a formula, Equation (30), which had been derived under the assumption that the principal axes remain stationary in space, and which therefore is not applicable to the case of simple shear.

THE EFFECT OF VARYING AMOUNTS OF MARTENSITE UPON THE ISOTHERMAL TRANSFORMATION OF AUSTENITE REMAINING AFTER CONTROLLED QUENCHING

By H. J. Elmendorf

Abstract

The transformation of austenite to martensite has been studied for four commercial steels by the Greninger-Troiano quench temper method. The resulting austenite-martensite microstructures formed by controlled quenching were employed to determine the effect of varying amounts of the two constituents on isothermal transformations at 600, 700, 800, and 900 degrees Fahr. The results are shown in chart form.

The effect of microstructure on isothermal transformation is discussed and the resulting mechanical properties are illustrated in graphs wherein it is seen that quench and tempered steels may be heat treated from the data contained in a series of time-temperature diagrams which are similar to the S-curve. The results show that a composite microstructure of bainite and tempered martensite in the proper proportions will produce the advantages of tempered martensite tensile strength and bainite ductility. In general, it may be stated that controlled quenching followed by immediate tempering will produce the optimum in mechanical properties.

Introduction

AUSTENITE at subcritical temperatures does not start to transform immediately and the character of the transformation products depends almost entirely upon the cooling rate imposed upon the steel. Extremely slow cooling produces transformation essentially at the equilibrium temperature; intermediate cooling lowers the transformation temperature and it then generally proceeds over a range of temperature; very rapid cooling markedly lowers the transformation temperature and the austenite will transform directly to martensite when the required conditions are met. Specifically these conditions are: (A) An imposed cooling rate sufficiently rapid to miss the upper region of rapid transformation on the cooling rate

A paper presented before the Twenty-fifth Annual Convention of the Society, held in Chicago, October 18 to 22, 1943. The author, H. J. Elmendorf, is research engineer, American Steel & Wire Co., Cleveland. Manuscript received June 21, 1943.

S-curve, and (B) a quenching bath low enough in temperature to allow the austenitic steel to transform into martensite as it progresses through the required range of temperature for the steel under consideration. These specifications are in accord with the concepts of the S-curve and austenite to martensite transformations.

E. S. Davenport and E. C. Bain (1)* investigated the isothermal transformation of austenite at a series of temperature levels which resulted in the development of the S-curve. Essentially these curves are time-temperature diagrams depicting the effect of temperature upon the time required for measurable beginning and ending of austenite transformation and the character and mechanical properties of the resulting microstructures.

H. Carpenter and J. M. Robertson (2) in England and A. B. Greninger and A. R. Troiano (3) in this country have shown that austenite transforms to martensite over a range of temperature which is characteristic for the steel under consideration. Specifically, a steel quenched to a temperature within the martensite formation range will start to transform as soon as the temperature for the beginning of martensite formation is attained and continues to form as cooling progresses. It has been stated that if cooling is interrupted at some intermediate point in this range, then transformation is interrupted and upon resumption of cooling, transformation proceeds. Likewise, if the steel is held at the intermediate temperature for sufficient time, transformation may proceed isothermally. A recent publication by A. B. Greninger (4) stated that the rapidity of the quench will have little or no effect upon the temperature for the beginning of martensite formation.

Therefore a method is presented to produce a reasonably controlled proportion of austenite and martensite in a steel by simply controlling the temperature of the quenching bath and simultaneously observe the effect of various proportions of austenite and martensite upon subsequent isothermal transformation at various temperature levels. In this paper we show the effects of various proportions of austenite and martensite upon the isothermal transformation completion time at temperature levels from 600 to 900 degrees Fahr. and the mechanical properties resulting therefrom. In the course of this paper it is noted that there is an optimum heat treatment which, when properly controlled, will result in a superior combination of tensile strength and ductility for quench and tempered steels.

*The figures appearing in parentheses pertain to the references appended to this paper.

Transformation of Austenite to Martensite

Austenite-martensite transformations have been well covered by numerous investigators who have employed various methods of determination. In this paper we have used the Greninger-Troiano method (3) which is briefly: Austenitize as required and follow by quenching to a series of temperatures to form martensite; follow by a short tempering to darken the martensite and then quench into a bath at room temperature and examine the resulting microstructures metallographically.

Throughout this investigation austenitizing consisted of heating in lead at 1550 degrees Fahr. for one minute. Quenching was carried out in controlled temperature oil and salt baths. Four commercial steels were employed and the pertinent data follow:

Table I
Analysis of Steels

Steel	Size Inches	Per Cent C	Mn	P	S	Si	Mo
AISI–c1065	0.120 D.	0.66	0.78	0.017	0.035	0.225	....
AISI–c1080	0.120 D.	0.80	0.87	0.012	0.023	0.295	....
AISI–c1095	0.120 D.	0.91	0.46	0.012	0.022	0.275	....
AISI–a4063	0.177 D.	0.64	0.61	0.014	0.017	0.198	0.25

Table II
Time-Temperature Cycles for the Martensite Determination

Quenching Temperature, ° F.	Quenching Time, Seconds	Tempering Temperature, ° F.	Tempering Time, Seconds
80–oil	60	530	5
180–oil	60	530	5
250–oil	60	530	5
320–oil	60	530	5
380–salt	60	700	3
450–salt	15	700	3
500–salt	15	700	3

A typical series of photomicrographs depicted the austenite-martensite transformation of steel AISI-c1065 are shown in Fig. 1 below. The same type of photomicrographs have been examined for the four steels investigated and have been rated independently for per cent of martensite by four persons and the averages plotted in Fig. 2. It should be pointed out that inasmuch as austenite may be heterogeneous in many respects, the initial and final transformations of austenite to martensite may be subject to some inaccuracies.

It is to be noted that the trends of the martensite transforma-

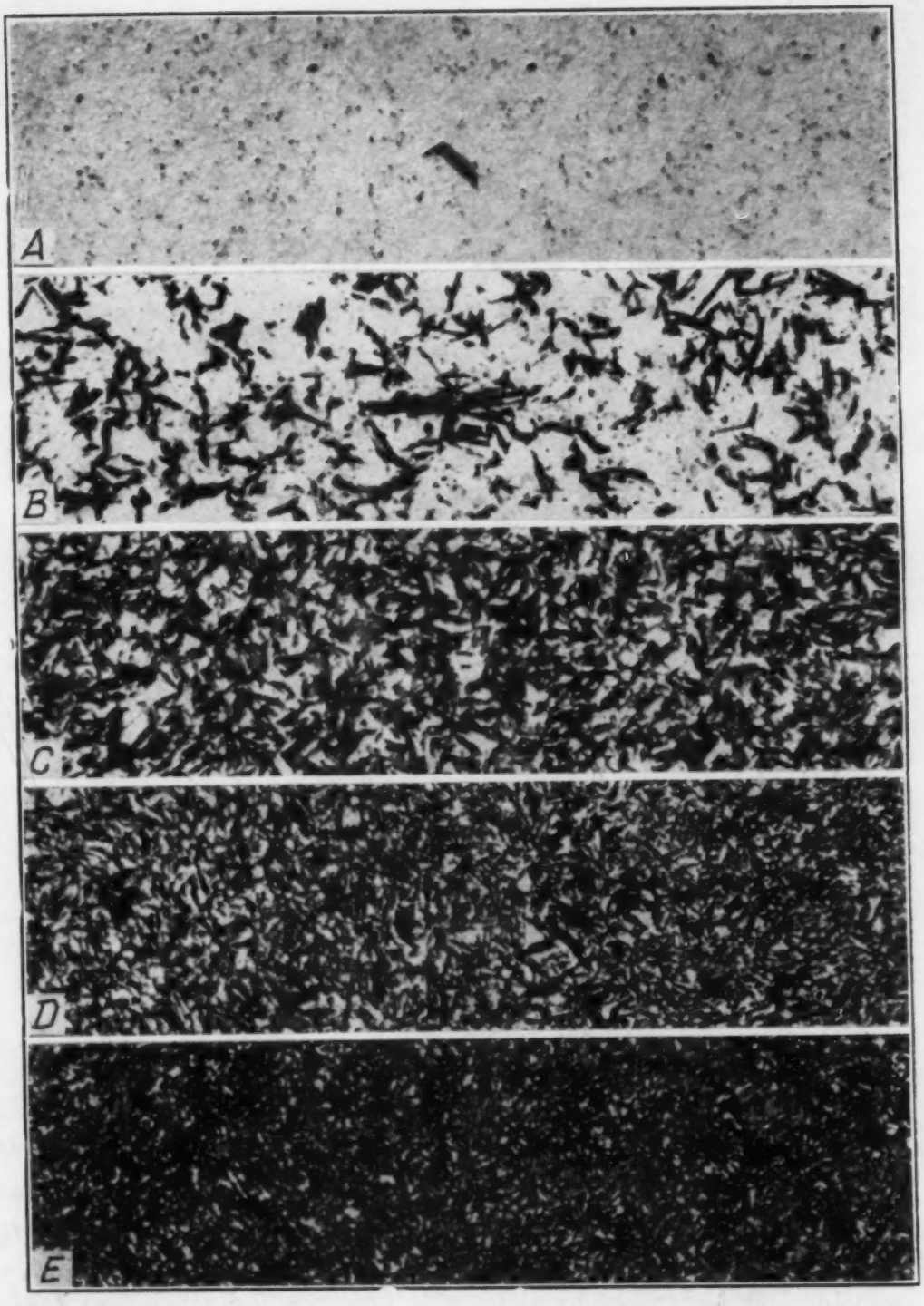

Fig. 1—Progress of Austenite-Martensite Transformation in AISI-c1065 Steel. (a) 500 Degrees Fahr., (b) 450 Degrees Fahr., (c) 380 Degrees Fahr., (d) 320 Degrees Fahr., (e) 250 Degrees Fahr. × 500.

tion curves are similar, and it is interesting to observe that there is little difference between the low alloy AISI-a4063 and the plain carbon AISI-c1065 steel. One would expect a slight difference,

however, it is entirely possible that the small amount of alloy (0.25 per cent molybdenum) might not be very potent in this respect. Some investigators have proposed correction factors for various alloying elements but it is believed that the factor for molybdenum in the amount investigated may be small.

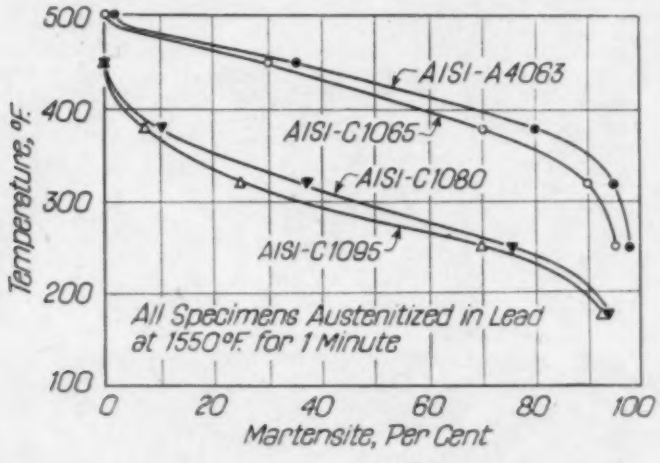

Fig. 2—Austenite-Martensite Transformation in Four Commercial Steels.

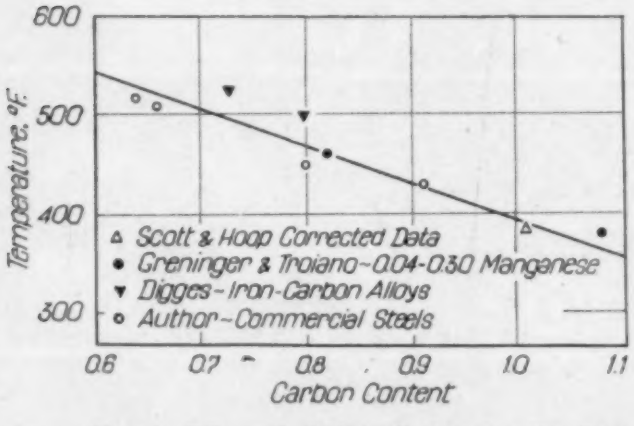

Fig. 3—Effect of Carbon Content on the Start of Martensite Transformation.

Fig. 3 illustrates the effect of carbon content on the temperature for the start of martensite transformation and in addition we have plotted the published data of other investigators. In this illustration, we have made no effort to separate the effects of varying manganese or alloy content which exist in the steels investigated; however, in spite of this we believe the points to show very close agreement. The data reported by T. G. Digges (5) is for iron-carbon alloys; H. Scott and Hoop (6) for corrected high manganese steels; A. B. Greninger and A. R. Troiano (3) for a low manga-

nese steel in one case and a commercial steel in another and all show very consistent agreement; should the steels investigated be corrected for alloying elements, it is very probable that all data would be very comparable.

Isothermal Transformation of Various Austenite-Martensite Mixtures

The isothermal transformation of austenite to ferrite and carbide structures has been reported by Davenport and Bain (1) and others and the methods employed for the construction of the S-curve are well known. In this study the same technique has been

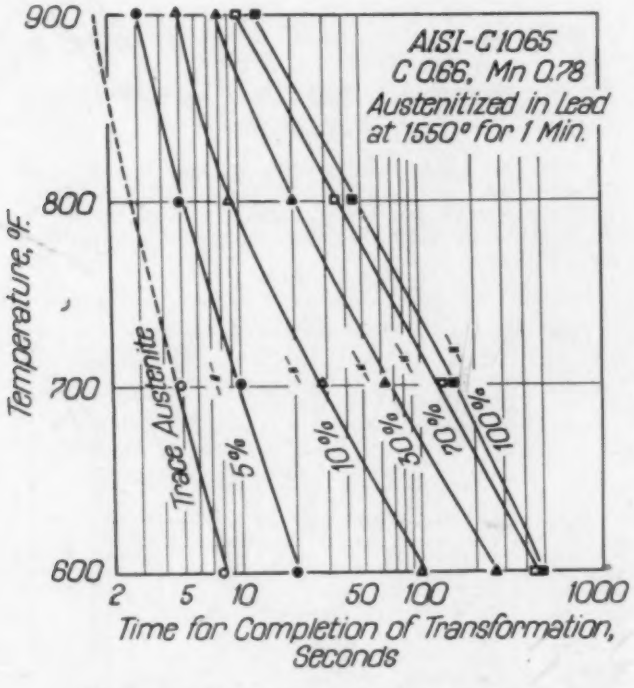

Fig. 4—Effect of Varying Amounts of Austenite on the Time for Completion of Isothermal Transformation for AISI-c1065 Steel. Amounts of Austenite Remaining After Controlled Quenching Noted on Individual Curves.

employed deviating only in the respect that our starting structures for transformation are various mixtures of austenite and martensite rather than all austenite. These mixtures are produced by the use of controlled quenches which are then followed by isothermal transformation studies to determine the required times for completion of the austenite remaining in the quenched steel. A martensite determination specimen was treated for each quench employed as

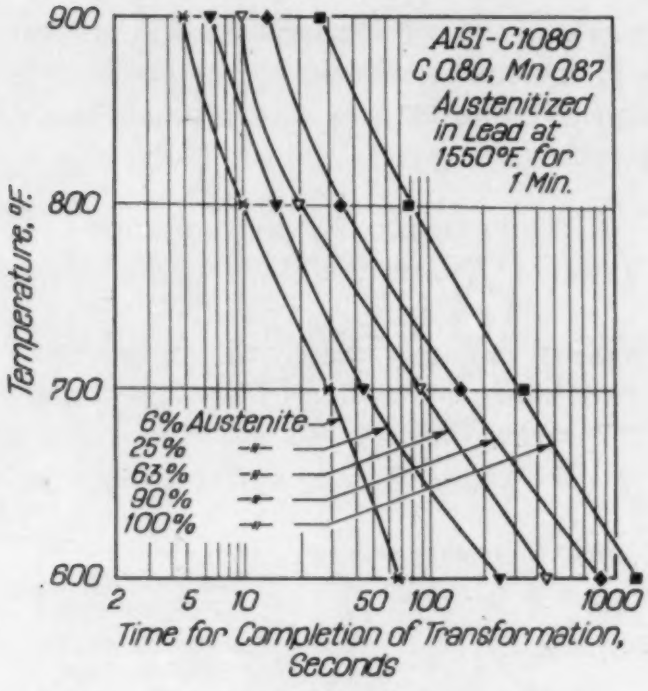

Fig. 5—Effect of Varying Amounts of Austenite on the Time for Completion of Isothermal Transformation for AISI-c1080 Steel. Amounts of Austenite Remaining After Controlled Quenching Notes on Individual Curves.

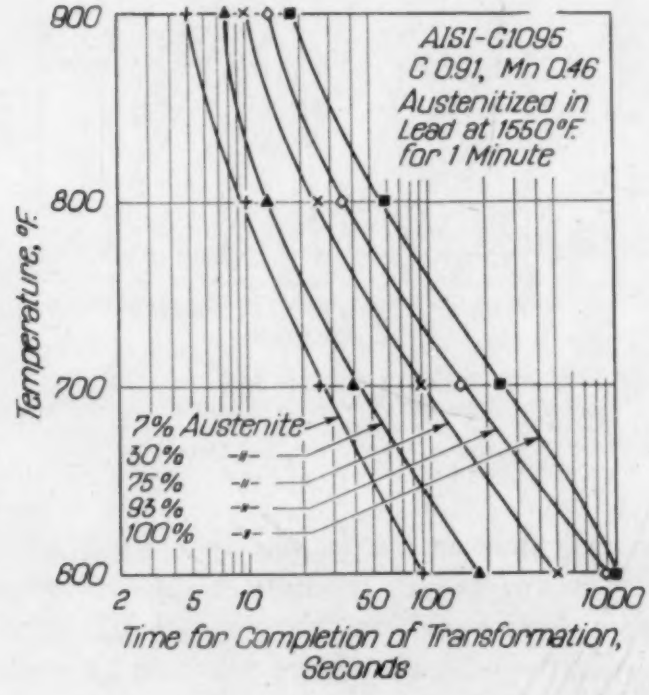

Fig. 6—Effect of Varying Amounts of Austenite on the Time or Completion of Isothermal Transformation for AISI-c1095 Steel. Amounts of Austenite Remaining After Controlled Quenching Noted on Individual Curves.

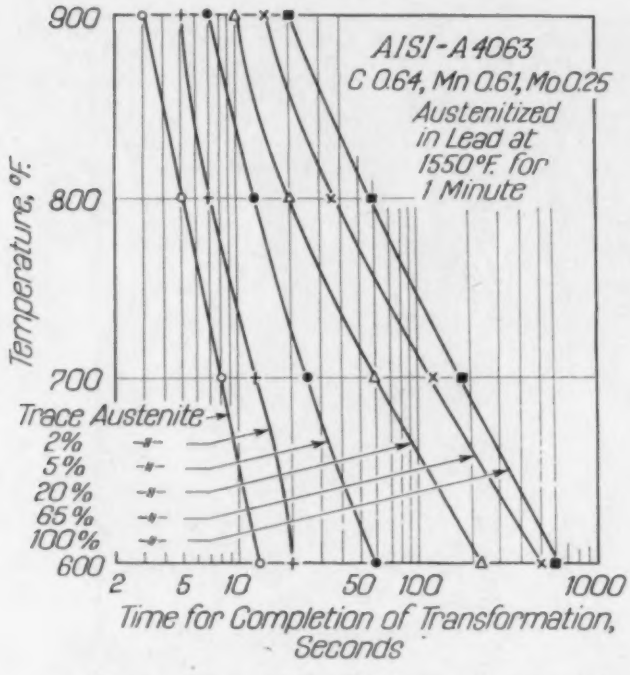

Fig. 7—Effect of Varying Amounts of Austenite on the Time for Completion of Isothermal Transformation for AISI-a4063 Steel. Amounts of Austenite Remaining After Controlled Quenching Noted on Individual Curves.

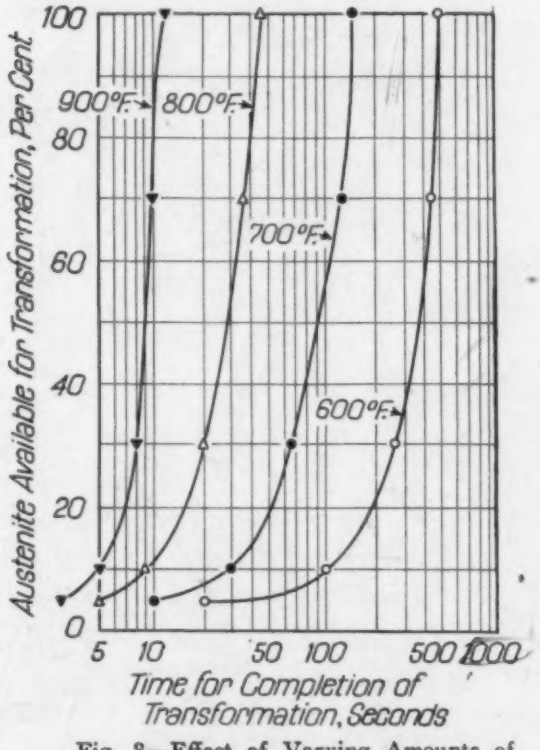

Fig. 8—Effect of Varying Amounts of Austenite on the Time for Completion of Isothermal Transformation for AISI-c1065 Steel. Amounts of Austenite Are Those Remaining After Controlled Quenching.

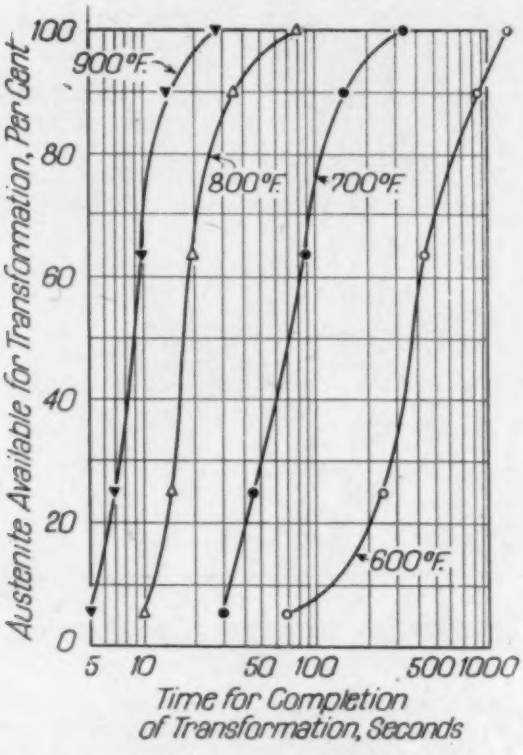

Fig. 9—Effect of Varying Amounts of Austenite on the Time for Completion of Isothermal Transformation for AISI-c1080 Steel. Amounts of Austenite Are Those Remaining After Controlled Quenching.

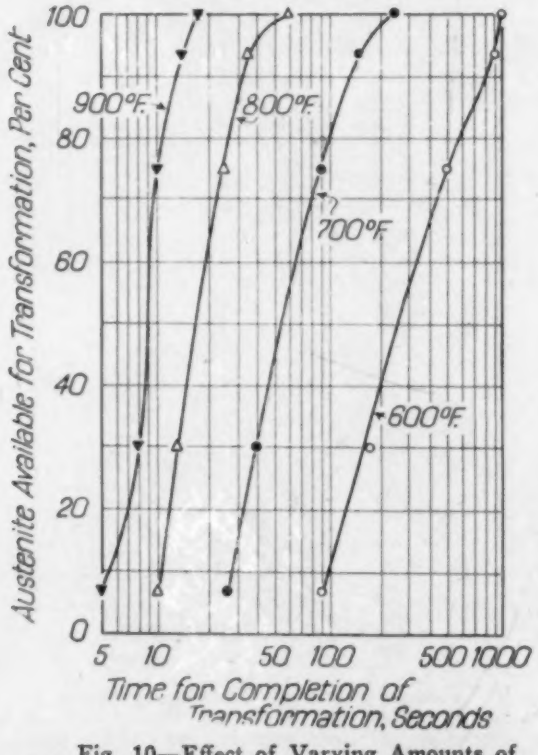

Fig. 10—Effect of Varying Amounts of Austenite on Time for Completion of Isothermal Transformation for AISI-c1095 Steel. Amounts of Austenite Are Those Remaining After Controlled Quenching.

a control for the amount of austenite in the reported isothermal transformation specimens. The data for the various mixtures have been plotted by two methods, namely: (a) Temperature versus time for the various mixtures and (b) per cent of austenite in the specimen versus time for the temperature levels investigated. We wish to point out that inasmuch as we are starting with a mixed microstructure of austenite and martensite, any immediate tempering will produce a mixed microstructure of bainite and

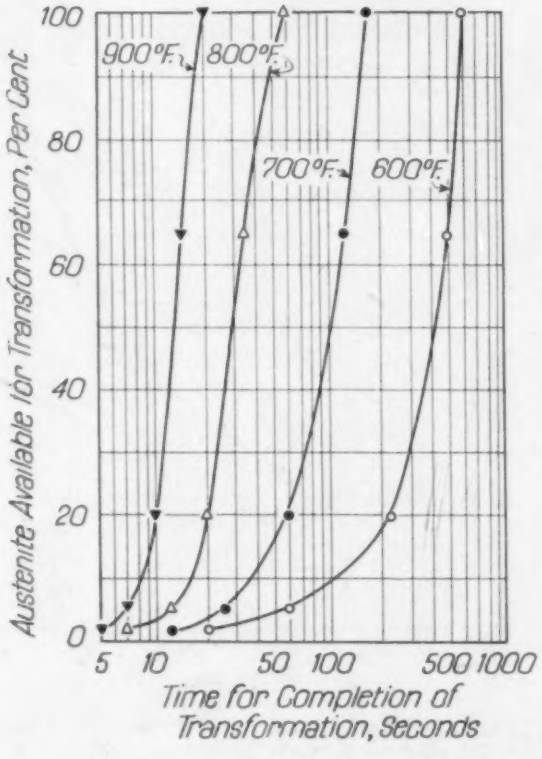

Fig. 11—Effect of Varying Amounts of Austenite on the Time for Completion of Isothermal Transformation for AISI-a4063 Steel. Amounts of Austenite Are Those Remaining in Steel After Controlled Quenching.

tempered martensite, with the proportions of the final mixture dependent on the amounts of each formed in the quench. Figs. 4-11 follow showing the isothermal transformation data. In Figs. 4-7 it is observed that the amounts of austenite for each curve is the amount remaining in the quenched specimen for subsequent isothermal transformation. In all cases these varying amounts of austenite have been transformed completely to bainite and the times for the completion of transformation are shown. In Figs. 8-11, the remaining amounts of austenite in the quenched steel for

subsequent transformation to bainite by isothermal transformation are plotted as a function of the amount of time required for transformation completion.

These curves lead to some very interesting conclusions on the effect of martensite in an austenite-martensite mixture on subsequent transformation. It is observed that the time for the completion of transformation for all temperature levels is appreciably shortened by

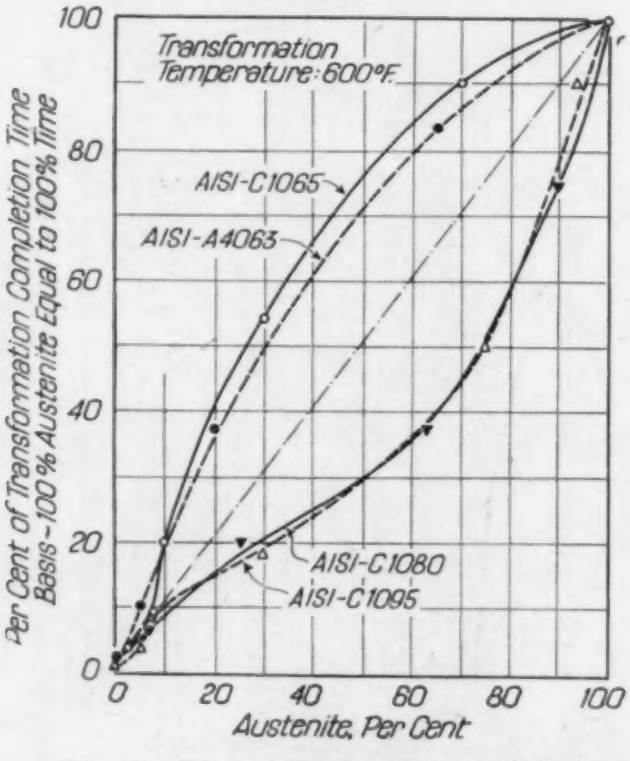

Fig. 12—Effect of Varying Amounts of Austenite on the Per Cent of Time for the Completion of Isothermal Transformation.

the presence of the martensite in the austenite matrix. Likewise, as the amount of martensite increases, the time for completion is shortened until 100 per cent martensite should require zero time for completion. The acceleration of completion transformation may be explained by two hypotheses, namely: (a) As mentioned by J. M. Robertson in one of his earlier publications, the micro stress imposed on the system by the formation of the martensite might very well influence the transformation of the remaining austenite and therefore produce the acceleration. (b) When we consider the specimen which is totally austenitic to require the maximum time for completion of transformation, we might expect specimens containing smaller

amounts of austenite to require a time for completion of transformation in relation to the amount of austenite present. If the latter is true we should expect to have a straight line relationship between the amount of austenite present for transformation and the per cent of time required for completion of transformation. We have made a plot of these data and as a result we do not believe that the latter hypothesis explains the results illustrated in Fig. 12, while the former more nearly approximates the data.

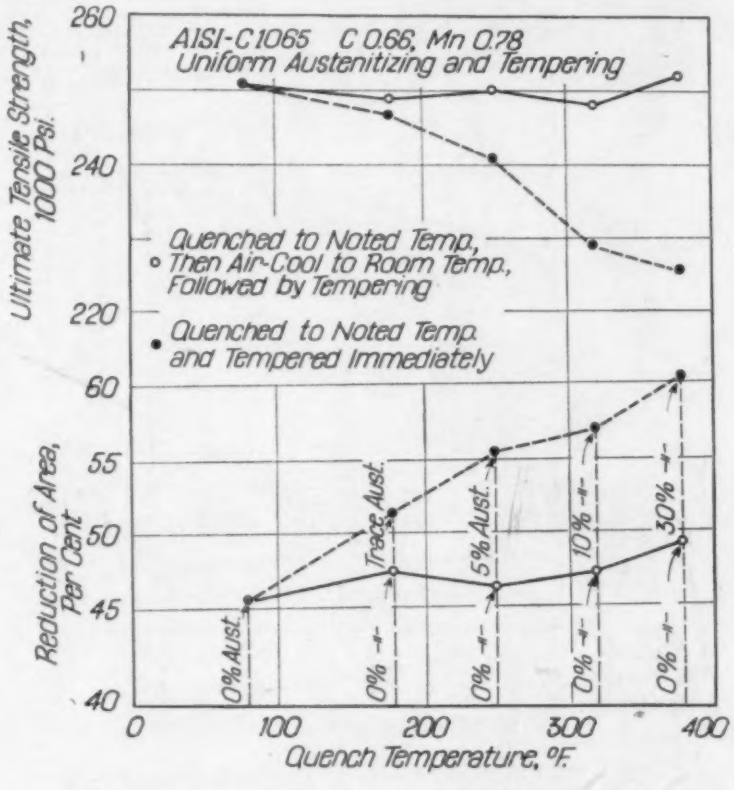

Fig. 13—Comparison of Mixed Structure and Macro Stress Theories to Account for Increase in the Ductility for Hot-Quenched Steels.

This figure is for the 600 degree Fahr. transformation level; the other temperature levels show some variation. In general AISI-c1065 and AISI-a4063 steels tend to lie above the straight line relationship while the AISI-c1080 and AISI-c1095 steels tend to lie below and in both cases the curves for the pairs of steels lie very close together. If we can assume higher carbon martensite to exert a greater micro stress on the system, we are then able to account for the different displacement for the various steels; however, before this can be definitely stated more study must be given to the subject.

Mechanical Properties

We have studied the effect of various mixtures of austenite and martensite (Present as bainite and tempered martensite) on tensile strength, hardness, and ductility properties.

The mechanical properties investigation follows the isothermal transformation study as a natural sequence in that we have used

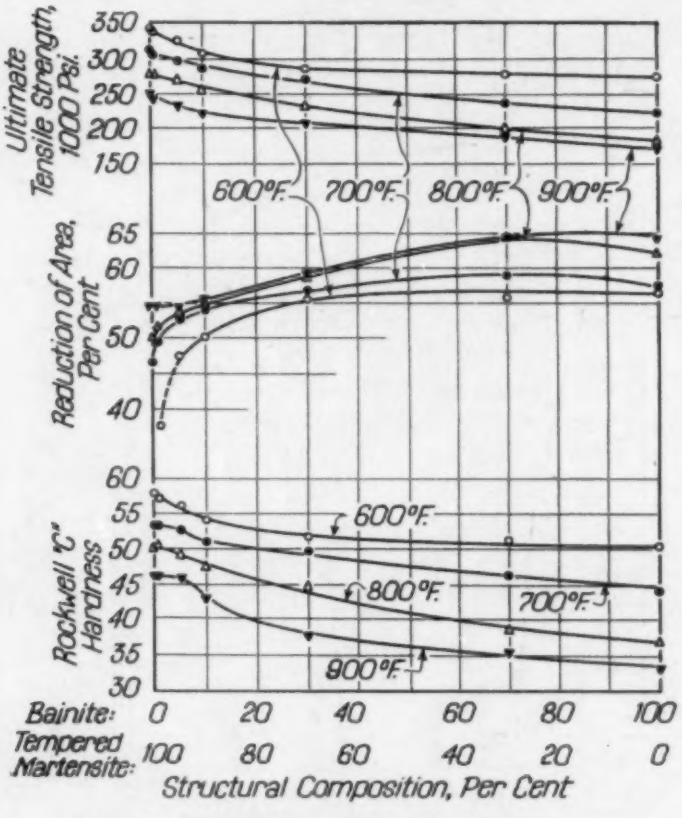

Fig. 14—Effect of Structural Composition on the Mechanical Properties of AISI-c1065 Steel. Composition Variations Regulated by Controlled Quenching.

the determined time and temperature cycles evolved from that work with the one exception of allowing 10 per cent overtime in the tempering operation to provide for any non-homogeneities in the quenched steels. According to the martensite formation theory used throughout this investigation a steel treated by quenching into a controlled temperature bath would have a mixed microstructure of austenite and martensite and after suitable subsequent tempering the bainite and tempered martensite structure might logically have the advantages of high tensile strength resulting from the tempered martensite and high ductility resulting from the

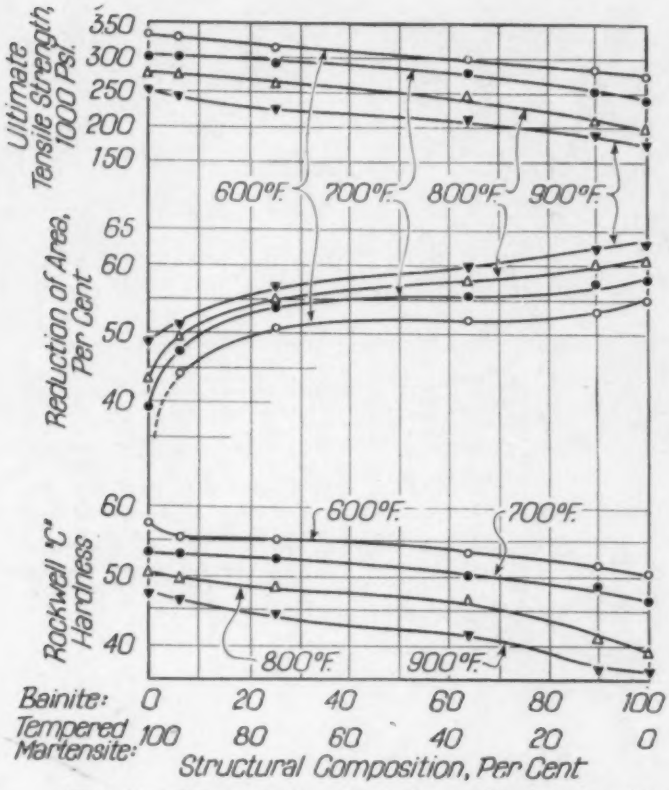

Fig. 15—Effect of Structural Composition on the Mechanical Properties of AISI-c1080 Steel. Composition Variation Regulated by Controlled Quenching.

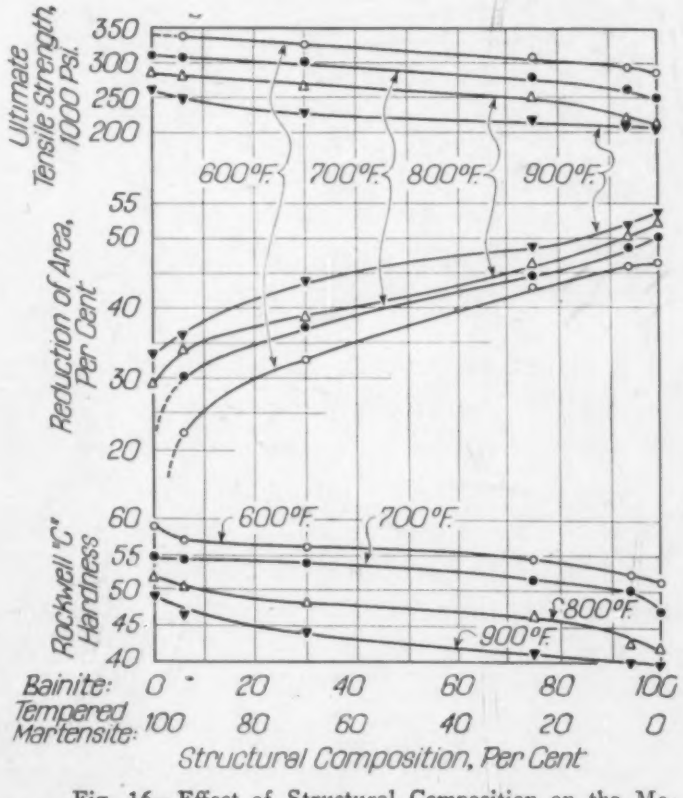

Fig. 16—Effect of Structural Composition on the Mechanical Properties of AISI-c1095 Steel. Composition Variations Regulated by Controlled Quenching.

bainite, the main point being to determine the optimum proportion necessary to produce the desired mechanical properties.

During the course of this investigation the question was raised many times that the increase in ductility for a hot-quenched steel might be associated with a lower macro stress in the steel due to the elevated temperature quench rather than to the presence of bainite. This question led to a series of treatments wherein we

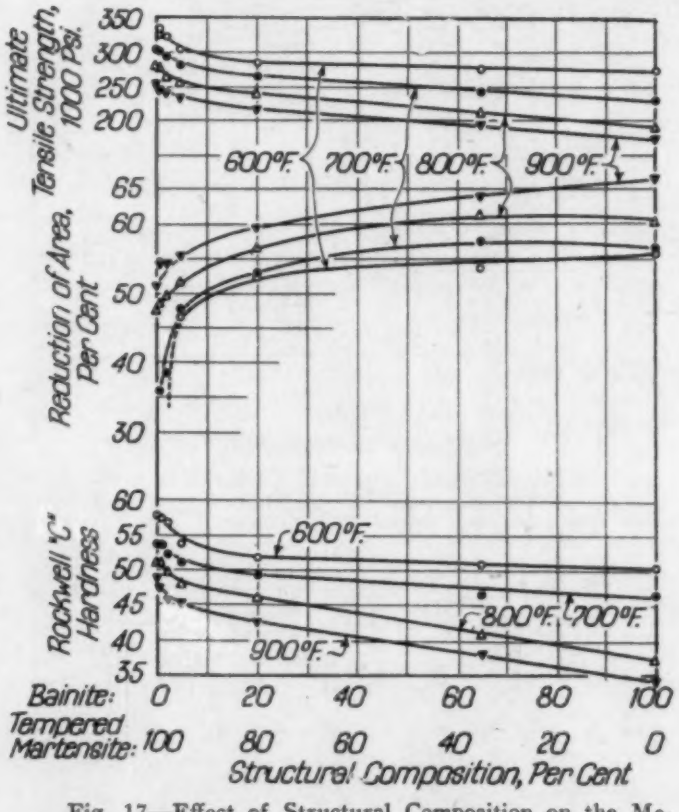

Fig. 17—Effect of Structural Composition on the Mechanical Properties of AISI-a4063 Steel. Composition Variations Regulated by Controlled Quenching.

have produced a structure typical of the quenching treatment followed in one case by immediate tempering and in the other by air cooling the quenched steel to room temperature and then tempering. According to the macro stress theory the air-cooled specimens should show the same mechanical properties as the immediately tempered specimens while according to the mixed structure theory we would expect the immediately tempered specimens to have progressively lower tensile strengths and higher ductilities as the quenching temperature was raised, due of course to larger amounts of bainite being present as a result of more austenite in the quenched steel. Likewise, according to the mixed structure theory we would ex-

pect all of the air-cooled steels to have the same tensile strength and ductility regardless of the initial quenching temperature inasmuch as the air cooling naturally allows any austenite remaining in the quenched steel to proceed to martensite on cooling. Fig. 13 shows the results of this study and it is clear that the macro stress theory does not hold entirely and that the mixed structure theory appears very tenable. It is however believed that the elevated temperature

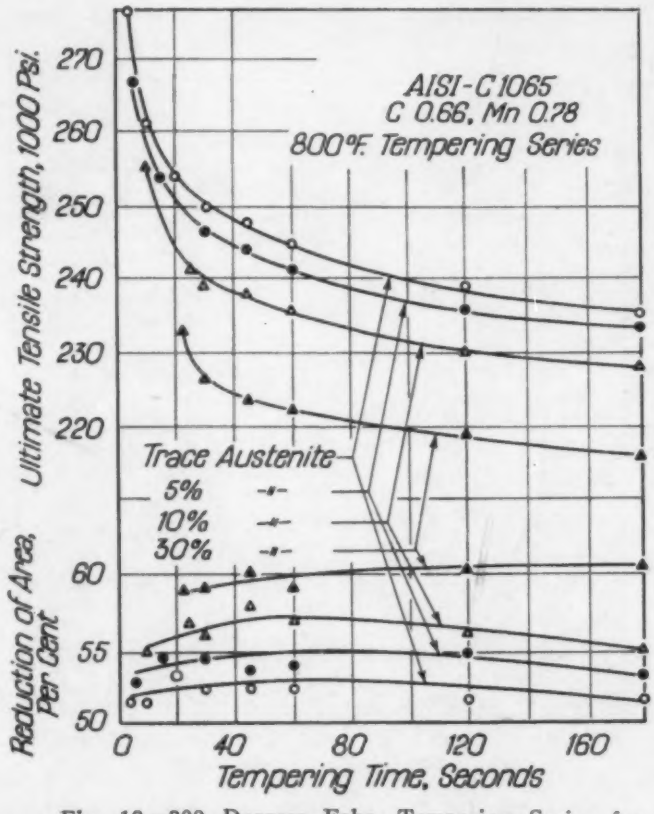

Fig. 18—800 Degrees Fahr. Tempering Series for AISI-c1065 Steel. Amount of Austenite Remaining After Controlled Quenching Noted on Individual Curves.

quench in many cases is very useful in the avoidance of cracks formed during quenching.

The mechanical properties of the four steels studied have been plotted as a function of the structural composition of the steel, namely, bainite and tempered martensite, and we have used 100 per cent bainite and 100 per cent tempered martensite steels as the two base points. The results are shown in Figs. 14 to 17. It is seen from these plots that the lowest tensile strength, lowest hardness and the highest ductility for any one temperature level are generally associated with the fully bainitic steel with slight variances

in some instances. A decrease in the quenching temperature synonymous with a decrease in the amount of austenite remaining in the quenched steel (hence less bainite in the tempered steel) always raises the tensile strength and hardness, and lowers the ductility; furthermore, the transformation time for completion is always decreased. Likewise, there are instances where a suitable combination of bainite and tempered martensite with the same

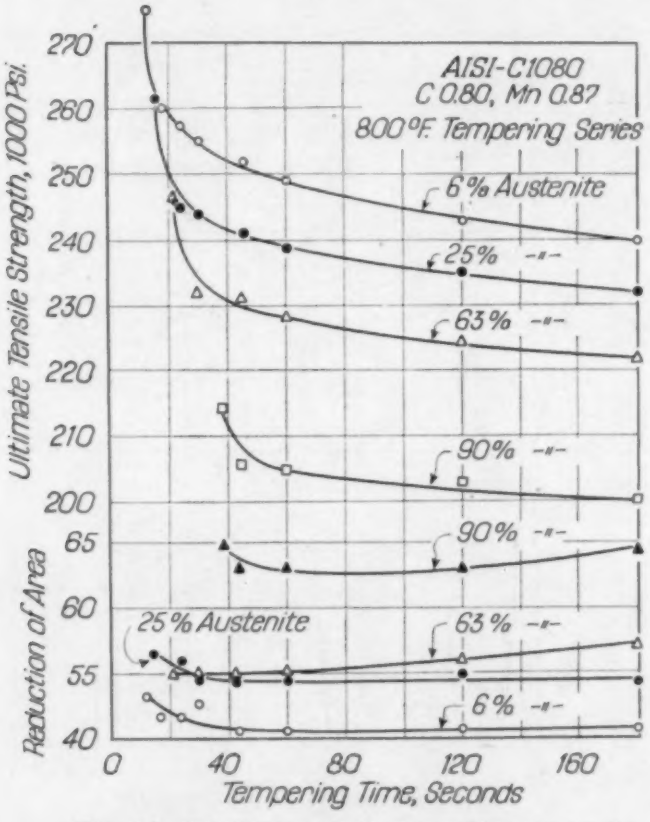

Fig. 19—800 Degrees Fahr. Tempering Series for AISI-c1080 Steel. Amount of Austenite Remaining After Controlled Quenching Noted on Individual Curves.

hardness as a wholly bainitic structure will exhibit higher tensile strength and ductility with an appreciably shorter transformation time. Generally this difference exists due to a difference in the temperatures involved for the production of the two systems.

While the quenching times used in this study are very short, a few quenches in the order of one hour were investigated and it was found that the long time had no great effect on either the tensile or ductility properties. Accordingly it is believed that the main prerequisite consists of quenching to a suitable elevated temperature, properly controlled, followed by immediate tempering.

It is realized that the tempering cycles reported in this paper are very short and in Figs. 18 to 19 we show the results of longer times for AISI-c1065 and c1080 steels, austenitized in lead at 1550 degrees Fahr. for one minute, quenched at a series of temperatures, and tempered at 800 degrees Fahr. As might be expected the longer times lower the tensile strength and seem to have very little effect on the ductility. This is to be expected when it is considered that the additional tempering time will have little or no effect on the bainite and probably affects only the martensite.

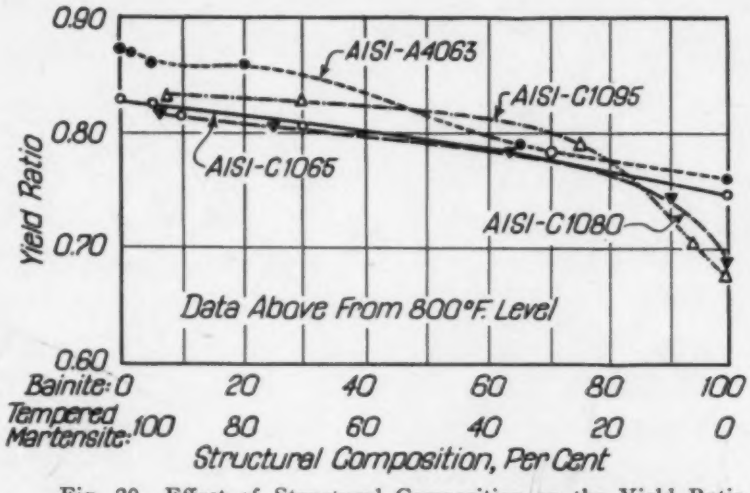

Fig. 20—Effect of Structural Composition on the Yield Ratio of Four Commercial Steels.

A few tests using the same cycles as above were carried out for 0.01 per cent yield strength values and it is observed from Fig. 20 that the yield ratio is lowest in all cases for the fully bainitic steels and that a combination of approximately 50 per cent tempered martensite and 50 per cent bainite or higher amounts of tempered martensite exhibit the highest ratios. It is observed that the AISI-a4063 steel shows the highest ratio for practically all structural combinations studied.

From the results of the mechanical property study it is believed that optimum heat treating cycles for quench and tempered steels may be arrived at with the same simplicity as was previously associated only with the use of the S-curve for the determination of the proper austempering heat treating cycles. As in austempering, the complete heat treatment may be arrived at from simple time-temperature diagrams illustrated in Figs. 4 to 7. However, we wish to reaffirm that the elevated quench must be immediately followed by tempering to obtain the full measure of success.

Summary and Conclusions

The mechanism of martensite transformation as reported by Carpenter and Robertson and others has been confirmed and it is believed that the transformation may be reasonably controlled with suitable equipment. It is thought that the carbon content of the steel under consideration exerts the greatest influence on the temperature for the beginning of martensite transformation and probably is of major importance throughout the range of transformation. On the basis of this work it is evident that the molybdenum content of 0.25 per cent has very little effect on the start of martensite transformation.

The presence of martensite, formed on cooling, in an austenite matrix will materially shorten the time for completion of transformation and the greater the amount of martensite the shorter the time. It is possible that the acceleration of completion transformation may be due to a micro stress imposed on the system by the martensite formed during the quench. The fact that the higher carbon steels investigated transformed at a faster rate than the lower carbon steels may tentatively be explained on the basis that high carbon martensite may exert a greater micro stress on the system.

For the same transformation level, fully bainitic steel exhibits the lowest tensile strength and hardness, and in most cases the highest ductility. Transformation of an austenite-martensite specimen will result in a mixed microstructure of bainite and tempered martensite which, when properly controlled, may exhibit the high tensile properties of a tempered steel and the high ductility of an austempered steel. In addition the required time for completion of transformation will be very materially shortened.

Other investigations have shown that quenching times as long as one hour have no harmful effects on the mechanical properties of the steel. Longer tempering times result only in a lowering of the tensile strength with very little effect on the ductility.

It may be stressed that to obtain the advantages of an elevated temperature controlled quench, it must be immediately followed by tempering to realize the stated improvements in mechanical properties. Also sufficient transformation time must be allowed for the decomposition of the austenite into bainite otherwise the heat treated steel may be brittle due to the retained austenite which would be present as untempered martensite.

ACKNOWLEDGMENTS

The author gratefully acknowledges the contributions made to this paper by the other members of the staff of the American Steel and Wire Company Research Department, particularly Mrs. M. B. Hall who assisted in obtaining some of the experimental data, and Mr. Stanley Curtin in the preparation of the charts. Mr. R. E. Griffiths and Mr. G. T. Spare likewise assisted in the course of the study. Dr. E. C. Bain, Carnegie-Illinois Steel Corp., Mr. E. S. Davenport, Dr. R. L. Rickett, Mr. J. R. Vilella, and Mr. R. A. Grange, U. S. Steel Corp. Research Laboratory aided the author with constructive criticism and advice.

References

1. E. S. Davenport and E. C. Bain; "Transformation of Austenite at Constant Sub-critical Temperatures", *Transactions,* American Institute of Mining and Metallurgical Engineers, Iron and Steel Division, 1930, p. 117-144.
2. H. Carpenter and J. M. Robertson; Metals, Oxford University Press, 1939.
3. A. B. Greninger and A. R. Troiano; "Kinetics of the Austenite to Martensite Transformation in Steel", TRANSACTIONS, American Society for Metals, Vol. 28, 1940, p. 537-574.
4. A. B. Greninger; "Martensite Thermal Arrest in Iron-Carbon Alloys and Plain Carbon Steels", TRANSACTIONS, American Society for Metals, Vol. 30, 1942, p. 1-26.
5. T. G. Digges; "Transformation of Austenite on Quenching High Purity Iron-Carbon Alloys", TRANSACTIONS, American Society for Metals, Vol. 28, 1940, p. 575-607.
6. H. Scott and Hoop; Discussion on "Transformation of Austenite on Quenching High Purity Iron-Carbon Alloys", TRANSACTIONS, American Society for Metals, Vol. 28, 1940, p. 604.

DISCUSSION

Written Discussion: By G. M. Foley, research engineer, Battelle Memorial Institute, Columbus, Ohio.

The author presents a technique and results of great value to those interested in the martensite and isothermal transformations.

I should like to ask if the effect of martensite on the beginning of isothermal transformation of the remaining austenite was observed, and whether any generalizations regarding the effect of martensite on the induction period can be made.

It seemed of interest to replot the author's data after the method used to compare S.A.E. steels by Janitzky and Baeyertz in the A.S.M. Metals Handbook, 1939 edition. Figs. A and B show plots of ultimate strength versus reduction of area, the only other tension test properly reported by the author, for various mixtures of martensite and bainite.

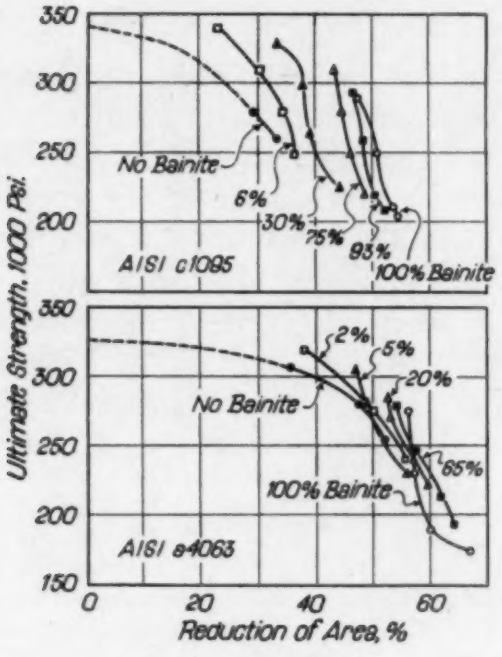

Fig. A

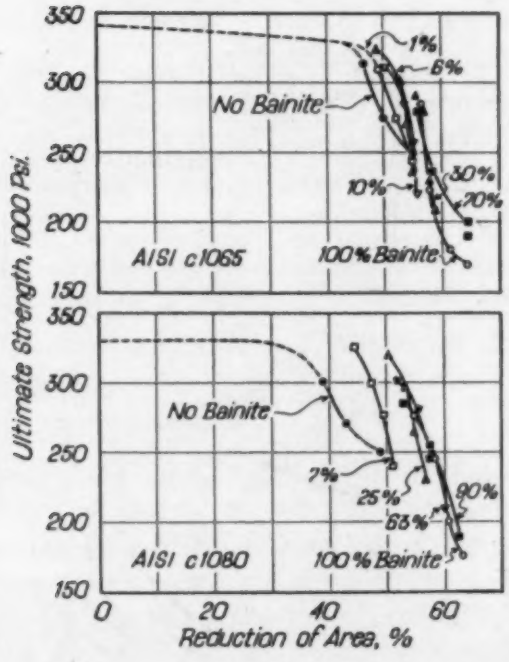

Fig. B

The diagrams for the two higher carbon steels show the potent effect of small amounts of bainite in increasing the ductility of tempered martensite. On the other hand, in the case of these high strength materials, for any given ultimate strength, the maximum ductility is obtained from bainite. Higher strengths are shown for mixtures of martensite and bainite than for any pure

bainite, but stronger bainite could be had by transformation at a lower temperature than was done by the author. The heat treating time might, in this case, become excessive.

In the two lower carbon steels shown the effect of varying the proportions of tempered martensite and bainite is less pronounced and, as has been noted frequently, the relative ductility of bainite decreases at lower hardness.

The major question about the practicability of the heat treatments described thus depends upon the relative advantages of shorter heat treating times, involving a reduction of austempering time for high strength from 25 minutes to 4 minutes as against the loss of ductility which may occur in some materials, and the complications of the double quenching technique involved.

Written Discussion: By B. R. Queneau, lieutenant commander, U.S.N.R., U. S. Naval Proving Ground, Dahlgren, Va.

The author has added some valuable data to the information on the transformation of austenite to martensite and bainite. The effect of the presence of martensite on the austenite-bainite transformation is of particular interest.

However, when discussing the mechanical properties of various mixtures of bainite and tempered martensite, the author confuses the picture to some extent by comparing structures varying both in hardness and in ductility. For a given steel, bainite formed at one temperature is softer than martensite tempered at that temperature. For instance in steel AISI-c1065 treated by the author, bainite formed at 600 degrees Fahr. (315 degrees Cent.) had a hardness of R_C51 as compared to R_C58 for martensite tempered at the same temperature. To obtain a hardness of R_C51, a tempering temperature of 800 degrees Fahr. (425 degrees Cent.) was required for an initial structure of 100 per cent martensite and a temperature of 700 degrees Fahr. (370 degrees Cent.) for a mixture of 30 per cent bainite and 70 per cent martensite. From the curves shown in Fig. 14, the following hardness and per cent reduction of area data can be obtained:

Structural Composition, Per Cent	Temperature of Transformation and Tempering—Degrees Fahr.	Hardness, Rockwell C	Per Cent Reduction of Area
100 Bainite	600	51	56
20 Bainite	700	51	56
0 Bainite	800	51	50
100 Bainite	700	44	57
30 Bainite	800	44	57
10 Bainite	900	44	56
100 Bainite	800	37	62
40 Bainite	900	37	62

It can be seen that for steel AISI-c1065 the ductility of mixtures of bainite and tempered martensite is equal to that of a homogeneous bainite of equal hardness unless the per cent of tempered martensite is over 80 per cent. For the steels of higher carbon content investigated by the author, much lower percentages of martensite result in a loss of ductility.

It has been shown (from the work of Bain, Davenport and others), that for high carbon steels bainite has greater ductility than tempered martensite of equal hardness. The importance of the present paper is that it indicates that considerable time of heat treatment can be saved by partially transforming the austenite to martensite prior to the austempering treatment without loss of ductility.

Written Discussion: By Charles Nagler, Department of Metallography, University of Minnesota, Minneapolis, Minn.

Mr. Elmendorf is to be complimented for the fine work he did on gathering information for this paper. It was with much interest that the writer read in the conclusions the statement: "Molybdenum content of 0.25 per cent has very little effect on the start of martensite transformation."

This conclusion is in line with some work carried out by the writer in studying the effect of molybdenum on austenite transformation rate in cast iron at relatively low subcritical temperatures of 400 to 700 degrees Fahr. (205 to 370 degrees Cent.). It was found that molybdenum content up to approximately one-half per cent had little or no effect on the position of the beginning or end portion of the isothermal transformation curves in the temperature range of 400 to 700 degrees Fahr. (205 to 370 degrees Cent.).

The cast irons used in this investigation were approximately of the 3.00 carbon 2.00 silicon variety. These studies were carried out on a commercial heat of iron made in a cupola. There is no reason to believe that molybdenum would have any different effect in cast iron than it would have in steel, for it appears that the carbon content is somewhat of a major factor in determining the beginning and end point on the isothermal transformation curves of any alloy, be it either a steel or a cast iron in the low temperature subcritical range of 400 to 700 degrees Fahr. (205 to 370 degrees Cent.).

Written Discussion: By E. P. Klier, assistant instructor, University of Notre Dame, Notre Dame, Ind.

The subject matter covered in this paper is of broad theoretical as well as practical importance. Thus the data given in Fig. 2 affirm the results of Förster and Scheil[1] that the formation of martensite begins at a low rate (dV/dT), attains a maximum then decreases, all on continuous cooling. Further it is indicated that the rate of martensite formation is not purely a function of the distance below Ar", but may well be dependent on the composition of the steel, i.e., the martensite range is not a constant temperature interval.

It is believed that the author's remarks regarding the effect of martensite on subsequent transformation by isothermal holding are somewhat ambiguous. From a theoretical point of view it is far more important that the rates of transformation be determined than the actual times for completion. Since these data for the purpose at hand need be only qualitatively correct, the information contained in the author's Fig. 12 will suffice. The tangent to any of these curves indicates the rate of transformation at that point. It is interesting to note that for the two medium carbon steels the rate of austenite decomposition decreases with decreasing austenite present. This does not appear to be true, however, for the high carbon steels, in which instances the rate curves pass through points of inflection. For these steels then the maximum rate of austenite decomposition takes place when about 60 to 80 per cent austenite is present.

After a consideration of the results of Zmeskal and Cohen[2] on high carbon high chromium steels it appears that the results for the two high carbon steels may be in error. Reference to their Fig. 4 indicates that the steels containing

[1]F. Förster and E. Scheil, *Z. Metallkde.*, Vol. 28, 1936, p. 245-247.

[2]O. Zmeskal and M. Cohen, "The Tempering of Two High Carbon-High Chromium Steels," TRANSACTIONS, American Society for Metals, Vol. 31, 1943, p. 380-408.

the greatest amounts of austenite transformed at the highest rates. The data of Zmeskal and Cohen are preferred for the high carbon steels because of the method used in determining the course of the transformation. The micro-stress theory which demands an increase in the rate of austenite decomposition with increasing amounts of martensite present cannot be considered correct. That the austenite in mixed structures of various sorts transforms at a lower rate than 100 per cent austenite has been shown repeatedly.[3, 4, 5]

The work on the mechanical properties of steels composed of mixtures of tempered martensite and isothermal decomposition products is very interesting, but it is believed that certain work of this nature which has already been done should be given consideration.

Griffiths, Pfeil and Allen[6] have shown that frequently structures composed in part of intermediate transformation products are very low in impact properties. It has been shown in numerous instances that it is not possible to completely transform austenite in the upper intermediate range[4, 6, 7] while the physical properties thus developed are inferior to those developed in tempered martensite structures of the same hardness.[6] Continued holding at constant temperature to ensure complete transformation has in some instances been shown to have deleterious effects.[7, 8]

Author's Reply

The author is grateful to those who have contributed discussions to this paper.

Mr. Foley has commented upon the possible effects of martensite on the start of isothermal transformation. While we have not reported on this effect of martensite, we do believe there may well be a definite effect, however, due to the similarity of two of the products present—bainite and tempered martensite—it is very difficult to differentiate between them and this is particularly true at the temperature levels investigated, namely, 600 to 900 degrees Fahr. (315 to 480 degrees Cent.). We might add that we have observed that the isothermal transformation product seems to start at the martensite needle interface.

We have found that the two-step heat treatment is not at all impractical and requires only a controlled temperature quench bath wherein the steel is allowed to remain until it has approximated the bath temperature and is then followed by an ordinary tempering treatment. The excellent mechanical properties obtained and the short tempering times involved are believed to be well worth the requirements of controlled quenching.

Commander Queneau rightly calls attention to the fact that the final heat treated steel is composed of two microstructural constituents differing markedly in hardness. We believe this combination to be of value as it permits us to take

[3] D. P. Antia, Discussion, TRANSACTIONS, American Society for Metals, Vol. 31, 1943, p. 408.

[4] H. Lange and K. Matieu, *Mitteilungen aus dem Kaiser Wilhelm Institut für Eisenforschung*, Vol. 20, 1938, p. 125-134.

[5] V. Sadovski and N. Chuprakova, *Metallurg*, Vol. 14, 1939, p. 88-89.

[6] W. T. Griffiths, L. B. Pfeil and N. P. Allen, Iron and Steel Institute. Second Report of the Alloy Steels Research Committee, 1939, p. 343-367.

[7] H. Döpfer and H. J. Wiester, *Archiv. Eisenhüttenwesen*, Vol. 8, 1935, p. 541-548.

[8] A. Rose and W. Fischer, *Mitteilungen aus dem Kaiser Wilhelm Institut für Eisenforschung*, Vol. 21. 1939, p. 133-145.

advantage of the high tensile strength of the high hardness tempered martensite and the high ductility of the bainite and to so combine the two that a very desirable result is achieved.

Mr. Nagler's comments on the effects of molybdenum on the isothermal transformation of cast iron are very interesting. Isothermal transformation data for steel have shown that the molybdenum predominantly affects the portion of the S-curve from about 800 degrees Fahr. (425 degrees Cent.) and higher—that is, in the region of the "nose" of the S-curve, with lesser effects observed at the lower temperatures of 500 to 700 degrees Fahr. (260 to 370 degrees Cent.). The effect of molybdenum on the Ar" point has been corroborated by Chiswik and Greninger in their recent paper.

Mr. Klier's comments are greatly appreciated and the points are well taken. We would like to say that from a commercial point of view, the effect of martensite on the acceleration of complete transformation is of prime importance in that it offers practical methods of achieving high tensile strength coupled with high ductility with a minimum of time consumed.

We would like to point out that the data of Zmeskal and Cohen offered as a refutation of our high carbon transformation data may well be at variance when it is considered that the Zmeskal and Cohen paper was concerned with the transformation of retained austenite in 1 to 1.5 per cent carbon, 5 to 12 per cent chromium steels while our investigation was primarily concerned with plain carbon steels whose austenite definitely transforms on cooling. The above variances coupled with the complete dissimilarity in the investigational methods may well account for the noted differences.

The data quoted from Griffiths, Pfeil and Allen are primarily concerned with low carbon alloy steels whose intermediate transformation structures are not particularly adapted to the production of good mechanical properties; however, this does not hold for the plain carbon steels over 0.50 per cent carbon as has been shown by Davenport and Bain and others. The Griffiths et al. data are primarily for hardnesses under 45 Rockwell C for low carbon alloy steels and in the author's experience we have never considered these hardnesses or carbon contents to be satisfactory for the constant temperature type of heat treatment. Rather, we have always confined this type of heat treatment to plain carbon steels between 0.50 and 1.10 per cent carbon at hardnesses of approximately 45 to 55 Rockwell C.

Numerous instances are at hand which clearly show that the time for completion of transformation at some of the upper intermediate temperature levels is a very time consuming job. However, the temperatures are in the range of 800 to 1000 degrees Fahr. (425 to 540 degrees Cent.) and are generally associated with the low carbon high alloy type of steel. We have never noted this behavior in the plain carbon steels for which this treatment is contemplated. Likewise, we have seen examples of overtime transformation high as 2400 per cent and upon subsequent testing showed no deleterious effects. We might add that disastrous results are always obtained when insufficient time is allowed for the completion of the transformation of the austenite.

MARTENSITE REACTIONS IN ALLOY STEELS

By Peter Payson and Charles H. Savage

Abstract

By means of the Greninger-Troiano quench-temper procedure, the effects of manganese, silicon, nickel, chromium, molybdenum and tungsten on the temperatures of the start of the martensite reaction in 0.50 carbon steels have been determined. From these data and those of Greninger on the effect of carbon a formula has been developed from which the Ms points of alloy steels may be calculated with a fair degree of accuracy. Since carbon has a very marked effect on the Ms point, the temperature of the martensite reaction can be used as a measure of the carbon content of the steel. The quench-temper procedure may therefore be used for measuring depth of decarburization (or carburization) in steels.

Introduction

IT has become clear in recent years that the reactions which occur in steels during their heat treatment can be understood thoroughly only through an understanding of the transformations of the austenites of the steels. These transformations are best summarized in the transformation temperature time curves, many of which have been published. The curves of the alloy steels differ widely among themselves as might be expected. However, these differences are not haphazard, but follow an orderly change depending on the alloying elements dissolved in the austenite. For example, from the data of Davenport (1),* and Parke and Herzig (2), (3), (4), the following conclusions may be reached on the effects of alloying elements on the shapes of the transformation curves:

1. Carbon has little effect on the transformations from about 1300 to 900 degrees Fahr. (705 to 480 degrees Cent.) but markedly retards the transformations from about 900 to 400 degrees Fahr. (480 to 205 degrees Cent.).

2. Manganese and nickel retard the transformations both at the upper as well as the lower temperature ranges.

*The figures appearing in parentheses refer to the bibliography appended to this paper.

A paper presented before the Twenty-fifth Annual Convention of the Society, held in Chicago, October 18 to 22, 1943. The authors, Peter Payson and Charles H. Savage, are associated with the Eastern Research Laboratory, Crucible Steel Company of America, Harrison, N. J. Manuscript received July 19, 1943.

3. Chromium and molybdenum retard the transformations from about 1300 to 1100 degrees Fahr. (705 to 595 degrees Cent.) appreciably, and have a very marked retarding effect on the reactions from about 1100 to 900 degrees Fahr. (595 to 480 degrees Cent.), but have little effect on the reactions from about 900 to 400 degrees Fahr. (480 to 205 degrees Cent.).

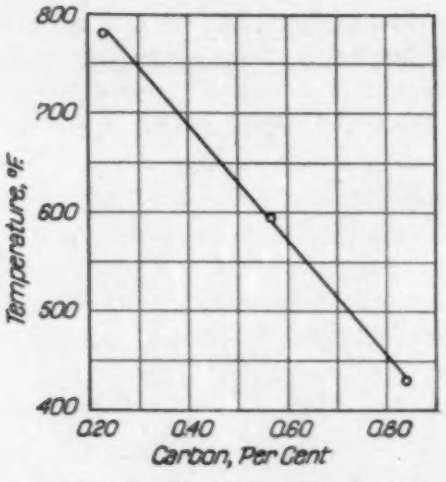

Fig. 1—The Effect of Carbon on the Ms of Plain Carbon Steel (6).

It was natural to expect that the alloying elements would have similar orderly effects on the martensite reactions in steels. However, although a number of publications have presented data on martensite reactions (5), (6), (7), (8), (9), 10, only the effect of carbon has been studied quantitatively. It is shown in Fig. 1, reproduced from Greninger (6), that increasing carbon markedly lowers the temperature of the start of the martensite reaction, or the Ms point as designated by Shepherd (10). Since there were not already available sufficient data from which the effects of the different elements on the Ms point could be established, and since it has been indicated (9), (10) that a knowledge of Ms points is advantageous in carrying out the effective hardening of steels, an investigation was made to supply these data. This paper discusses this investigation as well as a method based on Ms determinations for measuring depth of decarburization (or carburization) in alloy steels.

Experimental Procedure

A series of 15-pound induction melted ingots was made up with varying amounts of manganese, silicon, nickel, chromium, molybde-

num and tungsten. These were forged to bars approximately 1 by 0.5 inch. The analyses of these bars are shown in Table I. All steels were specified approximately 0.50 carbon because first, it was desirable to eliminate any question of the effect of carbon by maintaining carbon constant; second, it was expected that with some alloy modifications, steels with less than 0.50 carbon might precipitate ferrite during the quench to the Ms temperature, and thus alter the composi-

Table I

The Effect of Alloying Elements on the Ms and Mf Points of 0.50 Per Cent Carbon Steel

Type %	C	Mn	Si	Ni	Cr	Mo	W	Austenitizing Treatment °F Mins.	Tempering Treatment in Quench-Temper Procedure °F	Ms °F	Approximate Mf °F
1 Mn	0.47	1.02	0.34	....	....	....	....	1800–10	600– 5 Secs.	590	200
3 Mn	0.47	3.33	0.26	....	....	....	....	1800–10	700–20 Secs.	445	— 25
5 Mn	0.44	4.87	0.29	....	....	....	....	1800–10	700–20 Secs.	370	—100
1 Si	0.47	0.40	1.06	....	....	....	....	1800–15	625–3 Secs.	610	275
1 Ni	0.45	0.36	0.31	1.16	....	....	....	1700–30	600–10 Secs.	590	275
3 Ni	0.46	0.34	0.28	3.36	....	....	....	1700–30	600–30 Secs.	540	150
5 Ni	0.46	0.35	0.30	4.83	....	....	....	1700–30	600– 1 Min.	495	125
1 Cr	0.50	0.32	0.27	....	0.98	....	....	2300–3	700–10 Secs.	595	175
3 Cr	0.51	0.35	0.31	....	3.16	....	....	2300–3	1200–30 Secs.	495	50
5 Cr	0.55	0.33	0.31	....	4.61	....	....	2300–3	1200–30 Secs.	415	0
1 Mo	0.50	0.34	0.32	....	....	1.05	....	2300–3	1200–15 Mins.	625	300
3 Mo	0.49	0.33	0.31	....	....	3.51	....	2300–3	1000– 1 Hr.	580	225
5 Mo	0.46	0.34	0.27	....	....	5.40	....	2300–3	1000– 1 Hr.	550	200
1 W	0.53	0.38	0.32	....	....	....	1.04	2300–3	1200–20 Secs.	625	300
3 W	0.46	0.34	0.27	....	....	....	3.42	2325–3	1200–30 Secs.	600	300
5 W	0.46	0.37	0.27	....	....	....	4.78	2325–3	1200–30 Secs.	590	275
3 Ni-1 Cr	0.46	0.30	0.28	3.36	0.99	....	....	2100–5	1000–10 Mins.	500	...

tion of the residual austenite; and third, with steels containing large amounts of the carbide-forming elements chromium, molybdenum and tungsten, it was expected that carbon over 0.50 might not be completely dissolved in the austenite even at extremely high temperatures. All steels also contained approximately 0.20 to 0.40 manganese and silicon (except in the cases of those steels in which these elements were purposely varied) so that any conclusions based on these experimental heats could be applicable to commercial alloy steels which always contain at least similar amounts of these two elements.

The Ms determinations were made by the Greninger-Troiano quench-temper metallographic procedure described in previous publications (5), (8), (9). The sections used were in no case over $\frac{3}{16}$ inch thick, and in many cases were not over 0.030 inch in thickness, the thinner sections being used when ever there was any tendency for ferrite to separate from the austenite during the quench to the Ms temperature. (It should be pointed out here that an attempt

was made to determine the Ms point of a 0.50 carbon steel containing only 0.30 manganese and 0.30 silicon and the results were not successful because it was not possible by this technique to avoid high temperature transformations even in sections only 0.030 inch thick when quenched into baths at about 600 to 650 degrees Fahr.)

The austenitizing temperatures used for the different steels were based on the solubilities of the carbides, since in order to determine

Table II
The Effect of Grain Size on the Ms of the 1 Per Cent Mn and 3 Per Cent Ni Steels

Type %	C	Mn	Si	Ni	Austenitizing Treatment °F Mins.	Fracture Grain Size	Ms °F
1 Mn	0.47	1.02	0.34	....	1600–30	5¾	590
1 Mn	0.47	1.02	0.34	....	1800–10	4¾	590
1 Mn	0.47	1.02	0.34	....	2000–10	3	595
3 Ni	0.46	0.34	0.28	3.36	1700–30	4¼	540
3 Ni	0.46	0.34	0.28	3.36	1800–20	4	540
3 Ni	0.46	0.34	0.28	3.36	2000–10	2½	535

the effects of the various elements, it was necessary to have them completely dissolved in the austenite. The austenitizing treatments for the different steels are shown in Table I. In every case it was established by examination of a quenched microsection that the selected austenitizing treatment was satisfactory for complete solution of carbides. The austenitizing treatments were carried out in a carbonaceous muffle in a globar furnace to minimize decarburization.

Since Greninger (6) had indicated that austenitizing temperature had a measurable effect on the Ms point, it was necessary that this effect be checked because a fairly wide range of austenitizing temperatures was used in this investigation. Accordingly, the Ms points of the 1 per cent manganese and the 3 per cent nickel steels were measured for three different austenitizing temperatures, viz., 1600, 1800, and 2000 degrees Fahr. (870, 980 and 1095 degrees Cent.) for the former, and 1700, 1800, and 2000 degrees Fahr. (925, 980 and 1095 degrees Cent.) for the latter. As shown in Table II, the Ms points were found to be within 5 degrees Fahr. for all of the austenitizing temperatures. It is to be concluded, therefore, that austenitizing temperature has a negligible effect on the Ms point, as long as the temperature is sufficiently high for complete solution of carbides.

The tempering treatment in the quench-temper procedure was determined by experiment. Its selection was based on the facts that it gave a satisfactory etching contrast between the

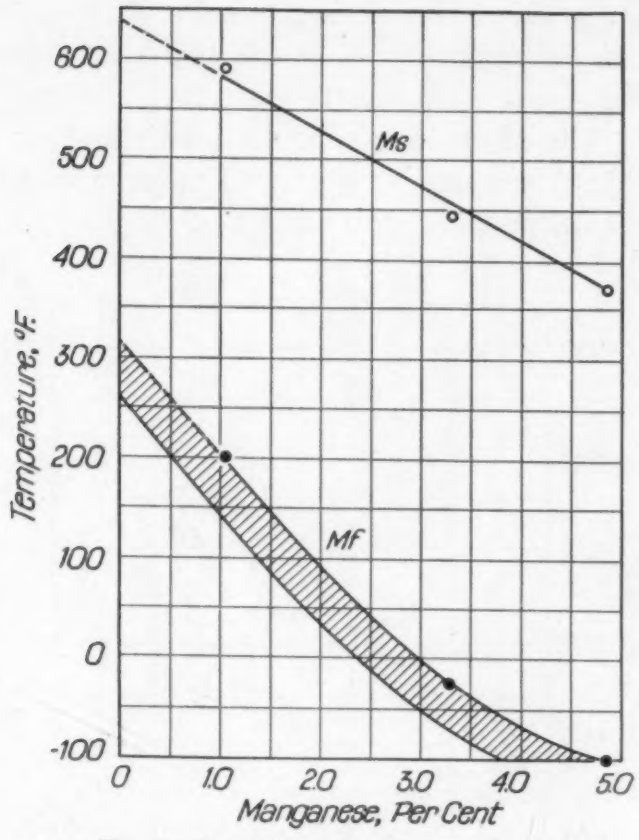

Fig. 2—The Effect of Manganese on the Ms and Mf of 0.50 Per Cent Carbon Steel.

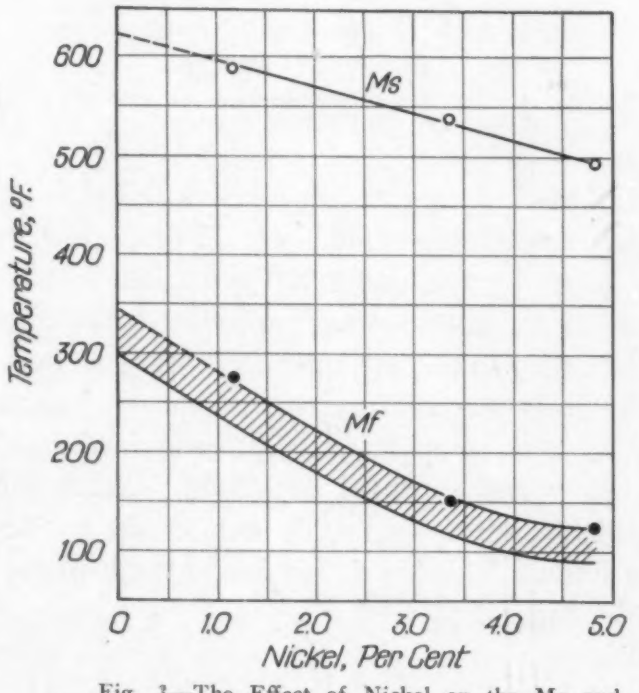

Fig. 3—The Effect of Nickel on the Ms and Mf of 0.50 Per Cent Carbon Steel.

tempered and untempered martensite, and that it would not permit transformation of the austenite. The selected treatments are shown in Table I. The pieces were always quenched in water after they were tempered. The Ms values were measured to about 10 degrees Fahr. To do this, a sample was quenched to an arbitrarily selected temperature, held in the bath for 15 seconds, then tempered and ex-

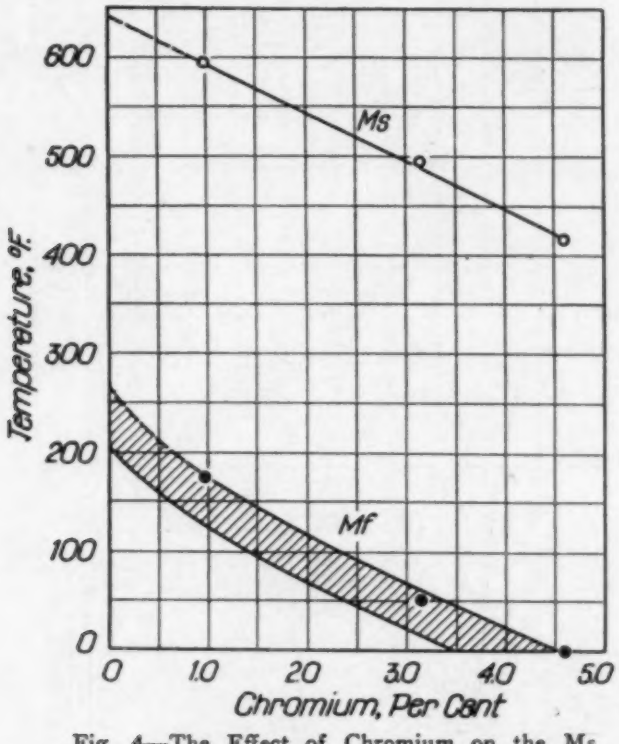

Fig. 4—The Effect of Chromium on the Ms and Mf of 0.50 Per Cent Carbon Steel.

amined. If it showed tempered martensite, another sample was quenched to a higher temperature, held for 15 seconds, then tempered and examined. Thus by cut and try, the region in which the Ms temperature was to be found was gradually established. In the final determination, the sample was quenched first to a bath somewhat above the expected Ms temperature so that most of the heat would be abstracted from the sample before it was introduced into the bath held just below the expected Ms point. With this two-step quench, the temperature of the final bath could be controlled to within 2 degrees Fahr. The Ms determinations are given in Table I and are plotted in Figs. 2 to 6.

Since the designation of the Ms point by the metallographic method is somewhat arbitrary, the photomicrograph in Fig. 7 is

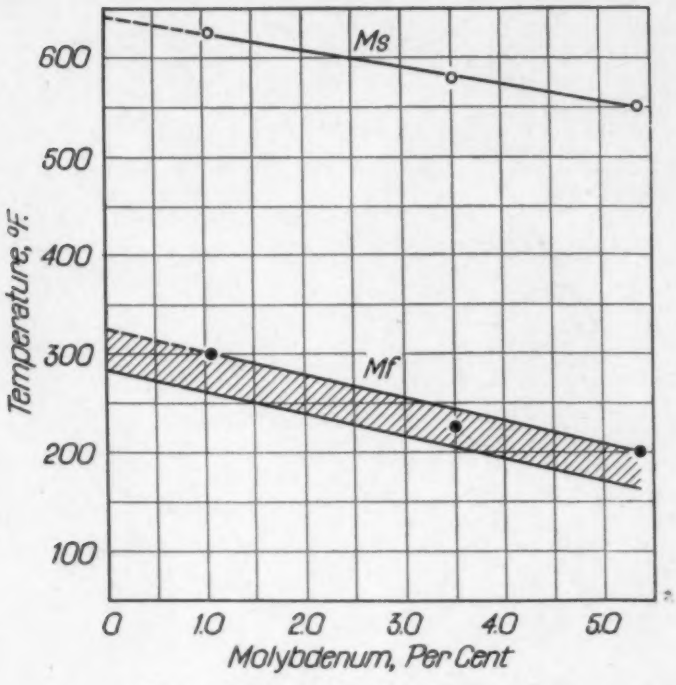

Fig. 5—The Effect of Molybdenum on the Ms and Mf of 0.50 Per Cent Carbon Steel.

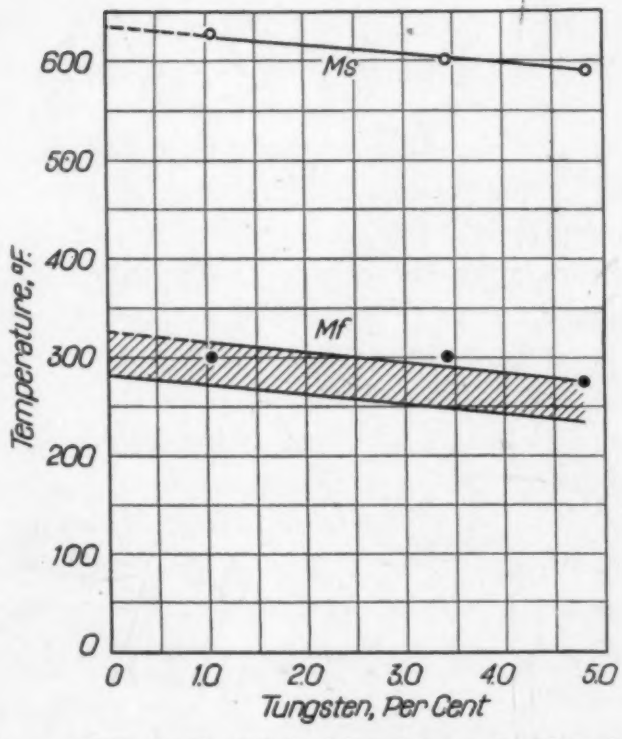

Fig. 6—The Effect of Tungsten on the Ms and Mf of 0.50 Per Cent Carbon Steel.

Fig. 7—Amount of Tempered Martensite Considered Necessary to Indicate Ms Point in Quench-Temper Procedure. × 1000.

shown to illustrate the amount of tempered martensite which was established as the limit. A dark etching needle here or there in the section was considered insufficient evidence that the sample had been quenched below the Ms point. If the number of dark etching needles in any field of the microsection was definitely in excess of the amount shown in the photomicrograph, the temperature to which the piece had been quenched was considered to be below the Ms point.

To make the data on the effects of the alloying elements on the martensite reactions more complete, determinations were also made of the temperatures of the finish of the martensite reaction, or the Mf points. These determinations were made by the metallographic method which it is admitted is less reliable for the finish of the reaction than for the start of the reaction. (See discussions of references (8) and (9).) The approximate Mf values are shown in Table I and in Figs. 2 to 6. For bath temperatures below room temperature, mixtures of dry ice and methanol were used.

Discussion of Results

The data of Table I and the curves of Figs. 1 to 6 show that

within the limits of analyses studied, all elements tend to lower the temperature of the martensite reaction. Carbon is by far the most effective, the order of the other elements from most to least effective being manganese, chromium, nickel, silicon, molybdenum and tungsten. The latter three have approximately equal effects. The decrease in the Ms temperature appears to be directly proportional to the amount of the element in the steel. A gratifying fact is that all the Ms lines of Figs. 2 to 6 when extrapolated to 0 per cent of each element indicate the Ms temperature of a plain carbon steel of about 0.50 carbon to be 635 to 645 degrees Fahr. (335 to 340 degrees Cent.) which is in good agreement with the Ms point for a 0.50 carbon steel as indicated by Greninger's curve reproduced in Fig. 1.

When data are found to have linear relationships, it is natural that an attempt should be made to combine them into a simple for-

Table III
Comparison of Measured and Calculated Values of Ms Points

Steel	Austenit. Temp., °F	C	Mn	Si	Ni	Cr	Mo	Ms Point–°F Meas.	Calc.	Deviat.
4042	1500	0.43	0.90	0.23	0.23	0.27	0.26	610	600	—10
4063	1500	0.64	0.85	0.29	0.19	0.24	0.27	445	490	+45
8442	1500	0.40	1.43	0.22	0.23	0.29	0.32	600	590	—10
8949	1500	0.49	1.01	0.20	0.54	0.56	0.38	535	530	— 5
8749	1500	0.52	0.85	0.21	0.53	0.50	0.26	540	535	— 5
4142	1500	0.41	0.86	0.30	0.11	1.06	0.23	590	575	—15
4160	1575	0.61	0.59	0.24	0.16	0.94	0.33	500	485	—15
4342	1500	0.42	0.68	0.18	1.74	0.81	0.29	530	550	+20
Special	1650	0.30	1.63	0.49	....	0.44	0.33	655	625	—30

NOTE: Of the above, all but the last value were published in Reference (10). The last appeared in Reference (7).

mula. The result of this attempt is the following, which may be applied to the prediction of the Ms temperature of any low alloy steel providing of course that the austenitizing temperature used is one at which all carbides will be completely in solution in the austenite.

Ms in °F = 930—570C—60Mn—50Cr—30Ni—20Si—20Mo—20W.

There are not many published Ms points against which this formula may be tested. Those in references (8) and (9) cannot be used because all steels discussed are tool steels and the conventional austenitizing temperatures used for these steels are not high enough to dissolve all carbides. The calculated values of Ms points for these steels would therefore be much lower than the measured values, as indeed they are. However, the Ms values published in references

(7) and (10) may serve to test this formula. These are shown in Table III together with values calculated from the formula. It will be noted that six of the calculated values are within 5 to 15 degrees Fahr. of the measured values, one is off by 20 degrees Fahr., one by 30 degrees Fahr., and one by 45 degrees Fahr. For most practical purposes it appears therefore that values of Ms points calculated from this formula should be satisfactory.

Of the Mf points there is very little to be said because of the uncertainty of these values. It may be stated generally however that the Mf points are approximately 325 to 475 degrees Fahr. (165 to 245 degrees Cent.) below the Ms points, the spread between the Ms and Mf points being greater for the elements that are most effective in depressing the Mf point, namely, manganese, chromium, and nickel.

Measurement of Decarburization by Means of the Martensite Reaction

From Fig. 1 which shows the effect of carbon on the Ms point of plain carbon steel it is very clear that the martensite reaction can be used to measure the carbon content in steel. By the quench-temper procedure it is easy to distinguish between a 0.60 and a

Table IV

Effect of Carbon Content on the Ms Points of 18-4-1 and 5-4-4-1 High Speed Steels

The 18-4-1 samples were austenitized at 2350 degrees Fahr., and the 5-4-4-1 samples at 2225 degrees Fahr. After being quenched to salt baths at appropriate temperatures, the samples were tempered immediately at 1100 degrees Fahr. for 10 minutes, then quenched in oil.

Type	C	Mn	Si	Cr	V	W	Mo	Ms Point °F
18-4-1	0.33	0.32	0.13	3.65	1.33	17.98	....	670
18-8-1	0.51	0.34	0.20	3.70	1.12	17.77	....	510
18-4-1	0.70	0.43	0.33	3.84	1.08	17.58	....	380
18-4-1	0.84	0.49	0.24	3.88	1.07	17.67	....	275
5-4-4-1	0.38	0.33	0.26	3.87	1.43	5.44	3.96	570
5-4-4-1	0.59	0.35	0.32	3.90	1.50	5.31	4.08	425
5-4-4-1	0.81	0.35	0.25	3.97	1.43	5.36	4.02	320
5-4-4-1	0.84	0.31	0.22	4.05	1.71	5.41	4.52	305
5-4-4-1	1.00	0.34	0.31	3.92	1.52	5.35	4.08	220

0.70 carbon steel because the Ms points are about 60 degrees Fahr. apart. All that is necessary is that the steel be heated to a temperature at which all carbides are in solution and that the austenite thus formed be cooled sufficiently rapidly to the martensite temperature to avoid any high temperature transformation. As has been indicated above, the martensite reaction can be measured by the quench-temper procedure to within at least 10 degrees Fahr., and therefore

the carbon content of the steel can be measured to about 0.02 per cent.

This procedure somewhat modified can also be applied to high alloy steels in which carbides are not completely dissolved at any austenitizing temperature. The modification involves merely the use of a constant austenitizing temperature. To demonstrate this, two series of steels were made up, one consisting of the 18-4-1 high

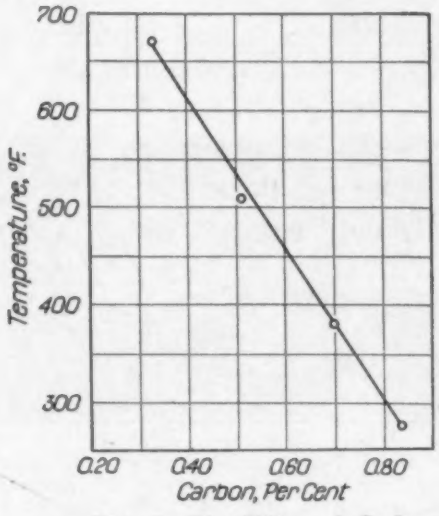

Fig. 8—The Effect of Carbon on the Ms of 18-4-1.

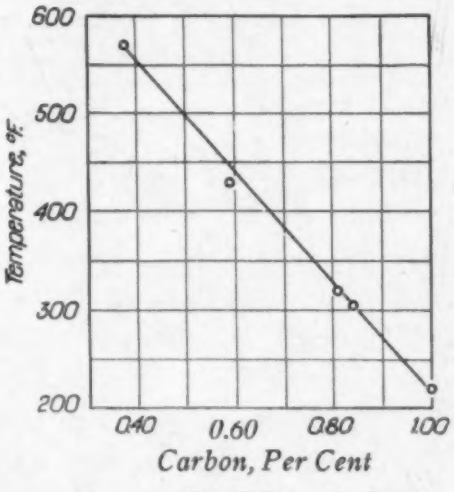

Fig. 9—The Effect of Carbon on the Ms of 5-4-4-1.

speed steel base with variable carbon, and the other of the 5-4-4-1 high speed steel base with variable carbon. The analyses of these steels are given in Table IV. The Ms temperatures were determined as described above, an austenitizing temperature of 2350 degrees Fahr. (1290 degrees Cent.) being used for the 18-4-1 series and an austenitizing temperature of 2225 degrees Fahr. (1220 degrees Cent.)

being used for the 5-4-4-1 series. The Ms points for these steels for the austenitizing temperatures mentioned are given in Table IV and are plotted in Figs. 8 and 9. The linear relationships between Ms temperatures and carbon contents are again visible in these two series. The slope of these two carbon - Ms temperature lines is almost the same as that of the Greninger curve shown in Fig. 1. It is obvious then that by means of these lines, the carbon content in these two high speed steels can be measured within a few points by the quench-temper procedure.

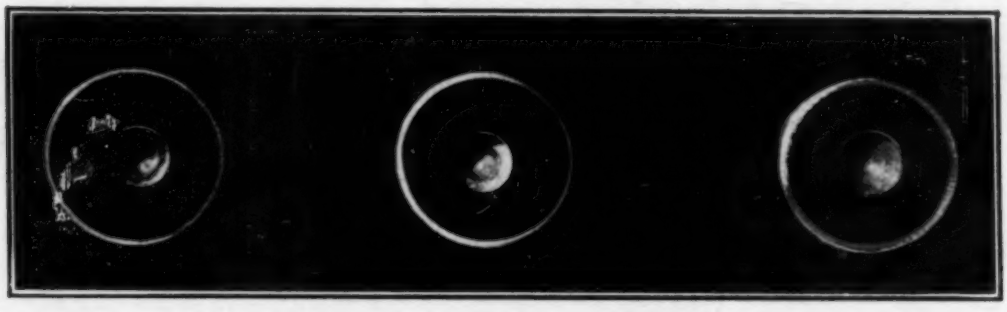

Fig. 10—Bars of 5-4-4-1 High Speed Steel Showing Different Amounts of Decarburization as Indicated by the Quench-Temper Procedure. Samples After Being Decarburized were Heated in a Carbonaceous Muffle at 2225 Degrees Fahr., Quenched to a Bath at 310 Degrees Fahr., Tempered at 1100 Degrees Fahr., then Polished, and Etched in 5 Per Cent Nital. Central Hole Drilled to Provide Fresh Cut Edge for Control. Natural Size. (Although the microstructure of the decarburized rim actually is dark etching, and that of the core is light etching, the photograph makes the relationship appear reversed. This is attributable to the fact that macroscopically, only the rim appears etched and the core appears to be polished and not etched. The reflection of light from the polished surface into the lens of the camera causes the photograph of the core of the sample to be completely dark.)

This method has been applied to the measurement of depth of decarburization in high speed steels. (Evidently, the method could also be applied to other steels, and for measurement of depth of carburization as well.) The decarburized samples are heated in a carbonaceous muffle at 2350 degrees Fahr. (1240 degrees Cent.) for 18-4-1 and 2225 degrees Fahr. (1220 degrees Cent.) for 5-4-4-1. They are then quenched to the appropriate bath temperature for the base carbon content of the steel, 380 degrees Fahr. (195 degrees Cent.) for 18-4-1, and 310 degrees Fahr. for 5-4-4-1, and held about 15 seconds at the bath temperature, then tempered immediately at about 1100 degrees Fahr. (595 degrees Cent.) for 10 minutes. A very sharp contrast is then obtained in the polished and etched microsection between the dark etching tempered martensite in the low carbon rim and the light etching untempered martensite in the high carbon core. This is illustrated in Fig. 10, which is a photomacrograph of three artificially decarburized samples of ¾-inch round

Fig. 11—Decarburized Rim 0.025 Inch Deep, in 18-4-1 High Speed Steel as Indicated by Quench-Temper Procedure. Sample Austenitized at 2350 Degrees Fahr., Quenched to 380 Degrees Fahr., Then Tempered at 1100 Degrees Fahr. for 10 Minutes and Etched in 5 Per Cent Nital. Composite Taken at × 500, Then Reduced About One-half.

5-4-4-1 high speed steel which have been given the quench-temper treatment. The holes in the center of each sample are drilled purposely to provide fresh cut edges in the microsection as a control to establish whether or not any decarburization had been introduced during the austenitizing of the sample prior to the quench-temper procedure. Fig. 11 is a reduced composite of several adjacent fields of a decarburized rim after the quench-temper treatment, photographed originally at × 500 to show how clearly the decarburized layer is delineated by this method. However, although the principle of this method of measuring decarburization is quite simple, it is necessary that all heating and transformation temperatures be carefully controlled to get reliable results.

Summary

It has been shown that carbon, manganese, silicon, nickel, chromium, molybdenum and tungsten all tend to lower the Ms point of steel, the decrease in the Ms point being proportional to the amount of the element dissolved in the austenite. Of these elements, carbon has by far the greatest effect in depressing the Ms point, manganese, chromium, and nickel follow in that order, and silicon, molybdenum, and tungsten, are least effective, and are about equivalent in this respect. On the basis of experimental data, the following formula can be used for calculating Ms points of low alloy steels providing that the austenitizing temperatures used are sufficiently high to permit solution of all the carbides in the steel:

Ms in °F = 930—570C—60Mn—50Cr—30Ni—20Si—20Mo—20W.

Since the Ms temperature of a steel is very sensitive to its carbon content, the quench-temper procedure used for measuring the Ms temperature can also be used for establishing the depth of decarburization, or carburization, in steels. As an example, the application of this method to the measurement of decarburization in high speed steel has been shown.

Acknowledgments

The authors are grateful to the executives of Crucible Steel Co. of America for permission to present these data. Messrs. J. L. Klein, C. K. Baer, C. T. Roberts, F. Baureis, and G. Stefanelli all contributed to the preparation of this paper, and the authors are glad to acknowledge this aid from their colleagues at Eastern Research Laboratory. All induction melted ingots were made at Crescent Laboratory under the supervision of Mr. K. Metcalfe.

Bibliography

1. E. S. Davenport, "Isothermal Transformation in Steels," TRANSACTIONS, American Society for Metals, Vol. 27, 1939, p. 837-886.
2. R. M. Parke and A. J. Herzig, "Hardenability of Molybdenum S.A.E. Steels," *Metals and Alloys,* Vol. 11, p. 6-13.
3. J. R. Blanchard, R. M. Parke and A. J. Herzig, "The Effect of Molybdenum on the Isothermal Subcritical Transformation of Austenite in Low and Medium Carbon Steels," TRANSACTIONS, American Society for Metals, Vol. 29, 1941, p. 317-335.
4. J. R. Blanchard, R. M. Parke and A. J. Herzig, "The Effect of Molybdenum on the Isothermal Subcritical Transformation of Austenite in Eutectoid and Hypereutectoid Steels," TRANSACTIONS, American Society for Metals, Vol. 31, 1943, p. 849.
5. A. B. Greninger and A. R. Troiano, "Kinetics of the Austenite to Martensite Transformation in Steel," TRANSACTIONS, American Society for Metals, Vol. 28, 1940, p. 537-574.
6. A. B. Greninger, "The Martensite Thermal Arrest in Iron Carbon Alloys and Plain Carbon Steels," TRANSACTIONS, American Society for Metals, Vol. 30, 1942, p. 1-26.
7. R. A. Flinn, Earnshaw Cook and J. A. Fellows, "A Quantitative Study of Austenite Transformation," TRANSACTIONS, American Society for Metals, Vol. 31, 1943, p. 41-70.
8. Paul Gordon, Morris Cohen and Robert S. Rose, "The Kinetics of Austenite Decomposition in High Speed Steel," TRANSACTIONS, American Society for Metals, Vol. 31, 1943, p. 161-217.
9. P. Payson and J. L. Klein, "The Hardening of Tool Steels," TRANSACTIONS, American Society for Metals, Vol. 31, 1943, p. 218-256.
10. B. F. Shepherd, "Martempering," *Iron Age,* Vol. 151, Jan. 25, 1943.

DISCUSSION

Written Discussion: By H. H. Chiswik, research metallurgist, Battelle Memorial Institute, Columbus, Ohio.

On page 269, the authors state the Ms lines of Figs. 2 to 6 when extrapolated to 0 per cent of each element indicate the Ms temperature of a plain carbon steel of about 0.50 carbon to be 635 to 645 degrees Fahr. (335 to 340 degrees Cent.) and that this value is in good agreement with that reported by Greninger (Fig. 1). I should like to point out that the extrapolated value of the manganese curve to 0 per cent manganese (Fig. 2) should not correspond to the value reported by Greninger, 625 degrees Fahr. (330 degrees Cent.), since the latter dealt with a steel containing 0.42 to 0.62 per cent manganese. The extrapolated value of that curve should rather correspond to the Ms point of a nearly pure iron-carbon alloy containing 0.50 per cent carbon (the 0.26-0.34 per cent silicon may be disregarded, since its maximum effect, if any, on the Ms point can only be about 6 degrees Fahr. on the basis of the authors' work). The Ms point of a 0.50 per cent carbon pure iron-carbon alloy is reported by Greninger to be 690 degrees Fahr. (365 degrees Cent.) which is considerably higher than the extrapolated value 635 degrees Fahr. (335 degrees Cent.) obtained by the authors. The discrepancy becomes even greater when one considers the fact that the values plotted on the manganese curve (Fig. 2) are for carbon contents of 0.44-0.47 per cent rather than 0.50 per cent, in view of the considerable effect of carbon on the Ms point (6 degrees Fahr. per 0.01 per cent carbon).

A similar discrepancy exists in the extrapolated value of the nickel curve

(Fig. 3). When corrected to a 0.50 per cent carbon content, the nickel curve yields a value of 585 degrees Fahr. (307 degrees Cent.) for the Ms point of a steel containing 0.35 per cent manganese. Allowing 20 degrees Fahr. for the manganese content (on the basis of the authors' work, 1 per cent manganese depressed the Ms point 60 degrees Fahr.), a value of 605 degrees Fahr. (320 degrees Cent.) is obtained as the Ms point of a 0.50 per cent carbon pure iron-carbon alloy, as contrasted to Greninger's value of 690 degrees Fahr.

On the basis of the above, it appears that considerably more data would be necessary, especially in the low alloy content range (<1 per cent), before one could conclude that the effects of the alloying elements on the Ms points are purely algebraically additive, as suggested by the authors in their empirical formula on page 269. It may well be that at low alloy contents (<1 per cent) the Ms curves are not strictly linear. Furthermore, it would be well to emphasize that the formula suggested by the authors is definitely not applicable to steels with carbon contents above 0.80 per cent where the effect of carbon ceases to be linear.

Written Discussion: By B. F. Shepherd, chief metallurgist, Ingersoll-Rand Co., Phillipsburg, N. J.

The Society is again indebted to Mr. Payson and his associates for continuing their work on the formation of martensite.

Being interested in current specifications, I have used Mr. Payson's formula to plot the Ms points of a number of standard specifications, using the mean of

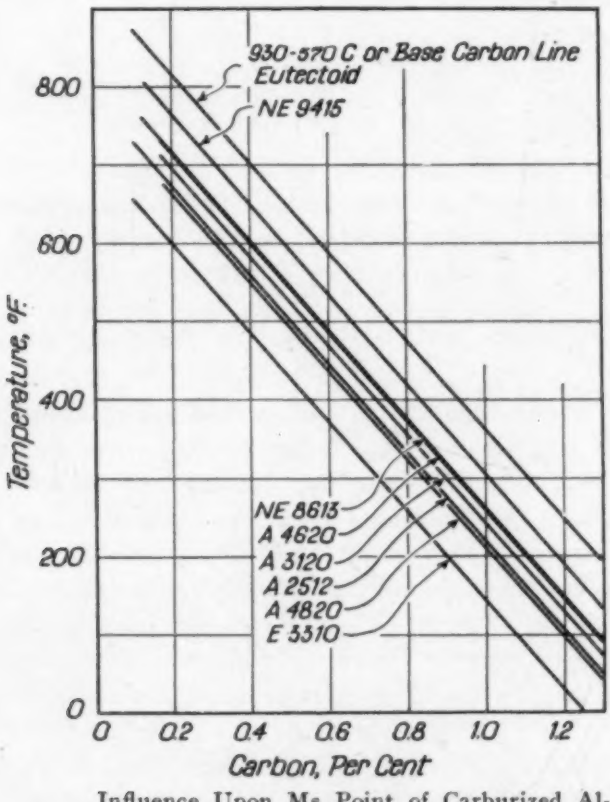

Influence Upon Ms Point of Carburized Alloy Steels Calculated on Mean of Specification According to Payson's Formula.

the specification analysis. The range of temperature is only 30 or 40 degrees from low of all elements to high of all elements.

Using a carburizing steel, we see the influence of carbon content as shown in the accompanying illustration. The authors have pointed out that the formula is good only when carbides are in solution and the lower portion of these curves should be blocked out below the percentage of carbide which is placed in solution at the commonly used hardening temperatures and soaking times.

The eutectoid for alloy steels is shifted to the left so that increasing percentages of alloy have more free carbide. It would be valuable to know just what the eutectoids are for the standard compositions.

Written Discussion: By Louis A. Carapella, Mellon Institute of Industrial Research, Pittsburgh.

The fact that the Ar" temperatures or Ms points of steels can be established from the chemical analysis alone is indeed useful for "Martempering" or other heat treatments where the knowledge of such a temperature is important. There-

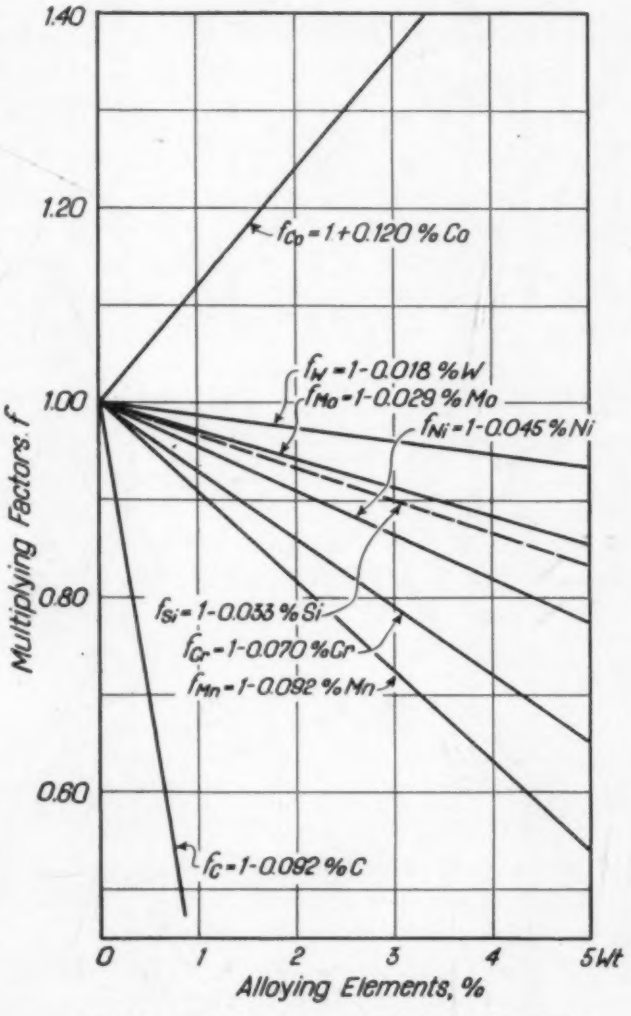

Multiplying Factors for Calculating Ms Points of Steels.

Table A

A Comparison of the Observed and Calculated Values of Ms Points for Both Methods

Steel No.	C	Mn	Si	Ni	Cr	Mo	Ms °F. obs.	Algebraic Method Ms calc.	Algebraic Method diff.	Multi. factor Method Ms calc.	Multi. factor Method diff.
4042	0.43	0.90	0.23	0.23	0.27	0.26	610	600	—10	600	—10
4063	0.64	0.85	0.29	0.19	0.24	0.27	445	490	+45	490	+45
8442	0.40	1.43	0.22	0.23	0.29	0.32	600	590	—10	580	—20
8949	0.49	1.01	0.20	0.54	0.56	0.38	535	530	— 5	535	0
8749	0.52	0.85	0.21	0.53	0.50	0.26	540	535	— 5	540	0
4142	0.41	0.86	0.30	0.11	1.06	0.23	590	575	—15	580	—10
4160	0.61	0.59	0.24	0.16	0.94	0.33	500	485	—15	500	0
4342	0.42	0.68	0.18	1.74	0.81	0.29	530	550	+20	545	+15
Special 3Ni-1Cr*	0.30	1.63	0.49	---	0.44	0.33	655	625	—30	610	—45
	0.46	0.30	0.28	3.36	0.99	---	500	495	— 5	500	0

*See Table I.

by eliminated is the laborious experimentation often required to determine this information. The authors, therefore, should be commended for this contribution.

It is of interest to bring out that a little better agreement may be obtained between the calculated and observed values of the Ms points by using the "multiplying-factor-principle" instead of the algebraic method given by the authors. This procedure is preferred by the writer because of the ease with which Ms points can be computed by a successive multiplication of factors with a slide rule.

In both methods, however, it is assumed that the influence of each element on the lowering or raising of the Ms points of steels is independent of the presence of others. Thus, shown in the accompanying figure are the factor-curves derived judiciously from the authors' data presented in Table I. The carbon factors, however, were computed from the data published by Greninger (6) (see Fig. 1), while the cobalt factors were derived from the recent work of Chiswik and Greninger.[1] By extrapolating the curve shown in Fig. 1 to 0 per cent carbon content, a value of about 925 degrees Fahr. (495 degrees Cent.) was obtained. Although the real physical significance of this temperature is unknown, it is useful as a "datum-temperature" upon which to base the computation of actual Ms points. This value is slightly lower than the one used by the authors. The multiplying-factor-principle may now be expressed as

$$M_s = 925 \times f_C \times f_{Mn} \times f_{Si} \times f_{Ni} \times \ldots\ldots \text{etc. (degrees Fahr.)}$$

A comparison of the observed and calculated values of Ms points for both methods is made in Table A. There is generally good agreement between the algebraic and multiplying-factor methods; the latter, however, does show a little better agreement with the observed values. Whenever the computed values of the Ms points are excessively lower than those observed, it may indicate inaccuracy or incompleteness of chemical analysis or both; whereas, higher values may suggest that the effectiveness of all elements is not being fully realized. Furthermore, the possibility of the presence of errors in observations must not be overlooked in this account.

Finally, this paper offers us some idea of the empirical nature of martensitic reactions in steels. More systematic work of this type should be undertaken in studying the influence of vanadium, titanium, columbium, copper, boron, aluminum, phosphorus, beryllium, and other elements in order to give us a more complete knowledge of martensitic reactions in alloy steels.

Authors' Closure

Mr. Chiswik very properly has pointed out that the manganese and nickel curves, Figs. 2 and 3, when extrapolated to 0 per cent of each element should not correspond to the value reported by Greninger for a 0.50 per cent carbon steel. It may be as Mr. Chiswik has indicated that other factors so far not considered account for the coincidence that the lines for each element as shown in Figs. 2 to 6 actually do intersect the temperature axis at approximately the same value. In regard to Mr. Chiswik's reference to the formula on page 269, the authors did not

[1]H. H. Chiswik and A. B. Greninger, "Influence of Nickel, Molybdenum, Cobalt and Silicon on the Kinetics and Ar" Temperatures of the Austenite to Martensite Transformation in Steels," TRANSACTIONS, American Society for Metals, Vol. 32, 1944, p. 483.

intend to imply that the formula should be used in place of actual determinations of Ms points. A formula of this kind is useful only to approximate the values, and not to measure them. In the authors' laboratory Ms determinations are still being carried out and these determinations practically always check the formula. For those who do not find it convenient to measure Ms values, the formula should be reasonably helpful. Among the papers presented at this meeting there are two determinations of Ms values which serve further to check the validity of the formula. In the paper by Cruciger and Vilella[2] the measured value of Ms for the case of the carburized 4815 steel is given at 200 to 205 degrees Fahr.—the calculated value is 240 degrees Fahr. (115 degrees Cent.). In the paper by Chiswik and Greninger[3] the measured value for the commercial 2345 steel is about 520 degrees Fahr. (270 degrees Cent.)—the calculated value is 530 degrees Fahr. (276 degrees Cent.).

Mr. Shepherd's curves are welcome additions to the paper. By means of these curves it should be possible to estimate from Ms determinations the carbon content in the carburized portions of these steels, as well as the depth of case.

Mr. Carapella's multiplying-factor formula provides those who are interested in calculating Ms values another method of getting these results, which is perhaps better than the algebraic method of the authors.

The authors have already tried to supply some of the data on martensitic reactions for which Mr. Carapella asks in the last paragraph of his discussion. It was found that vanadium carbides in steels of about 0.50 per cent carbon did not dissolve completely even at 2350 degrees Fahr. (1290 degrees Cent.), and that in low carbon-low vanadium steels the bainite reactions interfered with the determination of the Ms point by metallographic methods. Apparently the effect of vanadium on the Ms point is going to be difficult to establish. About 0.5 per cent copper depresses the Ms temperature only slightly. Both cobalt and aluminum were found to raise the Ms temperature as has been reported by Chiswik and Greninger[3] and by Zyuzin, Sadovski, and Baranchuk[4]. The present authors found that 0.4 per cent aluminum lowered the Ms slightly while 1.45 per cent aluminum definitely raised it. The additional data on Cu, Co and Al are as follows:

Type	C	Mn	Si	Addition	Aust. Temp. °F.	Ms °F.
0.50 Cu	0.45	0.35	0.29	0.56 Cu	1700	620
0.90 C	0.90	0.32	0.38	---	1700	425
1.40 Co	0.88	0.33	0.36	1.39 Co	1700	460
0.40 Al	0.88	0.34	0.41	0.40 Al	1700	420
1.45 Al	0.87	0.33	0.38	1.45 Al	1700	470

[2]J. R. Cruciger and J. R. Vilella, "The Isothermal Transformation of Case-Carburized S.A.E. 4815," TRANSACTIONS, American Society for Metals, Vol. 32, 1944, p. 195.

[3]H. H. Chiswick and A. B. Greninger, "Influence of Nickel, Molybdenum, Cobalt and Silicon on the Kinetics and Ar" Temperatures of the Austenite to Martensite Transformation in Steels," TRANSACTIONS, American Society for Metals, Vol. 32, 1944, p. 483.

[4]V. Zyuzin, V. Sadovski and S. Baranchuk, "Influence of Alloy Elements on Position of Martensite Point, Quantity of Retained Austenite, and Stability of Retained Austenite During Tempering," *Metallurg*, Vol. 14, 1939, p. 75-80.

AN X-RAY STUDY OF THE TIME-RATE OF PRECIPITATION FROM A SOLID SOLUTION OF COPPER IN ALUMINUM

By Charles H. Townes

Abstract

The age hardening of aluminum-copper alloys has been studied by many investigators using density, elastic limit, elongation, hardness, electrical conductivity, and lattice parameters. Results are summarized elsewhere.[1] *The present work (using balanced filters and Geiger-Müller counters) shows the time rate of change of the diffracting powers of the atomic planes of the aluminum-copper solid solution and of its decomposition products (Θ′ and Θ). Prestrained 25S alloy was heated for 24 hours at 540 degrees Cent. (1005 degrees Fahr.) (to dissolve all the copper in the aluminum) and then water-quenched at 20 degrees Cent. The copper was then allowed to migrate at 309 degrees Cent. (590 degrees Fahr.). It was found that: (a) In the aluminum "solid solution" phase the diffracting power of the (111) planes decreased to a constant value in 120 hours; the (100), (110), and (311) planes showed a decreased diffracting power followed by a considerable increase. (b) The (112) (2) plane of Θ decreased to a constant diffracting power in 120 hours. (c) The (001) (3), (101) (2), (112), (110) (2), and (211) planes of Θ increased in diffracting power to a constant value in approximately 120 hours. Definite interpretations of the above are offered.*

PRECIPITATION from a binary (or even ternary) solid solution has been studied for many years by many investigators using many methods[1]. We may use the aluminum-copper system as a typical example. It appears that the precipitation of an aluminum-copper intermetallic compound from a solid solution of copper in aluminum, takes place in two steps. The first step yields a tetragonal material, called Θ′, considered by metallurgists to be an allotropic

From a thesis submitted to the Physics Department of the Graduate School of The Pennsylvania State College in partial fulfillment of the requirements for the degree of Doctor of Philosophy.

[1] "Age Hardening of Metals," published by the American Society for Metals, 1940.

The author, Charles H. Townes, is associated with the department of physics, Virginia State College, Ettrick, Va. Manuscript received June 7, 1943.

form of $CuAl_2$, whose lattice constants are, a_o=8.20, b_o=11.6 Å, A=a/b=0.71. This material is supposed to change into a second tetragonal material, called Θ ($CuAl_2$), whose lattice constants are, a_o=6.04 Å, b_o=4.86 Å, A=a/b=1.24. It is the purpose of the present investigation to add to the above a rather detailed knowledge of the time-rate of growth of individual crystallographic planes in the precipitate ($CuAl_2$). This was made possible by the use of Geiger-Müller quantum counters to measure the intensities of X-ray beams diffracted by the precipitate.

Apparatus, Material and Technique

A molybdenum target Coolidge (G. E. X-ray Corp.) tube was operated at 25 ma., 42 $Kv_{(max.)}$ with balanced ZrO_2 and $SrCO_3$ (Patterson Screen Co.) filters. The filters contained respectively 0.072 gram Zr and 0.138 gram Sr per square centimeter. Three lead slit systems, each 0.01 inch wide and 0.75 inch high and 6 inches long, were mounted on a Spencer Lens Co. (No. 818) spectrometer. One of these was the customary collimating slit system; a second system, mounted on the swinging arm, was used in the usual way to measure the angle of diffraction for various diffracted beams; the third was mounted rigidly to admit the beam from the (311) planes of the solid solution of copper in aluminum. The beam passed by this third slit system served, therefore, as a standard or pilot to indicate that all operating conditions were constant while readings were being taken on the beams passed by the second slit system. The (311) planes of the solid solution were chosen merely because the intensity was high and the angle was large enough to avoid contact with the slit system on the swinging arm.

The two Geiger-Müller quantum counters were of the argon-oxygen type. Each was provided with its own high voltage supply and with its own amplifying and pulse-leveling circuit, etc. These circuits were of the usual type, such as have become semi-standard in this laboratory. Counts were made on Cenco impulse counters (Central Scientific Co. No. 73511). A mercury switch taped to the handle of a Cenco interval timer (No. 73405) was inserted in series with the impulse counter so that all data were taken over 5 ± 0.02 minute intervals. Experience has shown that over this time interval the counts on the third (stationary) counter were substantially uniform.

The electric furnace used for heating the specimens was operated on a constant voltage circuit so that it was easy to maintain a substantially constant temperature. Temperatures were measured by a chromel-alumel thermocouple.

Specimens for examination were cut from a sheet of 25S alloy kindly furnished by Drs. R. F. Mehl and C. S. Barrett. The composition of 25S is given (Metals Handbook) as 4.5 per cent copper, 0.8 per cent manganese, 0.8 per cent silicon, balance aluminum. The presence of these elements and the substantial absence of others was confirmed by the spectroscope. The strips cut from the original sheet were pulled through a die-plate to give cylindrical wires, 0.043 inch in diameter. The wires were then heated in the air in the furnace at 540 degrees Cent. (1005 degrees Fahr.) for 24 hours, in order to put all the copper in solid solution in the aluminum, and were then quenched in water at 20 degrees Cent.[2]

They were then polished on fine emery cloth to remove traces of oxide. Then they were put back in the furnace at 309 degrees Cent. in order to facilitate the migration of copper in the aluminum, and were kept at that temperature except when under examination. Each time the wires were taken out of the furnace, they were quenched in water at 20 degrees Cent. No evidence of oxidation could be found in these quenched specimens. Time of aging was reckoned from the time of first insertion into the furnace at 309 degrees Cent. and included all the time at 309 degrees Cent. (590 degrees Fahr.). Time at 20 degrees Cent. was not counted as part of the aging time. In many cases, the examination with the Geiger-Müller counter was paralleled by an exposure of a duplicate specimen on another X-ray outfit, using a photographic film. In some cases, further checks were made with a microscope at $\times$ 100, since the precipitate was indicated by brown patches. All specimens were given identical time-temperature histories. The time required for the complete examination at 20 degrees Cent. varied from 90 to 270 minutes.

Experimental Results

The Geiger-Müller counter proved to be more sensitive than the photographic film, since it often indicated clearly the presence of

[2] A.S.M. Metals Handbook, 1939 edition, p. 1222 shows that at 4 per cent copper, 96 per cent aluminum, 540 degrees Cent. lies in the solid solution range and that this range is very narrow. The present work seems to show that small amounts of manganese and silicon do not alter this diagram greatly since the approximate temperature limits for 25 S turned out to be 505 and 550 degrees Cent. (940 and 1020 degrees Fahr.).

lines which could not be seen with certainty above the background on the film. The time history of a typical specimen is shown in Figs. 1, 2, and 3.

In all cases, the ordinate is expressed in terms of quantum counts per minute, i.e., one fifth of the counts made during the standard 5-minute counting period.

The diffraction pattern of the (224) planes of the Θ' phase could be found easily by photographic means at heating times (309 degrees Cent.) between 20 and 60 minutes with an apparent maximum intensity at about 60 minutes, but the line could not be found photographically if the time were increased to 9 hours. This line could, however, be detected easily by the quantum counter for heating times up to 280 hours—long after the Θ phase had become constant. No other lines of the Θ' phase could be found, indicating perhaps that the particle size was small or that the Θ' phase was oriented within rather narrow limits.

Discussion of Results

It is to be assumed, of course, that the presence of copper in solid solution in the aluminum will tend to produce distortions in the crystals of aluminum. In a cubic crystal these distortions should "average out" so that the crystals of the solid solution should still be cubic, but with a lattice parameter somewhat different from that of the Al. Migration of copper in the solid solution must result in the formation of nuclei of an intermetallic compound, Θ' (considered by metallurgists to be $CuAl_2$). Succeeding atoms of copper will find it more difficult to migrate away from these nuclei than to migrate in the free solid solution. This should tend to produce an enormous number of nuclei of Θ' scattered pretty uniformly throughout the aluminum. It is to be expected, therefore, that the atomic planes of the solid solution should become very badly distorted during the first part of the "aging" at 309 degrees Cent. (590 degrees Fahr.), and that therefore their diffracting power should decrease markedly. Fig. 1 shows that, for all four crystallographic planes of the solid solution that were investigated, this was indeed the case.

It has been assumed above that the growth of nuclei of Θ' is due, not to a unidirectional flow of copper toward the nuclei, but only to the fact that there is less chance for flow of individual atoms

of copper away from the nuclei. The larger the nuclei the more stable they must become, and this leads at once to the conclusion that the large nuclei must grow at the expense of the smaller nuclei. If we once grant this, it is evident that, except in the immediate neighborhood of the segregations of the precipitate, the distortions

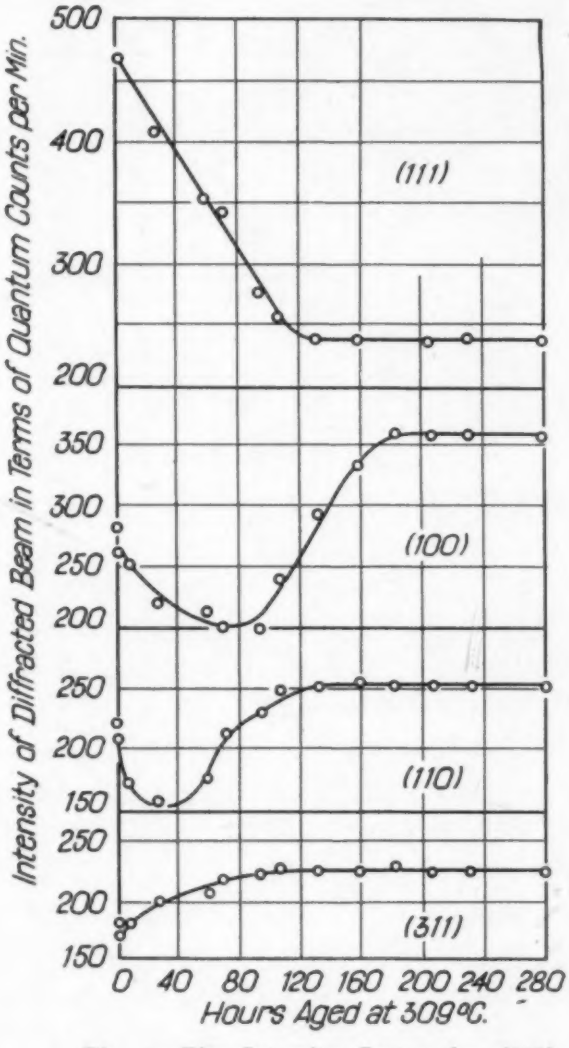

Fig. 1—Time-Intensity Curves for (111), (100), (110), and (311) Planes of the Solid Solution of Copper in Aluminum.

of the aluminum lattice must become less and less until eventually, when practically all the copper has been converted into precipitate, the diffraction power of the aluminum lattice must become nearly normal. We may expect, therefore, that some one or more planes of the aluminum lattice (which will be the planes along which the precipitate forms) will continue to show impaired diffracting power, while the rest of the planes will show a recovery or even a final

increase in diffracting power. Examination of Fig. 1 shows that this is the case, for the (111) planes (with the biggest interplanar spacing in the whole aluminum lattice, and therefore the planes along which a precipitate might be expected to segregate), show a constantly decreasing diffracting power for about 120 hours, after which the diffracting power remains constant. Fig. 1 shows also that all the

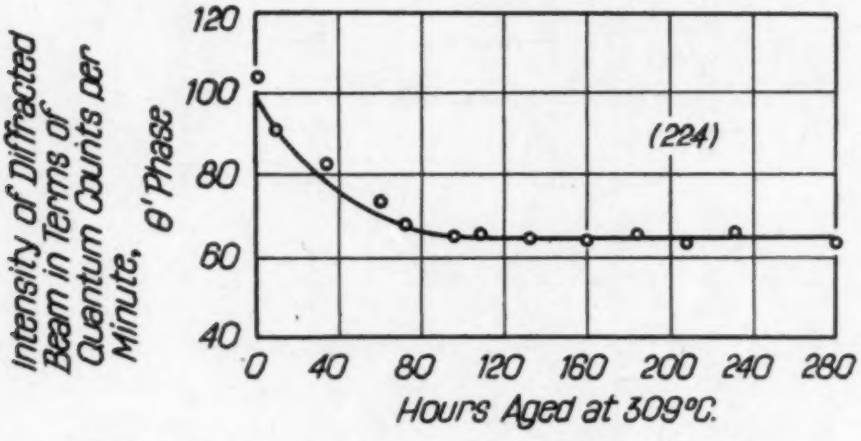

Fig. 2—Time-Intensity Curves for (224) Planes of the Θ′ Phase.

other planes of the aluminum investigated showed a decrease in diffracting power followed by a substantial rise. In the case of the (110) and (100) planes the final diffracting power became considerably more than at the beginning.

Fig. 2 shows that only one plane of Θ′, (224), could be found to diffract X-rays and that its diffracting power was weak in comparison with that of the planes of the Θ phase. This may mean that the amount of Θ′ was small, or that its particle size was very small, or that the range of orientation of most of its crystals was not favorable. The data from Fig. 2 do not enable us to decide between these alternatives. The data from Fig. 2 are, however, of peculiar interest because of the fact that a small portion of the Θ′ is shown to persist at 309 degrees Cent. (590 degrees Fahr.) for at least 280 hours.

Fig. 3 shows diffraction from the (211), (220), (112), (310), (202) and (003) planes of the Θ phase. No diffraction could be found for (110) and (200) of Θ, which are the two larger interplanar spacings which can be calculated for the unit prism of Θ. The planes found represent consecutive spacings in the tetragonal crystals of Θ. Obviously, there is no zone axis common to all these planes, and we must assume, therefore, that they have a substantially

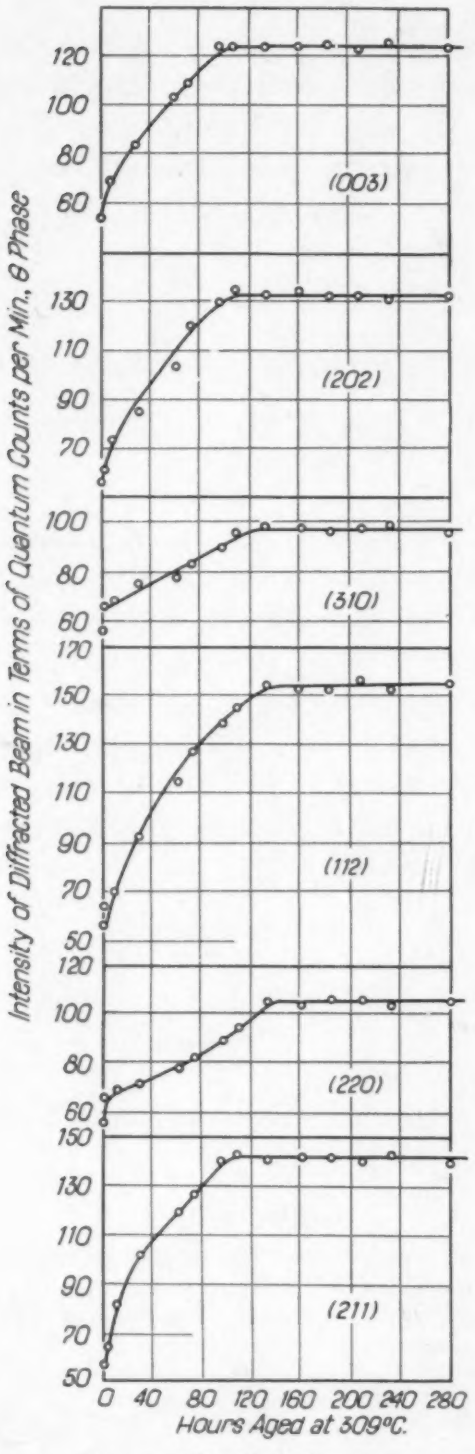

Fig. 3—Time-Intensity Curves for (211), (220), (112), (310), (202), (003) Planes of the θ Phase.

random orientation. This makes it easy to assume that diffracting power is, to some extent at least, a measure of the amount of mate-

rial present. With this assumption, Fig. 3 can be interpreted as showing that the Θ phase of the precipitate did not exist at the moment the specimens were first put in the furnace at 309 degrees Cent. (590 degrees Fahr.), but that it commenced to form at once at that temperature, and reached a maximum, stable, amount in about 100 hours. But this is the length of time required for Θ' to reach its minimum, stable amount.

The following picture, then, predicts the experimental facts as stated above.

1. In a specimen of 25S alloy, precipitation from a solid solution of copper in aluminum forms a crystalline material (called by metallurgists Θ'), until an *equilibrium* is reached between the solid solution and Θ'.

2. The Θ' phase changes quickly to a compound having randomly oriented tetragonal crystals (called by metallurgists Θ), until an equilibrium is reached. At 309 degrees Cent. (590 degrees Fahr.) equilibrium is reached in about 100 hours.

3. The 25S alloy, completely aged at 309 degrees Cent. (590 degrees Fahr.), consists of three phases, (a) solid solution, (b) the Θ' phase, (c) the Θ phase, all in equilibrium with each other.

4. The Θ phase crystallizes in such a manner as to distort the (111) planes of the solid solution.

ACKOWLEDGMENT

I wish to express my gratitude and thanks to Dr. Wheeler P. Davey for his direction and interest during the course of this work.

It is a pleasure to express my thanks to the General Education Board and to the Rosenwald Foundation for fellowships which made it possible to undertake this work.

Bibliography

1. Dix and Richardson, *Transactions,* American Institute of Mining and Metallurgical Engineers, Vol. 13, 1926, p. 560.
2. Gwyer, Phillips and Mann, *Journal,* Institute of Metals, Vol. 40, 1928, p. 297.
3. R. F. Mehl, *Transactions,* American Institute of Mining and Metallurgical Engineers, Vol. 76, 1928, p. 405.
4. Goler and Sachs, *Metallwirtschaft,* Vol. 8, 1929, p. 671.
5. Gayler and Preston, *Journal,* Institute of Metals, Vol. 41, 1929, p. 191.
6. G. Wassermann, *Zeit. Metallk.,* Vol. 22, 1930, p. 160.
7. Dix, Sager and Sager, *Transactions,* American Institute of Mining and Metallurgical Engineers, Vol. 99, 1932, p. 119.
8. Gayler and Preston, *Journal,* Institute of Metals, Vol. 48, 1932, p. 197.
9. Philip and Brick, *Journal,* Franklin Institute, Vol. 215, 1933, p. 557.
10. Schmid and Siebel, *Zeit. Phys.,* Vol. 85, 1933, p. 36.

11. P. Wiest, *Zeit. Phys.,* Vol. 81, 1933, p. 121.
12. Phillip and Brick, *Transactions,* American Institute of Mining and Metallurgical Engineers, Vol. 111, 1934, p. 94.
13. E. Schoenchen, *Metallwirtschaft,* Vol. 13, 1934, p. 665.
14. P. Wiest, *Zeit. Phys.,* Vol. 74, 1934, p. 225.
15. Wiest and Dehlinger, *Zeit. Metallk.,* Vol. 26, 1934, p. 150.
16. Becker and Döring, *Ann. Phys.,* Vol. 24, 1935, p. 719.
17. Fink and Smith, *Mining and Metallurgy,* 1935, p. 228.
18. Fink and Smith, *Mining and Metallurgy,* 1935, p. 513.
19. Mehl and Smith, *Transactions,* American Institute of Mining and Metallurgical Engineers, Vol. 116, 1935, p. 330.
20. E. Schoenchen, *Metallwirtschaft,* Vol. 14, 1935, p. 205.
21. O. Stranski, *Zeit. Physik,* Vol. 36, 1935, p. 393.
22. Wassermann and Weerts, *Metallwirtschaft,* Vol. 14, 1935, p. 605.
23. Fink and Smith, *Transactions,* American Institute of Mining and Metallurgical Engineers, Vol. 122, 1936, p. 284.
24. Fink and Smith, *Mining and Metallurgy,* 1936, p. 101.
25. R. F. Mehl, *Transactions,* American Institute of Mining and Metallurgical Engineers, Vol. 122, 1936, p. 11.
26. R. Becker, *Zeit. Metallk.,* Vol. 29, 1937, p. 245.
27. R. Becker, *Metallwirtschaft,* Vol. 16, 1937, p. 573.
28. M. Gayler, *Journal,* Institute of Metals, Vol. 60, 1937, p. 249.
29. Fink and Smith, *Transactions,* American Institute of Mining and Metallurgical Engineers, Vol. 124, 1937, p. 162.
30. R. Becker, *Ann. Phys.,* Vol. 32, 1938, p. 128.
31. Fink and Smith, *Transactions,* American Institute of Mining and Metallurgical Engineers, Vol. 128, 1938, p. 223.
32. Fink and Smith, *Transactions,* American Institute of Mining and Metallurgical Engineers, Vol. 128, 1938, p. 244.
33. Mehl and Rhines, *Transactions,* American Institute of Mining and Metallurgical Engineers, Vol. 128, 1938, p. 185.
34. G. Preston, *Phil. Mag.,* Vol. 26, 1938, p. 855.
35. G. Preston, *Proceedings,* Royal Society, Vol. A167, 1938, p. 526.
36. G. Wasserman, *Zeit. Metallk.,* Vol. 30, 1938, p. 62.
37. Calvet, Jacquet and Guinier, *Journal,* Institute of Metals, Vol. 55, 1939, p. 121.
38. M. Cohen, *Transactions,* American Institute of Mining and Metallurgical Engineers, Vol. 133, 1939, p. 95.
39. W. L. Fink, D. W. Smith and L. A. Willey, Age Hardening of Metals Symposium, published by American Society for Metals, 1940, p. 31.
40. Gordon and Cohen, Age Hardening of Metals Symposium, published by American Society for Metals, 1940, p. 161.
41. H. Y. Hunsicker, Age Hardening of Metals Symposium, published by American Society for Metals, 1940, p. 56.
42. L. W. Kempf, Age Hardening of Metals Symposium, published by American Society for Metals, 1940, p. 8.
43. R. F. Mehl and L. K. Jetter, Age Hardening of Metals Symposium, published by American Society for Metals, 1940, p. 342.
44. W. P. Skyes, Age Hardening of Metals Symposium, published by American Society for Metals, 1940, p. 82.
45. Fink and Smith, *Transactions,* American Institute of Mining and Metallurgical Engineers, Vol. 137, 1940, p. 102.
46. Fink and Smith, *Transactions,* American Institute of Mining and Metallurgical Engineers, Vol. 137, 1940, p. 110.
47. C. Samanars, *Transactions,* American Institute of Mining and Metallurgical Engineers, Vol. 137, 1940, p. 85.
48. Barrett, Geisler and Mehl, *Nature,* Vol. 143, 1941, p. 134.
49. W. L. Fink, *Journal of Applied Phys.,* Vol. 13, 1942, p. 75.
50. Evans, *Review of Scientific Instruments,* Vol. 5, 1934, p. 359.

BRIGHT GAS QUENCHING OF S.A.E. X-4130 AND NE 8630 WELDED AIRCRAFT TUBES

By Wm. Lehrer

Abstract

The physical properties stipulated by the AN-T-3 specifications for normalized S.A.E. X-4130 welded aircraft tubing are secured in large production furnaces by bright gas quenching in a superfast cooling zone which is located immediately adjacent to the heating zone. The paper gives a brief description of the evolution of the gas quenching zone and of its construction and discusses in detail the results obtained with it.

The attainment of the desired physical properties is controlled by the rate of quenching gas recirculation, by the conveyor speed and by the temperature from which the tubes are gas-quenched. The adjustment of these variables is governed primarily by the carbon content of the steel and by the tube wall thickness. The effect of the various factors involved is shown by a number of figures and tables.

The physical properties are further improved by following the gas quenching with an accelerated aging treatment. The results produced by gas quenching S.A.E. X-4130 steel are applicable to NE 8630 steel.

DURING normal peace times and up to May 1940, the production of airplanes in the U.S.A. was such that all steel tubing required in their construction could be supplied by the Seamless Tube Industry. Because the German Blitzkriegs in Poland and in the Low Countries of Europe had demonstrated the tremendous importance of the airplane in modern warfare, the President of the United States on May 28, 1940, asked Congress in his National Defense Program for 50,000 planes a year. This seemingly impossible increase in the rate of aircraft production taxed the Seamless Steel Tube Industry beyond its maximum production facilities. The Welded Tube Industry stepped into the picture and in a relatively short time succeeded in eliminating this threatening bottleneck in aircraft production.

A paper presented before the Twenty-fifth Annual Convention of the Society, held in Chicago, October 18 to 22, 1943. The author, Wm. Lehrer, is associated with the Development Department, Surface Combustion Co., Toledo, Ohio. Manuscript received June 19, 1943.

Structural Aircraft Steels

Steel tubing is one of the principal materials from which the main structural members of airplanes such as fuselage structures, wing beams, engine mounts, etc., are fabricated. Since lightness is a primary requirement in airplane construction, the tubing is made of high quality steels and is invariably heat treated to develop high physical properties. The common aircraft tubing steels are S.A.E. 1025, X-4130, X-4135, X-4340, X-6150, and of late NE 8630. Of these, X-4130 or NE 8630 is by far the most widely employed steel. Better than 90 per cent of the aircraft tubing structures consist of S.A.E. X-4130 steel which is processed by the tube mills in rounds, ovals, streamlined, square and rectangular shapes.

AN-T-3 Specifications

The Army-Navy specifications for aeronautical chrome-molybdenum (X-4130) welded steel tubing are covered in detail by the AN-T-3 specifications. They list the following requirements:

Table I
Chemical Composition

Steel No.	Carbon	Manganese	Phosphorus (Max.)	Sulphur (Max.)	Chromium	Molybdenum
	Per Cent					
X4130	0.25-0.35	0.40-0.60	0.040	0.050	0.80-1.10	0.15-0.25

"After the last forming operation, the tubing shall be normalized, stress relieved, or otherwise heat treated to develop the physical properties specified in Table II."

Fundamental Principles

Although main consideration will be given in this paper to bright gas quenching of welded S.A.E. X-4130 aircraft tubing, a brief outline of the essential fundamental principles and of the evolution of the gas quenching apparatus appears advisable.

Normalizing of X-4130 Tubing

As disclosed by Table II, the AN-T-3 specifications for normalized X-4130 welded aircraft tubing are:

Table II
Physical Properties

Condition and Wall Thickness Inch	Tensile Strength (Min.) Lb. Per Sq.In.	Yield Strength at 0.2 Per Cent Set or at Extension Indicated (Min.) Lb. Per Sq. In.	Extension Under Load Inch in 2 Inches	Elongation in 2 Inches Full Tube (Min.) Per Cent	Elongation in 2 Inches Strip (Min.) Per Cent
(A) All sizes	95,000*	.....	.....	..	.
(N)					
Up to 0.035 incl.	95,000	75,000	0.0090	10	5
Over 0.035 to 0.188 incl.	95,000	75,000	0.0090	12	7
Over 0.188	90,000	70,000	0.0087	15	10
(HT-125)					
All Walls	125,000	100,000	0.0107	12	7
(HT-150)					
All Walls	150,000	135,000	0.0130	10	6
(HT-180)					
All Walls	180,000	165,000	0.0154	8	5
(HT-200)					
All Walls	200,000	165,000	0.0154	7	4

*Maximum.

Minimum Yield Strength—75,000 pounds per square inch measured at 0.009 inch extension in 2 inches.

Minimum Tensile Strength—95,000 pounds per square inch.

Minimum Elongation in 2 inches—10 to 12 per cent on the full tube, 5 to 7 per cent on the strip.

"Normalizing is generally defined (1)[1] as a heat treatment, comprising heating iron-base alloys to approximately 100 degrees Fahr. above the critical temperature range followed by cooling to below that range in still air at ordinary temperature."

Cooling in Still Air

It is quite probable that the foregoing heat treatment will produce the above physical properties on most heats of X-4130 steel as long as single tubes are handled or as long as the heat treating operation is carried out on a small scale.

Extensive determinations made on large production continuous heat treating furnaces, however, have disclosed that the normalizing treatment executed in accordance with the above definition produces the specified physical properties only in few specific instances. The carbon content of the steel must be on the high side of the allowable carbon range and even then only thin wall tubing responds to cooling

[1]The figures appearing in parentheses refer to the bibliography appended to this paper.

in still air. Furthermore, the production rate of the furnace has to be greatly reduced by suitable spacing of the tubes on the furnace conveyor and by adequate conveyor speeds so as to prevent an excessive temperature rise of the air surrounding the tubes and thus a retardation of the rate of cooling to a detrimental degree.

Forced Cooling

For the average carbon analysis and for the average tube sizes and wall thicknesses, however, cooling in still air is inadequate for producing the physical properties specified for normalized S.A.E. X-4130 aircraft tubing. The rate of cooling must be considerably faster and can be secured only by forced cooling in a continuous stream of cold gases so arranged that the gases being heated by the immediate contact with the hot steel are constantly replaced by a fresh supply of cold gases.

Cooling Medium

It is well known that a scaled surface of the work to be cooled or quenched reduces the rate at which heat can be removed from the steel by a cooling medium; that is, it decreases the rate of cooling and thus affects the physical properties. A scaled surface is conducive also to nonuniformity of the metallurgical results obtained in cooling or quenching. Obviously cooling in still air produces scale and consequently does not facilitate the attainment of the best possible physical properties.

The use of air as the cooling medium has another disadvantage. The rate of cooling of metals is to an appreciable extent dependent upon the heat capacity of the quenching medium applied (2). Air having a specific heat of 0.2374 is a comparatively slow cooling medium, particularly if the cooling process is carried out in still air.

A marked improvement of the cooling rate and of the resultant physical properties of steel is obtained by the application of a bright annealing gas in place of air. Such a gas eliminates any scale or oxide film on the surface of the steel to be treated not only during the rapid cooling cycle but also during the much longer heating and soaking periods at elevated temperatures. The most frequently encountered bright annealing gas which is produced by the partial combustion of a fuel gas and which contains approximately 5.0 per

cent CO_2, 10 per cent CO, 12 per cent H_2 and a moisture content equivalent to a 40 degrees Fahr. dew point has the added advantage that its heat capacity is 13 per cent higher than that of air, its specific heat being 0.2686. Besides promoting a faster rate of cooling for the two reasons just outlined, the use of a bright annealing gas results in considerable saving of time, labor and material because no removal of scale is required subsequent to the heat treating operation.

It is obvious, therefore, that a bright annealing gas as a cooling medium is superior to air.

The utilization of a nonoxidizing gas as the cooling medium necessitates special precautions in the construction of the fast cooling chamber and in the handling of the gaseous cooling medium.

Evolution of Gas Quenching Apparatus

The heat treating furnace most prevalent in the steel tube mill is the continuous roller hearth bright annealing furnace, since the roller hearth is ideally suited for continuously conveying elongated material such as tubes through the heating and cooling chambers. The heating zone of these furnaces varies in length from 17 to 60 feet and in width from 3.5 to 6 feet, depending on the desired hourly rate of production. Their capacities range from 2500 pounds per hour to 15,000 pounds per hour for the average tube sizes handled. The work is invariably heated by heating elements located above and below the roller hearth line. Because of the application of a bright annealing atmosphere, the furnaces are equipped with a slow cooling chamber, the length of which falls within a range of from 1.25 to 2 times the length of the heating zone and is governed by the number of accelerated cooling zone sections employed to bring the overall length of the furnace within the limits of floor space available in the tube mill.

Fast Cooling Zone for Seamless Aircraft Tubes

The fast cooling zone used for rapid cooling of the tubes is located immediately adjacent to the discharge end of the heating zone and forms one continuous work chamber with the heating zone on its work entering side and with the slow cooling zone on its discharge side. This general arrangement is illustrated by Fig. 1. The same protective atmosphere is maintained throughout the entire length of

the furnace. Whereas the work in the heating zone and in the slow cooling zone is surrounded by the protective gases in an almost quiescent condition, the gases in the fast cooling zone are forced against and around the work at accelerated velocities. The gases are withdrawn from the bottom of the zone and are pulled over a suitable water-cooled coil by means of a fan which delivers the cooled gases under pressure to a large plenum chamber located above the work. From the plenum chamber the gases are discharged onto the work and, having absorbed their quota of heat from the hot work, are

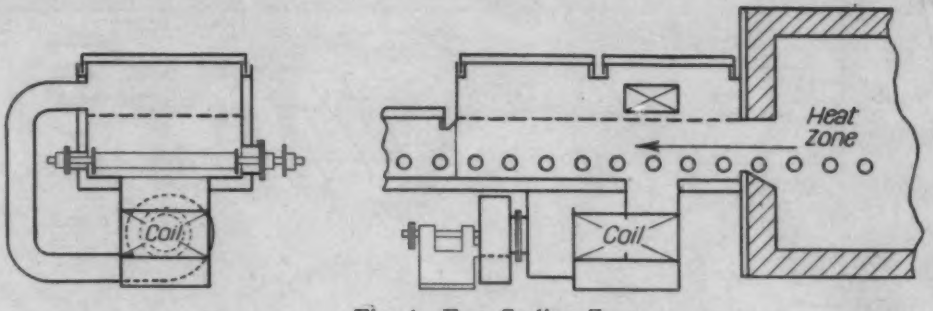

Fig. 1—Fast Cooling Zone.

again removed from the work cooling chamber, are cooled and returned to the plenum chamber. The atmosphere gases are thus being recirculated over the work to be cooled in a single pass arrangement. Since, as is well known, the enclosures separating the protective atmosphere from the ambient room atmosphere must be gas-tight in any controlled atmosphere furnace, it is obvious that, in view of the sub-atmospheric pressures created at the suction side of the recirculating fan, particular care must be exercised in making the fast cooling zone 100 per cent gas-tight.

Performance of Fast Cooling Zone on Seamless Aircraft Tubes

Fast cooling zones of this type have been used in conjunction with continuous roller hearth furnaces for several years and on seamless S.A.E. X-4130 aircraft tubing have produced satisfactory physical properties as specified for normalized tubing. Two precautions were essential. First, the tubes had to be spaced on the conveyor so as to allow the recirculated cold gases to pass between the tubes and to completely envelop each individual tube. Secondly, the carbon content of the steel had to be on the high side of the permissible carbon range, that is, above 0.30 carbon.

A typical heating and cooling cycle obtained with this type of fast cooling zone is presented by the normalizing curve shown in Fig. 2.

Physical properties produced on S.A.E. X-4130 seamless tubes by these rates of fast cooling are listed in Table III.

The results obviously better the minimum requirements for normalized S.A.E. X-4130 seamless tubes by a good margin; they are, however, being secured only with a considerable sacrifice in production and economy. The necessary spacing of the tubes on the con-

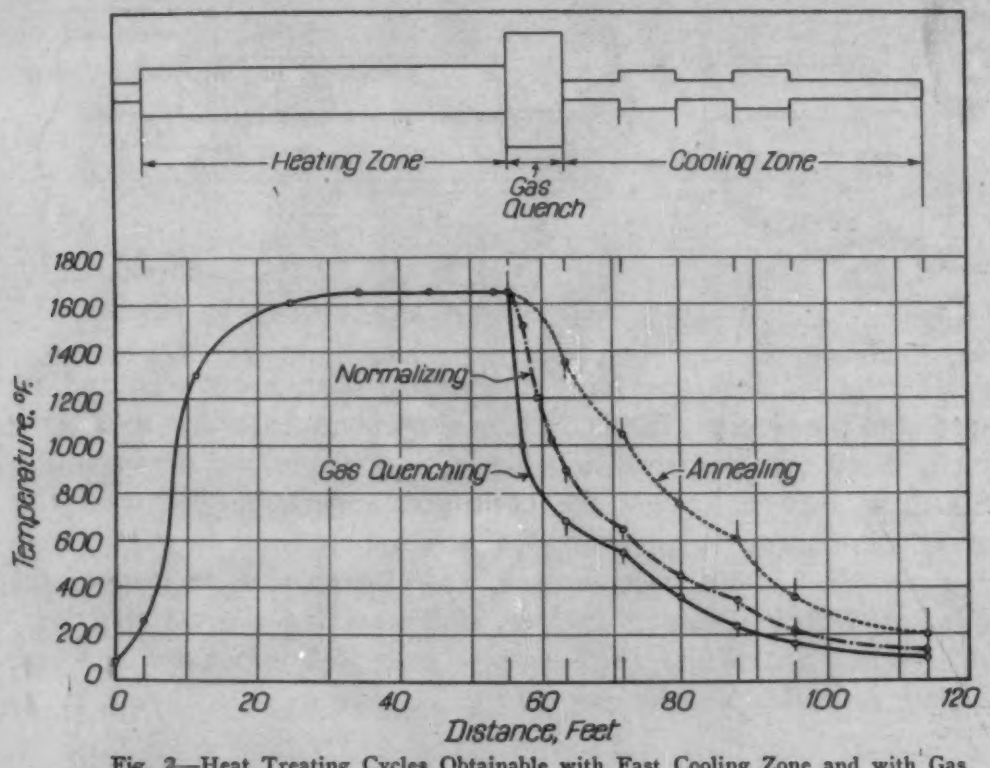

Fig. 2—Heat Treating Cycles Obtainable with Fast Cooling Zone and with Gas Quenching Zone.

veyor reduces the hourly rate of production for normalizing to approximately 50 per cent of that obtainable when operating the furnace on annealing in which case the conveyor hearth is fully loaded. Greater care and additional labor are required in spacing the tubes. Furthermore, it was in most instances found advantageous to fast cool from 1700 degrees Fahr. (925 degrees Cent.) instead of 1650 degrees Fahr. (900 degrees Cent.) which lowers the efficiency of heating to some degree as well as contributes to a shortening of the life of the heat-resisting alloy employed in the heating zone.

Table III
Physical Properties of Seamless S.A.E. X-4130 Normalized Tubes

Tube Size	Yield Strength P.S.I.	Tensile Strength P.S.I.	Elongation Per Cent
½" O.D. x 20 ga.	88,800	119,200	19.5
¾" O.D. x 20 ga.	95,300	116,500	19.5
1⅛" O.D. x 18 ga.	94,800	121,800	20.3
1½" O.D. x 17 ga.	99,600	121,700	18.7
1" O.D. x 11 ga.	89,700	107,800	24.2

In any event, the fast cooling zone just described has successfully met the normalizing requirements for S.A.E. X-4130 seamless aircraft tubing.

Super-Fast Cooling Zone for Welded Aircraft Tubes

The heat treatment of welded S.A.E. X-4130 aircraft tubing had presented a more difficult problem.

Welded tubes are produced from a flat-rolled steel strip formed by a series of rolls into a practically perfect cylinder the seam of which is joined by a continuous welding process. It is a well-established fact that the welding difficulties increase with progressively higher carbon contents of the steel and that alloy steels such as the chromium-molybdenum series further complicate the welding operation (3). In order to assure a soundly welded seam, the carbon content of the steel used for welded X-4130 aircraft tubing is, therefore, normally held on the low side of the permissible carbon range, that is, 0.30 per cent carbon or lower.

The lower carbon content, on the other hand, makes it harder to secure the desired physical properties by heat treatment. Furthermore, the degree of cold working which invariably increases the tensile properties is in the case of welded tubes negligible compared to seamless drawn tubes. The cooling rates produced by the fast cooling zone and giving satisfactory physical properties on seamless S.A.E. X-4130 aircraft tubing were found to be entirely too slow for welded tubing. It became necessary to resort to still faster rates of cooling of the heated tubes, the cooling rates being more in the nature of a quench.

Description of Apparatus

The desired result was accomplished in the super-fast cooling zone which is shown in Fig. 3. For the sake of ready comparison

the same scale applies to Fig. 3 as to Fig. 1. The super-fast cooling zone is again placed immediately adjacent to the discharge end of the heating zone but blasts the tubes, as they leave the heating chamber, from both top and bottom by large volumes of cold gases issuing from a series of high velocity gas nozzles. The arrangement of the gas nozzles, which are located above and below the work and which extend the full width of the hearth, necessitates a withdrawal of the gases from the cooling chamber through a series of outlet openings provided on both sides of the chamber and also placed above and

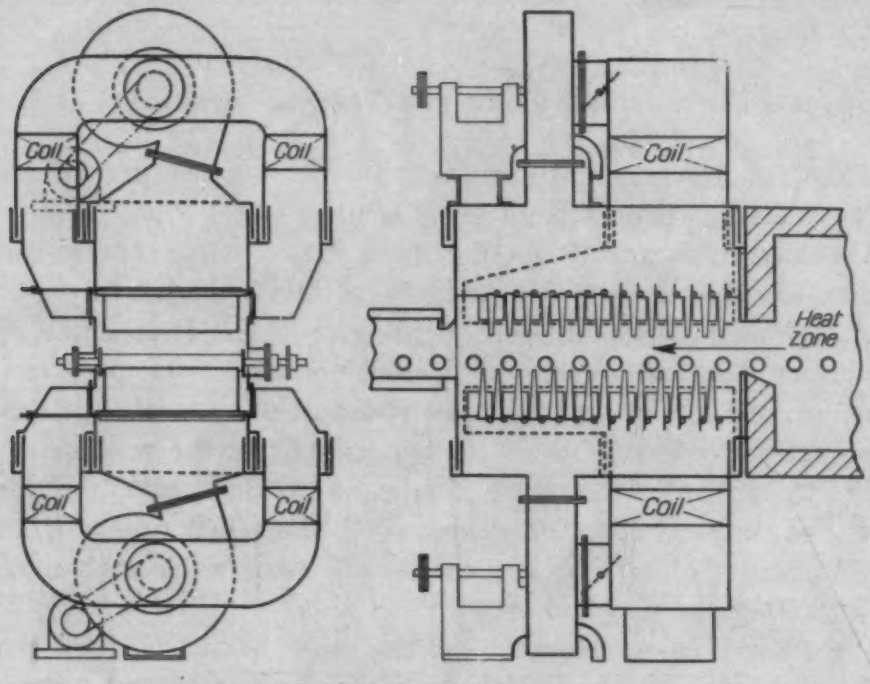

Fig. 3—Gas Quenching Zone.

below the hearth line. Having absorbed heat from the hot work, the gases are cooled by pulling them over four water cooled coils by means of two large recirculating fans which then deliver the cold gases back to the high velocity discharge gas nozzles. The side outlet openings as well as the gas nozzles are equipped with individual dampers which facilitates any desired concentration and distribution of the recirculated gases in the 8-foot total length of the super-fast cooling zone.

The gas recirculating system consists of two separate units—one being placed above the work and the other one below the work. The construction of each unit is such that the fan suction ducts, dis-

charge ducts and cooling coils can readily be removed as one complete assembly for any necessary repairs. The joints between the removable assemblies and the stationary middle portion of the cooling chamber are made gas-tight by the use of suitable liquid seals.

Gas Recirculating Capacity

The combined gas recirculating capacity of both fans is more than 10 times that of the fast cooling zone applied for normalizing seamless aircraft tubing.

The three identical furnaces, in which the gas quenching results presented in this paper were secured and which have a heating zone 4 feet wide by 50 feet long, are each provided with a maximum gas recirculating capacity of 22,000 cubic feet per minute.

The resultant high rate of heat removal is obviously due to the rapid circulation of the relatively cool gas. The two most vital requirements for quick gas cooling are met, and the most rapid gas quenching rates are thus made possible.

Gas Quenching Replaces Normalizing

For the reasons just disclosed the term "Normalizing" no longer is applicable in the heat treatment of welded S.A.E. X-4130 aircraft tubing but has been replaced by "Gas Quenching". Since the gas quenching medium produces a bright surface of the quenched work, the new heat treatment is commonly referred to a "Bright Gas Quenching". The super-fast cooling zone section in which the drastic cooling is performed is known as the "Gas Quenching Zone".[2]

Flexibility of Gas Quenching Zone

Before going into the details of the physical properties secured by bright gas quenching S.A.E. X-4130 welded aircraft tubing, a few words appear appropriate concerning the flexibility of the gas quenching apparatus.

A very desirable feature of any heat treating furnace is its adaptability to various heat treating cycles. The continuous roller hearth furnace employed in the tube mill covers a wide range of

[2]The gas quenching furnaces described above are commercially available and are being built by the company with which the author is associated.

operating temperatures from a minimum of 800 degrees Fahr. (425 degrees Cent.) to a maximum of 1800 degrees Fahr. (980 degrees Cent.). Thus, the same furnace is used for tempering, stress relieving, sub-critical annealing, full annealing, normalizing and gas quenching. To maintain the high standard of this universal tube mill furnace, the control of the heating had to be matched by an equally flexible control of the cooling rates.

For this reason two master dampers are placed in the main path of the recirculated gases, one damper in the top system and the second one in the bottom system. They allow a ready adjustment of the volume of the recirculated gases to suit the different heat treatments to be performed. It will be shown in a later section that a control of the rate of gas recirculation is necessary also in gas quenching tubes of varying sizes and wall thicknesses.

The difference in the rate of cooling obtained is illustrated by Fig. 2.

With the dampers in the closed position the rate of cooling is sufficiently slow to produce a full anneal as is shown by Table IV.

Table IV
Softness of Various Annealed Steels in Terms of Rockwell B Scale
Annealing Temperature: 1550 Degrees Fahr.

Type of Steel	S.A.E. 1010	S.A.E. 1020	S.A.E. 1025
Rockwell Before Annealing	78–84	76–80	76–78
Rockwell After Annealing	48–51	60–63	71–73
Rockwell Specifications for Annealed Tubes	45–55	65–75	70–80

Tensile tests were made on the S.A.E. 1025 steel tubes only with the following results:

Yield Strength:	44,000 to 47,000 pounds per square inch
Ultimate Tensile Strength:	64,000 to 68,000 pounds per square inch
Elongation:	35.5 to 37.5 per cent

The physical properties secured with the dampers in a partly open or in a fully open position are given in the following sections.

Performance of Gas Quenching Zone

The AN-T-3 specifications for "normalized" X-4130 welded aircraft tubing are readily met by bright gas quenching. The attainment of the desired results is not hampered by special precautions in tending the furnace. The conveyor is fully loaded across its width

and length. The conveyor speeds for the different tube sizes are at least equal to and in many instances faster than the speeds required for annealing.

In the furnace equipped with the small fast cooling zone, the work has to be run through the furnace at reduced speeds to allow adequate cooling time. Therefore, the hourly production rate of the furnace when operating on normalizing is limited by the cooling capacity of the fast cooling zone. The gas quenching zone having a tremendous cooling capacity has completely eliminated any production restrictions from this source. The tubes are conveyed through the furnace at approximately twice the speed formerly possible with the small fast cooling zone. The increased conveyor speed and the above mentioned full loading of the conveyor account for the high rates of production obtained when bright gas quenching.

Production Limitations

However, there are three noteworthy limitations.

1. *Soaking Time*—The first one concerns the heating operation. Compared to seamless drawn tubes, welded tubes have very little cold working prior to the final heat treatment. Consequently, a longer soaking period has to be allowed in the heating zone (4). As a rule, about one-third of the length of the heating zone is utilized for soaking whenever the furnace is operating on a gas quenching cycle.

2. *Quenching Time*—Secondly, the time in the gas quench is as important as the time at maximum heat treating temperature. Certain fundamental principles underlie all forced cooling. Heat can be removed from a solid object only by dissipation from its surface. By maintaining the surface at substantially the same temperature as the cooling medium, the cooling time is reduced to a minimum; the rate of cooling then depends entirely on the thermal conductivity of the metal to be cooled. It is obvious, then, that the time in the quench must be sufficiently long to allow the heat from the center of the object to flow to the cooled surface and that the quenching time is a function of the thickness of the object (5).

3. *Loading of Tubes*—Finally in order to secure uniform results, the tubes must be loaded on the conveyor in a single layer. This method of loading is conducive to uniformity not only in quenching but also in heating; it is for this reason desirable for all various heat treating operations performed in the furnace.

Rate of Gas Quenching

In spite of the above precautions, the gas quenching zone of a 4-foot effective width is capable of bright gas quenching at a continuous rate 4500 to 5000 pounds per hour of X-4130 welded aircraft tubing from 1650 degrees Fahr. (900 degrees Cent.) to black heat in less than 1 minute. The actual quenching time depends on the rate of gas recirculation and on the conveyor speed which in turn is governed by the tube size and wall thickness. Tubes having a wall thickness of 0.049 inch are gas-quenched from 1650 degrees Fahr. (900 degrees Cent.) to black heat in 30 seconds. Lighter gage tubes require a shorter quenching time and heavier gage tubes a longer quenching time.

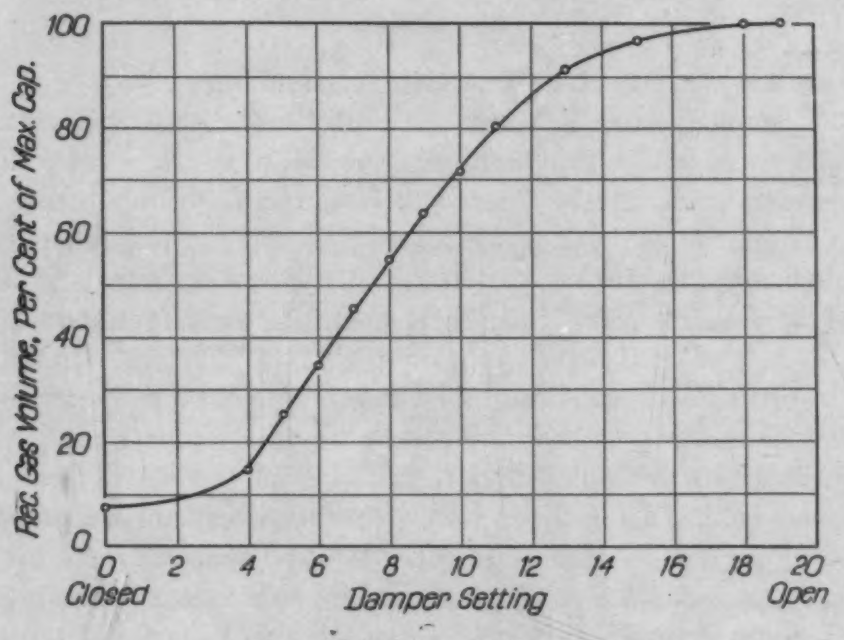

Fig. 4—Calibration of Main Dampers.

Discussion of Results

The following sections deal with the results obtained by gas quenching and with the effect of the various factors involved on the physical properties of S.A.E. X-4130 welded tubes. These factors are rate of gas recirculation, conveyor speed, temperature and carbon content of the steel.

Rate of Gas Recirculation

As mentioned above, master dampers are provided in the two gas recirculating systems for adjusting the rate of gas recirculation. The volume of recirculated gases can thus be varied at will and since the port area of the high velocity gas discharge nozzles is fixed after some preliminary tests, the velocity of the gases striking the work is adjustable.

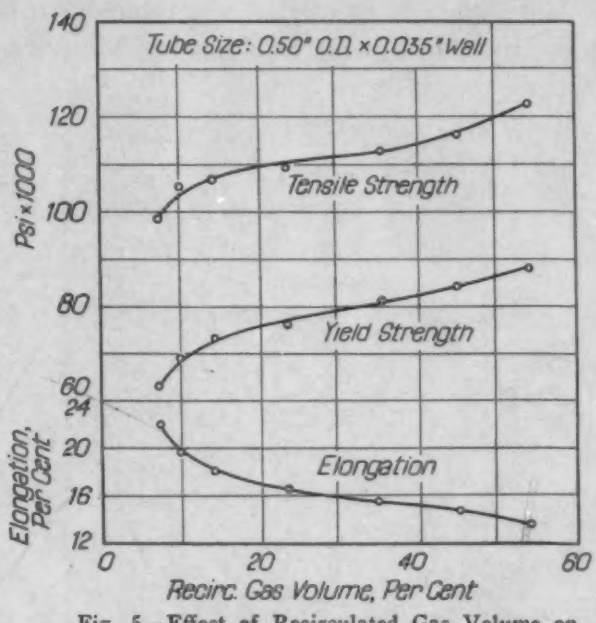

Fig. 5—Effect of Recirculated Gas Volume on Physical Properties of S.A.E. X 4130 Steel Tubes. Carbon Content of Steel 0.29 Per Cent. Conveyor Speed Constant 6 Feet Per Minute. Gas Quench Furnace Temperature 1650 Degrees Fahr.

1. Calibration of Master Dampers—It is, of course, extremely important that the arrangement of the dampers is practicable for duplication of exactly the same damper settings in order to assure reproduction of the same physical properties of the work treated. The use of damper quadrants which are divided into a number of equal spaces and which are equipped with suitable locking devices readily facilitates such duplication of results. The calibration of the damper quadrants is presented by Fig. 4 which discloses the change of the recirculated gas volume, given in per cent of the maximum provided capacity, for various damper settings. The figure shows that with the dampers in the closed position a small volume of gases is still being recirculated which is due to intentional leakage around the dampers and which is necessary for preventing the structural

members of the gas quenching zone from becoming damaged by overheating at any time. This leakage is not of such magnitude that it impairs the desired softness of the tubes when operating the furnace on an annealing cycle, as is proven by the Rockwell readings listed in Table IV.

2. *Individual Dampers*—The individual dampers provided for each gas inlet nozzle and for each gas outlet port are not being utilized for varying the recirculated gas volumes or the gas velocities. Although some beneficial effect might be gained by their adjustment for different tube sizes and wall thicknesses, simplicity of furnace

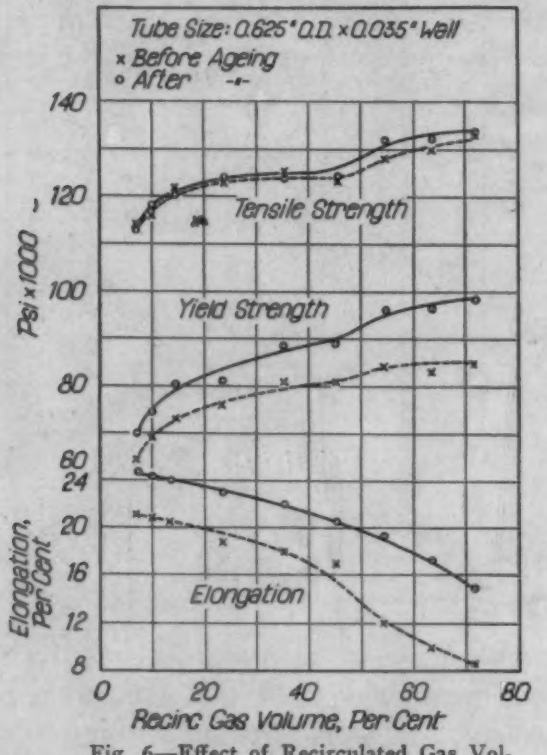

Fig. 6—Effect of Recirculated Gas Volume on Physical Properties of S.A.E. X 4130 Steel Tubes. Carbon Content of Steel 0.29 Per Cent. Conveyor Speed Constant 6 Feet Per Minute. Gas Quench Furnace Temperature 1650 Degrees Fahr.; Aging Furnace Temperature 600 Degrees Fahr.

operation has dictated a fixed setting of these individual dampers. They are essential nevertheless for proper balancing the atmosphere within the furnace and with respect to the ambient room atmosphere. By a series of preliminary tests and by actual operating experience it has been found that an optimum average operating condition suitable for all tube sizes run through the furnace is secured by concentrating

the entire gas recirculation over the first half of the gas quenching zone immediately adjacent to the heating zone.

3. Effect of Gas Recirculation Rate on Physical Properties— The two factors controlling the necessary adjustment of the rate of the recirculated gas flow appear self-explanatory. First, the higher the physical properties desired, the faster has to be the cooling rate; that is, the dampers must be opened to allow a greater volume of recirculated gases. The effect of the rate of the gas recirculation on the physical properties of welded X-4130 aircraft tubes is illus-

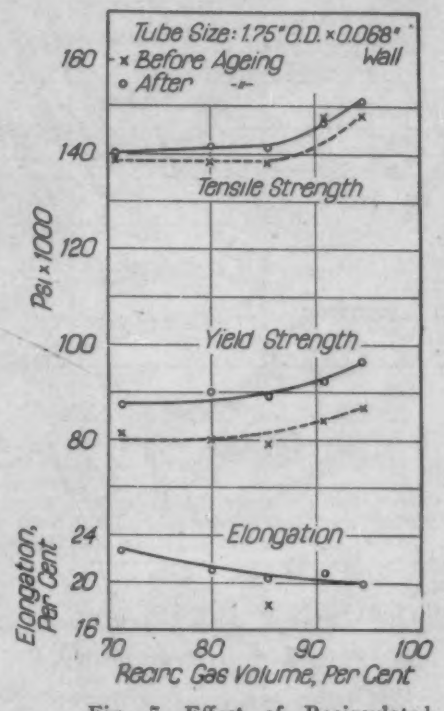

Fig. 7—Effect of Recirculated Gas Volume on Physical Properties of S.A.E. X 4130 Steel Tubes. Carbon Content of Steel 0.35 Per Cent. Conveyor Speed Constant 3 Feet Per Minute. Gas Quenching Furnace Temperature 1700 Degrees Fahr.; Aging Furnace Temperature 600 Degrees Fahr.

trated by Figs. 5, 6, 7 and 8. All four figures which present the results of tests conducted on four different tube sizes under actual production conditions disclose the same general pattern; the yield strength and the tensile strength rise and the elongation decreases with increasing rates of gas recirculation. The specified minimum physical properties are exceeded by a safe margin which obviously is desirable from the standpoint of production since some variations

are to be expected due to unavoidable differences in the analysis of the various heats of steel obtained from the steel mill.

4. Recirculating Gas Volume Requirements for Various Tube Wall Thicknesses—A comparison of the four Figs. 5, 6, 7 and 8 discloses also the differences in the range of the recirculated gas

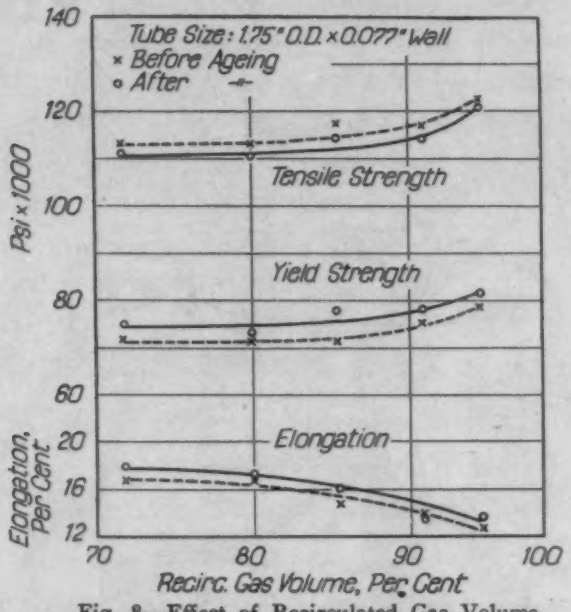

Fig. 8—Effect of Recirculated Gas Volume on Physical Properties of S.A.E. X 4130 Steel Tubes. Carbon Content of Steel 0.29 Per Cent. Conveyor Speed Constant 2.5 Feet Per Minute. Gas Quench Furnace Temperature 1700 Degrees Fahr.; Aging Furnace Temperature 600 Degrees Fahr.

volumes required for the various wall thicknesses of the tubes. This is the second vital consideration in the control of the rate of gas recirculation. Very thin tube walls cool rapidly by radiation alone since the entire enclosure of the gas quenching zone is substantially at room temperature (6). As the tube wall becomes heavier, more forced cooling by means of a cooling medium has to be applied. Figs. 5 and 6 show, for instance, that on 0.035-inch tube wall the desired physical properties are secured with less than 50 per cent of the total available gas recirculation capacity, whereas a 0.068-inch wall thickness (Fig. 7) requires about 75 per cent of the maximum recirculating capacity and still heavier tubes a correspondingly higher recirculation.

The physical properties produced on tubes of different wall thickness by a constant rate of gas recirculation are illustrated by Fig. 9. In order to obtain the same physical properties on all tube

wall thicknesses, it is obviously necessary to increase the gas recirculation for the heavier walls.

The rates of gas recirculation normally applied in actual production to the various tube wall thicknesses are plotted on Fig. 10 which clearly shows the requirements in this respect.

Conveyor Speed

Of equal importance in the attainment of the physical properties is the length of time the tubes remain in the gas quenching zone.

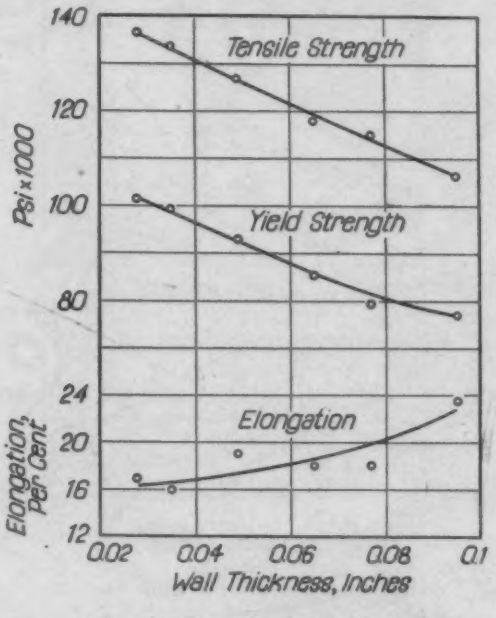

Fig. 9—Change of Physical Properties of S.A.E. X 4130 Steel Tubes of Various Wall Thicknesses for Constant Gas Recirculation. Rate of Gas Recirculation 70 Per Cent of Maximum Available Capacity.

Since tubes of any particular size travel through the continuous furnace at a constant rate, the time in the gas quench is governed by the conveyor speed.

1. Conveyor Speed Proportional to Tube Wall Thickness—It has already been pointed out that even though the surface of the tubes is cooled to substantially the same temperature as the gas quenching medium which is made possible by the high rates of gas recirculation, the tubes must be held in the blast of cold gases sufficiently long to permit the heat from the center of the tube to be conducted to the chilled surface. The quenching time, that is, the

conveyor speed, is, consequently, dependent on the wall thickness of the tube.

2. Thermal Conductivity of Tubes—The thermal conductivity of the metal plays a significant part in the continuous bright gas quenching of tubes for another reason also. As the tubes leave the heating zone and enter the gas quenching zone, the leading end of the

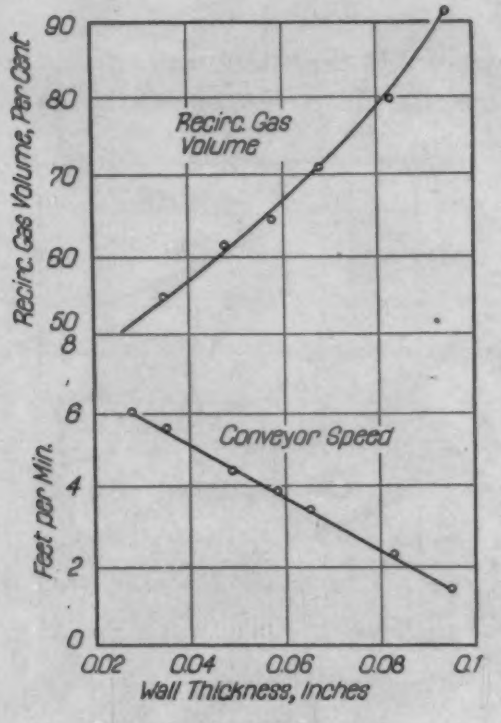

Fig. 10—Normal Rates of Gas Recirculation and Normal Conveyor Speeds for Various Tube Wall Thicknesses.

tube is cooled while the trailing end is still at maximum furnace temperature. There is, therefore, a considerable flow of heat by conductivity from the hot portion of the tube to the cooled portion. It is apparent that the heavier the tube wall, the more heat is conducted lengthwise to the tube.

3. Limitation of Conveyor Speeds—The conveyor speeds employed in the test runs which are presented by Figs. 5, 6, 7 and 8 are given in the respective titles. For the sake of convenience, the conveyor speeds normally used in actual production are shown graphically in Fig. 10. As can be seen, the conveyor speed is a straight line function of the tube wall thickness, the highest speeds being applicable to the lightest tube walls. Faster speeds than those shown

in Fig. 10 are possible by increasing the rates of gas recirculation; however, conveyor speeds in excess of 6 feet per minute were found to be impractical because of the difficulties experienced in keeping the conveyor loaded, particularly when handling small diameter tubes or tubes of short length.

The effect of the conveyor speed on the physical properties of two welded X-4130 welded tubes of heavy wall thickness under constant gas recirculating conditions are plotted in Fig. 11. The curves indicate that higher yield and tensile strengths could have been ob-

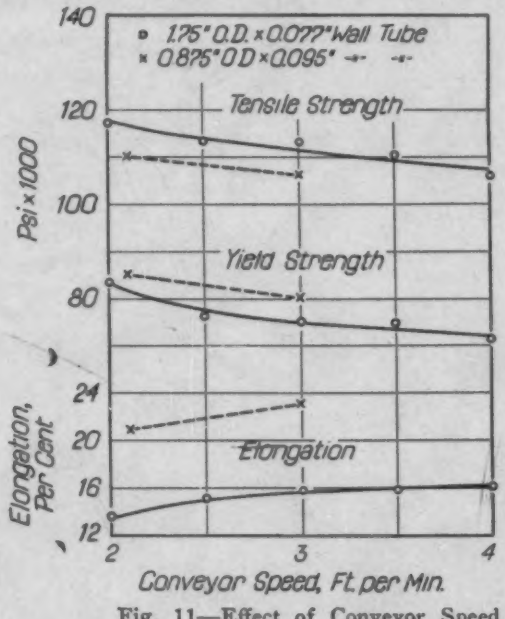

Fig. 11—Effect of Conveyor Speed on Physical Properties of S.A.E. X 4130 Steel Tubes. Rate of Gas Recirculation Constant 80 Per Cent of Maximum Available Capacity.

tained at conveyor speeds slower than 2 feet per minute which was the lowest speed possible at the time the tests were conducted.

Temperature of Gas Quenching Furnace

For gas quenching, welded S.A.E. X-4130 tubes are as a general rule heated and soaked in the heating chamber at a temperature of 1650 degrees Fahr. (900 degrees Cent.). This temperature is adequate for producing the desired physical properties on the most common welded tube sizes which range from ⅜ to 2 inches in diameter and from No. 22 gage (0.028 inch) to No. 16 gage (0.065 inch) in wall thickness.

1. 1700 Degrees Fahr. for Heavy Wall Tubes—For heavier wall tubes, on the other hand, it was found advantageous and in some cases even necessary to heat the tubes to 1700 degrees Fahr. (925 degrees Cent.). The reason for this higher temperature becomes apparent when giving consideration to the following conditions existing in the furnace.

The gas quenching zone is of necessity placed immediately adjacent to the discharge end of the heating zone. Since the gas quenching zone is at substantially room temperature and since a definite minimum opening is required between the heating chamber

Table V

Physical Properties Obtained at 1650 and at 1700 Degrees Fahr. Furnace Temperature

Furnace Temp. Degrees Fahr.	Tube Size O.D. x Wall	Conveyor Speed Ft. Per Min.	Yield Strength P.S.I.	Tensile Strength P.S.I.	Elongation Per Cent
1650	1¾" x 0.077"	2.5	70,000	110,000	18.0*
1700	1¾" x 0.077"	2.5	77,900	113,900	13.3*
1650	1¾" x 0.077"	2.0	76,200	112,000	14.8*
1700	1¾" x 0.077"	2.0	83,000	121,200	11.5*
1650	⅞" x 0.095"	3.0	74,400	103,300	23.0†
1700	⅞" x 0.095"	3.0	79,500	109,700	21.5†
1650	⅞" x 0.095"	2.0	76,100	105,000	22.6†
1700	⅞" x 0.095"	2.0	84,800	107,200	21.0†

*Tested on Strip
†Tested on Full Tube.

and the quenching chamber so as to facilitate the continuous travel of the tubes through the furnace, a considerable portion of heat is lost by radiation from the discharge end of the heating zone. This obviously results in an unavoidable temperature drop or gradient in the last few feet of the heating zone.

In order to offset as much as possible the heat loss at this vital point in the furnace, additional heating elements are being utilized and a refractory-lined door is provided for separating the heating zone from the quenching zone. The door opening is adjustable so as to reduce to a minimum the height of the opening and thus the heat loss by radiation.

As has been outlined in the last section, the conveyor speed has to be lowered for heavier wall tubes. The reduction of the conveyor speed reaches a point where the tubes cool slowly in the discharge end of the heating zone and, before reaching the blast of cold gases, may drop to a temperature too low for proper quenching. These adverse temperature conditions are overcome by raising the furnace

temperature to 1700 degrees Fahr. (925 degrees Cent.) or even somewhat higher, if necessary.

2. 1650 Degrees Fahr. for Medium and Light Gage Tubes—When gas quenching light and medium wall welded tubes, the conveyor speed is sufficiently fast to prevent the tube temperature from dropping to a detrimental degree before the tubes are struck by and quenched by the cold recirculated gases. As a matter of fact, it has been observed that the fast traveling medium and light gage tubes actually aid in maintaining the desired 1650 degrees Fahr. tempera-

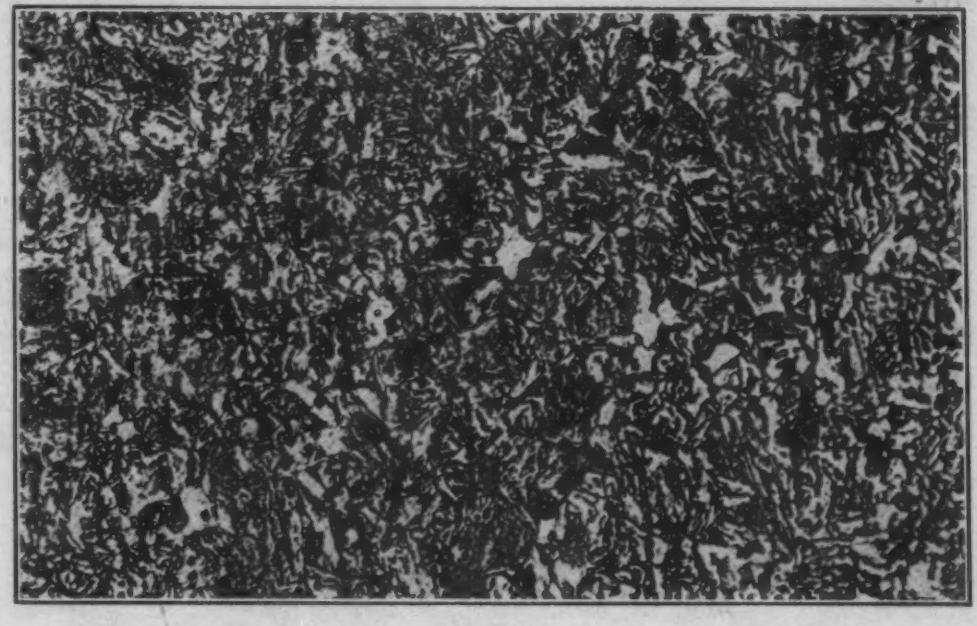

Fig. 12—Structure of Gas Quenched S.A.E. X 4130 Steel Tube of 0.29 Per Cent Carbon Content. × 500.

ture at the discharge end of the furnace. The tubes are, therefore, gas-quenched from the proper temperature and the specified physical properties are secured without any difficulties.

The results obtained on two heavy wall tube sizes before and after raising the furnace temperature from 1650 to 1700 degrees Fahr. (900 to 925 degrees Cent.) are listed in Table V.

Carbon Content of X-4130 Steel

The three preceding sections dealt with the outstanding factors in the operation of the furnace which have a decided influence on the physical results produced. The most vital single factor control-

ling the physical properties of the tubes unquestionably is the composition of the steel itself used in making the tubes and, in this respect, the carbon content of the steel is of prime importance.

Table I shows the permissible carbon range of S.A.E. X-4130 steel which varies from 0.25 to 0.35 per cent carbon. It has already been pointed out that with the carbon content on the low side the attainment of the specified physical properties is more difficult whereas steels in the upper carbon range are heat treated with comparative ease. The effect of the carbon content on the weldability of the

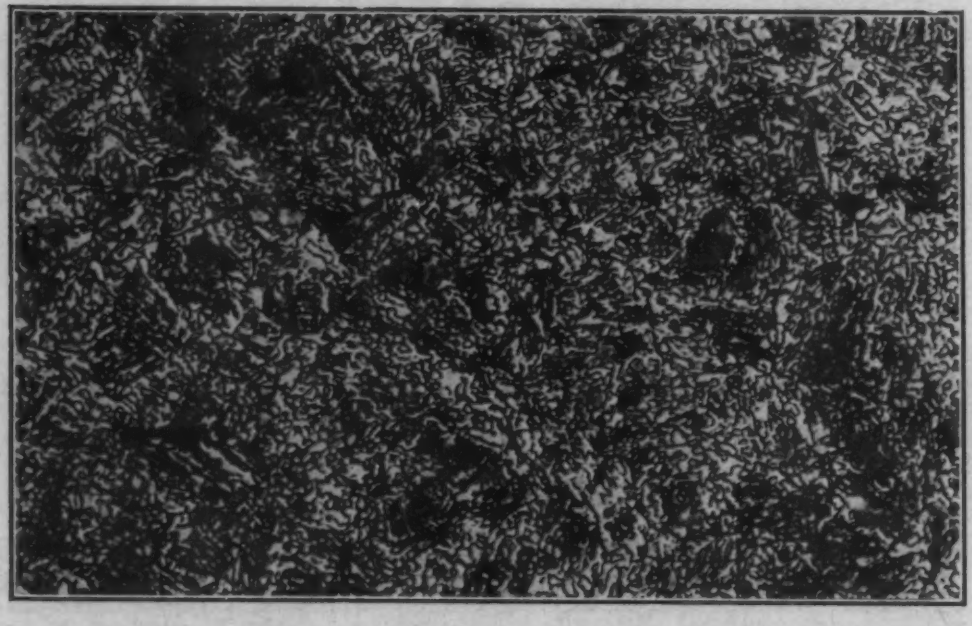

Fig. 13—Structure of Gas-Quenched S.A.E. X 4130 Steel Tube of 0.35 Per Cent Carbon Content. × 500.

steel, on the other hand, has been mentioned also in an earlier section. As a general rule, welded S.A.E. X-4130 aircraft tubes are produced from steels having an average carbon content of between 0.28 to 0.30 per cent. Most of the test results presented in this paper on physical properties as well as the furnace operating data concerning rates of gas recirculation, conveyor speed and temperature hold good for these carbon percentages.

Some modifications are being introduced, however, by carbon contents deviating from the above percentages. Fig. 7, for instance, shows the physical properties obtained on a 0.35 carbon steel. The high yield and tensile strengths are obviously the result of the higher carbon content of the heat of steel available for the particular tube size used in these tests.

Photomicrographs representing the structure of the above S.A.E. X-4130 steel tube of 0.29 carbon content and also the structure of a 0.35 carbon S.A.E. X-4130 tube, both in their gas-quenched condition, are shown in Figs. 12 and 13, respectively. A comparison of the two structures discloses a pronounced difference, the gas-quenched

Table VI
Physical Properties of Seamless Drawn X-4130 Steel Tube Obtained for Various Carbon Contents of the Steel

Per Cent Carbon	Tube Size O.D. x Ga.	Yield Strength P.S.I.	Tensile Strength P.S.I.	Elongation Per Cent
0.231	1½" x No. 20	77,200	127,600	27
0.245	1" x No. 22	80,500	129,000	18
0.297	1½" x No. 20	90,100	140,500	12

structure of the higher carbon steel approaching more closely the structure secured by conventional liquid quenching followed by tempering.

The effect of the carbon content of the X-4130 steel tubes on the physical properties appears evident; the lower the carbon, the more drastic must be the gas quench, that is, the greater must be the rate of gas recirculation. Similar considerations are to be given to the adjustment of the other factors in the furnace operation which influence the physical properties such as conveyor speed and temperature.

Since all tests presented in this paper were conducted on production furnaces in full operation, it was impossible to secure additional data in sufficient quantity which would have shown in greater detail the relationship between the carbon content of welded X-4130 steel tube and the physical properties obtained. Considerable information had been gathered, however, in this respect on seamless drawn X-4130 aircraft tubes. Even though the latter tests were carried out in a continuous roller furnace equipped with the old single pass fast cooling zone in which the specified physical properties could be produced only under favorable conditions as has been outlined in the section on the "Performance of the Fast Cooling Zone," the test data on the seamless drawn tube is listed here in Table VI. They show the effect of the carbon content of the steel on the physical properties of seamless drawn tubes and indicate the general trend to be expected in this respect in case of welded X-4130 aircraft tubes.

Aging of X-4130 Gas-Quenched Tubes

The bright gas quenching of welded X-4130 aircraft tubes is usually followed by an aging treatment. Aging of steel manifests itself as a change in the physical properties and is caused by precipitation of the solute which has been retained in supersaturated solution by very rapid cooling. It takes place slowly at room temperature but can be accelerated to a considerable degree by raising the temperature to within the tempering color range of steel (7).

From the test data presented in the previous sections it is apparent that the physical properties stipulated by the AN-T-3 specifications for S.A.E. X-4130 welded aircraft tubing can be met by gas quenching in the super-fast cooling zone without any further treatment. In the first continuous roller hearth furnace applied to gas quenching of welded S.A.E. X-4130 tubing, the same single pass fast cooling zone which produced satisfactory results on seamless drawn S.A.E. X-4130 tubes was utilized. The physical properties obtained were below the specified limits. They were raised, however, to within the specifications by aging the tubes at 800 degrees Fahr. (425 degrees Cent.) in a separate aging furnace.

Description and Arrangement of Aging Furnace

The latter is a forced convection heating furnace such as is conventionally employed for low temperature drawing operations. The products of combustion generated in one or two individual direct fired heaters are recirculated throughout the entire length of the work heating chamber. The aging furnace is as a rule placed in straight line with the gas quenching furnace and for this reason is equipped with a roller hearth conveyor also. Both furnaces are separated by a power driven roller table of such length as to accommodate the maximum length of tube to be heat treated. This arrangement of the aging furnace with respect to the gas quenching furnace eliminates any additional handling of the tubes which are placed on the charge table in front of the high temperature furnace and are unloaded from the discharge table at the outlet of the aging furnace. The two furnaces have separate drive stations so as to facilitate the same or different conveyor speeds in both units.

Being direct fired, the aging furnace produces a blue temper colored surface on the aged tubes. This surface film of oxidation

Table VII
Physical Properties of Welded S.A.E. X-4130 Tubes Gas-Quenched in Super Fast Cooling Zone Before and After Aging

Gas Quench Furnace Temperature: 1650 Degrees Fahr.
Aging Furnace Temperature: 800 Degrees Fahr.

Tube Size O.D. x Gauge	Before Aging — Yield Strength P.S.I.	Before Aging — Tensile Strength P.S.I.	Before Aging — Elongation Per Cent	After Aging — Yield Strength P.S.I.	After Aging — Tensile Strength P.S.I.	After Aging — Elongation Per Cent
¾" x No. 22	79,600	156,000	24	101,000	136,000	17
1" x No. 20	81,500	146,000	23	95,000	128,000	15
1" x No. 18	75,500	138,000	28	94,500	130,000	20
⅞" x No. 16	79,000	143,000	23	96,000	131,000	18
1¼" x No. 16	76,000	139,000	28	90,000	127,000	28

Table VIII
Physical Properties of Welded X-4130 Aircraft Tubes Bright Gas-Quenched and Aged at Normal Production Rates of 5000 Pounds Per Hour

Tube Dia. Inches, O.D.	Wall Thickness — Gauge	Wall Thickness — Decl. Inches	Yield Strength P.S.I.	Tensile Strength P.S.I.	Elongation (On Full Tube)
¾	22	0.028	101,000	136,000	17
1⅛	20	0.035	102,000	137,000	15
1	20	0.035	92,500	127,000	21
⅞	20	0.035	94,600	130,200	15.5
¾	20	0.035	94,000	125,000	14
⅝	20	0.035	96,000	132,000	19
½	20	0.035	95,800	131,000	13.5
⅜	20	0.035	92,000	122,700	12
1⅜	18	0.049	93,000	127,000	20
¾	18	0.049	92,000	125,000	20
1¼	17	0.058	90,000	124,000	19
⅞	17	0.058	99,800	134,000	15
1¼	16	0.065	90,000	127,000	22
⅞	16	0.065	94,000	131,000	18
1½	..	0.068	87,600	141,000	22.7
1¼	..	0.077	82,700	120,800	13.8
2	13	0.095	86,200	107,500	11%*
⅞	13	0.095	85,500	108,000	21%

*Tested on the strip.

has not been found objectionable in the further processing of the tubes but is by many considered advantageous because it forms a protective coating against rusting.

Aging Effect at Room Temperature

The effect of aging at room temperature has been observed on many occasions in the heat treatment of welded S.A.E. X-4130 tubes. Test samples pulled of the same tube immediately after gas quenching and after a 24-hour period normally showed a difference of between 2000 and 4000 pounds per square inch in the yield strength in favor of the aged tube.

solution by very rapid cooling. It takes place slowly at room temperature but can be accelerated to a considerable degree by raising the temperature to within the tempering color range of steel (7).

From the test data presented in the previous sections it is apparent that the physical properties stipulated by the AN-T-3 specifications for S.A.E. X-4130 welded aircraft tubing can be met by gas quenching in the super-fast cooling zone without any further treatment. In the first continuous roller hearth furnace applied to gas quenching of welded S.A.E. X-4130 tubing, the same single pass fast cooling zone which produced satisfactory results on seamless drawn S.A.E. X-4130 tubes was utilized. The physical properties obtained were below the specified limits. They were raised, however, to within the specifications by aging the tubes at 800 degrees Fahr. (425 degrees Cent.) in a separate aging furnace.

Description and Arrangement of Aging Furnace

The latter is a forced convection heating furnace such as is conventionally employed for low temperature drawing operations. The products of combustion generated in one or two individual direct fired heaters are recirculated throughout the entire length of the work heating chamber. The aging furnace is as a rule placed in straight line with the gas quenching furnace and for this reason is equipped with a roller hearth conveyor also. Both furnaces are separated by a power driven roller table of such length as to accommodate the maximum length of tube to be heat treated. This arrangement of the aging furnace with respect to the gas quenching furnace eliminates any additional handling of the tubes which are placed on the charge table in front of the high temperature furnace and are unloaded from the discharge table at the outlet of the aging furnace. The two furnaces have separate drive stations so as to facilitate the same or different conveyor speeds in both units.

Being direct fired, the aging furnace produces a blue temper colored surface on the aged tubes. This surface film of oxidation

O.D. x Gauge	P.S.I.		Per Cent	P.S.I.		Per Cent
¾" x No. 22	79,600	156,000	24	101,000	136,000	17
1" x No. 20	81,500	146,000	23	95,000	128,000	15
1" x No. 18	75,500	138,000	28	94,500	130,000	20
⅞" x No. 16	79,000	143,000	23	96,000	131,000	18
1¼" x No. 16	76,000	139,000	28	90,000	127,000	28

Table VIII

Physical Properties of Welded X-4130 Aircraft Tubes Bright Gas-Quenched and Aged at Normal Production Rates of 5000 Pounds Per Hour

Tube Dia. Inches, O.D.	Wall Thickness Gauge	Wall Thickness Decl. Inches	Yield Strength P.S.I.	Tensile Strength P.S.I.	Elongation (On Full Tube)
¾	22	0.028	101,000	136,000	17
1⅛	20	0.035	102,000	137,000	15
1	20	0.035	92,500	127,000	21
⅞	20	0.035	94,600	130,200	15.5
¾	20	0.035	94,000	125,000	14
⅝	20	0.035	96,000	132,000	19
½	20	0.035	95,800	131,000	13.5
⅜	20	0.035	92,000	122,700	12
1⅜	18	0.049	93,000	127,000	20
¾	18	0.049	92,000	125,000	20
1¼	17	0.058	90,000	124,000	19
⅞	17	0.058	99,800	134,000	15
1¼	16	0.065	90,000	127,000	22
⅞	16	0.065	94,000	131,000	18
1½	..	0.068	87,600	141,000	22.7
1¼	..	0.077	82,700	120,800	13.8
2	13	0.095	86,200	107,500	11%*
⅞	13	0.095	85,500	108,000	21%

*Tested on the strip.

has not been found objectionable in the further processing of the tubes but is by many considered advantageous because it forms a protective coating against rusting.

Aging Effect at Room Temperature

The effect of aging at room temperature has been observed on many occasions in the heat treatment of welded S.A.E. X-4130 tubes. Test samples pulled of the same tube immediately after gas quenching and after a 24-hour period normally showed a difference of between 2000 and 4000 pounds per square inch in the yield strength in favor of the aged tube.

Accelerated Aging

The increase in yield strength becomes considerably higher by subjecting the gas-quenched tubes to the accelerated aging treatment in the aging furnace. Figs. 6, 7 and 8 present graphically the physical properties obtained on three different sizes of S.A.E. X-4130 tubes before and after aging. A comparison between these three figures discloses that the increase in yield strength due to aging is more pronounced on the lighter gage tubes than on the heavier gage tubes, indicating that the aging effect depends to a large degree upon the rapidity of the gas quenching. Unquestionably, the results secured by aging are influenced also by the chemical composition of the steel. Aside from invariably showing an increase in yield strength due to the accelerated aging treatment, the test data plotted in Figs. 6, 7 and 8 did not allow definite conclusions regarding the effect of the aging on the tensile strength and on the elongation. These tests had been run primarily to determine the relationship between the physical properties and the rate of gas recirculation in the gas quenching zone.

Results of Accelerated Aging

A special series of tests was conducted, therefore, on various sizes of tubes to clarify the effect of aging on the physical properties of gas-quenched S.A.E. X-4130 aircraft tubes. The results of the latter tests are listed in Table VII.

From the test data tabulated above, the following conclusions may be drawn:

1. Accelerated aging increased the yield strength of gas-quenched S.A.E. X-4130 welded tubes by more than 10,000 pounds per square inch.
2. Accelerated aging lowers the tensile strength by more than 10,000 pounds per square inch.
3. Accelerated aging decreases the elongation by an average of 5 per cent.

Even though the specified physical properties can be secured by the gas quenching treatment alone in the super-fast cooling zone, the effect of the accelerated aging is beneficial to such a degree that it warrants the use of an aging furnace on all welded S.A.E. X-4130 aircraft tubes.

Table IX
Chemical Composition

Steel No.	Carbon	Manganese	Sulphur	Phosphorus	Silicon	Chromium	Nickel	Molybdenum
	Per Cent							
X-4130	0.32	0.53	0.028	0.014	....	0.92	....	0.18
NE 8630	0.29	0.71	0.020	0.019	0.25	0.50	0.59	0.20

Table X
Comparison of Physical Properties of S.A.E. X-4130 and NE 8630 Welded Tubes

Tube No.	S.A.E. X-4130 Yield Strength P.S.I.	S.A.E. X-4130 Tensile Strength P.S.I.	S.A.E. X-4130 Elongation Per Cent	NE 8630 Yield Strength P.S.I.	NE 8630 Tensile Strength P.S.I.	NE 8630 Elongation Per Cent
1	96,400	144,000	15.0	96,400	138,400	14.0
2	98,700	149,200	15.0	87,300	137,200	15.0
3	85,000	149,600	15.0	90,500	135,200	16.5
4	90,900	142,500	16.0	86,500	136,400	15.0
5	86,500	141,000	16.0	87,500	137,600	13.0
Average	91,500	145,000	15.40	89,650	137,000	14.70

Tabulation of Average Physical Properties Produced by Gas Quenching and Aging

A complete tabulation of the average physical properties obtained in normal production on various tube sizes by gas quenching and aging is given in Table VIII. These results disclose a progressive decrease of the yield and tensile strengths as the tube wall thickness increases but in all cases the physical properties are well above the low limits stipulated by the AN-T-3 specifications.

NE 8630 Versus X-4130

The tests presented in this paper were conducted during the fall of last year and during the early months of the present year, when an ample supply of S.A.E. X-4130 steel was available. At the time of this writing, however, S.A.E. X-4130 steel is no longer being produced by the steel mills but is being replaced by the National Emergency Steel NE 8630. It thus appears safe to anticipate that, at the time of presentation of the paper, NE 8630 steel will be used exclusively in place of X-4130 steel.

Comparison of Physical Properties of Both Steels

A comparison of the physical properties of both types of steel tubes obtained by bright gas quenching in the super-fast cooling zone

is, therefore, of paramount interest and importance. A production test run was made on both steels under practically identical conditions. The tube sizes were the same, namely, 0.50 inch O.D. by 0.034 inch tube wall thickness. The temperature from which both steel tubes were gas-quenched was 1650 degrees Fahr. (900 degrees Cent.) and the aging temperature was held constant at 600 degrees Fahr. (315 degrees Cent.). The conveyor speeds were 5 feet per minute through the gas quenching furnace and 5.5 feet per minute through the aging furnace. The composition of both steels used in these tests is given in Table IX.

Five tubes were picked out at random from each production run; their physical properties are compiled in Table X.

The table shows a somewhat higher average yield and tensile strength for the S.A.E. X-4130 steel than for the NE 8630 steel. Two factors account for this difference. First, the carbon content of the S.A.E. X-4130 steel was slightly higher than that of the NE 8630 steel. Secondly, the rate of gas recirculation in the gas quenching zone was somewhat greater for the former steel than for the latter. 63 per cent of the maximum available gas recirculating capacity was used in the first test as compared to 55 per cent in the case of the National Emergency Steel.

Taking into consideration these two factors, it must be concluded that, for all practical purposes, the NE 8630 steel is capable of developing the same physical properties upon gas quenching as the S.A.E. X-4130 steel and that the heat treatment involved in gas quenching and in aging is identical for both types of steel.

Summary and Conclusions

The foregoing data justify the following conclusions:

1. Bright gas quenching in the super-fast cooling zone makes it possible to meet the AN-T-3 specifications for the physical properties of welded S.A.E. X-4130 aircraft tubing on a large production scale.
2. The physical properties are controlled by the rate of gas recirculation, by the conveyor speed and by the temperature from which the tubes are gas quenched.
3. The adjustment of the above variables in the furnace operation is governed by the carbon content of the steel and by the tube size, particularly by the wall thickness of the tubes.

4. Accelerated aging of the gas quenched tubes has an additional beneficial effect on the physical properties of the heat treated welded aircraft tubes.
5. Gas quenching allows the tubes to be welded to finish size and thus eliminates any cold drawing either for sizing or for attainment of the desired physical properties.
6. The application of a bright annealing atmosphere as the gas quenching medium increases the rate of cooling and, at the same time, makes unnecessary any cleaning or pickling of the heat treated tubes.
7. Main dampers provided in the path of the recirculated cooling gases facilitate the use of the same furnace for process or for finish annealing of other classes of tubes.
8. Welded NE 8630 aircraft tubes develop the same physical properties upon gas quenching as welded S.A.E. X-4130 tubes.

Acknowledgment

The generous co-operation of the Heat Treating Departments and of the staffs of the Metallurgical Departments of the Michigan Steel Tube Products, of the Steel and Tubes Division of Republic Steel Corp. and of the Bundy Tubing Company in carrying out the production test runs and in determining the physical properties of the test tubes is gratefully acknowledged. The author wishes to especially express his sincere appreciation to Mr. R. O. Berg, Mr. S. Gorom and Mr. F. Monroe of the Michigan Steel Tube Products, to Mr. M. Thomas of the Steel and Tubes Division, and to Dr. R. H. Hobrock, Dr. A. DiGuilio and Mr. J. F. McMaster of the Bundy Tubing Company.

Bibliography

1. Dr. Eng. Albert Sauveur, "The Metallography and Heat Treatment of Iron and Steel.
2. R. S. Archer, "Heat Treatment of Metals," A.S.M. Metals Handbook.
3. A.S.M. Metals Handbook, "Welding of Metals."
4. R. F. Mehl, "Recrystallization," A.S.M. Metals Handbook.
5. R. S. Archer, "Heat Treatment of Metals," A.S.M. Metals Handbook.
6. R. S. Archer, "Heat Treatment of Metals," A.S.M. Metals Handbook.
7. S. Epstein and H. L. Miller, "Aging in Iron and Steel," A.S.M. Metals Handbook.

DISCUSSION

Written Discussion: By Armand DiGiulio, head, Research Division, Bundy Tubing Company, Detroit.

The author should be congratulated for presenting informative data on welded steel tubing. There are, however, several points which need to be clarified.

From the discussion of Spec. AN-T-3 on page 291 and again on page 297, the impression may be gained that tubes, to meet condition N requirements, must be "normalized". If we use the term as defined in A.S.M. Handbook, 1939, page 4, we see that this is not the case. The Spec. AN-T-3 establishes a minimum value for mechanical properties to be produced by any one of the methods listed in paragraph E-2 of the specification as reported on page 291 of this paper.

It is mentioned on page 315 that a change in yield strength, "aging", has been observed on welded X-4130 tubes within 24 hours after gas quenching. No data is presented to support this statement and the literature does not reveal any similar occurrence on X-4130 heat treated the conventional way. It would be desirable to have the author present data to support his statement.

The author refers to the low temperature treatment to which the tubes are subjected after gas quenching as "accelerated aging" and the conclusions are drawn that accelerated aging increases yield strength, and decreases tensile strength and percentage elongation. In our plant, we found that the low temperature treatment results in an increase in yield strength and elongation and a decrease in tensile strength and hardness. The increase in elongation and the lowering of tensile strength is shown to occur in Figs. 6 and 8 of this paper, while the author's conclusions seem to be based on Table VII.

Unfortunately, not sufficient data are presented showing furnace speeds, amount of quenching gas, chemical composition and the structural composition before and after quenching.

In view of these facts, the author's conclusion seems hardly justifiable.

Written Discussion: By Morse Hill, assistant metallurgist, Materials Lab., Engineering Division, Materiel Command, Army Air Forces, Wright Field, Dayton, Ohio.

The author's description of the gas quenching and heat treatment of aircraft tubing will certainly serve to clear up some misconceptions as to the significance of the term "normalized", which sometimes arise in the minds of those who are unacquainted with tubing manufacture practice.

Did the author intend to imply that carbon is the only important agent in changing the physical properties of the gas-quenched tubing or are chromium and molybdenum and manganese also important? The fact that 8630 responds to the same treatment as 4130 would seem to indicate on first thought that only carbon is important, but in that case we are dealing with a change in the whole balance of elements rather than with variation in any one of them.

Can the author give any further information as to the nature of the change on aging? Is it a precipitation effect or a stress relief action raises the yield point on aging or some other effect? In the laboratory it has been found that the change is accompanied by a change in the nature of the stress-strain curve. As this figure shows, normalized tubes have a smooth curve with no well defined yield point, while aged tubes have a very distinct break in the curve. This

rounding of the curve is almost certainly due to some internal stress in the metal which may as easily be caused by the presence of a super-cooled material as by unrelieved volume changes resultant on rapid cooling.

Oral Discussion

J. B. R. ANDERSON:[3] Mr. Lehrer, while he had a very interesting paper, was talking low side and high side of analyses. During the past year the American Iron and Steel Institute has endeavored to get our steel making working ranges down to about what we would consider a practical minimum. Now, when you start talking about 0.28 to 0.30 carbon as necessary to accomplish the desired physical properties you are beyond the means of a steel maker. In other words, it is not practical for a steel maker to work to such close limits. It would seem more logical, particularly in these times, to design your heat treating equipment to take care of the standard article. Perhaps a little faster cooling or something like that could secure your desired physical properties.

SAM TOUR:[4] I simply want to point out one item which has not been emphasized sufficiently in this paper, and that is the higher effective cooling obtained with hydrogen than with any of the other gases. If it is desired to increase the rate of cooling, and that is presumably what is desired in this case, then the atmosphere should be such as to contain as high a percentage of hydrogen as possible. Carbon monoxide and carbon dioxide are not fast cooling gases and neither is nitrogen. Hydrogen is. Instead of creating an atmosphere containing only 12 per cent hydrogen it would be desirable to use an atmosphere with hydrogen as high as possible.

ARMAND DIGIULIO: I would like to ask Mr. Tour if he has any figure which would indicate the increase in cooling effectiveness by, let us say, a doubling of the hydrogen content of the composition in the paper.

MR. TOUR: That would have to be determined upon the particular equipment and circulative system which you have, which I have not, so I could not give you the figure, but I can say the cooling rate of straight hydrogen is about five times the cooling rate of carbon monoxide, about five to one in effectiveness in absorbing heat between hydrogen and carbon monoxide.

JOHN J. TURIN:[5] I should like to point out, with reference to securing fast cooling rates, that one is not quite free to choose any type of atmosphere which he would like to have. Pure gases like hydrogen and nitrogen are things that cannot be obtained economically. The bright annealing atmosphere is relatively cheap atmosphere which does perform the required cooling action in a very satisfactory manner. As has been shown in the paper, this cooling action is more than sufficient to meet the requirements which have been set by the specifications. In answer to Mr. Anderson, one ought to point out that the cooling system is very flexible, and that the reason for this flexibility of the superfast cooling zone is to allow the control of the tubing physical properties regardless of whether the carbon contents are on the nose or whether they are on the low side, which

[3]Metallurgist, Carnegie-Illinois Steel Corp., Pittsburgh.
[4]President, Sam Tour & Co., Inc., New York City.
[5]Physicist, Surface Combustion, Toledo, Ohio.

would be from 0.25 to 0.30 per cent of carbon, or whether on the high side, which would be from 0.30 to 0.35 per cent of carbon.

Author's Reply

The author is grateful to those who have offered their comments and suggestions concerning this work. This paper can be considered as a progress report on the adaptability of a gaseous medium for the bright quenching of carbon and alloy steels. As such, it presents a method for successfully developing, in S.A.E. X4130 and NE 8630 welded aircraft tubing, the physical properties which satisfy condition N of Specification AN-T-3.

In view of the increasing demand for such tubing as well as the attendant difficulties in applying conventional heat treating methods, it was believed that the information thus far obtained in commercial gas quenching applications should be passed on without delay.

More complete data on the bright gas quenching method of heat treating will require considerably more research and development work. Such work will be aided by the remarks and constructive criticism of these men who are familiar with the problems involved.

Dr. DiGuilio questions the apparent aging of welded X4130 tubes within 24 hours after gas quenching as evidenced by increase in yield strength. The author agrees that the literature reveals no similar occurrence in X4130 after heat treating in the conventional manner. Such aging, however, has apparently occurred after gas quenching. The data obtained on this subject are meager, and while the total increase is usually small, the trend has always been towards increased yield strength. This room temperature aging was mentioned as being of academic rather than of practical value.

Accelerated aging by heating to considerably above room temperature is of considerable importance and the results of carefully conducted tests are shown in Table VII. Increased yield as well as decreased elongation is consistently noted in these results.

Mr. Hill inquires into the causes of the change in the yield point values during the aging process. It is the author's opinion that such change is due to a precipitation effect. As Mr. Hill points out, either precipitation from a supercooled material or unrelieved volume changes due to rapid cooling could cause a break in the stress-strain curve. When noticeable loss in elongation accompanies the increase in yield, we would expect the change to be brought about by precipitation rather than stress relief. Additional data on this subject should be available in the near future.

The author wishes to assure Mr. Hill that he is in full accord with the opinion that elements such as chromium, molybdenum and manganese have a definite influence on the physical properties of gas-quenched tubing. While carbon was specifically mentioned as being of major importance, it was not intended that the other elements should be ignored.

The fact that NE 8630 steel responded to the same treatment as X4130 was fully expected in view of the demonstrated ability of the metallurgist to accurately balance the elements so that two steels of widely different analysis are comparable in physical properties.

The remarks of Mr. Tour and Mr. Anderson have been discussed by Dr. Turin. Mr. Tour's mention of the increased cooling effects of hydrogen as compared to the usual atmospheres suggests that considerable range of cooling rates may be obtained by proper choice of the gas quenching medium. This is true since the cooling rate of any hot body is a function of the heat transfer coefficient between the hot body and the cooling medium, and this heat transfer coefficient increases in value with the specific heat of the cooling medium as well as with its velocity.

We are familiar with the high heat capacity of hydrogen gas and are making use of this valuable property to a limited extent in the atmospheres described on page 293 of this paper. However, the use of too high a hydrogen concentration in a furnace of the type required for tubing presents a hazard due to the explosive nature of the hydrogen. We prefer to obtain our rapid cooling rates by using a comparatively safe gas at extremely high velocity. In the commercial units described in the paper we are able to obtain satisfactory cooling rates on all sizes of tube up to about 0.095 inch wall thickness with less than the maximum recirculating capacity of 22,000 cubic feet per minute. This is explained on page 306 and is graphically shown in Fig. 9.

Mr. Anderson's description of some of the difficulties besetting the steel manufacturer is fully appreciated, and the gas quenching equipment described in this paper has been designed with the idea of accommodating these difficulties.

SOME EFFECTS OF HEAT TREATMENT ON LOW ALLOY TITANIUM STEELS

By George F. Comstock

Abstract

Heat treatment of titanium steels above about 2000 degrees Fahr. (1095 degrees Cent.) is shown in this paper to be capable of producing a marked increase in strength, due evidently to the solubility of titanium carbide in the austenite at high temperatures. Instances of this effect are described in 0.13 per cent carbon steel, 0.37 per cent carbon steel, chromium-molybdenum steel (S.A.E. 4140), and a 1.24 per cent manganese-copper-phosphorus plate steel. The increased strength produced by titanium can be utilized in steels used in the as-rolled condition, or stress-relieved at sub-critical temperatures, because billets are generally heated above 2000 degrees Fahr. (1095 degrees Cent.) for rolling, and quenching is not required to retain titanium in the strengthening form. Without mechanical working after the high-temperature heat treatment the steel is coarse-grained and may have low impact value. Normalizing between the critical range and about 2000 degrees Fahr. (1095 degrees Cent.) generally obliterates most of the strengthening effect of titanium, which then improves the ductility and impact value.

MOST of the available information on titanium steels, exclusive of austenitic stainless steels, has been obtained from small ingots which were converted into bar form for testing without the same high temperature soaking-pit treatment as is generally used for full-sized commercial ingots. It has not been sufficiently well appreciated that such a difference in the high temperature heat treatment of the ingots may have a very important effect on the properties of titanium steel, especially if the rolled or forged shapes are not normalized. Accordingly, the object of this paper is to explain and illustrate the influence of that processing factor on the final results obtained.

High temperature heat treatment has a more important effect on the properties of titanium steels than on those of other alloy steels

A paper presented before the Twenty-fifth Annual Convention of the Society, held in Chicago, October 18 to 22, 1943. The author, George F. Comstock, is metallurgist, The Titanium Alloy Manufacturing Co., Niagara Falls, N. Y. Manuscript received April 10, 1943.

because it is only at the very highest heat treating temperatures that titanium carbide dissolves in austenite. Furthermore titanium carbide, unlike the carbides of most other elements used in alloy steels, does not mix with cementite or form double carbides with iron (1), (2).* But the stability of titanium carbide is greater than that of cementite or most other carbides in steel, so that when titanium is added to steel practically all of it combines with carbon, leaving that much less carbon available to form cementite and other similarly soluble carbides. Since the solution of cementite, and the other carbides associated with it, in austenite above the critical temperature is the chief factor in the hardening and strengthening of steel by heat treatment, it is evident that titanium, in forming relatively insoluble titanium carbide, will reduce the effective amount of the hardening and strengthening agent and produce the same result as a reduction in carbon content. This, of course, is an over-simplification of the total action of titanium in steel, which is complicated by grain-size effects, deoxidation, intensification of other alloys, etc., but the above may be accepted as a useful though rough outline of the normal influence of titanium on the properties of low-alloy engineering or structural steels heat treated at the usual temperatures.

This matter of heat treatment is a point that should not be overlooked, because titanium carbide is only relatively insoluble in steel, and can be caused to dissolve appreciably at higher temperatures than are generally used in heat treatment. When this solution occurs, the steel is strengthened and hardened by titanium in much the same way as by other carbide-forming elements that dissolve in the austenite. At lower temperatures, such as are used in normal heat-treating practice, the titanium carbide is precipitated, so that most of the effect of its solution is lost. Both precipitation and solution are sluggish, however, and their results depend as much upon the time allowed for the action as upon the temperatures involved.

Equilibrium Relations Between Carbon and Iron with Low Titanium

The equilibrium relations beween titanium, iron and carbon in steel have been disclosed by Buttinghaus in Germany (2), and are compared for low-carbon steel containing 0.0, 0.3, and 0.7 per cent titanium in Fig. 1. Here it is seen how increasing titanium contents

*The figures appearing in parentheses pertain to the references appended to this paper.

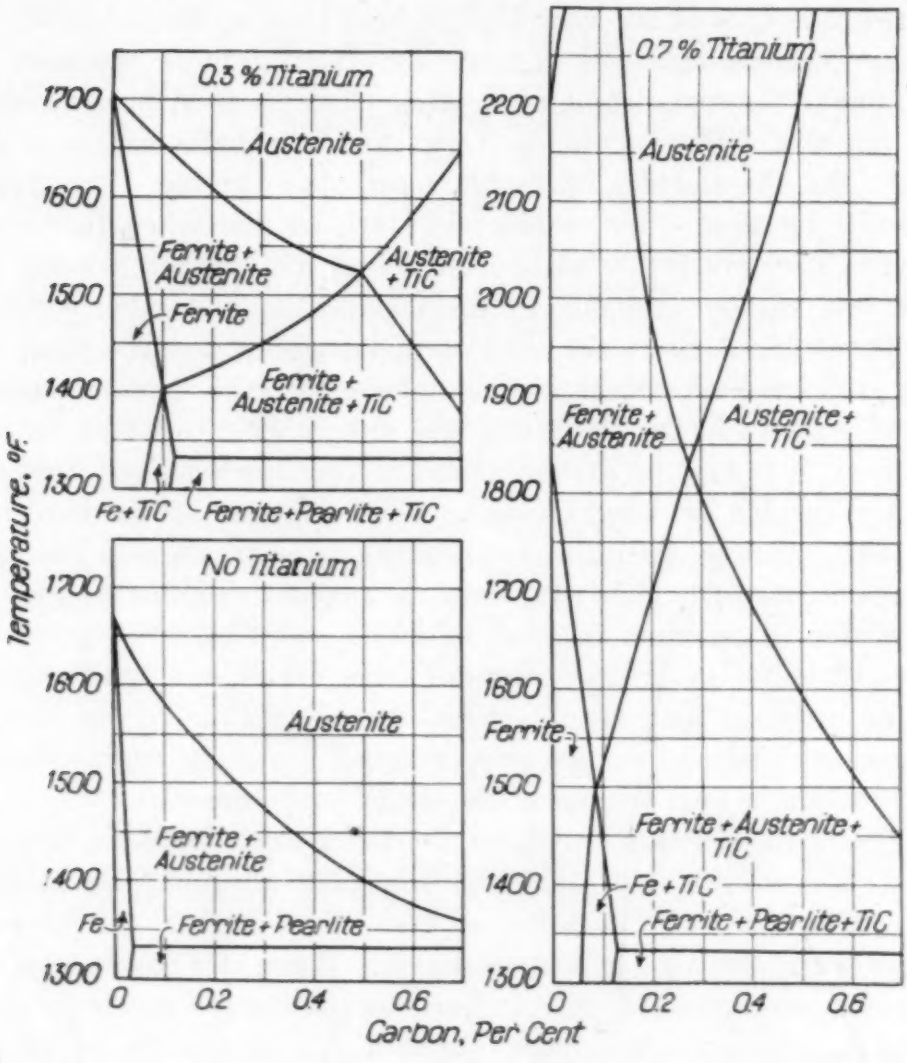

Fig. 1—Iron-Carbon Equilibrium Diagrams with 0, 0.3 and 0.7 Per Cent Titanium, Respectively, According to Buttinghaus.

restrict the pure austenite field, expand the range of alpha iron or ferrite, and extend the occurrence of titanium carbide. However, even with as much as 0.7 per cent titanium and 0.2 to 0.4 per cent carbon, there is an extensive field of pure austenite solid solution under equilibrium conditions above about 2000 degrees Fahr. (1095 degrees Cent.), which means of course that all the titanium carbide in such a steel can be made to dissolve completely by sufficient time at those temperatures. Some metallographic evidence on the partial solution of titanium in 18 per cent chromium steel was offered by Bannon in 1936 (3), but his soaking period at high temperature was only 1 hour, and complete solution was not attained.

Low-Carbon Titanium Steel

A good illustration of the marked influence of high temperature heat treatment on the properties of titanium steel can be found in the data reported elsewhere on the strain aging of low-carbon steel (4). Table I shows the tensile properties of two steel bars containing about 0.13 per cent carbon, 0.48 per cent manganese, and 0.18 per cent silicon, and with about 5 times as much titanium as carbon, each forged from a 17-pound ingot. One ingot was forged at about 1750 degrees Fahr. (985 degrees Cent.), and the other was first soaked for 4 hours at 2150 degrees Fahr. (1175 degrees Cent.), both being finished at about the same temperature.

Table I
Properties of Forged Low-Carbon Titanium Steel

Heat Treatment before forging, Degrees Fahr.	1750	2150	1750	2150
Normalizing Temperature after Forging, Degrees Fahr.	None	None	1700	1700
Yield Strength, Lbs. per Sq. In.	28,500	51,100	21,000	20,400
Tensile Strength, Lbs. per Sq. In.	60,000	64,900	56,300	53,000
Elongation in 6 in., Per Cent	21.0	11.8	23.2	25.7
Reduction of Area, Per Cent	69.9 (seams)	77.0	79.6	83.0

The marked increase in yield strength due to soaking this titanium steel at 2150 degrees Fahr. (1175 degrees Cent.) can readily be appreciated from Table I, but it is also evident that the effect was lost on normalizing. The latter treatment gave the titanium carbide an opportunity to separate from the solid solution in the previously superheated bar, which then reverted to the condition and properties of the other bar made from the normally heated small ingot. The difference in properties between the two specimens tested in the as-forged condition shows that the solid solution was preserved, however, during the cooling of the steel while forging, at least to an effective degree, the precipitation being sufficiently sluggish so that *quenching* from 2150 degrees Fahr. (1175 degrees Cent.) was not necessary.

S.A.E. 1040 Steel with Titanium or Vanadium

A more extensive investigation of the effects of high-temperature heat treatment was made on an S.A.E. 1040 steel with 0.35 per cent titanium in comparison with two similar steels without titanium, one,

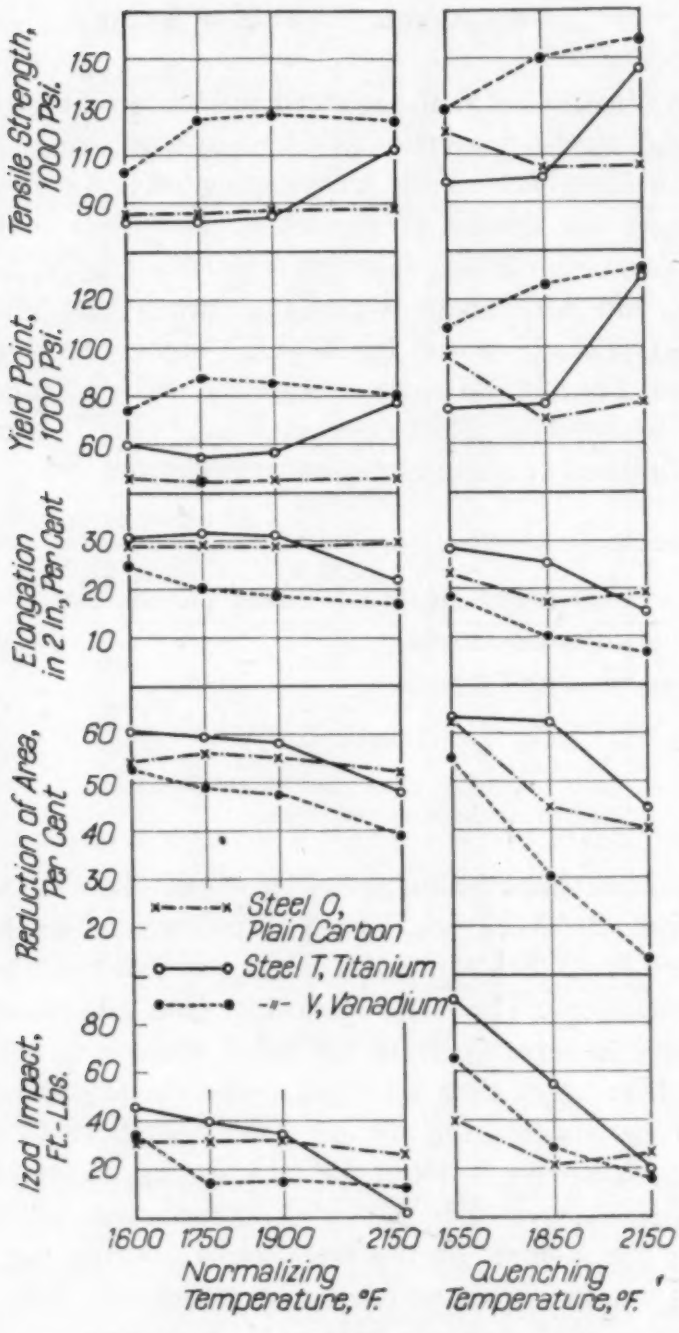

Fig. 2—Tensile and Impact Test Results on S.A.E. 1040 Steels Normalized or Quenched from Various Temperatures, the Quenched Specimens All Having Been Subsequently Tempered at 1050 Degrees Fahr.

however, containing 0.10 per cent vanadium. These steels were received in the form of 1.5-inch round bars rolled from large ingots, and tests were made on forged 7/8-inch rounds heat treated after forging. The titanium steel was made by adding aluminum and

ferrotitanium in the ingot mold, while the untreated steel was from a coarse-grained heat made without aluminum deoxidation. The analyses and austenitic grain sizes of these steels at various temperatures are given in Table II, while Fig. 2 shows how their tensile and impact properties varied with heat-treating temperature.

Table II
Analyses and Austenitic Grain Sizes of S.A.E. Steels with and without Titanium

Steel	Chemical Analysis				A.S.T.M. Grain Size Normalized at			
	C	Mn	Si	Alloys	1600° F.	1750° F.	1900° F.	2150° F.
O	0.36	0.68	0.22	None	3	3–4	2–3	1–2
T	0.37	0.63	0.26	0.35 Ti	8–9	8	7–8	3–4
V	0.40	0.66	0.19	0.10 V	8–9	6–7	3	0–1

In performing the heat treatments indicated on Fig. 2, the ⅞-inch round specimens were held at temperature for 1 hour. The curves show quite consistently how the titanium steel became stronger but less ductile or tough as the titanium carbide passed into solution above 1850 or 1900 degrees Fahr. (1010 or 1040 degrees Cent.), while similar changes occurred in the vanadium steel below 1750 or 1850 degrees Fahr. (955 or 1010 degrees Cent.), and the non-alloy steel did not become stronger after high temperature treatment.

S.A.E. 4140 Steel with Titanium

Similar changes due to solution effects at high temperature have been found in S.A.E. 4140 steel containing much smaller amounts of titanium. With even as little as 0.053 per cent titanium there was an appreciable increase in strength as the normalizing temperature was raised from 1650 to 2150 degrees Fahr. (900 to 1175 degrees Cent.), but more interesting results were obtained with titanium contents above 0.07 per cent. Examples of tensile and impact results on steel of this kind, forged from small induction-furnace heats to ⅞-inch round bars are given in Table III. The ingots contained about 0.38 per cent carbon, 0.85 per cent manganese, 0.30 per cent silicon, 1 per cent chromium, 0.25 per cent molybdenum, and 0.10 per cent titanium. Various heat treatments were applied to the ingots or bars as noted, though all these results were obtained with specimens finally tempered 2 hours at 1175 degrees Fahr. (635 degrees Cent.).

It may be noted from Table III that in every instance where treatment of 2000 degrees Fahr. (1095 degrees Cent.) or over was

Table III
Properties of S.A.E. 4140 Steel with 0.1% Titanium, Tempered at 1175 Degrees Fahr. (635 Degrees Cent.)

Test No.	Heating Temperature for Forging, Degrees Fahr.	Normalizing Temperature, Degrees Fahr.	Lbs. per Sq. In. Yield Strength	Lbs. per Sq. In. Tensile Strength	Per Cent Elongation in 2 in.	Per Cent Reduction of Area	Izod Impact Value, Ft. Lbs.
1	1750	1650	95,300	118,000	21.0	59.0	32
2	1750	2000	111,200	133,400	17.5	51.6	5
3	1750	2150	114,000	139,900	15.5	46.7	7
4	2050	None	103,800	124,400	19.5	53.9	34
5	2050	1650	98,200	121,400	20.7	55.5	18
6	2150	None	116,300	133,200	15.0	46.8	33
7	2150	1600	93,000	119,800	19.5	56.1	18

the last heat treatment applied, except for sub-critical tempering, the yield strength was appreciably higher than when normalizing was used. Generally the tensile strength also was better, but the ductility and impact resistance were low when the high temperature treatment was applied after forging. Thus to take advantage of the higher yield strength conferred by titanium and high-temperature heat treatment, without the occurrence of low notched-bar impact values, it is necessary to work the steel mechanically after that treatment, to reduce the grain size, as was done in Tests 4 and 6. If the grain refinement is accomplished by normalizing, the strengthening effect of the titanium is lost, presumably because the titanium carbide then is given an opportunity to precipitate from the solid solution or to agglomerate into particles too coarse to be effective for strengthening.

Low Alloy High-Strength Plate Steel with Titanium

A better illustration of this action was afforded by a trial of titanium in a low-alloy high strength plate steel, where mold additions of titanium in various amounts were used in a single open-hearth heat. The heat analysis was 0.14 per cent carbon, 1.24 per cent manganese, 0.36 per cent copper, 0.125 per cent phosphorus, 0.078 per cent silicon, and 0.023 per cent sulphur. The heat was deoxidized in the ladle with ¾ pound of aluminum per ton, and when the 8500-pound ingots were poured, low-carbon 40 per cent ferro-titanium was thrown into the stream entering some of the molds. These ingots were heated for about 12 hours at 2200 degrees Fahr. (1205 degrees Cent.) and rolled into slabs. The slabs were reheated for about 1.75 hours to 2150 degrees Fahr. (1175 degrees Cent.)

and rolled to half-inch plates. The slabs and plates from various parts of the ingots were sampled for analysis and agreed closely with the heat analysis given above, except of course for their titanium contents which varied from zero up to about 0.25 per cent.

These plates were tested in tension and impact both as-rolled and after normalizing 2 hours at 1650 degrees Fahr. (900 degrees

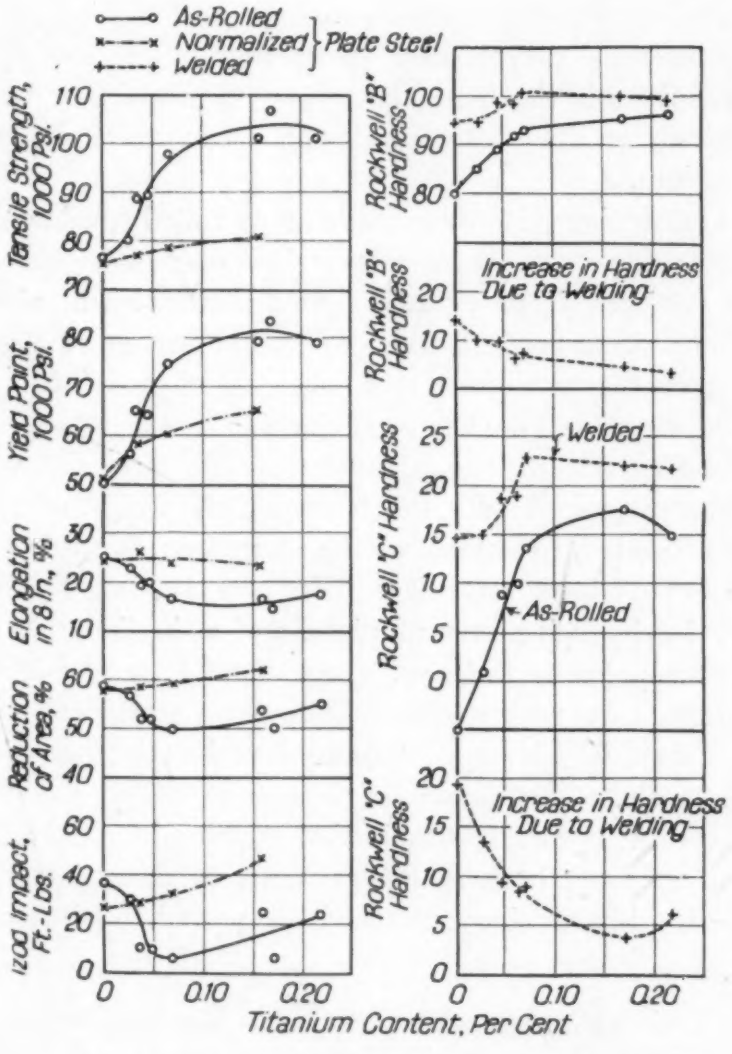

Fig. 3—Tensile, Impact and Hardness Test Results on Plate Steel with Various Amounts of Titanium.

Cent.). The tensile specimens were the full thickness of the plate, 1.5 inches wide, and 9 inches long between shoulders. They were cut lengthwise from both middle and edge of the plate, and also transversely, and the results were averaged for each titanium content since there was but little difference between the properties at the

various locations. Impact tests were made with standard Izod specimens at room temperature, and were likewise averaged for each titanium content. The results of these tests are shown plotted against the titanium content of the steel in Fig. 3.

The very marked increase in yield and tensile strength found in this plate steel with increasing titanium content is readily appreciated from Fig. 3, and it is seen that it is accompanied by an increase in hardness and decreases in ductility and notched-bar impact resistance. After normalizing, the increase in strength with titanium was still perceptible, though much smaller, but the reduction of area and impact values of the normalized specimens were improved with higher titanium.

Weld hardening tests were made on as-rolled specimens by means of hardness surveys on cross-sections of single beads deposited on scale-free surfaces from $\frac{3}{16}$-inch coated electrodes at about 55 degrees Fahr. at a rate of 6 inches per minute, using 55 volts and 175 amperes. All the sections tested were at least 2 inches from the ends of the beads. The Rockwell hardness was measured at four points in the hardened zone just beneath the weld deposit, and the average was compared with the hardness of the plate at the same location not welded, to determine the increment due to weld hardening. One set of tests was made using the Rockwell B scale, with welds on 7 by 10-inch pieces of plate, and a duplicate set was made using the diamond penetrator and C scale on 3.5 by 4.75-inch samples.

The results by both methods are shown graphically on Fig. 3, the C scale method giving perhaps a more distinct comparison between the steels. The maximum hardness below the weld beads did not increase as much with increasing titanium content, at least up to about 0.15 per cent, as the as-rolled hardness before welding, so that the weld-hardening was much decreased by titanium in such amounts.

Comparison with Previous Results on Phosphorus-Titanium Steel

The relative properties of these titanium steels illustrate very distinctly the marked effect of small titanium additions on the strength and hardness of steel tested in the as-rolled condition without heat treatment other than that applied in the ingot soaking pits or slab-heating furnaces at or above 2150 degrees Fahr. (1175 degrees Cent.). It is also clearly shown how this effect may be reduced or

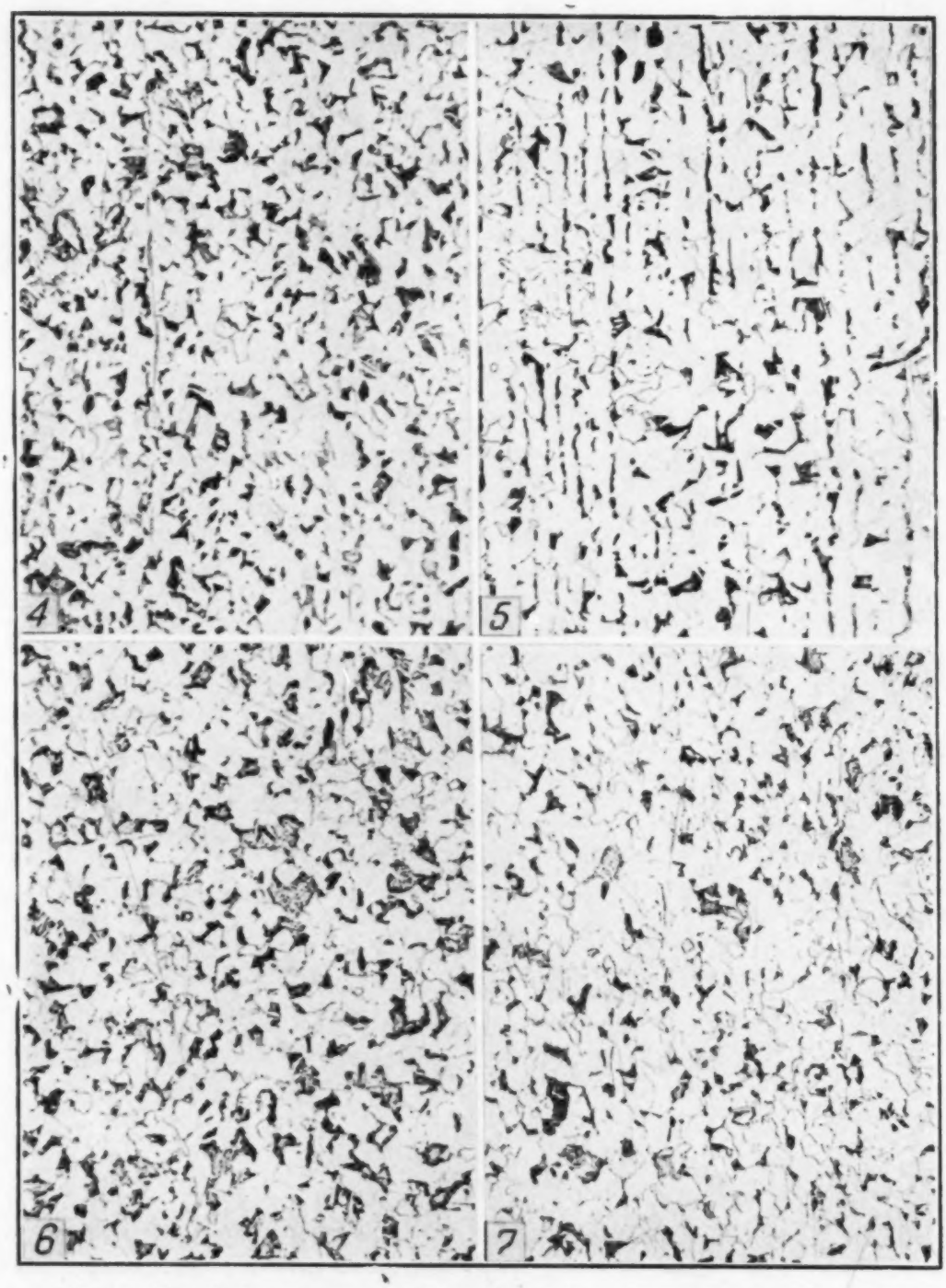

Fig. 4—Lengthwise Structure of Plate Rolled From Upper Part of Ingot Without Titanium, Magnified 100 Diameters, Etched with Nital.

Fig. 5—Same as Fig. 4, Except From Lower Part of Ingot.

Fig. 6—Lengthwise Structure of Plate Rolled From Upper Part of Ingot with 0.07 Per Cent Titanium, Magnified 100 Diameters, Etched with Nital.

Fig. 7—Same as Fig. 6, Except From Lower Part of Ingot, with 0.06 Per Cent Titanium.

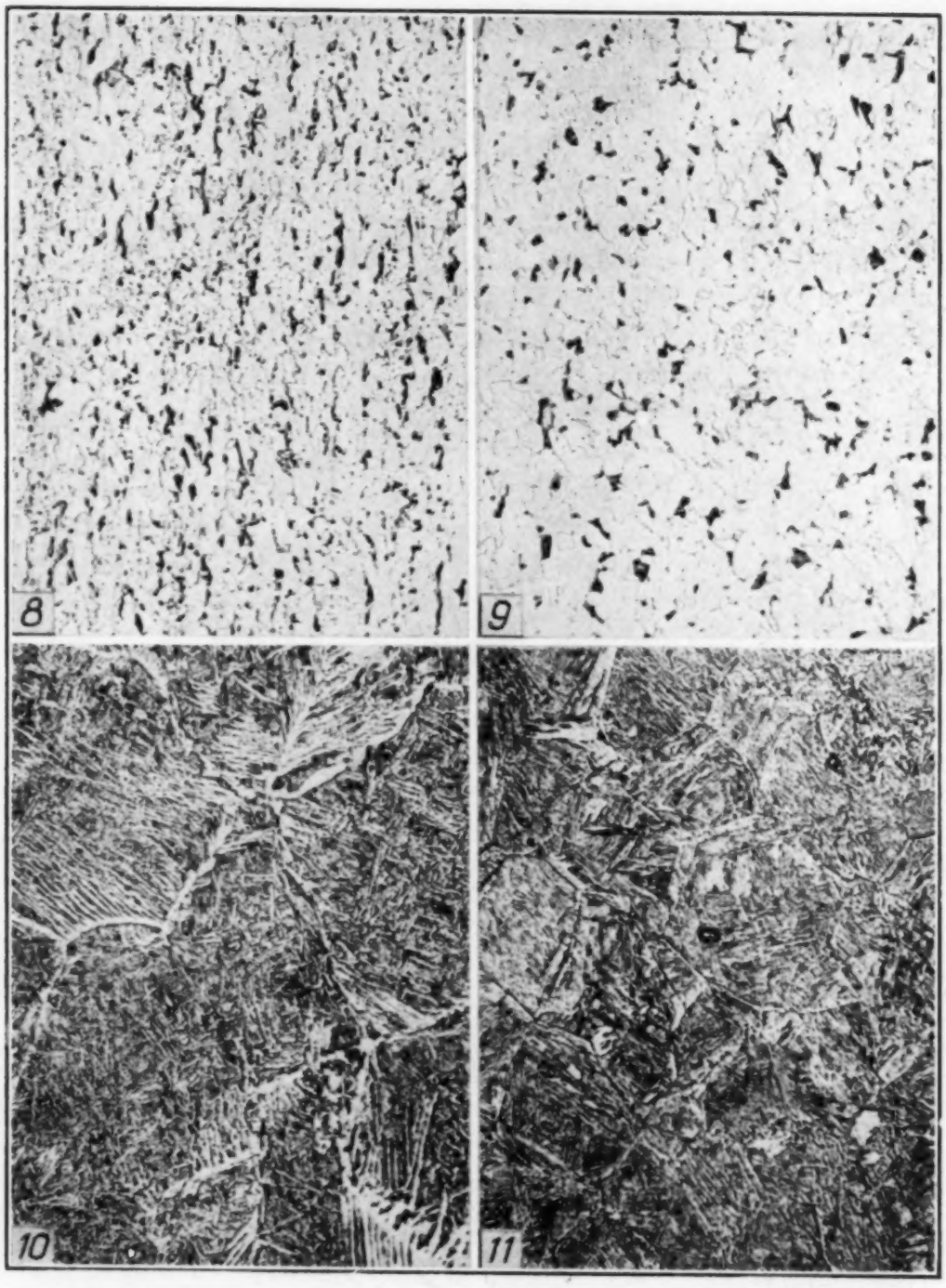

Fig. 8—Lengthwise Structure of Plate Rolled From Upper Part of Ingot with 0.24 Per Cent Titanium, Magnified 100 Diameters, Etched with Nital.

Fig. 9—Same as Fig. 8, Except From Lower Part of Ingot, with 0.17 Per Cent Titanium.

Fig. 10—Structure of the Coarsest Zone Beneath a Single-Bead Weld Deposit on the Plate with No Titanium, Magnified 200 Diameters, Etched with Nital.

Fig. 11—Structure of the Coarsest Zone Beneath a Single-Bead Weld Deposit on the Plate with 0.24 Per Cent Titanium, Magnified 200 Diameters, Etched with Nital.

eliminated by subsequent normalizing. These features, which are important in the practical application of titanium steels, were unfortunately not considered in the author's recent paper on phosphorus-titanium steel (5), because the experience then reported was acquired only with small ingots that were not soaked at a high temperature before forging. The titanium carbide was thus not taken into solution in the steels studied at that time, and did not increase the strength and hardness.

Another factor should be considered, however, in comparing the results shown in Fig. 3 with those in the previous paper (5), and that is the amount of titanium present. Most of the steels studied in the former paper contained 0.40 per cent or more titanium, while in Fig. 3 half as much is nearly the maximum. There is a perceptible tendency in Fig. 3 for the strengthening to fall off, and the ductility and toughness to improve, even in the as-rolled steel, as the titanium content approaches or exceeds 0.20 per cent. This is probably due to the fact that there then appears a definite decrease in the amount of pearlite in the steel, and this factor begins to counteract the hardening effect of the titanium carbide dissolved in the ferrite. With steels containing over 0.40 per cent titanium there would, of course, be much less pearlite in the structure, and better ductility with lower strength would naturally follow.

The microstructures of some of the steels included in Fig. 3 are of interest in this connection and are shown in Figs. 4 to 11 inclusive. The plate structures with low titanium are seen to be less banded than the others, and with titanium around 0.20 per cent there is decidedly less pearlite. The weld structures in the coarse zones show less coarsening with about 0.20 per cent titanium.

Conclusions

Thus two especially important factors governing the properties and usefulness of titanium steels are, first, the percentage of titanium in relation to the carbon content, which influences the amount of pearlite in the structure, and second, the temperature and time of the last heat treatment above the critical range. That heat treatment determines in which of the two following ways titanium will affect the properties and usefulness of a low alloy steel:

(A) With normalizing *below* about 2000 degrees Fahr. titanium improves the ductility and impact resistance but with comparatively limited, if any, increase in yield and tensile strengths.

(B) With heat treatment *above* about 2000 degrees Fahr. (1095 degrees Cent.) titanium increases the yield and tensile strengths, sometimes as much as 50 per cent, but gives lower ductility and impact resistance. The decrease in the latter properties may be corrected by mechanical work, such as forging, without serious impairment of the improved strength.

The differences in properties resulting from these two methods of heat treatment are probably due to a difference in the mode of titanium carbide dispersion. Under the conditions of the first method, titanium carbide is not appreciably soluble, and a coarse dispersion results. Under those of the second method, the titanium carbide is dissolved, and either held in solution or precipitated in a finely dispersed condition. This may be achieved with moderate cooling rates, quenching not being necessary.

ACKNOWLEDGMENTS

Acknowledgment is made to the Titanium Alloy Manufacturing Company for supplying the facilities required for making the tests here reported, and for permission to publish the results. The author also wishes to record his appreciation of the capable assistance of numerous associates on the technical staff of the same Company, especially Mr. A. S. Yocco, who made many of the experimental ingots and most of the mechanical tests. Further thanks are due to Dr. R. H. Aborn, of the Research Laboratory, United States Steel Corporation, for supplying the 1.5-inch rounds of the 0.35 per cent titanium steel used in the investigation; and to the Otis Works of the Jones and Laughlin Steel Corporation, and Mr. S. W. Whitelaw, metallurgist, for treating the plate-steel ingots with titanium and furnishing the plates that were tested.

References

1. W. Hume-Rothery, G. V. Raynor, and A. T. Little, "On the Carbide and Nitride Particles in Titanium Steels," *Journal,* Iron and Steel Institute, Vol. 145, 1942, No. 1, p. 129.
2. A. Buttinghaus, "The Iron End of the Iron-Titanium-Carbon System," *Technische Mitteilungen Krupp A, Forschungsberichte,* 1938, p. 67.
3. R. E. Bannon, "Effect of Titanium on the Hardness and Microstructure of Heat Treated 18 Per Cent Chromium Steel Ingots," TRANSACTIONS, American Society for Metals, Vol. 25, Sept., 1937, No. 3, p. 737.
4. G. F. Comstock, "The Strain Aging of Killed Low-Carbon Steel, with Particular Reference to the Effect of Titanium," A. S. T. M. Preprint, June, 1943.
5. G. F. Comstock, "Some Properties of Phosphorus-Titanium Steels," TRANSACTIONS, American Society for Metals, Vol. 30, June, 1942, No. 2, p. 337.

DISCUSSION

Written Discussion: By J. W. Price, Jr., metallurgist, Carnegie-Illinois Steel Corp., Munhall, Pa.

Mr. Comstock's paper has been read with considerable interest, and it is believed that the author should be complimented for drawing the attention of a group such as this to the fact that titanium is a useful hardening element in steels, as well as a deoxidizer and a carbide stabilizer.

During the past several years, we have been experimenting with titanium as an alloying element in low alloy high tensile steels, and our results are in close agreement with those pointed out in this paper. When we began to work with titanium as an alloying element, it was with the idea of using it as a substitute for vanadium in high tensile welding steels. Our experience with vanadium had shown that on cooling from rolling temperatures, considerably higher physical properties were obtained than could be obtained on the same material after normalizing. It was reasoned that this was due to the circumstance that, at the relatively high temperature to which the steel was heated for rolling, the vanadium would be largely in solution in the austenite, and could therefore act as a hardening element upon cooling, whereas on subsequent normalizing, the temperature is not sufficiently high to put all of the vanadium carbide into solution and on cooling from the normalizing temperature it would be inactive as a hardening element.

A number of heats of plain carbon structural plate steel were made with titanium additions varying from 0.02 to 0.08 per cent, and it was found that, as the titanium addition increased, the as-rolled physical properties also increased. Likewise, as the titanium addition increased, the drop in physical properties after normalizing increased. We believe that this is due to the fact that titanium carbide behaves in about the same manner as vanadium carbide.

Weldability tests on these titanium bearing heats indicated a considerably superior weldability to that of some steels which rely on more easily soluble carbide-forming elements for their physical properties. This was also attributed to the solution characteristics of the titanium carbide. In other words, a narrower zone of the plate than that which is heated above the ordinary critical range in welding is heated sufficiently high to permit much titanium carbide solution, and also the time at such temperature is sufficiently short that solution may be incomplete. We have believed for some time that the good weldability of manganese-vanadium structural steels could, at least in part, be accounted for by this explanation, and we now believe that it can be applied even more definitely to the titanium-bearing steel.

In order to produce an appreciable increase in physical properties by the addition of titanium it is necessary to add an amount sufficient to give a ladle analysis of 0.03 per cent titanium or greater. Heats containing 0.05 to 0.07 per cent titanium show in the as-rolled condition an increase in yield point of 10,000 to 15,000 pounds per square inch, and a similar increase in ultimate strength.

It is believed that these results offer some evidence in support of Mr. Comstock's contention that titanium has considerable hardening power when the austenitizing temperature is sufficiently high to put it in solution.

We would like to ask the author whether or not he considers some of the titanium contents he has discussed in his paper (0.30 and 0.70 per cent) commercially practical for basic open-hearth steel. Our experience indicates that mold additions do not give uniformly satisfactory results, nor have we been able to obtain titanium contents over about 0.10 per cent consistently by means of ladle additions.

Oral Discussion

RICHARD W. HARGIS:[1] I would like to ask the author if he has had any experience with titanium treated steels of about 0.01 per cent in heavy forging work ranging up to 20 inches in diameter, particularly relative to refining the grain size in short heat treatments either normalizing or annealing after forging.

JOHN F. ECKEL:[2] Mr. Comstock's presentation led me to believe that he felt the increase or change in physical properties was the result of possible solution hardening in the alpha phase. I wonder if he has any information on how titanium may affect the solubility of carbon in the alpha phase.

SAMUEL L. HOYT:[3] Mr. Comstock is dealing with very interesting subject matter here. I believe titanium is a rather difficult element to handle properly in steel and requires careful experimental work, such as Mr. Comstock has presented this morning. For welding applications, the manganese-titanium steel is well known and I should like to ask Mr. Comstock if, in that case, the peculiar behavior of titanium is not utilized? That is, not until the steel is heated to some fairly high temperature is the titanium carbide dissolved, and in that way becomes an effective hardening aid. In other steels air cooling is not always sufficient to give the strength needed.

Other applications which involve about the same behavior are brazing, silver soldering, and so forth, particularly where it is desirable to keep the cost down. In other words, by utilizing the air hardening capacity which titanium steel acquires upon heating to temperatures above those normally used, it may be possible to secure good properties without subsequent heat treatment.

W. E. JOMINY:[4] One of the subjects that has always intrigued me in connection with most elements is the effect on resistance to wear. It was a pet subject of mine four or five years ago. Wear resistance is something about which we know very little, because we do not seem to have any standard method for measuring it. In the description of the properties of elements in the days before these elements were scarce, there was usually a statement that it develops resistance to wear. I have not heard that denied about titanium. As a matter of fact, in my own experience, titanium as an addition agent to cast iron seems to give very good wear resistance, apparently titanium carbide being the reason for that behavior. It has the added advantage in that in cast iron the material is not hard to machine since it does not increase the hardness of the cast iron. It does seem to increase the abrasion on the tool in cutting, however, as you would expect a wear-resisting material to do. I have not seen many data on the effect of titanium carbide on wear resistance in steel. I have found it to be very

[1]Engineer, Isaacson Iron Works, Seattle, Wash.
[2]Associate professor of metallurgy, Purdue University, Lafayette, Ind.
[3]Technical adviser, Battelle Memorial Institute, Columbus, Ohio.
[4]Metallurgist, Dodge Chicago Plant, Division of Chrysler Corp., Chicago.

satisfactory in piston rings and cylinder iron. I wonder whether Mr. Comstock would be able to give us any comments in that regard?

Author's Reply

I would like to express my appreciation to all those who have shown their interest in the paper by the various discussions that were offered. I am especially grateful to Mr. Price for his very interesting remarks in support of the paper. In regard to his question as to whether it is practical to secure more than 0.1 per cent residual titanium in basic open-hearth practice, I will have to admit that is a difficult problem and that we can only offer possible suggestions as to how it might be done in practice with commercially attractive results. I believe that the open-hearth men will have to find out the best way to do that for us, and I think it probably will be done in a few years. The trouble seems to be the oxidizing effect of the open-hearth slag on top of the ladle, and if that is controlled in some practical way, so the titanium is not oxidized out of the steel by the slag on top of the ladle, I believe it will be possible to secure higher recoveries of larger amounts of titanium from ladle additions.

Mr. Hargis asked if we had any experience with titanium in very large forgings, and I am afraid I will have to admit that we do not have any special data to offer particularly on that subject, but when titanium treatment is applied to steel, so that you get an amount of titanium recovered on the order of 0.01 per cent, it has somewhat the same effect as aluminum in giving a finer grain size. Probably with aluminum that is due to the formation of aluminum oxide; in the case of titanium I believe it is due to the formation of titanium-carbo-nitride. This compound forms nuclei in the steel before the steel freezes, so that more primary crystals of steel start to form in a given volume of melt and none of them can therefore attain such a large size.

Mr. Eckel asked for the effect of titanium on the solubility of carbon in the alpha phase. All we know about that is expressed in the diagrams that are shown in the preprint, which are taken from German records, and which seem to show that the solubility of carbon in ferrite is slightly increased by the presence of titanium.

Dr. Hoyt spoke about the weldable manganese-titanium steels. It is true that in these steels, which are generally used in the form of as-rolled plate, advantage is taken of the strengthening effect of titanium. Mr. Price's remarks throw some light on this subject, and he mentioned that the weldability of the titanium steel was found to be superior to that of similar steels without titanium.

Dr. Hoyt's suggestion that the titanium steels, strengthened by high-temperature heat treatment, should maintain their properties well on brazing or silver soldering is an interesting one that seems plausible, and should be carefully investigated.

In regard to the wear resistance that Mr. Jominy mentioned, that has been extremely interesting to us, but the few wear tests that we made on titanium cast irons did not seem to support Mr. Jominy's experience very well. Possibly that was because all our tests were made without any lubrication, and were therefore not comparable to normal service in an engine cylinder. We did find, however, that titanium is very effective for decreasing the grain size of the cast iron, particularly the size of the graphite, and for improving machinability.

NOTCHED BAR TENSILE TEST CHARACTERISTICS OF HEAT TREATED LOW ALLOY STEELS

By G. Sachs, J. D. Lubahn and L. J. Ebert

Abstract

Previous tests on notched alloy steel tensile test bars revealed severe embrittlement if the strength level of the steel exceeded 200,000 pounds per square inch. However, the notch strength values of such high strength steels scattered considerably. Therefore, a systematic investigation was initiated in order to determine the influence of various factors on the results of the notched bar tensile test.

In order to eliminate bending stresses which considerably reduce the notch strength, a new "concentric" test fixture was developed.

Decarburization was found to increase the notch strength; while careful grinding and polishing of the notch fillet, in combination with the concentric test fixture, yielded throughout uniform results. Thus, the results of the notched bar tensile test can be used to obtain reliable additional metal characteristics, which cannot be obtained by any other method.

The first part of this investigation dealt with the effects of notch radius. The transverse elastic strain, the notch strength, and the notch ductility, of a notch-ductile steel, having a strength level below 200,000 pounds per square inch, were almost independent of the notch radius, between zero and $\frac{1}{32}$ inch. This indicated that the transverse stress, or triaxiality, in the restrained notch section was little affected by the notch radius, within this range. Only when the notch radius became rather large, the notch strength, and correspondingly the transverse tension, decreased with increasing radius, while the notch ductility simultaneously increased. The notch strength of a steel having a high strength level, however, was larger the larger the notch radius, because of the correspondingly smaller stress-concentration in the notched section. The notch strength increased up to a notch radius of $\frac{1}{32}$ inch, and then decreased, because of the

This paper represents the third and fourth reports on the research program conducted at Case School of Applied Science under the sponsorship of the International Nickel Company.

A paper presented before the Twenty-fifth Annual Convention of the Society, held in Chicago, October 18 to 22, 1943. Of the authors, G. Sachs is professor of physical metallurgy, J. D. Lubahn and L. J. Ebert are research assistants, department of metallurgical engineering, Case School of Applied Science, Cleveland. Manuscript received May 12, 1943.

decreasing transverse tension. The stress concentration also explained the varying shapes of the stress-strain curves for the notched section.

In the second part of the investigation, results of tests with an "eccentric" test fixture were discussed. The superposition of bending on tension generally reduced the notch strength more the higher the strength level (or the smaller the notch ductility), and the larger the eccentricity. Above a certain eccentricity, the notch strength of a steel became smaller, the higher the strength level; i.e., the eccentric notch strength measured primarily the inherent (notch) ductility of the steel. This could be explained readily by theoretical conceptions.

Introduction

PREVIOUS investigations on notched tensile test bars (1)[1] were made with the immediate purpose in view of comparing various types of low alloyed steels regarding their relative tendency toward "embrittlement" under unfavorable circumstances. It was found that for a 60-degree sharp notch, the behavior of the metal was distinctly one of two types. For steels having a strength level below 200,000 pounds per square inch, approximately, the notch ductility was relatively high, above 2 per cent, say, and the notch strength was consistent and above the ultimate strength. For steels having a strength level above 200,000 pounds per square inch, approximately, the notch ductility was nearly zero and the notch strength scattered widely between values close to the ultimate strength and values as low as 30 per cent of the ultimate strength. The scattering of the notch strength values and the inaccuracies of measuring the notch ductility by the method used at that time made it impossible to draw definite conclusions regarding the behavior of the metal and to make comparisons between different steels.

In view of the difficulties encountered in the investigation made heretofore, it was considered advisable to continue the investigation along new and more fundamental lines. The aim of the new program might be summarized as an effort to determine what variables are responsible for the scattering mentioned above, to investigate the effect of these variables on the behavior of the metal, and thus eventually to devise a testing method in which these variables can be controlled, for the final purpose of comparing the reaction of different steels to various conditions.

[1]The figures appearing in parentheses refer to the bibliography appended to this paper.

It was also thought that only a detailed systematic study of these variables, eventually clarifying the stress-strain relations in notched bar tensile tests, would eliminate the many uncertainties regarding the practical significance of the metal characteristics revealed by this test.

Of those variables which can be readily investigated, the ones which seemed most likely to be responsible for the scattering were as follows:

1. Variations in surface conditions at the root of the notch.
2. Variations in notch radius.
3. Eccentricity of loading.

This paper deals with the effects of these factors on the results of notched bar tensile tests on heat treated low alloy steels. In order to obtain reproducible results, it was found necessary to develop new procedures of testing.

Regarding surface effects, such as decarburization, it is well known that the use of forming gas (80 per cent N_2, 20 per cent H_2) as a controlled atmosphere for hardening results in decarburization at the surface of the specimen. In the earlier tests (1) the decarburized metal at the root of the notch was not removed after heat treatment, and consequently this soft layer might well have had a pronounced effect on the overall behavior of the notch. Therefore, a few tests, using the newly developed equipment, were made in order to determine the magnitude of this effect; and a technique of preparing the specimens was developed, which eliminated the scattering of the results caused by a varying surface condition.

Regarding the notch radius, it was previously observed that a presumably "sharp" notch actually had a small radius, somewhat less than 0.001 inch. Since there was no way of controlling the size of this small radius, it was thought that variations of the notch radius might be a partial cause of the observed scattering, particularly in view of the large effect of variations in radius on the stress concentration factor in the elastic range of straining (2). In addition, the "sharpness" of a notch is considered generally as a factor of considerable practical and theoretical significance for the strength properties of a steel structure. Consequently, the effects of the notch radius were made the object of an extensive investigation.

For this purpose, a new testing fixture was built which per-

mitted the testing of notched bar tensile test specimens without any superimposed bending. The results of such "concentric notched bar tensile tests" were consistent; this test method appeared to yield characteristics of a heat treated steel which cannot be obtained by means of any other test method.

The previous tests (1) were made with standard ball fixtures similar to those recommended by the A.S.T.M. Standards. The fact that these fixtures resulted in a considerable eccentricity of loading was verified by eccentricity measurements on a number of specimens tested in these fixtures. Thus the importance of eccentricity as a cause of the observed scattering was definitely established.

Several previous investigations (3), (4), (5), dealing with the effect of eccentric loading on the strength of notched and threaded tensile test bars, have used a tapered shim underneath the head or nut. This method is not definite, but creates eccentric loading during a test only as long as the head has not been bent to such an extent that it rests on both sides of the shim.

In order to obtain more exacting conditions, experimentation along new lines was conducted. A testing fixture was designed for applying combined tensile and bending loads to notched tensile test bars. The notch strength in an "eccentric notched bar tensile test" depended primarily on the inherent ductility of the metal, and can be used as a measure of ductility, which apparently is more readily obtained by this method than by any other used at present.

Material and Preparation of Specimens

Five different low alloy steels, previously investigated (1), were available. Only the results obtained on S.A.E. 3140 steel, which was selected as a representative material, are reported here, but some additional tests on the other steels showed that all steels of a similar carbon content behaved fundamentally in the same manner.

The S.A.E. 3140 steel was heat treated, by oil quenching and tempering for 1 hour at different temperatures (1), to different "strength levels", i.e., average tensile strengths ranging from 130,000 to 270,000 pounds per square inch. The properties of cylindrical test bars are assembled in Table I.

Table I

Properties of S.A.E. 3140 Steel Oil-Quenched from 1525 Degrees Fahr.
(0.40% C, 1.37% Ni, 0.66% Cr, 0.76% Mn, 0.26% Si, 0.015% S, 0.020% P)

Tempering Temperature (1 hour) Degrees Fahr.	Specimen Diameter In.	Yield Strength 1000 Psi	Tensile Strength 1000 Psi	Contraction In Area Per Cent	Strength Level 1000 Psi
500	0.351	233	273	52	
	0.351	233	273	52	270
650	0.350	216	241	55	
	0.350	218	242	55	240
740	0.501	200	211	..	
	0.501	198	215	..	
	0.301	...	222	54	220
830	0.500	181	188	57	
	0.500	178	186	57	190
	0.300	185	196	58	
	0.299	185	195	58	
1000	0.500	133	147	60	
	0.500	130	144	60	145
1200	0.500	110	128	62	
	0.500	112	129	62	130

A notch depth of 50 per cent (50 per cent of the cross sectional area removed) was chosen arbitrarily for these tests.[2]

It was first thought that the final machining of the notch might have some surface effects due to the extremely severe cold work at the surface during machining. To determine whether this factor had any effect, a series of concentric notched bar tensile tests was made in which pairs of specimens having a strength level of 240,000 pounds per square inch were tested, each pair being identically prepared in all respects, as described later, except that one of the two had the effects of the final machining (before lapping) removed by an additional pickling. The notch was made 0.003 inch deeper by the pickling operation, thus removing any effects of machining (6). To avoid possible hydrogen embrittlement due to the pickling, the pickled specimens were tempered for 15 minutes at 400 degrees Fahr. (205 degrees Cent.) after pickling. The result of this comparison is represented in Table II. It is possible that the cold working of the surface by machining would have an effect, but that sufficient stock is subsequently lapped off (as described later) to remove the cold-worked metal, or to eliminate any differences introduced by the machining, thus accounting for the failure of the comparison in Table II to show any effects of the cold work by machining.

The effect of decarburization at the root of the notch was deter-

[2]The effects of notch radius should be similar for other notch depths to those for a 50 per cent notch. These relations will be made the subject of another investigation.

Table II
Effect of Pickling on the Notch Strength of 50 Per Cent Notched Tensile Test Bars of 240,000 Pounds Per Square Inch Strength Level

Radius In.	Notch Strength Pickled 1000 Psi	Notch Strength Unpickled 1000 Psi
0.000	210	183
0.002	225	234
0.006	259	298
0.008	306	295
0.016	317	329
0.031	326	326

mined for a single condition by a few additional tests on specimens which were not machined after heat treatment. The depth of decarburization was estimated from a microsection to be about 0.002 inch. The results in Table III show an increase in notch strength by approximately 70,000 pounds per square inch because of the presence of the decarburized surface layer. This effect corresponds to that of a notch radius of 0.004 inch (see Fig. 9). Thus, decarburization relieves the embrittling effect of sharp notches on steels having a high strength level, as was to be expected; and variations in surface conditions, particularly decarburization, at the root of the notch were partly responsible for the scattering observed in earlier tests.

Table III
Effect of Surface Decarburization on the Notch Strength of a 50 Per Cent, Sharply Notched Tensile Test Bar of 240,000 Pounds Per Square Inch Strength Level

Notch Strength with decarburization present — 1000 psi	Notch Strength with decarburization removed — 1000 psi
268	210
272	183
279	

The elimination of these surface effects as a variable resulted in the procedure outlined below.

1. Rough machining of the specimens allowing 0.010 inch for grinding the cylindrical surface after heat treating. 0.010 inch in diameter of stock was left at the notch bottom to be removed after the heat treatment.

2. Heating for 1 hour at 1525 degrees Fahr. (830 degrees Cent.) in a vertical, controlled atmosphere furnace and oil quenching in an air-lift quenching tank (1).

3. Tempering for 1 hour in an electric Lindberg Cyclone forced-convection furnace.

4. Machining of the notch to the final depth and approximate

radius desired, thus removing the surface effects due to heat treatment, such as decarburization.

5. Lapping of the radius at the notch bottom to a smooth contour, using piano wire or a sharpened file for the sharp notch (1) and valve grinding compound.

6. Grinding of the cylindrical surface to 0.500 inch diameter, and of the under side of the head to a flat seat.

Preliminary Tests With Ball Seat Tensile Test Fixtures

In the previous notch bar tensile tests on heat treated steels (1), a gripping device was used, according to A.S.T.M. Standards E8-36, which was supposed to be effective in avoiding bending stress on the specimens.

A number of preliminary tests were made in order to determine the bending stress introduced by this fixture and its effects on the results of notched bar tensile tests. In these tests a number of threaded end specimens having a total length of 3 inches, and provided with a 50 per cent sharp notch (cylindrical diameter 0.50 inch, notched diameter 0.35 inch), were tested in the usual manner.

During such tests the elastic strains at two opposite elements were measured by means of two Huggenberger lever-type strain gages over a gage-length of 1 inch with the notch in center. Circumferentially scribed lines, 0.997 inch apart, were provided to serve as seats for the knife edges of the extensometers, see Fig. 7. Before any measurements were made, each specimen was loaded to 10,000 pounds to permit the specimen to be seated and to preclude the possibility of any shift in position during the actual test. At no time from this point on was the load allowed to fall below 1500 pounds again, so that there was no possibility of a shift in position that might change the eccentricity. With the gages in opposite positions on the specimen the load was increased from 1500 to 9900 pounds, in 300-pound increments. The gage readings were plotted against the load, and the slopes of the straight lines so obtained, Fig. 1, were used to calculate the component of eccentricity in the plane of the two measured strains.[3] The eccentricity measurements were repeated with the gages in positions 90 degrees away from their original positions. Thus, the components of eccentricity were determined in two directions at right angles, and they were added vectorially to give the total eccentricity.

[3] See Appendix I.

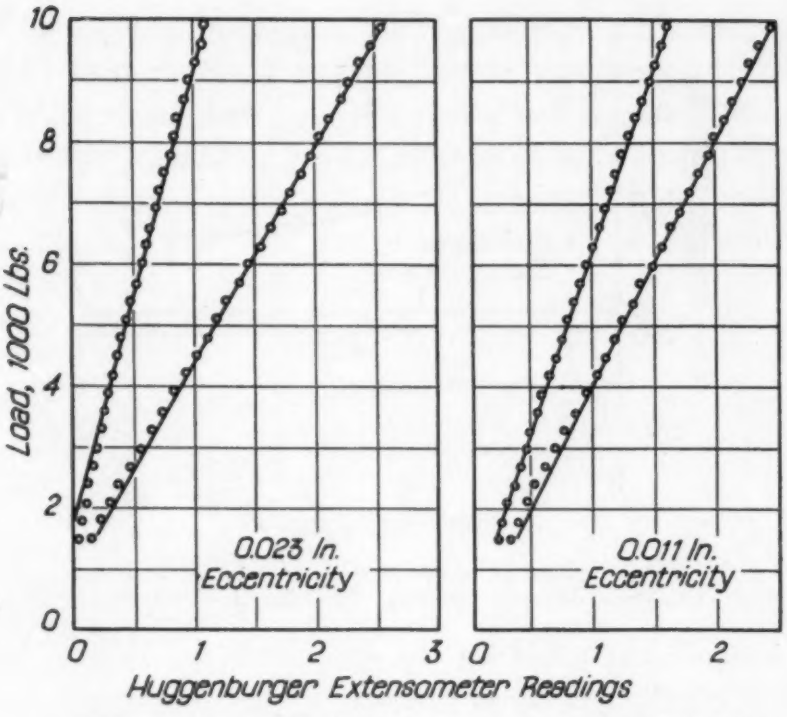

Fig. 1—Examples of Stress-Strain Curves for Opposite Sides of Common Notched Tensile Test Specimens Illustrating the Effect of Eccentricity on Tensile Tests with Ball Seat Fixtures.

Also, in order to reveal the effect of larger eccentricities than those obtainable with ball seat fixtures, a few tests were made with the balls removed and the fixtures displaced to one side as far as possible. Eccentricities of approximately 0.1 inch were measured in such tests. However the stress-strain curves showed a certain curvature which rendered these eccentricity values uncertain.

Two conditions of the S.A.E. 3140 were tested in this manner. The test bars were of two types, differing in the radii at the notch bottom, which were zero and 0.008 inch respectively.

The effect of eccentricity on the notch strength as derived by this method is illustrated in Fig. 2. The notch strength of the notch brittle condition, having a strength level of 240,000 pounds per square inch, and tested in the form of bars provided with a sharp notch, decreases considerably with increasing eccentricity. The range of eccentricity in regular tests, between 0 and 0.020 inch, thus accounts for a scattering of the notch strength by $\pm$ 20 per cent.

This explains part of the scattering encountered in the previous tests (1). The influence of eccentricity decreases with both increasing notch radius and decreasing strength level, and the possible variations in eccentricity during testing with the self-aligning fixture have

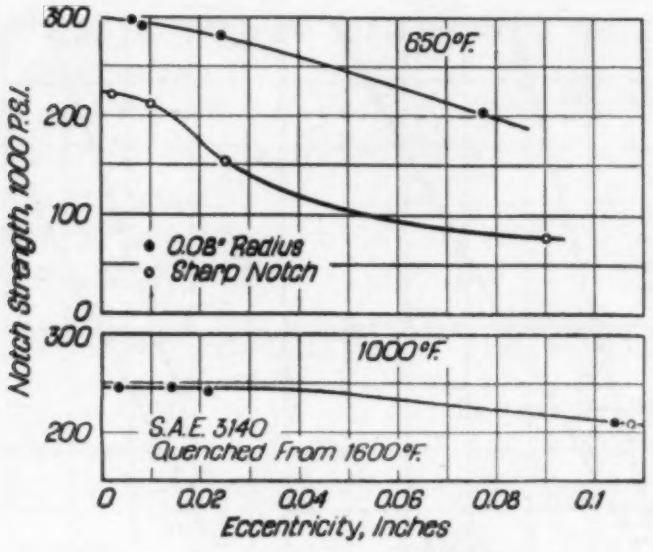

Fig. 2—Effect of Eccentricity and Notch Radius on Notch Strength for Two Tempering Temperatures.

only an insignificant effect on the notch strength of test bars possessing a strength level below 200,000 pounds per square inch, or a high notch ductility.

The presence of considerable bending stress in testing with the self-aligning fixture can be attributed to either the presence of friction in the ball seats which is particularly large in testing very strong metals and/or the irregular seat and force transmission of threaded-end specimens.

The results of these preliminary tests with large eccentricity confirm the previous view that the differences in notch strength of various conditions of the steel, and provided with notches of varying sharpness, may be considerably increased by superimposing a certain amount of bending to the applied tension.

Stress and Strain Measurements

In the earlier tests (1), the transverse strain was determined from measurements with a special micrometer equipped with one chisel-shaped anvil. The readings were tedious and inaccurate and required correction for the wearing away of the metal at the bottom of the notch during the tests. Also, measurements of the diameter after fracture were made previously by means of a measuring microscope. This method also proved very time-consuming and so inaccurate that the errors ($\pm$ 1 per cent) were often larger than were the desired values of reduction of area after fracture, or contraction in area, introduced as "notch ductility".

For the purpose of measuring the average transverse strain in the notched section during the test and at the moment of fracture, a special transverse strain gage was built, which gave more accurate results in less time. This gage consisted of two knife edges which fitted into the notch on each side of the specimen, Fig. 3. One knife edge was allowed to slide freely on a pair of horizontal rods, lubricated with heavy machine oil; the other was fixed with respect to the rods. The knife edges were pulled down into the notch by

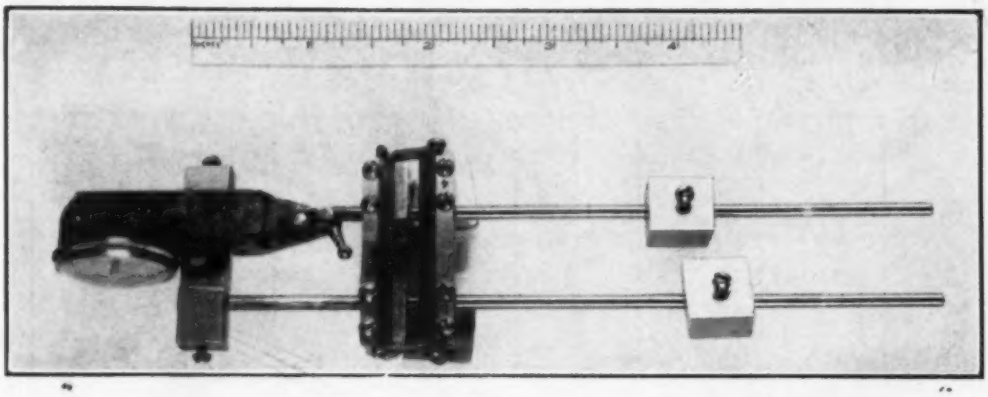

Fig. 3—Gage for Measuring the Average Transverse Strain Across the Bottom of the Notch.

springs connecting them at each end. A Last Word dial gage was mounted on a bar which was clamped to the rods, and had its pin in contact with the movable knife edge. Thus it measured directly the relative movement between the fixed and movable knife edges, i.e., the change in diameter at the root of the notch. The Last Word gage was graduated in such a way that one division represented 0.0002 inch. Reliable results could not be obtained on sharp notches unless the knife edges for the gage were kept sharp.

Load and gage readings were recorded at intervals during the test and up to the breaking point. Damage to the gage at the breaking point of the specimen was prevented by supporting the gage with a string from the head of the testing machine. At the moment of fracture, the two parts of the specimen were projected directly away from the gage with considerable velocity, leaving it hanging on the string. Thus, transverse strain readings could be taken at various intervals during the test, up to point of failure. Fig. 4 shows typical curves obtained when the load is plotted against the gage readings.

From the load measurement and gage readings, the stress and

strain quantities are given by the following equations:

$$S = \frac{4P}{\pi d_o^2} \qquad [2]$$

$$e = \frac{200\,RK}{d_o} \qquad [3]$$

where: S = average longitudinal stress in the notched section, pounds per square inch.
P = load, pounds.
d_o = original diameter of the cross section at the root of the notch, inch.
e = per cent reduction in cross-sectional area at the root of the notch.
R = change in gage reading from the beginning of the test, divisions.
K = value of one division on the gage = 0.0002 inch.

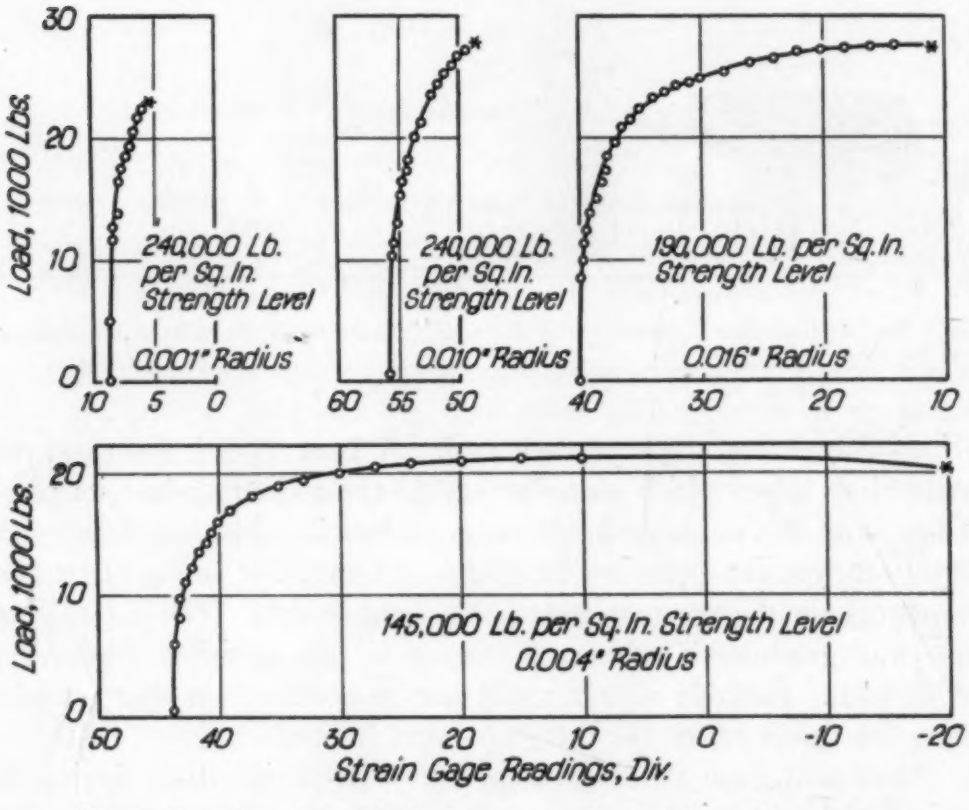
Load, 1000 Lbs.
240,000 Lb. per Sq. In. Strength Level
0.001" Radius
240,000 Lb. per Sq. In. Strength Level
0.010" Radius
190,000 Lb. per Sq. In. Strength Level
0.016" Radius
145,000 Lb. per Sq. In. Strength Level
0.004" Radius
Strain Gage Readings, Div.

Fig. 4—Examples of Load-Deflection Curves Obtained from Notched Bar Tensile Tests.

From curves like Fig. 4, "stress-strain curves" were derived, in which the stress is the average longitudinal stress in the notched section and the strain is defined as the per cent of plastic reduction in cross-sectional area at the root of the notch. If the total strain had been used as the abscissa, the curves would have various slopes, depending on the notch radius, and thus would be difficult to represent for convenient comparison. The use of the plastic strains

eliminates this difficulty, but gives essentially the same shape of stress-strain curve. For the purpose of computing these quantities, it is necessary to know the original area, or the diameter, of the cross section at the root of the notch. This diameter was determined, as in previous tests (1), with the aid of micrometers with one chisel-shaped anvil.

The two principal quantities discussed in this paper are the "notch strength", i.e., the average longitudinal strength of the notched section, and the "notch ductility", i.e., the per cent reduction in cross-section at the root of the notch (or contraction in area) at the breaking point. The "fracture stress" is the ratio of breaking load to the area of the notched section after failure. As "notch strength ratio," the ratio of notch strength to regular tensile strength (strength level) is introduced.

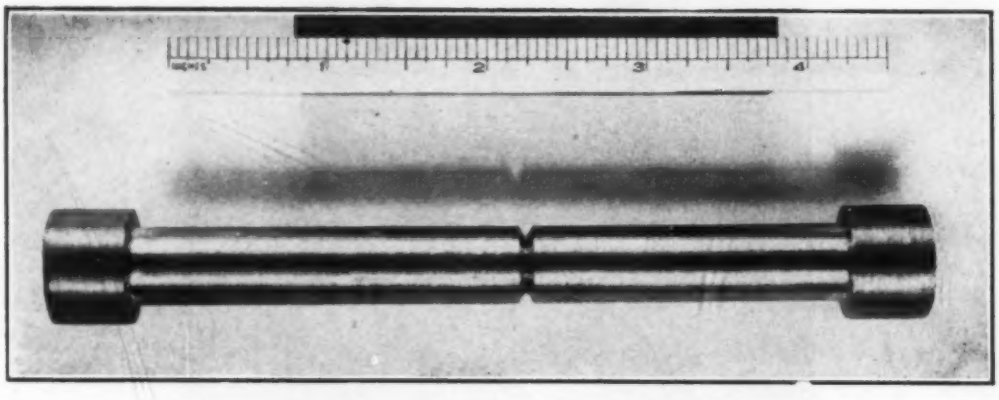

Fig. 5—Specimen Used for Concentric Loading Tests.

Part I
Concentric Notched Bar Tensile Tests and the Effects of Notch Radius

Test Procedure—In this investigation, the scattering influence of eccentricity was kept at a minimum (a) by the use of special accuracy in the final machining of the specimens, and (b) by testing the specimens in fixtures which were designed and constructed with the primary objective of obtaining concentricity of loading.

Button-head specimens, Fig. 5, were used instead of the threaded end specimens for which the earlier fixtures were adapted. These were ground to size on the cylindrical surface, so that they had a snug fit in split adapters. Also, the surface under the head was ground to a plane surface perpendicular to the cylindrical surface.

The use of button-head specimens, prepared with the above precautions, eliminated errors arising from the difficulty of making accurate and reproducible threads to fit the adaptors.

The concentric test fixtures, Figs. 6 and 7, employed several features not present in earlier fixtures, all of which probably contributed to the observed improvement in concentricity of loading. Highest accuracy was extended to those parts of the fixtures which

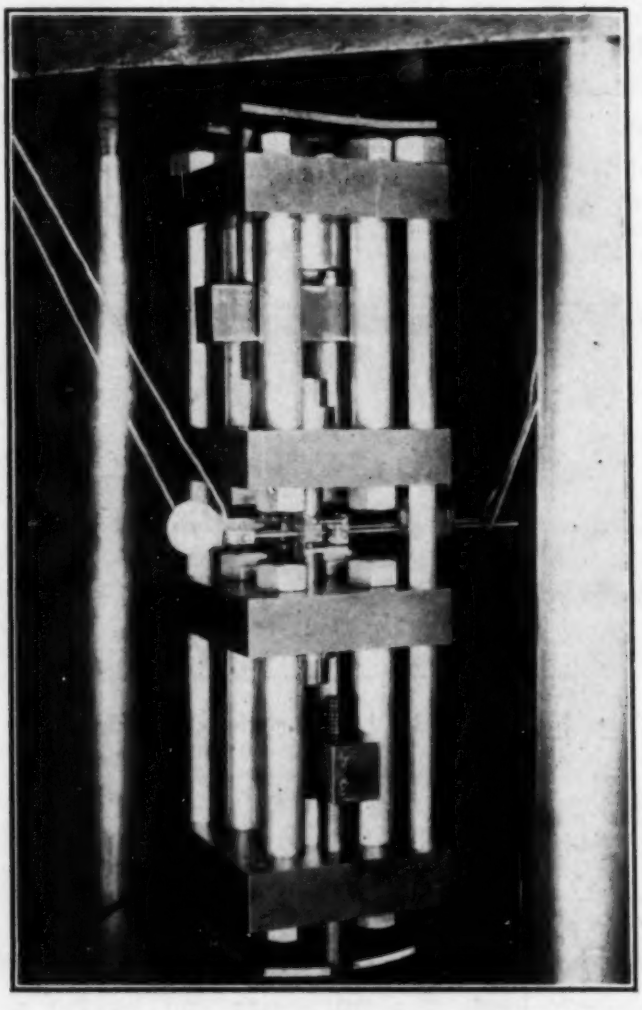

Fig. 6—Fixtures for Concentric Loading with Specimen and Transverse Strain Gage in Place.

connected the specimen to the balls at each end. The fixtures were made from a non-deforming steel in such a way that the centers of the balls were as nearly in line with the axis of the specimen as is possible with regular machining equipment. This was accomplished by careful machining, including grinding and lapping, where necessary.

However, the condition obtained by the best possible machining is not sufficient to produce concentricity of loading because it is possible to have a bending moment in the specimen. Such a condition arises as a result of a misalignment of the parts at the beginning of the test, which cannot be entirely eliminated because of the friction of the balls. To remove the possibility of such an initial misalignment, the parts of the fixture were made to slide on guide rods, which per-

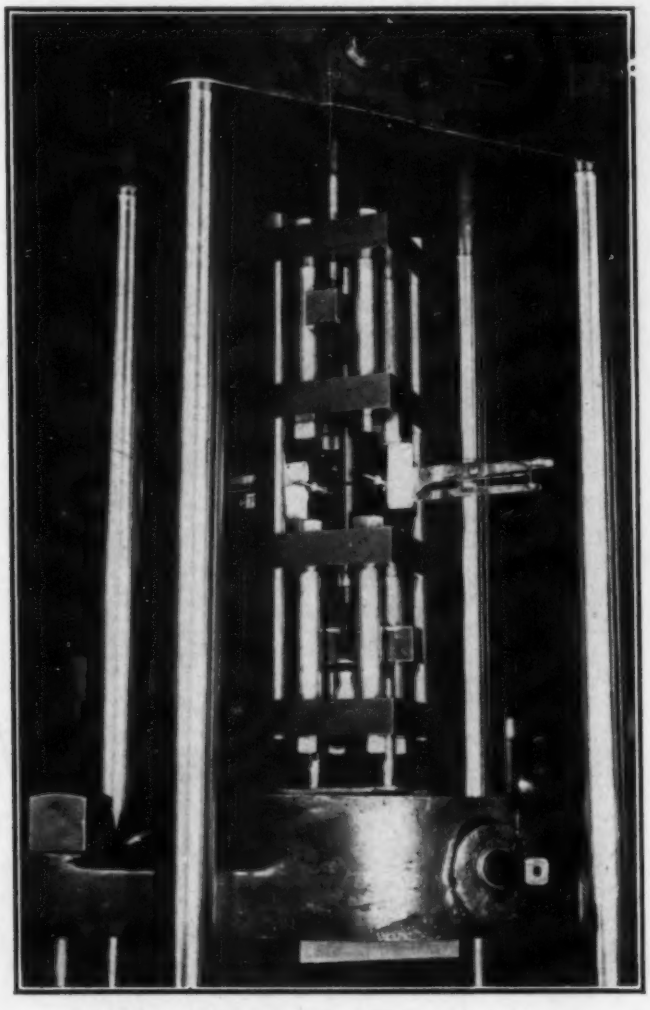

Fig. 7—Experimental Setup for Measuring Eccentricity of Loading.

mitted freedom of motion parallel to the axis of the specimen, but which prevented any misalignment.[4]

In the earlier fixtures the ball seat consisted of a shallow spherical

[4]The smoothness of the various load-deflection curves (see Fig. 4) is an indication of the fact that the fixtures did not stick on the guide rods during the test. Some difficulty in this respect was encountered in early tests because the rods were scored by very small burrs on the edges of the holes. Careful stoning of the corners removed this difficulty.

recess of the same radius as the ball. After several tests had been made, flattened places were observed on the edges of the ball seats. These were apparently caused by the hammering effect of the ball at the moment of breaking of the specimen, and had the effect of shifting the effective position of the ball seat. In the new fixtures used for this investigation, the possibility of damaging the ball seats was precluded by using a special part for the seat, with a deep cylindrical recess just fitting the ball. With this type of arrangement, the ball could never bear against the seat in any other position but the concentric position.

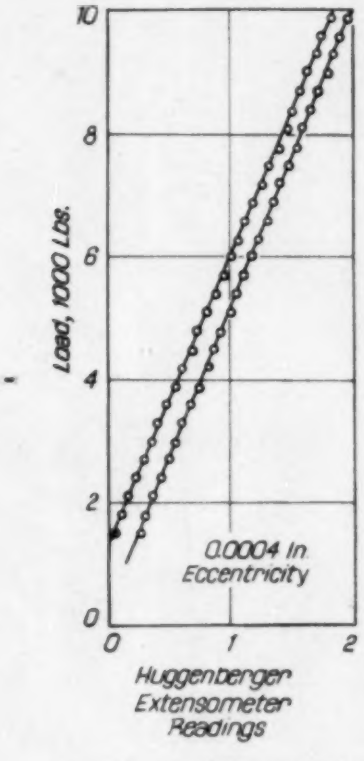

Fig. 8—Examples of Stress-Strain Curves for Opposite Sides of Button Head, Tensile Test Specimens Loaded in the New Concentric Test Fixture.

The amount of eccentricity likely to be caused by the fixtures was again determined by measurements on three specimens prepared for this purpose.[5] They were 7 inches long and were provided with circumferentially scribed lines, 0.997 inch apart, to serve as seats for the knife edges of the extensometers, see Fig. 7. The stress-strain curves of various elements of the test bars were practically

[5] See Appendix I.

identical, Fig. 8, resulting in eccentricities of less than 0.001 inch for all three specimens.

In each series, the radius was varied from zero (sharp notch) to infinity (unnotched specimen) in steps that were determined by available sizes of piano wire and drill rod used for lapping the radius to its final size.

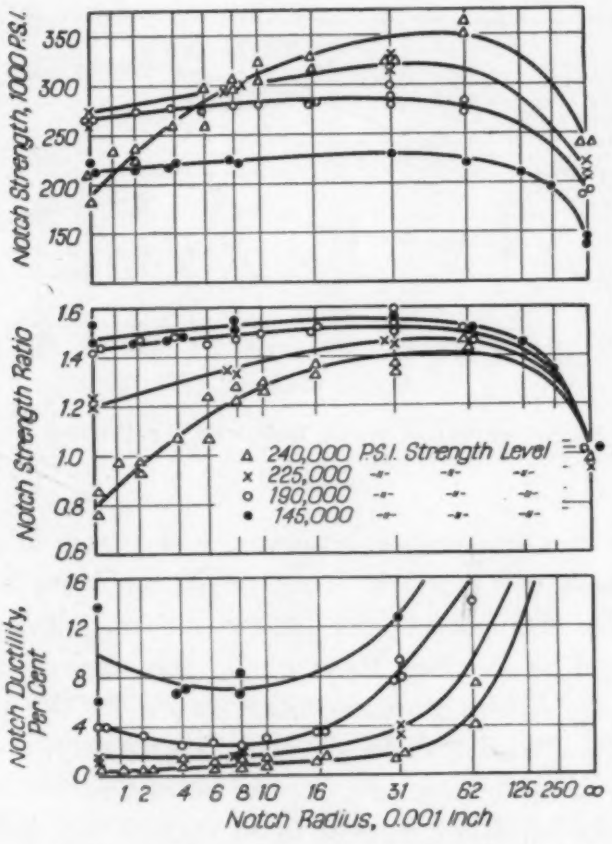

Fig. 9—Effect of Notch Radius on the Notch Characteristics of Heat Treated S.A.E. 3140 Steel.

The notch strength, the notch ductility, and the fracture stress were determined in each test, if possible. The results are represented in various manners in Figs. 9 and 10. The notch strength values obtained by the new method scatter considerably less than results of earlier tests. Whereas previously the notch strength varied by $\pm$ 30 per cent from a mean value for a 50 per cent sharply notched test specimen of 250,000 pounds per square inch strength level (1), in the present investigation, the variations in notch strength did not exceed $\pm$ 8 per cent for the same conditions, Fig. 9. This greater consistency of results must be caused by the concentricity of loading and the elimination of surface effects, thus confirming the opinion

that the earlier scattering was due to a lack of control of these variables. The previously observed scattering increased with increasing brittleness. The magnitude of scattering of the present results, however, is apparently independent of the brittleness, but it is caused rather by the generally expected variations in composition and homogeneity.

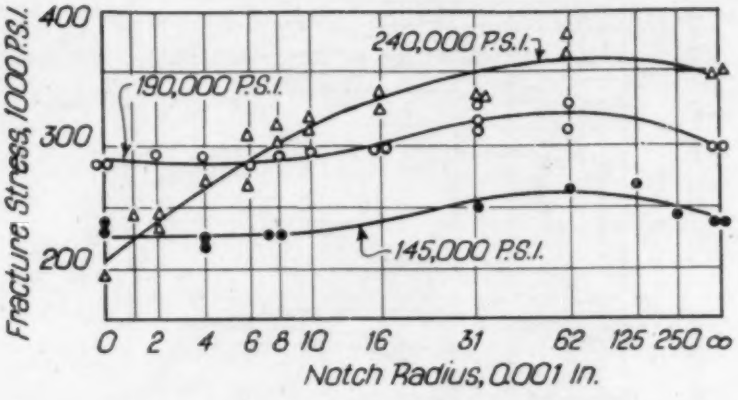

Fig. 10—Effect of Notch Radius on the Fracture Stress of Notched, Heat Treated S.A.E. 3140 Steel.

The notch ductility values, however, still scatter widely (Fig. 9), showing as much as ± 50 per cent deviation from a mean value, even for the 145,000 pounds per square inch strength level. These variations cannot be ascribed to errors in the strain gage, since such errors are negligible in comparison, as shown by the consistency of the points on the load-deflection curves. Apparently, even though the notch strength is quite consistent, the amount of strain up to the breaking point is highly dependent upon factors which have not been discovered and controlled as yet.

The stresses and strains during each test were determined as previously discussed. From the stress-strain curves, see Fig. 14, the yield strength values for various strains were taken, see Fig. 16. It was evident that the scattering of the yield strength values, i.e., variations in the shape of the stress-strain curve, is greatest for both the smaller strains and for the higher strength levels, being as high as ± 20 per cent for 0.1 per cent strain and 240,000 pounds per square inch strength level. Even for the 190,000 pounds per square inch strength level, the variations in the shape of the stress-strain curve for a given notch radius are as great as the variations due to a change in radius from zero to 0.062 inch. The significance of these variations will be discussed later.

Experimental Results

Regarding the effects of the radius at the notch bottom, it is known that the stress distribution during elastic straining (2), or the stress concentration at the notch bottom, is decidedly influenced by the radius, or rather by the ratio of the radius to the outside diameter,

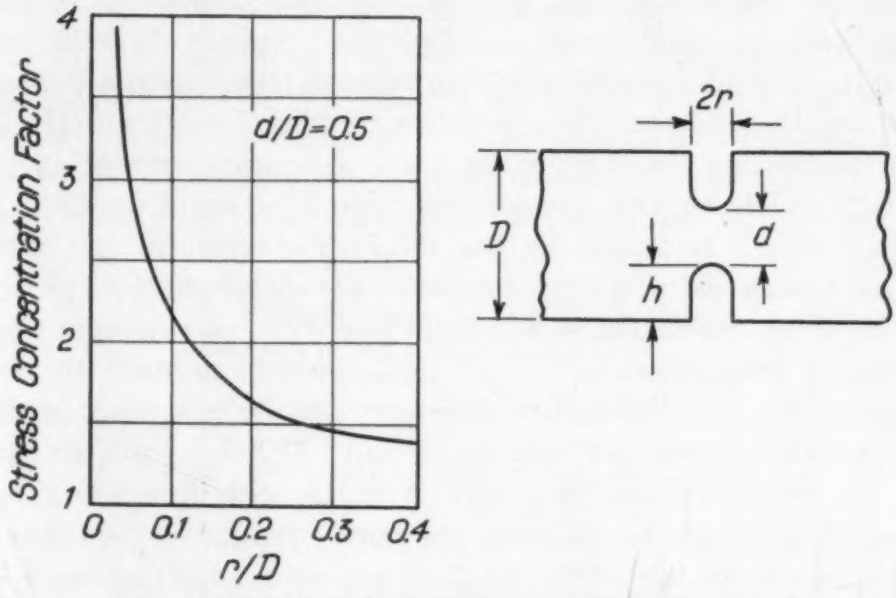

Fig. 11—Effect of Notch Radius on the Stress Concentration in a Flat Notched Bar. (Derived from Frocht).

other factors being constant, Fig. 11. The effect of radius on the results of notched bar tensile tests, however, apparently has not attracted any attention as yet.

The effect of radius on the notch strength and notch ductility for the four investigated strength levels is illustrated in Fig. 9. In order to represent all radii from zero (sharp notch) to infinity (no notch), an abscissa scale was used in which the quantity $\frac{r}{0.2 + r}$ (r in inches) was plotted as uniform scale. Whether this quantity has any physical significance is not known.

The notch ductility varies with both strength level and notch radius, being smaller in general for smaller radii and higher strength levels. Regarding the variation with notch radius, there is little change for notch radii between zero and $\frac{1}{32}$ inch. Above $\frac{1}{16}$ inch radius, the ductility begins to increase more and more rapidly, approaching the value of 50 to 60 per cent for the unnotched condition. For the 240,000 pounds per square inch strength level the

ductility increased gradually and continuously with radius from about 0.3 per cent to about 1.5 per cent. For the lower strength levels there is apparently a minimum in the ductility for a radius of approximately 0.005 inch.

For a notch of infinite radius (unnotched bar) the notch strength is, of course, identical with the tensile strength. With decreasing radius, the notch strength gradually increased above the tensile strength to a value as much as 50 per cent greater than the tensile strength. For all three investigated strength levels, such a maximum value was reached for a notch radius of approximately 0.031 inch. With still smaller notch radii, the notch strength decreases again by amounts which become greater for higher strength levels. This decrease, which is caused by the embrittling effect of the sharper notches, can be more readily compared for different strength levels by using a representation in which the notch radius is plotted against the "notch strength ratio" (or ratio of notch strength to tensile strength), Fig. 9. This figure illustrates for the two lower strength levels, 145,000 pounds per square inch and 190,000 pounds per square inch, the small decrease in notch strength with decreasing notch radius, which is nearly the same for both strength levels, while the notch strength for the 240,000 pounds per square inch strength level decreases markedly with decreasing radius. Thus the embrittling effect of sharp notches is insignificant for strength levels up to 190,000 pounds per square inch but very pronounced for a strength level of 240,000 pounds per square inch.

This decrease in notch strength with decreasing notch radius in the vicinity of zero radius is not sufficient to account for the scattering of previous results (1), even for the 240,000 pounds per square inch strength level. In earlier tests the radius might have varied between zero and as much as 0.0005 inch. This would explain a scattering of only $\pm$ 2 per cent, whereas the previously observed variations were as much as $\pm$ 35 per cent.

As observed previously, values of notch strength ratio below 1.0 are definitely connected with the variations in notch ductility. As long as the ductility is above 2 per cent, approximately, the notch strength for a fairly sharp notch (zero to $\frac{1}{32}$ inch) radius is 40 to 50 per cent higher than the ultimate strength, such as for the 145,000 pounds per square inch and 190,000 pounds per square inch strength levels. If the ductility is less than about 2 per cent, the notch strength falls below this ideal value by amounts which are

greatest for the sharpest notches, which in turn yield the lowest values of notch ductility.

The fracture stress, defined as the breaking load divided by the cross-sectional area at the moment of failure, is represented in Fig. 10. The curves clearly demonstrate that this fracture stress has no simple physical meaning. If the notch ductility again exceeds the value which is the dividing line between the notch-brittle and the notch-ductile conditions, the fracture stress depends only slightly upon the notch radius. However, all conditions, including the condition which has a strength level of 240,000 pounds per square inch, exhibit a definite maximum of fracture stress if the notch radius is approximately $\frac{1}{16}$ inch. This cannot be explained at present. With

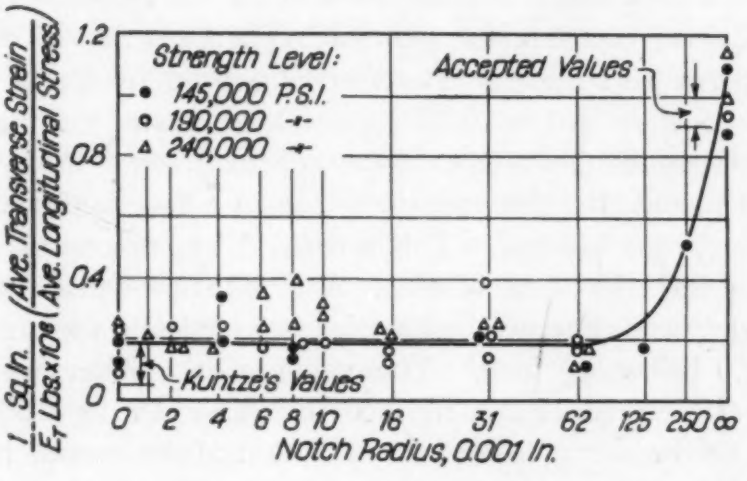

Fig. 12—Effect of Notch Radius on Elastic Contraction of the Notched Section.

small notch radii, the fracture stress of the steel having the high stress level is very considerably reduced, obviously because of the presence of the high initial stress concentration. The effect of this stress concentration on the fracture stress, however, is almost completely eliminated if a strain of as little as 2 per cent precedes the failure.

Theoretical Relations

The increase of strength, above the value of the tensile strength, by notching has been ascribed to the development of transverse tension which restricts the flow of the metal under the action of the applied longitudinal tension (1). This conception is confirmed by a study of the elastic characteristics of the notched section of the

test bars provided with notches of various radii. If the inverse slope of the stress-strain curve for a notched bar, see Fig. 4, i.e., the ratio of the average transverse strain to the average longitudinal stress, is determined for low loads where the stress-strain curve is straight, within the limits of accuracy the inverse transverse modulus is obtained, Fig. 12. This value depends upon the elastic modulus, and Poisson's ratio of the steel, and also upon the average transverse stress in the notched section (7), (8). The experimental values in Fig. 12 scatter considerably, because of the limited sensitivity of the transverse gage, which was designed primarily for the measurement of small plastic strains, i.e., of strains at least 10 times as large as the greatest elastic strains. However, the large number of tests determines a sufficiently definite trend of the curve of inverse transverse modulus versus notch radius. The presence of transverse stress reduces this specific elastic contraction from the ratio of Poisson's constant ($m = 0.28$ approx.) to elastic modulus ($E =$ 30,000,000 pounds per square inch approx.), or 9×10^{-8} square inches per pound, for the unnotched bar to a fraction of this value for a sharply notched bar. This is caused by the restraint of contraction by the transverse tension. Fig. 12 shows that the average transverse stress in the notched section is practically the same for all notch radii below $\frac{1}{32}$ inch. The value of the inverse transverse elastic modulus $1/E_T$ in this range of notch radii (for a 50 per cent notch) is, on the average, 19 per cent of that of the inverse transverse elastic modulus of an unnotched bar $\frac{m}{E}$. The average transverse stress S_T can be determined from this value according to the following relations for the elastic transverse strain e_T (2):

$$e_T = -\frac{S_L}{E_T} = \frac{1}{E}(S_T - mS_L - mS_T)$$

$$-\frac{S_L}{E_T} + \frac{mS_L}{E} = \frac{S_T}{E} - \frac{mS_T}{E}$$

$$S_L\left(\frac{m}{E} - \frac{1}{E_T}\right) = S_T\left(\frac{1}{E} - \frac{m}{E}\right)$$

$$\frac{S_T}{S_L} = \frac{E}{1-m}\left(\frac{m}{E} - \frac{1}{E_T}\right) = \frac{1}{1-m}\left(m - \frac{E}{E_T}\right)$$

$m = 0.284$
$E = 30{,}000{,}000$ psi.
$1/E_T = 0.19 \times 10^{-4}$ (see Fig. 11)

$$\frac{S_T}{S_L} = \frac{1}{1-0.284}(0.284 - 3 \times 10^7 \times 0.19 \times 10^{-8}) = 32 \text{ per cent}$$

Thus, for the investigated sharp notches, an average transverse stress (S_T) of approximately 32 per cent of the applied longitudinal stress (S_L) results from this conception. If the metal flows under a constant shear stress:

$$t = \frac{S_L - S_T}{2} = \frac{Sn}{2}$$

where Sn is the flow stress in pure tension, the longitudinal stress required to stretch the notched section would be

$$S_L = Sn + S_T,$$

or a value equal to the sum of the stress in pure tension plus the transverse stress. In the present case, this would mean that 1.47 times the stress in tension is necessary to stretch correspondingly the notched bars.

This relation readily explains the effect of sharp notching on the tensile strength, Fig. 9, provided that the notch ductility is sufficiently high. In such a case, the notch strength is only a particular value of the longitudinal stress, determined by identical differential relations between strain-hardening and reduction in area as those of unnotched bars (1). It is particularly interesting that the plastic flow preceding the point of maximum load does not reduce materially the magnitude of the transverse stress. The shape of the notch strength versus notch radius curve for sufficiently ductile specimens is thus also accounted for by the presence of a transverse stress, proportional to the difference between notch strength and tensile strength. Consequently, there is little change in the magnitude of transverse stress with notch radius up to a radius of $\frac{1}{32}$ inch.

On the contrary, the measurements of elastic stress have established definitely the presence of a stress concentration, or stress-peak, which increases tremendously if the notch radius decreases to small values, Fig. 11. Thus, this stress concentration has only an insignificant influence on the notch strength as long as the notch ductility is sufficiently large. Evidently the large plastic strain occurring before failure, for low strength levels, is sufficient to cause a redistribution of the stress, resulting in a more uniform distribution, which differs only little for various, but small, notch radii.

On the other hand, the stress concentration must be responsible for the loss of notch strength for the 240,000 pounds per square inch strength level in the region of small radii. Under these conditions the inherent lack of ductility of the metal makes it impossible to even out the nonuniform stress distribution before failure, and consequently the specimen breaks at a lower average stress than would be present for a uniform stress distribution.

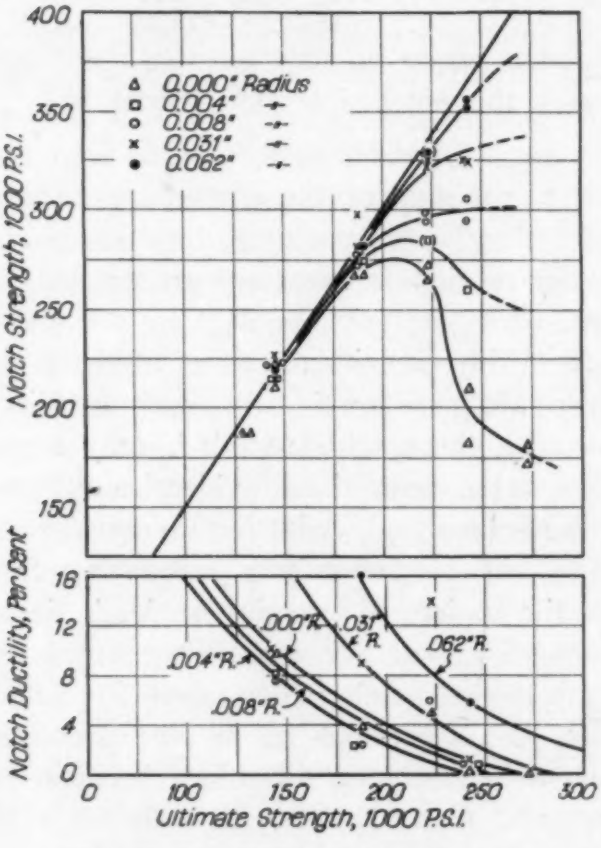

Fig. 13—The Effect of Strength Level and Notch Radius on the Notch Strength and Notch Ductility of S.A.E. 3140 Steel Specimens with 50 Per Cent Notches.

The effects of strength level on the notch strength and notch ductility can be perceived more readily by using a representation in which these quantities have been plotted against the ultimate tensile strength of an unnotched bar of the same material, Fig. 13. The notch ductility varies almost linearly with strength level, becoming very small at 250,000 pounds per square inch for all radii up to $\frac{1}{32}$ inch.

As discussed previously, variations in the notch ductility are reflected in the notch strength. For the 0.062-inch radius, the notch

strength is nearly 50 per cent greater than the ultimate or tensile strength, even for the highest strength level. This behavior is characteristic of steels with a high notch ductility; and consequently the conditions represented by the straight line with the slope of 1.5 are described as "ideal" with regard to ductility.

The notch strength for each of the smaller radii deviates from the "ideal" condition at strength levels which are smaller for the sharper notches. The progressive deviation from the

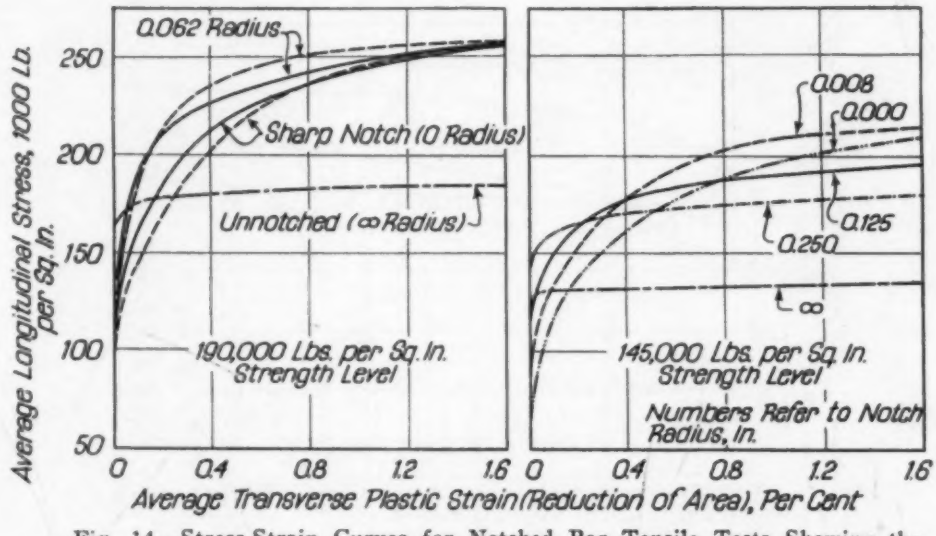

Fig. 14—Stress-Strain Curves for Notched Bar Tensile Tests Showing the Effect of Strength Level and Notch Radius.

ideal condition is characterized first by a gradual decrease in the slope of the curve from 1.5 to zero, then to negative values, resulting in an actual decrease of notch strength with increasing strength level, and finally, a condition where the notch strength becomes less than the ultimate strength. This latter condition occurs for the 0.000-inch radius at a strength level of 220,000 pounds per square inch (for S.A.E. 3140 steel).

Stress-Strain Curves

The two main factors discussed previously that influence the notch characteristics, namely, the presence of an average transverse tension and an uneven distribution of longitudinal stress in the elastic state, are also responsible for the "stress-strain" characteristics of notched tensile test bars in the semiplastic and plastic range, Fig. 14.

The effect of the notch radius on the shape of the stress-strain curves may be observed readily for the lowest strength level, but the variations for the higher strength are so large that they obscure the effects of notch radius. For the 190,000 pounds per square inch strength level, for example, there is almost as much variation between two curves for zero radius or between two curves for 0.062-inch radius as there is between two curves one of which is for zero radius and the other for 0.062-inch radius. The cause of these variations is not known definitely, but a possible

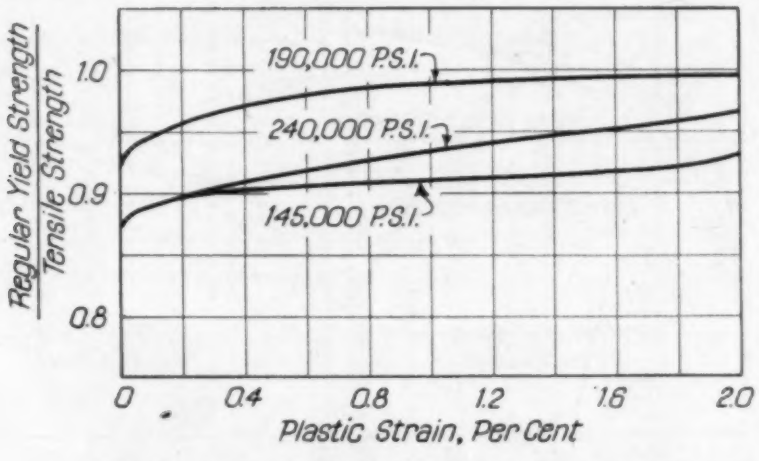

Fig. 15—Strain Hardening Characteristics of S.A.E. 3140 Steel Having Various Strength Levels.

explanation is the presence of residual quenching stress in oil-quenched and tempered steel (9). The magnitude of the residual stress decreases considerably with the increasing tempering temperature or decreasing strength level; and it can be assumed that variations in residual stress also decrease simultaneously. The presence of such varying residual stress, superimposed upon the elastic stress distribution, readily accounts for variations in the stress-strain relations corresponding to the magnitude of the residual stress.

According to the previously discussed conceptions, the shape of each stress-strain curve should depend upon the following factors:

1. The stress concentration factor
2. The average transverse stress
3. The strain hardening characteristics of the steel
4. The residual stresses

The high longitudinal stress at the bottom of the notch, or the "stress peak", is primarily responsible for the shape of the

stress-strain curves in the early part. When the stress peak reaches the yield strength of the metal at the bottom of the notch, plastic flow occurs in that region. Consequently, the stress-strain curve begins to deviate towards higher strains at a low average stress, and this effect continues to a greater extent as a larger proportion of the metal at the notch bottom undergoes plastic strain. Since the stress concentration factor is higher for the sharper notches, the bending off of the stress-strain curve is more pronounced and begins at a lower load for the sharper notches.

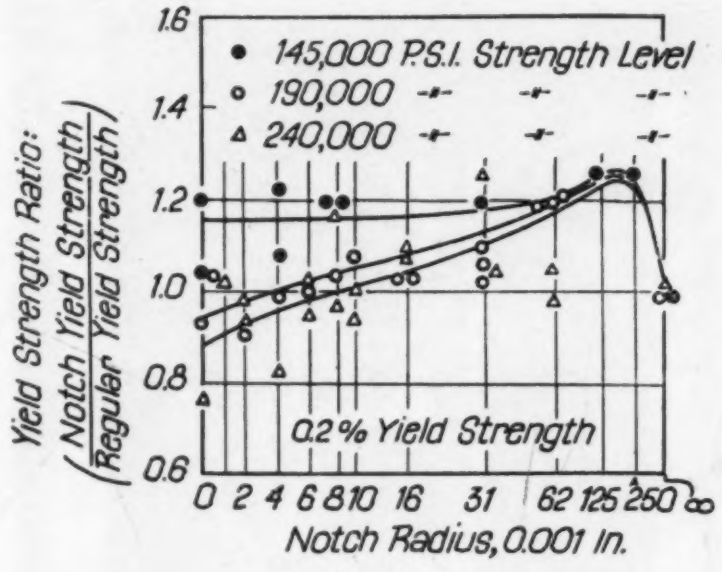

Fig. 16—Variation of Yield Strength Values with Strength Level and Notch Radius.

The transverse tension in the notched section affects not only the elastic part of the stress-strain curve, but it also has a pronounced effect on the rest of the curve. If transverse tension is superimposed upon longitudinal tension, a higher stress is required to produce a given amount of plastic flow. Thus the entire curve tends to be higher than would be the case if no transverse stress were present.

The strain-hardening characteristic of the unnotched metal, as it exists in the three conditions of strength level investigated, are represented in Fig. 15. For the sake of comparison, the ordinates have been brought to a common basis by dividing the stress for a given strain by the tensile strength of the metal. Fig. 15 shows that the metal having the intermediate strength level strain hardens little by small plastic strains, whereas the metal having either a low or a high strength level strain hardens to a considerably

greater degree. These two strength levels differ primarily in the fact that the metal of highest strength level does most of its strain-hardening for strains less than 2 per cent, while the metal of lowest strength level strain hardens little in this region. These differences in strain hardening characteristics among the various strength levels should influence the ordinates of the stress-strain curves for a given strain, but probably to a considerably smaller degree than the presence or absence of transverse stress.

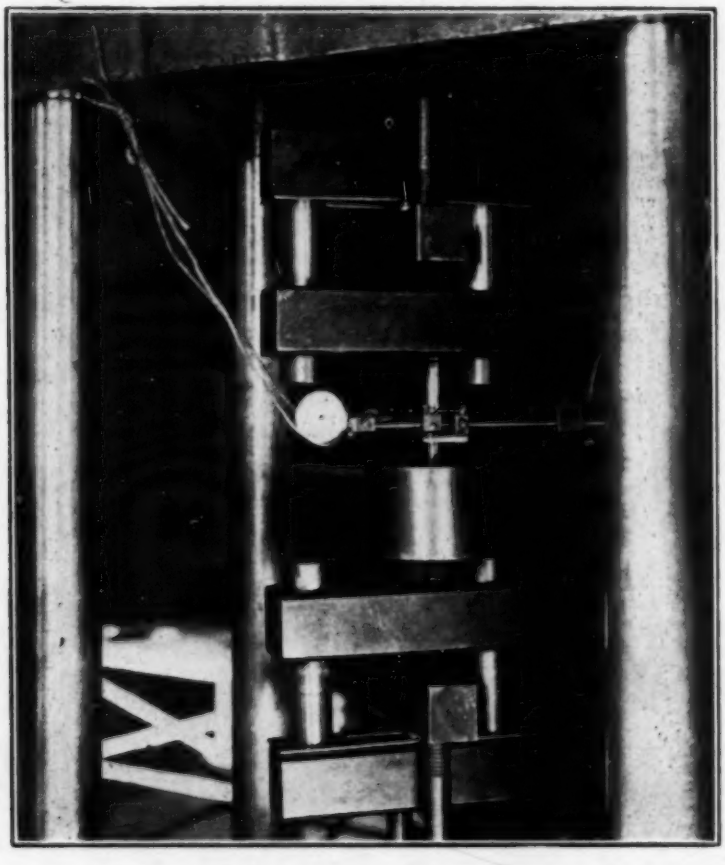

Fig. 17—Tensile Test Fixtures for Producing a Controlled Eccentricity up to 1.5 Inches.

The yield strength values for the sharply notched bars clearly decrease with increasing strength level, Fig. 16. Also, the scattering of the values or their deviation from a trend curve increases with the strength level, as previously discussed. These two phenomena can be explained only by the presence of residual quenching stresses, the magnitude and variations of which decrease with increasing tempering temperature or decreasing strength level.

Part II
Eccentric Notched Bar Tensile Tests and the Effects of Eccentricity

Test Procedure — In order to subject tensile test specimens to a definite additional bending load, a new, rather simple fixture was developed, Fig. 17. It consisted of a modification of the usual ball-seat type, incorporating certain features that made it possible to produce different amounts of eccentricity by only minor adjust-

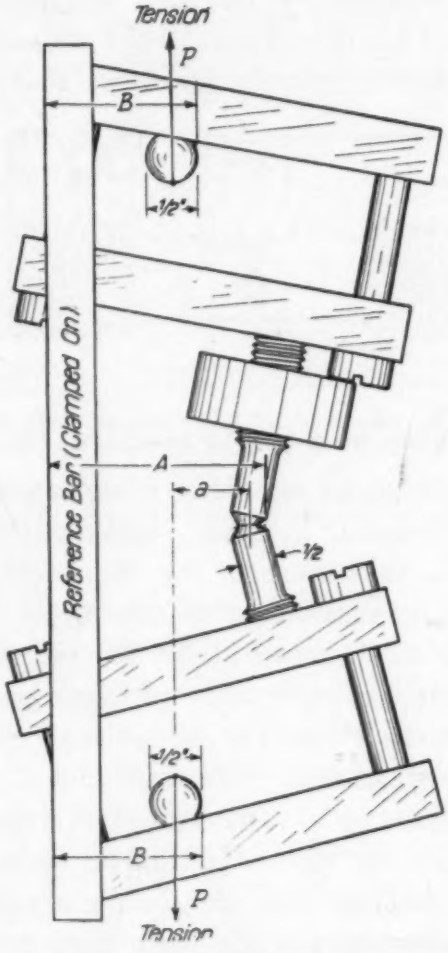

Fig. 18—Method of Measuring Eccentricity. (Fixtures Shown in Exaggerated Position for Sake of Clearness).

ments. The common threaded-end test specimen was held between the cross members of two rectangular frames, and in each test had the same position with respect to the frames. The load was applied to the other cross member of each frame by means of a hardened steel ball which was seated in a second frame connected

with the cross heads of the tensile machine. The hardened balls were seated in the frame that held the specimen by means of hardened steel seats, which had the same radius as the ball. These seats fitted into slots and could be shifted with respect to the specimen by means of shims. By using shims of different widths, the specimen could be shifted from the axis of loading by amounts varying from 0.00 to 1.50 inches. All parts of the fixture were made of heat treated, low alloy steel.

Because of some play between the threaded end and the grips, the actual initial eccentricity deviated slightly from that which would be determined by the shims of the fixtures, i.e., the nominal eccentricity. The initial eccentricity was therefore measured by

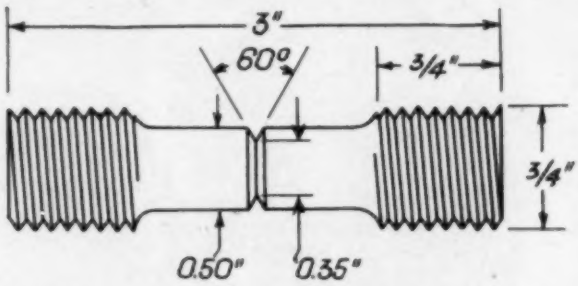

Fig. 19—Threaded End Specimen with 50 Per Cent Sharp Notch Used in Eccentric Testing.

a method which probably sacrifices some accuracy for the sake of simplicity. The results, however, indicate that the accuracy of these measurements is sufficient for the desired purpose. The measurement of the eccentricity was essentially a correction of the nominal eccentricity as determined by the size of the shim placed between the ball-seat and the axis of the specimen. The shims were ground to size as closely as possible by ordinary machining. Since all parts were made very accurately, and since the specimen had the same position with respect to the frames of the fixture for each test, the only deviation which could occur from the nominal eccentricity was caused by improper lining up of the specimen in the frames. This resulted particularly from undersize threads on the specimen or from other incongruencies in the specimen. To determine the actual eccentricity, a bar was clamped across the ends of the fixtures to be used as a reference plane. From this plane, the distances A and B, Fig. 18, were measured with micrometers. The eccentricity (a) was then calculated from the relation:

$$a = (A - \tfrac{1}{4}\text{ inch}) - (B - \tfrac{1}{4}\text{ inch}) = A - B$$

In each series of tests, the eccentricity was varied from zero (concentric tests) to approximately 0.50 inch, and for a few strength levels, to 1½ inches. The test bars for the concentric tests were of the button-head type, as previously described, while those for the eccentric tests were provided with threaded ends, Fig. 19.

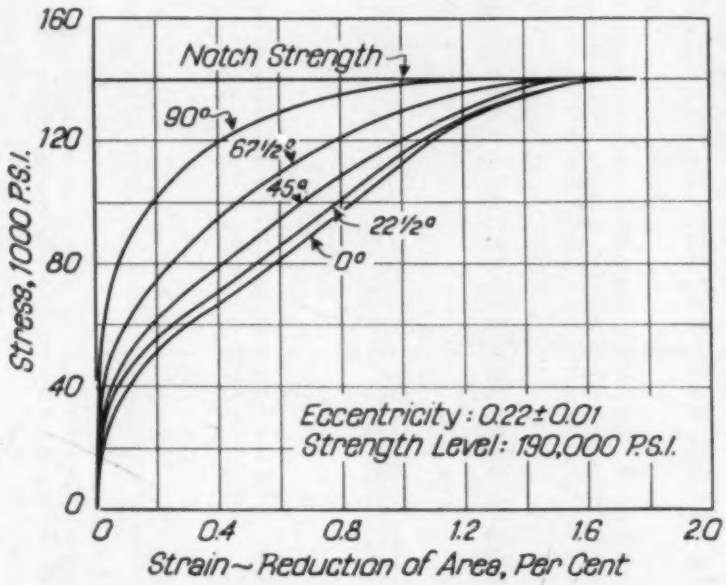

Fig. 20—Stress-Strain Curves Showing the Effect of the Angle Between the Plane of the Eccentricity and the Direction of Strain Measurement.

The average transverse strain across the notched section was measured during the test by means of the transverse gage, previously described. The measurements were made in a direction perpendicular to the plane of bending. It was intended to use the transverse strain at failure as a criterion of the "notch ductility" by calculating from it the change in cross-sectional area, or "contraction in area", corresponding to the measured change in diameter. An attempt was made to determine the significance of this value and its relation to the true contraction in area, or "notch ductility", by determining the stress-strain curves in different directions with respect to the plane of bending, Fig. 20. This investigation showed that the transverse strain in the plane of bending was much larger than the minimum strain perpendicular to the plane of bending, so that the contraction in area based on this latter value is always smaller than the true contraction in area, which depends on the strains in all directions. Consequently, the measured transverse

Table IV

Results of Notched Bar Tensile Tests on S.A.E. 3140 Steel Provided with 50 Per Cent Sharp Notches and Oil-Quenched from 1525 Degrees Fahr.

Strength Level 1000 Psi.	Initial Eccentricity In.	Notch Diameter In.	Notch Depth Per Cent	Notch Strength 1000 Psi.	Contraction In Area (Gage) Per Cent	Contraction in Area (Measuring Microscope) Per Cent	Notch Strength Ratio
130	0.00	0.354	50	187	....	11.5	1.44
	0.00	0.355	50	187	....	11.5	1.44
	0.04	0.348	52	194	1.19*	10.5	1.49
	0.04	0.350	49	188	1.75*	9.0	1.45
	0.08	0.346	50	186	1.35*	10.6	1.43
	0.11	0.347	50	186	0.52*	11.2	1.43
	0.22	0.348	49	167	2.66*	9.0	1.28
	0.24	0.350	49	172	4.58	10.6	1.32
	0.48	0.347	52	56	1.51	4.0	0.43
	1.44	0.354	50	12	1.14*	2.7	0.09
145	0.00	0.354	50	211	13.80	9.3	1.45
	0.00	0.348	49	223	5.76	8.3	1.54
	0.08	0.354	50	206	3.39	8.7	1.42
	0.22	0.354	50	152	4.18	8.2	1.05
	0.22	0.354	50	154	1.95	6.1	1.06
	0.46	0.354	50	53	1.13	5.6	0.37
	0.47	0.354	50	54	0.23	5.0	0.37
	0.95	0.354	50	20	0.11	....	0.14
	1.46	0.354	50	14	0.09	7.2**	0.10
190	0.00	0.348	49	266	3.80	6.2	1.40
	0.00	0.348	49	268	3.89	6.7	1.41
	0.03	0.354	50	258	0.62	5.0	1.36
	0.08	0.354	50	210	1.25	9.8	1.11
	0.21	0.354	50	143	1.34	2.7	0.75
	0.23	0.354	50	128	0.71	5.0	0.67
	0.46	0.354	50	60	0.14	5.6	0.32
	0.47	0.354	50	56	0.24	6.1	0.30
	1.46	0.354	50	16	0.07	3.8	0.08
	1.45	0.354	50	13	....	0.5	0.07
240	0.00	0.348	51	210	....	2.3	0.88
	0.00	0.354	50	183	0.33	3.3	0.76
	0.09	0.354	50	137	0.11	2.6	0.57
	0.22	0.354	50	79	0.00	1.6	0.33
	0.47	0.354	50	30	0.00	2.7	0.12
	1.45	0.354	50	10	0.00	6.1**	0.04
270	0.00	0.355	49	173	0.19	0.6	0.64
	0.00	0.357	49	182	0.18	1.6	0.67
	0.04	0.345	50	156	0.18	0.6	0.58
	0.12	0.345	50	92	0.03	0.0	0.34
	0.24	0.332	50	51	0.00	0.0	0.19
	0.48	0.351	51	22	0.00	0.0	0.08

*Gage stopped before fracture.
**Specimen not completely fractured in test. Broken by hand.

strain cannot be used as a criterion of the notch ductility for an eccentric test, unless the relation between the contraction in area and the minimum transverse strain is clarified by further work. The notch ductility was determined from the area after failure by means of a micrometer microscope for all specimens except button-head specimens having small ductility values. For such concentric specimens, the value determined from the reading on the transverse strain gage, however, was considered to be more reliable. For ductilities smaller than 3 or 4 per cent, the measuring microscope gives values which are not sufficiently accurate, because of the inherent errors of at least ± 1 per cent. For larger ductilities, the transverse

strain gage is not reliable because of the difficulty of extrapolating to the breaking strain.

The results of the tests are assembled in Table IV. No attempts will be made, however, to evaluate the notch ductility, as further tests appear necessary in order to obtain a more complete conception of this characteristic of an eccentric notched bar tensile test.

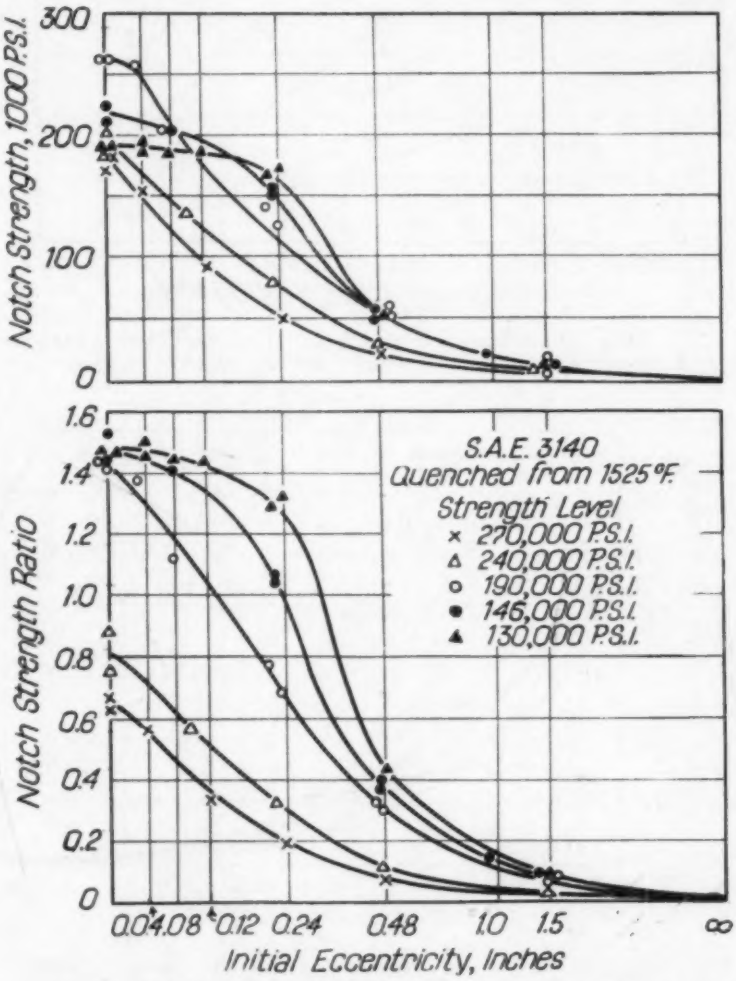

Fig. 21—Results of Eccentric Notched Bar Tensile Tests on S.A.E. 3140 Steel Specimens with 50 Per Cent Sharp Notches.

Experimental Results

The values of notch strength and notch strength ratio are represented in various manners in Figs. 21 to 26. In order to spread the most interesting range of eccentricities, between 0 and 0.5 inch, an abscissa scale was used for the eccentricity (e) in which the quantity $e/(.6+e)$ was plotted as uniform scale. Whether this quantity has any physical significance is not known.

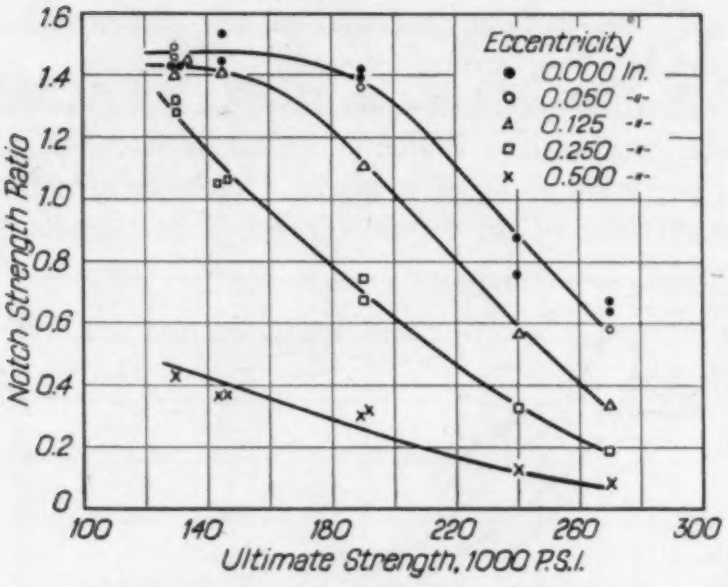

Fig. 22—Effect of Strength Level on the Notch Strength Ratio of Eccentrically Loaded Test Specimens.

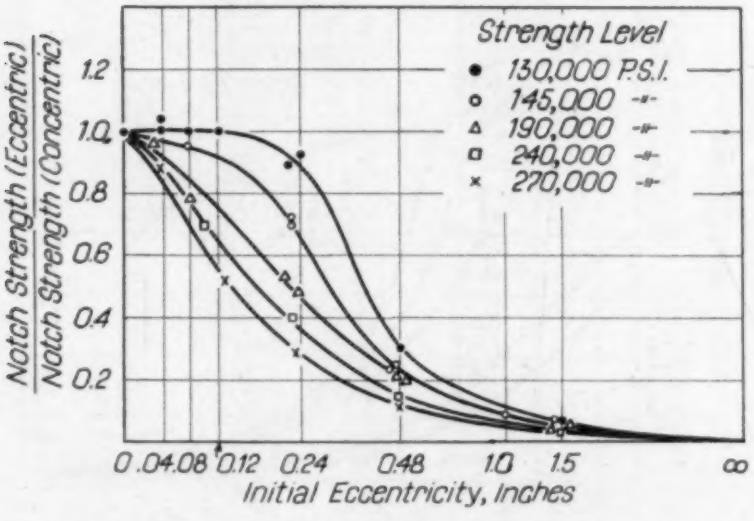

Fig. 23—Effect of Eccentricity on the Ratio : Notch Strength of Eccentric Specimen Divided by Notch Strength of Corresponding Concentric Specimen.

For any strength level, the notch strength decreases with increasing initial eccentricity and becomes very small if the eccentricity is very large, Fig. 21. The most interesting range of eccentricities is that from zero to ¼ inch. In this range, the notch strength of high strength levels decreases rapidly with increasing eccentricity, while that of the lowest investigated strength level is affected only slightly. Consequently, at an eccentricity of ¼ inch, the lower the strength is, the higher the notch strength becomes.

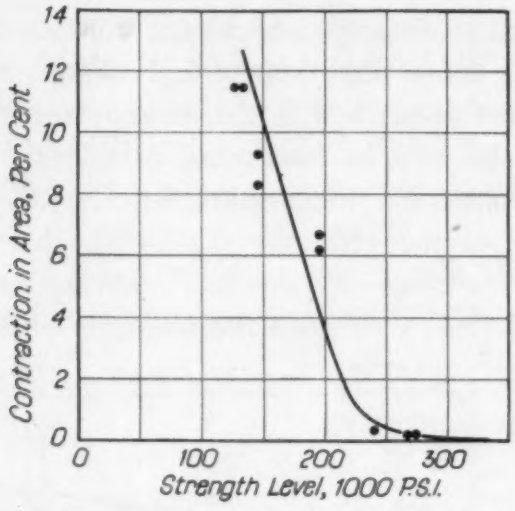

Fig. 24—Effect of Strength Level on the Ductility of 50 Per Cent Sharp Notched Specimens Tested Concentrically.

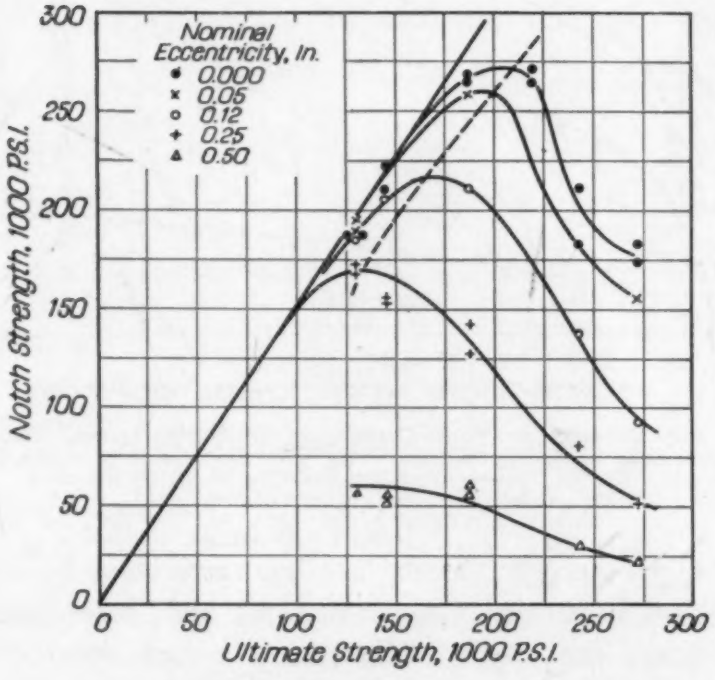

Fig. 25—Effect of Strength Level and Eccentricity on Notched Bar Tensile Tests of S.A.E. 3140 Steel Specimens with 50 Per Cent Sharp Notches.

This holds true for higher eccentricities also, but the absolute values of notch strength are then rather small for all strength levels, and their differences cannot be determined accurately.

The notch strength ratio, Fig. 22, of concentric test specimens is almost constant for strength levels below 200,000 pounds per square inch, and above this limit it decreases with increasing

strength level, as previously discussed. For eccentricities above a small amount, say more than 0.10 inch, however, the notch strength ratio increases continuously with decreasing strength level, Fig. 22. The above relations may be illustrated further by the ratios of the eccentric to the concentric notch strengths, Fig. 23. This representation shows, beyond the relations discussed, that the strength-decreasing effect of eccentricity on steels having very high strength levels only slightly increases with the strength level.

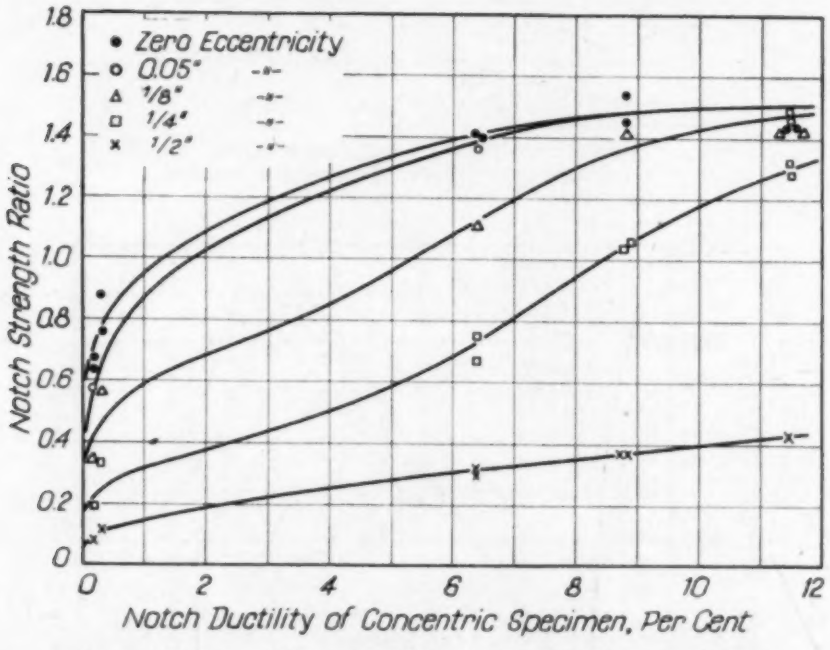

Fig. 26—Effect of Notch Ductility on the Notch Strength Ratio of Eccentrically Loaded Specimens, Using Contraction in Area of the Concentrically Loaded Specimens as the Criterion of Notch Ductility.

Such high strength levels are characterized by very small values of notch-ductility. According to the investigations with concentric loads, the notch ductility of the heat treated steels decreases with increasing strength level, almost linearly, Fig. 24, and becomes very small if the strength level reaches approximately 200,000 pounds per square inch. The notch strength is nearly proportional to the ultimate strength at strength levels below this limit, but decreases with decreasing notch ductility if the notch ductility is very small, or the strength level high, Fig. 25. Thus, in the high strength range, the (concentric) notch strength is primarily a function of the notch ductility. However, the values of notch ductility being very small, the relation between notch

ductility and notch strength would be difficult to establish accurately.

On the other hand, if the eccentricity is high, the notch strength (and the notch ductility) decreases continuously with increasing strength level, Fig. 25. This is true, for the investigated steel, if the eccentricity is anywhere over $\frac{3}{16}$ inch; while at lower eccentricities the notch strength still exhibits a maximum at a certain strength level, which is lower the higher the eccentricity.

Thus, the experimentation on sharply notched tensile-test bars

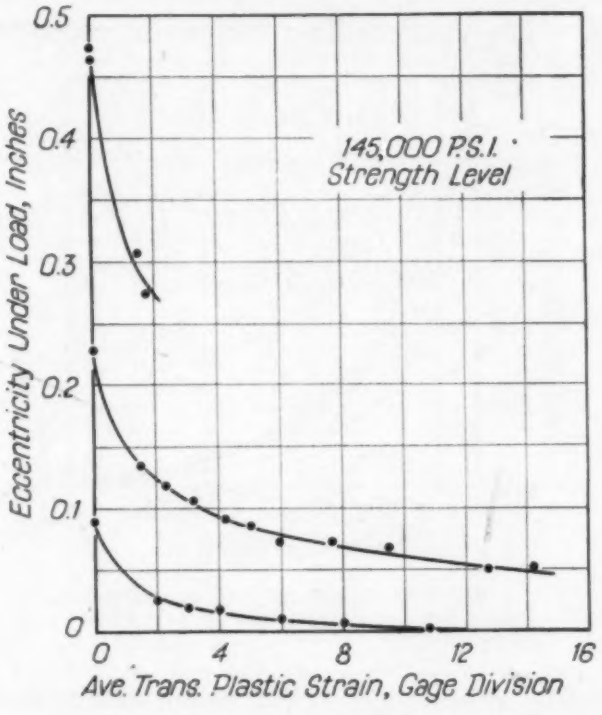

Fig. 27—Change in Eccentricity with Progressive Straining of Eccentrically Loaded Notched Tensile Test Bars.

has revealed, so far, two interesting relations. First, the strength level which exhibits the maximum strength, if sudden section changes are present, is approximately 200,000 pounds per square inch, or much lower than the maximum tensile strength of approximately 300,000 pounds per square inch attainable with such steels. Second, if the strain is not pure tension, but bending is superimposed, the heat treated steel may exhibit a higher actual strength the lower its strength level is.

These relations are more clearly represented if the notch strength ratio is plotted versus the notch ductility of the concentrically tested specimens, Fig. 26.

As previously discussed, the notch strength ratio was not affected by eccentricities up to ¼ inch, if the notch ductility was sufficiently large, say over 15 per cent.

For such high ductility steels, the previously observed law applies, that the notch strength ratio is constant. For ductility values less than 13 per cent, however, the notch strength deviates from this law, the deviation being greater, the lower the notch ductility (or the higher the ultimate strength), and the larger the eccentricity. This results in notch strength ratio versus notch ductility curves of varying shapes. The intermediate range of eccentricities, e.g. ¼

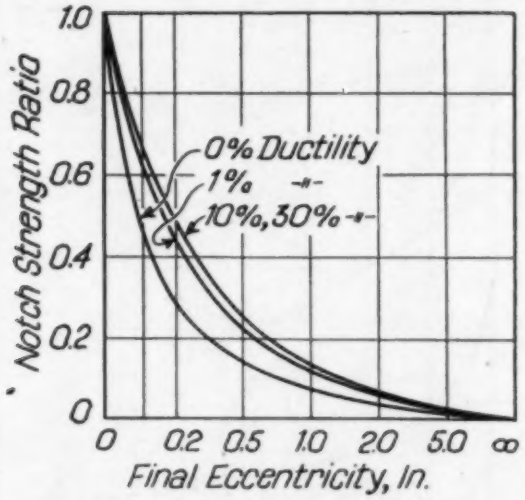

Fig. 28—Theoretical Relation Between Notch Strength Ratio and Final Eccentricity.

inch, is particularly interesting, as the notch strength ratio increases progressively with increasing notch ductility, and becomes, therefore, a suitable measure for the notch ductility. Regarding the very high strength levels, possessing a notch ductility of less than 1 per cent, the results obtained so far are not quite conclusive. Theoretically, the notch strength ratio should still be a suitable measure for small ductilities, as long as unnotched specimens fail in a ductile manner. Such curves for small eccentricities show an effect of ductility only if the notch ductility is small, while the notch strength ratio for very high eccentricities, e.g. ½ inch, is small and difficult to measure accurately.

Thus, it appears that such a test presents a possibility of measuring the notch ductility both in a more simple and more accurate manner than any conceivable strain gage. This conclusion, probably, has considerable practical significance. At present, it appears that

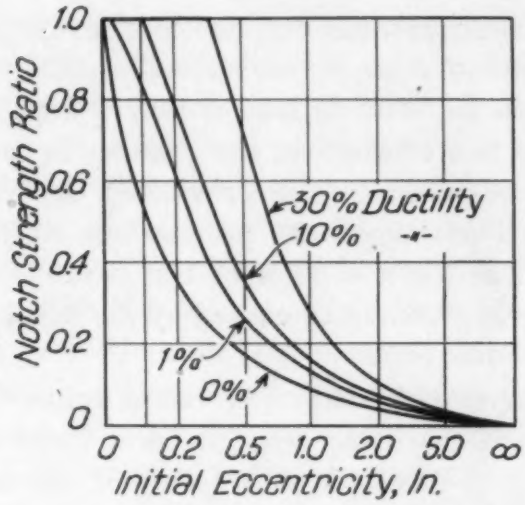

Fig. 29—Theoretical Relation Between Notch Strength Ratio and Initial Eccentricity.

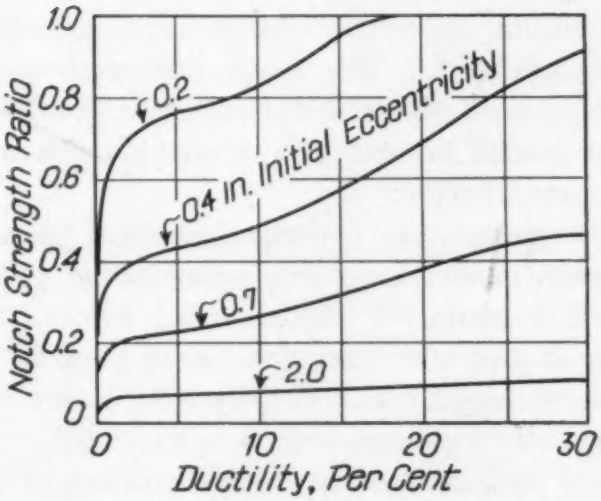

Fig. 30—Theoretical Relation Between Notch Strength Ratio and Ductility.

the evaluation of a steel based on the very high values of the contraction in area in regular tensile tests is entirely misleading, while the notch ductility is representative for its practically useful ductility. The eccentric notched bar tensile test now offers a simple method for accurately measuring this ductility.

Theory of the Eccentric Notched Bar Tensile Test

The above relations between notch ductility and eccentric notch strength can be explained readily. In an eccentric test, any plastic flow in the notched section (or anywhere else) will reduce the

eccentricity. Consequently, the test does not reveal the notch strength for the initial combination of tension and bending, but for a final combination where the bending load is only a fraction of the initial. In order to prove this conception, the changes in eccentricity during such tests were measured by the previously described method, see Fig. 18, after various increments prestraining. These changes are illustrated in Fig. 27 for a number of test bars. They show clearly the large decrease in eccentricity caused by the small plastic deformations in the notched section.

Thus, the curves notch strength versus initial eccentricity, Fig. 21, would represent the notch strength as a function of the actual eccentricity at the moment of failure only if the notch ductility is zero. If the notch ductility is very small, i.e., at high strength levels, the curves' notch strength versus eccentricity will be affected only slightly by changes in ductility; while for the lower strength levels, eccentricities within a certain range are completely eliminated before failure, and within this range the notch strength becomes practically independent of the initial eccentricity. If the ductility is larger, the horizontal branch of the curve notch strength versus eccentricity becomes longer.

Attempts were made to develop theoretical conceptions regarding the strength of a metal which is being subjected to an eccentric tensile load. The treatment of a notched bar is too complicated, even if the stress and strain relations were known. However, the conditions in a notched bar eccentrically loaded may be simulated by considering an unnotched bar with a short length at the center in which the plastic flow is localized; and introducing further simplifying assumptions, the strength of a bar subjected to an eccentric tensile load can be calculated as a function of the amount of eccentricity.[6] Various curves, Fig. 28, were obtained by such a method, for metal conditions characterized by a constant strength level, 150,000 pounds per square inch, and a ductility varying between 0 and 30 per cent. The ductility is defined hereby as the maximum, longitudinal, plastic strain at failure.

These theoretical curves for various ductilities differ only slightly, as the strength was calculated as a function of the final eccentricity. This eccentricity is smaller than the original, because of bending of the specimen and the tilting of the test fixture, and can be calculated also on the basis of the previously introduced assump-

[6]See Appendix II.

tions. Thus, finally the strength can be obtained as a function of the initial eccentricity and the ductility of the metal. Such curves, Fig. 29, possess fundamentally the same trend as the experimental curves, Fig. 23, and this can be considered as a proof for the validity of the assumptions used in the theoretical analysis. This agreement of experimental results and theoretically derived values also applied to the representations of notch strength versus ductility, see Fig. 30 and 26. It is not possible, as yet, to evaluate the actual stress and strain distributions in notched specimens subjected to plastic flow. However, the results of the analysis also indicate that any average of the strains over the cross section, such as the contraction of area, can be considered as a suitable criterion of ductility under the most severe stress conditions which can be controlled and tested at present.

Summary and Conclusions

1. In order to obtain reproducible results of notched bar tensile tests on high strength, low alloy steels, the testing conditions must be controlled considerably more closely than usual in the testing of materials. This should apply also to the tensile testing of any brittle metal.

2. The results of the notched bar tensile tests confirmed previously drawn conclusions that a sharp notch embrittles severely any heat treated steel. The ductility of notched tensile test bars decreased continuously with increasing strength level and became very small if the strength exceeded 200,000 pounds per square inch. The strength of a notched bar, possessing an average ductility of more than a few per cent in the notched section, was considerably higher than the ultimate strength, primarily depending upon the notch depth. On the contrary, the notch strength of a metal possessing a low notch ductility may be considerably lower than the ultimate strength.

3. The investigation of a steel heat treated to various strength levels and provided with notches of various radii revealed that the notch strength characteristics of a metal are complex functions of several fundamental factors:

(a) The stress peak at the notch bottom is eliminated gradually by plastic flow. This explains that the tensile strength and fracture stress of notched steel bars are adversely and severely affected by a sharp notch only if the notch ductility is low. The stress concentration also accounts for the low yield strength and

the smooth stress-strain curves of sharply notched bars.

(b) The magnitude of the transverse stress, or triaxiality, present in the notched section, depends little upon the notch radius, unless the fillet becomes very shallow. This explains that extremely high notch strength values can be obtained in test bars of high strength steels provided with a smooth, deep notch, which consequently possess a low stress concentration and sufficiently high ductility.

(c) The presence of residual stresses, the magnitude of which increases with increasing strength level, accounts for the fact that the yield strength ratio of a sharply notched bar is lower and scatters more the higher the strength level.

(d) The stress-strain and other conventional characteristics obtained by means of a regular tensile test have no relation to the behavior of a metal subjected to nonuniform, triaxial tension.

4. The superposition of a bending moment during a notched bar tensile test yielded results which can be explained by the following conceptions:

(a) The strength of a brittle material decreases rapidly with the magnitude of a superimposed bending moment.

(b) In a ductile material, the bending moment caused by eccentricity of loading decreases during the plastic flow to an extent determined by the ductility of the material.

(c) A material possessing a certain ductility will possess a practically constant (notch) strength if the eccentricity does not exceed a certain value.

(d) These relations permit to select an eccentricity which will range the notch strength values of various conditions of a heat treated steel according to their ductility.

Appendix I

Determination of Eccentricity From Load-Extension Diagrams

Consider a cylindrical bar of a given radius (r) subjected to a tensile load (P) acting at an eccentricity (a), see Fig. 18. This will cause a maximum tensile stress (S_1) at a position (1) at the surface closest to the direction of tension and a minimum stress (S_2) at a position (2) at the surface diametrically opposite to the first position.

In the elastic state, the stress distribution is linear, the stress at any point consisting of two components, caused by the tensile load (P) and the bending moment, M = Pa, respectively. Thus, the maximum stress is:

$$S_1 = \frac{P}{A} + \frac{Par}{I}, \tag{1}$$

where $A = \pi r^2$, and $I = \pi r^4/4$.
Considering that:

$$\frac{P}{A} = \frac{S_1 + S_2}{2}, \tag{2}$$

the following relation results:

$$a = \frac{\pi r^3}{P} \cdot \frac{S_1 - S_2}{8} \tag{3}$$

If strain measurements are made at positions 1 and 2, curves representing the load (P) versus the strain gage readings, $\triangle_1$ and $\triangle_2$ respectively, are obtained. For a gage length of 1 inch, the corresponding strains, e_1 and e_2, are, on the one hand:

$$e_1 = K_1\triangle_1, e_2 = K_2\triangle_2 \tag{4}$$

where K_1 and K_2 are the two gage constants, and on the other hand:

$$e_1E = S_1, e_2E = S_2 \tag{5}$$

where E is the modulus of elasticity. Let the slopes of the curves P versus $\triangle_1$ and P versus $\triangle_2$ be:

$$a_1 = P/\triangle_1, a_2 = P/\triangle_2 \tag{6}$$

From equations (4), (5), and (6), the stresses become:

$$S_1 = PE\,(K_1/a_1), S_2 = PE\,(K_2/a_2) \tag{7}$$

And substituting (7) into (3) yields the final relation:

$$a = E \cdot \frac{\pi r^3}{8}\,(K_1/a_1 - K_2/a_2) \tag{8}$$

Although equation (8) applies only to a plain cylindrical bar, it may be applied to a notched bar approximately by using an "effective" diameter (2r), which is the mean diameter over the gage length.

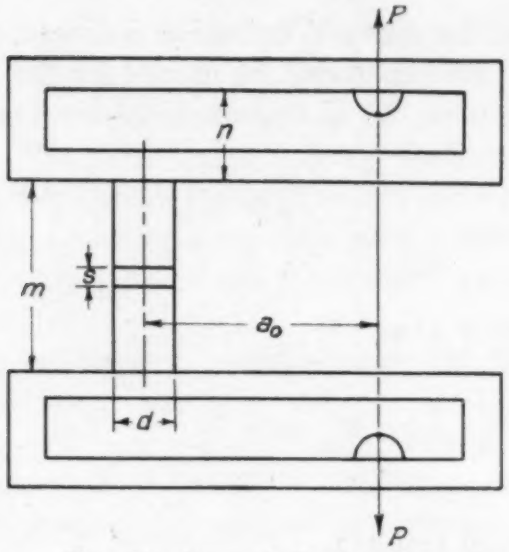

Fig. 31—Assumed Testing Setup for Theoretical Analysis.

Appendix II

Theoretical Analysis of a Notched Tensile Test Specimen Subjected to Eccentric Loading

The object of these calculations is the determination of the strength (N) of a test bar subjected to a tensile load (P) acting at a certain initial eccentricity (a_o), Fig. 31. In order to simplify the problem, the test bar shall behave according to the assumptions listed in Table V. The solution applies to a prismatic bar provided with a notch of infinitely small depth; but should represent also qualitatively the conditions present in a deeply notched, cylindrical tensile test bar. The (notch) strength of the prismatic bar, for concentric loading, is equal to its regular tensile strength or flow stress (K), since there shall be no strain hardening, and the notch strength ratio (Y) shall be therefore defined as $Y = N/K$. For a probable linear distribution of the strain (e) over the cross section, the stress (S) distribution may be one of three cases, Fig. 33.

Table V
List of Assumptions, See Fig. 31

1. Constant flow stress, K.
2. Rigid fixtures.
3. Square cross section.
4. No distortion of cross section.
5. Zero friction at the ball surfaces.
6. Maximum elastic deflection along length m.
7. Plastic flow restricted to length s.
8. Eccentricity constant over the length m.
9. Metal fails when plastic strain reaches ductility R.

Case I. The first part of the notch strength ratio versus initial eccentricity curve, corresponding to Case I of Fig. 33, is horizontal, since the notch strength ratio is unity. The final eccentricity is zero, but the initial eccentricity depends upon the strain distribution. The bending strain at the surface is half the difference of the edge strains or $\frac{R+\frac{K}{E}-e_s}{2}$. This is related to the radius of curvature, r_s, of the portion S, Fig. 31, by:

$$\frac{R+\frac{K}{E}-e_s}{2}=\frac{d}{2r_s} \quad \ldots\ldots(1)$$

The corresponding angle, Θ_s, subtended by the arc s, Fig. 32, is:

$$\theta_s=\frac{s}{r_s} \quad \ldots\ldots(2)$$

Solving (1) for r_s and substituting in (2):

$$\theta_s=\frac{s}{d}\left(R+\frac{K}{E}-e_s\right) \quad \ldots\ldots(3)$$

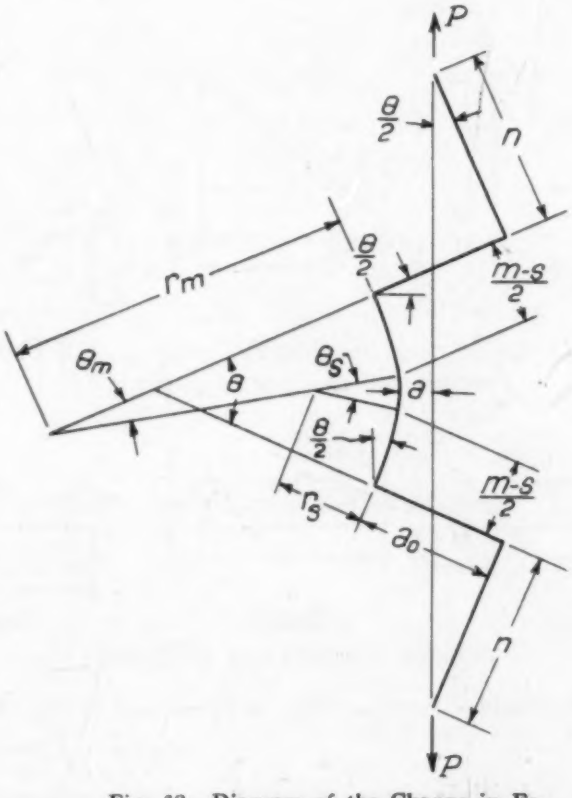

Fig. 32—Diagram of the Change in Eccentricity Due to Curvature of the Specimen and Displacement of the Fixtures.

Since the final eccentricity is zero for Case I the stress distribution is uniform in all parts of the specimen. By assumption 6, Table V, the strain is elastic in the region m, and thus the strain distribution will be uniform. Then the bending is zero in region m and $\Theta_m = 0$. By the geometry of Fig. 32:

$$\Theta = 2\Theta_m + \Theta_s \quad \ldots\ldots (4)$$

Substituting $\Theta_m = 0$, (4) becomes:

$$\Theta = \Theta_s \quad \ldots\ldots (5)$$

The angular displacement of the fixtures is then $\frac{\Theta_s}{2}$ and from the schematic diagram of Fig. 32, the initial eccentricity can be calculated as a function of the final eccentricity. From the figure:

$$\left(\frac{m-s}{2}\right) \sin\frac{\Theta}{2} + a + n\sin\frac{\Theta}{2} = \frac{a_o}{\cos\frac{\Theta}{2}} \quad \ldots\ldots (6)$$

For small values of Θ:

$$(m-s)\frac{\Theta}{4} + a + \frac{n\Theta}{2} = a_o \quad \ldots\ldots (7)$$

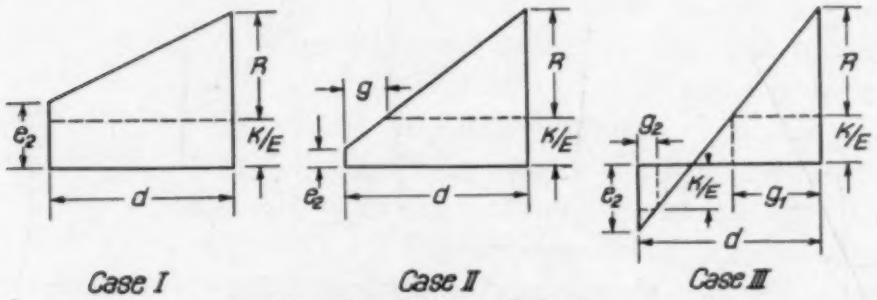

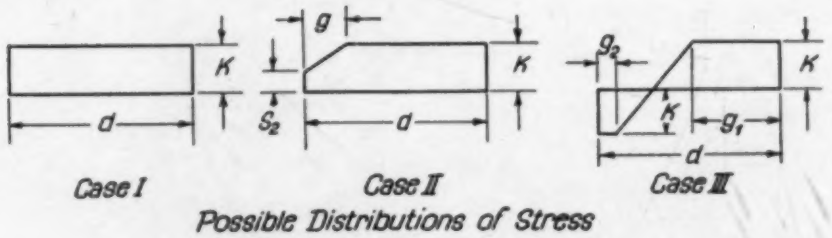

Fig. 33—Various Possible Types of Stress and Strain Distributions in an Eccentrically Loaded Bar.

The limiting initial eccentricity for the horizontal part of the notch strength ratio versus eccentricity curve is determined by a

strain distribution at the limit between Cases I and II, Fig. 33, where $e_2 = \frac{K}{E}$, E being the modulus of elasticity. Then (3) becomes:

$$\Theta_0 = \frac{sR}{d} \quad \ldots\ldots (8)$$

Noting (5) and substituting Θ in (7):

$$a_0 = \frac{sR}{d}\left(\frac{m-s}{4}\right) + \frac{nsR}{2d} \quad \ldots\ldots (9)$$

The dimensions of the fixture and specimen used in the experimental work are approximately:

$s = 0.25$ inch
$d = 0.50$ inch
$m = 1.70$ inch
$n = 3.70$ inch

Assuming a value of K of 150,000 pounds per square inch and E = 30,000,000 pounds per square inch, (7) becomes:

$$A_0 = 1.106R \quad \ldots\ldots (10)$$

which gives the allowable initial eccentricity without loss of strength.

Case II. The second portion of the notch strength versus initial eccentricity curve is characterized by the stress and strain distributions of Case II, Fig. 33. The load is the integral of the stress across the diameter of the bar. This integration requires the stress distribution in the region g. This is:

$$S = S_2 + \frac{x}{g}(K - S_2) \quad \ldots\ldots (11)$$

where x is the distance from the left edge of the specimen. Integrating from $x = 0$ to $x = g$, the load P_1, due to the stress in region g, is:

$$P_1 = d\left[S_2 g + (K - S_2)\frac{g}{2}\right] \quad \ldots\ldots (12)$$

The load, P_2, due to the remaining uniform stress, K, is:

$$P_2 = Kd(d - g) \quad \ldots\ldots (13)$$

and the total load, P, is:

$$P = P_1 + P_2 = \frac{dg}{2}(S_2 - K) + Kd^2 \quad \ldots\ldots (14)$$

The notch strength is then:

$$N = \frac{P}{d^2} = \frac{g}{2d}(S_2 - K) + K \quad \ldots\ldots (15)$$

and the notch strength ratio is:

$$Y = \frac{N}{K} = 1 - 1/2\frac{g}{d}\left(1 - \frac{S_2}{K}\right) \quad \ldots\ldots (16)$$

The eccentricity is determined from the condition that the summation of moments is zero when there is no motion. Taking the left edge of the specimen as the center of moments:

$$P\,(d/2 + a) = \int_o^d SxdA \quad \ldots\ldots (17)$$

Since the stress distribution is discontinuous, the integral must be divided into two parts. Also noting that:

$$dA = d\,(dx) \quad \ldots\ldots (18)$$

$$P\left(\frac{d}{2} + a\right) = d\int_o^g [S_2x + (K - S_2)\frac{x^2}{g}]\,dx + d\int_g^d Kxdx \quad \ldots\ldots (19)$$

Integrating, inserting the value for p, and solving for "a":

$$a = \frac{\frac{Kd^2}{2} - \frac{g^2}{6}(K - S_2)}{Kd - \frac{g}{2}(K - S_2)} - \frac{d}{2} \quad \ldots\ldots (20)$$

Since the notch strength ratio and the eccentricity both involve the unknown quantity, S_2, this quantity must be replaced by a function of known quantities and g. From the geometry of the strain distribution diagram, Fig. 33:

$$\frac{R}{d - g} = \frac{\frac{K}{E} - e_2}{g} \quad \ldots\ldots (21)$$

Solving for e_2 and noting that $e_2 = \frac{S_2}{E}$:

$$S_2 = E\left[\frac{K}{E} - \frac{R}{\frac{d}{g} - 1}\right] \quad \ldots\ldots (22)$$

Inserting this value in (16) and (20) and simplifying:

$$Y = 1 - \frac{ER\left(\frac{g}{d}\right)^2}{2K\left(1 - \frac{g}{d}\right)} \quad \ldots\ldots (23)$$

$$\frac{a}{d} = \frac{1/2 - 1/3\frac{g}{d}}{\frac{2K}{ER}\left(\frac{d}{g}\right)^3\left(1-\frac{g}{d}\right)-1} \quad \ldots\ldots(24)$$

Equation (24) may be simplified still further by combining with (23) to give:

$$\frac{a}{d} = \left(\frac{1-Y}{Y}\right)\left(1/2 - 1/3\frac{g}{d}\right) \quad \ldots\ldots(25)$$

Equations (23) and (25) now give the eccentricity and notch strength ratio as functions of the parameter g. This quantity may vary within certain limits which are determined by the values of S_2. S_2 may vary from $-K$ to $+K$. Solving (22) for $\frac{g}{d}$ and inserting $+K$ and $-K$, it is found that $\frac{g}{d}$ may vary from zero to $\frac{2K}{2K+RE}$.

The initial eccentricity may be determined from the final eccentricity as before by a consideration of the curvature of the specimen and the angular displacement of the fixtures. However, the curvature of the elastic part of the specimen must be taken into account also when the final eccentricity is not zero. According to assumptions 6 and 8 of Table V, the stress distribution in the region m will be linear, varying from S_2 at one edge to K at the other.

The average stress or notch strength is:

$$N = \frac{S_2 + K}{2} \quad \ldots\ldots(26)$$

and the notch strength ratio is:

$$Y = \frac{N}{K} = \frac{1}{2}\left(1+\frac{S_2}{K}\right) \quad \ldots\ldots(27)$$

The stress distribution is:

$$S = S_2 + \frac{x}{d}(K - S_2) \quad \ldots\ldots(28)$$

from which the eccentricity may be determined by the equation:

$$P\left(\frac{d}{2}+a\right) = Nd^2\left(\frac{d}{2}+a\right) = \int_0^d xSdA \quad \ldots.(29)$$

Inserting (26), (28), and (18), integrating, and solving for S_2:

$$S_2 = K\left(\frac{d-6a}{d+6a}\right) \quad \ldots\ldots(30)$$

Then

$$e_2 = \frac{S_2}{E} = \frac{K}{E}\left(\frac{d-6a}{d+6a}\right) \quad \ldots\ldots(31)$$

and the bending strain, from which the radius of curvature is determined, is $\frac{1}{2}\left(\frac{K}{E} - e_2\right)$. Using the value of e_2 from (31) and equating to $\frac{d}{2r_m}$ as in the bending of a beam:

$$\frac{K}{E}\left(\frac{a}{a+d/6}\right) = \frac{d}{2r_m} \quad \ldots\ldots(32)$$

The angle subtending the curved part of the specimen between the fixtures and the plastic region at the center is:

$$\theta_m = \frac{m-s}{2r_m} \quad \ldots\ldots(33)$$

Solving (32) for r_m and inserting in (33):

$$\theta_m = \left(\frac{m-s}{d}\right)\left(\frac{K}{E}\right)\left(\frac{\frac{a}{d}}{\frac{a}{d}+\frac{1}{6}}\right) \quad \ldots\ldots(34)$$

To find Θ_s from (3), e_2 is required. This can be found from the relation:

$$e_2 = \frac{S_2}{E} \quad \ldots\ldots(35)$$

Substituting the value of S_2 from (22):

$$e_2 = \frac{K}{E} - \frac{R}{\frac{d}{g}-1} \quad \ldots\ldots(36)$$

Now substituting (36) in (3) and simplifying:

$$\theta_s = \frac{sR}{d}\left(\frac{1}{1-\frac{g}{d}}\right) \quad \ldots\ldots(37)$$

Θ_s from (37) and Θ_m from (34) may now be used to determine the

initial eccentricity by means of equations (4) and (7).

The notch strength ratio versus final eccentricity curve for zero ductility can also be determined now from equations (27) and (30) using S_2 as a parameter varying from +K to −K. Solving (30) for a:

$$a = \frac{d}{6}\left(\frac{1-\frac{S_2}{K}}{1+\frac{S_2}{K}}\right) \qquad \text{.....(38)}$$

The initial eccentricity depends only upon r_m for the entire length of the specimen. Thus:

$$\theta = \frac{m}{r_m} \qquad \text{.....(39)}$$

Solving (32) for r_m and inserting in (39):

$$\theta = \left(\frac{2m}{d}\right)\left(\frac{K}{E}\right)\left(\frac{\frac{a}{d}}{\frac{a}{d}+\frac{1}{6}}\right) \qquad \text{.....(40)}$$

which can be used in (7) to determine the initial eccentricity.

Case III. For the general case where R has a finite value, the third part of the curve corresponding to Case III of Fig. 33 is determined in the same way as the second part. By integration of the stress

$$Y = \frac{g_1 - g_2}{d} = \frac{g_1}{d} - \frac{g_2}{d} \qquad \text{.....(41)}$$

The eccentricity is determined by the condition of equilibrium of moments

$$P\left(\frac{d}{2}+a\right) = \int_o^d SxdA \qquad \text{.....(42)}$$

which yields upon integrating and solving for "a":

$$\frac{a}{d} = \left[\frac{\frac{g_1}{d}\left(1-\frac{g_1}{2d}\right) - \frac{1}{2}\left(\frac{g_2}{d}\right)^2 + \frac{1}{6}\left(1-\frac{g_2}{d}\right)^2\left(\frac{2K}{RE+2K}\right)^2}{\frac{g_1}{d}-\frac{g_2}{d}}\right] - \left[\frac{1}{2}\right] \qquad \text{..(43)}$$

Equations (41) and (43) involve two parameters, g_1 and g_2, which can be related by an equation if the geometry of the strain distribution is considered. From Fig. 33:

$$\frac{g_1}{R} = \frac{d - g_2}{R + \frac{2K}{E}} \qquad \text{.....(44)}$$

Solving for $\frac{g_1}{d}$:

$$\frac{g_1}{d} = \frac{RE\left(1 - \frac{g_2}{d}\right)}{RE + 2K} \qquad \text{.....(45)}$$

Considering g_1 as a function of g_2, the only independent variable in (41) and (43) is g_2. This may vary between zero and a value which corresponds to infinite eccentricity. For infinite eccentricity, g_1 and g_2 are equal. Substituting g_2 for g_1 in (44) and solving for $\frac{g_2}{d}$:

$$\frac{g_2}{d} = \frac{RE}{2RE + 2K} \qquad \text{.....(46)}$$

which is the limiting value for $\frac{g_2}{d}$.

The initial eccentricity is determined with equations (4), (7), and (34), applying equally well to Case III. Θ_s, however, must be expressed in terms of the new parameters g_1 and g_2. Again, if (3) is to be used to find Θ_s, the value of e_2 must be expressed in terms of g_1 and g_2. From Fig. 33, by symmetrical triangles:

$$\frac{-e_2 - \frac{K}{E}}{g_2} = \frac{R}{g_1} \qquad \text{.....(47)}$$

Solving for e_2 and substituting in (3):

$$\Theta_s = \frac{s}{d}\left(R + R\frac{g_2}{g_1} + \frac{2K}{E}\right) \qquad \text{.....(48)}$$

Bibliography

1. G. Sachs and J. D. Lubahn, "Notched Bar Tensile Tests on Heat Treated Low Alloy Steels," TRANSACTIONS, American Society for Metals, Vol. 31, 1943, p. 125-160.
2. G. Sachs and J. D. Lubahn, "Effects of Notching on Metals Strained in Tension," *Iron Age*, Vol. 150, 1942, Oct. 8, p. 31-38; Oct. 15, p. 48-52.

3. K. Matthaes, "Notch Effects Under Static Stress," *Luftfahrtforschung,* Vol. 14, 1938, p. 28-40; *Metal Treatment,* Vol. 4, 1938, p. 15-23.
4. H. Kiessler and W. Connert, "Notched Bar Tensile Tests with Superposed Bending Strain," *Archiv für das Eisenhüttenwesen,* Vol. 14, 1940-41, p. 555-560.
5. G. Sachs, P. S. Cole and R. A. Roth, "The Strength of Heat-Treated Alloy Steel Bolts," this volume, p. 396.
6. H. Moeller and A. Roth, "Cold-Working of the Metal Surface by Various Machining Conditions," *Mitteilungen,* Kaiser Wilhelm Institut für Eisenforschung, Düsseldorf, Vol. 19, 1937, p. 127-130.
7. W. Kuntze, "Cohesive Strength," *Mitteilungen,* D. Materialprüfungsamt, Special Issue No. 20, 1932.
8. W. Kuntze, "Transverse Elastic Strain and Triaxial Stress States in Notched Specimens," *Zeit. Physik,* Vol. 72, 1931, p. 785-792.
9. G. Sachs, "Forging Stresses, Heat Treating Stresses, and Heat Stresses," *Metallwirtschaft,* Vol. 8, 1929, p. 343-347.

DISCUSSION

Written Discussion: By E. S. Jenkins, chief of structures department, Curtiss-Wright Corp., Buffalo.

The authors are to be commended for their extremely interesting study of the notched bar tensile test and of the notch characteristics of heat treated, low-alloy steels. They have improved the testing technique and they have made an important contribution to the interpretation of the test results on this type of specimen. The writer would, however, like to discuss certain minor features of the paper and the general significance of this type of test.

In connection with the discussion of the "average transverse stress" and the "inverse transverse modulus", several questions arise. To begin with, the authors develop the relations for the average transverse stress by assuming that the state of stress is tri-axial and consists of the longitudinal stress, in the direction of the axis of the bar, and two tensile stresses of equal magnitude, acting on the bar cross section in the radial and tangential directions, respectively.

There is, as a matter of fact, no theoretical justification for this assumption. The analytical results of Neuber are in contradiction to it, indicating the presence of radial and tangential stresses of variable magnitude over the bar cross section in the notched region. The radial stresses must be zero at the surface of the notch, while the tangential stresses have their maximum values at such points. The relatively large degree of variation of these stresses over the bar cross section makes an "average stress" determination of slight practical significance. The same would seem to be true of the "inverse transverse modulus", defined as the ratio of the unit diametral contraction and the mean longitudinal stress.

The results obtained for the inverse transvere modulus (Fig. 12) do, however, bring out an interesting point. It is found by the authors that the value of this modulus does not vary for a wide range of very sharply notched specimens. This probably indicates that the excessively large stress concentrations introduced at the roots of very sharp notches cause early yielding of the root material, resulting in an effective increase in the notch radius even at low loads. The plastic shape readjustment seems to proceed until a definite minimum effective notch radius is attained. While the data of Fig. 12 do not decisively prove that this change of notch radius is the cause for the invariance of the inverse transverse

modulus for sharply notched specimens, the possibility is not too remote.

It should be noted that, whereas the state of stress in the root region of a notched round bar is tri-axial, the state of stress near the root of a notch cut in a flat plate is bi-axial. A comparison of the two, relative to the effects of the third principal stress, might conceivably be of some value.

The development in Appendix II of the paper, regarding the analysis of a notched tensile test specimen subjected to eccentric loading, seems to describe the nature of the phenomenon with sufficient accuracy for general purposes. It is of interest to note, however, that a more exact calculation could be made. Such a calculation would be based on the theory for the bending of beams under combined flexure and axial loads. The calculation could be extended to the plastic range without introducing severe difficulties and could be based on a strain-hardening stress-strain curve of arbitrary shape for the specimen material. Although it is recognized that the addition of bending will make the test more sensitive to notch effects it is questioned whether this advantage would offset the added difficulty of interpreting the results.

In conclusion, the writer would like to raise the question of the significance of notched bar tensile test results in general. Customarily the notch test is taken to indicate the toughness of a material. But the toughness is not defined or measured quantitatively. It seems that behind the idea of toughness is a characteristic which can be measured. It is the strain which the material can undergo without fracture when subjected to complex states of stress. We are well aware at this time that the structural behavior of a material is dependent on the three-dimensional state of stress to which it is subjected. Pure (as opposed to notched) tension tests give results applicable to a one-dimensional state of loading; hence they form only a special case of the general law of behavior. It is not possible, for example, to extrapolate from the pure tension test results to the more general cases of bi-axial or tri-axial stress. However, since the tension test forms a successful basis for many of the fundamental laws of modern structural design its use is justified on practical grounds.

The notched bar tensile test is an attempt to modify the simple tension test so as to obtain results for the material behavior under a more complicated state of stress. There is sincere doubt, however, as to the state of stress introduced by the notch. The bar stress distribution continuously varies through the bar volume. Furthermore, a new distribution appears for each increment of plastic strain. Moreover, these distributions are critically dependent on the shape of the notch. Any quantitative interpretation of the notched bar results thus seems to be extremely difficult.

It would perhaps be of advantage to replace the notched bar tensile test by a different test, also designed to give data on the bi-axial and tri-axial behavior of the material, and more readily adaptable to broader interpretation.

Written Discussion: By R. B. Bland, structures research engineer, Lockheed Aircraft Corp., Burbank, Cal.

The authors are to be congratulated on their work, especially in regard to the reduction of test scatter reported in a previous paper (Ref. 1 of this paper).

It is unfortunate that the original load deflection curves, as well as stress-strain curves for the basic material, were not presented in this paper. These data would have been decidedly interesting to us.

The statement that "... the plastic flow preceding the point of maximum load does not reduce materially the magnitude of the transverse stress" appears to us to be founded on somewhat debatable assumptions. The results of tests at the Lockheed Aircraft Corporation, in which the value of the transverse stress was actually measured, indicate that the value of the transverse stress reaches a maximum at the yield and thereafter continually decreases as the amount of plastic deformation increases.

The tests under eccentric load would perhaps be of more value if they were conducted with a constant bending moment.

Oral Discussion

G. C. RIEGEL:[7] While not having had the advantage of previously studying this paper by Dr. Sachs, I am sure it merits very careful perusal and I certainly feel that it has much intellectual "meat" in it for those of us who are concerned with states of stress imposed by a notch.

At the risk of being presumptuous and possibly diverting the original thought, I should like to ask Dr. Sachs if he thinks there would be any virtue in using a notched specimen, such as a Charpy type, stressing it somewhere below the elastic deformation range, but rather highly, and then measuring the energy absorption figures in the same manner we usually do in the so-called notched-bar impact test?

In other words, to take an example from experience (and that after all is why we came here, I think, as metallurgists and engineers to learn something that can be applied), we have the instance of a gun carriage rolling along at 45 miles an hour on the proving ground with an axle made of S.A.E. 4340 steel of a section probably 2-5/16 diameter at the radius where the bearing is carried. When the carriage falls into a chuck hole, the fine ductile 4340 axle, at Rockwell C-32 or 33, breaks with a brittle fracture with no elongation and no reduction of area. We have here then a state of tension with a rapid loading of the specimen at some "sore" spot, as Prof. H. F. Moore, I think, has called it. The energy has no time for distribution in the ductile material and therefore the axle appears to break with a brittle fracture. That is just one analogy that comes to my mind and I think many of us have that experience and often wonder what to do with it. If we test the material after it has broken, we cannot find, either with tension or notched-bar tests, that it is unsatisfactory, and still it breaks.

A. E. FOCKE:[8] After listening to this paper, it seems to me that to the same extent that we agree that the wear capacity of a material cannot be measured in absolute units, since it does not exist apart from the conditions of service, we are forced to admit that "strength" is subject to the same limitations.

All our testing is done on the chain itself or on chain parts because we have found by experience that tests made on regular test specimens give us little information from which we can predict the practical value of a material or a process for chain.

It is interesting that our empirical results based on tests of chains or chain parts confirm the conclusion one draws from this work of Dr. Sachs. We know that steels heat treated to strengths much greater than 200,000 psi are not safe for chain sideplates for general application and even this value must be reduced

[7]Chief metallurgist, Caterpillar Tractor Co., Peoria, Ill.

[8]Research metallurgist, Diamond Chain & Mfg. Co., Indianapolis, Ind.

if the chain is to perform satisfactorily under unusual conditions of fatigue or corrosion.

This is important to us for we are under constant pressure to build chains of greater tensile strength using the same dimensions as those of our standard chains and it is not always easy to convince others that this cannot be safely accomplished by simply increasing the hardness of the material in the sideplates.

It is for this reason that we appreciate these contributions of Dr. Sachs since they emphasize so definitely the perils of attempting to use data obtained on uniform test pieces to predict the value of a material in service.

R. L. TEMPLIN:[9] Unfortunately not having had the opportunity to preview the paper with the thoroughness which the work seems to warrant, there are a couple of general comments that I think are worth while. I believe that a number of us are interested in getting at the type of test that will shed further light on the notched ductility or perhaps sensitivity of various metals. The difficulties contingent upon making good tensile tests with specimens of the type indicated are indeed rather difficult. They vary, of course, with the materials to be tested. This applies not only to the preparation of specimens with the desired dimensions of notch, but also to the difficulties contingent upon getting axial loads on the specimens.

As I understood the test procedure as followed with the lateral extensometer, the authors had very sharp, hardened knife edges that bore on the bottom of the notch and on opposite sides of the specimen and it would seem even though a light spring pressure was used on this apparatus that the additional stresses caused in the specimens might have an effect on the results obtained in some of the tests.

We prefer in our own work, for notch sensitivity tests in the normal elastic range, to use the dynamic or fatigue test as being somewhat more satisfactory than the static test. It is admitted, however, this type of test is not entirely satisfactory in the higher portions of the plastic ranges of materials.

Authors' Reply

Mr. Jenkins has expressed objections to results obtained from tests with nonuniform stress distribution. However, we have found that any feasible homogeneous test on steel does not yield commercially significant metal characteristics; and this is particularly true for regular tensile tests on heat treated high strength steels. Consequently, for the purpose of practical evaluation, more complex tests must be used, at present, approaching practical conditions of straining, even if the actual local stress and strain states are not recognized and average values constitute the metal characteristics. However, we cannot agree with the conclusion that such average values are without significance. Averaging of stresses and strains in the elastic state appears entirely possible, and the "inverse transverse modulus" should be, therefore, a definite measure of the average triaxiality. The fact that the radial stress is zero in a thin surface layer is apparently of less importance than assumed by Mr. Jenkins.

Mr. Jenkins, however, agrees with us that a number of relations have been revealed which cannot be obtained by other tests, at present. If he is in a position

[9]Assistant director of research and chief engineer of tests, Aluminum Company of America, New Kensington, Pa.

to devise another, more lucid and not too tedious test, which will yield similar information, we will be glad to follow up such a suggestion.

We were interested to learn from Mr. Bland that plastic flow reduces the amount of triaxiality. The degree of triaxiality in the plastic range for a notched specimen can be estimated from the notch strength ratio, i.e., the per cent increase in strength by notching. An investigation of the effect of increasing plastic flow on the notch strength ratio possibly indicates a decrease of triaxiality. However, the effect is small within the range of strains encountered in our notched-bar tensile tests, hardly greater than the limits of accuracy of the tests.

At the time the eccentric loading test was developed, a constant bending moment test, requiring a more complex apparatus, was considered. Later, the simpler test was preferred as a preliminary approach to the problem, reserving the other test for further investigation, if necessary. However, the eccentric loading test now appears to be more revealing than a constant bending moment test. It measures the ability of the steel to eliminate eccentricity, i.e., the inherent ductility of the metal under adverse conditions. This important metal characteristic would not influence appreciably the results of a constant bending moment test.

The experience related by Messrs. Riegel and Focke on very different fields of application indicates that the service strength is much more frequently determined by stress-raisers than is generally recognized. For reasons not known as yet, stress-raisers that are too mild to produce brittle failures in present laboratory tests apparently cause service failures of the brittle type. Corrosion, fatigue, section size, fiber direction, low temperature, etc., may augment the effects of a mild stress-raiser. In the example of the axle cited by Mr. Riegel, the principal augmenting factor may have been the section size, as the other factors mentioned are not likely present under the manufacturing and service conditions of the example.

Impact, or high-speed loading, is another embrittling factor (2), but the magnitude of its effect in combination with multi-axial stress should not be sufficient to account for the failure mentioned. Notched bar impact tensile tests should yield results which differ only slightly from those of notched bar static tensile tests; and the results of the latter tests agreed with those of conventional notched bar impact bending tests (1).

Since the knife-edges of the extensometer make contact with the bottom of the notch at a point, there will be a high, localized, transverse compression at the knife edges, as pointed out by Mr. Templin, even for a very small spring pressure. The average transverse stress due to the knife edges would be extremely small, however, since the small load is distributed over a large area within the specimen. Consequently, there would be no effect on the breaking conditions, which are determined by the stress state somewhat below the bottom of the notch.

We have not attempted to correlate static notched bar properties with notch fatigue. We would like, however, to advance the theory that the notch effect is of much the same nature in fatigue tests as in static tests, but becoming apparent in fatigue tests at much lower strength levels.

THE STRENGTH OF HEAT TREATED ALLOY STEEL BOLTS

By G. Sachs, P. S. Cole and R. A. Roth

Abstract

S.A.E. 2330 steel exhibits its highest tensile strength and hardness if tempered at 200 to 400 degrees Fahr. (95 to 205 degrees Cent.) after oil quenching. This applies also to bolts in this alloy, if tested in the regular manner. However, if bending is superimposed to tension, the strength of high strength bolts will be considerably reduced, the maximum strength being 160,000 pounds per square inch, after tempering at 1000 degrees Fahr. (540 degrees Cent.). Higher strength bolts break underneath the head in a brittle fashion, rather than in the generally weaker threaded part. This embrittlement and loss in strength can be eliminated by providing a fillet under the head of the bolt.

Introduction

THIS paper deals with the strength of heat treated alloy steel bolts which were subjected to testing conditions simulating a wide range of service conditions.

In recent investigations on various alloy steels, it was observed that sharp notches (1)[1] reduced materially the strength and ductility of cylindrical test bars if the ultimate strength or "strength level" of the steel exceeded a value of approximately 200,000 pounds per square inch (2). Tubing subjected to internal pressure exhibited a similar, but not quite as pronounced, "embrittling effect" if the strength level of the steel exceeded a value of approximately 150,000 pounds per square inch (3). Cylindrical notched bars (4) and bolts (5) were also found to break at reduced loads, in a brittle fashion, if their strength level was above 150,000 pounds per square

[1]The figures appearing in parentheses pertain to the bibliography appended to this paper.

Abstract from a thesis presented to Case School of Applied Science by P. S. Cole and R. A. Roth in partial fulfillment of the requirements for the B. S. Degree. This paper also incorporates the results of a thesis presented to Case School of Applied Science by R. P. Frohmberg and L. G. Hernecheck in partial fulfillment of the requirements for the B. S. Degree. The authors are also indebted to Mr. J. D. Lubahn for frequent advices.

A paper presented before the Twenty-fifth Annual Convention of the Society, held in Chicago, October 18 to 22, 1943. Of the authors, G. Sachs is professor of physical metallurgy, Case School of Applied Science, Cleveland, P. S. Cole and R. A. Roth are in the armed forces. Manuscript received February 15, 1943.

inch, and if a bending strain was superimposed upon the applied tension by means of shims placed under the heads of the test bars or under the nuts of the bolts.

It was the particular purpose of the investigation reported on to clarify some of the factors which might cause embrittlement of high strength alloy steel bolts. Commercial aircraft bolts, fabricated from S.A.E. 2330 steel, were selected for the investigation.[2]

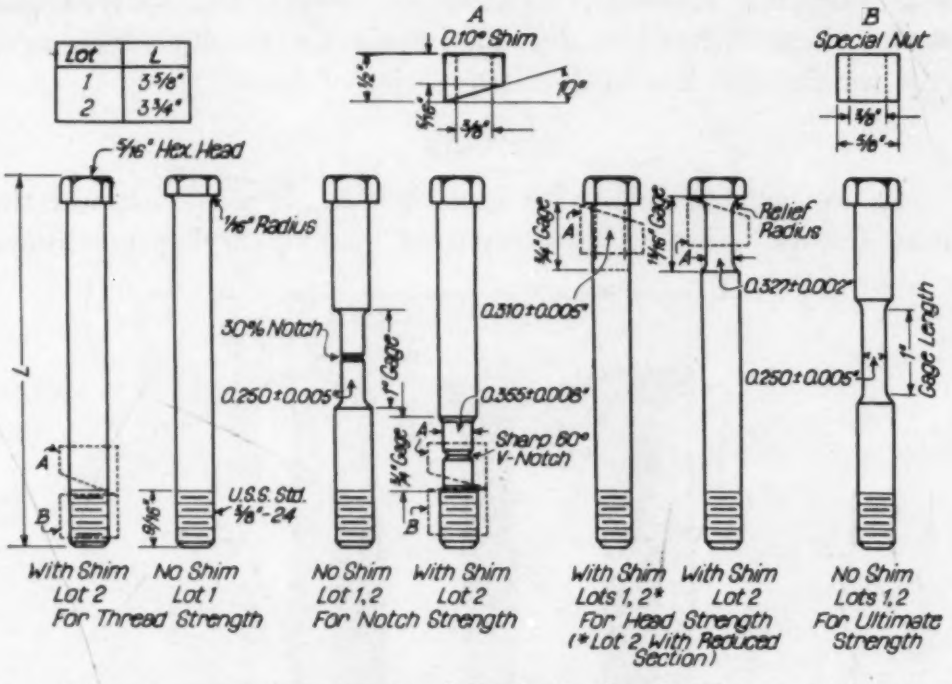

Fig. 1—Dimensions and Arrangement of Specimens for the Various Series of Tests.

The variations were as follows, representing the most important fundamental factors influencing their strength:

1. Various strength levels, as determined by the tempering procedure after proper hardening,

2. Various shapes of the head, which was found more prone to rupture than the thread, in the range of conditions conducive to brittle breaks, and

3. Various types of loading, i. e., regular tension and tension with superimposed bending.

Two lots of S.A.E. 2330 bolts, 3/8 inch diameter and 3 5/8 and 3 3/4 inch total length, respectively, Fig. 1, were used for the investigation. They were heat treated by quenching from a vertical furnace containing forming gas into an airlift quenching tank with oil

[2]We are indebted to Mr. Carl Harvey, chief metallurgist, Lamson and Sessions Co., Cleveland, Ohio, for the bolts used in this investigation.

and tempering at various temperatures for an hour in an electric forced air convection type furnace (1). The hardening temperature, 1500 degrees Fahr. (815 degrees Cent.), was maintained for one-half hour. All specimens were machined before heat-treating; and the results, therefore, apply to a steel with a decarburized surface.

The two lots of bolts showed a slightly different response to heat treating. This is probably explained by a varying content in residual alloying elements, such as chromium and molybdenum. However these differences did not impair the results which agree closely for the two lots in duplicate series of tests.

Results

In an early stage of the investigation, it was observed that various failures of the bolts occurred under varying conditions.

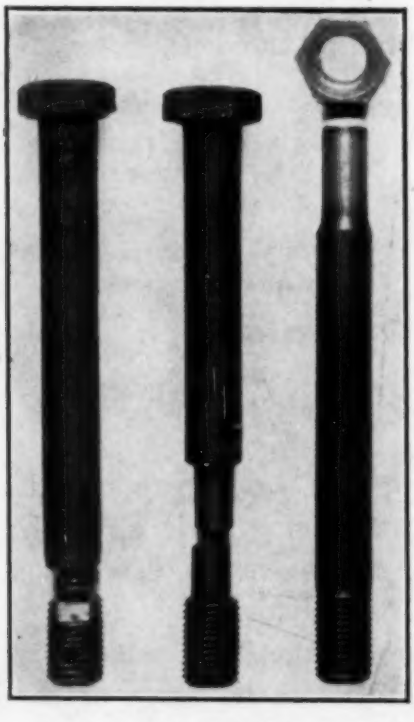

Fig. 2—Typical Failures. Left —Thread Break. Center—Notch Break. Right—Head Break.

Fig. 2. Two major types of failure were recognized:

(a) Breaks through the thread, and

(b) Breaks under the head.

Also minor failures by (c) stripping of the thread and (d) through the cotter-pin hole of the bolts, lot 1, occurred occasionally. Such failures were disregarded in most instances, see later.

Consequently, each test supplied, fundamentally, two values:

(a) The strength of one of the two sections, the thread root section or the section under the head, and

(b) A stress below the strength of that section which did not fail.

In addition to tests on bolts in the shape as supplied, tests were made also on bolts reduced in section at various points, Fig. 1. Some such specimens were provided with a 60-degree sharp notch,

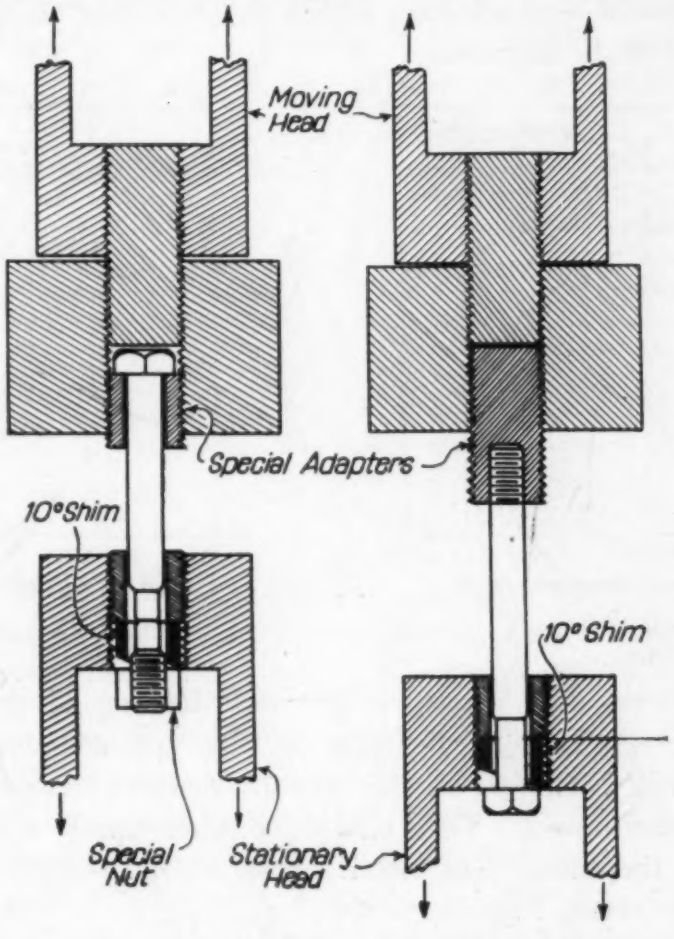

Fig. 3—Tensile Testing Fixture for Testing Bolts Under Combined Tension and Bending.

which removed 30 per cent of the cross-sectional area of the reduced section. Further series of tests were made on bolts with an increased radius machined under the head. Also, the ultimate strength was determined by testing specimens with a reduced cylindrical section.

Thus, four different strength characteristics of the 2330 steel in various conditions of heat treating were determined:

(a) The strength through the thread, or "thread strength",

(b) The strength under the head, or "head strength",

(c) The strength through the notched section or "notch strength", and

(d) The ultimate strength or "strength level" of a cylindrical section.

With the exception of the cylindrically machined bars, all other types of test bars were subjected to tensile tests in two ways, Fig. 1:

(a) By means of regular ball-seat fixtures, and

(b) provided in addition with a tapered shim or washer having an angle of 10 degrees.

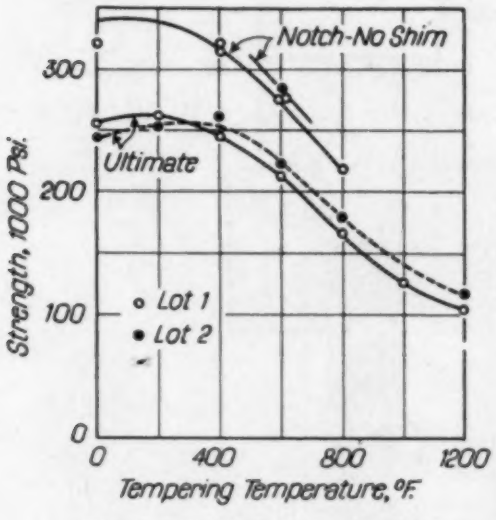

Fig. 4—Ultimate Strength and Notch Strength—No Shim.

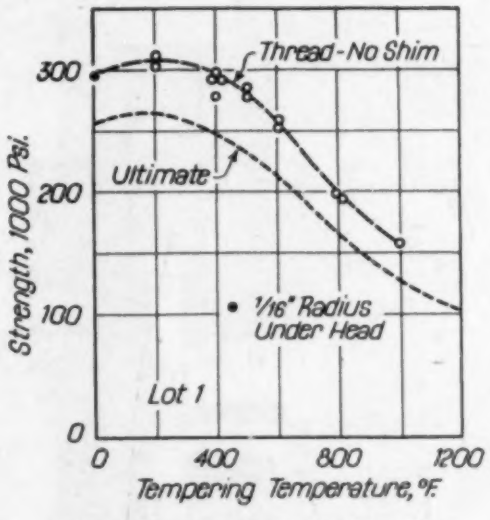

Fig. 5—Thread Strength—No Shim.

The tapered shim results in eccentric loading of the test bar, or in a superposition of bending on the applied tension. This eccentricity will be higher in the sections close to the shim than in sections farther away. This enables one to apply a higher eccentricity to the thread (or notch) than to the section under the head and vice versa, Fig. 3.

The rolled thread, as well as the corners under the head, and also the machined sharp notch and machined head fillet had a radius of approximately 0.002 to 0.003 inch.

The results of the various series of tests are plotted in Figs. 4 to 11 against the tempering temperature.

The ultimate strengths of the two lots of bolts, Fig. 4, differed slightly, as previously mentioned. A maximum ultimate strength of approximately 260,000 pounds per square inch was obtained by tempering at 200 to 400 degrees Fahr. (95 to 205 degrees Cent.).

The thread strength, Fig. 5, and notch strength, Fig. 4, in tests without shim, were almost identical for a given condition. This confirms the previously recognized fact that threads (6) and compound notches (7) behave much the same way as a single notch of the same contour and depth.

Throughout the whole range of the investigated strength levels, both the thread strength and notch strength are 30 ± 5 per cent higher than the ultimate strength. The notched section appears slightly stronger than the threaded section, but this may be explained by various factors, such as differences in contour, in decarburization, etc. The absence of low strength values in these

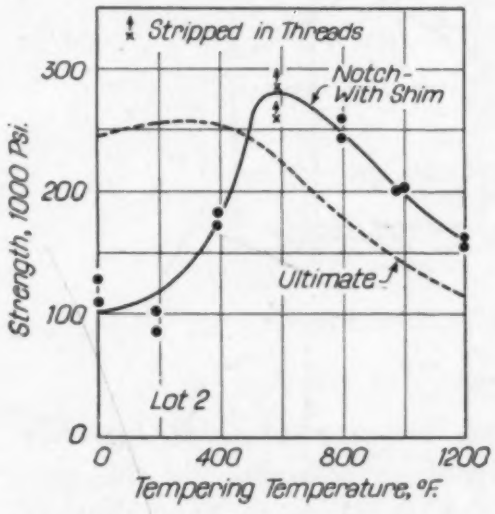

Fig. 6—Notch Strength—With Shim.

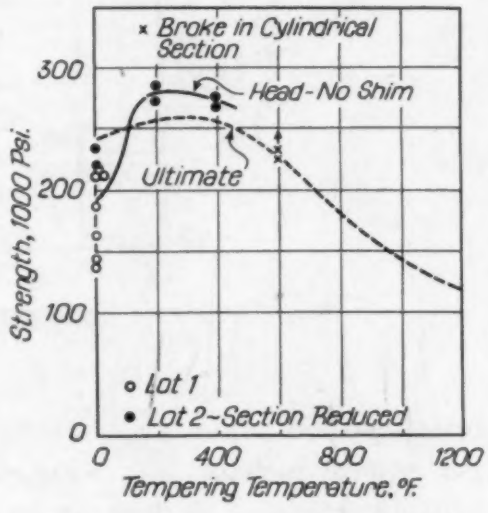

Fig. 7—Head Strength—No Shim.

series of tests, Fig. 4 and 5, means that the threaded section of S.A.E. 2330 steel bolts is not susceptible to an embrittlement for any possible heat treatment or strength level, if subjected to regular tension with little or no eccentricity.

However, if a shim is added under the nut, the bolts were found to possess a much lower strength than without a shim. In the series on threaded bolts, very irregular results were obtained and the thread stripped in all tests. This is rather peculiar, as for similar previous tests (5) results are reported which agree with previous results (4) and the present tests on notched bars. No attempts were made to reveal the reasons for the stripping of the thread in the present tests.

Thus, a shim under the nut of bolts provided with a notch close to the thread resulted in low notch strength values of the

highest strength levels, being less than 40 per cent of the ultimate strength, Fig. 6. With increasing strength level, the notch strength increased rapidly, and became practically the same as that of bars

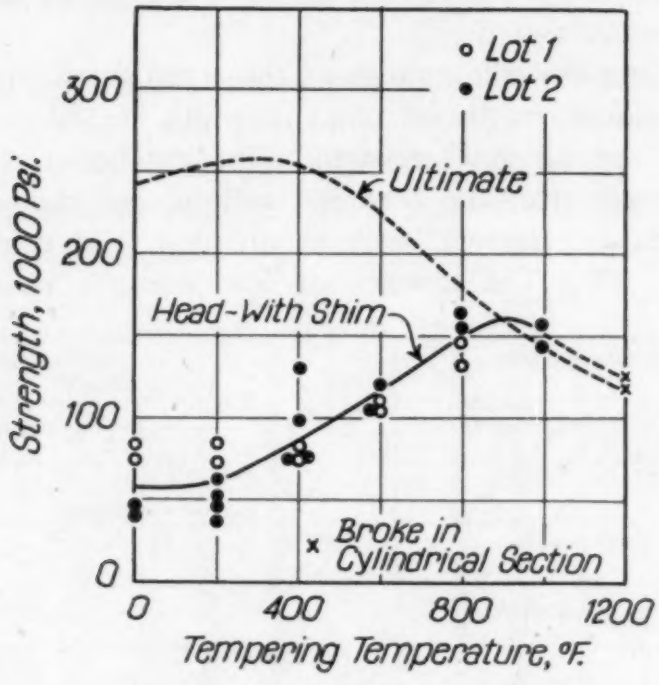

Fig. 8—Head Strength—With Shim.

tested without shim if the strength level decreased to 225,000 pounds per square inch or less. Fig. 10 illustrates schematically this embrittling effect of a shim under the nut on the notch (and thread) strength.

The section under the head was found to be more susceptible to embrittlement than the thread, Fig. 7. In the as-quenched condition, all test bars failed in a cup-like fashion, Fig. 2, underneath the head, rather than through the generally weaker section through the thread. Also, if the section was reduced under the head, the as-quenched bars still failed under the head in a brittle fashion, rather than through the cylindrical section. This is interesting in that it proves that the embrittlement of the head is not primarily dependent upon the fiber as determined by the heading process but upon the notch effect of the head contour.

In order to obtain a thread failure for the as-quenched condition, the radius under the head was increased by machining off a part of the head, from a few thousandths of an inch to $\frac{1}{16}$ inch, Fig. 1. Thus, such a stress relief radius increased considerably the

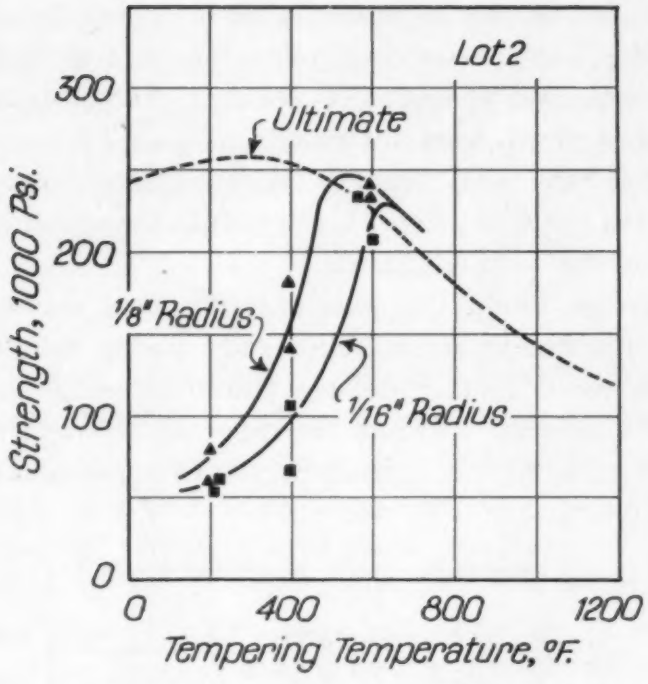

Fig. 9—Effect of Stress Relief Radius Under Head—With Shim.

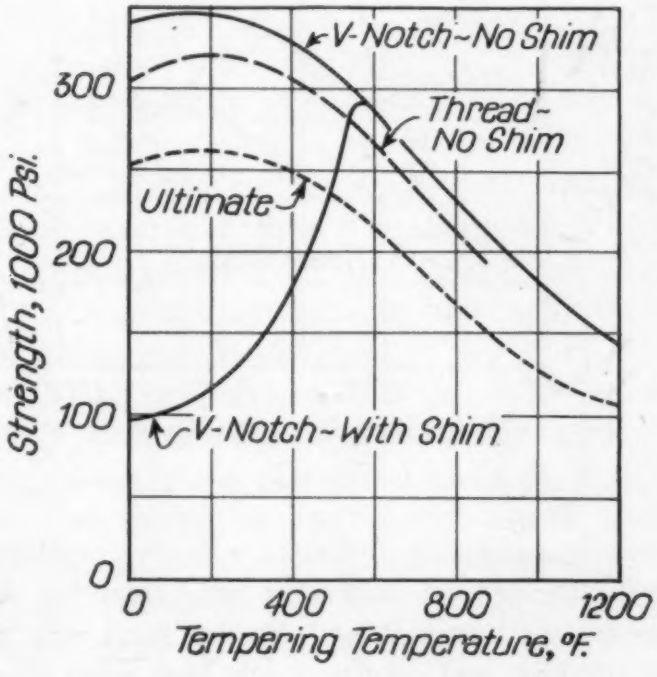

Fig. 10—Results of Various Thread and Notch Tests (Schematic).

strength of the section under the head, if the conditions are conducive to brittle failures.

The tests with a shim under the head also showed that the

section under the head was more liable to embrittlement than the thread, Fig. 8. The head strength for the high strength levels, if tested with a shim, was as low as 20 per cent of the ultimate strength. Only when the strength level decreased to 160,000 pounds per square inch or lower did the head strength become identical for bolts tested with and without the shim, Fig. 11, the failure then occurring through the thread or in the reduced section.

Again, it was found that this embrittlement could be reduced materially by machining stress relief radii under the head, Fig. 9. But even a radius of 1/8 inch did not eliminate completely the effect of the shim. However, it raised the range of strength levels which were not susceptible to brittle head breaks to approximately 240,000 pounds per square inch, Fig. 11.

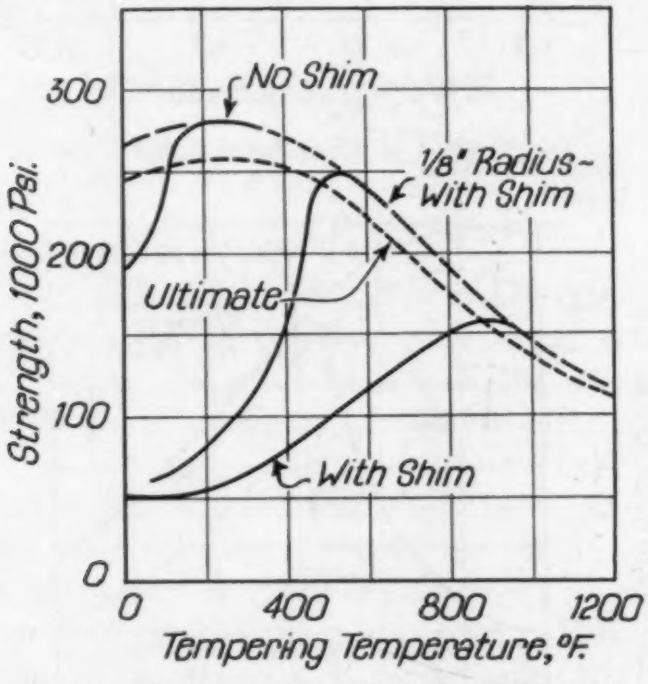

Fig. 11—Results of Various Head Tests (Schematic).

The present investigation indicates a higher tendency towards embrittlement for the section under the head than for the threaded section. However, as clean thread breaks were not obtained in these tests with shims, and as the notch was some distance away from the shim, the actual properties of the threaded section were not revealed by these tests. Previous experimentation on some alloy steels (4) (5) in which thread and notch breaks occurred close to the shim yielded low strength values if the strength level was

160,000 pounds per square inch or higher, while in the present tests low notch strength values were obtained only for strength levels above 220,000 pounds per square inch. It will therefore be attempted in further tests to clarify this discrepancy and to determine in a more accurate manner the respective sensitivity of the two sections to superimposed bending.

Conclusions

1. In tension, with little or no superimposed bending, ductile breaks through the threads occur except in the as-quenched bolts.

2. As-quenched bolts show brittle failures under the head at low and widely scattered loads, thus indicating greater notch sensitivity at this point than in the threads.

3. Failures under the head can be prevented by adding a "stress-relief" radius from shank to head. If necessary in practical cases, this may take the form of a semicircular groove having a radius of one-eighth to one-sixth of the shank.

4. Superimposed bending at either the head end or thread end causes brittle failures in these sections at considerably reduced loads. For a 10-degree shim under the head, brittle failures occur at the head for tempering temperatures below 800 degrees Fahr. (425 degrees Cent.) or strength levels above 160,000 pounds per square inch.

5. For a shim under the nut, failures occurred at very low loads by stripping of the threads in an apparently brittle manner. Only for tempering temperatures above 1200 degrees Fahr. (650 degrees Cent.) did the thread reach approximately the same strength when tested with a shim as without.

For tempering temperatures less than 400 degrees Fahr. (205 degrees Cent.) (strength levels above 250,000 pounds per square inch), brittle failures were obtained through a 0.002-inch-radius notch placed near the nut and tested with a shim under the nut.

6. Brittle breaks under the heads are suppressed by the use of a relief groove. Commercially feasible radii ($\frac{1}{16}$ inch) permit superimposed bending without impairment at strength levels up to 225,000 pounds per square inch.

7. The as-quenched bolt showed a lower tensile strength and a greater tendency toward brittle failures with superimposed bending than a bolt stress relieved by tempering at 200 to 400 degrees Fahr. (95 to 205 degrees Cent.).

8. Bolts of the selected steel and size may be heat treated to 250,000 pounds per square inch if the straining in service is to be in pure tension, but 175,000 pounds per square inch is the maximum safe limit if superimposed bending is present.

9. A greater strength level may be used in the presence of superimposed bending if a fillet is used under the head. Possible improvement may result from the use of fillets in the thread bottoms.

Bibliography

1. G. Sachs and J. D. Lubahn, "Notched-Bar Tensile Tests on Heat Treated Low Alloy Steels", TRANSACTIONS, American Society for Metals, Vol. 31, 1943, p. 125.
2. G. Sachs and J. D. Lubahn, "Effects of Notching on Strained Metals", *Iron Age*, Vol. 150, 1942, Oct. 8, p. 31-38; Oct. 15, p. 48-52.
3. G. Sachs and J. D. Lubahn, "Bursting Tests on Notched Alloy Steel Tubing", TRANSACTIONS, American Society for Metals, Vol. 31, 1943, p. 71.
4. H. Kiessler and W. Connert, "Notched-Bar Tensile Tests with Superimposed Bending Strain", *Arch. Eisenhuettenwesen*, Vol. 14, 1940-41, p. 555-560.
5. K. Matthaes, "Notch Effects Under Static Stress," *Luftfahrtforschung*, Vol. 14, 1938, p. 28-40; *Metal Treatment*, Vol. 4, 1938, Spring Issue, p. 15-23.
6. W. Kuntze, "The Strength of Threads", *Zeit. V. D. Ing.*, Vol. 73, 1929, p. 469-471.
7. E. A. Davis, "Combined Tension-Torsion Tests on 0.35 Per Cent Carbon Steel," *Transactions*, American Society of Mechanical Engineers, Vol. 62, 1940, p. 577-586.

DISCUSSION

Written Discussion: By E. S. Jenkins, chief of structures department, Curtiss-Wright Corp., Buffalo, N. Y.

From the standpoint of the airplane designer the paper can best be summarized as showing that standard aircraft bolts may possibly have too low a strength rating. It is shown that for heat treatments up to 200,000 pounds per square inch ultimate tensile strength, the bolts can withstand considerable static eccentric load. If the designer feels that the static load strength is a sufficient criterion he may easily convince himself that he can rerate the bolts by increasing their strength by a different heat treatment. It is interesting to note that the standard heat treatment for commercial aircraft bolts is at the highest tempering temperature studied in the paper. Although the static strength may be raised substantially by lowering the tempering temperature, it is believed that repeated load tests will be required to convince the designers that it will be wise to go very far in this direction.

Written Discussion: By R. B. Bland, structures research engineer, Lockheed Aircraft Corp., Burbank, Cal.

The results given in the subject paper have already been applied in a qualitative way. When making acceptance tests of castings, we usually find it nec-

essary to heat treat the attaching bolts to high strength levels in order to obtain failure in the casting. When the loads result in purely tensile stresses in the bolt, we can use strength levels of 250,000 pounds per square inch; but where bending stresses are present in the bolt it is necessary to use lower strength levels of the order of 180,000 pounds per square inch or less.

In conducting fatigue tests of bolts, we sometimes obtain failures in the threads, and sometimes under the head, especially if any eccentricity is present. Fatigue failures in the threads can readily be combatted by rolling the threads, but fatigue failures under the head can best be met by giving a radius to the junction of head and shank.

The low thread-strength values for eccentric loading are undoubtedly due to the fact that the threads are too brittle to allow sufficient deformation so that all the thread around the bolt circumference can share in carrying the load.

In general, the authors are to be congratulated on their paper, which gives results of direct value to the airplane industry. In only two instances can this paper be criticized:

(1) It should have been specified, as in Ref. 1 of the paper, that the impact strength is a minimum for tempering temperatures of 1110 degrees Fahr. (600 degrees Cent.). This strength range of 220,000 pounds per square inch, which appears to be the best except for head failures, is not the best from the standpoint of impact strength. However, if impact strength is not a consideration, and if fatigue loads are unimportant, the use of heat treatment in this region might result in small but definite weight savings in the airplane structure.

(2) The tests under eccentric loading do not mean much except insofar as they furnish us with a "floor" to the worst conditions we are likely to meet. For many practical applications, it is possible to compute the bending moments, and hence tests under a constant bending moment would probably be of greater value. The test setup, as shown, yields a bending moment that, when we consider local deformations, must vary in an extremely complex manner with load. An interaction curve, from pure bending to pure tension, would be highly desirable.

Oral Discussion

RAY VINES:[3] Some practical work we did in connection with hydrogen embrittlement of zinc plated, hardened steel screws may be of interest in connection with this paper. We were running into trouble with breakage on high strength screws and to determine safe limits we zinc plated and tested several types of screws which had been heat treated and drawn to various hardness levels. Simulating service conditions, the treated screws were used to tighten a spring clamp to a bar, some bending being superimposed upon the tension by the nature of the clamp. The imposed stress was sufficient to cause breakage if the screw had been embrittled by plating, the number of screws broken after an overnight period serving as a guide to the degree of embrittlement. Although various types of screws were tested, the significant features can be shown by the results obtained on screws made by upsetting the head and rolling the thread. One set of these screws had a radius, which was formed during upsetting, at

[3]Metallurgist, Ford Instrument Co., Long Island City, N. Y.

the head-shank junction while the other set was machined after forming to a sharp corner at the head-shank junction.

When tested immediately after zinc plating and without the benefit of a hydrogen relief treatment, severe breakage occurred on screws with and without radii if the hardness was above about Rockwell "C" 40. The amount of breakage increased with increase in hardness, reaching 100 per cent (all out of a minimum of 10 screws tested) at a hardness of Rockwell "C" 43. It was observed that the screws without radii usually broke at the head-shank junction while those with radii usually broke in the threads. Furthermore, the incidence of head-shank breakage increased with increase in hardness as shown below.

Screws with Radii		Screws Without Radii	
Hardness Rockwell "C"	Percentage of Breaks at Head-Shank Junction	Hardness Rockwell "C"	Percentage of Breaks at Head-Shank Junction
52.5	18 per cent	51.5	92 per cent
43.0	0 per cent	43.0	78 per cent
39.0	None Broken	39.0	15 per cent

It should perhaps also be noted that for any given hardness and plating condition, the screws without radii suffered a much greater percentage breakage than the screws with radii. Furthermore, relieving treatments (400 degrees Fahr. for two or more hours) were successful in eliminating the breakage in the screws with radii even at Rockwell "C" 52.5 but they did not reduce the breakage on the screws without radii at a Rockwell of "C" 51.5.

There is one other point that I would like to mention, namely, the effect of hydrogen embrittlement in increasing the severity of a given notch or increasing the notch sensitivity of a given steel. Professor Sachs mentioned, in connection with the other paper given here this morning, that the shape of the part and notch, the speed and temperature of testing and almost everything else were important in notch sensitivity tests. I was wondering, if in connection with these studies, hydrogen embrittlement might not be used as a substitute for high testing speeds or very sharp notches.

SAM TOUR:[4] I wish to compliment Dr. Sachs on both of these papers. They are very valuable contributions to our knowledge.

I wish to assume some of the prerogatives of the author and discuss one of the discussions to the paper before the author does. Particularly my remarks are directed against the suggestion made by Mr. Vines of superimposing hydrogen embrittlement upon other tests. In all sharp notch work there are numerous variables, as Dr. Sachs has tried to point out and has demonstrated. Variables of thickness, variables of radius of notch and numerous other variables make the situation almost bewildering. I would certainly hesitate to superimpose upon this the most bewildering thing, hydrogen embrittlement. If we only knew something about hydrogen embrittlement we might be able to control it a little better. Knowing so little about it, its mechanism and what really causes it, how to get away from it, how to decrease it, we certainly are in no position to use it as a multiplying factor to enhance some other faults.

In zinc plating, hydrogen embrittlement occurs in one factory to a decided extent, in another factory to a much less extent—apparently both factories using the same practice. The reasons for the variation are certainly not clear. Such

[4]President, Sam Tour & Co., Inc., New York City.

minor details as a change in temperature of 10 degrees, the pH of the plating solution, a change of only a minute or two in the pickle dip, a change in the acid concentration of the pre-dip, all affect this hydrogen embrittlement. A 24-hour layover after plating seems to have an effect. Summer has an effect as against winter. There are so many variables in hydrogen embrittlement that I would very much hesitate to draw that red herring across the trail of any other physical property.

RAY VINES: I can agree with Mr. Tour that hydrogen embrittlement is very confusing but I am inclined to disagree with him on the fact that one plant encounters hydrogen embrittlement while another one using the same practice does not. Differences in "ductility" do in fact occur from plant to plant and also from time to time in the same plant but since we do not have a good test for hydrogen embrittlement we cannot say that these differences are in hydrogen embrittlement. A slight change in design on the screws mentioned above was the factor determining whether or not they were embrittled by exposure to hydrogen. As with notch sensitivity, some of the confusion of hydrogen embrittlement will disappear when the usual superimposed variables are eliminated.

R. E. CHRISTIN:[5] I appreciate Dr. Sachs' last paper. It brings to mind some of the designs we have had to work with. We had to take a cold-headed bolt or upset bolt and machine under the head, which brings it into the classification of a machined bolt. Dr. Sachs made the remark in his paper about a cold-headed bolt not showing up as well as a machined bolt and it may have been due to the fact that it may have been machined after cold heading. We must take that into consideration. An aircraft quality bolt calls for a 0.005 to 0.015 radius under the head. It also calls for a ground finish. You must put the undercut under the head to allow for the grinding wheel. I feel that more work probably could be done about a design that would allow us to take the cold-headed bolt and grind it without doing any machining under the head, by permitting the larger radius under the head so these stress raisers wouldn't be placed in there. I believe all the undercutting under the head is dangerous, because in putting a 0.005 to 0.015 radius under the head with a tool, it is pretty difficult to keep your tools in apple pie order. I have rejected bolts in process due to this condition where the tools would wear down and leave a lot of tool marks. In the magnaflux test those tool marks will show up like a crack. Well, if you cut the bolt head and place it under the microscope you will find out that those marks under the head appear to be 0.002 to 0.003 deep. That may not seem very bad but they do show up under a magnaflux. It leaves the consumer in doubt as to whether those bolts shall pass. I believe, like you probably read in Mr. Almen's papers, that design plays such an important part in this failure. We are asking the bolt manufacturers to hold those radii as far as possible to 0.005 to 0.015. I believe with such a low radius that it is very difficult to keep your tools sharp and to prevent any more tool marks. Sometimes you end up with a bolt, although you have a 0.015 radius, with more tool marks than you started with and those are the bolts that usually show up under magnaflux. And I should like to add to Dr. Sachs' paper that a little more effort be made to get away from these stress radii. Why should a machined bolt stand up better than a cold-headed bolt after heat treatment? I would think that a cold-

[5]Metallurgist, Columbus Bolt Works Co., Columbus, Ohio.

headed bolt without tool marks would be just like a machined bolt without tool marks. The less machining, the better.

Authors' Reply

As far as my understanding goes, Mr. Jenkins and Mr. Bland draw the conclusion from our tests that the use of bolts having a strength of 200,000 pounds per square inch should be safe if concentric loading is secured. The tests with eccentric loading are considered as representing a condition which will be more severe than any likely to be met in practice. However, while eccentricity may be controlled within certain limits, other embrittling factors, such as section size, for instance, may affect considerably the maximum strength level which is safe.

Another such embrittling factor is hydrogen embrittlement, according to Mr. Vines. His experience indicates that steel screws having a strength level as low as 180,000 pounds per square inch (Rockwell C hardness 39) are likely to break in a brittle fashion, under the head, if tested under practical conditions. Regarding Mr. Vines' suggestion to utilize hydrogen embrittlement for testing purposes, we agree with Mr. Tour that other factors, such as eccentricity or notch sharpness, may be controlled more readily.

One peculiar result, which I would like to mention in relation to Mr. Christin's remarks, is that we found specimens with machined square shoulders less likely to break under the head than upset bolts. The two series of tests were not entirely comparable, but it appeared to us that headed bolts may or may not be superior to machined bolts, depending upon as yet unknown features of their fabrication.

It may be mentioned again that the results of notched bar tensile tests are in agreement with those of notched bar impact bending tests, at present. We also wonder whether repeated stresses can be evaluated as an embrittling factor in much the same manner as other such factors. In general, there are two types of embrittling factors: external factors, such as discussed primarily in the two papers presented by us; and internal or structural factors, such as strength level and hydrogen embrittlement. It appears possible that the action of all external factors could be explained fundamentally in the same manner, being primarily a function of the ductility of the metal.

EFFECT OF QUENCHING-BATH TEMPERATURE ON THE TEMPERING OF HIGH SPEED STEEL

By Paul Gordon, Morris Cohen and Robert S. Rose

Abstract

The relationship between the quenching-bath temperature and the tempering kinetics of 6-5-1.5 high speed steel was studied by means of magnetic, dilatometric and hardness measurements. In particular, the retained austenite decomposition on tempering was followed as a function of time and temperature during single, double and multiple tempering.

If the austenitized steel is cooled to room temperature prior to tempering, the retained austenite can be essentially decomposed by tempering for about 2.5 hours at 1050 degrees Fahr. (565 degrees Cent.), but if the hardening quench is arrested above room temperature, correspondingly large quantities of austenite are transferred to the tempering process and appreciable amounts remain after the above tempering treatment. Extending the time at 1050 degrees Fahr. (565 degrees Cent.) beyond 2.5 hours does little to reduce the residual austenite, while higher tempering temperatures result in considerable softening. However, practically complete decomposition of the retained austenite can be achieved in 2.5 hours at 1050 degrees Fahr. (565 degrees Cent.) by double or multiple tempering, even if the quenching-bath temperature is high. A tentative explanation for this marked difference between single and repeated tempering after arrested quenching has been presented.

Transverse bend tests demonstrate that arrested quenching followed by single tempering yields inferior strength properties. On the other hand, if repeated tempering is used in accordance with principles described, very satisfactory transverse strength values can be attained despite high quenching-bath temperatures.

THE tempering of high speed steels as reported in previous publications was conducted upon specimens hardened by cooling from the austenitizing temperature to *room temperature*. It is now

A paper presented before the Twenty-fifth Annual Convention of the Society, held in Chicago, October 18 to 22, 1943. Of the authors, Paul Gordon is research assistant, and Morris Cohen is associate professor of physical metallurgy, Massachusetts Institute of Technology, Cambridge, Mass., and Robert S. Rose is sales metallurgist, Vanadium-Alloys Steel Co., Boston. Manuscript received July 12, 1943.

essential to inquire whether deviations from this practice materially alter the tempering characteristics and thereby affect the ultimate properties of the steel. This issue was raised by the recent work of Gordon and Cohen (1)* who showed that subatmospheric cooling of hardened high speed steel prior to normal tempering causes improved mechanical properties. The merits of such low-temperature treatment have since been confirmed by actual performance tests. Consequently, it may be inferred that the lowest temperature which the austenitized steel attains as a part of the hardening operation has considerable influence on the ultimate behavior of the steel in service.

Now, in the commercial heat treatment of high speed steel, it frequently happens that in the hardening operation the tools are not allowed to reach even room temperature—let alone subzero temperatures—before being transferred to the tempering furnace. This procedure is commonly adopted in the case of complicated tools which are particularly susceptible to distortion and cracking, and is accomplished by arresting the quench from the high heat temperature, whether the cooling be conducted in air, oil, or in molten salt followed by air. It is also likely that many hardened tools fail to attain room temperature because of inadvertent reasons. Quenching oils often become heated due to continuous usage, and if the tempering is carried out directly after quenching into such oil, the minimum temperature between austenitizing and tempering may become relatively high. In fact, room temperature itself may vary through wide limits from time to time.

It has been amply demonstrated (2), (3) that, in the hardening of high speed steel, the austenite-martensite transformation takes place characteristically on cooling below the M-point, and thus the austenite : martensite ratio that goes into the tempering process depends upon the temperature to which the steel is cooled in the hardening operation. One immediately begins to wonder whether the mechanism of tempering is affected by the presence of unusual amounts of austenite resulting from limited cooling through the martensite range. There is no assurance, for example, that the kinetics of retained austenite decomposition on tempering, as established for steels hardened to room temperature (4), remain the same when the hardening quench is stopped above room temperature. As a matter of fact, it is conceivable that our lack of basic information concerning this interesting tempering problem is responsible for

*The figures appearing in parentheses refer to the bibliography appended to this paper.

unnecessarily inferior properties in those instances where the austenitized tools are not cooled "all the way".

The present paper attempts to lay the scientific groundwork for the answers to these important questions. Magnetic, dilatometric, hardness, and metallographic studies are reported here for high speed steel during tempering after austenitizing and quenching to bath temperatures between 80 and 500 degrees Fahr. (25 and 260 degrees Cent.), thus simulating various degrees of arrested cooling in the hardening operation. In particular, the retained austenite decomposition on tempering is followed as a function of time and temperature with single, double and multiple* tempers. The detrimental consequences of the arrested cooling treatments, and the beneficial effect of the proposed corrective measures, are demonstrated by transverse bend tests.

Experimental Details

Material Studied—The composition of the high speed steel forming the basis of this investigation is given in Table I. It is a standard commercial grade, commonly referred to as 6-6-2, although it might be more accurately designated as 6-5-1½. The steel was obtained in the form of annealed, centerless-ground, ¼-inch diameter rods through the courtesy of Mr. James P. Gill of the Vanadium-Alloys Steel Company.

Table I
Chemical Analyses

Heat No.	C	Mn	Si	W	Cr	V	Mo
5360	0.805	0.26	0.33	5.87	4.07	1.50	4.84

Heat Treatment — In all cases, the specimens were austenitized at a temperature of 2225 degrees Fahr. (1220 degrees Cent.) in a carbonaceous muffle, then dipped momentarily into molten lead at 1050 degrees Fahr. (565 degrees Cent.) to abstract the major part of the heat, and quenched into hot oil or molten metal at the predetermined arrested cooling temperature for about ten minutes. This period of time was sufficient to bring the specimens to the quenching-bath temperature without introducing any appreciable isothermal transformation of the austenite (2). Then, *without further*

*The term "multiple tempering" is used in this paper to indicate three or more tempering cycles.

cooling to room temperature, the specimens were transferred directly to a suitable lead bath for the tempering treatment. In general, the cooling from the tempering bath to room temperature was conducted in air. For the double and multiple tempering experiments, the first tempering cycle was performed just as described, while each of the succeeding tempers consisted of heating from room temperature to the tempering temperature, holding for the specified interval of time, and cooling in air to room temperature. All temperatures were controlled to ±5 degrees Fahr. (±3 degrees Cent.).

Types of Measurements — The specimens for all the measurements were ¼ inch in diameter with lengths as follows: ⅜ inch for the hardness and metallographic studies, 2 inches for the dilatometric runs, 4¼ inches for the magnetic determinations, and 5 inches for the bend tests. The hardness readings were made with a Rockwell machine, and are believed accurate to ±0.3 units on the C-scale. Complete descriptions of the dilatometric and magnetic apparatus are given elsewhere (2), (5). In the bend tests, the specimens were supported on a 4½-inch span, and loaded transversely at two intermediate points to provide a uniform bending moment over the middle third of the span. The breaking strength or modulus of rupture was calculated from simple beam theory and the maximum transverse load which the specimen could sustain. These measurements were carried out in triplicate, and the average values reported here are probably accurate to ±5 per cent.

In this investigation, the progress of the retained austenite decomposition as a result of tempering was observed by means of magnetic measurements at room temperature after the tempering treatment. This method was selected in preference to others available because of its high sensitivity and rapid execution. It was also thought desirable to ascertain the amounts of retained austenite on a quantitative basis, and hence the magnetic measurements were calibrated with the aid of variously-treated 6-5-1½ specimens whose austenite contents were known from independent dilatometric experiments (2). The resulting correlation is shown in Fig. 1. It will be noted that the intensity of magnetization becomes zero at about 93 per cent austenite (rather than at 100 per cent) because the austenitizing treatment leaves approximately 7 per cent of undissolved, non-ferromagnetic carbides. While the magnetic measurements can be made very accurately (±0.2 per cent), the conversions

to austenite contents using Fig. 1 are no more accurate than the dilatometric method employed for the calibrating specimens in the first place. This experimental error is estimated at ±2 per cent austenite.

It is known that the curve in Fig. 1 does not hold for 18-4-1 high speed steel, and therefore its application to compositions other than the one under discussion is not recommended. Also, the state of stress influences the magnetization values somewhat, and stress relief during tempering may cause an increase in magnetization even

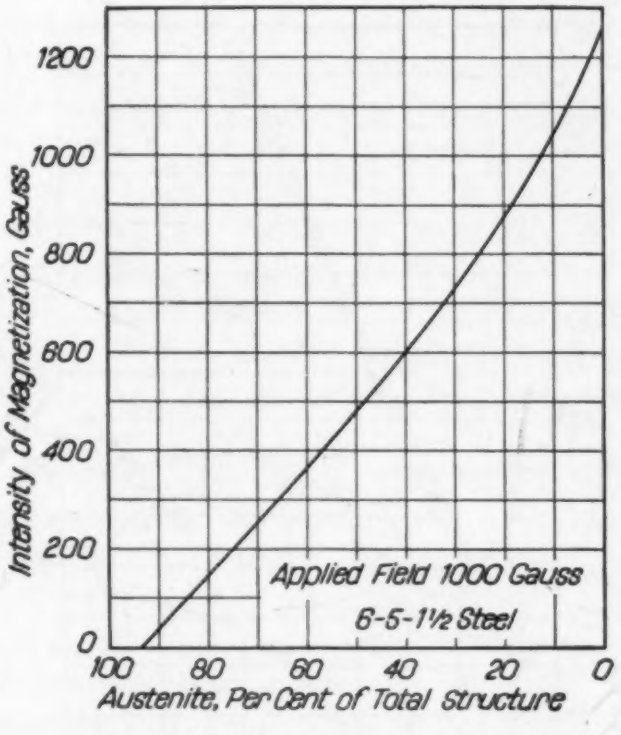

Fig. 1—Calibration Curve for Converting Intensity of Magnetization into Per Cent Austenite.

though the austenite content does not change. Fortunately, however, these stress effects, as observed at an applied field of 1000 gauss, are well within the ±2 per cent uncertainty stated above. Moreover, within these limits, Fig. 1 is valid whether the ferromagnetic constituent co-existing with the austenite is tetragonal martensite, tempered martensite, bainite or pearlite. Again, it should be cautioned that this fortuitous circumstance does not necessarily prevail in other steels.

Discussion of Results

Effect of Quenching-Bath Temperature Followed by Normal Tempering—A set of specimens for magnetic and hardness measurement was austenitized at 2225 degrees Fahr. (1220 degrees Cent.), cooled to temperatures between 80 and 500 degrees Fahr. (25 and 260 degrees Cent.), and tempered directly at 1050 degrees Fahr. (565 degrees Cent.) for 2½ hours. This tempering treatment may be considered as normal since it has been shown to convert virtually all of the retained austenite in room temperature quenched high

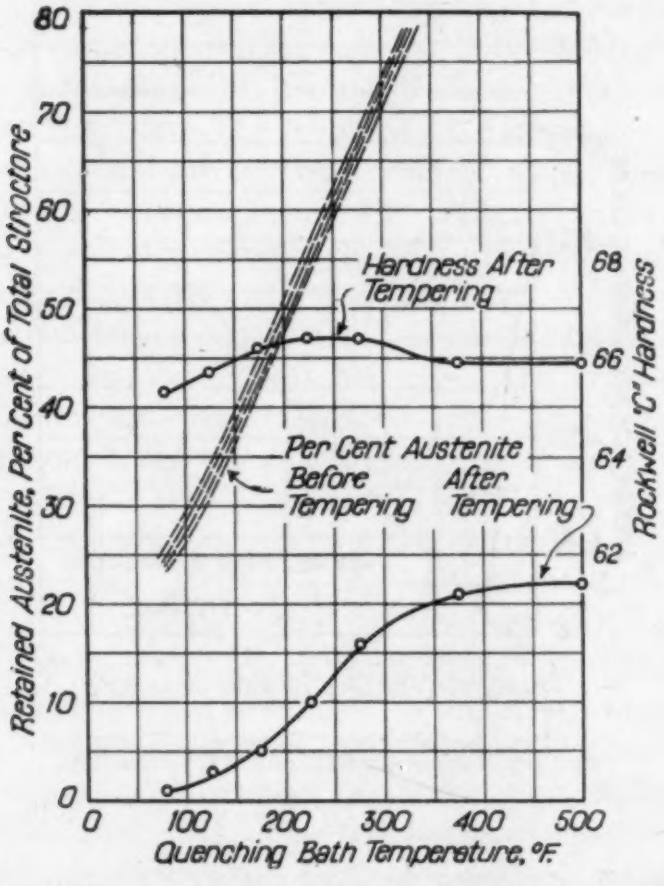

Fig. 2—Per Cent Austenite and Hardness after Quenching to Indicated Temperatures and Single Tempering Directly for 2.5 Hours at 1050 Degees Fahr.

speed steel (6). The austenite contents and hardness values resulting from the above cycles are plotted in Fig. 2 as a function of the quenching-bath temperature. For the sake of easy comparison, the amounts of austenite existing in the steel *at* the quenching-bath

temperature before tempering are also shown in Fig. 2. The latter data were taken from previous work of the authors (2).

According to Fig. 2, the 2½-hour tempering treatment at 1050 degrees Fahr. (565 degrees Cent.) reduces the retained austenite content to about 1 per cent if the austenitized steel is first cooled to room temperature during the hardening operation. However, when the hardening quench is arrested at higher temperatures, not only are there increasing amounts of austenite present before tempering but there is also more and more austenite remaining in the steel *after* tempering. For example, if the quenching-bath temperature is 225 degrees Fahr. (105 degrees Cent.), about 53 per cent of austenite is carried over into the tempering process, and 10 per cent of austenite remains (at room temperature) after tempering for 2½ hours at 1050 degrees Fahr. (565 degrees Cent.). whereas if the hardening quench is continued to 80 degrees Fahr. (25 degrees Cent.), there is only about 23 per cent of austenite available for tempering, and practically none after tempering. The maximum austenite content (22 per cent) retained after such tempering occurs when the quenching is arrested above the martensite range (M-point = 420 degrees Fahr., 215 degrees Cent.). In other words, quenching to a temperature such as 500 degrees Fahr. (260 degrees Cent.) and then tempering yields approximately the same amount of retained austenite as quenching to room temperature without subsequent tempering. It appears, then, that with regard to the transformation of the last portion of the austenite, tempering becomes less efficacious as the quenching-bath temperature is raised.

The hardness after tempering increases from R_c 65 with a quenching-bath temperature of 80 degrees Fahr. (25 degrees Cent.) to R_c 66½ when the bath temperature is 225 to 275 degrees Fahr. (105 to 135 degrees Cent.), and then decreases to about R_c 66 as the bath temperature approaches and exceeds the M-point. At first glance, the enhanced hardness up to 225 to 275 degrees Fahr. (105 to 135 degrees Cent.) appears anomalous in view of the accompanying increase in the amount of austenite which persists after tempering. However, the reasons for this behavior are quite clear. It must first be remembered that the residual austenite brought over into the tempering process transforms on cooling from the tempering temperature (cf. Fig. 6), and the secondary martensite thus formed is untempered. On the other hand, the primary martensite developed during the hardening quench *is* subjected to the tempering heat, and

hence undergoes some softening. It is evident that as the quenching-bath temperature is raised, the amount of primary martensite formed diminishes and the amount of residual austenite becomes greater. Consequently, after tempering, the structural effect of raising the quenching-bath temperature is to decrease the amount of tempered martensite and to increase the amount of untempered martensite. This behavior is accompanied by a finite increase in hardness. However, above 275 degrees Fahr. (135 degrees Cent.), the trend is counteracted by the comparatively large amounts of austenite retained after tempering, and the hardness begins to fall off. The foregoing dependence of structural constitution on the quenching-bath temperature is tabulated quantitatively in Table II.

Another way of interpreting the hardness data in Fig. 2 is in terms of the maximum secondary hardness attainable on tempering at 1050 degrees Fahr. (565 degrees Cent.) after arresting the hardening quench at various temperatures. It will be demonstrated later (page 431) that the tempering time to reach maximum secondary hardness becomes longer as the amount of austenite retained on hardening is increased. For example, when the quenching-bath temperature is below 225 degrees Fahr. (105 degrees Cent.), a 2½-hour temper at 1050 degrees Fahr. (565 degrees Cent.) brings the steel into the softening stage beyond the secondary hardness peak, while with quenching-bath temperatures between 225 and 275 degrees Fahr. (105 and 135 degrees Cent.), maximum secondary hardness is reached in just about 2½ hours at 1050 degrees Fahr. (565 degrees Cent.). By the same token, when the bath temperature lies above 275 degrees Fahr. (135 degrees Cent.), 2½ hours at 1050 degrees Fahr. (565 degrees Cent.) is not sufficient to achieve the secondary hardness peak. It will be noted that the hardness values in Fig. 2 vary accordingly.

A study of Table II shows quite clearly that arresting the hardening quench at temperatures above 80 degrees Fahr. even when followed by normal tempering (2½ hours at 1050 degrees Fahr.) leaves appreciable quantities of retained austenite as well as much larger amounts of untempered martensite. Considering these effects plus the fact that the large amounts of untempered martensite form on cooling from the tempering temperature with attendant stress-raising volume changes, one would reasonably expect that arrested cooling on hardening might have serious consequences. This is confirmed by the results of the bend tests, listed in Table III. The transverse

Table II

Structure of High Speed Steel After Quenching to Indicated Temperatures and After Tempering Directly for 2½ Hours at 1050 Degrees Fahr. Percentages are on Volume Basis

	At Bath Temperature			At Room Temperature After Tempering			
Quenching-Bath Temperature Degrees Fahr.	a Per Cent Undissolved Carbide	b Per Cent Austenite (From Fig. 2)	c Per Cent Martensite (100–a–b)	d Per Cent Undissolved Carbide (= a)	e Per Cent Tempered Martensite (= c)	f Per Cent Austenite (From Fig. 2)	g Per Cent Untempered Martensite* (b–f)
80	7	23	70	7	70	1	22
125	7	31	62	7	62	3	28
175	7	41	52	7	52	5	36
225	7	53	40	7	40	10	43
275	7	65	28	7	28	16	49
375	7	89	4	7	4	21	68
500	7	93	0	7	0	22	71

*The amount of untempered martensite is taken as equal to the per cent of austenite which transforms as a result of tempering since this transformation takes place principally on cooling from the tempering temperature.

breaking strength is definitely lowered by not cooling all the way to room temperature before tempering.

Table III
Transverse Strength After Quenching to Indicated Temperatures and Tempering Directly for 2½ Hours at 1050 Degrees Fahr.

Quenching-Bath Temperature Degrees Fahr.	Modulus of Rupture Lbs. per Sq. In.	Comparative Strength Per Cent
80	434,000	100
125	363,000	84
175	287,000	66
225	309,000	71

Effect of Tempering Temperature After Arrested Quenching—Since a 2½-hour temper at 1050 degrees Fahr. (565 degrees Cent.) was found inadequate to decompose all of the retained austenite when the hardening quench was stopped above room temperature, it seemed of both technological and practical importance to study the effect of tempering temperature as an independent variable. Accordingly, a series of specimens was quenched to a bath temperature of 225 degrees Fahr. (105 degrees Cent.), and then tempered directly for 2½ hours at temperatures ranging from 80 to 1250 degrees Fahr. (25 to 675 degrees Cent.). The resulting hardness and retained austenite determinations are plotted in Fig. 3. On tempering between 80 and 225 degrees Fahr. (25 and 105 degrees Cent.) (after quenching to 225 degrees Fahr., 105 degrees Cent.), both the hardness and per cent of retained austenite remain constant. The final condition of the steel at room temperature after such treatment is essentially the same as that produced by direct quenching to room temperature.

In the tempering range between 225 and 750 degrees Fahr. (105 and 400 degrees Cent.), however, there is a marked decrease in hardness and a substantial increase in the amount of austenite. As a matter of fact, after tempering at temperatures between 450 and 750 degrees Fahr. (230 and 400 degrees Cent.), the austenite content (50 to 57 per cent) is approximately that existing in the steel at the quenching-bath temperature of 225 degrees Fahr. (105 degrees Cent.). Consequently, it must be concluded that tempering above 225 degrees Fahr. exercises a potent stabilizing influence on the available austenite. If it were not for this stabilization much of the existing austenite would transform on cooling from the quenching-bath temperature, i.e., if the tempering were omitted only 23 per cent

of austenite would remain in the steel at room temperature—the same amount as that retained on normal hardening. This stabilizing effect is actually strong enough when the tempering is conducted above 450 degrees Fahr. (230 degrees Cent.) to prevent any austenite decomposition from occurring on subsequent cooling to room temperature inasmuch as the M-point is suppressed to subatmospheric temperatures. The concurrent decrease in hardness is further evidence that tempering in this range leads to structures at room tem-

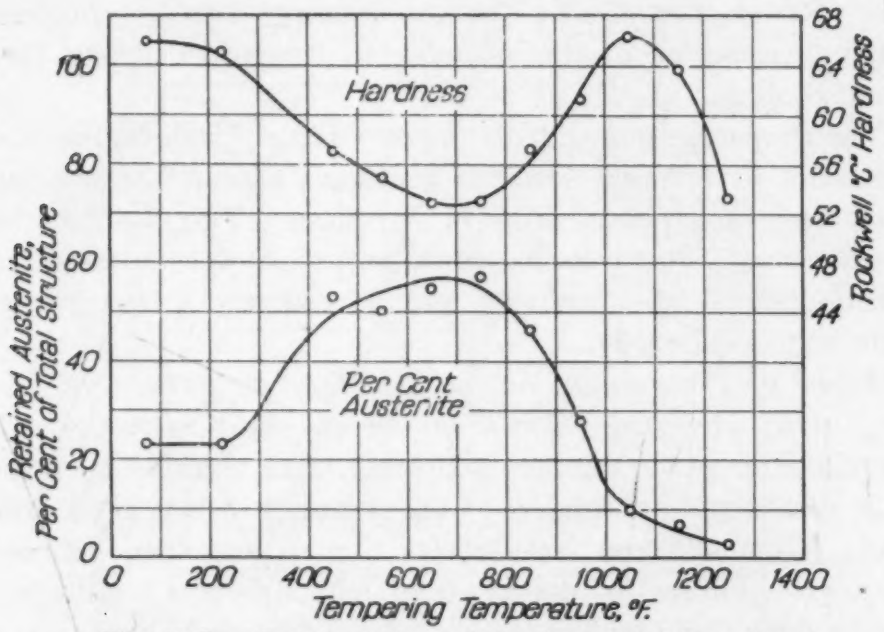

Fig. 3—Per Cent Austenite and Hardness after Quenching to 225 Degrees Fahr. and Single Tempering 2.5 Hours at Indicated Temperatures.

perature containing large proportions of austenite. Of course, part of this drop in hardness is due to the progressive tempering of the martensite formed during the hardening quench to 225 degrees Fahr. (105 degrees Cent.), but this softening effect is only of limited importance here. Even in steel quenched all the way to room temperature, thus containing some 70 per cent of martensite compared to the 42 per cent in the steel cooled to 225 degrees Fahr. (105 degrees Cent.), complete tempering of the martensite at 750 degrees Fahr. (400 degrees Cent.) is accompanied by a softening of only 4 points on the Rockwell "C" scale (4), whereas the softening shown in Fig. 3 amounts to almost 14 points.

When the tempering temperature is raised to 750 to 1050 degrees Fahr. (400 to 565 degrees Cent.) (Fig. 3), there is a sharp

increase in the hardness and a simultaneous reduction in the austenite content. Although the stabilizing effect described above is undoubtedly active at these tempering temperatures, the range is sufficiently high to cause carbide precipitation from the austenite and thereby condition the austenite for transformation during the cooling to room temperature. This conditioning becomes more marked as the tempering temperature is raised, until at temperatures above 950 degrees Fahr. (510 degrees Cent.) the stabilizing influence becomes completely obscured. However, even on tempering at 1050 degrees Fahr. (565 degrees Cent.) the conditioning does not proceed far enough to cause all of the austenite to transform during the subsequent cooling.

On tempering above 1050 degrees Fahr. (565 degrees Cent.), the amount of retained austenite continues to decrease but there is also a very precipitous drop in hardness. This combination of changes strongly suggests that some isothermal decomposition of the austenite takes place, probably into a relatively soft aggregate of ferrite and carbide (2).

Effect of Tempering Time at 1050 Degrees Fahr. (565 Degrees Cent.) After Arrested Quenching—In an effort to secure a better understanding of the tempering process after arrested quenching, a set of specimens was cooled to temperatures between 80 and 500 degrees Fahr. (25 and 260 degrees Cent.), and then tempered at 1050 degrees Fahr. (565 degrees Cent.) for different lengths of time, each specimen being tempered once. 1050 degrees Fahr. was selected for this study because of its common use in practice, and because it yields very high hardness after arrested hardening (Fig. 3). The austenite contents remaining after these treatments are shown in Fig. 4. Some results after tempering at 750 degrees Fahr. (400 degrees Cent.) are included as an illustration of what might be expected if extremely short times at 1050 degrees Fahr. (565 degrees Cent.) could be studied. The percentages of austenite at the quenching-bath temperatures are also indicated for comparison purposes.

The unusual trends in Fig. 4 are readily explained on the basis of the stabilizing and conditioning effects previously noted. The stabilizing influence is most clearly evident after quenching to temperatures up to 225 degrees Fahr. (105 degrees Cent.) followed by tempering at 750 degrees Fahr. or for very short times at 1050 degrees Fahr. (565 degrees Cent.). In fact, all of the austenite present in the steel at bath temperatures up to 225 degrees Fahr. (105 de-

grees Cent.) can be stabilized by tempering for 2½ hours at 750 degrees Fahr. (400 degrees Cent.). However, when the quenching-bath temperature is progressively raised above 225 degrees Fahr., the amount of austenite retained after tempering at 750 degrees Fahr. begins to diminish rapidly (curve 3, Fig. 4). Since relatively little conditioning occurs at 750 degrees Fahr., the decreasing amounts of

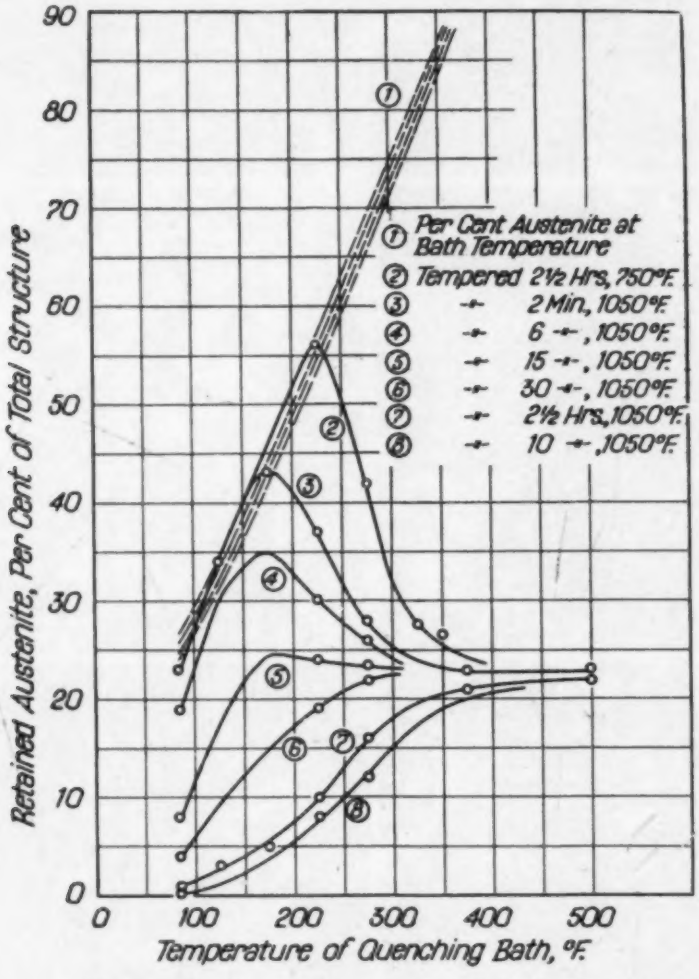

Fig. 4—Per Cent Austenite as a Function of Quenching-Bath Temperature and the Subsequent Tempering Treatment.

retained austenite cannot be entirely accounted for in this way. Consequently, it appears that the stabilizing action due to the tempering treatment becomes less and less potent as increasing quantities of austenite are carried into the tempering operation. In the extreme case where the bath temperature is above the M-point and the steel is completely austenitic (except for excess carbides) on being trans-

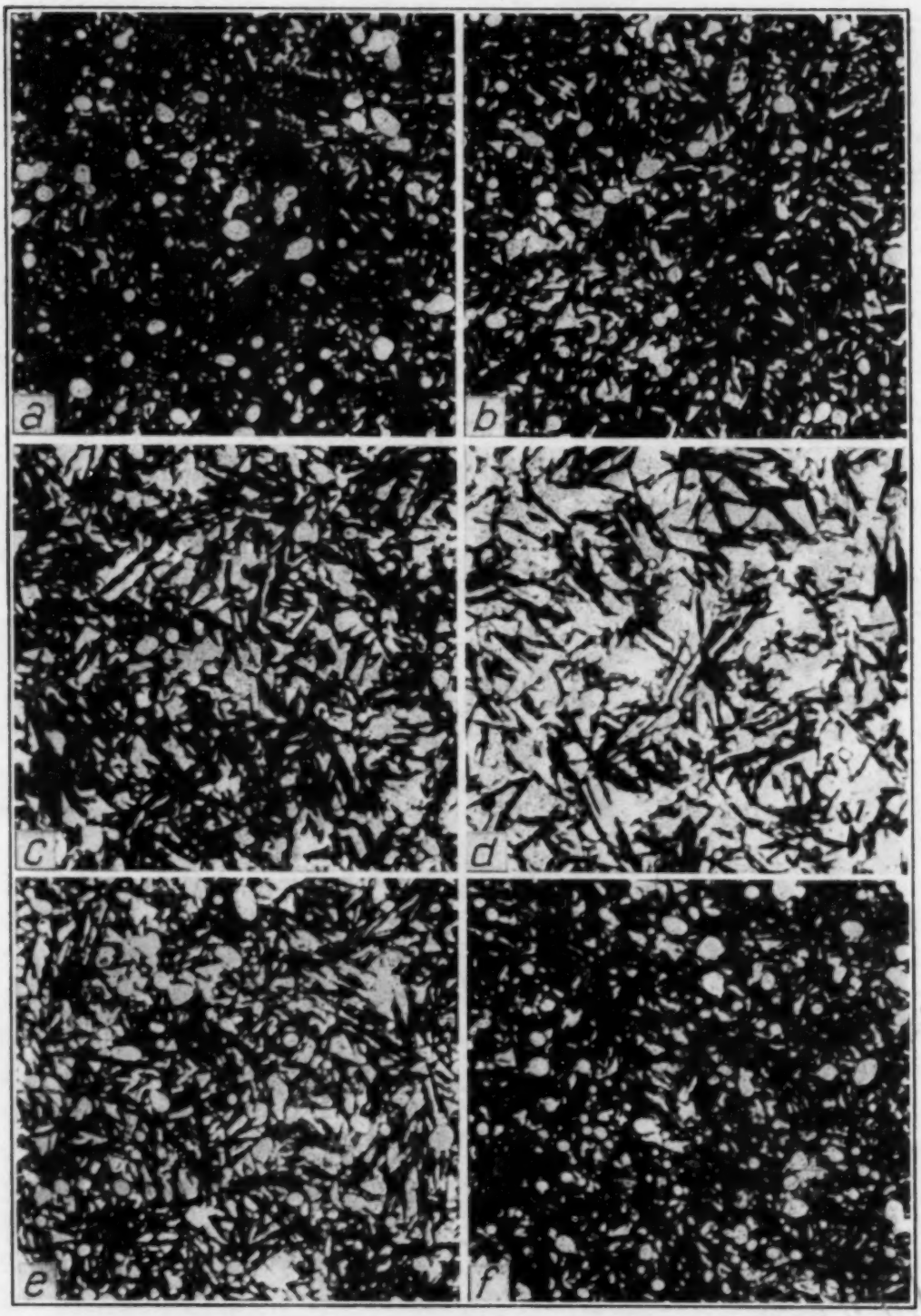

Fig. 5—Microstructures of 6-5-1.5 Steel after Quenching to Indicated Bath Temperatures and Single Tempering for 2.5 Hours at 750 Degrees Fahr. Nital Etch. × 1000. Quenching Bath Temperatures (a) 80 Degrees Fahr. (b) 125 Degrees Fahr. (c) 175 Degrees Fahr. (d) 225 Degrees Fahr. (e) 275 Degrees Fahr. (f) 325 Degrees Fahr.

ferred to the tempering furnace, no appreciable stabilization is found. Conditioning *does* make itself felt when the tempering temperature is raised to 1050 degrees Fahr. (565 degrees Cent.). For each bath temperature, the austenite retained after tempering at 1050 degrees Fahr. decreases as the tempering time is increased (curves 3-8, Fig. 4). This means that sufficient conditioning takes place to vitiate at least part of the stabilizing effect, and corresponding amounts of austenite decomposition occur on cooling from the tempering temperature. Nevertheless, if the quenching bath temperature is above 125 degrees Fahr. (50 degrees Cent.) considerable quantities of austenite persist even after tempering at 1050 degrees Fahr. for 10 hours (curve 8, Fig. 4).

In order to substantiate the surprising effects illustrated by Fig. 4, a number of metallographic and dilatometric studies were made. The photomicrographs shown in Fig. 5 represent a series of specimens quenched to temperatures between 80 and 325 degrees Fahr. (25 and 165 degrees Cent.), directly tempered for 2½ hours at 750 degrees Fahr. (400 degrees Cent.) and then retempered for 1 hour at 1050 degrees Fahr. (565 degrees Cent.) to darken the existing martensite.* The microstructures of Fig. 5 demonstrate very clearly the increasing amounts of austenite retained after cooling to bath temperatures up to 225 degrees Fahr. (105 degrees Cent.) followed by tempering at 750 degrees Fahr. (400 degrees Cent.). Furthermore, the amount of austenite begins to decrease as the quenching bath temperature is raised above 225 degrees Fahr. (105 degrees Cent.), in accordance with curve No. 2 of Fig. 4.

The dilation curves of Fig. 6 are also in good agreement with the data in Fig. 4. Curve A-1 shows no sign of austenite decomposition during cooling from a tempering treatment of 2 minutes at 1050 degrees Fahr. (565 degrees Cent.) (after arrested hardening at 175 degrees Fahr., 80 degrees Cent.). In this case, the stabilization is completely effective in retaining to room temperature all of the austenite brought over into the tempering treatment. However, as the quenching bath temperature is raised, and/or as the tempering time is lengthened, increasing amounts of austenite undergo decomposition on cooling from the tempering operation.

*The purpose of this heat treatment is to reveal the amount of austenite after arrested quenching and tempering at 750 degrees Fahr. (400 degrees Cent.). The subsequent tempering at 1050 degrees Fahr. (565 degrees Cent.) is primarily intended to darken any martensite which may have formed on cooling from the 750 degrees Fahr. (400 degrees Cent.) temper. Undoubtedly, the second temper causes further decomposition of the austenite on cooling but this product, being untempered, etches light and is indistinguishable from the austenite whose presence is being sought.

To summarize the implications of the foregoing experiments, there is now good evidence that, on tempering, the retained austenite in high speed steel is subjected to a stabilizing influence which acts to prevent decomposition during the subsequent cooling. However, this stabilizing action gradually becomes inoperative as the quantity of austenite exposed to tempering is increased. Conceivably the stabilizing tendency may be enhanced by raising the tempering temperature or lengthening the tempering time, but then the condition-

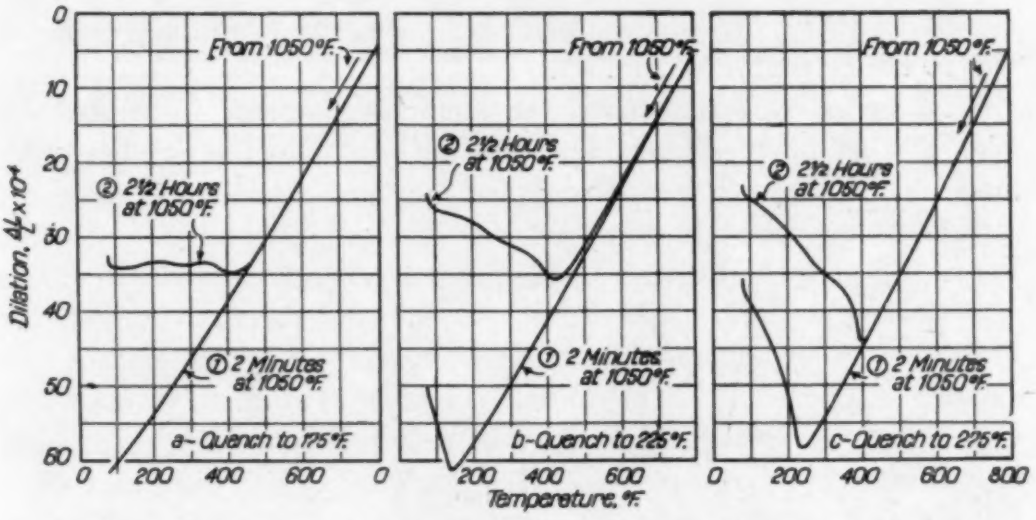

Fig. 6—Dilation Curves for Cooling from the Tempering Treatment after Quenching to 175, 225 and 275 Degrees Fahr.

ing reaction (carbide precipitation) sets in, and begins to counterbalance the stabilizing effect. Accordingly, in all likelihood, there is an upper limit to the amount of austenite which can be retained at room temperature by means of stabilization. This limit is probably somewhat above the maximum austenite content of 56 per cent retained during the course of this work.

Effect of Single, Double and Multiple Tempering After Arrested Quenching—The data described thus far were based on single tempers, that is, the tempering treatments were carried out for the required length of time without intermediate coolings to room temperature. It has already been demonstrated elsewhere (4) that, in normally hardened high speed steel, there is practically no difference between single and repeated tempering in their effect on the rate of retained austenite decomposition. However, it is not known whether

this situation remains the same when the hardening quench is arrested *above* room temperature. Therefore, the next step in this research was to investigate the rate of austenite decomposition as a function of tempering time in single, double and multiple cycles after quenching to various bath temperatures. The curves in Figs. 7 to 11 represent the results of retained austenite and hardness determinations made on specimens cooled to bath temperatures of 80, 125, 175, 225 and 275 degrees Fahr. (25, 50, 80, 105 and 135 degrees Cent.) and

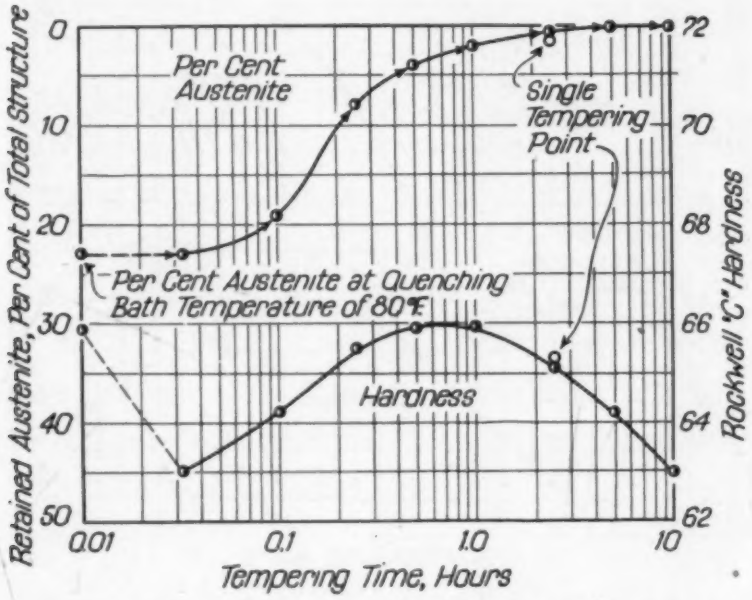

Fig. 7—Per Cent Austenite and Hardness after Quenching to 80 Degrees Fahr. and Tempering at 1050 Degrees Fahr.

then tempered directly at 1050 degrees Fahr. (565 degrees Cent.) as indicated. The measurements for the multiple tempering curves were obtained on specimens that were quenched to the designated bath temperatore, tempered at 1050 degrees Fahr. (565 degrees Cent.) for the first interval of time (2 min.), cooled to room temperature for the measurements, heated again to 1050 degrees Fahr. (565 degrees Cent.) for a period sufficient to bring the total tempering time to that represented by the next point on the curve, cooled to room temperature for measurements corresponding to the accumulated tempering time, heated again to 1050 degrees Fahr. (565 degrees Cent.), and so on. The steps in this multiple tempering process are illustrated by the arrow heads running along the retained

austenite curves in Figs. 7 to 11. The points on the single tempering curves were obtained by cooling specimens to the designated bath temperature, then directly tempering each specimen *once* at 1050 degrees Fahr. (565 degrees Cent.) for the appropriate length of time, and cooling to room temperature for the measurements. Comprehensive single tempering experiments were performed after hardening to 225 and 275 degrees Fahr. (105 and 135 degrees Cent.) (Figs. 10 and 11), while only 2½-hour single tempers were con-

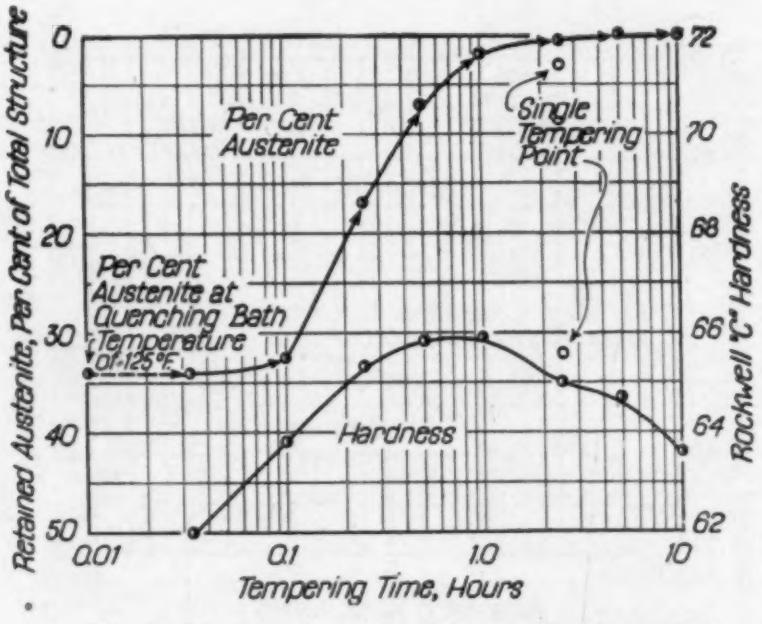

Fig. 8—Per Cent Austenite and Hardness after Quenching to 125 Degrees Fahr. and Tempering at 1050 Degrees Fahr.

ducted after hardening to 80, 125 and 175 degrees Fahr. (25, 50 and 80 degrees Cent.). (This explains the individual single tempering points in Figs. 7, 8 and 9.) To secure the double tempering results shown in Figs. 10 and 11, the specimens which had been single tempered were each retempered once more for a suitable length of time to bring the cumulative time up to that signified by the next point on the curve. The dashed lines portray the method of using the single tempered specimens for the additional temper so as to yield the data for the double tempering curves.

A number of important observations may be drawn from the curves in Figs. 7 to 11. (A) If the steel is hardened by cooling to room temperature (Fig. 7), a subsequent temper of 2½ hours at 1050 degrees Fahr. (565 degrees Cent.) results in virtually complete

transformation of the retained austenite regardless of whether the tempering is conducted in one or in several operations. This confirms the previous findings of Cohen and Koh (4). (B) However, if the hardening quench is arrested above room temperature, then a marked difference develops between double and multiple tempering on the one hand and single tempering on the other. In particular, single tempering for 2½ hours at 1050 degrees Fahr. (565 degrees

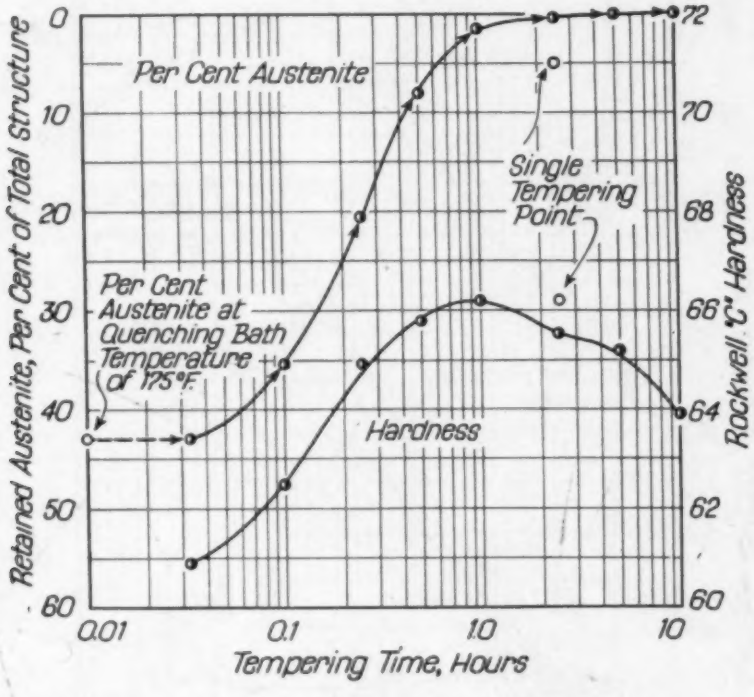

Fig. 9—Per Cent Austenite and Hardness after Quenching to 175 Degrees Fahr. and Tempering at 1050 Degrees Fahr.

Cent.) after hardening to temperatures above 80 degrees Fahr. (25 degrees Cent.) leaves considerable quantities of austenite in the steel —the higher the quenching-bath temperature,* the greater is the amount of residual austenite after such tempering. Furthermore, from the shape of the single tempering curves in Figs. 10 and 11, it is evident that single tempering, even if prolonged for days, will not condition the austenite sufficiently to achieve total decomposition. On the other hand, either double or multiple tempering for a cumulative time of 2½ hours after quenching to any temperature up to 275 degrees Fahr. (135 degrees Cent.) (and probably higher) does result in essentially complete decomposition of the retained austenite.

*Up to the M-point.

In other words, no matter how large the amount of austenite transferred to the tempering operation because of arrested hardening, its entire conversion can be accomplished by tempering for 2½ hours at 1050 degrees Fahr. (565 degrees Cent.) if the tempering is carried out in two or more operations. (C) As far as the retained austenite decomposition is concerned, multiple tempering is somewhat more effective than double tempering when compared at equivalent temper-

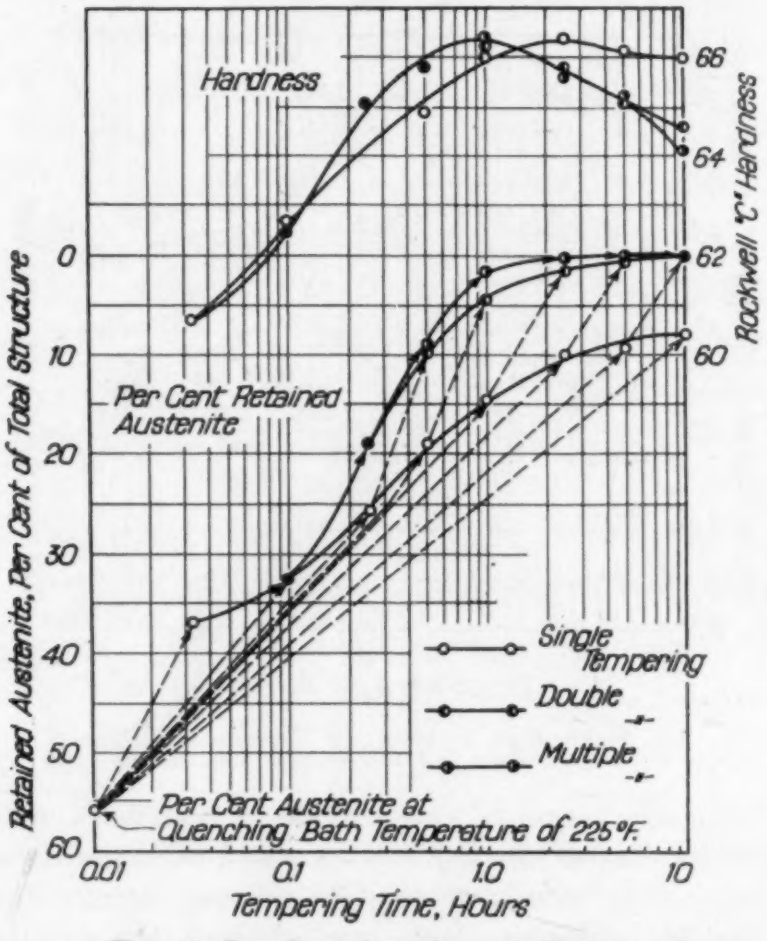

Fig. 10—Per Cent Autsenite and Hardness after Quenching to 225 Degrees Fahr. and Tempering at 1050 Degrees Fahr.

ing times, but the difference may be regarded as negligible for practical purposes. (D) The time to reach maximum secondary hardness on tempering at 1050 degrees Fahr. (565 degrees Cent.) is only slightly affected by the quenching-bath temperature if double or multiple tempering is used (being about ½ hour), but in the case of single tempering, the hardness peak is shifted from ½ hour after a room temperature quench to 2½ hours after quenching to 225 to

275 degrees Fahr. (105 to 135 degrees Cent.). Table IV lists the approximate tempering times at 1050 degrees Fahr. (565 degrees Cent.) for maximum secondary hardness and for complete austenite transformation in relation to the quenching-bath temperature.

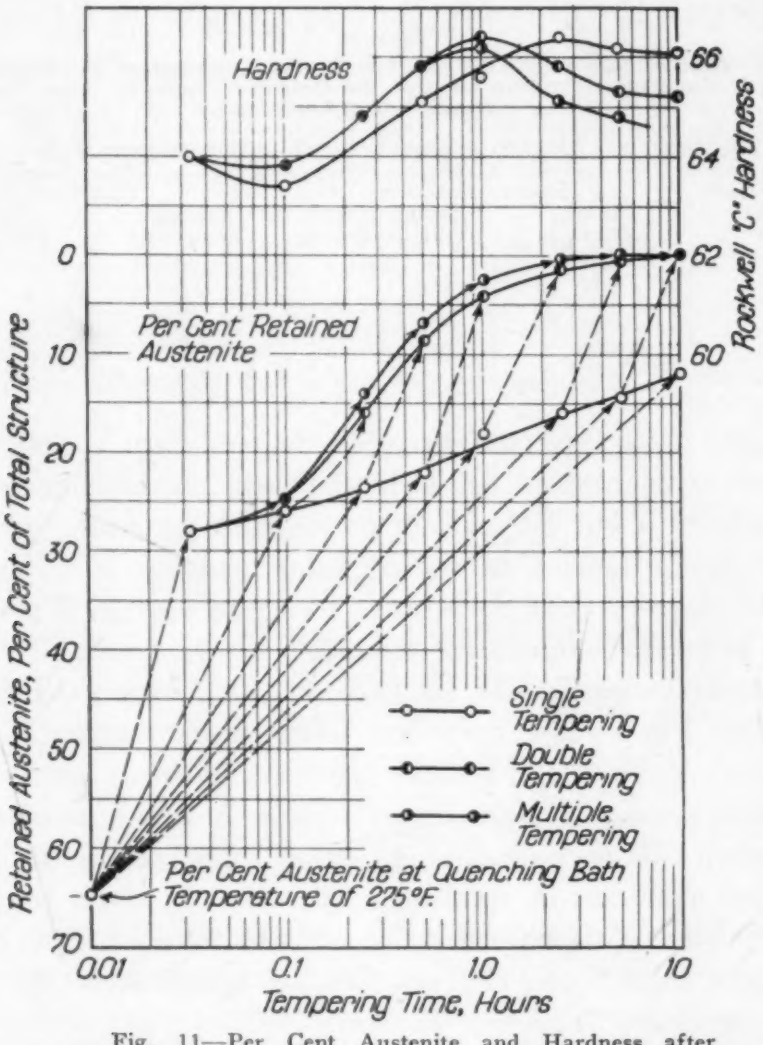

Fig. 11—Per Cent Austenite and Hardness after Quenching to 275 Degrees Fahr. and Tempering at 1050 Degrees Fahr.

Scientific Considerations—The basic reason for the sluggishness of the austenite decomposition on single tempering after arrested hardening is worthy of considerable thought, particularly in view of the comparative effectiveness of double and multiple tempering. Therefore, an attempt was made to throw some light on these unusual phenomena. At first, it might be assumed that, since the retained austenite transforms during the cooling from the tempering temperature, intermittent coolings would tend to stimulate the conversion

of the austenite for any given cumulative tempering time. This possibility, however, was ruled out as a general explanation by the following experiments. Two specimens were austenitized and quenched to 225 degrees Fahr. (105 degrees Cent.), tempered for

Table IV
Tempering Time at 1050 Degrees Fahr. for Maximum Secondary Hardening and for Practically Complete Transformation of the Retained Austenite After Quenching to Various Bath Temperatures

Quenching-Bath Temperature Degrees Fahr.	Tempering Time at 1050 Degrees Fahr., Hours			
	For Maximum Secondary Hardening		For Complete Transformation	
	Single Tempering	Double or Multiple Tempering	Single Tempering	Double or Multiple Tempering
80	½	½	2½	2½
125	..	½	...	2½
175	2½	1	...	2½
225	2½	1	>10	2½
275	2½	1	>10	2½

2½ hours at 1050 degrees Fahr. (565 degrees Cent.), and cooled in air to room temperature. In each specimen, the magnetic measurements disclosed about 10 per cent of residual austenite. One specimen was then subjected to six 5-minute tempers at 1050 degrees Fahr. (565 degrees Cent.), and was found to contain 3 per cent of austenite after this cumulative exposure of ½ hour. The second specimen was tempered for ½ hour at 1050 degrees Fahr. (565 degrees Cent.) in a single operation, and it also contained 3 per cent of austenite. From this, it is clear that the number of actual heatings and coolings, per se, have no detectable effect on the rate of austenite decomposition. This conclusion is further supported by the fact that the retained austenite in specimens quenched to room temperature can be completely transformed by a total time of 2½ hours at 1050 degrees Fahr. (565 degrees Cent.) regardless of the number of tempering cycles (4).

Another tentative explanation, which was tested and then rejected, is concerned with the possible formation of bainite instead of martensite during the cooling from the tempering temperature. It is known that when bainite is allowed to form at the expense of martensite (2), the over-all austenite decomposition attained by the time room temperature is reached may be considerably less than when the bainite transformation is avoided. It is quite conceivable, then, that long single tempering might well result in bainite formation expecially when large amounts of austenite are involved, whereas shorter repeated tempers might merely condition the austenite for

increments of martensite formation. To test this hypothesis, two specimens were first quenched to 225 degrees Fahr. (105 degrees Cent.), single-tempered for 2½ hours at 1050 degrees Fahr. (565 degrees Cent.) and then cooled to room temperature in a dilatometer. In one run, the dilatometer containing the specimen was cooled in air, and in the other, the cooling was conducted much more slowly in a furnace. The corresponding dilation curves are shown in Fig. 12. On furnace cooling, there is definite evidence of a split transformation, the upper step being due to bainite formation, and the

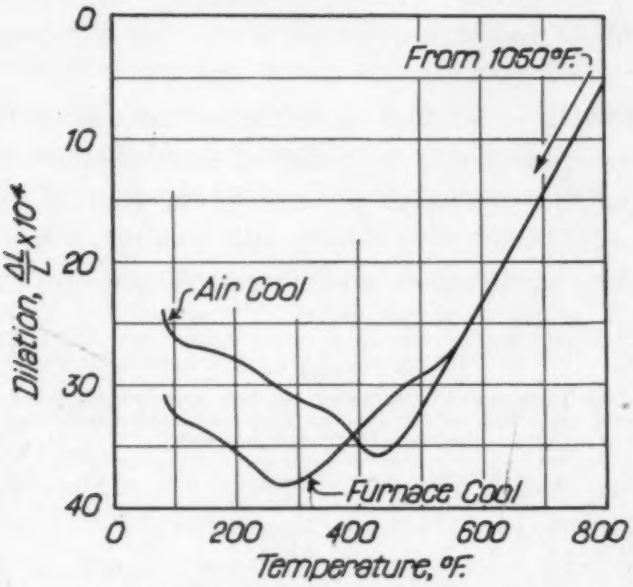

Fig. 12—Dilation Curves Showing Effect of Rate of Cooling from the Tempering Treatments after Quenching to 225 Degrees Fahr. and Tempering Directly for 2.5 Hours at 1050 Degrees Fahr.

lower to martensite formation. On air cooling, however, the bainite transformation is suppressed, and only martensite forms. Yet more austenite decomposition occurs in the latter event than when the bainite comes into the picture, as is demonstrated by the fact that air cooling results in a substantially greater transformational expansion than furnace cooling (Fig. 12).

Since these findings indicate that the rate of cooling may influence the extent of austenite decomposition after certain tempering treatments because of bainite formation, further variations in cooling rate were investigated. A series of specimens was quenched to 225 degrees Fahr. (105 degrees Cent.), tempered once at 1050 degrees Fahr. (565 degrees Cent.) for 2½ hours, and cooled to room temperature at the rates indicated in Table V. A double temper of

1 + 1½ hours is also included for comparison purposes. From the amounts of residual austenite listed in Table V, it is manifest that the magnitude of the cooling transformation increases with the faster rates of cooling, and the quantity of austenite remaining diminishes correspondingly. Nevertheless, even water quenching, which is undoubtedly rapid enough to suppress all traces of bainite formation, leaves much more austenite than the equivalent double temper with air cooling. Hence, although bainite may form under some conditions on cooling from the tempering temperature, it certainly cannot account for the slower decomposition of the retained austenite achieved by single tempering compared to that achieved by repeated tempering.

The authors have reached the tentative conclusion that the reason for this difference between single and repeated tempering is associated with the carbide precipitation process which conditions the retained austenite for transformation during the cooling. When high speed steel is normally hardened to room temperature, the 23 per cent of

Table V

Effect of Cooling Rate After Tempering on the Amount of Retained Austenite. Specimens quenched to 225 degrees Fahr. and tempered once at 1050 degrees Fahr. for 2½ hours.

Tempering Treatment	Cooling Medium	Per Cent Austenite After Tempering
Single Temper, 2½ hours	Furnace	22
Single Temper, 2½ hours	Lime	12
Single Temper, 2½ hours	Air	10
Single Temper, 2½ hours	Oil	7
Single Temper, 2½ hours	Water	7
Double Temper, 1 + 1½ hours	Air	<½

retained austenite can be conditioned for essentially complete conversion by tempering at 1050 degrees Fahr. (565 degrees Cent.) for 2½ hours. Yet if the steel is quenched to 1050 degrees Fahr. (565 degrees Cent.) in the first place, and held there for 2½ hours, about 22 per cent of austenite remains after cooling to room temperature. In other words, the latter exposure at 1050 degrees Fahr. (565 degrees Cent.) causes very little conditioning of the austenite for additional decomposition. Therefore, it becomes necessary to account for the occurrence of carbide precipitation when the *retained* austenite is exposed to 1050 degrees Fahr. (565 degrees Cent.) and the absence of any such amount of precipitation when the *primary* austenite is heated in the same way. Since the chemistry of the austenite and the rate of diffusion are presumably the same in both cases, it is reason-

able to believe that the difference in the rate of carbide precipitation is due to a difference in the rate of nucleation. It appears that the presence of martensite formed during the hardening quench provides nuclei for the carbide precipitation, and that when no martensite is allowed to form because of stopping the quench above the M-point, the rate of carbide nucleation becomes very small. Proceeding along these lines, it would follow that the rate of austenite conditioning on tempering increases with the amount of co-existing martensite.

If this picture is accepted, the difference between single and repeated tempering is readily explained. As the quenching-bath temperature is raised, the amount of martensite carried into the tempering process is decreased, while the amount of austenite is increased. Consequently, the nucleating effect due to the martensite is lessened, and even prolonged single tempering does not prepare the last portion of the austenite for decomposition. But, on repeated tempering, the situation is greatly altered. For example, suppose the steel is cooled to 225 degrees Fahr. (105 degrees Cent.) and then tempered for 1 + 1½ hours at 1050 degrees Fahr. (565 degrees Cent.). Under these conditions, the magnetic data indicate that 56 per cent of austenite and only 37 per cent of martensite go into the first tempering cycle. On heating for 1 hour, enough conditioning occurs so that about 41 per cent of austenite transforms into martensite on cooling, thus leaving 15 per cent of residual austenite (Fig. 10). With the 78 per cent of martensite now available for aiding the carbide nucleation, the remaining austenite can be conditioned for decomposition in another 1½ hours at 1050 degrees Fahr. (565 degrees Cent.). If the tempering had been carried out as a single temper for 2½ hours, only 37 per cent of martensite would be present during tempering to enhance the nucleation process, and therefore, the austenite would not be completely converted on cooling. Fig. 10 shows that about 10 per cent of austenite remains as a result of this 2½-hour single temper, whereas a double or multiple temper for 2½ hours decomposes virtually all the austenite.

Practical Considerations—It has been demonstrated (Table III) that arresting the hardening quench of high speed steel prior to tempering leads to inferior strength properties. Unfortunately, however, hardening all the way to room temperature is not always feasible because of the danger of cracking. This is particularly true in the case of complicated sections, where one might well be inclined to compromise on the strength rather than risk the entire loss of an

expensive tool by cracking. Obviously, it would be of great practical importance if the tempering process could be adjusted to nullify the detrimental weakening effect of arrested hardening; then there would be no disadvantage in stopping the quench above room temperature, and such a treatment could be applied freely whenever potential cracking was inherent in the design of the tool.

A clue for the solution of this dilemma is provided by the unexpected differences revealed between single and repeated tempering when arrested hardening is employed. Accordingly, it was decided to ascertain the comparative influence of single, double and triple tempering on the transverse strength. Several bend test specimens were quenched to 80 and 225 degrees Fahr. (25 and 105 degrees Cent.), and were subjected to various combinations of tempering cycles, all at 1050 degrees Fahr. (565 degrees Cent.). The average results are tabulated in Table VI.

Table VI

Transverse Strength of 6-5-1½ High Speed Steel Quenched to 80 and 225 Degrees Fahr., and Tempered in Single, Double and Triple Combinations at 1050 Degrees Fahr.

Desig-nation	Quenching-Bath Temperature Degrees Fahr.	Treatment at 1050 Degrees Fahr. No. of Tempers	Time of Tempering, Hours	Modulus of Rupture Lbs. per Sq. In.	Per Cent Improvement over Single Tempering
1	80	1	2½	434,000	..
2	80	2	2½ + 1	490,000	13
3	225	1	2½	309,000	..
4	225	2	2½ + 2½	402,000	30
5	225	3	2½ + 2½ + 1	450,000	46
6	225	2	1 + 1½	377,000	22
7	225	3	1 + 1½ + 1	445,000	44

It is immediately evident from Table VI that double and triple tempering markedly enhance the transverse strength. After hardening to room temperature, the improvement is definite, but relatively moderate (Treatments 1 versus 2); here the *second* heating acts to relieve the stresses induced by the transformation of some 22 per cent of austenite during the cooling from the *first* operation (Table II), as well as to toughen the untempered martensite thus formed. Further transformation stresses are not generated during the cooling from the *second* temper since there is practically no austenite remaining after the *first* cycle.

After quenching to 225 degrees Fahr. (105 degrees Cent.), however, the advantage of more than one tempering operation becomes quite striking. In this case, there is a large improvement as a result of *double* tempering, but a *triple* temper provides further

benefit. After the *first* temper of 2½ hours (Treatment 3), the steel contains on the basis of the magnetic data about 46 per cent of untempered martensite in addition to the internal stresses produced by the formation of this martensite on cooling. Both of these factors tend to detract from the strength. Consequently, the *second* heating (Treatment 4) raises the strength by toughening the untempered martensite and reducing the internal stresses. Moreover, the *second* temper achieves the decomposition of the final 10 per cent of austenite (Table II) not converted by the *first* temper. Therefore, a *third* heating (Treatment 5) is necessary to relieve the transformation stresses and toughen the last increment of martensite. This nicely explains the higher strength obtained after triple tempering (Treatment 5) than after double tempering (Treatment 4).

Thus it appears that multiple tempering in accordance with the principles reported here does much to correct the adverse effect of arrested hardening on the strength properties. In fact, an improvement in strength of almost 50 per cent is attained when the proper tempering practice is adopted instead of the normal or single tempering. In addition, this paper presents the scientific data for selecting the proper combination of tempering cycles. Stated briefly, when the quenching-bath temperature is sufficiently high so as to cause the transfer of large quantities of austenite to the tempering operation, a tempering temperature of 1050 degrees Fahr. (565 degrees Cent.) is quite satisfactory (just as for normal hardening), but the austenite cannot be adequately conditioned during a *single* temper to achieve its entire conversion on cooling back to room temperature. At the same time, during this cooling, a large amount of austenite does transform into untempered martensite with attendant stress-raising volume changes. While a second temper can "take care" of these detrimental factors, further austenite decomposition into untempered martensite results during the second cooling, and this makes a third heating desirable. If, as in the case of hardening to room temperature, the total austenite decomposition can be accomplished by a single tempering treatment, then, of course, no austenite is left to transform on cooling from the second temper, and a third operation becomes unnecessary.

Therefore, in selecting a combination of tempering cycles, two treatments should be used if the retained austenite can be substantially converted by the first temper, but if two cycles are required to achieve complete decomposition of the austenite (as

is the case when the hardening quench is arrested appreciably above room temperature), then triple tempering is justified. However, the times selected are quite flexible. The triple temper corresponding to Treatment 5 (2½+2½+1 hours) involves an accumulated time of 6 hours at temperature. This time element may be materially reduced by studying the austenite decomposition curves in Figs. 7 to 11. For example, after cooling to a quenching-bath temperature of 225 degrees Fahr. (105 degrees Cent.) the retained austenite can be almost totally transformed by a double temper of 1+1½ hours. Then by applying a third temper of 1 hour for stress relieving and toughening purposes, one would expect quite satisfactory results even though this combination involves an effective tempering time of only 3½ hours instead of 6 hours. This prediction is substantiated by Treatment 7 in Table VI which shows just about as much improvement over single tempering as does the longer Treatment 5.

Despite the corrective action of multiple tempering when applied to steels whose hardening is arrested above room temperature, the fact still remains that the highest strength values are secured when the quenching-bath temperature is as low as possible. In fact, even higher strengths than obtainable on quenching to room temperature may be secured if the cooling is continued to sub-zero temperatures (1). Nevertheless, wherever such low temperature cooling jeopardizes the steel because of possible cracking, arrested hardening may be safely employed in conjunction with multiple tempering with the assurance that very respectable strength properties will be attained.

Conclusions

1. A 2½ hour single temper at 1050 degrees Fahr. is sufficient to cause complete transformation of the retained austenite in 6-5-1½ high speed steel if the previous hardening quench is carried to room temperature.

2. If, however, the hardening quench is arrested above room temperature, then appreciable quantities of austenite remain in the steel after single tempering for 2½ hours at 1050 degrees Fahr. The amount of austenite thus retained is greater, the higher the quenching-bath temperature.

3. The transverse strength of the 6-5-1½ steel after arrested

hardening and single tempering for 2½ hours at 1050 degrees Fahr. decreases considerably as the quenching-bath temperature is raised.

4. Raising the tempering temperature above 1050 degrees Fahr. decreases the amount of austenite retained after arrested quenching and single tempering, but such tempering is accompanied by large decreases in hardness.

5. After arrested quenching, even prolonged single tempering at 1050 degrees Fahr. does not cause the decomposition of all the austenite.

6. On the other hand, complete austenite decomposition after arrested quenching can be achieved in 2½ hours at 1050 degrees Fahr. provided that double or multiple tempering is used. A tentative explanation for this striking difference between single and repeated tempering after arrested quenching has been presented.

7. Repeated tempering after arrested quenching, and also after quenching to room temperature, causes a significant increase in the transverse strength of the steel. Whenever the quenching-bath temperature is appreciably above room temperature and, hence, double tempering is needed to accomplish complete decomposition of the retained austenite, a third temper results in further improvement of the strength properties. In spite of the highly acceptable values of transverse strength thus obtained, however, the highest strength values are secured when the quenching-bath temperature is as low as possible.

Acknowledgment

The authors are indebted to Mr. J. P. Gill and the Vanadium-Alloys Steel Company for permission to publish this work.

References

1. P. Gordon and M. Cohen, "The Transformation of Retained Austenite in High Speed Steel at Subatmospheric Temperatures," TRANSACTIONS, American Society for Metals, Sept. 1942, Vol. 30, p. 569-591.
2. P. Gordon, M. Cohen, and R. S. Rose, "The Kinetics of Austenite Decomposition in High Speed Steel," TRANSACTIONS, American Society for Metals, March, 1943, Vol. 31, p. 161-217.
3. P. Payson and J. L. Klein, "The Hardening of Tool Steels," TRANSACTIONS, American Society for Metals, March, 1943, Vol. 31, p. 218-256.
4. M. Cohen and P. K. Koh, "The Tempering of High Speed Steel," TRANSACTIONS, American Society for Metals, December, 1939, Vol. 27, p 1015-1051.

5. O. Zmeskal and M. Cohen, "Simultaneous Measurements of Magnetic and Dilatometric Changes," *Review of Scientific Instruments,* Vol. 13, 1942, p. 346-348.
6. J. P. Gill and R. S. Rose, "Molybdenum High Speed Steels," METAL PROGRESS, Vol. 40, 1941, p. 283-288.

DISCUSSION

Written Discussion: By Bernard S. Lement, assistant metallurgist, Watertown Arsenal, Watertown, Mass.[1]

The authors are to be congratulated for their latest contribution to the steadily increasing knowledge of the various factors affecting the austenite transformation which occurs in high speed steel. In this paper they have brought to light hitherto unsuspected effects connected with the minimum temperature reached during the quenching of high speed steel. Their work has practical significance in that scientific principles have been established which will enable heat treaters to insure near optimum strength properties in high speed steel tools subjected to varying quenching conditions encountered in practice. As a result of this investigation, multiple tempering has taken on new and added importance in the heat treatment of high speed steel tools.

Although the authors have furnished what appears to be a satisfactory explanation of the effectiveness of multiple tempering as compared with single tempering in causing the complete transformation of the austenite existing at the quenching bath temperature, no explanation is offered as to why stabilization of the austenite should take place as a result of single tempering. This stabilizing effect appears to be related to a similar phenomenon observed by Gordon and Cohen in their investigation[2] of the transformation of retained austenite in high speed steel during cooling to subatmospheric temperatures. It was found that both aging at room temperature and tempering after reaching room temperature had the effect of suppressing the austenite transformation which would normally occur on direct cooling to the temperature of liquid nitrogen. The explanation offered by the authors for this phenomenon was that both aging at room temperature and tempering after reaching room temperature probably result in relief of the internal stresses set up by the hardening transformation. This explanation may account for the stabilizing effect described in the present paper although it is not clear why the stabilizing action due to the tempering treatment should become less and less potent as increasing quantities of austenite are carried into the tempering operation.

Another possible explanation for this stabilizing effect lies in the possible isothermal formation of a small amount of bainite at the tempering temperature. As was shown by the authors in their investigation[3] of the S-curve of 6-6-2 high speed steel, hot quenching to temperatures in the range of 400 to 700 degrees

[1]Released for publication by the Bureau of Publications, War Department, Washington, D. C. The statements or opinions expressed in the discussion are to be considered those of the discusser and do not necessarily express the views of the Ordnance Department.

[2]P. Gordon and M. Cohen, "The Transformation of Retained Austenite in High Speed Steel at Subatmospheric Temperatures", TRANSACTIONS, American Society for Metals, Vol. 30, 1942, p. 569-591.

[3]P. Gordon, M. Cohen and R. S. Rose, "The Kinetics of Austenite Decomposition in High Speed Steel," TRANSACTIONS, American Society for Metals, Vol. 31, 1943, p. 161-217.

Fahr. (205 to 370 degrees Cent.) caused the austenite to transform to bainite and that this bainite formation had a stabilizing effect on the untransformed austenite. Since this temperature range corresponds fairly well with the tempering range of maximum stabilization as indicated in Fig. 3 for a hot quenching temperature of 225 degrees Fahr. (105 degrees Cent.), it is possible that some isothermal transformation to bainite may occur. It is desired to know what consideration was given to this possibility.

The effectiveness of double tempering as compared with single tempering in causing austenite transformation has been emphasized in this paper. It would be of interest to know the maximum amount of retained austenite (resulting from a quench-temper treatment) that could be transformed by a second tempering treatment consisting of 2.5 hours at 1050 degrees Fahr. (565 degrees Cent.). It would be of further interest to know how much austenite could be transformed by a tempering treatment consisting of 2.5 hours at 1050 degrees Fahr. (565 degrees Cent.) in the case where stabilization of the austenite has been accomplished by hot quenching into the temperature range of isothermal bainite formation above the M-point.

Written Discussion: By Otto Zmeskal, research metallurgist, Universal-Cyclops Steel Corp., Bridgeville, Pa.

This paper is another in the series of important contributions made by Dr. Cohen and his co-workers to the steadily growing scientific knowledge of the heat treatment of high speed steel.

The desirability of completing the quench before tempering has been scientifically demonstrated. The necessity of multiple tempering to obtain complete transformation of the retained austenite in tools that have not been allowed to go cold prior to tempering has been conclusively demonstrated.

The writer would like to ask this question of the authors: "Is complete transformation of the retained austenite a general objective to be always aimed at in the tempering of high speed steel?" In a previous publication,[4] Dr. Cohen has shown that the peak in hot hardness of 18-4-1 high speed steel is obtained when the tempering time is long enough to completely transform the residual austenite. The room temperature hardness of the steel so treated is at least one Rockwell C point below that of the state wherein five per cent retained austenite is present. It has been expressed that a small amount of retained austenite acts as a cushion to the martensite which forms during the cooling from the draw, and thus the internal stress condition is somewhat alleviated. Have the authors data to state what is the effect on the transverse strength of high speed steels, of completing the austenite transformation at temperatures other than 1050 degrees Fahr. (565 degrees Cent.)?

A commercial practice in the heat treatment of large objects made of high speed steel, such as rolls, is to quench to temperatures approximately 500 degrees Fahr. (260 degrees Cent.) and then to bring the object to the drawing temperature and cool to not lower than 500 degrees Fahr. (260 degrees Cent.) between repeated draws. From the work of the authors, it seems that the above practice should be modified, and that an improved cycle would require quenching from temperatures approximately 225 degrees Fahr. (105 degrees Cent.), followed by multiple tempering, with complete cooling between the draws.

[4]E. C. Bishop and Morris Cohen, METAL PROGRESS, March 1943, Vol. 43, p. 413.

The authors have not discussed the matter of the temperature to which a tool should be cooled between draws. Presumably the same principles that govern the stability of the residual austenite from the quench would also govern the stability of the residual austenite from the temper.

It is hoped that Dr. Cohen and his co-workers will gradually develop the scientific bases for the long list of modifications used in the heat treatment of high speed steel.

Written Discussion: By M. J. Weldon, metallurgist, The Henry G. Thompson & Son Co., New Haven, Connecticut.

It is with a deep sense of gratification that we welcome this further contribution of the authors to the technical literature on high speed steel. The writer is particularly interested in the results of the transverse bend tests shown in Tables III and VI respectively. We understand through Dr. Cohen that the specimens were centerless ground prior to testing. This practice is to be highly recommended since the test by its very nature is purely a surface test, that is, we are really measuring the ultimate strength of the outermost fibers in tension. The removal of surface that was probably altered in carbon content to a variable extent in heat treatment is consequently imperative. It is trusted that the specific results of Table VI will constitute the fundamental bases for modifications that should most certainly be made in the next revision of the National Metals Handbook dealing with the recommended quenching practice of high speed steels (p. 1000-1006, 1939 Edition).

One of the most perplexing problems confronting the tool steel metallurgist today is that of diagnosing premature failures of high speed cutting tools. In too many cases, such failed tools will be accompanied by the laconic report that: "... it dubbed over", or that: "... it didn't stand up." In cases where it is possible to progressively examine the tool during its service life, observation has disclosed the presence of weak cutting edges and failure was promoted by fine chipping and crumbling of the cutting edges followed by a rubbing action the sum total of which was finally termed "premature wear". Close inspection of such tools has shown that the so-called failures can only be observed by examination of the cutting points shortly after the tools are placed in service even though post mortem observation of the used tool would lead one to believe that undue wear was the actual cause of failure.

We sincerely trust that this contribution by the authors may be the direct means of encouraging other investigators to make more frequent use of this highly useful method of predicting performance properties of high speed steel cutting tools. It is indeed unfortunate that fuller advantage is not taken of the transverse bend test in evaluating tool performance because ample evidence discloses that for any type analysis of high speed steel there is an optimum strength which combined with hardness fits the alloy for a particular operation. Studies have proved that the carbon content is the most important variable to consider and its effect far outweighs that of any other element as measured by this test. We feel confident in stating that, as more work is published along the avenues approached by the authors, a change from one type analysis to another can be more freely made once the effect of carbon on transverse bend strength is fully recognized.

There is a healthy tendency in recent years to discuss type analyses in terms of edge strength rather than "toughness". We must compliment the authors from this standpoint in that the ambiguous term "toughness" is almost absent from the paper. This term, it seems to us, could be dispensed with when dealing with the mechanical properties of high speed steel because it has been generally so loosely employed in the past that it has lost any fundamental meaning perhaps ever intended to be conveyed. We suggest for future research that more attention be directed to the so-called "interrupted quench", a method that has saved many a tool from breakage during the heat treating cycle. We refer primarily to the well-known practice of oil quenching complicated and massive shapes that are either square or rectangular in cross section. Here, where contraction and expansion can take place in different parts of the same tool as it cools below 900 degrees Fahr. (480 degrees Cent.), it is customary to withdraw the tool from the oil bath when the edges have blackened. From that point on, hardening is allowed to proceed under relatively mild conditions of cooling in air until the entire cross section of the tool reaches the vicinity of room temperature. Rather oddly, peripheral and symmetrical tools even of massive sections do not require this degree of interrupted cooling and, in many cases, large twist drills and taps may be quenched in oil "all the way down". There appears to be a certain aging effect not always recognized in this mild cooling period following removal from the oil bath, the nature of which could be studied to advantage. To state the problem somewhat differently, the edge strength of the completely heat treated tool appears to be influenced not solely by its actual temperature attained prior to tempering but rather by the mode of cooling employed to "bring it down" from the superheat. For example, a series of specimens taken from the oil quenching bath at approximately 1000 degrees Fahr. (540 degrees Cent.) and then cooled in still air to 150 degrees Fahr. (65 degrees Cent.) prior to tempering will show superior edge strength when tested against a series cooled directly in oil to 150 degrees Fahr. (65 degrees Cent.) before tempering. We believe that additional studies by the authors may serve to clarify numerous difficulties the causes of which are probably related to this interesting but neglected phase.

Written Discussion: By K. J. Trigger, assistant professor of mechanical engineering, University of Illinois, Urbana, Ill.

When asked to discuss this paper, the writer anticipated a manuscript packed with absorbing data, and indeed, such is the case. It is gratifying to know that multiple tempering is such an effective panacea for quenching ills. The authors are to be congratulated on their splendid paper.

A point for discussion is brought up on page 434 of this paper in the following statement made with reference to hot quenching at 1050 degrees Fahr. (565 degrees Cent.): "Yet, if the steel is quenched to 1050 degrees Fahr. (565 degrees Cent.) in the first place and held there for 2.5 hours, about 23 per cent of austenite remains after cooling to room temperature." This is essentially the same amount of austenite that is retained on an oil quench to room temperature, 80 degrees Fahr. (25 degrees Cent.).

Investigations [5, 6] have shown that hot quenching in the vicinity of 1000 de-

[5]Gordon, Cohen, and Rose, "The Kinetics of Austenite Decomposition in High Speed Steel," TRANSACTIONS, American Society for Metals, Vol. 31, 1943, p. 161-197.

[6]Discussion by K. J. Trigger on "The Kinetics of Austenite Decomposition in High Speed Steel" TRANSACTIONS, American Society for Metals, Vol. 31, 1943, p. 198-200.

grees Fahr. (540 degrees Cent.) for periods of from 1 hour to 24 hours causes a "split" transformation on subsequent (slow) cooling to room temperature. After hot quenching at 1050 degrees Fahr. (565 degrees Cent.) for 24 hours, the subsequent room temperature structural composition has been indicated[5] as consisting of 38 per cent martensite, 38 per cent bainite, and 18 per cent retained austenite in addition to the undissolved carbides. According to the same paper, oil quenching to 80 degrees Fahr. (25 degrees Cent.) results in 71 per cent martensite, 23 per cent retained austenite, in addition to the undissolved carbides. (Considering the difference in holding time in the hot quench, the amount of retained austenite essentially agrees with that presented in the paper under discussion.)

In working with a steel of practically the same chemistry as that used by the authors, the writer using an austenitizing temperature of 2250 degrees Fahr. (1230 degrees Cent.), and a hot quench at 1025 degrees Fahr. (550 degrees Cent.) has always found that the "as-quenched" hardness is higher for hot quenching than that obtained if oil quenching is used. Typical values are 64.3 R_c for oil quenching compared to 65.2 R_c for a 2-hour hot quench, and 66.1 for a 24-hour hot quench, all cooled to 80 degrees Fahr. (25 degrees Cent.) prior to testing.

The secondary hardening capacity is considerably greater in the oil-quenched steels than in those hot-quenched for 24 hours as shown in the following tabulation:

Quench (all cooled to 80 degrees Fahr. prior to testing)	Hardness Rockwell C		
	As Quenched	After Double Temper at 1030°F.—2-hr total time	Increase due to Tempering
Oil at 80° F. (25° C.)	64.3	66.4	2.1
Lead at 1025° F. (550° C.) for 2 hr.	65.2	66.7	1.5
Lead at 1025° F. (550° C.) for 24 hr.	66.1	66.8	0.7

Considering the hardness "as quenched" in the light of the structural composition previously reported, it seems anomalous that the presence of 38 per cent untempered martensite, 38 per cent bainite, and 18 per cent retained austenite should be harder than 71 per cent untempered martensite and 23 per cent retained austenite unless it is that martensite and bainite, as herein referred to, are of essentially equal hardness.

The increase in hardness on tempering is due principally to carbide precipitation and transformation of retained austenite. If the amount of retained austenite is nearly the same for both oil-quenched and 24-hour hot-quenched steels, why is it that the oil-quenched samples show three times as much increase due to tempering?

If we examine Fig. 1, of this paper, it is noticed that the 7 per cent undissolved carbides have displaced the calibration curve from the origin (0 intensity of magnetization). Might there not be precipitation of non-ferromagnetic carbides from the austenite while holding at a 1000 degrees Fahr. (540 degrees Cent.) quench which would add to those already present? Would not such precipitation have the effect of further displacing the calibration curve frora the origin? Under this condition, any given intensity of magnetization would indicate more austenite than was actually present. The indicated difference may be relatively negligible from the standpoint of the amount of retained austenite, but the effect of the precipitated carbides would be much more pronounced as far as the hardness is concerned.

Table VI contains some very interesting results.

The writer in evaluating the effect of single versus double tempering of oil quenched test beams has found a similar improvement for double tempering. Briefly, the test conditions were as follows:

Steel: C, 0.82; Mn, 0.30; Si, 0.33; Cr, 4.01; W, 5.65; Mo, 4.99; V, 1.56.
Austenitizing Temperature: 2230 ± 5 degrees Fahr. (1220 degrees Cent.) Carbonaceous Muffle.
Quench: Oil at 80 degrees Fahr. (25 degrees Cent.).
Single Temper: 1025 degrees Fahr. (550 degrees Cent.) 2 hours, furnace cool.
Double Temper: 1025 degrees Fahr. (550 degrees Cent.) 1 hour—air cool.
1025 degrees Fahr. (550 degrees Cent.) 1 hour—furnace cool.

The test beams, approximately 0.375 inch square, were supported on 4-inch centers and loaded at the quarter points in such a manner that the middle 2 inches were subjected to a constant bending moment. The rate of loading was from 600 to 700 pounds per minute until (and if) failure occurred. Since the absolute capacity of the testing machine was 12,800 pounds, two of the test specimens were not broken.

The average results were as follows:

Tempering Treatment	Modulus of Rupture, p.s.i	Improvement over Single Tempering, Per Cent	Hardness Rc
Single	454,000	---	65.5
Double	>538,000	>18.5	

The differences between these values and those reported by the authors are not great and may be due to beam geometry, loading conditions, and slight differences in temperatures and times. Included are photographs of two tested beams along with appurtenant data. (Figs. A and B.)

The improvement is of the same order as that reported by the authors, and the conclusion is the same; i.e., a definite but moderate improvement.

While on the subject of transverse strength as influenced by heat treatment the writer presents the following summary of the effect of hot quenching time. Test beams were hot-quenched for various times and double tempered at 1025 degrees Fahr. (550 degrees Cent.). The mechanical conditions—i.e., beam geometry and loading—were as just related for the oil-quenched series. The data presented represent average values, believed conservative, of four tests under each condition.

Quenching Treatment		Modulus of Rupture, p.s.i	Per cent of "Standard"	Hardness Rc
Oil at 80°F (25°C)		>538,000	100.0	65.7
Hot-Quenched at 1025°F (550°C) for 2 min. and held as shown.	0 min.	455,000	< 84.5	66.3
	15 min.	432,000	< 80.2	66.4
	1 hr.	434,000	< 80.6	66.5
	2 hr.	436,000	< 81.0	66.4

It is noted that hot quenching time, within the range investigated, has negligible effect upon the transverse strength and any than hot quenching procedure results in lower strength than obtains in oil quenching. The strength obtained by hot quenching is, however, very respectable and no serious weakening should be encountered. It is also noted that any of the hot quenching procedures investigated results in a higher tempered hardness than is obtained by oil quenching.

To evaluate more completely the advantage, if any, in hot quenching, the writer has been conducting a series of lathe cutting tests using oil-quenched tool bits and 2-hour hot-quenched [1025 degrees Fahr. (550 degrees Cent.)] bits. The test conditions are as follows:

METAL CUT: NE 9445 annealed.
Tensile strength, 105,000 p.s.i.; Yield Point, 58,000 p.s.i.; Elongation, 17 per cent in 2 in.; Reduction in area, 26 per cent; Brinell hardness, 204.
Cut: Dry, roughing. Depth ⅛ inch. Feed 1/66 inch rev.
Tool: Mo-W HSS: Nose radius 1/16 inch; side cutting edge angle, 0 deg.; end cutting edge angle, 6 deg.; side rake, 14 deg.; back rake, 8 deg.; relief, 6 deg.

The results of tool life vs. cutting speed tests when plotted on log-log coordinates give the following summary:

Quench	Equation of V vs. T Line	V for tool life of 60 min.	Per cent (based on V_{60}
Oil	$VT^{.159}=122$	63.8	100
2-hr. hot-quench	$VT^{.162}=129.5$	66.7	104.5

A previous series of tests on 0.35 C steel of 159 BHN revealed practically an identical improvement. A similar series of tests using shorter hot quenching times is in progress, and the indications are that the 30-minute hot quench is practically as effective as the 2-hour hot quench.

Based on the transverse strength and cutting tests the writer is of the opinion that hot quenching in the vicinity of 1000 degrees Fahr. (540 degrees Cent.) is

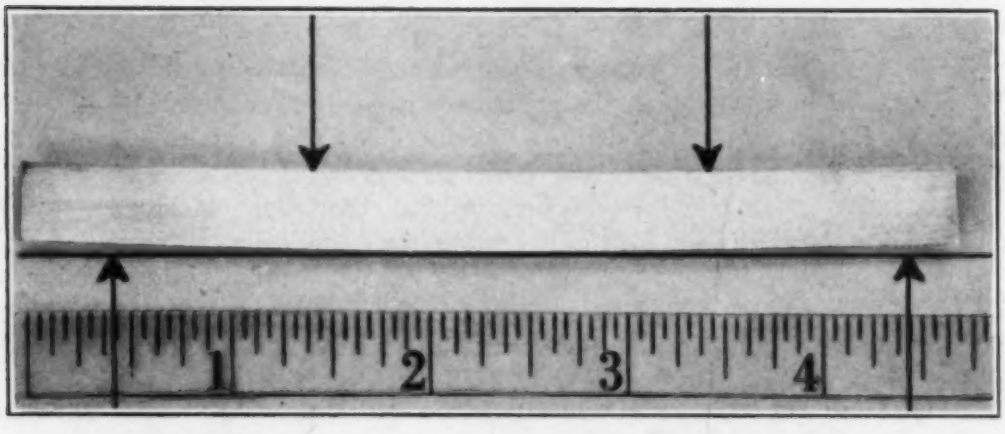

Fig. A—Specimen No. 1 of Oil Quench Double Temper Series. Extreme Fiber Stress—542,500 Pounds Per Square Inch. Yielding Began at Approximately 400,000 Pounds Per Square Inch. Hardness—Rockwell C—65.9. Maximum Deflection Under Load 0.23 Inch. Permanent Set—⅛ Inch. × 0.87.

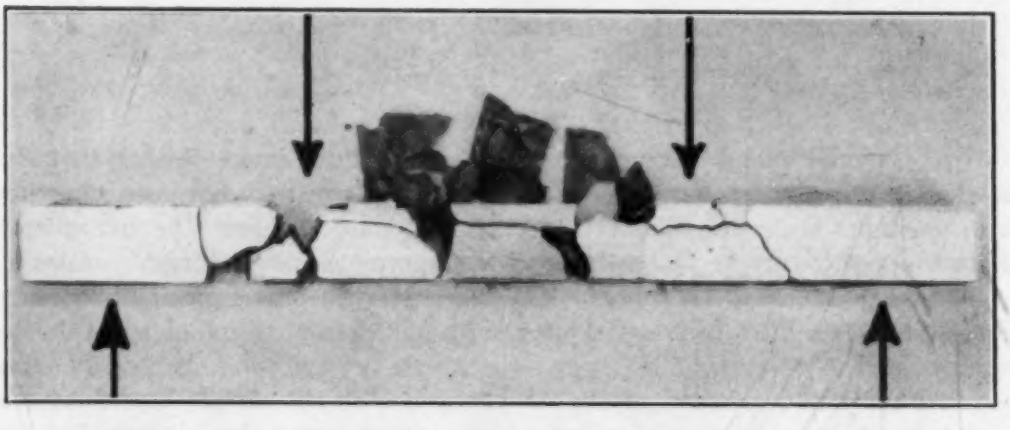

Fig. B—Specimen No. 2 of Oil Quench Double Temper Series. Extreme Fiber Stress—533,500 Pounds Per Square Inch. Yielding Began at Approximately 400,000 Pounds Per Square Inch. Hardness—Rockwell C—65.6. Note Fragmentation of Constant Bending Moment Section. × 0.87.

definitely advantageous. The optimum hot quenching time is still to be determined, but the indications are that 30 minutes will be adequate.

Written Discussion: By R. F. Harvey, Brown and Sharpe Manufacturing Co., Providence, R. I.

The results of tests conducted by the authors show that when the hardening of high speed steel is arrested above room temperature large amounts of austenite are transferred to the tempering furnace. It has been further demonstrated that repeated tempering is more effective than single tempering when considerably more than the normal quantity of austenite is present.

This information constitutes a valuable contribution to the knowledge that exists on the tempering of high speed steel. However, the authors' references to arrested quenching temperatures of 225 degrees Fahr. (105 degrees Cent.) and above is somewhat misleading as it is standard commercial practice to cool all high speed steel tools to at least below 130 degrees Fahr. (55 degrees Cent.) where they can readily be handled without gloves.

Several years ago the writer conducted a rather extensive investigation on the structural characteristics of high speed steel rapidly heated for hardening by high frequency induction methods. It was found that the resulting structures were characterized by (a) small grain size, (b) substantially complete carbide solution, (c) abnormally large quantities of retained austenite. It was also found that repeated tempering was necessary to accomplish complete decomposition of the large amount of retained austenite present in these structures. It would appear that the practical application of repeated tempering of highly austenitic structures will be more important as induction methods are applied to the hardening of high speed steels.

Regarding the theory advanced by the authors to explain the marked difference between repeated and single tempering of highly austenitic structures, I would like to ask whether the presence of primary and tempered martensite are equal in their effect in providing nuclei for carbide precipitation?

Written Discussion: By W. E. Bancroft, chief metallurgist Pratt & Whitney Div., Niles-Bement-Pond Co., W. Hartford, Conn.

This paper certainly constitutes another of the very valuable contributions to the literature on the behavior of high speed steel, which we have come to expect of Dr. Cohen and his associates at about this time each year. To my mind it adequately clarifies the situation concerning the behavior of high speed steel during and after arrested quenching. I have nothing but praise to express for the excellence of the procedure, and the presentation of the experimental results.

However, I think the principles developed here should be applied with some caution and due consideration as to the absolute necessity of arresting the quench at elevated temperatures and then tempering direct. I know that this practice has been advocated by some for many years and undoubtedly has some merit, especially, perhaps, as compared with quenching large and intricately designed tools right down to room temperature in cold oil. My own personal experience to date seems to indicate that quenching into a molten bath at between 1000 and 1200 degrees Fahr. (540 and 650 degrees Cent.) and then cooling to room temperature in air (not in oil) before tempering results in very little cracking which could conceivably be attributed to the thermal stresses developed in cooling down.

Therefore, while it might seem at first glance that the practice of quenching at elevated temperatures followed by triple drawing would be an easy way of handling all, even slightly hazardous, tools, I think the difference in strength should be carefully considered. As the authors themselves have pointed out, Table VI clearly shows that quenching to 80 degrees Fahr. (26.7 degrees Cent.) followed by double tempering gives superior strength to the best that can be obtained after quenching at 225 degrees Fahr. (105 degrees Cent.), and it is certainly preferable from an economic and practical viewpoint to complete the tempering in two draws rather than three.

I do not mean by the above to minimize in the slightest degree the importance of the present report. It definitely furnishes a much needed set of rules to be used in the event that quenching should be arrested above room temperature, but I believe this practice should be confined only to extreme cases where some sacrifice in final strength is clearly justified.

Written Discussion: By A. H. d'Arcambal, vice-president, Pratt & Whitney Div., Niles-Bement-Pond Co., W. Hartford, Conn.

It might be a good idea for Dr. Cohen and myself to visit a few chapters together this winter, discussing high speed steel at these meetings. Due to respect for old age, I undoubtedly would be called on to give the first paper, stressing as I have for many, many years the fact that hardened high speed steel should not be drawn until the same has reached room temperature. Dr. Cohen could then submit a prescription for tools that were drawn before reaching room temperature as undoubtedly some of our friends in the audience would not agree with my recommendations.

It has been our experience as a result of hardening many thousands of high speed steel tools daily that if a good quality high speed steel is employed and the proper hardening technique followed, such as the correct time and temperature at high heat, etc., high speed steel tools may be cooled to room temperature without any danger of cracking even in the case of complicated designs. In the case of large masses it is advisable to hot quench and then cool to room temperature before the drawing treatment.

Dr. Cohen has definitely shown in his interesting paper the detrimental effects of drawing before the tools reach room temperature, which can be overcome to some extent by multiple drawing. Considering, however, that one does not obtain the same strength even with three high draws on tools that have been drawn before reaching room temperature, as compared with tools that have been cooled to room temperature and given a double high draw it would seem as though the better practice would be to cool to room temperature before drawing. It has been definitely proven that tools drawn before reaching room temperature are very susceptible to grinding cracks and of course do not have the strength of tools properly hardened. In my opinion it is more hazardous to draw high speed steel tools before reaching room temperature than to allow tools to cool to room temperature before drawing.

Authors' Reply

The authors appreciate the many constructive comments and criticisms offered by the discussers. They particularly wish to thank Prof. Trigger for the valuable supplementary data he has presented.

Mr. Lement's questions are quite pertinent. The reason for the stabilizing effect of single tempering after arrested quenching has not yet been established. The answer is undoubtedly related to the question of why austenite transforms into martensite at all when cooled below the M-point. Although this process is not well understood, it is not unlikely that once the martensite formation is underway, the stress conditions set up by the transformation have an important accelerating effect on the transformation of each subsequent increment of austenite. If the austenite decomposition is interrupted and the steel reheated to some elevated temperature (for example, quenching to 225 degrees Fahr. and single tempering at 750 degrees Fahr.), the stresses present will be considerably alleviated. Upon subsequent cooling, with the stimulating effect of the stresses removed, the austenite in part or in toto may be sufficiently stable to resist decomposition all the way to room temperature. The nature of this stabilizing action is probably very much the same as that observed by two of the authors in their previous work on the transformation of austenite at subatmospheric temperature,[7] to which Mr. Lement has referred.

The stress relief theory also offers a possible explanation for the decreasing potency of the stabilizing action as the amount of austenite brought into the tempering treatment is increased. It is reasonable to suppose that the least stable portion of the austenite (that is, the austenite which decomposes earliest on cooling) requires little or no added impulse to undergo transformation other than the mere cooling below its transformation temperature. On the other hand, the most stable portions of the austenite (the last increments to transform during cooling) may be supposed to require for decomposition not only the persuasion of continued cooling, but the added stimulus of the stresses originating from the previous martensite formation. The requisite contribution of stresses to the continuation of austenite decomposition during cooling would, therefore, become larger as the amount of austenite left to transform becomes smaller. If this hypothesis is accepted, it is then not difficult to see that when the cooling is arrested very soon after the onset of the austenite-martensite transformation, relief of the incurred transformational stresses by reheating to, say, 750 degrees Fahr. (400 degrees Cent.) will have little influence on the resumption of decomposition during subsequent cooling. In other words, when the quantity of austenite brought into the tempering treatment is very large, the stabilizing effect is relatively small. On the other hand, as the arresting temperature is lowered, the quantity of austenite brought into the tempering treatment becomes smaller and the dependence of this austenite for decomposition upon the influence of transformational stresses becomes greater. Hence, when these stresses are relieved by tempering, the austenite is able to resist decomposition during subsequent cooling far below the temperatures at which it would originally have transformed, and in many cases is retained all the way to room temperature. Pursuing this picture further, if the steel is quenched directly to room temperature during hardening, the 20 to 25 per cent of retained austenite is so greatly dependent for additional decomposition upon the accelerating effect of the transformational stresses that even room temperature aging will accomplish sufficient stress relief

[7] P. Gordon and M. Cohen, "The Transformation of Retained Austenite in High Speed Steel at Subatmospheric Temperatures," TRANSACTIONS, American Society for Metals, Vol. 30, 1942, p. 569-591.

to lower the transformation point 50 to 100 degrees Fahr. below room temperature.[7] If, on the other hand, the hardening quench is arrested above or just below the M-point and the steel reheated to 1050 degrees Fahr. (565 degrees Cent.) for several hours, the formation of martensite during subsequent cooling indicates that practically no stabilization has occurred, as should be the case according to the above reasoning.

Mr. Lement has asked whether bainite forms during single tempering in the range of 450 to 750 degrees Fahr. (230 to 400 degrees Cent.) after quenching to, say, 225 degrees Fahr. (105 degrees Cent.). It may be said definitely that such bainite formation does not take place to any measurable extent. This is proven by the fact that the amount of austenite retained at room temperature after arresting the quench at 225 degrees Fahr. (105 degrees Cent.) and single tempering for 2.5 hours in the range 450 to 750 degrees Fahr. (230 to 400 degrees Cent.) is virtually the same as the quantity of austenite existing at 225 degrees Fahr. (105 degrees Cent.) during the hardening quench. The transformation curves for 6-6-2 high speed steel[8] indicate that isothermal bainite formation in the range 500 to 650 degrees Fahr. (260 to 345 degrees Cent.) will begin in approximately 9 minutes if the steel is quenched from the hardening temperature directly into this range. This fact, however, applies specifically to the situation in which 100 per cent austenite is originally present at the transformation temperature. In the case where the steel has first been quenched to 225 degrees Fahr. (105 degrees Cent.) and then reheated to 450 to 750 degrees Fahr. (230 to 400 degrees Cent.), only about 55 per cent of austenite is then available for transformation, and an entirely different set of transformation curves is needed to predict the time for the beginning of bainite formation.

Mr. Lement's last two questions can be answered by some data which the authors have obtained since the writing of this paper. Two series of experiments were carried out with 6-5-1.5 high speed steel. In the first, in order to determine the maximum amount of retained austenite which can be virtually completely transformed by a single temper of 2.5 hours at 1050 degrees Fahr. (570 degrees Cent.), several specimens were quenched from 2225 to 225 degrees Fahr. (1220 to 105 degrees Cent.), reheated to 750 degrees Fahr. (400 degrees Cent.) for 2.5 hours and cooled to room temperature. Each specimen, containing now about 55 per cent of retained austenite, was next given various short tempering treatments in order to bring their austenite contents to the values listed in column a of Table A. All the specimens were then given a single temper of 2.5 hours at 1050 degrees Fahr. (565 degrees Cent.) and their final austenite contents measured, as listed in column b of Table A. It may be seen from the data in Table A that virtually complete transformation after 2.5 hours at 1050 degrees Fahr. (565 degrees Cent.) is only obtained if the amount of retained austenite is not much over 25 per cent. The term "virtually complete transformation" is defined by the authors to mean not more than about 2 per cent of retained austenite.

The second series of experiments was carried out to determine whether the above figure of 25 per cent austenite would hold independently of the treatment used to bring the steel to that condition. Accordingly, several specimens were given the various treatments listed in column a of Table B resulting in the re-

[8] P. Gordon, M. Cohen and R. S. Rose, "The Kinetics of Austenite Decomposition in High Speed Steel," TRANSACTIONS, American Society for Metals, Vol. 31, 1943, p. 161-217.

Table A
Quantity of Retained Austenite Transformed by 2.5 Hour Single Temper at 1050 Degrees Fahr.

Specimen No.	Per Cent Austenite Before 2.5 Hour Single Temper at 1050° F. (a)	Per Cent Austenite After 2.5 Hour Single Temper at 1050° F. (b)
1	58	12
2	49	9
3	43	7
4	33	5
5	29	3
6	25	1

tained austenite contents indicated in column b. By appropriate short tempering treatments at 1050 degrees Fahr. (565 degrees Cent.), the austenite contents of the specimens were then reduced to approximately 25 per cent as indicated in column d. Finally all secimens were single tempered for 2.5 hours at 1050 degrees Fahr. (565 degrees Cent.). An examination of the retained austenite

Table B
Effect of Prior Treatment on Quantity of Retained Austenite Transformable by 2.5 Hour Single Temper at 1050 Degrees Fahr.

Specimen No.	Preliminary Treatment Austenitizing Temp.=2225°F (a)	Per Cent Austenite after Preliminary Treatment (b)	Structural Constituents after Prelim. Treatment (c)	Retempered to Per Cent Austenite asIndicated (d)	Per Cent Austenite after Final 2.5 Hr. Temp. 1050°F. (e)
7	Quench to 225°F. Temper 2.5 hrs. 1050°F.	10	Austenite Carbides, and Martensite	10	½
8	Quench to 225°F Temper 2.5 hrs. 850°F.	48	"	25	1
9	Quench to 225°F. Temper 2.5 hrs. 650°F.	55	"	23	1
10	Quench to 225°F. Temper 2.5 hrs. 550°F.	52	"	23	1.5
11	Quench to 225°F. Temper 2.5 hrs. 450°F.	54	"	24.5	1
12	Quench to 275°F. Temper 2.5 hrs. 750°F.	42	"	24	1
13	Quench to 325°F. Temper 2.5 hrs. 750°F.	27.5	"	26	2
14	Quench to 350°F. Temper 2.5 hrs. 750°F.	26.5	"	26.5	2
15	Hot Quench to 500°F. for 24 hrs.	43	Austenite Carbides, and Bainite	25	5.5
16	Hot Quench to 600°F. for 24 hrs.		"	18	2

contents in column e reveals that the final 1050 degrees Fahr. (565 degrees Cent.) temper was sufficient to cause the virtually complete decomposition of the

austenite in all specimens except specimen No. 15. This specimen, along with No. 16, differed from all the others in that it contained bainite instead of martensite. No. 16, containing only 18 per cent austenite before the final temper, *was* virtually completely transformed by the 2.5-hour temper at 1050 degrees Fahr. (565 degrees Cent.). A study of Table B leads to the following conclusions: A 2.5-hour single temper at 1050 degrees Fahr. (565 degrees Cent.) will cause the decomposition of up to about 25 per cent retained austenite in this high speed steel, regardless of how the steel is treated to obtain that quantity of retained austenite.[9] One exception to this statement, however, is the case when the austenite has been retained after isothermal bainite formation during hot quenching. Then the limit of residual austenite which will decompose completely after a 2.5-hour single temper at 1050 degrees Fahr. (565 degrees Cent.) is about 18 per cent instead of 25 per cent.

In reply to Dr. Zmeskal, it may be said that substantially complete transformation of the retained austenite in high speed steel is a general objective. In addition to the reason Dr. Zmeskal cited himself—that the peak in hot hardness corresponds to the condition of complete austenite transformation—it is a fact that retained austenite is generally co-existent at room temperature with some untempered martensite, unless intermediate drawing temperatures in the vicinity of 700 degrees Fahr. (370 degrees Cent.) have been used. The presence of untempered martensite and the concomitant unrelieved transformational stresses would be expected to have a deleterious effect on the mechanical properties of the steel. Furthermore, in the case of tools for which dimensional stability is of prime importance, the presence of untransformed austenite would be obviously undesirable because of the possibility of volume changes due to decomposition during use.

The authors have no data showing the effect on the transverse strength of high speed steels of completing the austenite transformation at temperatures other than 1050 degrees Fahr. (565 degrees Cent.).

Mr. Weldon's comments are most interesting. He has suggested that the rate of quenching be considered a variable as well as the temperature to which the steel is quenched. It is important to note that the mechanical properties of actual tools are influenced by the rate of cooling during the quench, even though it is hardly likely that the rate of cooling has much effect on the transformations studied here.

The authors agree with Mr. Weldon that the transverse bend test is useful in the studies of tool steels; that is why transverse bend strengths have been reported in this paper. It is not, however, felt that transverse strength alone can be directly correlated with tool performance. For example, Professor Trigger in his discussion has clearly demonstrated that improved tool life may be accompanied by inferior bend strength.

The authors are willing to grant Professor Trigger that some carbide precipitation may take place during a primary quench to 1050 degrees Fahr. (565 degrees Cent.), and the text has been changed accordingly. We have, however, found no dilatometric evidence of such precipitation, and our hardness measurements have not shown the difference between oil-quenched and hot-quenched samples indicated by Professor Trigger's data.

[9] That is, in 6-5-1.5 high speed steel austenitized at 2225 degrees Fahr.

From the hardness values given in his first table, Professor Trigger draws the conclusion that oil-quenched samples show three times as much secondary hardening as do hot-quenched samples, and implies that this signifies appreciably more retained austenite in the oil-quenched samples. This conclusion needs some modification. Professor Trigger has subtracted the as-quenched hardness values from the peak secondary hardness values and has called the result the increase in hardness due to tempering. Since, however, the hardened samples undergo considerable softening during tempering prior to the onset of secondary hardening, the true increase in hardness due to tempering must be derived by comparing the *minimum hardness during tempering* with the secondary hardness peak. If this is done, the increase in hardness due to tempering will undoubtedly be found to be nearly the same for oil-quenched and 1025 degrees Fahr. (550 degrees Cent.) hot-quenched samples. At the least, the ratio of 3 to 1 indicated by Professor Trigger will be reduced quite considerably.

Professor Trigger has suggested that the precipitation of non-ferromagnetic carbides during a 1000 degrees Fahr. (540 degrees Cent.) hot quench might affect the calibration curve given in Fig. 1 of the paper. The authors have found, however, that up to values of at least 50 to 60 per cent of austenite very large changes in the quantity of excess carbide present in the steel have no measurable effect upon the calibration curve. For example, the per cent of austenite in several specimens was determined dilatometrically. The per cent of excess carbide in those specimens varied widely, the lowest containing 6 per cent, and the highest 10 per cent, of free carbides. Yet, the measured magnetization of the specimens, when plotted against the dilatometrically determined austenite contents, were found to lie on the calibration curve given in Fig. 1.

It is hoped that Professor Trigger will continue his excellent work on the performance testing of actual tools, and that he will extend this work to include tests during interrupted, as well as continuous, cutting. The authors anticipate that the relationship between transverse strength and tool life will be materially affected by the amount of shock involved in the cutting tests.

We are very glad to learn of Mr. Harvey's experiments with the induction hardening of high speed steel, and trust that he will be able to publish the details soon. It is most interesting, from both scientific and practical points of view, that multiple tempering is effective in decomposing the large quantities of retained austenite resulting from induction hardening. The same principles apply as in the case of high austenite contents associated with arrested cooling.

Mr. Harvey feels that reference to arrested quenching temperatures of 225 degrees Fahr. (105 degrees Cent.) and above is misleading. That temperatures in this range are frequently used is indicated by the recommended quenching practice for high speed steels given on pages 1000 to 1006 of the 1939 Metals Handbook. The following is quoted from the section on tungsten high speed steels, page 1001, "...The tool may be quenched in oil and removed from the bath while still red or at approximately 1100 degrees Fahr. (595 degrees Cent.). The tool is then cooled slowly in air to 200 to 300 degrees Fahr. (95 to 150 degrees Cent.), then tempered immediately to avoid cracking." Furthermore Dr. Zmeskal, in his discussion of this paper, has stated that it is a commercial practice to arrest the quenching of large high speed rolls at 500 degrees Fahr. (260 degrees Cent.) before immediate tempering.

Mr. Harvey has asked whether primary and tempered martensite have the same effect upon the nucleation of carbide precipitation. This question cannot be answered. Whenever hardened high speed steel is tempered at temperatures high enough to permit carbide precipitation from the austenite, the martensite present will already have been tempered, for the breakdown of the primary tetragonal martensite occurs in the range 200 to 500 degrees Fahr. (95 to 260 degrees Cent.). Consequently, the nucleating effect of primary martensite on the carbide precipitation cannot be determined.

Both Mr. Bancroft and Mr. d'Arcambal seem to feel that the authors have implied a recommendation for arrested quenching. It should be emphasized that, quite to the contrary, the purpose of the present paper was to point out the disadvantages of arrested quenching, but at the same time, to indicate the corrective measures which could and should be adopted in the cases where arrested quenching is considered unavoidable or desirable. To put the matter another way, arrested quenching should not be used unless it is necessary, but for some types of tools and for some grades of steel, it is necessary if undue distortion and hazardous cracking are to be avoided.

AN OPTIMUM SILICON RANGE IN PLAIN AND 2.0 PER CENT CHROMIUM CAST IRONS EXPOSED TO ELEVATED TEMPERATURES

By C. O. Burgess and R. W. Bishop

Abstract

Plain and 2 per cent chromium cast irons in which the silicon content was varied between approximately 2.5 and 7.0 per cent have been subjected to high temperatures for extended periods. The carbon contents of the irons lie in the range of 2.9 to 3.5 per cent. Cyclic heating to a top temperature of 800 degrees Cent. (1470 degrees Fahr.) was employed, the irons being at this top temperature for a total period of approximately 500 hours. It was found that both the plain and chromium-bearing irons develop optimum resistance to growth and oxidation within a relatively narrow silicon range, namely, 3.0 to 4.5 per cent silicon. It appears that cast irons within this range exhibit maximum resistance to the combined effects of external and internal oxidation.

THE present study was undertaken to determine the effect of silicon content on the heat resistance of both plain and chromium-bearing cast irons. This problem of selecting the optimum silicon range for cast irons exposed to high temperatures has long engaged the attention of foundrymen and has been the subject of several investigations. Early tests were run by Rugan and Carpenter (1),* and more recently Norbury and Morgan (2) tested irons covering a wide silicon range. Some disagreement is evident in this earlier work. In the present investigation, results are obtained which indicate that a relatively narrow silicon range (3.0 to 4.5 per cent silicon) exists within which optimum resistance to high temperatures can be developed. Existence of such a range has apparently not been recognized by previous investigators.

*The figures appearing in parentheses refer to the bibliography appended to this paper.

A paper presented before the Twenty-fifth Annual Convention of the Society, held in Chicago, October 18 to 22, 1943. The authors, C. O. Burgess and R. W. Bishop, are research metallurgists, Union Carbide & Carbon Research Laboratories, Inc., Niagara Falls, N. Y. Manuscript received June 21, 1943.

Test Materials

The cast irons selected for this investigation possessed carbon contents that might normally be expected on cupola melting. In other words, the carbon content was held between about 2.9 and 3.5 per cent. The silicon range was deliberately limited to 2.5 to 7.0 per cent in that the purpose of the tests was to determine whether an optimum silicon range existed above the maximum 2.5 per cent silicon level usually employed by foundrymen and below the silicon level that might be expected to produce excessive brittleness or sensitivity to thermal shock. This maximum is not sharply defined, but for the purpose of our tests was assumed to be in the neighborhood of 6.0 to 7.0 per cent silicon.

In addition to plain cast irons, a series of 2.0 per cent chromium cast irons were included in the tests in view of earlier work (3), (4) that had shown that such irons possessed unusual heat resistance. It was thought that the presence of a special alloying agent, such as chromium, might affect the location of an optimum silicon range.

All the cast irons were prepared by melting malleable pig iron, Armco iron, and silicon metal in high frequency furnaces. Except in the case of specimen 2, the silicon metal was added to the initial charge to avoid any inoculating effect that might result from a late addition. In the 2 per cent chromium irons, the chromium was added as high carbon ferrochromium.

The analyses of the irons are shown in Table I. Turnings for analysis were obtained from standard 1.2-inch transverse bars. The phosphorus and sulphur contents in all specimens closely approximated the values shown for specimen 1 except in the three cases in which these constituents were deliberately varied.

From the above table, it appears that the combined carbon content of both plain and 2 per cent chromium cast irons decreases with silicon content although some evidence exists (Spec. 3 vs. Spec. 2) that even small variations in sulphur may delay pearlite breakdown. The combined carbon content of the 2 per cent chromium cast irons, which possess a rather uniform total carbon content, decreases progressively with increasing silicon content. It is significant to observe that increasing the silicon from 2.42 to 3.33 per cent was sufficient to lower the combined carbon content of the 2 per cent chromium cast iron from 2.15 to 0.81 per cent and to bring it within a readily machinable range.

Table I

Analysis of Test Irons

Specimen No.	Per Cent						
	Total Carbon	Combined Carbon	Silicon	Manganese	Chromium	Phosphorus	Sulphur
			Plain Irons				
1	3.54	0.40	2.51	0.56	....	0.115	0.043
2	3.31	0.22	3.32	0.64	....	.....	.....
3	3.28	0.31	3.35	0.54	....	.....	0.114
4	3.53	0.06	3.42	0.59	....	.....	.....
5	3.48	0.05	3.50	0.50	....	.....	0.131
6	3.35	0.03	3.50	0.58	....	0.580	.....
7	3.30	0.06	4.31	0.52	....	.....	.....
8	2.91	0.03	5.92	0.70	....	.....	.....
			2 Per Cent Chromium Irons				
9	3.16	2.15	2.42	0.54	2.04	.....	.....
10	3.08	0.81	3.33	0.49	1.91	.....	.....
11	2.96	0.58	4.72	0.55	1.78	.....	.....
12	3.06	0.60	5.46	0.60	1.90	.....	.....
13	2.88	0.29	6.32	0.62	1.90	.....	.....

Procedure Used in Oxidation and Growth Tests

The test specimens employed in the investigational work were 6-inch long bars cut from the middle portion of standard 1.2-inch diameter arbitration bars cast from the heats listed in Table I. The cut ends of the 6-inch bars were machined flat, and small stainless steel plugs were inserted into each of the machined faces. Such inserts or plugs permitted changes in true over-all length to be determined independently of errors normally brought about by scale formation. The specimens were placed on stainless steel racks. The racks were placed in a large Nichrome-wound furnace, and specimens and racks brought to a temperature of 800 degrees Cent. (1470 degrees Fahr.). The furnace was provided with openings that permitted ready entrance of air, and as a consequence the atmosphere was oxidizing.

In a typical heating cycle the furnace was brought to test temperature and the specimens inserted. One hour was allowed for the specimens to reach 800 degrees Cent. (1470 degrees Fahr.) and they were held at this temperature for 15 hours. The test specimens were then removed from the furnace and allowed to cool in still air to room temperature. This procedure was repeated 34 times until a total exposure time of 500 hours at 800 degrees Cent. (1470 degrees Fahr.) was attained. To avoid possible variations, all the specimens shown in Table I were heated simultaneously.

The growth bars were measured after each heating cycle with a vernier caliper capable of measuring accurately to 0.001 of an inch.

Results of Growth Tests

Previous work has shown that growth measurements are one of the most sensitive gages of the ability of a cast iron to resist heat effects. Thus in addition to the practical necessity, from a design standpoint, that cast iron members maintain constant or relatively constant dimensions, excessive growth also indicates a serious amount of internal oxidation and a general deterioration of physical properties.

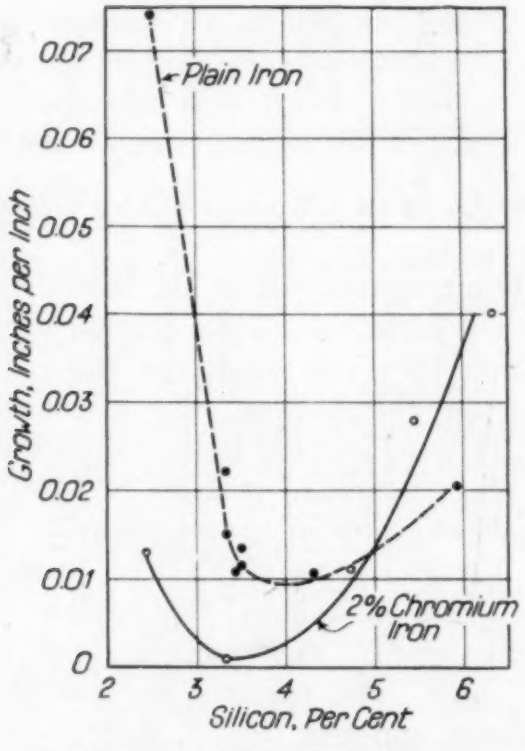

Fig. 1—Growth Versus Silicon Content After 500 Hours at 800 Degrees Cent.

Consequently, the over-all growth of the specimens during their 500-hour exposure is of primary importance. The results of the growth measurements are plotted in Fig. 1. It will be observed that growth of the plain irons reaches a minimum in the neighborhood of 3.5 to 4.5 per cent silicon. Unfortunately, there were not sufficient specimens in this critical silicon range to definitely establish the upper limit of the low growth range. However, the growth is still at a minimum at 4.31 per cent silicon, and rises sharply at a 5.92 per cent silicon content.

In the case of the 2 per cent chromium irons, a much lower

order of growth is encountered. For example, the growth of 2 per cent chromium iron even with a usual silicon content of 2.42 per cent is no greater than the minimum shown by a plain iron in the optimum silicon range. However, it is again evident that even in the 2 per cent chromium irons an optimum silicon range exists. The optimum range is similar to that for plain irons but appears to be slightly shifted to lower silicon contents, the lower limit being transposed closer to 3.0 per cent silicon than the 3.5 per cent exhibited by plain irons, and from the upward trend of the growth curve at 4.72 per cent silicon it appears that the upper limit of the optimum range in the case of the 2 per cent chromium irons may be closer to 4.0 per cent than the 4.5 per cent silicon estimated for the plain irons. The sharp rise in growth at a 5.46 per cent silicon level or above in the case of these 2 per cent chromium irons indicates that the protection against internal oxidation normally offered by the chromium content (4) can be destroyed by the use of excessive silicon contents.

It is significant that the growth of 2 per cent chromium irons is actually at a minimum when a sufficient amount of silicon (approximately 3.5 per cent) is introduced to lower the combined carbon content sufficiently to bring the irons into a machinable range.

Results of Oxidation Tests

In any discussion of the oxidation of cast iron, it should be recognized that both external oxidation, commonly known as scaling, and internal oxidation below the apparent metal surface may take place. It is this latter type of oxidation that is mainly responsible for growth (3), (4) and deterioration of physical properties.

External Oxidation—The formation of oxide constituents on the surface of a cast iron that can be removed by sandblasting or electrolytic pickling are considered to result from external oxidation. Some estimate of the resistance of irons to such external oxidation can be obtained from the general appearance of the bars after exposure. The typical appearance of plain cast iron growth Specimens 1 and 4 with silicon contents of 2.51 and 3.42 per cent silicon respectively, and 2 per cent chromium cast iron growth Specimens 9 and 10 with silicon contents of 2.42 per cent and 3.33 per cent silicon respectively, after 500 hours at 800 degrees Cent. is illustrated in Fig. 2. It can be noted that in the case of the plain irons the amount of scale

decreases with increasing silicon. This influence of silicon cannot be so clearly detected in the 2 per cent chromium specimens, as the presence of chromium confers considerable protection against scaling even on the lower silicon iron.

The most positive measure of external oxidation is, however,

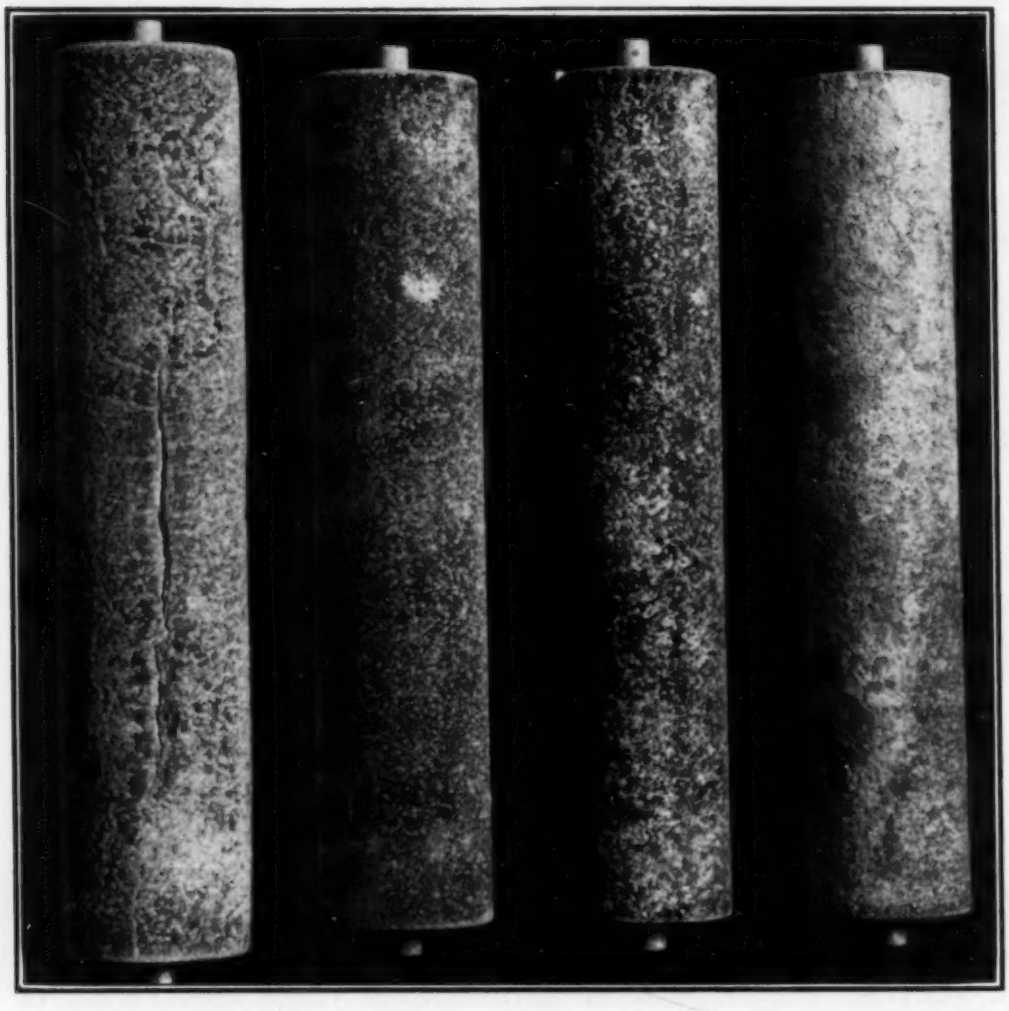

1 4 9 10

Fig. 2—Appearance of Typical Growth Bars After 500 Hours' Exposure at 800 Degrees Cent. Specimens 1 and 4 are Plain Irons. (1) 2.51 Per Cent Silicon. (4) 3.42 Per Cent Silicon. Specimens 9 and 10 are 2 Per Cent Chromium Irons. (9) 2.42 Per Cent Silicon. (10) 3.33 Per Cent Silicon.

the weight loss of the oxidized bars after sandblasting and electrolytic cleaning in 10 per cent ammonium citrate (5). This latter cleaning method had to be employed due to the formation of a very adherent scale on some of the higher silicon irons. The changes in weight in grams per square inch of both the plain and 2 per cent chromium irons are plotted against silicon content in Fig. 3.

As can be seen from these curves, the external oxidation or scaling loss drops sharply with increasing silicon in the case of the plain irons, and somewhat more slowly in the case of the chromium-bearing irons that have an initially high resistance to oxidation. It is remarkable that in both the plain and 2 per cent chromium irons when the weight loss finally reaches zero with increasing silicon content, a

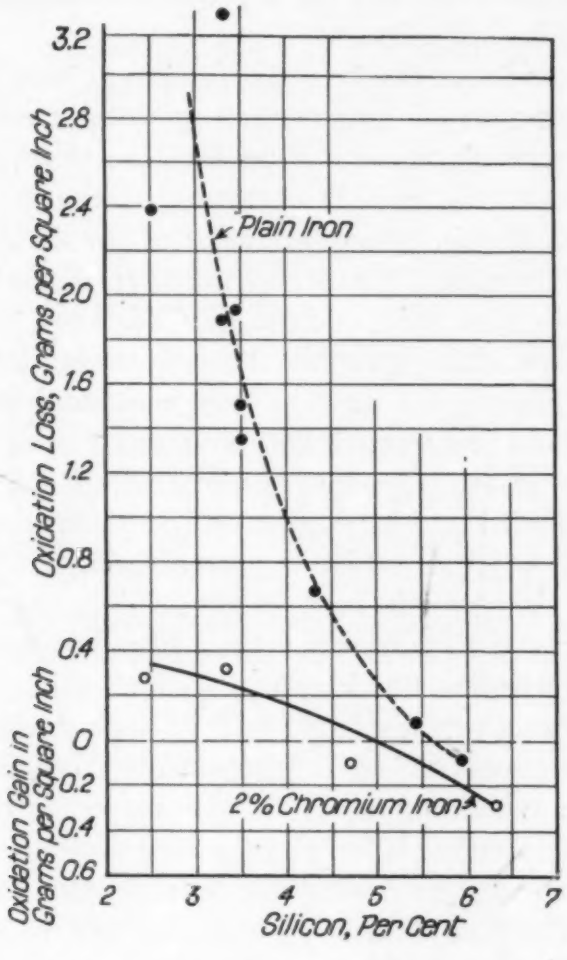

Fig. 3—Oxidation Loss or Gain Versus Silicon Content After 500 Hours at 800 Degrees Cent.

further silicon increase actually produces a weight gain. As the specimens were carefully cleaned of adhering scale, this weight gain can be due only to internal oxidation of the specimens. To some extent this weight gain due to internal oxidation must balance the scaling loss, although it is probably not significant until the scaling loss or external oxidation approaches a very small value. Fortunately, as will be described in the following section, the extent of internal oxidation can be closely estimated by other methods.

Internal Oxidation—The internal oxidation of cast iron through the formation of a "metal-oxide" constituent beneath the surface of the iron has been demonstrated in earlier papers (3), (4). Such internal oxidation is always accompanied by growth, and if extensive, by deterioration of the mechanical properties. The fact that chromium acts specifically to inhibit and prevent such "metal-oxide" penetration led to the use of the 2 per cent chromium cast iron series in the present investigation.

Internal oxidation can be recognized in at least four ways. First, by the phenomenon of progressive growth, second, by structural alterations observable under the microscope, third, by oxygen determinations on successive layers starting at the surface of exposed specimens, and fourth, by measurement of the decarburization of the specimens. The carbon content of the irons should, of course, vary inversely to their oxygen content, the absorbed oxygen or oxides undoubtedly eliminating graphite by converting it to CO and CO_2.

Relative growth has already been measured in Fig. 1, and on this basis it would be assumed that minimum internal oxidation occurs in irons lying in the range of approximately 3.0 to 4.5 per cent silicon. To check this observation and to determine the extent and penetration of internal oxidation, three successive layers were machined from the growth bars after sandblasting and electrolytic pickling to remove all adhering scale. The first metallic layer taken from the 1.2-inch diameter bars was $\frac{1}{16}$ inch thick; the second layer immediately beneath the first layer was $\frac{1}{8}$ inch thick. The last material for analysis consisted of turnings taken from the complete cross section of the remaining core. These respective layers called the outer layer, intermediate layer, and the core were analyzed for oxygen by the vacuum fusion method. The core samples were also analyzed for carbon. The results of the oxygen analyses are shown in Table II and Fig. 4. The results of the carbon analyses are shown in Fig. 5.

It is clear from Fig. 4 that the extreme outside $\frac{1}{16}$-inch layers of all specimens show a high oxygen content. The actual oxygen values obtained on these outer $\frac{1}{16}$-inch layers are not a true measure of the resistance of the irons to progressive internal oxidation. This is due to the fact that the quantity of oxygen or oxide in the surface layer is still influenced by the scaling process, i.e., scale adherence, and the resistance of the irons to complete conversion of the surface to a scale that can be mechanically removed. The oxygen contents of the intermediate $\frac{1}{8}$-inch layer and the core, however, give us a direct measure of the ability of a given iron to resist oxygen penetra-

tion and internal oxidation. It can be observed from Fig. 4 that the plain irons exhibit minimum oxygen values, i.e., maximum resistance to internal oxidation, in the range of about 3.35 to 4.31 per cent silicon. The amount of oxygen or internal oxidation in these inner layers rises sharply at points outside this range; for example, at a lower silicon level of 2.51 per cent and at a higher silicon level of

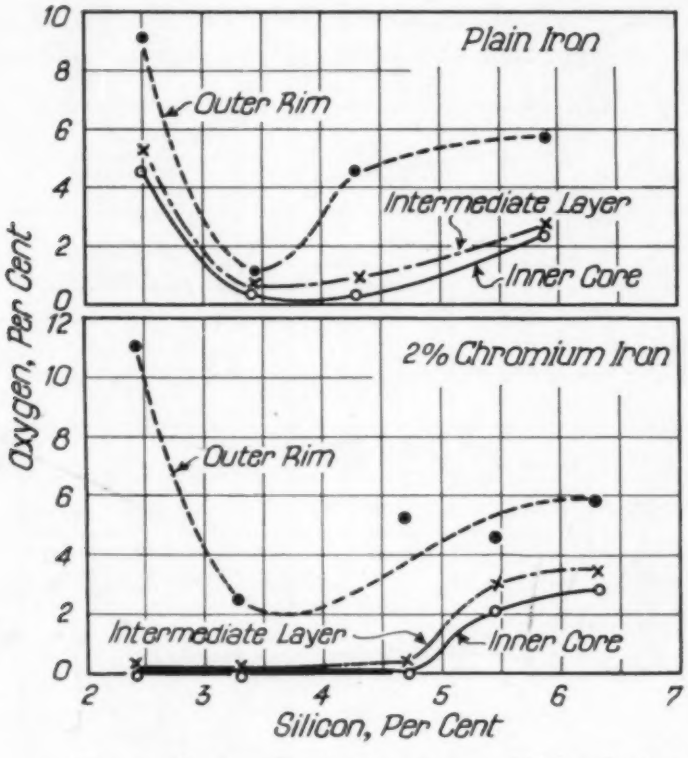

Fig. 4—Oxygen Penetration Versus Silicon Content After 500 Hours at 800 Degrees Cent.

5.92 per cent. In other words, the oxygen determinations confirm the growth tests as concerns the existence of a critical silicon range in which the irons possess optimum resistance to deterioration.

In the case of the 2 per cent chromium cast irons, as found previously, (3), (4) the presence of chromium alone is sufficient to largely prevent or inhibit oxygen penetration and internal oxidation of irons of normal silicon content. It is of interest, however, to observe that this ability of chromium-bearing irons to resist internal oxidation is not adversely affected by increasing the silicon content to 3.33 per cent, and a considerable proportion of the resistance to internal oxidation is maintained at a 4.72 per cent silicon level although the rise in oxygen content of the intermediate layer of this latter specimen indicates that at 4.72 per cent the upper silicon level for maximum resistance has been slightly exceeded.

In Fig. 5 the total carbon contents of the cores of the growth specimens are plotted against their silicon contents. Considering first the plain irons, it can be noted that internal oxidation has proceeded to such an extent in the 2.51 per cent silicon iron that its total carbon is appreciably lowered. In the range of 3.32 to 4.31 per cent silicon, however, only a minor loss in carbon content is evident, indicating that internal oxidation has not proceeded to a degree sufficient to decarburize the core of the irons. However, as the

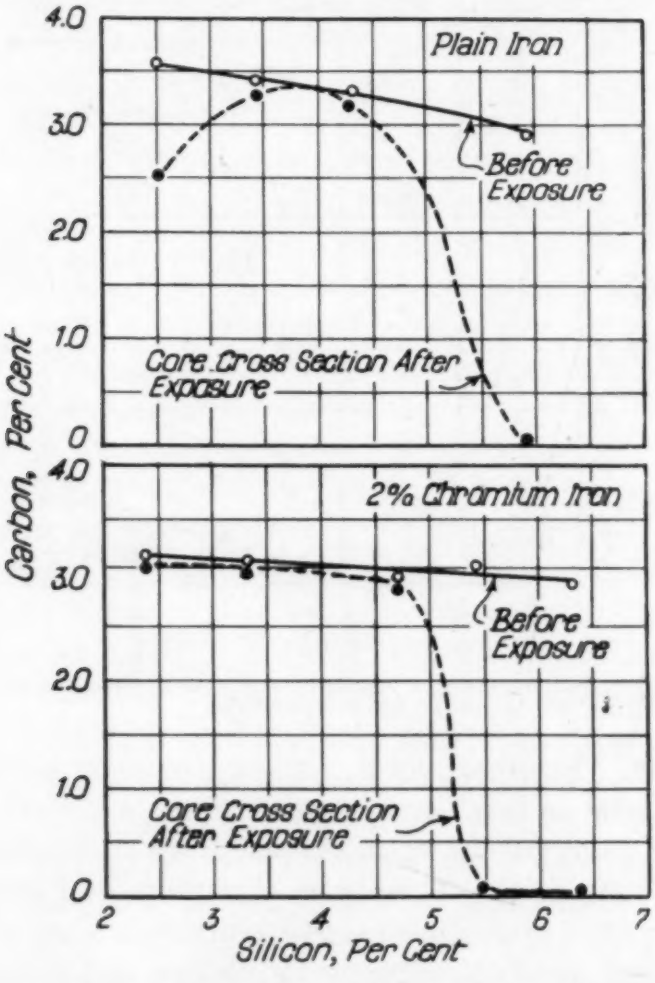

Fig. 5—Decarburization of Interior of Growth Bars After 500 Hours at 800 Degrees Cent.

silicon content of the plain irons is raised to a 5.92 per cent level, the core of the growth bar is almost completely decarburized, indicating that sufficient oxygen or oxide has penetrated this sample to combine with practically all the available graphite.

In the case of the 2 per cent chromium irons, it is clear from Fig. 5 that no appreciable drop in total carbon content occurs up to

Table II
Oxygen Determinations on Successive Layers of Growth Specimens

Specimen No.	Per Cent Silicon	Per Cent Chromium	Outer 1/16" Layer Per Cent Oxygen	Intermediate 1/8" Layer Per Cent Oxygen	Core Per Cent Oxygen
		Plain Irons			
1	2.51	....	9.15	5.41	4.57
2	3.32	....	1.26	0.97	1.22
3	3.35	....	1.07	0.54	0.40
4	3.42	....	1.44	0.68	0.27
5	3.50	....	0.99	0.75	0.48
6	3.50	....	1.22	0.58	0.27
7	4.31	....	4.30	1.09	0.39
8	5.92	....	5.71	2.88	2.38
		2 Per Cent Chromium Irons			
9	2.42	2.04	11.00	0.09	0.07
10	3.33	1.91	2.51	0.08	0.06
11	4.72	1.78	5.32	0.42	0.05
12	5.46	1.90	4.59	3.25	2.04
13	6.32	1.90	5.82	3.65	2.97

a 4.72 per cent silicon level. As the silicon content reaches 5.46 per cent however, there is a sharp decrease in carbon content to a negligible value. It is, therefore, evident that the chromium-bearing irons resemble the plain irons in that beyond a limiting value approximating 4.5 per cent silicon, further increase in silicon, for example up to 5.46 per cent, permits penetration of oxygen to the core of the specimen, and almost complete elimination of carbon results. These results check the growth tests and oxygen determinations in that they show that internal oxidation becomes a serious factor when a critical percentage of silicon is exceeded.

Microscopic Examination

It is reasonable to assume that structural changes would accompany the above phenomena. Metallographic specimens were, therefore, cut from the growth bars with the scale still adhering and mounted with Wood's metal inside annular rings. The typical appearance of such specimens is shown in Fig. 6. As the bars were sectioned approximately ¾ inch from the ends, in some cases the ¼-inch diameter stainless steel plugs, which extended an equal distance from the specimen ends, were intersected and appear in the center of the metallographic specimens. They should, of course, be disregarded.

The structure of the irons at critical silicon levels is shown before and after their 500-hour exposure at 800 degrees Cent. (1470 degrees Fahr.) in Fig. 7 at 100 diameters. It will be noted from the

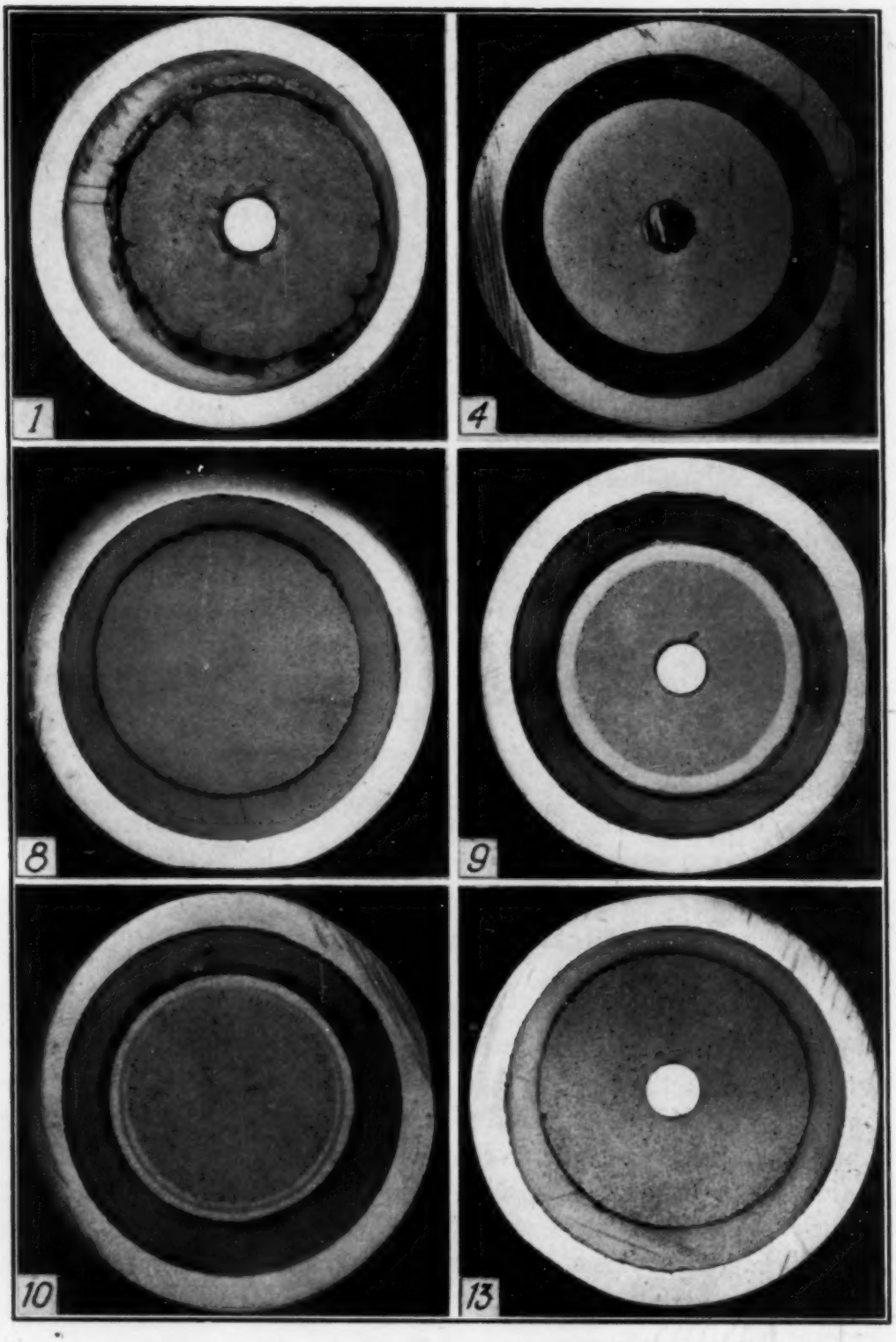

Fig. 6—Typical Sections of Growth Bars Used in Metallographic Examination. Specimens 1, 4 and 8 are Plain Irons. (1) 2.51 Per Cent Silicon. (4) 3.42 Per Cent Silicon. (8) 5.92 Per Cent Silicon. Specimens 9, 10 and 13 are 2 Per Cent Chromium Irons. (9) 2.42 Per Cent Silicon. (10) 3.33 Per Cent Silicon. (13) 6.32 Per Cent Silicon.

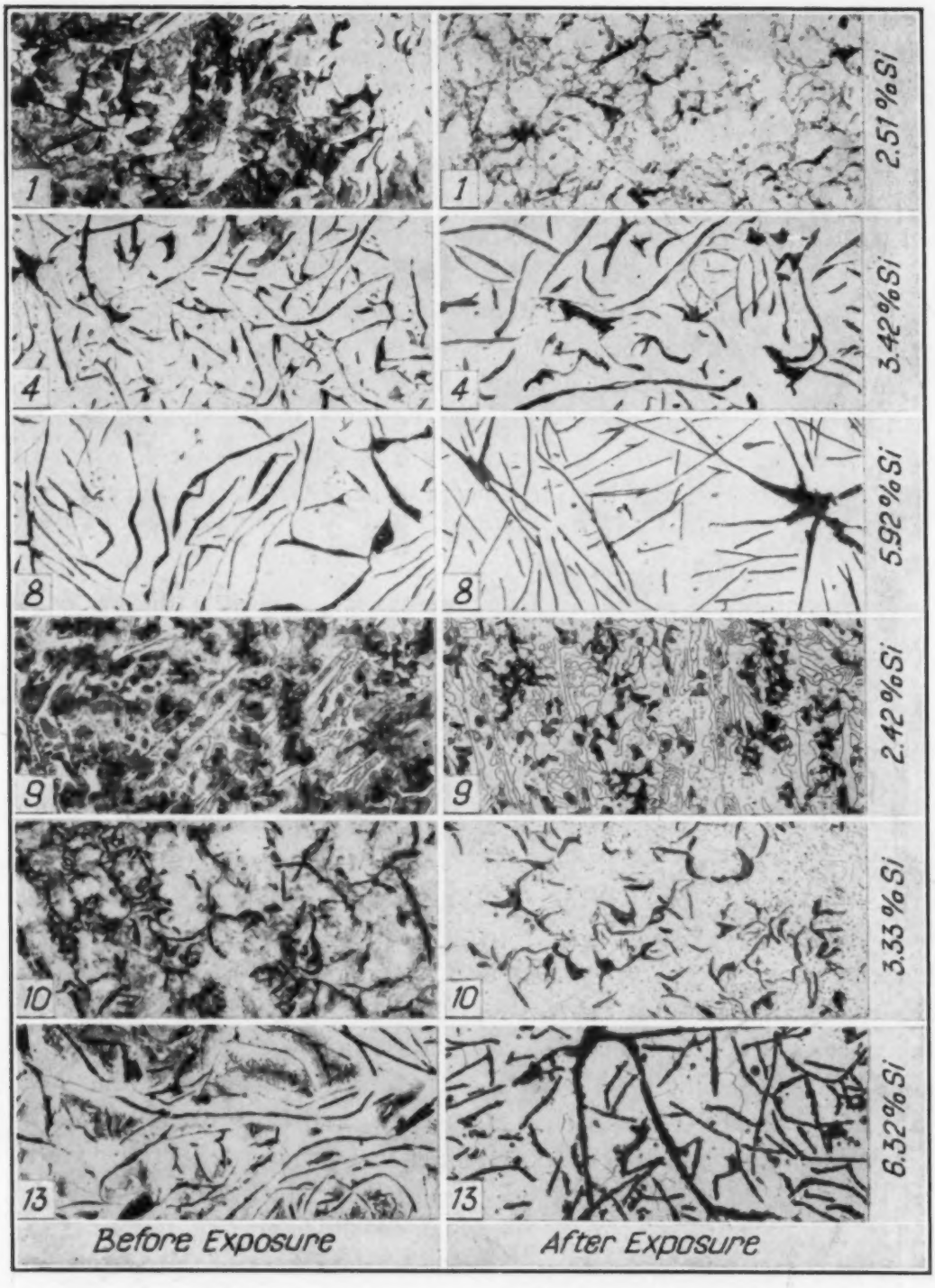

Fig. 7—Comparison of Structures of Growth Bar Cores Before and After Exposure to 800 Degrees Cent. × 100. Specimens 1, 4 and 8 are Plain Irons. Specimens 9, 10 and 13 are 2 Per Cent Chromium Irons.

left hand row of photomicrographs in Fig. 7 that increasing silicon decreases the quantity of pearlite or combined carbon, and increases the graphite size of both the plain and 2 per cent chromium irons as cast. Pearlite, for example, is almost completely eliminated in the plain irons at a 3.42 per cent silicon level. In the case of the chromium-bearing irons the pearlite is not completely eliminated even at a 6.32 per cent silicon level, but the amount of massive cementite is reduced to a negligible amount at a 3.33 per cent silicon level and practically eliminated at the 6.32 per cent silicon level. It is significant that graphite flakes, although generally increasing in size and quantity as silicon reaches values (3.33 and 3.42 per cent silicon) within the optimum range in both series of irons, show a further very marked increase in size and length when this range is exceeded and the silicon reaches high levels (5.92 per cent silicon and 6.32 per cent silicon). This is true despite the fact that the combined carbon in the plain irons has already reached a minimum value at a lower silicon content, and indicates that these very coarse graphite flakes may have originally precipitated prior to complete solidification of the irons. Such a mechanism would be indicated, as the carbon equivalents [per cent T.C. + 0.3 (per cent Si + per cent P)] of these latter high silicon irons considerably exceed the eutectic value of 4.3 per cent.

In the right hand row of photomicrographs, Fig. 7, the structures of the irons after exposure are illustrated. These photomicrographs were taken close to the center of the bars, and it can be noted that a gray constituent identified as metal-oxide has penetrated into the core of the plain iron specimen containing 2.51 per cent silicon. This constituent is not evident in either the 3.42 per cent silicon or 5.92 per cent silicon specimen. However, in the case of the 5.92 per cent silicon specimen we know from the oxygen analysis that considerable internal oxidation has taken place and the apparent graphite flakes in the groundmass actually consist of oxide products or voids, as the core analyzes only 0.05 per cent carbon. The 2 per cent chromium cast irons after exposure show some graphitization at the 2.42 per cent silicon level, and irons with 2.42 and 3.33 per cent silicon show spheroidization of pearlite with little or no change in any primary cementite that may be present. At the 6.32 per cent silicon level, however, pearlite is completely eliminated even in the presence of 2 per cent chromium, and the site of the original graphite flakes shows a widening and roughening that clearly indicate that internal oxidation has taken place. This is confirmed by the fact

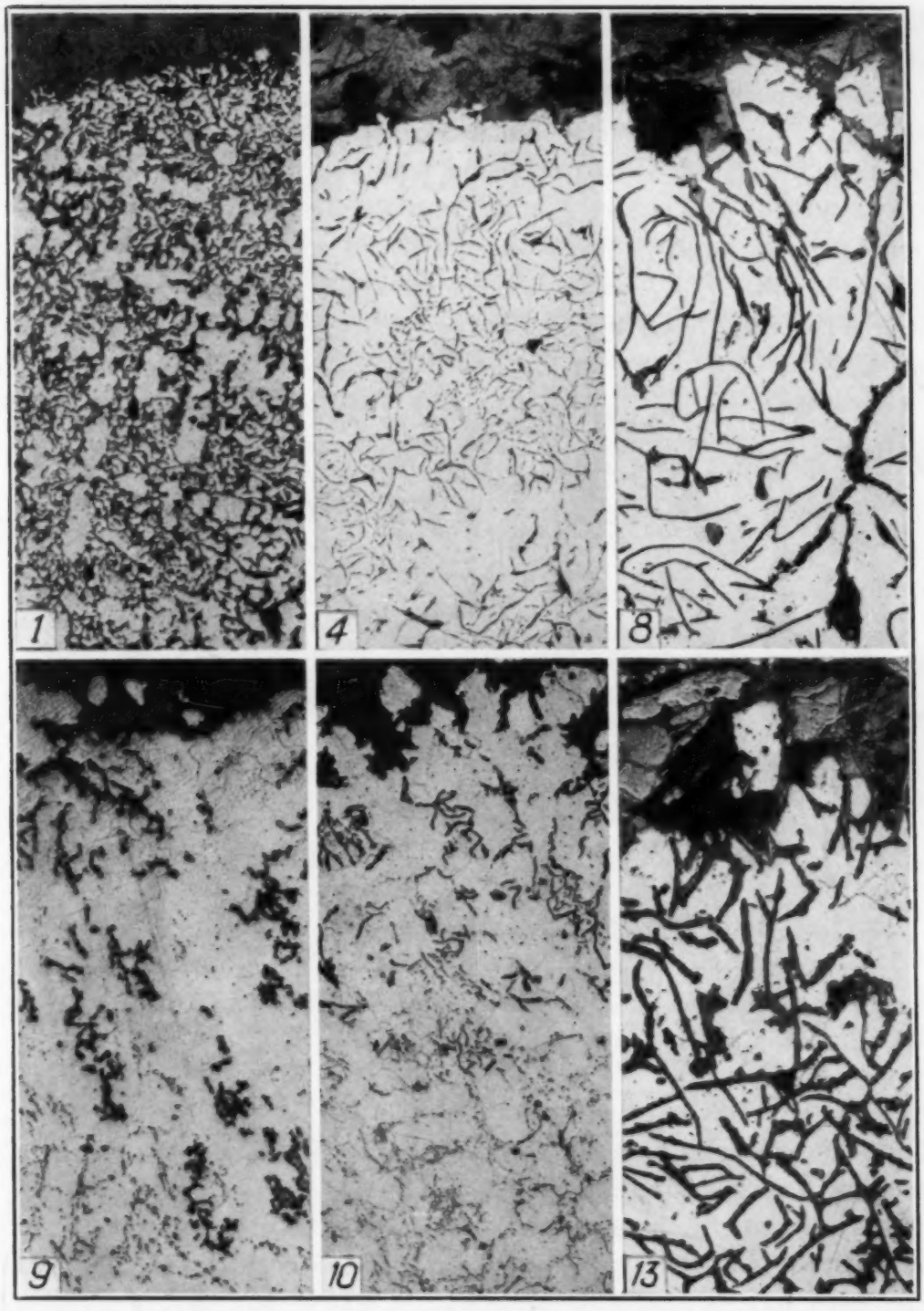

Fig. 8—Structure at Outer Rim of Growth Bars of Critical Silicon Content After Exposure at 800 Degrees Cent. × 100. Specimens 1, 4 and 8 are Plain Irons. (1) 2.51 Per Cent Silicon. (4) 3.42 Per Cent Silicon. (8) 5.92 Per Cent Silicon. Specimens 9, 10 and 13 are 2 Per Cent Chromium Irons. (9) 2.42 Per Cent Silicon. (10) 3.33 Per Cent Silicon. (13) 6.32 Per Cent Silicon.

that the total carbon content of the core of this specimen has dropped to 0.07 per cent.

The structures of these same specimens at the extreme surface adjacent to the scale give a clearer picture of the internal oxidation. Edge structures are shown at 100 diameters in Fig. 8 for plain and chromium irons of critical silicon content. It is evident in the case of the plain irons, that at a 2.51 per cent silicon level internal oxidation has proceeded to a point at which the original metal-oxide constituent has been replaced by oxide; at the 3.42 per cent silicon level penetration is confined to formation of a metal-oxide constituent

Fig. 9—Replacement of Graphite Flakes with Oxide at High Silicon Levels. × 500. Left—Specimen 8, Plain Iron, 5.92 Per Cent Silicon. Right—Specimen 13, 2 Per Cent Chromium Iron, 6.32 Per Cent Silicon.

layer too narrow to be readily detected; and at the 5.92 per cent silicon level the groundmass is relatively unattacked, but the graphite flakes have been replaced by oxide products. In some areas of this latter specimen, these oxide flakes have united so as to convert a whole area to oxide. In the case of the 2 per cent chromium irons the metal-oxide constituent is thinly scattered and confined to a narrow surface layer at a 2.42 per cent silicon level; at 3.33 per cent silicon, the depth of penetration is so narrow as to not be readily detected at this magnification, and at the 6.32 per cent silicon level the original graphite flakes are again replaced by oxide products and a thickening is evident. No intermediate metal-oxide formation

before conversion to oxide is evident in this high silicon iron. That the flakes in the 5.92 per cent silicon plain iron and the 6.32 per cent silicon-2 per cent chromium iron actually consist of oxide products is illustrated by the photomicrographs in Fig. 9, taken at 500 diameters.

Results of Tensile Tests

To determine the effect on the tensile strength of the prolonged exposure at 800 degrees Cent. (1470 degrees Fahr.) of the plain and 2 per cent chromium irons, standard A.S.T.M. tensile specimens were turned from the growth bars and their strength compared with

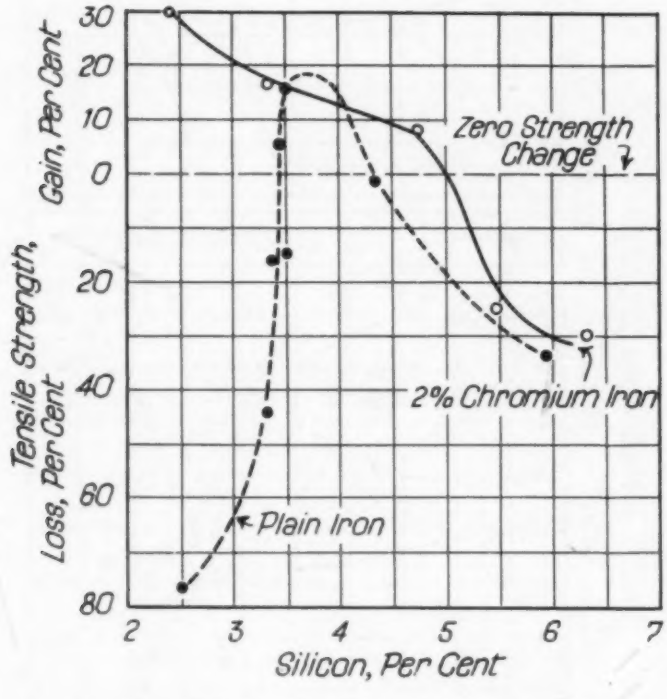

Fig. 10—Per Cent Change in Tensile Strength Versus Silicon Content After 500 Hours at 800 Degrees Cent.

the original strength exhibited by these irons in the as-cast condition. The per cent loss or gain in strength of the irons is plotted against their silicon content in Fig. 10, and the actual tensile values are shown in Fig. 11. The plain cast irons show a decided drop in strength at silicon levels below the optimum 3.3 to 4.3 per cent silicon range. Within this silicon range the strength remains approximately constant, and when it is exceeded, as at the 5.92 per cent silicon level, the strength again shows a decrease. The 2 per cent chromium irons actually show an increase in strength at all silicon levels up to 4.72

per cent. This phenomenon, noted in earlier work (3), (4) is presumably due to a softening following some graphitization and spheroidization of carbides. As the silicon increases to 5.46 per cent or above, the strength after exposure falls below the as-cast value.

Hardness values were determined on all specimens before and after exposure. The change in hardness of the irons is illustrated in Fig. 12. In the plain irons a decided drop in hardness is evident until a 3.5 per cent silicon level is reached. Between 3.5 and 4.3

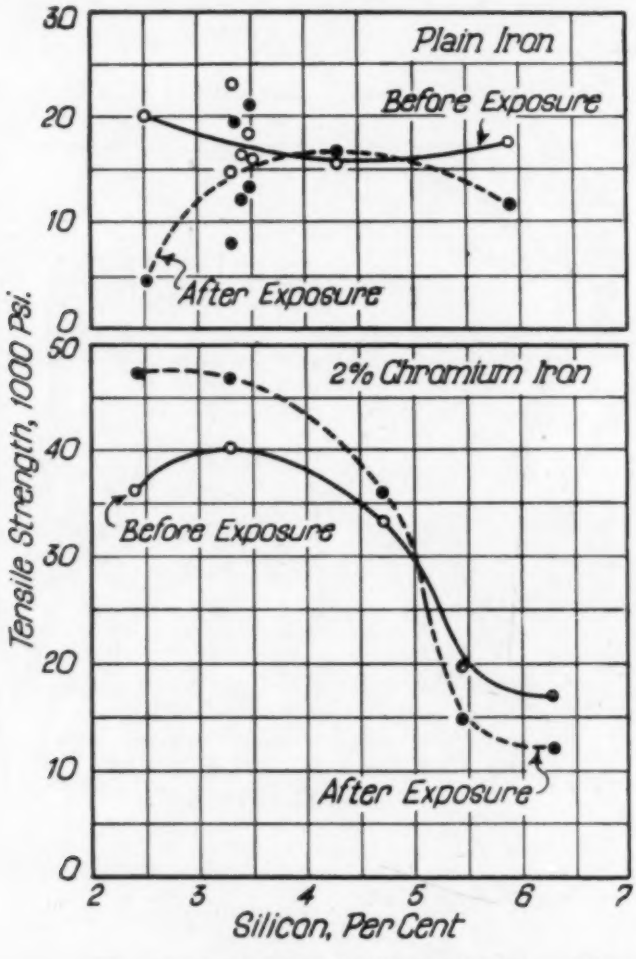

Fig. 11—Actual Tensile Strength Versus Silicon Content Before and After Exposure for 500 Hours at 800 Degrees Cent.

per cent silicon the hardness before and after treatment remains approximately constant. At the 5.92 per cent silicon level the hardness after exposure is actually higher than the as-cast value due presumably to strain set up by internal oxidation of the graphite flakes. A somewhat similar condition exists in the case of the 2 per cent chromium irons except that the hardness after exposure is below the

as-cast value until the silicon reaches 6.32 per cent, where an inversion again takes place.

General Observations

The existence of a preferred or optimum critical range (approximately 3.0 to 4.5 per cent silicon) has been established by the results recorded in this paper. Further increase in silicon above this range up to a level of approximately 7.0 per cent has been found to cause

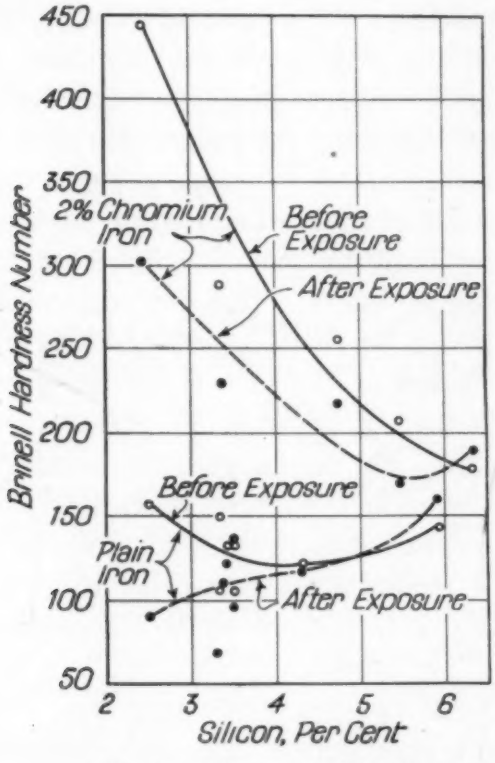

Fig. 12—Change in Brinell Hardness After Exposure at 800 Degrees Cent. for 500 Hours.

increased growth and internal oxidation. To this extent the results vary from those reported by previous investigators, notably Norbury and Morgan (2), who conducted a systematic investigation on the effect of silicon on the growth and scaling of cast irons and found a progressive improvement up to at least 6 per cent silicon. It is felt, however, that this discrepancy is more apparent than real, and rests upon a difference in the type of irons and exposure periods selected by these earlier investigators. These apparent discrepancies are worth further consideration, however, as they undoubtedly throw some light on the oxidation and growth phenomena.

First, as concerns oxidation, it has been found, in accordance with Norbury and Morgan's conclusions, that external oxidation or scaling decreases progressively as the silicon content is raised. Likewise, metal-oxide constituents that constitute an invariable preliminary step in the internal oxidation of lower silicon irons are limited to a very narrow surface zone and finally do not appear at all in the groundmass of the irons as their silicon content reaches the optimum range or exceeds it.

Despite this apparent resistance of the metal groundmass to oxidation, the present tests show that at least in irons possessing relatively coarse graphite flakes, decided internal oxidation takes place when the optimum silicon range is exceeded. This internal oxidation is evidenced by the eventual elimination of virtually all carbon or graphite from irons containing over approximately 5.0 per cent silicon. Metallographic examination at high magnification also confirms the fact that the graphite flakes in these irons have been replaced by oxide products. This internal oxidation cannot be readily recognized except by chemical analysis, as it is largely confined to the graphite flakes or the site of former graphite flakes and the groundmass immediately adjacent to them. Detection of this internal oxidation, using only metallographic examination and maximum exposure times of under 75 hours, is rendered particularly difficult since weight determinations indicate that during the first 45 to 75 hours of exposure, graphite alone is being oxidized in these high silicon irons, without the formation of any appreciable quantity of metal oxides.

As concerns dimensional changes, progressive measurements indicate that growth is a function of internal oxidation and therefore no appreciable growth occurs in the higher silicon irons until after they have been exposed to 800 degrees Cent. for periods of 45 to 75 hours. It appears that growth sets in only after the graphite has been largely removed and metal-oxide formation is initiated.

The fact that the internal oxidation is largely confined to the graphite flakes in very high silicon irons further means that the severity of such internal oxidation is doubtless a direct function of the length of the graphite flakes and their spacing in the groundmass. It can be readily appreciated that in low-carbon irons or irons containing fine, supercooled graphite such as were tested by Norbury and Morgan, internal oxidation would be inhibited or materially slowed up. Consequently, resistance to external oxidation becomes the controlling factor, and the selection by these authors of a silicon

range in excess of 4 per cent and up to 10 per cent is justified. In fact, these latter authors recognize this importance of graphite flake size and limit their conclusions to irons "not having too large graphite flakes".

Despite the existence of the optimum silicon range outlined in this paper, the suitability of higher silicon irons of the Silal type (for example, in a 5 to 10 per cent silicon range) for high temperature applications is not questioned. Previous observations by Norbury and Morgan that increasing silicon progressively reduces scaling loss was confirmed by the present tests, and the recommended use of low total carbon content and a fine graphite distribution undoubtedly retards or greatly inhibits the internal oxidation that takes place in the higher carbon, coarser flake graphite irons exceeding the optimum silicon range.

Conclusions

In drawing conclusions from the foregoing experimental work, several limiting factors should be borne in mind. First, the conclusions are based on irons close to the carbon saturation point, i.e., they approximate eutectic or hypereutectic compositions. Second, the tests were made at one temperature, namely, 800 degrees Cent., and although this temperature was selected as the most suitable for an accelerated test, it would be presumptuous to assume that the relationship of the irons would remain unaltered using lower or higher test temperatures. Bearing these limitations in mind, the following conclusions can be drawn from the experimental work.

1. It has been found that an optimum silicon range exists in which both plain and 2 per cent chromium irons exhibit maximum resistance to growth, maximum resistance to internal oxidation, and maximum resistance to general deterioration of their physical properties.

2. In the case of the irons tested, this optimum silicon range lies roughly between 3.5 and 4.5 per cent silicon in the case of plain cast irons, and between 3.0 and 4.0 per cent silicon in the case of 2 per cent chromium irons.

3. It has been found that if the silicon content exceeds this range to any considerable extent, both the plain and 2 per cent chromium irons become subject to serious internal oxidation. This oxidation proceeds along the graphite flakes and is sufficient to reduce the carbon contents of these irons to a negligible value.

4. The plain irons in the optimum silicon range develop low tensile strengths in the as-cast condition of the order of 15,000 to 20,000 pounds per square inch. Thus, such high silicon, plain irons would be normally employed only in sections in which oxidation resistance alone is the primary consideration.

5. The 2 per cent chromium irons maintain a high strength in excess of 35,000 pounds per square inch throughout the optimum silicon range. The use of high silicon contents in the optimum range of 3.0 to 4.0 per cent accomplishes the double purpose of bringing these high chromium irons within a machinable range, and of moderately improving their normally high resistance to deterioration at elevated temperatures. These irons possess a desirable combination of properties that make them eminently suitable for use in high temperature operations.

ACKNOWLEDGMENT

The generous aid furnished by the staff of the Union Carbide and Carbon Research Laboratories, Inc., in carrying out the present investigation is gratefully acknowledged.

Bibliography

1. H. F. Rugan and H. C. H. Carpenter, "The 'Growth' of Cast Irons After Repeated Heatings," *Journal,* Iron and Steel Institute, Vol. 80, No. 2, 1909, p. 29-125.
2. A. L. Norbury and E. Morgan, "The Effect of Carbon and Silicon on the Growth and Scaling of Gray Cast Iron," *Journal,* Iron and Steel Institute, Vol. 123, No. 1, 1931, p. 413-434.
3. C. O. Burgess, "Influence of Chromium on the Oxidation Resistance of Cast Iron," TRANSACTIONS, American Society for Metals, Vol. 39, 1939, p. 604-622.
4. C. O. Burgess and A. E. Shrubsall, "Machinable 1.5 and 2.0 Per Cent Chromium Cast Irons to Resist Deterioration at High Temperatures," *Transactions,* American Foundrymen's Association, Vol. 50, 1942, p. 405-442.
5. H. S. Rawdon, "Atmospheric Corrosion Testing"—Symposium on Corrosion Testing Procedures, 1937, American Society for Testing Materials, p. 37.

DISCUSSION

Written Discussion: By C. H. Lorig, metallurgist, Battelle Memorial Institute, Columbus, Ohio.

The paper by Burgess and Bishop on the growth and heat resistance of plain and 2 per cent chromium cast iron under cyclic heating at 800 degrees Cent. (1470 degrees Fahr.) is particularly valuable in view of the growing interest in the

use of cast iron for services at elevated temperatures. They have established with reasonable certainty the existence, in both types of iron, of a range between 3.0 per cent and 4.5 per cent silicon at which maximum resistance to growth at 800 degrees Cent. (1470 degrees Fahr.) is developed. Hence, when no property other than heat resistance is essential, one might readily take advantage of the higher silicon irons to obtain castings of markedly improved growth and oxidation resistance just so long as the temperature conditions in service do not greatly exceed those of the test. But as the authors pointed out, one should not interpret the results too broadly by assuming that the effect of silicon in the range mentioned will also hold for conditions of heating much above as well as much below the temperature of 800 degrees Cent. (1470 degrees Fahr.) employed in the study. Furthermore, atmospheres which differ from the atmosphere existing in the laboratory furnace may likewise affect the results materially. Yet, as a guide to a selection of cast iron for exposure in air at 800 degrees Cent. (1470 degrees Fahr.) or thereabouts, the results of the work are extremely helpful.

One factor not mentioned in the paper but likely to have had an important effect on the character of the growth curve for the plain iron is the fact that the temperature chosen for cyclic heating was just above the alpha-gamma transformation temperature for the 2.5 per cent silicon iron but below the transformation temperature for the remaining higher silicon irons of the series. Hence, the growth of the 2.5 per cent silicon iron was thus influenced by the transformation occurring during each cycle as well as by internal oxidation. Those who have conducted growth tests realize how profoundly the alpha-gamma transformation may speed up the growth of cast iron through solution and reprecipitation of graphite and through volumetric changes that prevail. Growth in the 2.5 per cent silicon iron must, therefore, have been greatly accentuated over that of the remaining irons.

Previous work by others has indicated a second range of silicon content within which the growth of cast iron at elevated temperatures is impeded. This range lies below the silicon contents of the irons employed in the present study. Thus, irons with silicon contents below 2 per cent have often shown less growth than irons of substantially similar composition but containing from 2 to 3 per cent silicon. Part of the improvement with low silicon contents probably stems from the increased stability of the pearlitic matrix and the general tendency for the graphite to be somewhat more refined in the lower silicon irons. At any event, growth of cast irons at temperatures above the transformation may be retarded appreciably with lower silicon contents. The following will illustrate this effect of silicon.

Growth tests were conducted on two plain cast irons, one of which contained 3.30 per cent carbon, 1.90 per cent silicon, 0.65 per cent manganese, 0.15 per cent phosphorus, and 0.05 per cent sulphur; the other contained 3.30 per cent carbon, 3.15 per cent silicon, 0.65 per cent manganese, 0.15 per cent phosphorus, and 0.05 per cent sulphur. The irons received a late treatment with ferrosilicon. Specimens 10 inches long, taken from sections of 1.2-inch transverse bars, were equipped with stainless steel plugs at the ends, in the same manner as the specimens used by Burgess and Bishop, so that length increases could be measured with a micrometer without an error from oxide accumulation. The specimens

were heated in an electric furnace for four hours at 870 degrees Cent. (1600 degrees Fahr.), a temperature well above the critical temperature for both irons, then furnace-cooled to room temperature, and measured for increase in length. This heating cycle was repeated 8 times. After the first two cycles, growth progressed uniformly at a substantial rate. The total growth over the 8-cycle period for the higher silicon iron was 0.038 inch per inch while that for the lower silicon iron was 0.025 inch per inch, or approximately two-thirds that for the higher silicon iron. Thus there appear to be situations when the lower silicon irons may be markedly superior to somewhat higher silicon irons in growth resistance, and the curve for plain iron shown by Burgess and Bishop in Fig. 1, if extended to lower silicon percentages, might have shown this to be the case.

Written Discussion: By A. J. Edgar, technical advisor, Gray Iron Founders' Society, Inc., Washington, D. C.

The work is excellent and the authors are to be congratulated on a definite contribution to the vast field that will have to be covered on gray iron metallurgy. However, would not the paper have been more convincing if the irons had been chosen over a wider range of silicons, say, starting at 1.50 per cent and advancing at 0.50 per cent increments up to 10 per cent silicon content. These silicon contents should also be tied up with the carbon content so that the carbon equivalent would be a factor in conclusions.

The temperature of 800 degrees Cent. (1470 degrees Fahr.) is about the ultimate that can be withstood normally by even high alloy cast irons. Could it be possible that the irons used would react differently and respond differently at temperatures of, say, 425, 540 or 650 degrees Cent. (800, 1000 or 1200 degrees Fahr.)?

In determining the oxidation loss there should have been some consideration of the condition of the bars after removing the scale. A certain bar might have shown a low scale loss per square inch and be pitted which would indicate that the loss would have been considerably greater had the test continued; whereas another bar could have a higher weight loss per square inch but the parent surface of the bar could still be smooth and sound, indicating that the deterioration had been uniform and much more predictable for practical purposes.

Authors' Reply

As usual, Dr. Lorig's comments are very much to the point and are a valuable contribution to the paper. Considering unalloyed cast irons in the normal silicon range, it has been generally recognized that to maintain high strength and stability on exposure to moderately high temperatures, it is desirable to hold the silicon level of such irons to a relatively low value. For example, an iron at a given carbon level with a silicon content of 1.5 per cent will normally maintain greater strength and constancy of dimensions than an iron containing 2.5 per cent silicon. The examples quoted by Dr. Lorig serve to confirm this general observation. The minimum silicon that may be employed is, of course, governed by the necessity to retain a gray iron of ready machinability. When maximum oxidation resistance and growth resistance are the primary considerations, however, rather than maximum strength, it has been found as described in this paper, that an optimum silicon range of about 3.5 to 4.5 per cent exists for unalloyed

irons, i.e., a silicon range somewhat above the maximum considered by Dr. Lorig.

The above observations apply to unalloyed cast irons but not necessarily to irons containing substantial amounts of a carbide stabilizer such as chromium. As shown in the paper, high chromium irons will retain high strength at the high silicon levels necessary for maximum oxidation resistance.

Dr. Lorig also suggested that the growth results may be influenced by the fact that the test temperature of 800 degrees Cent. (1470 degrees Fahr.) is such that the lowest silicon irons may pass through the Ac or alpha-gamma transformation on heating, while the higher silicon irons do not. It would appear from both our own previous work[1] and that of other investigators[2] in which various exposure temperatures were employed, that passing through the alpha-gamma transformation does not produce any unusual increase in growth or oxidation. In fact from the information available, the slope of the curve of growth versus exposure temperature generally shows some decrease when the Ac point is reached or exceeded.

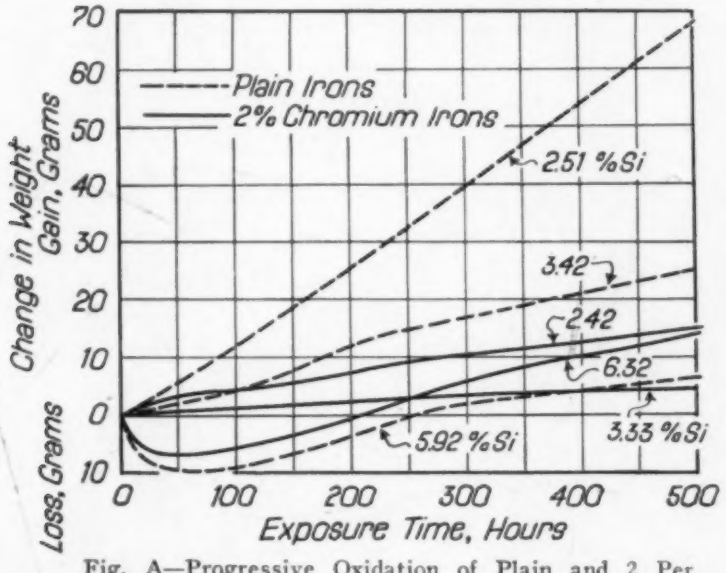

Fig. A—Progressive Oxidation of Plain and 2 Per Cent Chromium Irons.

Mr. Edgar inquires as to the condition of the cast iron bars after testing. The higher silicon bars showed no signs of pitting but on the contrary developed a very uniform adherent scale requiring the use of electrolytic pickling for its removal. Mr. Edgar also brings up the point that the reaction of the irons at lower temperatures might be different from that at the 800 degrees Cent. (1470 degrees Fahr.) test temperature. As noted in the paper, this possibility does exist but in the absence of specific information it is felt that a radically different behavior at these lower temperatures would not be anticipated.

[1]C. O. Burgess, "Influence of Chromium on the Oxidation Resistance of Cast Iron," TRANSACTIONS, American Society for Metals, Vol. 39, 1939, p. 604-622.

C. O. Burgess and A. E. Shrubsall, "Machinable 1.5 and 2.0 Per Cent Chromium Cast Irons to Resist Deterioration at High Temperatures," *Transactions*, American Foundrymen's Association, Vol. 50, 1942, p. 405-442.

[2]A. L. Norbury and E. Morgan, "The Effect of Carbon and Silicon on the Growth and Scaling of Gray Cast Iron," *Journal*, Iron and Steel Institute, Vol. 123, No. 1, 1931 p. 413-434.

In regard to the test temperature selected, namely, 800 degrees Cent. (1470 degrees Fahr.), this temperature happened to coincide with the temperature used in previous publications of one of the authors.[1] The temperature of 800 degrees Cent. (1470 degrees Fahr.) was also chosen to take advantage of the relatively high rate of oxidation and growth of ordinary cast irons at this temperature. It is thought that had a lower exposure temperature been used, these reactions would have taken place more slowly, in which case the significant behavior illustrated in Fig. A might have been missed. In this figure the progressive oxidation loss or gain in weight of the irons used in the investigation is plotted against exposure time. The high silicon irons, both plain and 2 per cent silicon, that is, the irons with over the optimum amounts of silicon, lose weight during the first 45 to 75 hours' exposure because of oxidation and elimination of a large percentage of their carbon content. Following carbon elimination, internal oxidation of the matrix takes place with a corresponding increase in weight. Growth coincides with this development of internal oxidation. Obviously, if the test temperature were decreased, it is doubtful whether this mechanism of progressive oxidation could have been detected within the 500-hour test period.

THE PARTITION OF MOLYBDENUM IN IRON-CARBON-MOLYBDENUM ALLOYS AT 1300 DEGREES FAHR. AND THE NATURE OF THE CARBIDES FORMED

By F. E. Bowman and R. M. Parke

Abstract

The partition of molybdenum in iron-carbon-molybdenum alloys of approximately eutectoid composition containing between 0.26 and 0.98 per cent molybdenum has been determined both for alloys prepared by transforming austentite directly and isothermally at 1300 degrees Fahr. (705 degrees Cent.) and for alloys quenched and tempered at 1300 degrees Fahr. (705 degrees Cent.). The data from the alloys prepared by these two methods support the opinion that partition is related to hardenability. The application of the findings to the use of steel is discussed briefly.

The identification of a face-centered cubic carbide [lattice parameter 10.5250Å, probable formula $(Fe, Mo)_{23}C_6$] in these alloys suggests that a re-examination of present iron-carbon-molybdenum diagrams is required.

Introduction

ALTHOUGH a large portion of the total steel consumed is employed in the annealed or normalized condition, the ultimate in properties is most conveniently attained by tempering a fully hardened material. In order to render such treatment applicable to relatively large sections it becomes necessary to increase the time required for the start of austenite transformation in the region of most rapid reaction, that is, in the vicinity of 1000 degrees Fahr. (540 degrees Cent.). This delay can best be obtained by additions of alloying elements and is graphically represented by the shift toward greater time of the Bain (1)[1] S-curves.

Rate of nucleation of the products of austenite decomposition, their rate of growth, the grain size of the parent austenite, and its homogeneity are among the factors known to influence the rate of

[1]The figures appearing in parentheses refer to the bibliography appended to this paper.

The authors are associated with the research laboratory, Climax Molybdenum Company of Michigan, Detroit. Manuscript received August 26, 1943.

austentite transformation. These have been well accounted for in the theory of hardenability. Composition, a most important factor, has thus far received only an empirical treatment. Sufficient data have been accumulated through years of physical testing to permit the prediction of properties from chemical composition with a reasonable degree of accuracy. Explanations for the role of single elements or combinations of elements in the hardening process are, however, still a matter of conjecture.

Hardenability is essentially a function of the rate of austenite transformation during the initial stages of the reaction. Therefore, a better understanding of hardenability will most likely be found in a study of the fundamental factors that influence the austenite decomposition reaction. For example, the precipitation of carbide from the solid solution austenite involves diffusion of carbon, from which it follows that an explanation of the rate of the austenite transformation reaction must take into account the rate of diffusion of carbon and any possible effect of third elements on this rate. Studies have been made of the effects of various elements upon the rate of diffusion of carbon in austenite. In the case of molybdenum, it has been found that 0.80 weight per cent molybdenum decreases the rate of diffusion of carbon at 1050 degrees Fahr. (565 degrees Cent.) by about five times (2). However, 0.80 per cent molybdenum increases by some 28,000 times the time necessary to transform a eutectoid austenite completely at 1050 degrees Fahr. (565 degrees Cent.) (3). From these facts it appears that additional explanations of the increased hardenability produced by molybdenum are needed. Wells and Mehl (4) have arrived at a similar conclusion as the result of corresponding studies with nickel and manganese.

It remains to consider diffusion of the alloying element itself as one of the important causes of the delay of transformation of alloyed austenite. This implies a segregation, during transformation, of the third element in either of the precipitated phases, ferrite or carbide. To prove a relation between the property of hardenability and partition of the third element between ferrite and carbide, it is required to show at least that (A) segregation occurs prior or during transformation and not after transformation, and that (B) segregation does not decrease to insignificance as the transformation temperature approaches 1000 degrees Fahr. (540 degrees Cent.). With these ideas in mind, an investigation of the partition of molybdenum between the ferrite and carbide phases in steel has been undertaken.

Additional discussion of the partition problem and the method of attack have been presented in an earlier paper (5).

Further Discussion of the Problem

Sufficient work has been done in fields closely related to partition to indicate that, in some instances, chemical separation of the carbides yields unreliable data. This has been found true in the authors' laboratory, particularly when the austenite has transformed below 1200 degrees Fahr. (650 degrees Cent.). For this reason, X-ray diffraction methods, seemingly applicable under all conditions, were adapted to the problem. The relationship existing between the molybdenum content and the alpha iron solid solution lattice parameter was determined from pure binary alloys (5). From this relationship the ferrite unit cell dimensions can be used to determine its composition. The carbide composition would thus be determined by difference, providing the molybdenum content is kept low enough to insure the formation of cementite only. Such a procedure is necessarily based on the currently accepted iron-carbon-molybdenum constitution diagrams (6), (7) which indicate that the orthorhombic Fe_3C is certainly the only carbide formed in alloys containing less then 1 per cent molybdenum.

Recently reported data, however, have given reason for questioning the accuracy of the current diagram. Morral, Westgren, and Phragmen (8) have found a face-centered cubic carbide in iron-rich iron-carbon-molybdenum alloys. While working with low carbon molybdenum steels, Crafts and Offenhauer (9) isolated a hexagonal carbide, the formation of which is apparently dependent upon the temperature at which quenched alloys are tempered. From these developments it is evident that a study of the nature of the carbides must be a part of the partition problem.

Certain restrictions were placed on the initial stages of the investigation so that data on both partition and carbide structure could be obtained most effectively. For example, the complications arising from proeutectoid constituents were minimized by limiting the alloys studied to approximately eutectoid carbon compositions, and the carbides were formed or homogenized at 1300 degrees Fahr. (705 degrees Cent.) to insure conditions most favorable for their isolation. Partition data on commercial steels are of recognized value and later studies will include such materials. Pure ternary alloys, however,

were used in the present work to establish a fundamental basis for subsequent investigations.

Experimental Procedure and Results

The alloys were prepared from electrolytic iron, pure molybdenum powder, and lampblack. One-thousand-gram heats were melted in magnesia crucibles in a vacuum induction furnace. All heats were held molten until visible evolution of gas had ceased and the pressure had returned to 500 microns (0.5 mm. Hg). Solidification took place in the crucible. The ingots were forged into strips approximately 3/4 by 1/8 inch. After removal of scale, sections of these strips were homogenized in vacuum at 2000 degrees Fahr. (1095 degrees Cent.) for 100 hours. This treatment eliminated all the usual evidence of segregation. The low pressure (less than 10 microns), under which the homogenization was carried out, effectively prevented decarburization, as shown by microscopic examination.

Only a state of metastable equilibrium between ferrite and iron carbide can be attained at 1300 degrees Fahr. (1095 degrees Cent.), for thermodynamic data indicate that between 1165 and 2190 degrees Fahr. (630 and 1200 degrees Cent.) cementite is unstable with respect to iron and graphite (10). The effect of a third element in the system upon the stability of the carbide has not been determined. But, since the approach to true equilibrium is extremely slow, this metastable state is generally accepted as representative of the ferrite-carbide equilibrium. In order to approach this metastable condition from two directions, it was decided to investigate the partition in iron-carbon-molybdenum alloys which resulted from (A) tempering martensite, and (B) the direct isothermal transformation of austenite. Such procedure provides a basis for comparing the rate of diffusion of molybdenum in ferrite and in austenite as well as a means of determining the difference, if any, in the ultimate partition resulting from the two modes of carbide formation.

Homogenized samples were given a solution treatment at 2000 degrees Fahr. (1095 degrees Cent.) for one-half hour followed by a water quench. Scale was removed by grinding. Metallographic examination of all materials failed to reveal the presence of undissolved carbides. The tempering treatments were carried out at 1300 degrees Fahr. (705 degrees Cent.) in a high vacuum. This temperature was selected to provide the most rapid diffusion rate attainable

at subcritical temperatures. It is also possible to separate by electrolysis the carbides formed at 1300 degrees Fahr. (705 degrees Cent.) and thereby to verify the X-ray data by an entirely independent method. Furthermore, for the alloys prepared by isothermally transforming austenite, the results of which are to be compared with those of the tempering treatment, the transformation time at this temperature (1300 degrees Fahr.) is not impractically long. The tempering times, 150 and 250 hours, were selected arbitrarily. Furnace cooling of all samples after tempering and after direct transformation insured complete precipitation of carbon from ferrite.[2] Carbides separated electrolytically in 5 per cent hydrochloric acid after each treatment provided samples for the determination of crystal structure. The materials tempered for 250 hours yielded sufficient amounts of carbide for complete chemical analysis. Thus a material balance on these alloys was obtained, the ferrite composition being determined by analysis of the electrolyte.

X-ray powder patterns of the carbides were taken in a 14-centimeter diameter camera. The precision determinations of the ferrite lattice parameters were made from patterns obtained in a 22.6-centimeter diameter back-reflection focusing camera. Cobalt radiation was employed in all cases. Cohen's method (12) of calculation as used in the case of the binary alloys (5) was used on the ferrite lattice determinations. The results are tabulated in Tables I and II.

The face-centered carbide noted in samples 11 and 30 has a lattice parameter of approximately 10.52 Å. From the analysis of the

Table I
Alloys Quenched and Tempered at 1300 Degrees Fahr. for 150 Hours

Alloy No.	25	28	11	30
Composition				
Carbon, Per Cent	0.82	0.78	0.74	0.83
Molybdenum, Per Cent	0.26	0.54	0.74	0.98
X-ray Determination				
Molybdenum in Ferrite, Per Cent	0.19	0.45	0.54	0.66
Molybdenum in Carbide, Per Cent	0.73	1.29	2.23*	2.81*
Carbide Structure	Orthorhombic	Orthorhombic	Orthorhombic + Face-cent. Cubic	Face-cent. Cubic + Orthorhombic

*The values given for the mixtures of the two carbides are the results of calculations based upon the relative proportions of the two materials present, as judged from the intensity of their diffraction patterns.

[2]Burns (11) has reported that the carbon soluble in ferrite at 1200 degrees Fahr. (650 degrees Cent.) produces appreciable expansion in the lattice which is retained by rapid cooling.

Table II
Alloys Quenched and Tempered at 1300 Degrees Fahr. for 250 Hours*

Alloy No.	25	28	11	30
Composition				
Carbon, Per Cent	0.82	0.78	0.74	0.83
Molybdenum, Per Cent	0.26	0.54	0.74	0.98
X-ray Determination				
Molybdenum in Ferrite, Per Cent	0.17	0.38	0.44	0.51
Molybdenum in Carbide, Per Cent	0.89	1.72	2.96†	3.70†
Chemical Analysis				
Molybdenum in Ferrite, Per Cent	0.17	0.36	0.43	0.50
Molybdenum in Carbide, Per Cent	0.90	1.74	3.01	3.74
Carbon in Carbide, Per Cent	6.64	6.59	6.23	5.34
Stoichiometric Composition of Carbide				
Theoretical Mol Per Cent C				
in $(Fe, Mo)_3C$	25.00	25.00	25.00	25.00
in $(Fe, Mo)_{23}C_6$	20.69	20.69	20.69	20.69
Experimental Mol Per Cent C	24.99	25.10	23.91	21.12
Carbide Structure	Orthorhombic	Orthorhombic	Orthorhombic + Face-cent. Cubic	Face-cent. Cubic + Orthorhombic

*A small loss of carbon is apparently inevitable in the electrolytic separation of the carbides, and the values given have been corrected to take this loss into account. In no case did these corrections alter the values of ferrite composition reported by the analytical laboratory by more than 10 per cent and, in most instances, considerably less. The agreement between the corrected values and those obtained from diffraction patterns is satisfactory.

†The values given for the mixtures of the two carbides are the results of calculations based upon the relative proportions of the two materials present, as judged from the intensity of their diffraction patterns.

material from sample 30, this carbide appears to correspond to that reported by Morral, Westgren and Phragmen (8), (13). They designate this carbide as $(Fe, Mo)_{23}C_6$ because of its structural analogy with $Cr_{23}C_6$ found in the chromium-carbon system (14).

From the results obtained it is evident that a definite migration of molybdenum from the ferrite to the carbide takes place during the spheroidization of martensite. Also, when sufficient molybdenum is present a new carbide is formed. Although equilibrium was evidently not reached within the times employed in the experiments described, the tendency toward equilibrium is apparent. The results indicate that, after long exposure to high, but subcritical, temperatures, the ferrite would be largely depleted in molybdenum if sufficient carbon were present. This is a significant fact in connection with the use of alloy steels for long times at elevated temperatures.

The partition of molybdenum between ferrite and carbide formed isothermally (at temperatures above 1000 degrees Fahr.) from austenite is more closely related to the problem of hardenability than the partition in tempered alloys. Here again interest in actual partition data is accompanied by the need for information regarding the carbides formed. In order to obtain the partition re-

sulting from the actual transformation reaction and to eliminate as far as possible any subsequent molybdenum diffusion, the times necessary for the completion of the reaction were obtained by the usual metallographic methods (1). The samples used in obtaining partition data remained at the reaction temperatures for this time only. Samples homogenized as previously described were austenitized at 1600 degrees Fahr. (870 degrees Cent.) for one-half hour in a completely deoxidized lead bath. Metallographic examination of water-quenched samples failed to disclose evidence of undissolved carbides. From the austenitizing bath the materials were quenched into lead at 1300 degrees Fahr. (705 degrees Cent.) and held for the time found necessary to complete the transformation.

Carbides from these completely transformed alloys were separated electrolytically and analyzed chemically in the manner described for the tempered materials. To obtain sufficient amounts of carbide for this purpose, it was not necessary to attack the entire sample. The portion of the alloy which remained unattacked was used to obtain the ferrite diffraction patterns. This insured that the ferrite lattice parameter was measured on material identical with that on which the carbide structure and composition, as well as the chemical determination of the ferrite molybdenum content, were made. The carbide diffraction patterns of the isothermally transformed alloys gave no evidence of a mixture of the orthorhombic and face-centered cubic structures noted in the tempered alloys. The results are listed in Table III.

Table III
Alloys Isothermally Transformed at 1300 Degrees Fahr.

Alloy No.	25	28	11	30
Composition				
Carbon, Per Cent	0.82	0.78	0.74	0.83
Molybdenum, Per Cent	0.26	0.54	0.74	0.98
Transformation Time, Seconds	850	1000	3000	4500
X-ray Determination				
Molybdenum in Ferrite, Per Cent	0.14	0.04	0.18	0.23
Molybdenum in Carbide, Per Cent	1.13	3.41	4.14	4.95
Chemical Analysis				
Molybdenum in Ferrite, Per Cent	0.13	0.04	0.19	0.23
Molybdenum in Carbide, Per Cent	1.21	3.42	4.02	4.96
Carbon in Carbide, Per Cent	6.63	5.23	5.20	5.19
Stoichiometric Composition of Carbide				
Theoretical Mol Per Cent C				
in $(Fe, Mo)_3C$	25.00	25.00	25.00	25.00
in $(Fe, Mo)_{23}C_6$	20.69	20.69	20.69	20.69
Experimental Mol Per Cent C	24.99	20.73	20.67	20.71
Carbide Structure	Orthorhombic	Face-cent. Cubic	Face-cent. Cubic	Face-cent. Cubic

The face-centered cubic carbide found in three of the isothermally transformed alloys provided material suitable for a thorough investigation. Back-reflection patterns were made and the lattice parameter was accurately determined. It was found to be 10.5250Å. No detectable variation in lattice parameter was found to have been produced by the three different molybdenum contents in the carbides as determined from chemical analysis. Morral (13) reports the results of a study of this type of carbide as it is found in the iron-tungsten-carbon system. He also reports the existence of a face-centered carbide in the iron-carbon-molybdenum system with a lattice parameter of 10.52_7 Å; beyond that no further work was done. The carbon contents of the carbides isolated in the present investigation indicate that the formula $(Fe, Mo)_{23}C_6$ can be accepted as representing its composition. Westgren (15) has shown that the corresponding iron-tungsten carbide contains 116 atoms per unit cell. As might be expected from the high iron content, this face-centered cubic carbide is strongly ferromagnetic.

A further investigation of the extent to which molybdenum follows the carbon during the actual transformation was made on alloys 50 per cent transformed. In all cases the carbides isolated from the alloys so treated displayed structures identical with those found to exist at the end of transformation. As indicated above, it is impossible to detect small changes in the composition of the carbide by lattice parameter measurements. Consequently, it cannot definitely be said that the molybdenum content remains unchanged during transformation . From the work on the partially transformed alloys it is apparent that molybdenum forms the cubic carbide in a very short time—not more than 600 seconds in the case of the 0.54 per cent molybdenum alloy. Comparing this with the results of the tempering treatments, which required as much as 250 hours, it seems highly improbable that the movement of molybdenum out of the ferrite during the time involved in the transformation would be detectable. Attempts to isolate sufficient amounts of carbides for chemical analysis from these partially (directly) transformed alloys were unsuccessful. The presence of martensite complicates the process in that the free carbon content of the residue is greatly increased. Apparently a portion of this carbon originates in the martensite, and consequently any adjustment of the analytical results is impossible. The application of diffraction methods is also unsatisfactory because of the lattice expansion produced by the excess carbon trapped in

solution in the ferrite by the quench from 1300 degrees Fahr. (705 degrees Cent.).

The stability of the face-centered cubic carbide is of utmost importance in considering the iron-carbon-molybdenum diagram. For this reason, a homogenized sample of the high-molybdenum alloy was treated, after transformation at 1300 degrees Fahr. (705 degrees Cent.), for an additional 150 hours at this temperature. The cubic structure found at the end of transformation was maintained, but a further concentration of molybdenum in the carbide occurred. The partition of molybdenum resulting from this treatment is noted in Table IV.

Table IV
Alloy Isothermally Transformed at 1300 Degrees Fahr. and Held 150 Additional Hours at That Temperature

Composition of the Alloy	0.92 Per Cent Molybdenum, 0.80 Per Cent Carbon
Molybdenum in Ferrite	0.092 Per Cent
Composition of Carbide	5.45 Per Cent Molybdenum, 5.18 Per Cent Carbon
Stoichiometric Composition of the Carbide	
Theoretical Mol Per Cent Carbon in $(Fe, Mo)_{23}C_6$	20.69
Experimental Mol Per Cent Carbon	20.79

Discussion of Results

It is apparent from the evidence at hand that molybdenum, when present in sufficient quantity, is capable of altering the structure as well as the composition of the iron-rich carbide. Further work will establish more definitely the concentration of this element necessary to effect the alteration. At present it can only be said that, under conditions most favorable for the migration of molybdenum atoms, 0.54 per cent molybdenum, or more, in austenite will yield this new phase in eutectoid steels. This value is appreciably lower than that of the alloys in which the existence of the cubic carbide was first noted, namely the 1 per cent carbon and 2 per cent molybdenum materials reported by Morral (13). It is also well within the range indicated by present equilibrium diagrams as containing only orthorhombic cementite. Without doubt a redetermination of the iron corner of the iron-carbon-molybdenum diagram is required, with greater emphasis placed on the purity and homogeneity of the alloys and a closer approach to equilibrium. It would be inadvisable to attempt any reconstruction of the diagram on the basis of present informa-

tion, but certain facts may be pointed out. A region of coexistence of ferrite, cementite, and the cubic carbide is required by the phase rule to exist between the ferrite-cementite and ferrite-cubic carbide fields. No evidence of such a condition was found in the isothermally transformed alloys studied, but the possibility of its existence cannot be eliminated on this evidence. Small portions of either carbide could easily be lost in the separation treatment. It is possible to identify the structure of the predominant carbide from diffraction patterns of the complete alloy, but the interference lines of the minor phase might be undetectable. The coexistence of the two carbide phases in the quenched and tempered samples of alloys 11 and 30 cannot be accepted as representative of the equilibrium conditions, for they obviously represent only a transitory state.

The degree to which molybdenum segregates in the carbide during the actual transformation of austenite to ferrite and carbide strengthens the suspicion that the migration of the alloying element is responsible for the decreased rate of transformation. The extent to which the two major factors involved—the rate of nucleation and rate of growth—are individually affected remains to be determined. However, the fact that in certain cases a carbide is formed which has much larger unit cell dimensions than cementite would naturally lead to the expectation of an influence on the nucleation rate. A decrease in the rate of growth seems obligatory in view of the much less rapid diffusion rate of molybdenum in austenite (16) as compared with that of carbon.

It is hoped that a complete explanation of the effects of molybdenum on hardenability will result from a correlation of diffusion rates of the element in austenite with partition data. It remains to be shown that a comparable concentration of molybdenum in the carbide also occurs when austenite is transformed in the vicinity of 1000 degrees Fahr. (540 degrees Cent.). If such is found to be true, then partition can most certainly be related to hardenability. This additional work will be attempted.

The complexity of the problem is readily apparent, and a thorough understanding of it will result only from a complete thermodynamic study of the system. The mechanism of the hardening process will be brought more clearly into focus, however, by continued studies of partition. In addition to the effect of transformation temperature on the distribution of the alloying element, the influence of proeutectoid constituents, both ferrite and carbide, must be

considered. The extent to which manganese, silicon, and other elements commonly found in steel influence the partition of the major alloying element must also be determined if partition data are to be applied to alloys of commercial analysis.

Summary and Conclusions

A study of the distribution of molybdenum in pure iron-carbon-molybdenum alloys of approximately eutectoid carbon content discloses that molybdenum concentrates in the carbides. This concentration occurs both in carbides formed directly from austenite at 1300 degrees Fahr. (705 degrees Cent.) and in carbides formed by tempering martensite at 1300 degrees Fahr. (705 degrees Cent.). The extent of this segregation is much greater in the isothermally transformed materials at the end of transformation (which in no case required more than 30 minutes) than is found in alloys quenched and tempered for as long as 250 hours at the same temperatures. In both cases, holding the alloys for extended times at 1300 degrees Fahr. (705 degrees Cent.) produces a continued migration of the molybdenum from the ferrite to the carbide.

A face-centered cubic carbide having a lattice parameter of 10.5250 Å was found, exclusively, after isothermal transformation in all alloys containing at least 0.54 per cent molybdenum. Chemical analysis indicates that the formula $(Fe, Mo)_{23}C_6$ can be considered as representing the composition. The quenched and tempered alloys contain this carbide only when the molybdenum content exceeds 0.75 per cent. In these cases it was found to exist simultaneously with the orthorhombic cementite. When molybdenum-containing austenite transforms at 1300 degrees Fahr. (705 degrees Cent.), the molybdenum diffuses through the austenite to the carbide and does so at a rate considerably greater than the rate at which it diffuses to the carbide through ferrite. The results of the work presented indicate that the partition of the alloying element may, through the necessity for its diffusion during the direct transformation of austenite, exert an important influence on hardenability.

The need for a redetermination of the iron-rich corner of the iron-carbon-molybdenum diagram is indicated by the confirmation of the existence of a carbide phase not considered in the diagrams currently accepted.

The tendency for the alloying element to migrate from the ferrite

to the carbide is a consideration of major importance in the use of steels at elevated temperatures for extended periods of time.

Excessive spheroidization of the carbides in steel during an annealing process is known to reduce the hardenability of the steel in the subsequent hardening treatment. The present work suggests that this fact is especially important in the heat treatment of molybdenum steels. The full capacity of molybdenum steels to harden may not be realized if the annealing treatments are performed merely to achieve a certain hardness.

ACKNOWLEDGMENT

The authors take pleasure in acknowledging their indebtedness to Dr. Lars Thomassen, of the University of Michigan, for his helpful suggestions and criticisms and for his kindness in reviewing certain of the X-ray data.

Bibliography

1. E. S. Davenport and E. C. Bain, "Transformation of Austenite at Constant Subcritical Temperatures," *Transactions,* American Institute of Mining and Metallurgical Engineers, Iron and Steel Division, 1930, p. 117.
2. J. L. Ham, R. M. Parke and A. J. Herzig, "The Effect of Molybdenum on the Rate of Diffusion of Carbon in Austenite," TRANSACTIONS, American Society for Metals, Vol. 31, December 1943.
3. J. R. Blanchard, R. M. Parke and A. J. Herzig, "The Effect of Molybdenum on the Isothermal Subcritical Transformation of Austenite in Eutectoid and Hypereutectoid Steels," TRANSACTIONS, American Society for Metals, Vol. 31, December 1943.
4. C. Wells and R. F. Mehl, "The Rate of Diffusion of Carbon in Austenite in Plain Carbon, in Nickel, and in Manganese Steels," *Transactions,* American Institute of Mining and Metallurgical Engineers, Iron and Steel Division, 1940, p. 279.
5. F. E. Bowman, R. M. Parke and A. J. Herzig, "The Alpha Iron Lattice Parameter as Affected by Molybdenum, and an Introduction to the Problem of the Partition of Molybdenum in Steel," TRANSACTIONS, American Society for Metals, Vol. 31, 1943, p. 487.
6. V. N. Svechnikov and N. S. Alferova, "Investigation of Alloys of the Iron-Carbon-Molybdenum System," *Teoriya i Praktika Metallurgii,* 1936, No. 4, p. 72-84.
7. T. Takei, "Equilibrium Diagram of the Iron-Carbon-Molybdenum System," *Kinzoku no Kenkyu,* Vol. 9, No. 3, March 1932.
8. F. R. Morral, G. Phragmen and A. Westgren, "Carbides of Low Tungsten and Molybdenum Steels," *Nature,* Vol. 132, 1933, p. 61.
9. W. Crafts and C. M. Offenhauer, "Carbides in Low Chromium-Molybdenum Steels," American Institute of Mining and Metallurgical Engineers, Technical Publication 1556, 1943.
10. S. Epstein, "The Alloys of Iron and Carbon," Vol. 1, p. 41. McGraw-Hill Book Co., Inc., New York, 1936.
11. J. F. Burns, "Classification of Alpha Iron-Nitrogen and Alpha Iron-Carbon as Age-Hardening Alloys," *Transactions,* American Institute of Mining and Metallurgical Engineers, Vol. 113, 1934, p. 239.

12. M. U. Cohen, "Precision Lattice Constants from X-ray Powder Photographs," *Review of Scientific Instruments,* Vol. 6, 1935, p. 68. *Errata,* Ibid., Vol. 7, 1936, p. 155.
13. F. R. Morral, Discussion, TRANSACTIONS, American Society for Metals, Vol. 31, 1943, p. 495.
14. A. Westgren, "Complex Chromium and Iron Carbides," *Nature,* Vol. 132, 1933, p. 480.
15. A. Westgren, "Crystal Structure and Composition of the Cubic Carbide of Chromium," *Jernkontorets Ann.,* Vol. 117, 1933, p. 501.
16. Climax Molybdenum Company, unpublished data.

INTERRUPTED QUENCH AND ISOTHERMAL TREATMENTS OF PRECIPITATION HARDENING ALLOYS: INTRODUCTORY NOTES

By R. H. Harrington

Abstract

Three industrial alloys were studied: (a), 97 copper-2.6 cobalt-0.4 beryllium, (b), 96 aluminum-4 copper and (c), 92.7 aluminum-7 silicon-0.3 magnesium. The rate of cooling from the solution temperature was not very critical, least so for the copper alloy. Interrupted quench treatments, for periods of minutes in the aging range, followed by standard aging treatments had practically no effect relative to the standard properties of the copper alloy; for the aluminum-silicon-magnesium alloy some very good properties were developed, all, however, slightly inferior to the maximum strength properties developed by quenching to room temperature. Isothermal (quench aging) treatments resulted in markedly lower properties for the copper alloy; with one exception the same effect resulted for the aluminum-copper alloy; while such treatments yielded good properties for the alloy aluminum-silicon-magnesium, these were all inferior in strength properties to the fully quenched and aged alloy. Microstructures, so developed, are not distinctly definitive although some differences may be noted. There are three chief results: (A), some very good properties can be developed by these treatments; (B), in full quenching, relatively rapid cooling from the aging range to room temperature is most important in the development of maximum tensile properties; (C), further research with wider ranges in time and temperatures for interrupted quench and quench aging treatments should evaluate the role of full-quenching strain relative to the nuclei number and quantity of precipitate evolved on subsequent aging. (By all previous experience, the rate of grain growth is dependent upon temperature alone after the early relief from strain.)

A GREAT deal of research has been done on the "isothermal heat treatments" of steels, the resulting data yielding the now

A paper presented before the Twenty-fifth Annual Convention of the Society, held in Chicago, October 18 to 22, 1943. The author, R. H. Harrington, is research metallurgist, General Electric Company, Schenectady, N. Y. Manuscript received June 24, 1943.

widely familiar S-curves for these materials. This method has been given little, if any, attention as a means for studying precipitation reactions in age hardening alloys.

Relative to precipitation hardening alloys, considerable work has been done in the study of the effect of the rate of cooling concluding the solution treatment. Several recent examples are as follows: Sykes (1)* compared the cooling rates for quenching iron-tungsten alloys in tap water and in air; Hunsicker (2) compared the cooling rates for aluminum-copper alloys quenched in cold and in boiling water; Fink and Smith (3) described the effect of thermal strain from fast rates of cooling upon subsequent preferred precipitation in aluminum alloys. Most of this work has been based on hardness measurements following final aging treatments. Hardness measurements are indicative but fail to show the inter-relationships of proportional limits, yield strengths, tensile strengths and elongations. It is interesting to note a statement by Hunsicker in his discussion of some of Sykes' work (1): "The effect of formation of nuclei during the quench on the ultimate mechanical properties of a precipitation hardening alloy is not certain."

The purpose of this report is to give briefly a few introductory notes upon the effects of some "isothermal treatments" upon the mechanical properties of three standard industrial alloys. The results indicate varying effects in the different alloys and justify continuing this type of research in more detail and with respect to other alloys as well.

General

Standard equilibrium diagrams yield only the information relative to the identity of the co-existing phases, the temperature range for precipitation for a given composition, and the quantity of the precipitated phase that can form for a given composition when the alloy is cooled so slowly as to be substantially free from strain.

Thus the factors most affected by strain from quenching (precipitation hardening alloys) are rate of nucleation, the number of nuclei, and rate of grain growth from these nuclei should quenching strains still persist. It is even possible for imposed strain

*The figures appearing in parentheses refer to the bibliography appended to this paper.

to shift the position and shape of the solvus line (4) and thus alter the quantity of precipitating phase from that indicated by the equilibrium diagram for strain-free material.

Heat Treatments

The "standard" heat treatment that yields the maximum strength properties, regardless of any practical significance, was chosen for basic consideration since it should be the most sensitive to effects of deviation from its standard performance.

Technically, any heat treatment that constitutes holding the material for any finite time at constant temperature is an "isothermal" heat treatment. For descriptive purposes, two types of isothermal treatments employed in this research are defined as follows:

Interrupted Quench—This consists of interrupting the continuity of the quench cooling, holding the material at a stated constant temperature for a given time interval, usually brief, after which the quench is completed to room temperature and the alloy is subsequently aged at room or elevated temperatures.

Quench Aging—This constitutes rapidly and continuously cooling the alloy from the solution temperature down to the desired aging temperature at which temperature the material is completely and directly aged. The final rate of cooling from this aging treatment is essentially without further effect.

For the purposes of this introductory investigation, interrupted quench treatments were employed involving only a few minutes at temperatures just above and just below the standard critical aging temperature, while quench aging treatments were made directly comparable to the standard aging treatment.

Alloy Materials

The copper-base alloy, containing 2.6 cobalt and 0.4 beryllium, in its various cast and wrought forms combines the following properties when heat treated: 45,000 to 55,000 pounds per square inch proportional limit; 50,000 to 60,000 pounds per square inch elastic limit; 90,000 to 125,000 pounds per square inch tensile strength; 92 to 105 Rockwell B hardness; 45 to 55 per cent of the electrical conductivity of copper; an endurance limit of 34 to 36,000 pounds per square inch for 100 million cycles; impact resistance (Charpy)

of 25 to 35 foot-pounds; and structural stability up to 500 degrees Cent. (930 degrees Fahr.).

The two aluminum alloys, containing respectively 4 per cent copper and 7 per cent silicon + 0.3 per cent magnesium, are well known and widely used and require no detailed introduction.

Test Samples

To eliminate as much as possible the confusing effects of previous history of the samples, these initial experiments were performed upon standard sand-cast tensile bars of each of the three alloys. Subsequent photomicrographs showed that the resulting grain sizes were as normally expected for each alloy so cast. The reported tensile properties are averages for results from 3 bars.

Methods

For the copper base alloy the interrupted quench and quench aging treatments were performed in a controlled-temperature, electrically-heated lead bath. In the case of the aluminum alloys, a stable quenching oil was substituted for the molten lead. For these treatments, quenching was done by direct immersion of the test samples into the molten lead or oil at the chosen temperatures. In the case of the copper base alloy, the samples were air-cooled at the conclusion of the interrupted-quench treatments whereas the aluminum alloys were water-quenched. All bars were air-cooled at the conclusion of the various aging treatments.

In each property table, the first line of properties is for the S (or standard) treatment with M or T (in the hardness column) indicating the minimum or typical properties normally specified. Heat treatment No. 1, in each case, gives the resulting properties for this specific lot of tensile bars when given the standard heat treatment, thus qualifying the quality of the particular lot of bars.

The Copper-Base Alloy: 97 Per Cent Copper-0.4 Per Cent Beryllium-2.6 Per Cent Cobalt

Treatment No. 1 shows that this lot of tensile bars was of very acceptable quality, the standard treatment, as usual, involving a water quench from the solution temperature. (Properties for this alloy are given in Table I.)

Table I

97 Copper—0.4 Beryllium—2.6 Cobalt (Trodaloy-1)

Heat Treat. No.	Solution Treatment Temp. °C.	Time	Intermediate or Isothermal Treatment Temp. °C.	Time	Aging Treatment Temp. °C.	Time	Proportional Limit P.S.I.	Tensile Strength P.S.I.	Elongation in 2" %	Rockwell Hardness B Scale
S	900	1 Hr. W.Q.	...	...	500	2 Hrs.	45,000	90,000	10	92 M
1	900	1 Hr. W.Q.	...	...	500	2 Hrs.	48,000	95,000	13	95
2	900	1 Hr.	450	2 Min. A.C.	500	2 Hrs.	46,900	94,000	13	93
3	900	1 Hr.	550	2 Min. A.C.	500	2 Hrs.	47,400	92,000	12	92
4	900	1 Hr.	500	2 Hrs. A.C.	...	...	29,800	70,450	17	80
5	900	1 Hr. W.Q.	...	...	500	1 Hr. W.Q.	43,800	90,350	13	93
					500	2 Hrs.				
6	900	1 Hr. W.Q.	...	...	600	10 Min. W.Q.	40,250	79,000	12	86
					500	2 Hrs.				

Treatments 2 and 3, for interrupted quenching at temperatures 50 degrees below and above the standard aging temperature, show that apparently the rate of nucleation, number of nuclei and grain growth of the precipitated phase during subsequent aging were relatively unaffected by these treatments. Also, it is indicated that this alloy is certainly insensitive to the rates of cooling employed over a rather wide range.

Treatment No. 4, with quench aging comparable to standard aging, showed marked depreciation in all properties and indicates that the alloy must be cooled nearly to room temperature before final aging in order to achieve its most useful properties.

Double aging at the standard aging temperature, treatment No. 5, had no appreciable effect relative to standard properties.

Double aging, with 10 minutes primary over-aging at 600 degrees Cent. (1110 degrees Fahr.), treatment No. 6, lowered the tensile strength and hardness but had much less depreciative effect than the direct quench aging (treatment No. 4).

Thus, for this alloy, strain is not critical from a wide range of cooling rates, but is required to develop efficient properties. That the quenching strain is not critical for various cooling rates from the solution temperature may be due to the fact that localized strain from the high degree of coring in the structure would take place anyway and, in this case, may be the predominant strain factor.

The Alloy of 96 Per Cent Aluminum-4 Per Cent Copper

Properties for some of the treatments given this alloy are shown in Table II. Treatment No. 1 shows that this lot of tensile bars qualifies satisfactorily on the basis of the standard treatment (line S).

Table II
96 Aluminum—4 Copper (Aluminum Alloy 195)

Heat Treat. No.	Solution Treatment Temp. °C.	Time	Intermediate or Isothermal Treatment Temp.	Time	Aging Treatment Temp. °C.	Time	Proportional Limit P.S.I.	0.2% Yield Strength P.S.I.	Tensile Strength P.S.I.	Elongation in 2" %
S	515	15 Hrs.	W.Q.	...	155	5 Hrs.	14,000	22,000	32,000 36,000	3M 5T
1	515	15 Hrs.	W.Q.	...	155	5 Hrs.	14,200	22,500	33,200	5.2
2	515	2 Hrs.	W.Q.	...	155	20 Hrs.	14,000	26,200	33,600	3.6
3	515	2 Hrs.	W.Q.	...	175	20 Hrs.	15,400	30,200	35,700	2.3
4	515	2 Hrs.	W.Q.	...	200	20 Hrs.	15,700	25,600	32,000	2.2
5	515	2 Hrs.	W.Q.	...	155	8 Hrs.	13,900	24,600	32,300	2.5
6	515	2 Hrs.	W.Q.	...	175	8 Hrs.	12,400	24,700	32,200	3.0
7	515	2 Hrs.	W.Q.	...	200	8 Hrs.	14,300	25,900	32,000	2.0
22	515	2 Hrs.	O.Q.	...	155	20 Hrs.	17,200	25,800	35,100	3.8
66	515	2 Hrs.	O.Q.	...	175	8 Hrs.	15,200	27,500	33,100	2.4
222	515	2 Hrs.	155 °C	20 Hrs.	A.C.	...	12,200	23,200	29,800	2.0
555	515	2 Hrs.	155 °C	8 Hrs.	A.C.	...	16,100	23,800	30,700	2.3
666	515	2 Hrs.	175 °C	8 Hrs.	A.C.	...	10,600	17,600	26,200	3.7
777	515	2 Hrs.	200 °C	8 Hrs.	A.C.	...	11,300	18,900	27,000	3 2
777A	515	2 Hrs.	200 °C	4 Hrs.	A.C.	...	11,100	18,200	27,400	3.6

Since it is usually difficult to determine the proportional limit from stress-strain data from aluminum alloys with more than ± 2000 pounds per square inch accuracy, specific comparisons are better based on the 0.2 per cent yield strength. Comparisons are especially valid when all three stress properties show increases or decreases in parallel.

It was found that heat treatment No. 2, with only 2 hours' solution treatment but with aging extended to 20 hours, yielded slightly higher stress properties and thus probably represented more critical precipitation for these bars. This solution treatment was arbitrarily chosen as the base for study of this alloy.

For soluton treatments 2 through 7, the strain from solution quench should be about the same. For this series of treatments it is considered that variations in elongation from about 2.5 to about 3.5 per cent are insignificant and comparisons are mainly based on the stress properties.

Heat treatments 2 through 7 yield the properties for various combinations of time with aging temperature. The highest strength

properties, and probably the maximum precipitation aging effect, were developed by an aging treatment of 20 hours at 175 degrees Cent. (350 degrees Fahr.) (No. 3).

Heat treatments 22 and 66 show the effect of a slower rate of cooling in an oil quench and should be compared respectively with water quench treatments Nos. 2 and 6. In both cases the oil quench treatments yielded the higher properties with heat treatment No. 22 resulting in the best properties for the whole series.

Heat treatments 222, 555, 666, 777 and 777A involve direct quench aging and, compared respectively with treatments 2, 5, 6, and 7, yield definitely lower properties. It appears necessary to completely cool this alloy to room temperature and age in the conventional manner in order to achieve maximum precipitation aging properties. Thus the strain from quenching appears to play a decisive role in developing maximum properties.

The Aluminum Alloy Containing 7 Per Cent Silicon and 0.3 Per Cent Magnesium

The properties for various heat treatments of this alloy are shown in Table III. There are two treatments available for this alloy and in use at this time. The widely used standard treatment with its minimum and typical properties are listed for heat treatment SO.

Heat treatment S1 (5), however, yields the maximum precipitation strengthening and was chosen as the base for this study. Heat treatment No. 1 yielded the high strength properties that, by comparison with S1, qualified this lot of standard tensile bars as being of good quality.

Treatments 1A1 and 1A2 show the effect of interrupted quench heats at 140 degrees Cent. (285 degrees Fahr.). Unfortunately, it was anticipated that the longer time of interruption at 140 degrees Cent. (285 degrees Fahr.) (1A2) would require less subsequent aging. This was not true and this treatment resulted in marked under-aging. Interrupted quench treatment 1B1, at 170 degrees Cent. (340 degrees Fahr.), also resulted in under-aging. However, interrupted quench treatments 1B2 and 1B3, having the basic aging treatment, give a direct comparison of 2 minutes versus 10 minutes interruption. For full aging treatments, this alloy is relatively insensible to brief interrupted quenches in the range of its critical

Table III

92.7 Aluminum—7 Silicon—0.3 Magnesium (Aluminum Alloy 356)

Heat Treat. No.	Solution Treatment Temp. °C.	Time	Intermediate or Isothermal Treatment Temp.	Time	Aging Treatment Temp. °C.	Time	Proportional Limit P.S.I.	0.2% Yield Strength P.S.I.	Tensile Strength P.S.I.	Elongation in 2" %
SO	538	15 Hrs.	W.Q.	...	160	4 Hrs.	12,000	22,000	30,000 32,000	3M 4T
S1	530	2 Hrs.	W.Q.	...	155	20 Hrs.	18,000 20,000	30,000 32,000	36,000 38,000	2M 3T
1	530	2 Hrs.	W.Q.	...	155	20 Hrs.	19,000	34,000	40,000	2.5
1A1	530	2 Hrs.	140°C	2 Min. W.Q.	155	20 Hrs.	20,000	30,500	36,500	2.5
1A2	530	2 Hrs.	140°C	10 Min. W.Q.	155	2 Hrs.	9,500	17,500	27,700	4.5
1B1	530	2 Hrs.	170°C	2 Min. W.Q.	155	5 Hrs.	13,250]	21,500	31,200	4.6
1B2	530	2 Hrs.	170°C	2 Min. W.Q.	155	20 Hrs.	16,250	32,250	37,700	3.0
1B3	530	2 Hrs.	170°C	10 Min. W.Q.	155	20 Hrs.	20,000	30,000	35,500	3.0
2	530	2 Hrs.	120°C 155°C	1.5 Hrs. 8 Hrs.	...	...	16,000	31,700	37,400	3.5
12	530	2 Hrs.	120°C 155°C	4 Hrs. 16 Hrs.	...	...	15,000	30,000	36,400	4.0
13	530	2 Hrs.	155°C	20 Hrs.	...	...	15,000	32,000	37,000	3.5
3	520	2 Hrs.	140°C	2 Min. W.Q.	155	20 Hrs.	17,000	31,500	36,100	3.1
4	540	2 Hrs.	140°C	2 Min. W.Q.	155	20 Hrs.	22,100	33,000	38,250	3.4

aging temperature although the basic "normal" treatment yielded slightly higher strength properties.

Heat treatments 2, 12, and 13 are three slightly different direct quench aging treatments and there are no essential differences in the resulting properties. The strength (or stress) properties of all three fall a little short of equalling those for the basic treatment, No. 1. (In the instances of Nos. 2 and 12, the tensile bars were interrupted quench-aged for the stated times at 120 degrees Cent. (250 degrees Fahr.) and then directly and quickly transferred to drawing ovens for completing the aging treatments at 155 degrees Cent.)

Heat treatment No. 3 is based on a solution treatment that, with normal quenching and aging, yields properties that are low. However, the interrupted quench (2 minutes at 140 degrees Cent.) effects increased properties in this case.

Heat treatment No. 4 shows a similar effect of interrupted quench (2 minutes at 140 degrees Cent.) for a solution treatment at 540 degrees Cent. (1005 degrees Fahr.) and subsequent aging at 155 degrees Cent. (310 degrees Fahr.) that normally yield lower properties.

Structures

For the Copper-Cobalt-Beryllium Alloy—Although minor variations in shape of precipitated phase, such as feathering and the beginning of "spheroidization" of the platelets, occur, these structures are not sufficiently definitive to lead to concise conclusions regarding the effect of specific treatments. There is a striking effect

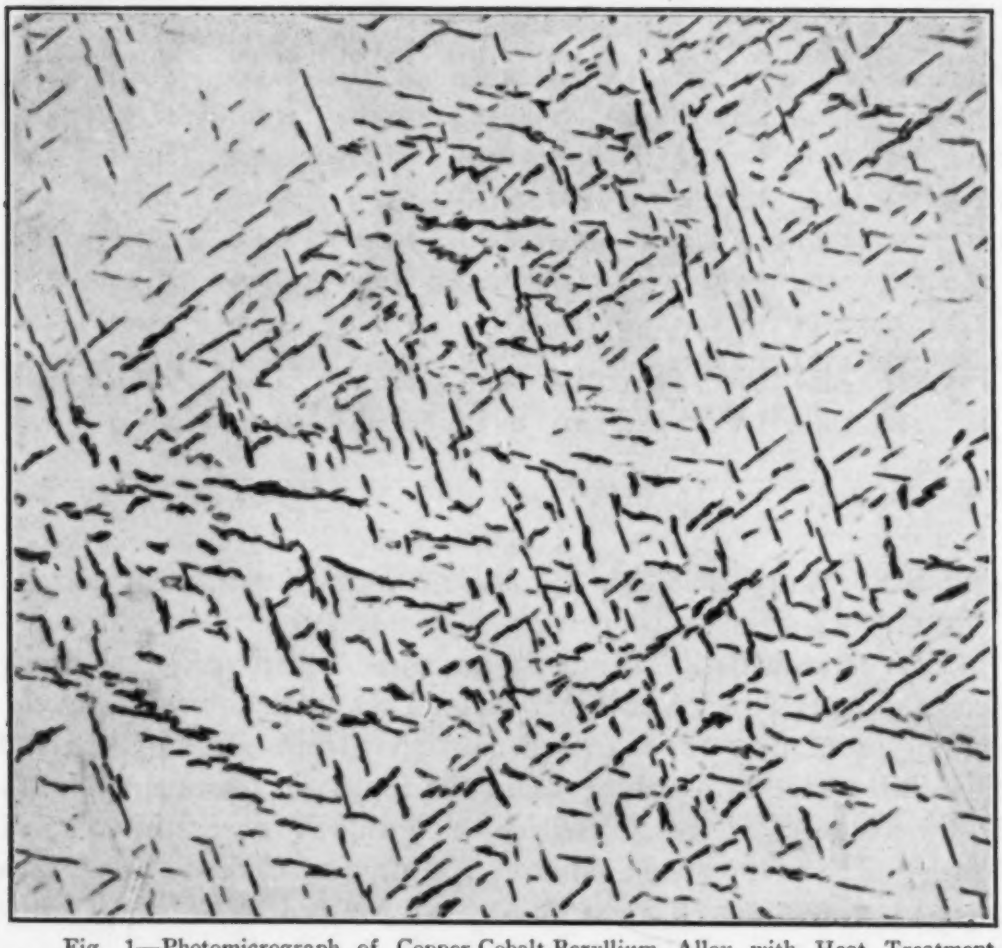

Fig. 1—Photomicrograph of Copper-Cobalt-Beryllium Alloy with Heat Treatment No. 4, Table I. × 1000.

of coring on the resultant location of the precipitated phase, cobalt-beryllium, along certain crystallographic planes. Ordinarily, the wrought and homogenized alloy of this composition yields a general distribution of small particles of cobalt-beryllium, just as would commonly be expected. Apparently the marked coring in the cast bars resulted in high localized strain (upon cooling) which, in turn, effected the "preferred", strain-induced precipitation. This is quite similar to the strain-induced precipitation along grain boundaries

and slip-planes in aluminum-copper alloys as described by Fink and Smith (3). Fig. 1 shows the structure for the copper-cobalt-beryllium alloy resulting from heat treatment No. 4 (Table I).

For the Aluminum Alloys—Samples of the aluminum alloys were normally polished, holding the sample by hand against the rotating wheel, etched with the standard "mixed-acid" micro etch,

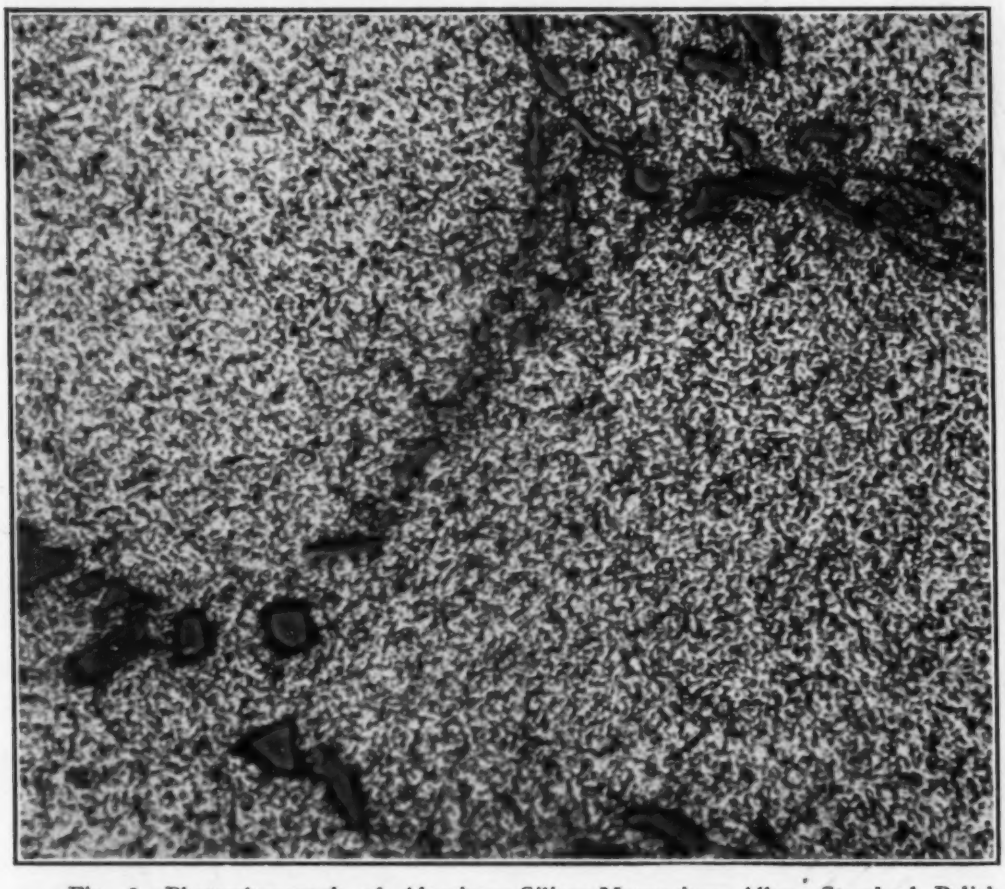

Fig. 2—Photomicrograph of Aluminum-Silicon-Magnesium Alloy, Standard Polish and Etch. × 1000.

and examined at × 1000. Regardless of treatment, all of the structures looked about identical, showing a fine, clearly outlined general distribution of small "precipitated particles", as indicated in Fig. 2, showing the "structure" for the aluminum-silicon-magnesium alloy with heat treatment No. 12. It has been proven that such a "precipitated particle" structure develops from segmented polishing scratches upon etching. Forty minutes polish with the final wheel, followed by a last polish by hand motion on a still wheel, yields the clear field matrix shown in Fig. 3. The fine, "precipitated-particle" structure, first developed in Fig. 2, was fictitious and has entirely

disappeared. Fig. 4 shows a similar clear field matrix after electrolytic polishing of another section. (The clear circles in Fig. 4 are vestiges of stain.)

Thus it must be assumed that the precipitation structures, developed by the various heat treatments of the aluminum alloys, are submicroscopic.

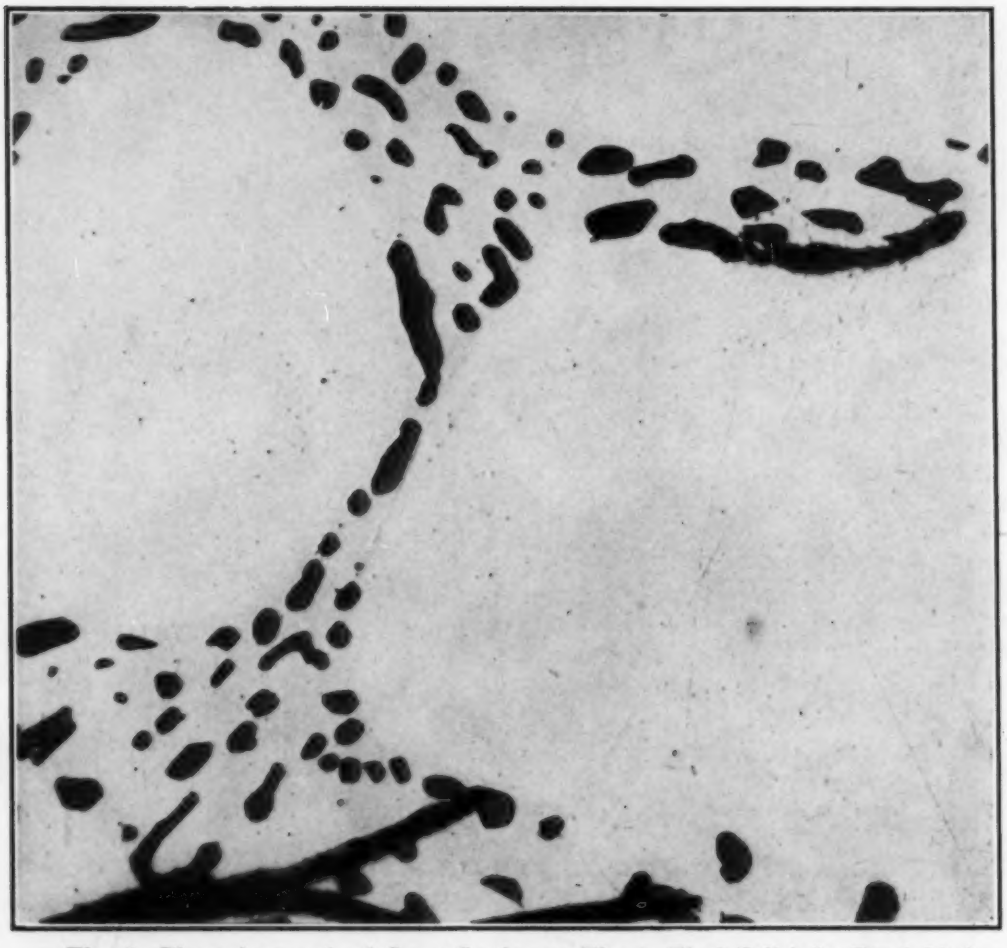

Fig. 3—Photomicrograph of Same Section as Fig. 2, Final Polish by Hand Motion Alone. Etched. × 1000.

Conclusions

In the absence of strain, the same principles should apply to precipitation as apply to solidification of a crystalline structure from the molten state:

(a) The rate of nucleation (or number of nuclei) would be a function solely of the aging temperature (in the absence of occlusions and inclusions).

(b) The rate of grain growth would be a function solely of the aging temperature.

The time relationship of (a) to (b) would determine the resulting structure and properties for any chosen aging temperature.

It would further be true, according to the equilibrium diagram, that, in the absence of strain, there would be no difference in structure and properties between (A), quenching to room temperature and subsequently aging at elevated temperature and (B) quenching

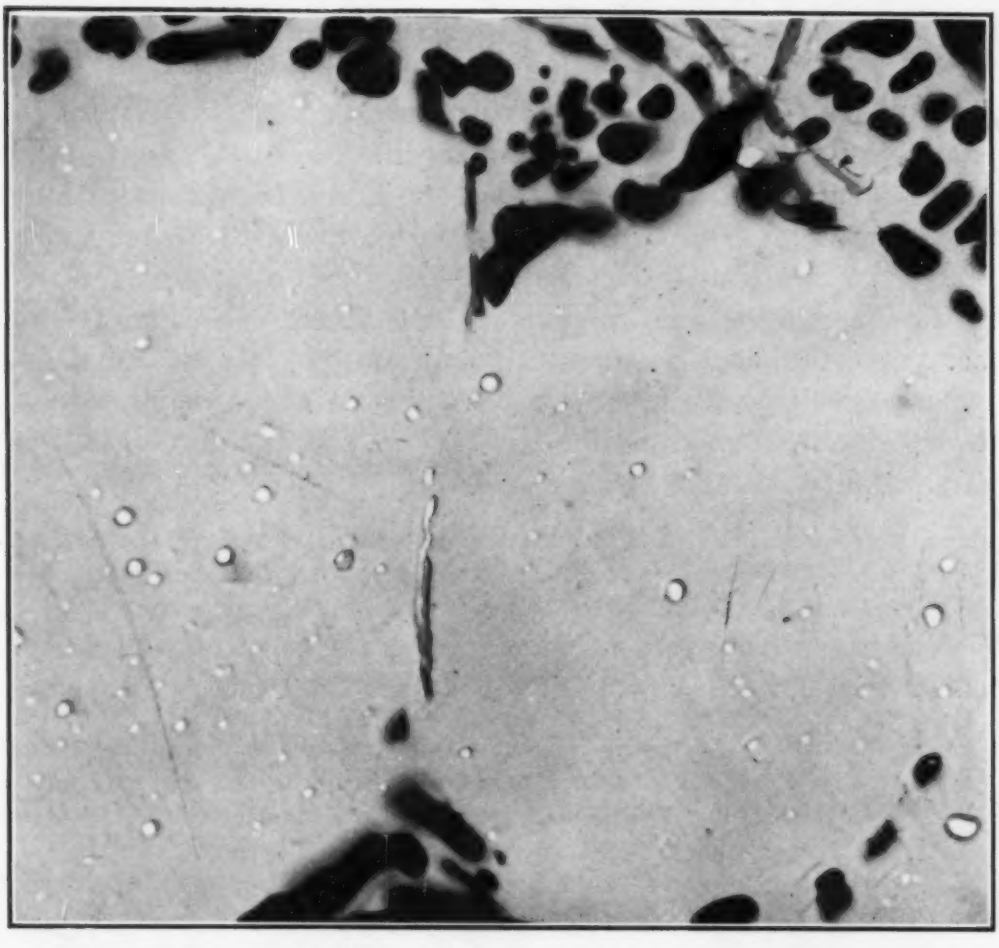

Fig. 4—Photomicrograph of Different Section of Aluminum-Silicon-Magnesium Alloy, Electrolytic Polish and Etch. × 1000.

at the same rate from the solution temperature to the same aging temperature and aging thereat for the same time.

The introductory experiments, reported herein, for interrupted quench and direct quench aging treatments, yield the following conclusions:

1. That, as indicated by previous studies of many investigators chiefly on the aging cycle, strain from the solution quench plays a critical role in determining the properties after subsequent aging.

2. That response to interrupted quench and direct quench aging will vary from one system to another.

3. That, for the alloys studied, the rate of cooling from the solution temperature to the temperature for subsequent critical aging, is not as critical as ordinarily supposed.

4. That the most important and strain effective part of the quenching cycle is the final cooling through the temperature range from that of subsequent critical aging down to room temperature.

5. That, unfortunately, the structures after subsequent critical aging are not generally useful (as they are in the case of steels) in the study of the effect of quenching strain.

6. That the effect of quenching strain and the results of interrupted quench and direct quench aging treatments are best studied through the means of mechanical properties that are thus developed.

The results of these preliminary experiments also indicate that other properties, such as electrical conductivity, must be included in further development. Over-aging treatments may prove useful in showing location and distribution of the precipitating phase and will also be included in further research.

Acknowledgments

The cast tensile bars of the copper-cobalt-beryllium alloy were furnished by Ampco Metal, Inc. The cast tensile bars of the two aluminum alloys were furnished by the foundry of the General Electric Co., Pittsfield Works. The heat treatments were applied by T. C. Jester and the photomicrographs made under the direction of Mrs. C. Brodie, both of the General Electric staff.

Bibliography

1. W. P. Sykes, "Further Notes on Precipitation Hardening in Heavy Alloys," Transactions, American Society for Metals, Vol. 28, 1940, p. 892 - 908.
2. H. Y. Hunsicker, "Precipitation Hardening Characteristics of High Purity Aluminum-Copper and Aluminum-Copper-Iron Alloys," Symposium of the Age-Hardening of Metals, published by American Society for Metals, 1940,
3. W. L. Fink and D. W. Smith, "Age-Hardening of Aluminum Alloys, III (Double Aging Peaks)," *Transactions,* American Institute of Mining and Metallurgical Engineers, Vol. 128, 1938, p. 223.
4. R. H. Harrington, "Role of Strain in Precipitation Reactions in Alloys," Symposium on the Age Hardening of Metals, published by American Society for Metals, 1940.
5. U. S. Patent No. 2,246,134.

DISCUSSION

DEL FREDERICKSEN:[1] What temperature of over-aging do you think would be necessary to observe the precipitated phase in the 195 alloy?

DR. HARRINGTON: You are speaking of a specific composition, I believe, that was the basis of work of a number of investigators in this country and also in England. The results indicated that aging in a range of 230 up to about 250 degrees Cent. will bring the particles of the precipitated phase up to microscopically visible size.

RALPH V. HILKERT:[2] I should like to ask Dr. Harrington whether the times at room temperature subsequent to the isothermal arrest but prior to artificial aging remained constant. If not, was there any difference found between specimens held for different lengths of time at room temperature prior to artificial aging?

DR. HARRINGTON: For the interrupted quench aging there is no specific test of time at room temperature reported, and with the interrupted quench aging I do not know for sure but it would seem to me that, with the interrupted quench temperature of aluminum alloy at 140 degrees Cent., the room temperature aging taking place before the subsequent completion of artificial aging might be entirely negligible as far as these aluminum alloys are concerned. They have thus been aged at a certain elevated temperature for a number of minutes and I hardly think that further aging at room temperature would be effective.

The data in this report are from bars that were artificially aged immediately after completion of the interrupted quench treatments.

WALTER BONSACK:[3] I know of only one application of such a treatment on aluminum alloys. This is 195 Alloy which is being quenched in boiling water and kept in boiling water for several hours. Properties equivalent to aging at room temperature are being obtained in this manner. It is a standard aging treatment now. From the experience I have on heat treating aluminum alloys, quenching at the lowest possible temperature gives superior results as measured in tensile strength, yield strength and better elongation.

DR. HARRINGTON: I do not believe that quenching at the lowest possible temperature always gives superior results. I do believe it may be true in the *absence* of plastic strain from quenching. If thermal quenching strains cause actual deformation at boundaries and along slip planes, as it may (Fink and Smith, loc. cit.), then subsequent aging may cause "preferred precipitation" along those boundaries and those affected planes. This could cause embrittlement and might adversely affect the tensile properties.

WM. L. FINK:[4] There is one minor point that I would like to discuss. Dr. Harrington raised the question as to whether strain hardening changes the solid solubility. We have a considerable amount of experimental evidence

---

[1]Research metallurgist Caterpillar Tractor Co., Peoria, Ill.

[2]Metallurgist, Carnegie-Illinois Steel Corp., Chicago.

[3]Director of Laboratories, National Smelting Co., Cleveland.

[4]Chief of Physical Metallurgy Division, Aluminum Research Laboratories, New Kensington, Pa.

on this point. In determining the solid solubility of various elements in aluminum, it is often difficult to obtain equilibrium at the lower temperatures. We generally use as a criterion of equilibrium the fact that the true solubility curves are usually straight lines when the reciprocal of the absolute temperature is plotted against the logarithm of the concentration. Usually there is no difficulty in obtaining a straight line at the higher temperatures, but at the lower temperatures experimental points are apt to fall off the straight line, indicating failure to obtain equilibrium.

The experimental procedure we use to attain equilibrium in such cases is to cold roll the sample, age it for an additional time at the same temperature and again determine the amount of material in solid solution. Sometimes we have to repeat that cycle of operations two or three times to attain equilibrium. We have never found any indication that the equilibrium is shifted by strain hardening.

There is one other point I would like to mention in connection with this work—the question of the size of the nuclei that form at different temperatures. If a sample is quenched rapidly from the solution heat treating temperature to room temperature, very small nuclei form during the room temperature aging between the quench and the artificial aging. On subsequent artificial aging these small nuclei are not stable, and most of them redissolve although some grow to a stable size, the percentage of those which grow depending upon the temperature and other experimental conditions. I think that effect may account for many of the results in Dr. Harrington's paper.

DR. HARRINGTON: Referring back to Mr. Bonsack's discussion, I was not directly concerned with the practical aspects of these treatments, I do not advise anyone to try any of these treatments in production, especially at this time, without thorough investigation of the practical results and the setting up of acceptable specifications. It is obvious that a number of these treatments are certainly impractical for production heat treatment.

I do wish to discuss Dr. Fink's statements regarding the effect of strain hardening on solid solubility. However, let us first consider his remarks on "size of nuclei that form at different temperatures." I do not believe that, by theoretical definition, "nuclei" may have "different sizes." A nucleus should, by primary definition, be that minimum lattice mass that will serve as a center for growth of a grain typified by the lattice of the nucleus. Theoretically the nucleus might be defined as a single lattice cell. Practically, a single cell seems a very frail thing and, for practical effects, a "nucleus" is probably an aggregate of a small number of such cells, a minimum number for real existence and real effect. Nuclei of different sizes merely mean to me that conditions have allowed some "true" nuclei to grow beyond their initial (or birth) size. Thus such questions are still debatable: What is a nucleus? May nuclei (of the same melt or solid phase) have different sizes? When does a nucleus cease to be a nucleus and become a growing grain? For the very small particle sizes involved, can "nuclei of different sizes" have different real effects on physical properties? How is the size of a nucleus truly measured? For these very small sizes of particles, isn't the number of "nuclei" far more effective on properties than size of nuclei? Finally, Dr. Fink states that: "If a sample is quenched rapidly from the solution heat treating temperature

to room temperature, very small nuclei form during the room temperature aging between the quench and the artificial aging. On subsequent artificial aging, these small nuclei are not stable, and most of them redissolve although some grow to a stable size, the percentage of those which grow depending upon the temperature and other experimental conditions. I think that effect may account for many of the results in Dr. Harrington's paper." The mechanics so stated by Dr. Fink are undoubtedly correct but the sequence of conditions is not, since no appreciable "room temperature aging" (beyond about 30 seconds) was allowed for any of the isothermal treatments. At least some hours of natural aging must be allowed for these alloys to show any real effects therefrom on their resultant tensile properties. Since all of the treatments involved final artificial aging, all the derived structures should be just as stable (in a practical sense) as those derived by "standard heat treatments". From my point of view, however, the very real and very probable effect of strain: on solute content of the parent solid solution, the number of nuclei of the precipitating phase, and the rate of grain growth, under certain conditions, has been almost entirely ignored.

A distorted lattice is a strained lattice whether the strain is caused by mechanical or thermal means. Hence the principles involved in an explanation of the effect of prerecrystallization aging of a cold-worked solid solution would apply similarly in degree to the reheating of a quenched (thermally strained) solid solution matrix of a precipitation hardening alloy. Studies of the past few years (by the author and others),[5, 6, 7, 8] have indicated that pronounced age hardening reactions can be induced in alloys that consist of single solid solution phases under normal (equilibrium, or relatively strain-free) conditions. In the case of the prerecrystallization-aged cold-rolled phosphor bronzes the strain-induced age hardening appears to be clearly due to precipitation. (The other cases may be either precipitation or order-disorder reactions). A rationalized picture, based on quantitative data, is presented in the accompanying figure for strain-induced precipitation in the alpha tin-bronzes.

These are the following points, relative to the diagram:

1. T-O-C represents the conventional equilibrium diagram for the Cu-Sn system, Alpha range, at constant pressure of the atmosphere.

2. P-P′ is the pressure axis for the 3-variable system of pressure, temperature and concentration described by the Phase Rule. For the solid state it is thus possible to use "+ pressure" for compressive strain and "— pressure" for strain in tension whereas, for gases and liquids, compression, or pressure on the system is the only rational concept.

3. The amount of cold reduction can be plotted along the P-axis with 90 per cent reduction at some point, D.

4. The strain resulting from cold working is wholly relieved only by

---

[5]"Role of Strain in Precipitation Reactions in Alloys," loc. cit.

[6]R. H. Harrington and R. G. Thompson, "The Precipitation Reaction in Cold-Rolled P-Bronze," TRANSACTIONS, American Society for Metals, Vol. 28, 1940, p. 933-949.

[7]R. H. Harrington and T. C. Jester, "The Precipitation Reaction in Aged Cold-Rolled Brasses," TRANSACTIONS, American Society for Metals, Vol. 30, 1942, p. 124-142.

[8]R. H. Harrington and L. E. Cole, "The Precipitation Reaction in Aged Cold-Rolled Cd-Cu," TRANSACTIONS, American Society for Metals, Vol. 31, 1943, p. 651-669. Inclusive of bibliographies and discussions therein.

complete recrystallization, say at about 300 degrees Cent. (570 degrees Fahr.). (The constant temperature plane O′ A′ B′ D′).

5. Just as a solution quench for some systems will retain a metastable supersaturated solid solution at room temperature, and artificial aging at some elevated temperature, is necessary to permit the required atomic diffusion for precipitation, strain, induced by plastic deformation (either mechanical or thermal), may exert a similar effect. Thus, if a possible precipitation (or else an order-disorder) reaction will result in lattice contraction, a localized volume under compressive strain would favor such a reaction whereas localized strain in tension would oppose such a reaction. The reverse effects of strain

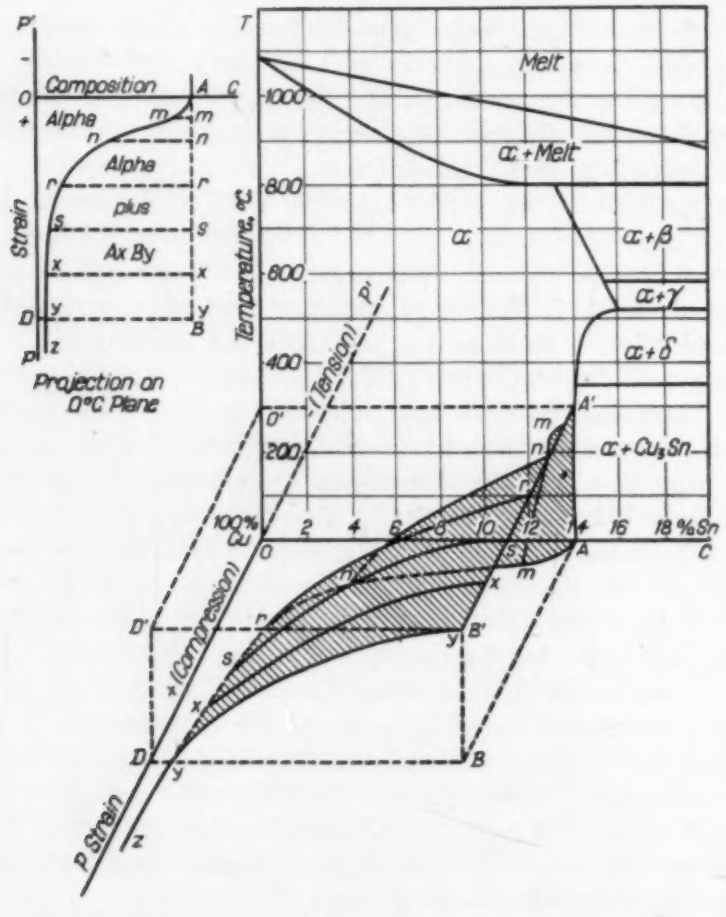

Fig. A—Possible Effect of Strain and Prerecrystallization Aging Relative to the Equilibrium Diagram for Solid Solutions.

apply to a reaction that results in lattice expansion. For certain systems, rates of diffusion at *room* temperature would be too slow for any practical effect, whereas elevated temperature (below that resulting in recrystallization) and time at temperature could effect strain-induced precipitation. Thus, in the diagram (Fig. A), the shaded curved "solvus surface" delineates the surface of temperature below which strain induced precipitation may take place and

above which re-solution takes place previous to structural recrystallization. Time at temperature may be a most important factor. The intersection of this "solvus surface" with the 0 degree Cent. temperature plane, P-O-C, shows the effect of strain on the solid solubility of tin in the alpha phase.

This diagram is submitted in very brief form only to illustrate the possible effects of "pressures", other than that of the atmosphere, on the equilibrium of the system. The same concept can be similarly applied to the solid solution phase of a "precipitation hardening system," one that yields precipitation under atmospheric pressure. Thus, such strain, in localized strain gradient volumes, whether caused by cold working or quenching, could induce "supernormal" precipitation. To save space in this discussion, interested readers may refer to other sources[9] for greater detail and a wider analysis.

F. N. RHINES:[10] I should like to take issue with Dr. Harrington with regard to the matter of invoking the phase rule to explain quenching effects, because I think that the phase rule cannot be applied in a case of this kind for several fundamental reasons. In the first place, the phase rule was set up upon the assumption that such variables as mechanical stress and particle size should be omitted from consideration. Secondly, the phase rule is built upon the assumption that the system being described is in equilibrium. It seems to me obvious that a mechanically strained condition is not an equilibrium condition; it is at least possible to imagine that in time a strained condition would settle back into an unstrained condition if we could afford to wait long enough. This does not mean, of course, that strain would not change the solubility. It simply means that we ought not to talk about the effects of strain on the basis of equilibrium diagrams.

I would like to differ with Dr. Fink also in his feeling that experiments conducted in the way described show that there is no effect of strain on solubility, because if the temperature is such that there is enough diffusion to bring about precipitation, it is hard to conceive that the internal stresses could also be maintained while precipitation was going on. I would rather see the question approached by using a condition whereby the strain was set up by something that could not diminish with time, such as the effect of grain size or the effect of embedded particles or something of that sort.

DR. FINK: My first remarks were not intended to indicate that it was impossible to get a change in solubility with pressure. I merely wanted to indicate that we had experimental evidence indicating that the effect of strain hardening is negligible in ordinary solubility determinations. I am not contending that very much higher pressures would not change the solubility.

With respect to Dr. Rhines' statements on the relieval of stress during the aging itself, it is true that there would be some recovery. In fact, we have made quite a number of measurements of relief of stress at temperature. If stress is plotted as ordinate and time as abscissa on a logarithmic scale, this type of curve is obtained (Fig. B). That is, initially the stress decreases along a straight line, then more slowly until a point is reached at which the

[9]"The Metallurgy of Modern Alloys," a current series of articles in *Steel Processing* (formerly *Heat Treating and Forging*), issues of Oct. and Nov., 1943, and Jan., Feb., March 1944.

[10]Assistant professor, Department of Metallurgy, Carnegie Institute of Technology, Pittsburgh.

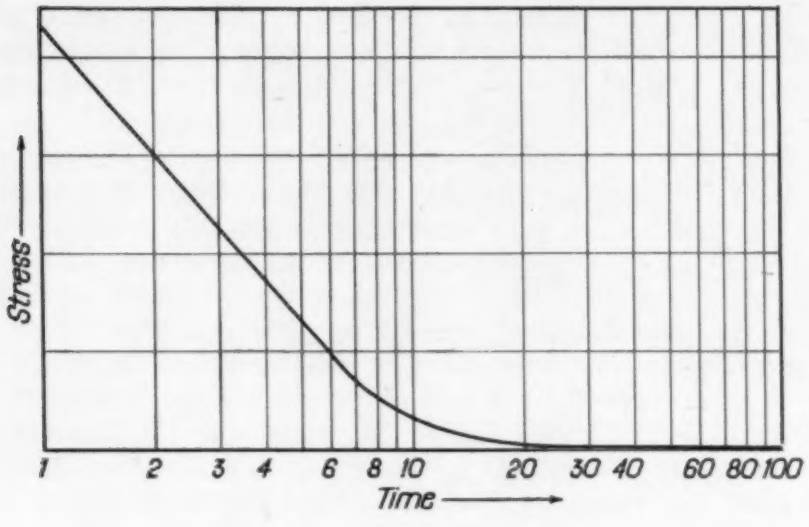

Fig. B

stress no longer changes. What we are determining, of course, in experiments involving long anneals, is the solubility of the solute in aluminum at the final constant stress rather than at the stress which was in the piece immediately after cold working.

Author's Closure

The author deeply appreciates the discussions contributed by various individuals and particularly those by Dr. Fink and Dr. Rhines as most pertinent.

It is worthwhile sometimes to "go pretty far" in order to bring out human reactions. We seldom have a chance to get together and the author took advantage to stir up something. Apparently he succeeded!

One conclusion seems to be agreement that *strain can* alter the solid solubility. It is to be noted also that Dr. Fink uses the terms "strain" and "pressure" interchangeably. It also appears, from the diagram submitted by Dr. Fink, that all strain, induced by cold working in his researches on solid solubility, was not relieved by the aging treatments (not true anneals) but was reduced to a constant value. Hence the measured data indicated the solid solubility under "non-equilibrium" conditions in those instances wherein an appreciable quantity of strain persisted.

Dr. Rhines takes issue on two points (a) that the phase rule cannot be applied to such variables as mechanical stress and particle size and (b) that the phase rule applies only to equilibrium and that a "mechanically" strained condition is not an equilibrium condition.

In reply to Dr. Rhines:

1. The author did not use the phase rule relative to particle size. However, it is true that, if strain can alter solid solubility, variation in strain will affect the number of nuclei and may, thereby affect subsequent particle size until temperature and time at temperature are altered to completely eliminate the effect of strain.

2. The author regards the *strained* lattice condition as comparable to

"pressure" on a gaseous system. This condition may *result* from mechanical forces, but, for this concept, the *cause* of the *strain* is no more important than the *cause* of other than atmospheric *pressure* on a gaseous system. One difficulty is that many words have multiple meanings. The engineering interpretation of "strain" is an extension of material under applied mechanical force. Material that is strained by cold working or by quenching is constituted of a multiple of minute strain-gradient volumes, each of which may act as an individual pressure system, unaware of its neighbors as long as the strain-gradient volumes persist. In the author's pressure, temperature, concentration diagram, the enclosed rectangular volume is inclusive of the effects of strain from plastic deformation by either cold working or by quenching. The range of strain so involved can be duplicated by hydrostatic pressure and it can be further extended only by some such externally maintained strain.

3. As to the use of the word "equilibrium", Marsh[11] offers the following concept: "Thermodynamic equilibrium may be said to be absolutely stable (equivalent to the atmospheric pressure phase diagram) *or* stable with respect to infinitesimal displacements but less stable than *another* equilibrium (and frequently called 'metastable'). Unstable equilibrium is seldom if ever realizable". Thus we have the concept of equilibria other than that of the *absolute*. Strained lattice is not the condition for absolute equilibrium and Dr. Rhines is certainly correct on this point. However, we do know that a strained lattice may have a practical stability. The distinction between absolute equilibrium of the T-O-C diagram and the equilibria of the P-T-C space diagram may be made by terming the latter "metastable."

The research of Bridgman on the effect of high *pressures* (compression) on metals and alloys has not received the attention of metallurgists and extrapolation to practical applications that it merits. Thus equilibria for pure metals have been plotted as T-O-P diagrams and pressures in the range of 10,000 to 20,000 atmospheres (147,000 to 294,000 pounds per square inch) induce allotropic modifications of metal lattices. The results, for instance, of Wilson's study[12] of the effect of elevated pressures (80,000 to 120,000 pounds per square inch, hydrostatic) and temperatures (40 to 400 degrees Cent.) on 75-25 Alpha brass show that an ordered phase in Alpha brass was promoted by pressure. It seems probable that variation of solid solubility in aluminum-alloys of the normally precipitation hardening class would be a comparatively slight effect and might be induced by strains in the range 2000 to 4000 atmospheres.

The author makes this presentation chiefly for the purpose of emphasizing the possibility of fostering real errors by too broad an application of the Metallurgists' abrogated phase rule wherein "pressure" is assumed to be always constant at 14.7 pounds per square inch.

---

[11] "Principles of Phase Diagrams," by J. S. Marsh, p. 14.
[12] T. C. Wilson, *Physical Review*, Vol. 56, 1939, p. 598.

THE VARIATION OF THE STRENGTH, RESISTANCE TO OXIDATION, AND ELECTRICAL CONDUCTIVITY OF METALS WITH TEMPERATURE

By D. J. McAdam, Jr. and G. W. Geil

Abstract

Additional evidence is presented that the strength of metals varies linearly with temperature represented on Kelvin's original thermodynamic scale. Diagrams derived from data presented in previous papers by the authors show that the logarithm of the oxidation-time is linearly related to temperature represented on the same scale. Data taken from the literature show that, on the same temperature scale, the logarithm of the electrical conductivity increases nearly linearly with decrease of temperature from the melting point down to the temperature of liquid air, and sometimes down nearly to the temperature of liquid hydrogen. This evidence considered in connection with the theory of the interatomic forces suggests that the strength of metals continues to increase with decrease of temperature far below that of liquid air.

The effect of temperature on electrical conductivity may be represented approximately by an equation of the same form as that representing the effect of temperature on the rate of oxidation.

Introduction

A RECENT paper by McAdam and Mebs (10)[1] discusses the variation of the strength of metals with temperature represented on a scale in which equal intervals correspond to equal thermodynamic efficiencies. This scale is the same [illegible]

reference to his second scale, which was proposed much later and is now in general use. Both scales are based on the principle of the Carnot cycle. According to the second law of thermodynamics,

$$(Q_1 - Q_2)/Q_1 = (T_1 - T_2)/T_1$$

where Q_1 is the heat added to a system at temperature T_1 (on Kelvin's second scale) and Q_2 is the heat removed at a lower temperature T_2. The term on the left of the equation represents the thermodynamic efficiency, the fraction of the transferred heat theoretically available as mechanical work. The equation may also be written in the form

$$\Delta Q/Q = \Delta T/T.$$

On Kelvin's first thermodynamic scale, equal temperature intervals correspond to equal thermodynamic efficiencies, and hence correspond to equal values of $\Delta T/T$, that is, to equal values of d log T. To represent temperature on a scale with equal intervals corresponding to equal thermodynamic efficiencies, it is not necessary to use the system of numbers proposed by Kelvin. It is necessary merely to plot on a logarithmic scale numbers taken from Kelvin's second scale. On this scale, consequently, temperature varies linearly with the logarithm of the volume of a perfect gas under constant pressure, and thus extends from $-\infty$ to $+\infty$.

As shown in the previous paper (10), the strength of metals varies linearly with temperature represented on this scale. The linear variation, however, probably is due to the influence of temperature alone. Upon the linear variation is superposed any variations of strength due to structural changes, such as strain aging. In the absence of such changes, the linear variation extends throughout a range at least from room temperature down to the temperature of liquid air (−188 degrees Cent.).

The evident advantages in the use of this scale in a study of the

THE VARIATION OF THE STRENGTH, RESISTANCE TO OXIDATION, AND ELECTRICAL CONDUCTIVITY OF METALS WITH TEMPERATURE

By D. J. McAdam, Jr. and G. W. Geil

Abstract

Additional evidence is presented that the strength of metals varies linearly with temperature represented on Kelvin's original thermodynamic scale. Diagrams derived from data presented in previous papers by the authors show that the logarithm of the oxidation-time is linearly related to temperature represented on the same scale. Data taken from the literature show that, on the same temperature scale, the logarithm of the electrical conductivity increases nearly linearly with decrease of temperature from the melting point down to the temperature of liquid air, and sometimes down nearly to the temperature of liquid hydrogen. This evidence considered in connection with the theory of the interatomic forces suggests that the strength of metals continues to increase with decrease of temperature far below that of liquid air.

The effect of temperature on electrical conductivity may be represented approximately by an equation of the same form as that representing the effect of temperature on the rate of oxidation.

Introduction

A RECENT paper by McAdam and Mebs (10)[1] discusses the variation of the strength of metals with temperature represented on a scale in which equal intervals correspond to equal thermodynamic efficiencies. This scale is the same in principle as the first of the two thermodynamic scales proposed by Kelvin (14). The principle of Kelvin's first scale may be most easily explained with

[1]The figures appearing in parentheses pertain to the references appended to this paper.

The views expressed in this paper are those of the authors, not of the National Bureau of Standards.

Of the authors, D. J. McAdam, Jr., is metallurgist, and G. W. Geil is associate physicist, National Bureau of Standards, Washington, D. C. Manuscript received September 4, 1943.

reference to his second scale, which was proposed much later and is now in general use. Both scales are based on the principle of the Carnot cycle. According to the second law of thermodynamics,

$$(Q_1 - Q_2)/Q_1 = (T_1 - T_2)/T_1$$

where: Q_1 is the heat added to a system at temperature T_1 (on Kelvin's second scale) and Q_2 is the heat removed at a lower temperature T_2. The term on the left of the equation represents the thermodynamic efficiency, the fraction of the transferred heat theoretically available as mechanical work. The equation may also be written in the form

$$\Delta Q/Q = \Delta T/T.$$

On Kelvin's first thermodynamic scale, equal temperature intervals correspond to equal thermodynamic efficiencies, and hence correspond to equal values of $\Delta T/T$, that is, to equal values of d log T. To represent temperature on a scale with equal intervals corresponding to equal thermodynamic efficiencies, it is not necessary to use the system of numbers proposed by Kelvin. It is necessary merely to plot on a logarithmic scale numbers taken from Kelvin's second scale. On this scale, consequently, temperature varies linearly with the logarithm of the volume of a perfect gas under constant pressure, and thus extends from $-\infty$ to $+\infty$.

As shown in the previous paper (10), the strength of metals varies linearly with temperature represented on this scale. The linear variation, however, probably is due to the influence of temperature alone. Upon the linear variation is superposed any variations of strength due to structural changes, such as strain aging. In the absence of such changes, the linear variation extends throughout a range at least from room temperature down to the temperature of liquid air (—188 degrees Cent.).

The evident advantages in the use of this scale in a study of the variation of mechanical properties with temperature suggested that the scale may be of value in a study of the variation of some physical and physico-chemical properties. For this purpose, curves of variation of atomic heat and total heat with temperature were included in the previous paper (10). These curves, however, show no significant correlation with the straight lines representing the variation of strength of metals with temperature represented on the principle of Kelvin's original scale.

The present paper presents results of additional study of the

variation of the strength of metals with temperature represented on this scale. The diagrams illustrating this variation are derived from data presented in the previous paper (10) and partly from the results of additional experiments. Attention is then given to the variation of the resistance of metals to oxidation at elevated temperatures. The diagrams illustrating this variation are derived from data in two previous papers by the authors (7, 8), but the diagrams have been modified so as to reveal the variation of resistance to oxidation with temperature represented in a scale of equal thermodynamic efficiencies. This relationship was not perceived at the time of publication of the two previous papers (7, 8). The paper then discusses the variation of electrical conductivity with temperature represented on this scale. The data on electrical conductivity were obtained by a survey of the literature.

The Variation of the Strength of Metals with Temperature

The investigation described in the previous paper (10) involved tension tests of notched and unnotched specimens at various temperatures. By the use of notched specimens a study was made of the influence of temperature and of the combination of principal stresses on the yield stress, ultimate stress, technical cohesion limit, and ductility. In this paper, attention will be given to strength indices obtained by tension tests of unnotched specimens. Tests of each metal were made at room temperature, in a mixture of carbon tetrachloride and chloroform cooled by solid CO_2 (—78 degrees Cent.), and in liquid air (—188 degrees Cent.). Some tests were made at 100 degrees or higher, and some were made at —110 to —128 degrees Cent. by use of the compound CCl_2F_2 cooled by liquid air. Details of the testing procedure are given in the previous paper (10).

To avoid local elevation of the temperature during plastic extension, the tensile load was applied more slowly than is usual in a tension test. Avoidance of local heating during a test at low temperature is important because work hardening increases with decrease in the temperature. Satisfactory results, therefore, cannot be obtained by loading rapidly at first and then decreasing the rate before the load reaches the maximum.

Some results of the investigation are shown in Figs. 1 and 2. The strength indices represented are the yield stress, ultimate stress, and "true" breaking stress. Temperature is represented on the pre-

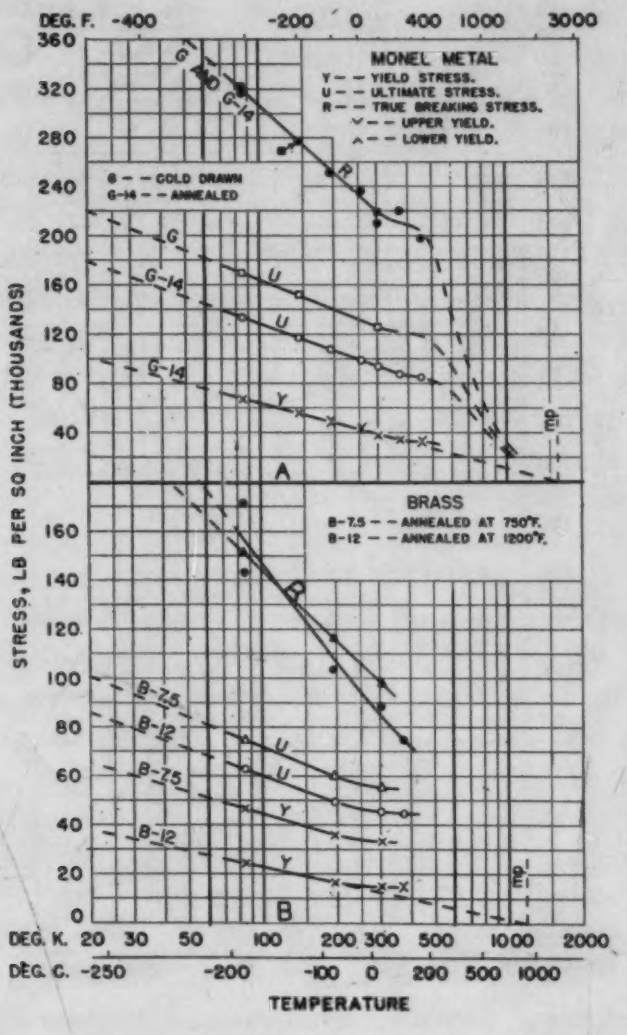
DEG. F. -400 -200 0 400 1000 3000
MONEL METAL
Y - - YIELD STRESS.
U - - ULTIMATE STRESS.
R - - TRUE BREAKING STRESS.
V - - UPPER YIELD.
Λ - - LOWER YIELD.
G - - COLD DRAWN
G-14 - - ANNEALED
BRASS
B-7.5 - - ANNEALED AT 750°F.
B-12 - - ANNEALED AT 1200°F.
STRESS, LB PER SQ INCH (THOUSANDS)
DEG. K. 20 30 50 100 200 300 500 1000 2000
DEG. C. -250 -200 -100 0 200 500 1000
TEMPERATURE

Fig. 1—Variation of the Strength of Monel Metal and Brass with Temperature.

viously mentioned scale. In future reference to temperature without qualification, it will be implied that temperature is expressed in terms of this scale.

Figs. 1A and 2B show results obtained with monel metal and oxygen-free copper. The data here shown are reproduced from Figs. 19A and 20, respectively, of the previous paper (10), but the temperature ranges have been extended so as to include the melting points of these metals. Throughout a range extending from —188 degrees Cent. (85°K) to room temperature (about 300°K) or higher, the ultimate stress of each of these metals, either in the cold drawn or in the fully annealed condition, varies linearly with the

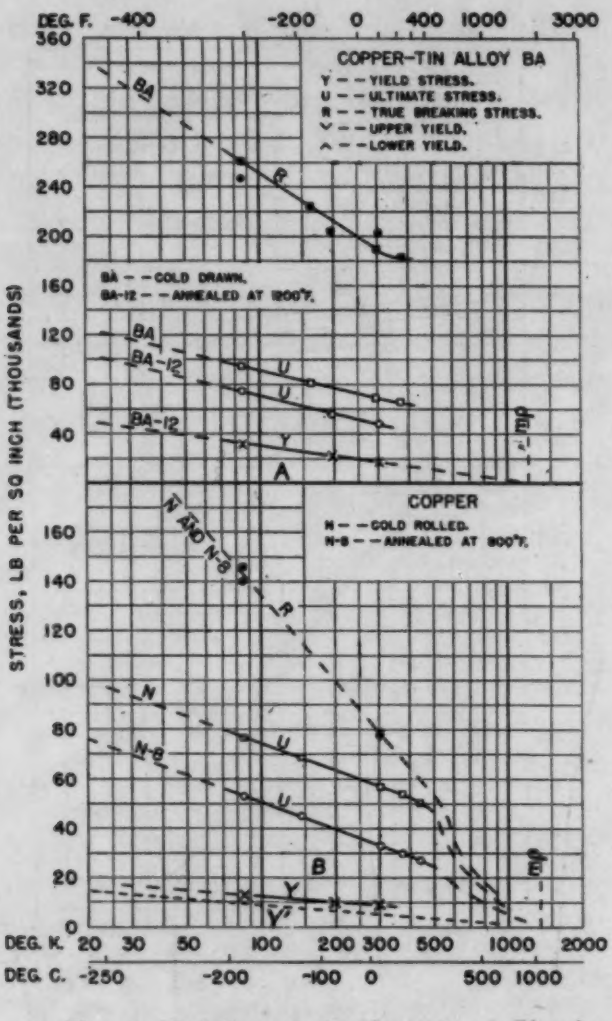
DEG. F. -400 -200 0 400 1000 3000
COPPER-TIN ALLOY BA
Y - - YIELD STRESS.
U - - ULTIMATE STRESS.
R - - TRUE BREAKING STRESS.
V - - UPPER YIELD.
Λ - - LOWER YIELD.
BA - - COLD DRAWN.
BA-12 - - ANNEALED AT 1200°F.
COPPER
N - - COLD ROLLED.
N-8 - - ANNEALED AT 800°F.
STRESS, LB PER SQ INCH (THOUSANDS)
DEG. K. 20 30 50 100 200 300 500 1000 2000
DEG. C. -250 -200 -100 0 500 1000

Fig. 2—Variation of the Strength of Phosphor Bronze and Copper with Temperature.

temperature. The exactness of this linear relationship is remarkable. In many tests made after discovery of the relationship, values of the ultimate stress were predicted accurately (frequently within about 0.5 per cent) either by long extrapolation downward to —188 degrees Cent. or by interpolation between the extremes of the temperature range. The yield stress of the monel metal (Fig. 1A) also varies linearly throughout the range between —188 and +100 degrees Cent. Moreover, the breaking stress values for both annealed and cold-drawn monel metal can be represented by a single line, which is practically straight between —188 degrees Cent. and room temperature. For the oxygen-free copper, the breaking stress can be determined only by indirect methods because of the delayed

progress of the fracture from the center to the circumference of the cross section (9). The evidence, however, seems to indicate that a single line can be used to represent the variation of the true breaking stress with temperature (Fig. 2B).

For the annealed copper (Fig. 2B), the linear relationship persists at least to 165 degrees Cent. For severely cold-rolled copper, however, softening evidently begins not far above 100 degrees Cent. For monel metal, the variation of the ultimate stress and yield stress becomes curvilinear with increase in the temperature above 100 degrees Cent. The breaking stress of both annealed and cold-drawn monel metal varies curvilinearly above room temperature. The evidence indicates that not far above room temperature the strength of monel metal is influenced by an elevating factor which is superposed on the variation of the strength due to temperature alone. This elevating factor is strain aging. Although strain aging is most prominent in low carbon steels, it influences the properties of many nonferrous metals. As shown in the previous paper (10), strain aging evidently has considerable effect on the properties of nickel and even of high purity aluminum. The strength of these two metals varies linearly with temperature from —188 degrees Cent. to above the temperature of solid CO_2 (—78 degrees Cent.). With further increase in temperature, however, a curvilinear relationship begins, which is qualitatively similar to that shown in the curves for annealed monel metal (Fig. 1). Strain aging evidently becomes appreciable at much lower temperatures for these metals than for monel metal.

Fig. 1B shows results of experiments with brass in two degrees of hardness caused by annealing cold-worked brass at two different temperatures, 370 and 650 degrees Cent. (700 and 1200 degrees Fahr.). Annealing at 370 degrees Cent. (700 degrees Fahr.) caused only partial softening; for full annealing, the higher temperature was required. The variation of the strength of the brass with temperature probably is linear from —188 degrees Cent. to about —78 degrees Cent.; above —78 degrees Cent., a curved relationship begins because of strain aging. (That brass is subject to strain aging has been shown by Broniewski and Wesolowski (1) and by others.

Fig. 2A shows results obtained with phosphor bronze. Results obtained with the cold-drawn alloy are reproduced from Fig. 23 of the previous paper (10); the diagram for the annealed alloy is the result of more recent experiments. With the cold-drawn alloy, an exactly linear relationship was found for both the ultimate stress and

the breaking stress between —188 degrees Cent. and room temperature. Above room temperature, a curved relationship begins because of strain aging. With the annealed alloy, an approximately linear relationship was found for ultimate stress and yield stress between —188 degrees Cent. and room temperature. The breaking stress, however, shows a curved relationship beginning at about —78 degrees Cent. It is probable, therefore, that a slight effect of strain aging becomes perceptible even for the yield stress and ultimate stress at some temperature between —78 degrees Cent. and room temperature, and thus causes a slight curvature within this range.

In the previous paper (10) evidence was presented to show the effect of temperature on the ultimate stress and breaking stress of heat treated 0.2 per cent carbon steel and of a heat treated 3 1/2T nickel steel (S.A.E. 2330). An exactly linear relationship was found for the ultimate stress of each of these steels between —188 degrees Cent. and room temperature. The breaking stress of the carbon steel also varied nearly linearly throughout the same temperature range, and the breaking stress of the nickel steel varied linearly between room temperature and —128 degrees Cent. Above room temperature, the ultimate stress of the nickel steel showed the elevating effect of strain aging. For notched specimens also, the ultimate stress was found to vary linearly throughout the range from —188 degrees Cent. to room temperature; this relationship was found with monel metal, copper, and 13:2 chromium-nickel steel (10).

The evidence suggests that the resistance of metals to plastic deformation, as expressed by either the yield stress or ultimate stress, varies linearly with temperature (on this scale) throughout a range from —188 degrees Cent. to room temperature or higher, provided that this relationship is not masked by the influence of structural changes such as strain aging. The technical cohesive strength also varies nearly, if not quite, linearly throughout the same temperature range.[2] This is shown by results obtained with notched specimens (10), and is suggested also by the linear variation of the breaking stress of unnotched specimens of some metals.

Speculation about the slopes of the straight portions of the lines of variation of strength with temperature led to the surmise that pro-

---

[2]As shown in the previous paper (10), the variation of the breaking stress of an unnotched specimen with temperature is due not only to the influence of temperature on the technical cohesive strengh, but also to the influence of temperature on three other variables: (a) the total plastic deformation (ductility), (b) the radial stress induced by the notch effect of the local contraction, and (c) the rate of work hardening during the tension test.

longations of these portions would be significantly related to the melting point of the metal. For this reason, the temperature range has been extended in Figs. 1 and 2 so as to include the melting points. The straight portions of the lines representing ultimate stress and breaking stress, if prolonged, would pass considerably above a point representing zero stress at the melting point. A similar relationship is found for lines representing the yield stress for cold-worked metal.[3] A different relationship, however, is found for the lines representing the yield stresses of annealed monel metal, annealed brass, and annealed phosphor bronze. Prolongations of the straight portions of these lines pass nearly, if not exactly, through the points representing zero stress at the melting point. For annealed copper (Fig. 2), line Y representing the yield stress as determined from an automatic diagram passes above the point representing zero stress at the melting point. These stresses, however, are far above the stress at which plastic deformation begins. Plastic deformation of 0.02 per cent is induced by a stress of only 5500 pounds per square inch at room temperature. Line Y′, drawn parallel to Y through the point representing this stress at room temperature, passes through the point representing zero stress at the melting point. The evidence thus suggests that, if plastic deformation of about 0.02 per cent is taken as a criterion for yield, the position of the melting point may determine the slope of the line representing yield of an annealed metal.

The actual course of a curve of variation of yield stress, ultimate stress or breaking stress between room temperature and the melting point, however, generally is not determined by the slope of the straight portion. The actual course is influenced not only by any strain aging that may occur within this temperature range, but also by another factor, the rate of plastic deformation. Throughout the range from —188 degrees Cent. to room temperature, the influence of the rate of deformation on the strength indices generally is slight.[4] With increase above room temperature, however, the influence of the rate of deformation becomes increasingly important. The variation of the resistance to plastic deformation within this range of temperature, therefore, cannot be represented by a single line, but must be represented by a series of lines, each corresponding to a specific rate of deformation. In Figs. 1 and 2, broken lines have been added

[3]The yield stress line for a severely cold-worked metal would be not far below the ultimate stress line.

[4]This statement does not apply to metals with low melting point, such as lead and tin.

to represent qualitatively the variation of the strength indices for a rate of deformation that is very high with reference to that of a creep test, but is not far from the rate generally used in an ordinary tension test.

The Variation of the Resistance of Metals to Oxidation with Temperature

Two previous papers by the authors discuss the influence of temperature and time on the resistance of metals to oxidation (7, 8). The resistance to oxidation is evaluated in terms of the times required for the oxide film to reach various definite thicknesses, which are indicated by interference colors. Diagrams of one of the three types presented show the relation between temperature and oxidation time for various constant interference colors (constant film thicknesses). Although temperature was then represented in terms of the logarithm of degrees K, the essential identity between this scale and Kelvin's original thermodynamic scale was not realized, and this identity was obscured by the logarithmic plotting of values of the tenth power of the number of degrees K. In this paper, data obtained with a number of metals have been replotted so as to show the relation between oxidation time and temperature represented on the principle of Kelvin's original thermodynamic scale.

Colors of oxide films are caused by interference between rays of light reflected from the inner and outer surfaces of the film. The coincidence of two waves differing in phase by 180 degrees causes the disappearance of light of a certain wave-length; if the incident light is "white", therefore, the reflected light is of the corresponding complementary color. Interference occurs when the film thickness is an odd multiple of one-fourth the wave-length of a component of the incident light. Interference, however, is determined by the wave-length in the film, not by the wave-length in air. The index of refraction, therefore, is a factor involved in the relation between wave-length, film thickness, and interference color.

As the film thickness increases, a light straw color appears first, and the color then changes gradually through reddish brown and purple to blue. With most metals, the series of colors is then repeated, and with some metals, third and even fourth order colors may be obtained. In the two previous papers (7, 8), a study is thus made of the rate of oxidation of steels and typical non-ferrous metals

as affected by composition, temperature, oxidation time, and film thickness. The results are presented in diagrams of three types. The first type shows the relation between temperature and oxidation time, for constant interference colors (constant film thicknesses). The second type shows the relation between oxidation time and film thickness for constant temperatures. The third type shows the relation between temperature and film thickness, for constant oxidation times. In the present paper, however, attention will be confined to diagrams of the first type, which are designed to reveal the relation between oxidation time and temperature. These diagrams are shown in Figs. 3 and 4.

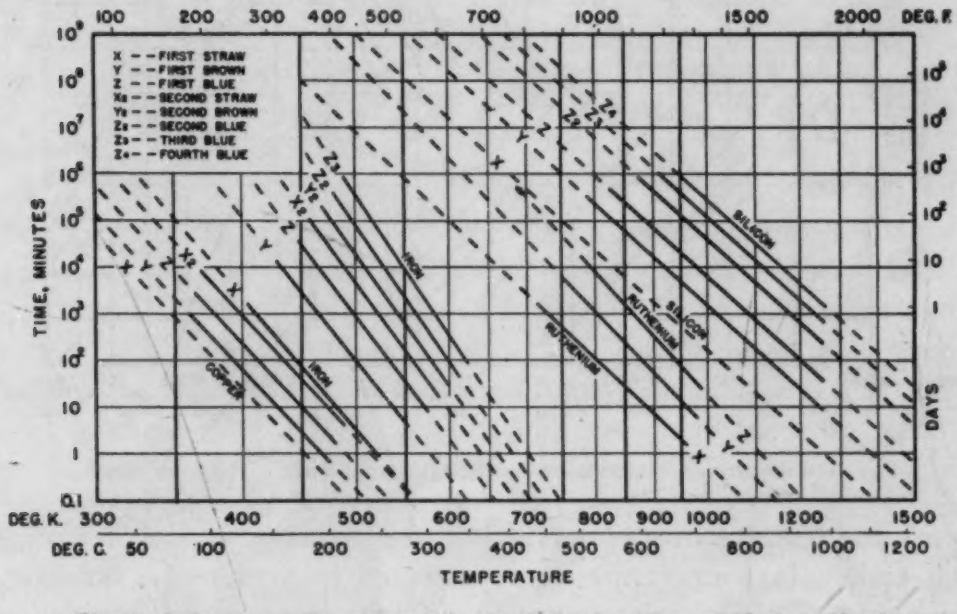
100 200 300 400 500 700 1000 1500 2000 DEG. F
X — FIRST STRAW
Y — FIRST BROWN
Z — FIRST BLUE
X2 — SECOND STRAW
Y2 — SECOND BROWN
Z2 — SECOND BLUE
Z3 — THIRD BLUE
Z4 — FOURTH BLUE
TIME, MINUTES
DAYS
COPPER
IRON
RUTHENIUM
SILICON
DEG. K. 300 400 500 600 700 800 900 1000 1200 1500
DEG. C. 50 100 200 300 400 500 600 800 1000 1200
TEMPERATURE

Fig. 3—Influence of Temperature on the Oxidation Time of Various Metals.

Temperatures are represented on a scale of equal thermodynamic efficiencies, and consequently in terms of logarithms of numbers of degrees K. Oxidation times also are represented on a logarithmic scale. To give a convenient slope to the lines representing the relation between temperature and oxidation time, the abscissa scale has been made 50 times the ordinate scale. This expedient is believed to be better than the one used in the previous papers, namely, plotting oxidation times against the tenth power of the temperatures (in degrees K).

Each diagram representing the resistance of a metal to oxidation consists of a number of lines, each showing the relation between

temperature and oxidation time for the indicated interference color. Each of these lines is straight. That this linear relationship is exact is well established in the original papers (*7*, 8) by numerous experiments covering wide ranges of temperature and oxidation time. The solid portions of the lines in Figs. 3 and 4 are the portions established by experiment; the broken portions are mere prolongations of the established lines. The lines show an exactly linear relationship between the logarithm of the oxidation time (for constant film thick-

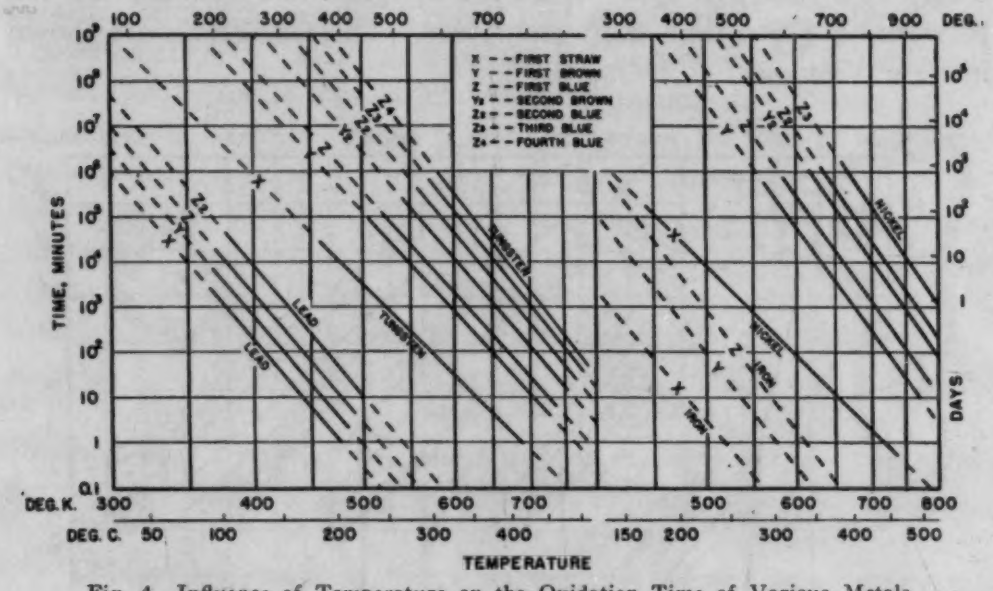

Fig. 4—Influence of Temperature on the Oxidation Time of Various Metals.

ness) and temperature represented on the principle of Kelvin's original scale. If temperature be represented in degrees K, however, the oxidation time varies inversely, and the mean rate of oxidation varies directly as a power of the temperature. This relationship may be derived from the equation:

$\log t_2 - \log t_1 = n (\log T_1 - \log T_2)$, where $\log t_1$, $\log T_1$, $\log t_2$ and T_2 represent the co-ordinates of two points on a straight line (Figs. 3 and 4), and "n" represents the cotangent of the angle of slope, with due allowance for the difference in scales. This equation may be changed to the form:

$t_2/t_1 = (T_1/T_2)^n$, which shows that the oxidation time (for constant film thickness) varies inversely as the nth power of the temperature in degrees K. The mean rate of oxidation, because it is proportional to the reciprocal of the oxidation time, varies directly as the nth power of the temperature in degrees K.

The evidence presented thus far shows linear variation of indices of two properties of metals with temperature represented on this scale. These indices are strength and the logarithm of the mean rate of oxidation. These variations will be discussed further after the presentation of evidence for an approximately linear variation of the logarithm of a third property with temperature represented on the same scale.

The Variation of the Electrical Conductivity of Metals with Temperature

Handbooks and other compilations generally give values of electrical resistance rather than values of conductivity. The values are generally given in tabular form and there are few curves of variation of either conductivity or resistance. Moreover, the generalizations made about the influence of temperature on electrical resistance frequently are inaccurate or incorrect. The authors, therefore, have made a search of the literature in order to assemble data on the influence of temperature on the electrical conductivity of many of the metallic elements and some alloys. Use has been made of the International Critical Tables (6), the Handbook of Chemistry and Physics (5), Landolt and Börnstein (11), etc. Considerable data, however, have been obtained from original publications. Results have been assembled in Figs. 5 to 12; the sources of the information have been indicated by means of the special symbols.

Brief attention will be given first to the variation of conductivity with temperature represented on the usual Kelvin scale. Typical curves on this scale are shown in Fig. 5. Because of the wide range of values of conductivity, these values are plotted on a logarithmic scale. Even on this scale of ordinates, the curves become so steep at low temperatures that they do not give a clear view of the variation of conductivity with temperature. The accelerated rise of these curves with decrease of temperature, however, is qualitatively similar to the rise of curves of variation of the strength of metals, when plotted on this scale (10).

Figs. 6 to 12 show the variation of the electrical conductivity of a number of metals and alloys with temperature. The curves in each figure have generally been placed on separate abscissa scales, which are indicated by numbers adjacent to each curve. Abscissas are logarithms of degrees K; ordinates are logarithms of electrical conductivities.

The curves are grouped in accordance with the periodic system of the elements. The distribution is as follows: Figs. 6 and 7, the two subdivisions of Group I; Fig. 8, Group II; Fig. 9, Groups III and IV; Fig. 10, Groups V and VI; Figs. 11 and 12, Group VIII. Curves for alloys are shown in Figs. 7, 11, and 12.

The graphs generally are approximately[5] straight throughout a temperature range from the melting point of the metal at least down to the boiling point of liquid air (—188 degrees Cent., 85°K), and

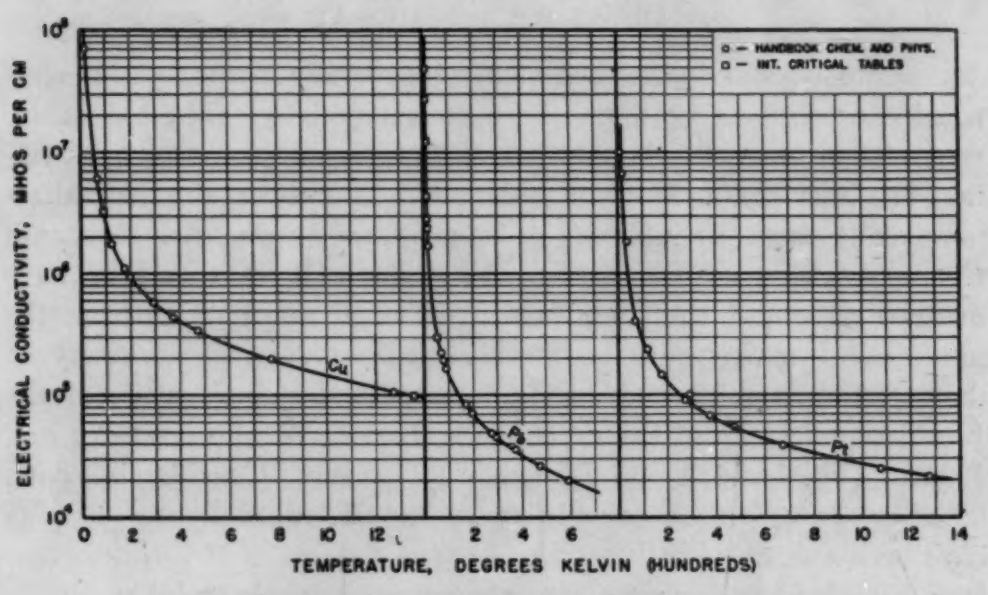

Fig. 5—Variation of Electrical Conductivity with Temperature.

sometimes down almost to the boiling point of liquid hydrogen (20.5°K). Some of the graphs then turn abruptly to the left and become practically horizontal. Such is the form of the graphs for lithium, potassium, rubidium, and cesium (Fig. 6), for beryllium and magnesium (Fig. 8), for indium (Fig. 9), for bismuth and molybdenum (Fig. 10), and for iron, cobalt, and nickel (Fig. 11). Some graphs, however, curve abruptly upward to a much higher level, and then become practically horizontal. Such is the form of the graph for sodium (Fig. 6), the graphs for zinc and cadmium (Fig. 8), for tin and lead (Fig. 9), for tungsten (Fig. 10), and for palladium, rhodium and platinum (Fig. 12).

The course of a graph at temperatures below the nearly straight portion, however, depends considerably on the purity of the metal.

[5]For platinum and copper, the use of the term "approximately" possibly is not justifiable.

As shown in Fig. 7, the graphs for high purity copper and gold turn upward to a much higher level, whereas the graphs for the less pure copper and gold turn to the left and become practically horizontal. A similar difference in purity probably is the cause of the difference between the graph for sodium and the graphs for the other metals of that group (Fig. 6). The graph for high purity iron, however, remains practically straight down almost to the temperature of liquid hydrogen, then abruptly ceases to rise. It is uncertain

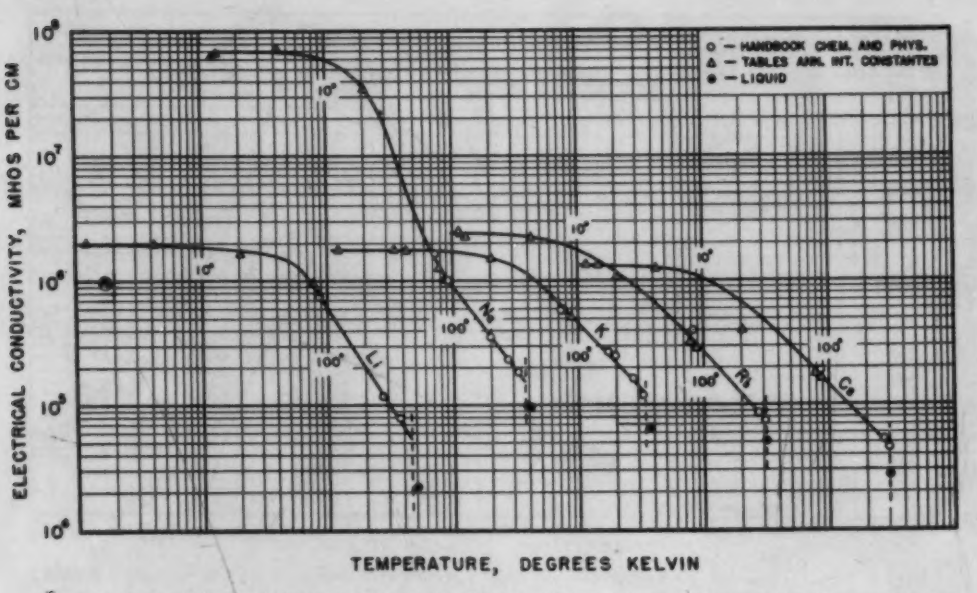

Fig. 6—Variation of Electrical Conductivity of the Alkali Metals with Temperature.

whether a graph for iron of still higher purity would eventually turn upward. Moreover, it is uncertain whether or not the curve for every metal of sufficient purity would be similar in form to the curve for sodium (Fig. 6).

A curve of this type does not necessarily imply that the metal will become superconducting[6] at sufficiently low temperature. Of the metals represented in Figs. 6 to 12, only zinc, cadmium, aluminum, indium, thallium, tin, and lead have proved to be superconducting.

Although the variation of electrical conductivity of metals with temperature generally can be represented approximately by straight lines such as those shown in Figs. 6 to 12, this variation generally is not exactly linear. For a few metals, such as silver, the relationship may be represented with considerable accuracy by a straight

[6]Superconductivity manifests itself by a nearly vertical rise of the curve at a certain temperature, and an abrupt drop at a slightly lower temperature.

line, on this scale. For most metals, however, the relationship is less simple, and an exact representation requires an equation with three or more terms. If the relationship were exactly linear, it could be represented by the equation $C_1/C_2 = (T_2/T_1)^n$, where C_1 is the electrical conductivity at temperature T_1 (in degrees K), C_2 is the conductivity at a higher temperature T_2, and "n" is the slope of the graph. The electrical conductivity, between the melting point and the lower limit of the linear relationship, would thus vary inversely

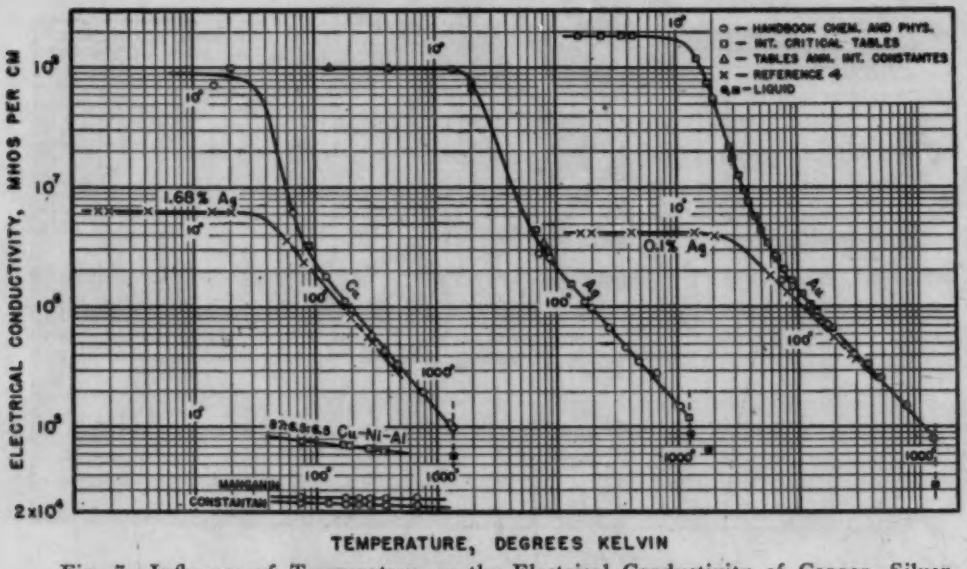

Fig. 7—Influence of Temperature on the Electrical Conductivity of Copper, Silver, Gold and Some of Their Alloys.

as a power (n) of the temperature in degrees K.[7] Values of "n" for the metals represented in Figs. 6 to 12 are listed in Table I. The value ranges from a small fraction for many alloys to nearly 2.0 for iron, cobalt, and nickel (Fig. 11). For many of the metals, "n" is only slightly greater than 1.0; the electrical resistance of these metals (throughout this temperature range) thus varies nearly linearly with T. For iron, cobalt, and nickel, however, the electrical resistance varies nearly as T^2.

General Discussion of the Variation of the Strength of Metals, the Rate of Oxidation, and the Electrical Conductivity with Temperature

For many physical and chemical reactions, investigators have found a linear relationship between the logarithm of the index of the

[7] If temperature is measured on a scale of equal thermodynamic efficiencies, the relationship would be represented by $C = e^{-n}L$, where "L" is the temperature on this scale.

Table I
Indices of Variation of Electrical Resistance with Temperature

I		II	III	IV	V	VI	VII		
Li 1.60	.....	Be 1.53	.....	.....	.....	.....	.....	.....	.....
Na 1.37	.....	Mg 1.29	Al 1.22	.....	.....	.....	.....	.....	.....
K 1.12	.....	.....	.....	.....	.....	.....	Fe 1.91	Co 1.59	Ni 1.98
.....	Cu 1.20	Zn 1.20	.....	.....	.....	.....	.....	.....	.....
Rb 1.12	.....	.....	.....	.....	.....	Mo 1.20	.....	Rh 1.14	Pd 1.11
.....	Ag 1.14	Cd 1.14	In 1.13	Sn 1.12	Sb 0.98	.....	.....	.....	.....
Co 1.04	.....	.....	.....	.....	.....	W 1.23	.....	.....	Pt 1.00
.....	Au 1.09	.....	Tl 1.27	Pb 1.14	Bi 0.98	.....	.....	.....	.....

property and the reciprocal of the temperature expressed in degrees K. Reported examples of such properties are: the equilibrium constant of a chemical reaction, the coefficient of viscosity of glass, and the rate of diffusion of metals into each other. The theoretical basis for such a relationship is Boltzmann's conception of the probability of occurrence of a physical phenomenon. On this basis, Becker developed a dynamic theory of the flow of metals and their resistance to plastic deformation. According to his equation, $U = C \cdot e^{-V(S-s)^2/2GkT}$, where U is the velocity of flow, V is a constant involving the modulus of elasticity, G is the shear modulus, C and k are constants, T is temperature in degrees K, S is the theoretical shearing stress, and s is the actual resolved shearing stress. From this equation, Orowan derived the following equation to represent the variation of the shearing stress with temperature. $\sigma = \sigma_0 - B\sqrt{T}$, where B is a constant, σ is the shearing stress at temperature T, and σ_0 is the shearing yield stress at absolute zero. According to this equation, the resistance of metals would be represented by a parabola starting from a finite ordinate at absolute zero. However, the actual variation of the strength of metals, as represented in Figs. 1 and 2, is very different. The straight sloping lines in these figures would not yield parabolas if transferred to Kelvin's second scale.

This correlation between the strength of metals and electrical conductivity appears to be of both theoretical and practical importance. According to the theory, both the forces of interatomic cohesion and the electrical conductivity are referable to the influence of the quasi-free electrons. The cohesion of the atoms of the space lattice is thought to be due to the attraction of the atoms for the electron "gas", and the electrical conductivity is due to the mobility of the electrons under the influence of an electromotive force. However, a comparison of the slopes of the lines of variation of strength

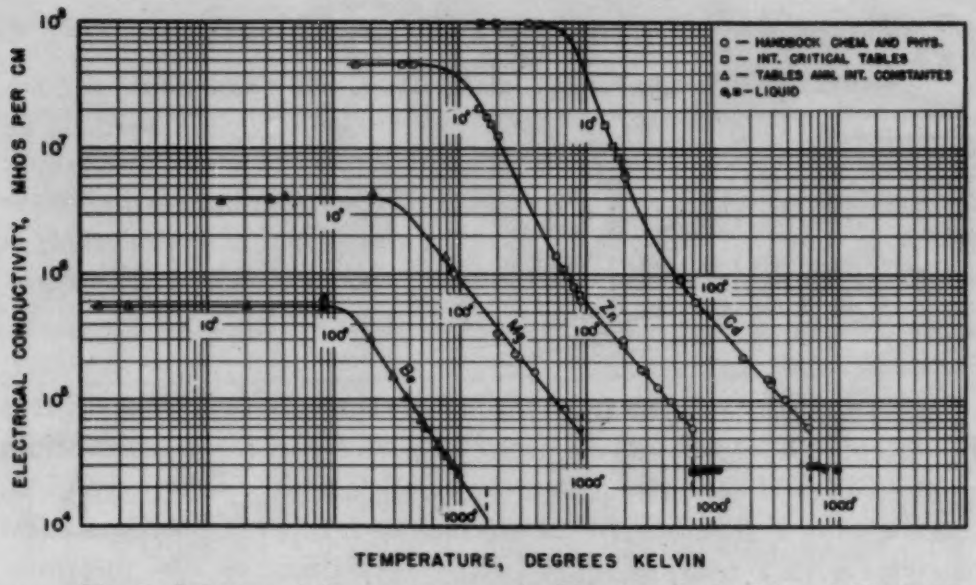

Fig. 8—Influence of Temperature on the Electrical Conductivity of Metals of Group II.

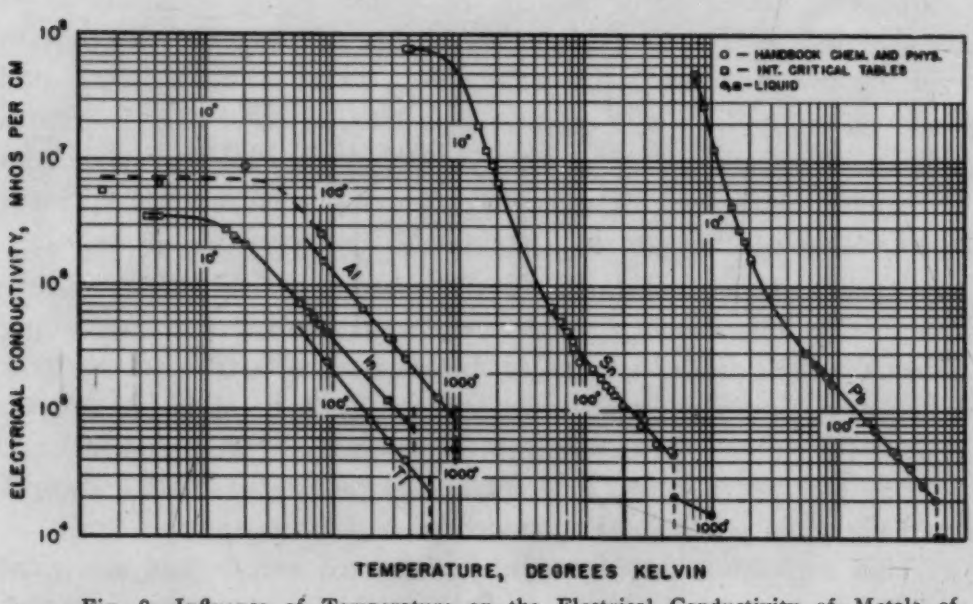

Fig. 9—Influence of Temperature on the Electrical Conductivity of Metals of Groups III and IV.

with the lines of variation of electrical conductivity (Figs. 6 to 12 and Table II) gives no basis for a supposition that the cohesive forces are a direct function of the electrical conductivity. Although the electrical conductivities of constantan, manganin, and aluminum bronze rise very little with decrease of temperature (Fig. 7), there is no reason to believe that the strength of these alloys rises much

Table II
Indices of Variation of Electrical Conductivity with Temperature

Alloy	n
Copper with 1.68% Ag	1.20
84:12:4 Cu-Mn-Ni[1]	0.015
60:40 Cu-Ni[2]	0.033
87:6.5:6.5 Cu-Ni-Al	0.12
Gold with 0.1% Ag	1.00
Fe (99.98% pure)	1.74
0.45% carbon steel	1.56
75:25 Fe-Ni	0.24
70:30 Ni-Fe[3]	1.30
90:10 Pt-Rh[4]	0.32
80:20 Pt-Ir[4]	0.16

[1]Electrical resistance alloy, Manganin.
[2]Electrical resistance alloy, Constantan.
[3]Alloy used in resistance thermometry.
[4]Thermocouple alloys.

less rapidly than the strength of monel metal, copper or nickel (10). Moreover, although the electrical conductivity of the 25:75 nickel-iron alloy (Fig. 11) and of the platinum alloys (Fig. 12) rises very slowly with decrease of temperature, the strength of these alloys probably rises much more rapidly.

The evidence, therefore, indicates that, although the strength of any given metal varies nearly linearly with the logarithm of its conductivity, the variation of the conductivity is not a quantitative index of the variation of the strength of that metal with temperature. Moreover, the relative strength of two metals at the same temperature cannot be deduced from a comparison of their electrical conductivities.

Two important factors tending to decrease electrical conductivity are: (a) space lattice distortion due to atoms of an alloying element, and (b) the thermal oscillations of the atoms. The increase of electrical conductivity with decrease of temperature is thought to be due chiefly to the decrease of the thermal oscillations. The increase in the interatomic cohesion with decrease in temperature, however, may be due chiefly to an increase in the frequency of interchange of electrons between adjacent atoms of the space lattice. According to theory (3), the cohesive force between the atoms of a molecule or between adjacent atoms of a space lattice depends largely on the frequency of the interchange of electrons between adjacent atoms. The frequency (ν) is proportional to the latent heat of evaporation (L). It appears possible that ν and L (like the logarithm of the electrical conductivity) increase linearly with decrease

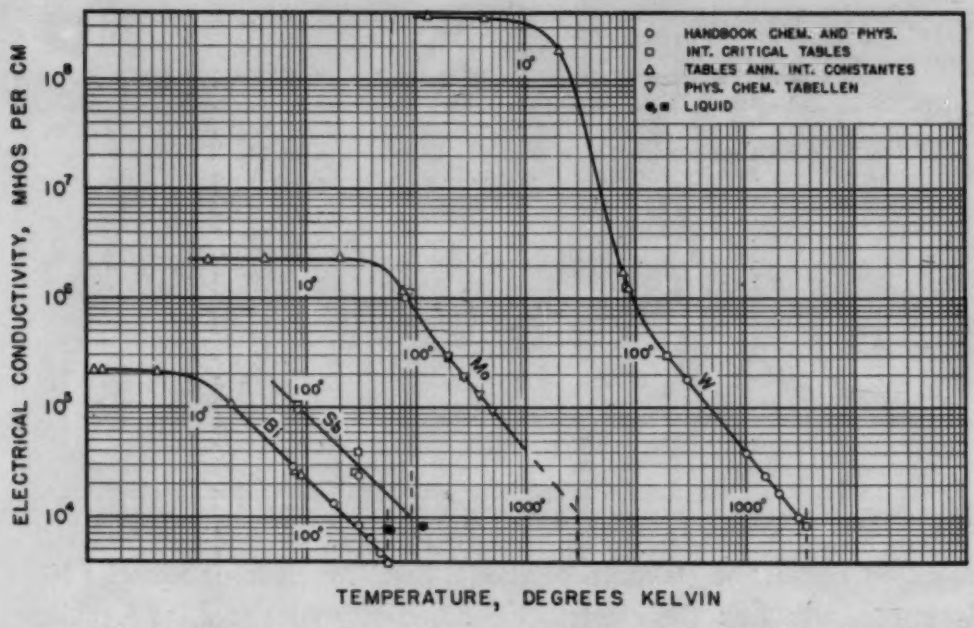

Fig. 10—Influence of Temperature on the Electrical Conductivity of Metals of Groups V and VI.

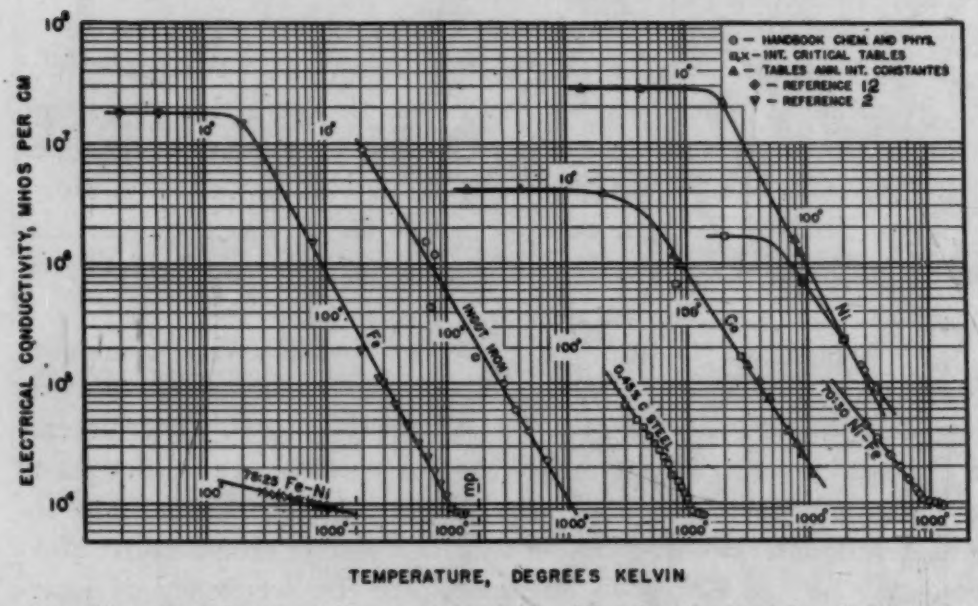

Fig. 11—Influence of Temperature on the Electrical Conductivity of Iron, Cobalt and Nickel.

of temperature, on a scale of equal thermodynamic efficiencies. If so, ν (for any given metal) would vary nearly linearly with log C. This subject, however, needs much additional investigation.

The generally continued increase in *electrical conductivity* with decrease in temperature below that of liquid air adds support to the

view that the strength of metals generally continues to increase with further decrease of temperature. It is uncertain, however, whether the steep upturn of some of the curves of electrical conductivity is associated with a similar rise of the strength of these metals. There is need for an investigation to determine whether or not the linear variation of the strength of metals continues down to the temperature of liquid hydrogen.

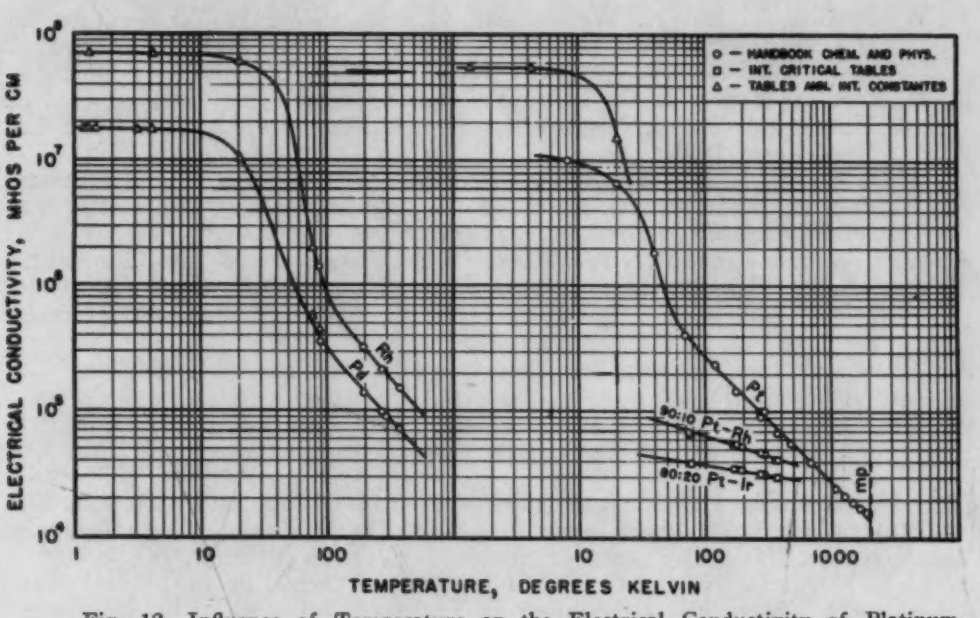

Fig. 12—Influence of Temperature on the Electrical Conductivity of Platinum Metals.

Oxidation of a metal, after the first adherent film of oxide has formed, proceeds by movement of ions and electrons through the film (7, 8). The film consists of a space lattice of electropositive metal ions and electronegative oxygen ions. During oxidation, metal ions and an equivalent number of electrons leave the metal, enter the film, and move outward toward the film-gas interface. The oxygen ions in the film, however, are too large to diffuse inward, because each oxygen atom has acquired two electrons on taking its place in the film. The growth of the film, therefore, consists chiefly in the meeting of oxygen ions and outwardly diffused metal ions at the film-gas interface.

The oxidation of a metal, therefore, involves electrical conductance, and the rate of oxidation depends in part on the electrical conductivity of the film. The evidence presented indicates that the effect of temperature on this electrochemical reaction may be repre-

sented by an equation of the same form as that representing approximately the influence of temperature on the electrical conductivity of a metal. For the rate of oxidation of a metal, however, the linear relationship with temperature (on this scale) is exact; for electrical conductivity, the relationship generally is only approximate.

References

1. W. Broniewski and K. Wesolowski, "L'influence de la Temperature sur les Propriétés Mecaniques des Laitons," *Rev. de Met.*, Vol. 30, 1933, p. 396-401, 453-457.
2. H. E. Cleaves and J. G. Thompson, "The Metal Iron," Alloys of Iron Monograph Series, Engineering Foundation. McGraw-Hill Book Co., New York, 1935.
3. S. Dushman, "Cohesion and Atomic Structure," Fourth Edgar Marburg Lecture, *Proceedings*, American Society for Testing Materials, Vol. 29, Pt. II, 1929, p. 7-64.
4. W. F. Giauque and T. W. Stout, "Induction Heaters for Calorimetry Below 1°K. An Investigation of the Electrical Resistance of Gold-Silver Alloys at Low Temperatures," *Journal*, American Chemical Society, Vol. 60, 1938, p. 388-392.
5. "Handbook of Chemistry and Physics," Chemical Rubber Publishing Co., Cleveland, Ohio.
6. "International Critical Tables of Numerical Data, Physics, Chemistry, and Technology," National Research Council, McGraw-Hill Book Co., N. Y.
7. D. J. McAdam, Jr. and G. W. Geil, "Rate of Oxidation of Steels as Determined from Interference Colors of Oxide Films," *Journal of Research*, National Bureau of Standards, Vol. 23, 1939, p. 63-124.
8. D. J. McAdam, Jr. and G. W. Geil, "Rate of Oxidation of Typical Nonferrous Metals as Determined by Interference Colors of Oxide Films," *Journal of Research*, National Bureau of Standards, Vol. 28, 1942, p. 593-635.
9. D. J. McAdam, Jr. and R. W. Mebs, "An Investigation of the Technical Cohesive Strength of Metals," American Institute of Mining and Metallurgical Engineers Technical Publication 1615; *Metals Technology*, Vol. 10, No. 5, Aug. 1943.
10. D. J. McAdam, Jr. and R. W. Mebs, "The Technical Cohesive Strength and Other Mechanical Properties of Metals at Low Temperatures," American Society for Testing Materials, Preprint No. 40, 1943 (Presented at annual meeting, 1943).
11. Landolt, Börnstein, Roth and Scheel, "Physikalische Chemische Tabellen," Julius Springer, Berlin.
12. G. C. Stauffer and M. A. Hunter, "Alloys of Iron and Nickel in Resistance Thermometry," Chapter 13 of "Temperature, Its Measurement and Control in Science and Industry," American Institute of Physics, Reinhold Publishing Corp., New York, 1941.
13. Gauthier Villars, "Tables Annuelles Internationales de Constantes et Données Numériques de Chimie, de Physique, de Biologie, et de Technologie," Paris; McGraw-Hill Book Co., New York.
14. W. Thompson, "On An Absolute Thermometric Scale Founded on Carnot's Theory of the Motive Power of Heat, and Calculated from Regnault's Observations," *Phil. Mag.*, Vol. 33, 1848, p. 313.

ARC WELDING OF ALLOY STEELS

By S. A. Herres

Abstract

Factors influencing the formation of cracks in the heat-affected zone of arc welded alloy steels were investigated. Root cracks (base metal cracks parallel and very close to the fusion zone) occur only when the weld heating and quenching cycle produces a martensitic type structure in the base metal immediately adjacent to the fusion line. They are observed only when moisture or hydrogen containing organic compounds are present in the welding atmosphere or electrode coating. Root cracks may be explained by assuming that stresses sufficient to cause the weld-hardened structure (already subject to thermal contraction and martensitic transformation stresses) to crack are contributed by precipitation of hydrogen which has dissolved in the weld metal and diffused into the weld heat-affected zone of the base metal during the welding cycle. Other types of base metal cracks are discussed.

Preheating the base metal prevents base metal cracking by slowing down the weld quenching rate, producing a more ductile heat-affected zone structure, relieving thermal contraction and martensitic transformation stresses, and permitting more opportunity for dissipation of trapped hydrogen.

Base metal cracks produced by welding process greatly accelerate failure of production weldments under shock, repeated high stress, or fatigue service loading.

IN the United States, arc welding of plain carbon structural steels was developed as a process of general importance during World War I. Since mechanical tests did not indicate any marked superiority in the quality of welds deposited with the fluxed electrodes of the time over welds made with bare electrodes, the practice of European countries in welding with fluxed electrodes was not followed. Welding equipment was modified to give a stable arc without use of

The statements or opinions expressed in this article are to be considered those of the author and do not necessarily express the views of the Ordnance Department.

The author, S. A. Herres, 1st Lieutenant, is associated with the Ordnance Department, Watertown Arsenal, Watertown, Mass. Manuscript received September 2, 1943.

fluxes, other than a superficial oxide coating, and a system of welding with bare electrodes was evolved and used almost exclusively for many years.

Bare electrode welding, while satisfactory for many purposes, results in a weld deposit with very low ductility and consequently slight resistance to shock loading. Development of electrode coatings containing combustible cellulosic matter, which surrounds the arc with a reducing atmosphere, as well as slag forming oxides, which protect the weld deposit during solidification and cooling, permitted deposition of weld metal with greatly increased ductility and shock resistance. Furthermore, the benefits of welding at greater speeds and in all positions were obtained. Arc welding application was thereby increased to include most low alloy steel structures where the steels are used in the as-rolled or normalized condition or after a subcritical stress relieving anneal (for machining and service stability). However, this process has been limited by the formation of a hard brittle martensitic zone adjacent to the weld wherein cracks very frequently occur during welding (1).[1] Thus, wherever the base metal contained sufficient alloy to form a martensitic area during the weld quenching cycle, a preheat of 300 to 500 degrees Fahr. (150 to 260 degrees Cent.) (2) was specified if the weld-affected base metal was to be free from cracks. Further, a post heat treatment at 1100 to 1200 degrees Fahr. (595 to 650 degrees Cent.) was considered desirable in order to temper the martensitic base metal zone and at the same time to relieve the thermal contraction stresses across the joint. In some instances, high alloy steels were welded with preheat to prevent formation of cracks during welding and the welded structure was given a full heat treatment. This practice is satisfactory provided that the weld metal is of suitable composition to develop similar properties to the base metal during heat treatment.

In very recent years, and particularly since this country became involved in World War II, American Industry has been called upon to apply the arc welding process to fabrication of alloy steel structures which must have considerable strength and resistance to impact loading. Steels which are commercially heat treated in heavy and sometimes complex sections must be used. Preheating and/or heat treatment after welding is often impractical.

A welding process which is applicable to heat treated, high hardenability steels without use of preheat or post heat treatment

[1]The figures appearing in parentheses refer to the bibliography appended to this paper.

and which results in a weld deposit of suitable strength and shock loading resistance was therefore required. This was accomplished through use of mineral coated austenitic electrodes of the modified 18 per cent chromium, 8 per cent nickel or 25 per cent chromium, 12 per cent nickel types. While a martensitic weld quenched zone is developed in the base metal on the first pass, base metal cracks do not ordinarily form during welding and the zone is tempered somewhat when later passes are deposited in a multiple layer weld. The weld metal deposit has the properties of reasonably high yield strength (measured at ordinary offset) and excellent ductility at any rate of strain.

Because of the obvious importance of base metal cracks which occur during or soon after welding on the performance of alloy steel weldments, and because existing theories did not entirely explain the facts, an investigation of the factors influencing formation of these cracks was undertaken at the Watertown Arsenal Laboratory.

Test Procedure

Weld bead deposits for the tests herein reported were laid down with a stick feed, automatic travel, and electrode feed welding machine. Direct current, reversed polarity, and a standard travel speed of 5 inches per minute was used for all tests. Details of test method and welding procedures are given in connection with the individual tests.

Data and Discussion

Examination of sections taken through single bead deposits on alloy structural steels of various thicknesses indicate that several different types of cracks may occur in the heat-affected base metal adjacent to a weld deposit. The three most commonly observed types of hard cracks are root cracks, toe cracks, and vertical cracks as illustrated in Figs. 1A, I B, and IC, respectively.

Fig. 2 is an attempt to list all possible factors which might influence susceptibility of a given base metal to hard cracking.

The weld bead hardness test frequently has been proposed (3) as a measure of susceptibility to hard cracking, the theory being that maximum hardness developed in the base metal under a single weld bead is a measure of the physical properties and cracking susceptibility of the base metal. Several investigators have attempted to

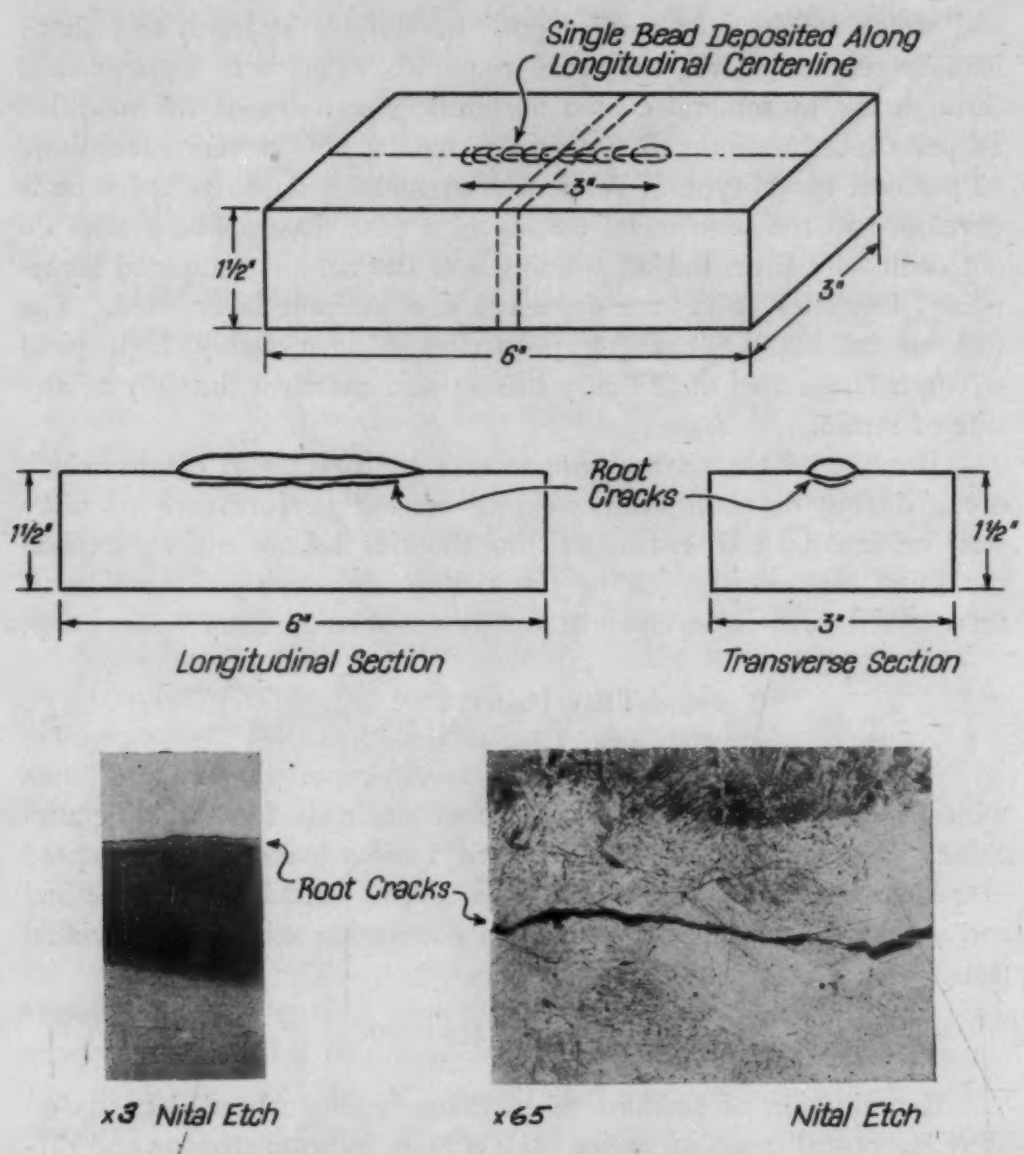

Fig. 1A—Root Crack System Under a Single Weld Bead on a 0.40 Per Cent Carbon Alloy Steel Plate.

correlate chemical composition with hardness and have given limits of chemical composition to avoid excessive hardening and limits of hardness to avoid base metal cracking.

A number of single bead tests were made on alloy structural steels using both ferritic electrodes, with and without base metal preheats, and austenitic electrodes without base metal preheats. Weld-hardenability curves were plotted by the method shown in Fig. 3A. Table I and Figs. 3B and 3C give representative results. No root cracks were found under any austenitic single bead deposits nor under any

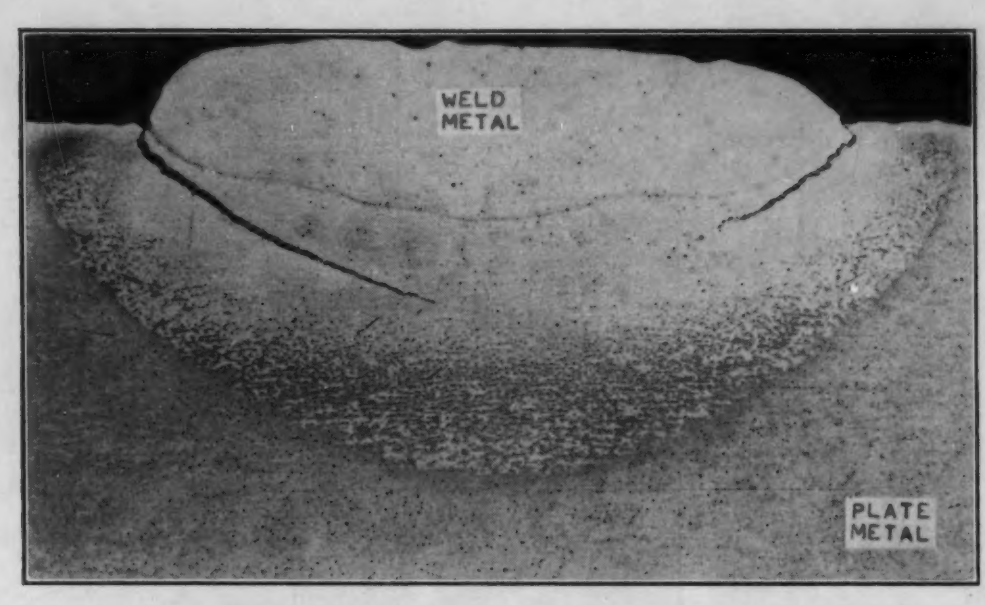

Fig. 1B—Toe Cracks in 0.5-Inch Section of 0.40 Per Cent Carbon Alloy Steel. Single Weld Bead Specimen Made with Ferritic Type Electrode. Nital Etch. × 5.

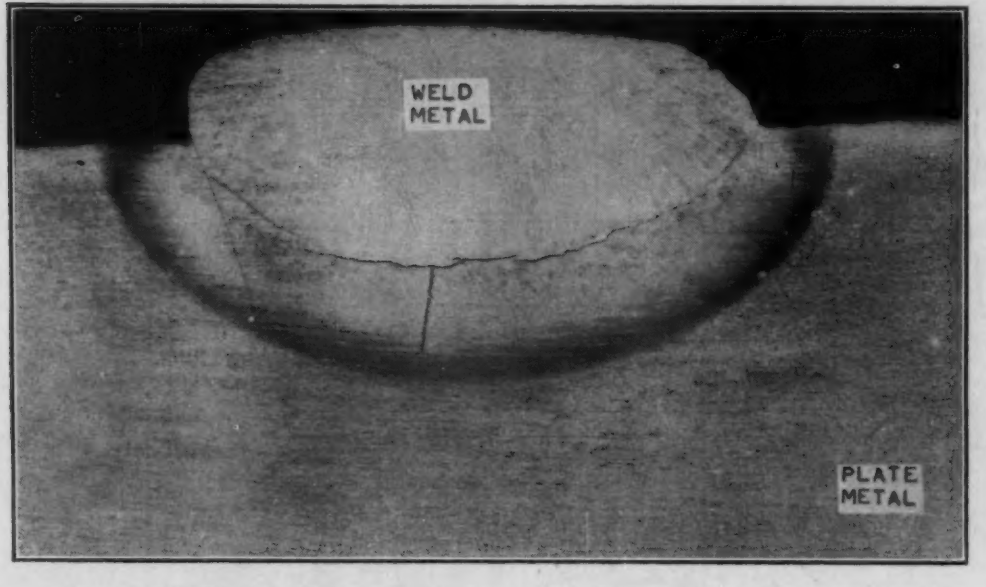

Fig. 1C—Vertical and Root Cracks in 1.5-Inch Section of 0.45 Per Cent Carbon Alloy Steel. Single Weld Bead Specimen Made with Ferritic Type Electrode. Nital Etch. × 5.

ferritic single beads deposited with base metal preheats of 250 degrees Fahr. (120 degrees Cent.) or higher. No adequate correlations were possible between cracking susceptibility and degree or depth of hardening in the heat-affected zone.

Microstructures in the heat-affected zones of a number of the hardness survey specimens were studied. Root cracks (Figs. 4A and

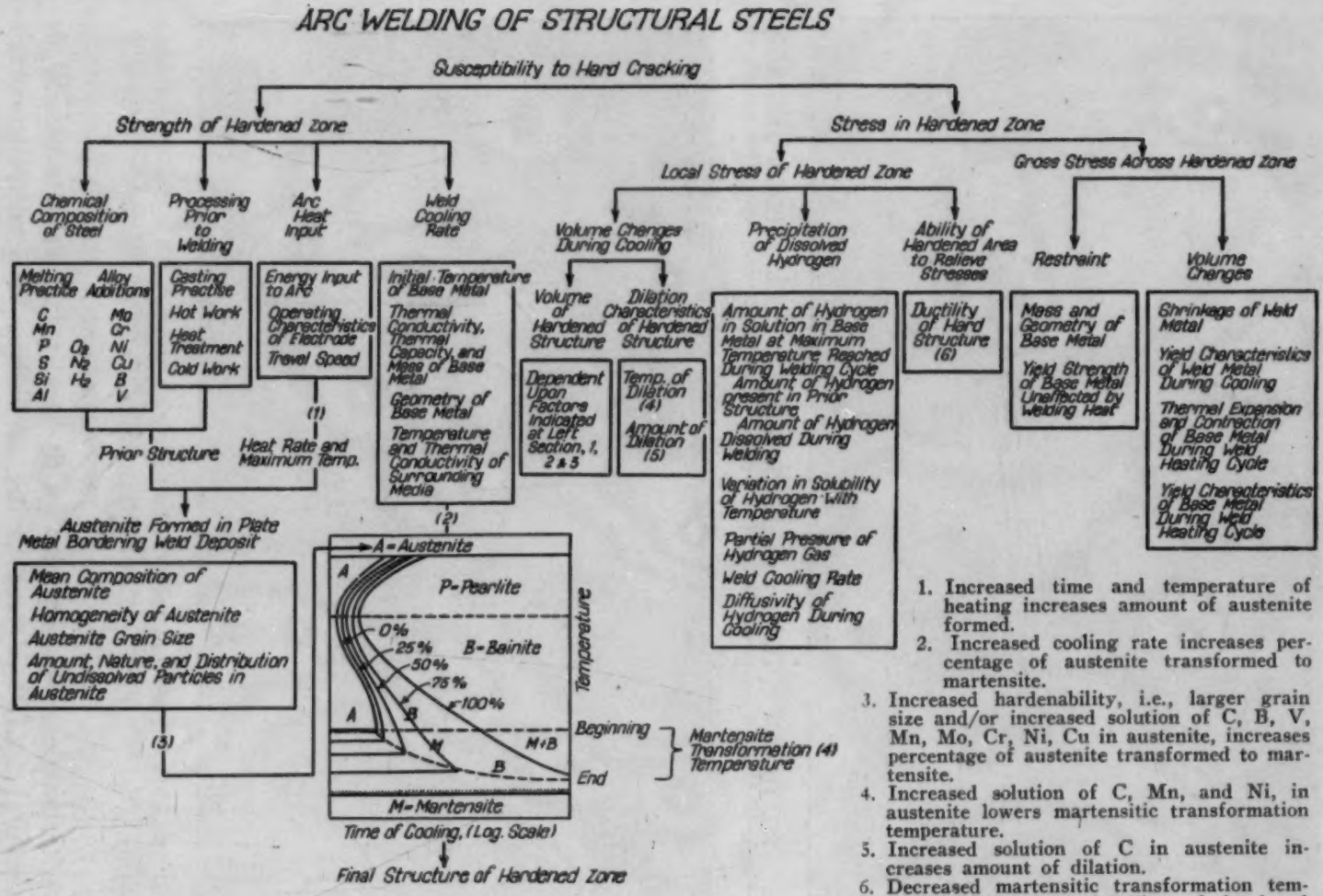

Fig. 2

1. Increased time and temperature of heating increases amount of austenite formed.
2. Increased cooling rate increases percentage of austenite transformed to martensite.
3. Increased hardenability, i.e., larger grain size and/or increased solution of C, B, V, Mn, Mo, Cr, Ni, Cu in austenite, increases percentage of austenite transformed to martensite.
4. Increased solution of C, Mn, and Ni, in austenite lowers martensitic transformation temperature.
5. Increased solution of C in austenite increases amount of dilation.
6. Decreased martensitic transformation temperature decreases ductility of hardened structure.

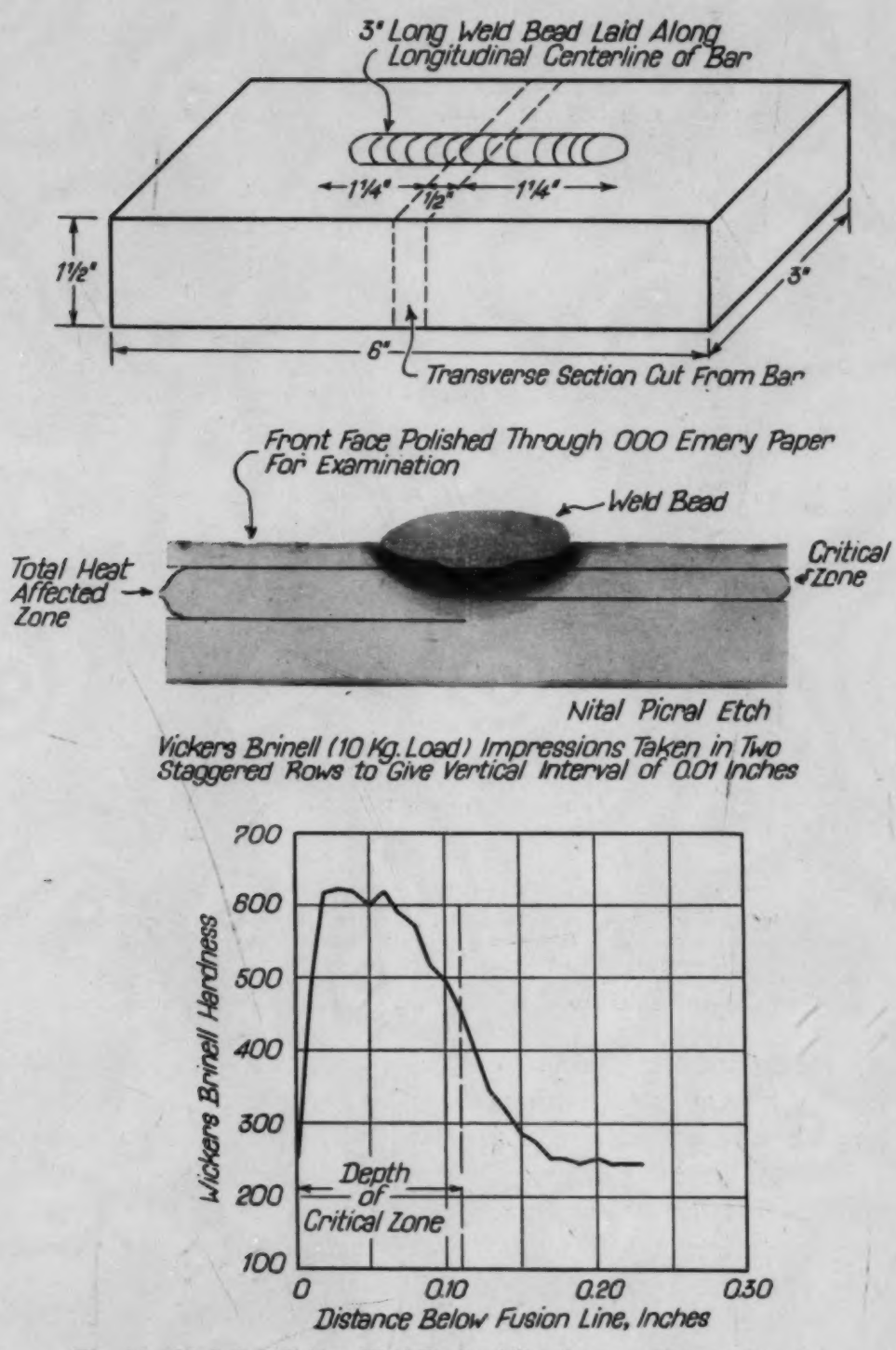

Fig. 3A—Method of Taking Weld-Hardenability Survey. Photograph × 1.5.

Table I
Results of Weld-Hardenability Surveys

Steel	Single Bead on 6 x 3 x 1½-Inch Block: Depth of Critical Zone* (Inches)	Max. Hard.	Cracking	Single Bead on 6 x 3 x ½-Inch Block: Depth of Critical Zone* (Inches)	Max. Hard.	Cracking
			Welded at Room Temperature			
WD 1020	....	208	None	....	190	None
1045	....	...	....	....	315	None
4820	0.075	400	None	0.21	430	None
6150	0.09	690	Small root crack	0.11	425	Root and toe cracks
4145	0.09	707	Small root crack	0.07	575	None
3140	0.10	605	Root crack	0.04	500	None
4340	0.125	665	Root crack	0.125	565	Root and toe cracks
2340	0.145	645	Root crack	0.105	597	None
			Welded at 250 Degrees Fahr. Preheat			
4820	0.05	380	None	0.09	380	None
6150	0.09	708	None	0.09	505	None
4145	0.12	605	None	0.075	490	None
3140	0.075	570	None	....	385	None
4340	0.145	640	None	....	...	....
2340	0.12	595	None	0.075	560	None
			Welded at 400 Degrees Fahr. Preheat			
4820	0.05	345	None	0.07	350	None
6150	0.08	530	None	0.06	465	None
4145	0.115	580	None	....	430	None
3140	0.055	465	None	....	350	None
4340	0.17	625	None	....	...	....
2340	0.12	560	None	0.045	500	None
			Welded at 600 Degrees Fahr. Preheat			
4820	....	...	....	....	335	None
6150	....	380	None	....	450	None
4145	....	435	None	....	345	None
3140	....	375	None	....	300	None
4340	0.135	515	None	....	...	....
2340	....	410	None	....	405	None
			Welded at 800 Degrees Fahr. Preheat			
6150	....	315	None	....	390	None
4145	....	315	None	....	...	....
4340	....	375	None	....	...	....
2340	....	295	None	....	400	None

*Vertical distance between fusion line and 50 per cent martensite line, determined by change in etching characteristics (see Fig. 3A), by maximum drop on hardness curve, or by hardness level corresponding to 50 per cent martensitic structure of steels of equivalent carbon content.

5A) were observed to occur only in those specimens which had a martensitic base metal structure in the zone bordering the fusion line. The absence of cracks in preheated and thin base metal sections, which cooled slowly following welding, could be explained by assuming that the austempered type structures (Fig. 4B) found in all such specimens had lesser transformation stresses and greater ability to relieve gross stresses than the martensitic structures in the hard cracked specimens. But the absence of hard cracks in the martensitic structures (Fig. 5B) under austenitic weld beads could not be explained.

An attempt was made to find a satisfactory inspection test for disclosing the presence of root cracks which, due to their discon-

Table I—(Continued)

Steel	Chemical Composition C	Mn	Si	Ni	Cr	Mo	V	Grossmann Hardenability†	Initial Plate Structure
WD 1020	0.22	0.47	0.03	....	....	....	....	0.550	Fine-grained, normal pearlite-ferrite
1045	0.435	0.86	0.19	....	....	....	....	1.37	Fine-grained, normal pearlite-ferrite
2340	0.43	0.60	0.29	3.56	0.12	Trace	....	3.24	Fine-grained, very fine pearlite-ferrite
3140	0.42	0.78	0.22	1.32	0.58	Trace	....	4.05	Fine-grained, normal pearlite-ferrite
4145	0.40	0.54	0.22	0.37	0.91	0.22	....	4.90	Fine-grained, very fine pearlite-ferrite
4340	0.38	0.68	0.20	1.75	0.87	0.28	....	8.47	Fine-grained, very fine pearlite-ferrite
4820	0.16	0.55	0.18	3.50	0.16	0.24	....	3.08	Fine-grained, spheroidal carbides-ferrite
6150	0.49	0.72	0.15	0.24	0.94	Trace	0.17	3.55	Fine-grained, very fine pearlite-ferrite

Welding Conditions

Three-inch single bead deposited on block with $\frac{3}{16}$-inch diameter Fleetweld No. 8, low carbon, low alloy ferritic electrode, organic type coating.
D. C. reversed polarity: 195-200 amperes, 23-25 volts.
Travel speed: 5 inches per minute.

†Grossmann hardenability calculated by assuming a grain size of 4. Actual weld grain sizes vary from 1-2 near the fusion line to 7-8 near edge of heat-affected zone for all of these steels. Although a difference of only one in as-quenched grain size makes a difference of approximately 10 per cent in Grossmann hardenability units, the relative rating of various steels will remain the same for any one assumed grain size.

tinuous nature, may be missed entirely on examining a single polished transverse section. The groove-bend test of Fig. 6A was developed. Tests were run to show effect of chemical composition of base metal on cracking tendencies (Fig. 6B). Root cracks may be observed to have opened up during bending of bars from all of the high hardenability steels but not in bars from WD-1020 or 1045 steels which failed entirely in the weld metal. Results of these and additional tests confirm the conclusion that cracks do not form unless there is sufficient alloy present in the base metal to effectively harden the heat-affected zone during the welding cycle. Compositions which contain carbide stabilizing alloys, such as chromium and vanadium, were found to show slightly less weld hardening and root cracking tendency, particularly when subjected to a prior heat treatment which would tend to stabilize carbides, than other alloys of equivalent Grossmann hardenability. This is presumably because the time available for austempering during the arc welding cycle is insufficient to permit complete solution of these carbide forming alloys.

Fig. 6C illustrates the application of the groove-bend test for determining the necessary preheat temperature to eliminate hard cracking when welding with ordinary ferritic electrodes. Under the conditions of these tests, a preheat of 300 degrees Fahr. (150 degrees

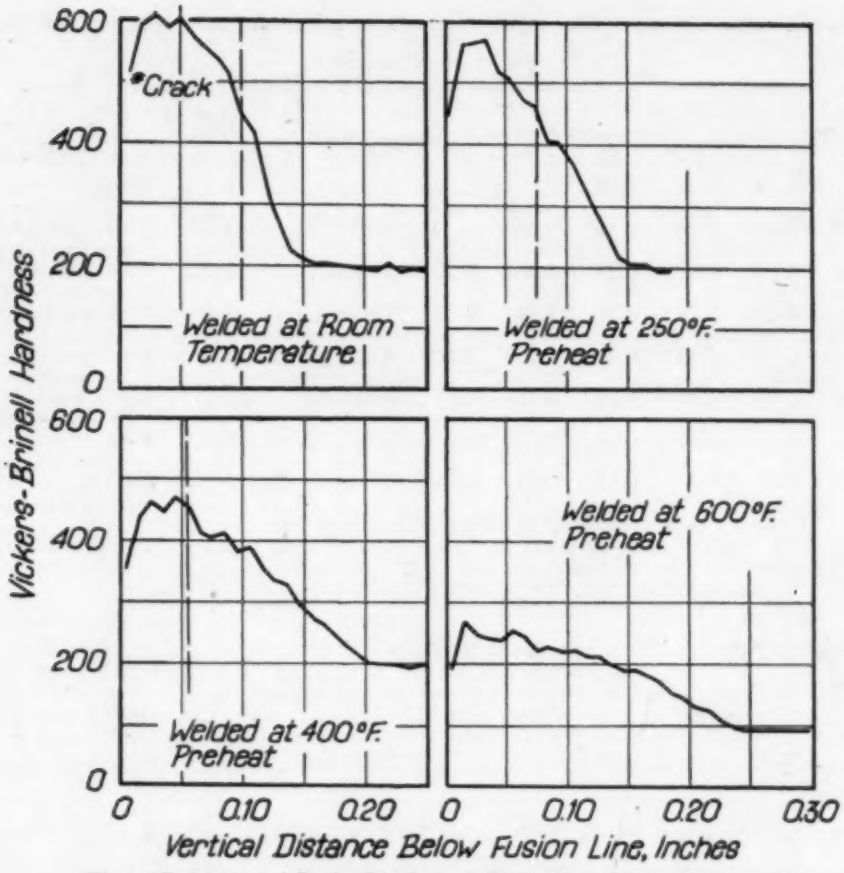

Fig. 3B—6x3x1½-Inch Blocks of WD 3140 Forged from Bar Stock. Annealed 3 Hours at 1650 Degrees Fahr., Furnace Cool. 3-inch single beads deposited with $\frac{5}{32}$-inch diameter Fleetweld No. 8, low carbon, low alloy ferritic electrode, organic type coating. Initial plate temperatures: 60 to 70 degrees Fahr., 250 degrees Fahr., 400 degrees Fahr., 600 degrees Fahr. D.C. reversed polarity; 195 to 200 amperes, 23 to 25 volts. Travel speed: 5 inches per minute.

Cent.) was required for complete elimination of hard cracking in two structural alloy compositions. A great improvement in ductility of the weld-hardened zone of these steels is also evident from the amount of bend before failure of the 300-degree Fahr. (150-degree Cent.) preheat sample. This improvement is presumably due to austempering effect.

In order to check the theory that absence of cracks in the heat-affected zone under austenitic weld bead deposits is due to greater ductility of weld metal and hence lesser overall stress across the region of cracking with austenitic than with ferritic weld deposits, an approximate determination of overall stresses was made by the method illustrated in Fig. 7. Restraint was varied by increasing or decreasing the depth of the slit at the base of the groove machined to receive the weld bead deposit. In two series of tests higher overall stresses were found for austenitic than for ferritic deposits. In a

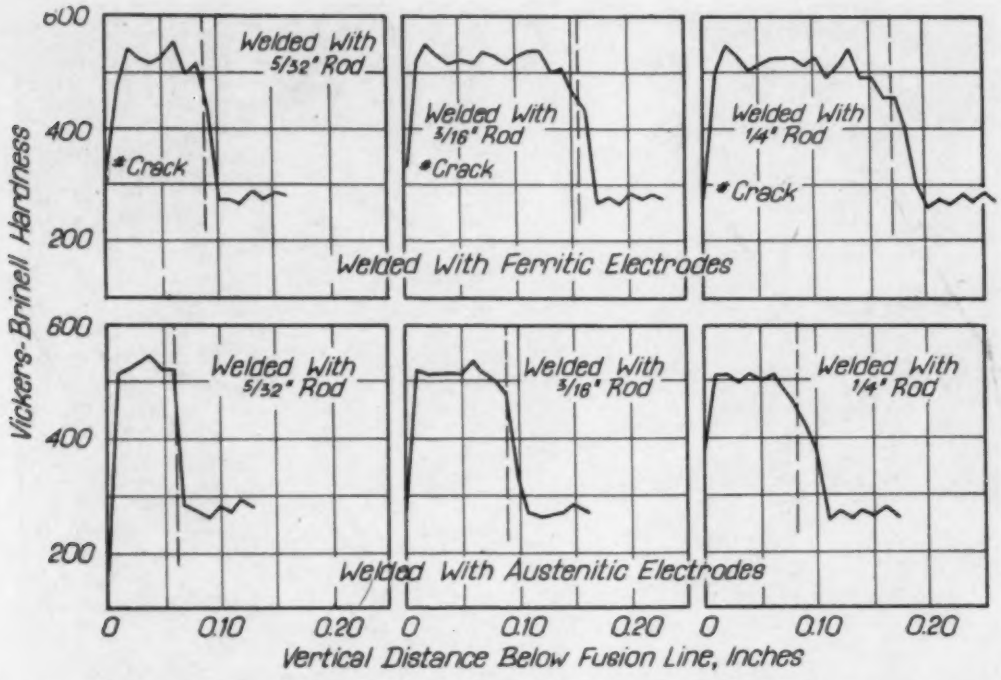

Fig. 3C—6x6x1½-Inch Blocks of 0.26 Carbon Medium Alloy Steel Plate. Quenched and Tempered. Three 3-inch single beads deposited respectively on one block with $\frac{5}{32}$, $\frac{5}{16}$, and ¼-inch diameter plain carbon Murex Fillex electrodes, organic type coating; and on another block with $\frac{5}{32}$, $\frac{5}{16}$, and ¼-inch diameter austenitic electrodes, mineral type coating. Initial plate temperature: 60 to 70 degrees Fahr. D.C. reversed polarity.

Electrode Diameter	Amperes	Volts
$\frac{5}{32}$ inch	100–110	22–23
$\frac{5}{16}$ inch	195–210	26–29
¼ inch	300	28

Travel speed: 5 inches per minute. Blocks set in water ½ inch deep during welding—allowed to cool to room temperature between beads.

third series with higher restraint (less depth of slit) cracks occurred in the weld metals. Austenite is known to have a higher thermal contraction than ferritic metal, and while these tests are not regarded as conclusive, the experiment served to indicate that the difference in overall stresses across a weld bead is not sufficient to explain the presence of root cracks when mild steel electrodes are used, and the absence of root cracks when austenitic electrodes are used.

Because of the many anomalies the results of these tests present to existing theories concerning root cracks, the effect of hydrogen introduced by moisture and organic matter in the electrode coating was investigated. Heating of ferritic type electrodes in an oven for 1 hour at a temperature of 600 degrees Fahr. (315 degrees Cent.) or higher immediately prior to welding was found to eliminate root cracking under single bead deposits and in groove-bend tests on a number of hardenable alloy steels. Figs. 8A and 8B show that root cracks have occurred under deposits made with untreated electrodes,

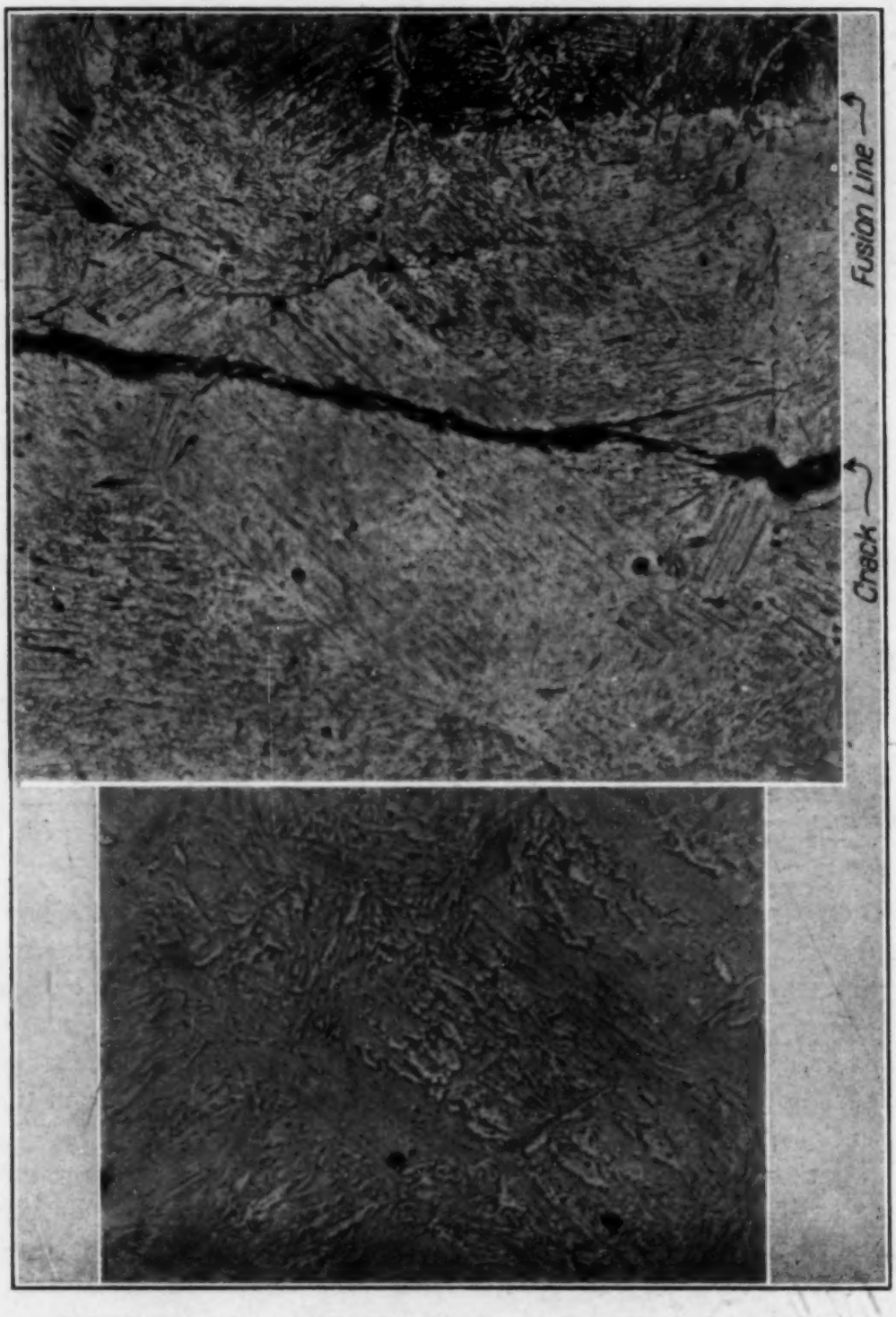

Fig. 4A—WD 3140, 1½-Inch Plate Welded at Room Temperature. Upper—Coarse-Grained Structure in Plate Metal Immediately Beneath Weld Bead, Principally White Martensite. × 200. Lower—Portion of Martensite Grain in Region of Crack. × 1500.

but are absent when the electrode has been heated prior to use. Specimens welded with the treated electrodes fail through the weld

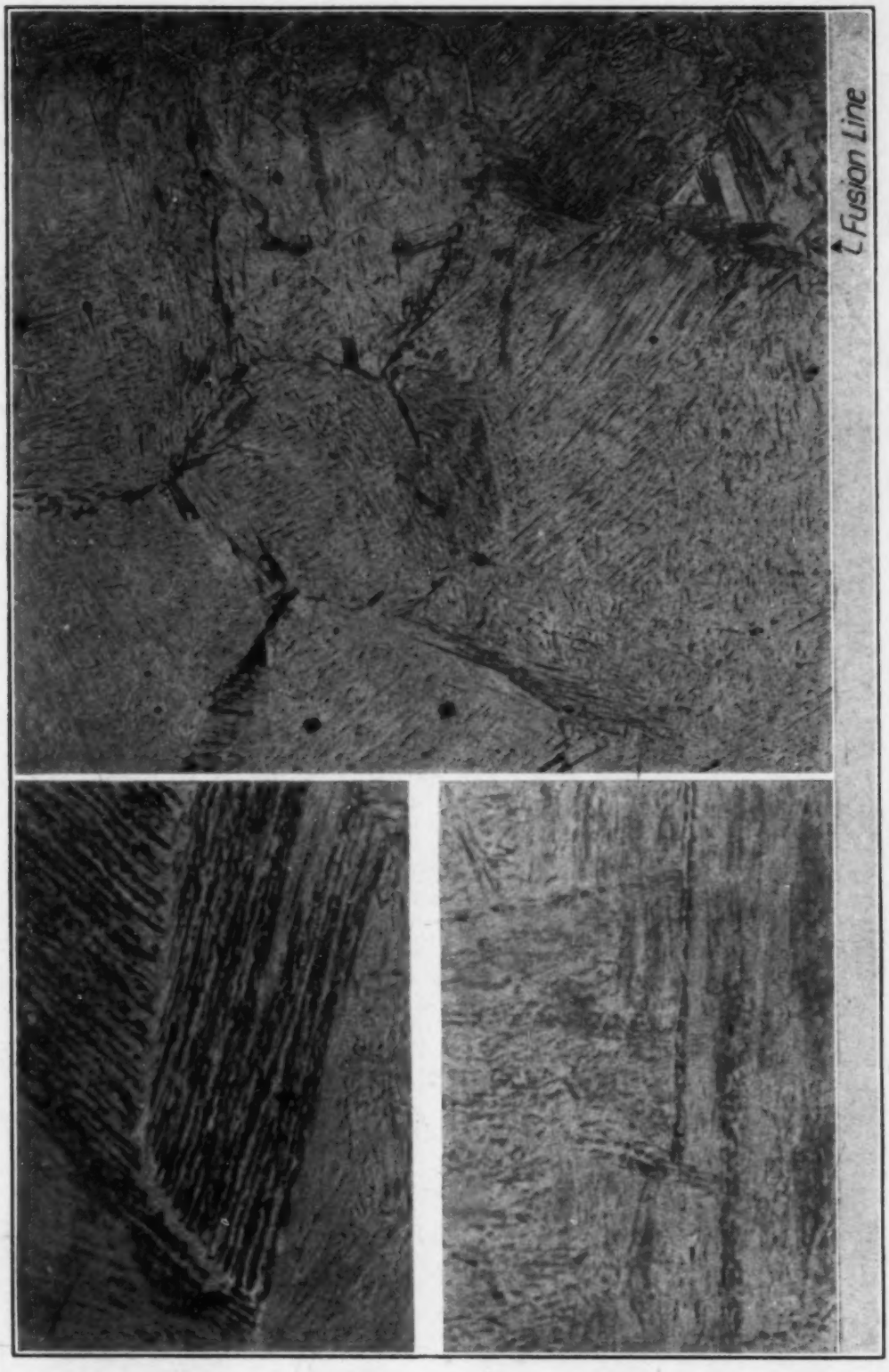

Fig. 4B—WD 3140, 1½-Inch Plate Welded at 250 Degrees Fahr. Preheat. Upper —Coarse-Grained Structure in Plate Metal Immediately Beneath Weld Bead, Upper Bainite at Grain Boundaries, Remainder Principally Lower Bainite. × 200. Lower Photomicrographs × 1500.

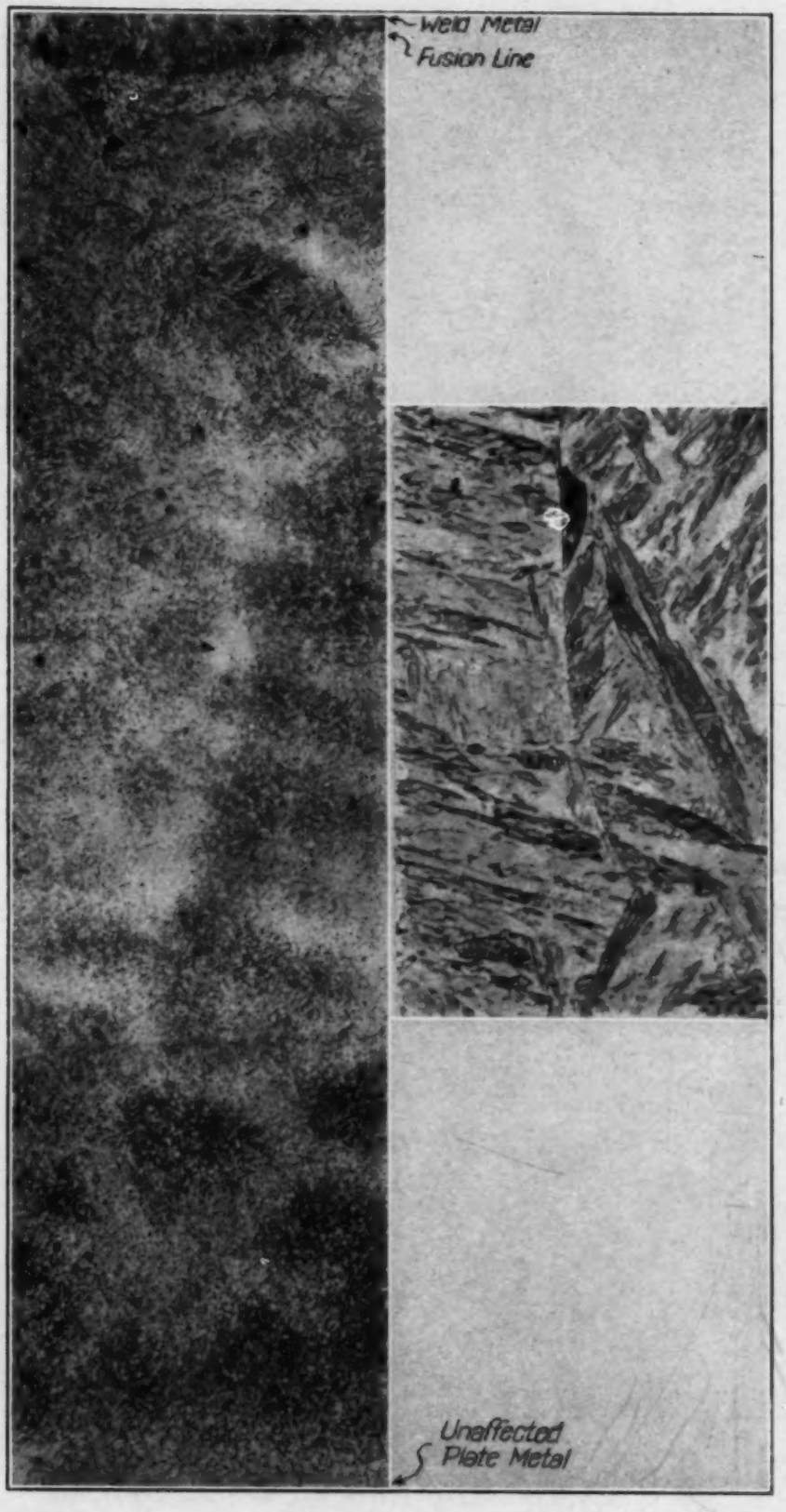

Fig. 5A—Photomicrographs Showing Structure of Heat-Affected Zone Under Single Weld Bead Deposited with Ferritic Electrode on 0.30 Per Cent Carbon Alloy Steel Plate. × 50. Inset—Structure 0.01 Inch Below Fusion Line. × 1500.

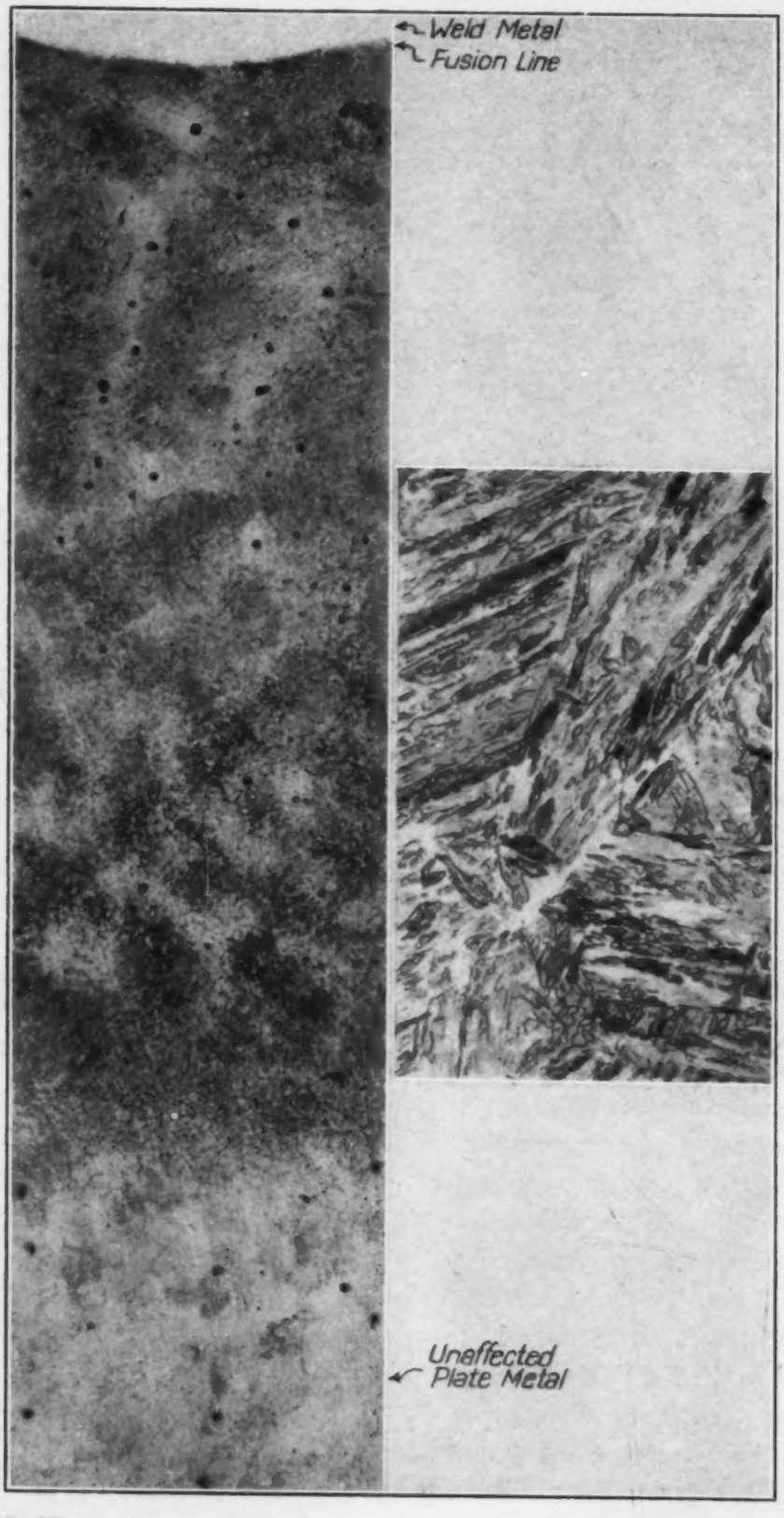

Fig. 5B—Photomicrographs Showing Structure of Heat-Affected Zone Under Single Weld Bead Deposited with Austenitic Electrode on 0.30 Per Cent Carbon Alloy Steel Plate. × 50. Inset—Structure 0.01 Inch Below Fusion Line. × 1500.

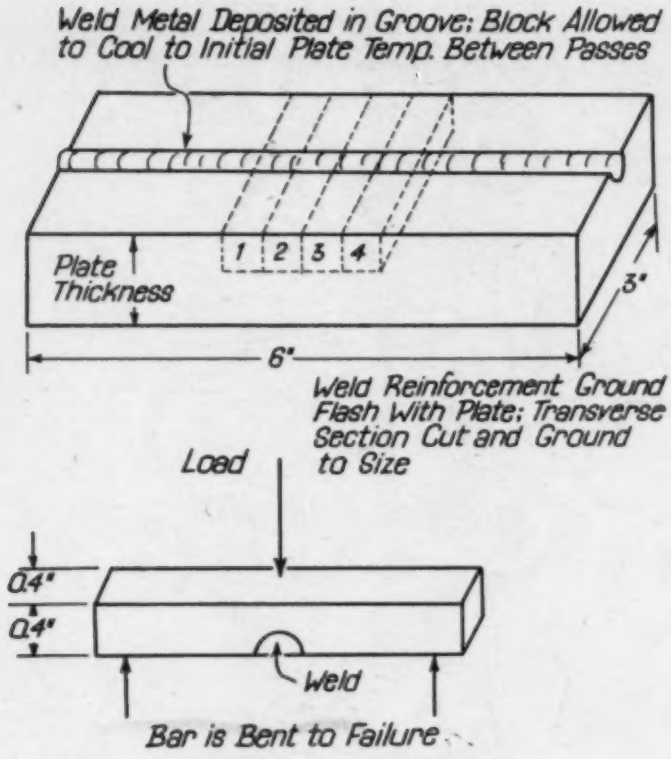

Fig. 6A—Groove-Bend Test.

metal and across the weld heat-affected zone at a much higher load than that required to open up the root cracks parallel to the fusion zone in specimens welded with untreated electrodes. However, heating of the electrode coating has destroyed the protective properties of the coating and exposed the weld metal to the same influences that cause bare electrode deposits to lose their ductility.

The effect of moisture is further illustrated in Fig. 9A where transverse sections of single beads deposited with four commercial ferritic electrodes were given a deep acid etch which tends to exaggerate presence of hard cracks. Adding moisture to the coating by immersing the electrodes in water or wrapping moist paper around them before welding was found to slightly increase root cracking. A temperature of at least 600 degrees Fahr. (315 degrees Cent.) (Fig. 9B) for heating electrodes is necessary to eliminate base metal cracking; hence, it is assumed that hydrogen present as combined moisture and in cellulosic compounds ($C_6H_{10}O_5$) must be driven off as well as absorbed moisture.

Austenitic electrodes, which have been observed to eliminate root cracking, are given an all-mineral type coating containing no cellulosic matter. These coatings are often high in calcium carbonate

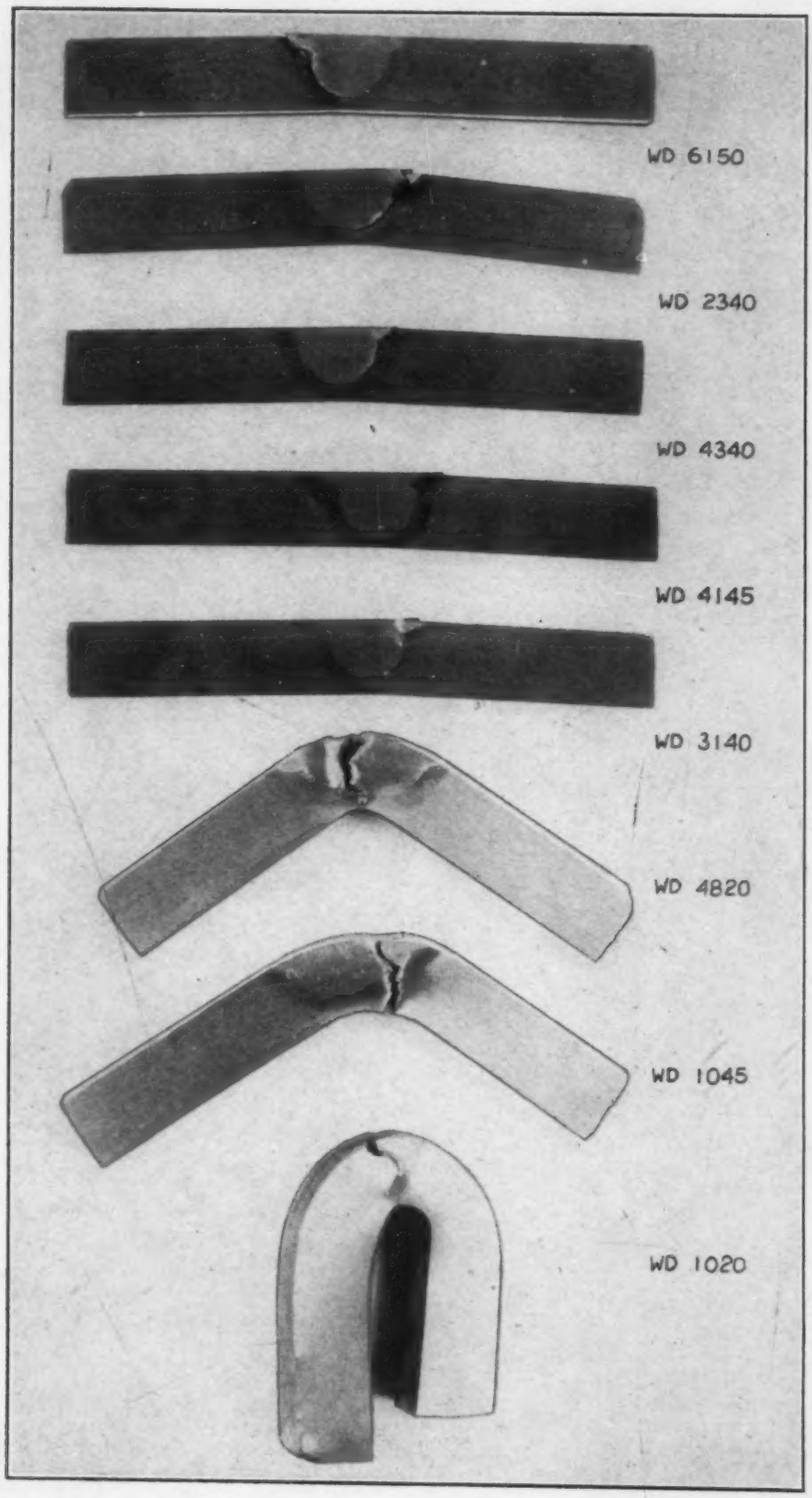

Fig. 6B—Groove-Bend Tests Showing Effect of Chemical Composition on Base Metal Cracking Tendencies. See Table I for Compositions. Three Passes with $\frac{1}{8}$-Inch Diameter Fleetweld 8 Electrode Deposited in Grooves on 1½-Inch Thick Blocks.

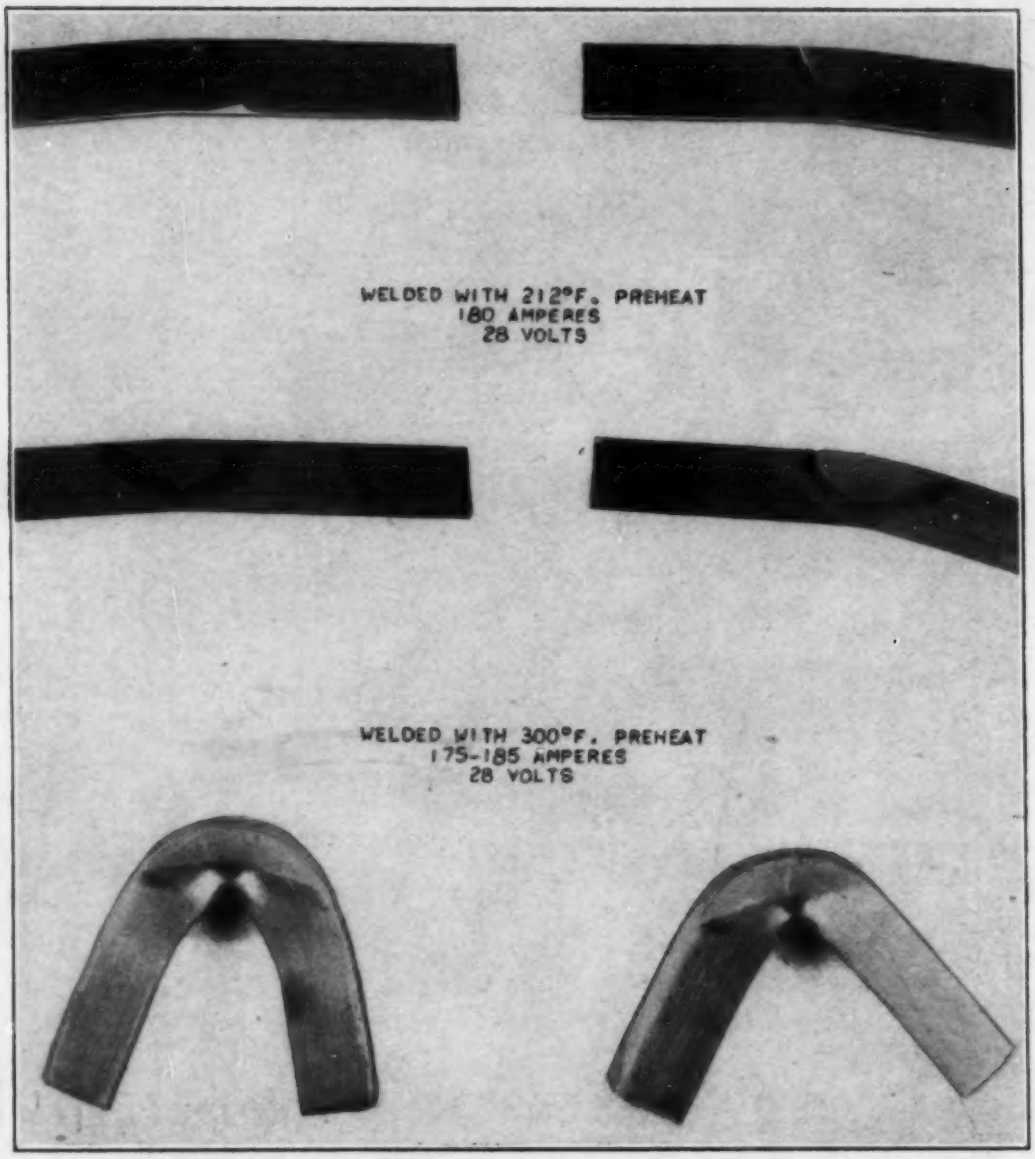

Fig. 6C—Groove-Bend Tests Showing Effect of Preheat on Base Metal Cracking Tendencies of 26 C Medium Alloy Steel. Two Passes with $\frac{1}{4}$-Inch Diameter Arcrods 0.001 Ferritic Electrode Deposited in Groove on 1½-Inch Thick Blocks. (Upper Specimens Welded at Room Temperature, 180-190 Amperes, 26-27 Volts.)

which evolves carbon dioxide in the arc heat. Carbon dioxide would be expected to reduce the hydrogen concentration in the weld metal by both chemical and mechanical reactions. Commercial ferritic electrode coatings, even of the so-called "mineral" type, contain a certain percentage of cellulose, combined moisture, or sometimes acetylene associated with ferro alloys. Special ferritic electrodes with a stainless type lime or titania base coating are now becoming available. Fig. 9C illustrates the fact that root cracking reoccurs when a fer-

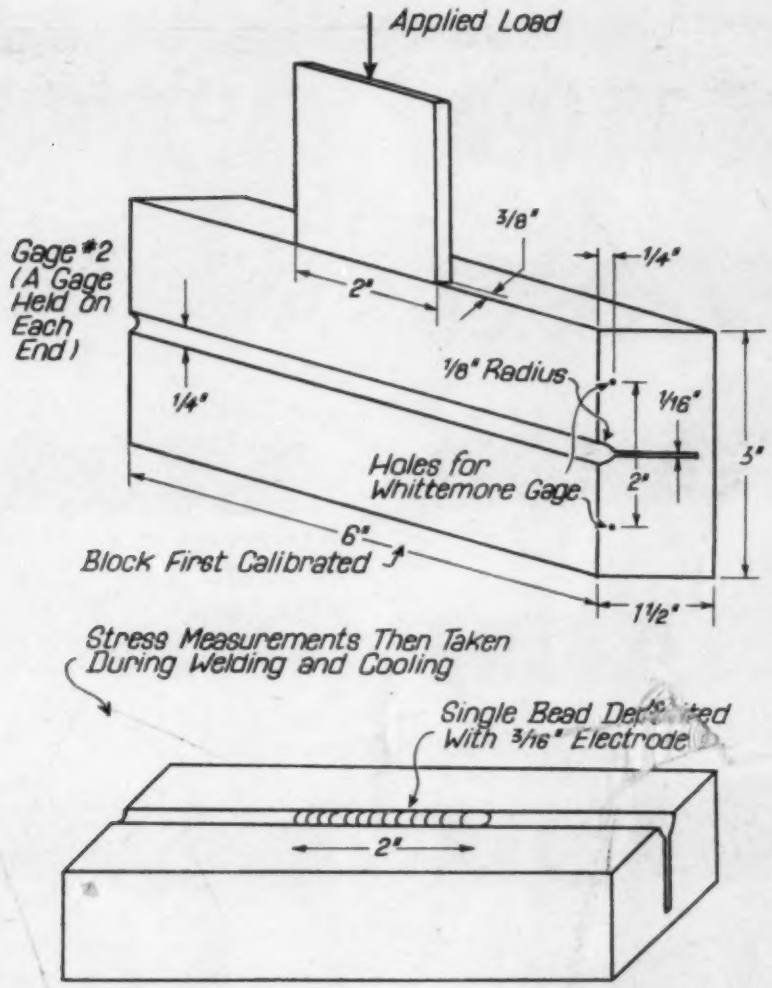

Fig. 7—Method of Measuring Over-all Stress During Welding and Cooling of a Single Weld Bead.

ritic electrode which has once been dried is again moistened, and that root cracks do not ordinarily occur when either an austenitic or ferritic electrode is coated with a stainless type coating. Further experiments have revealed that root cracks do not ordinarily occur when welding alloy steels with mild steel electrodes having either no coating or a "sul" (light oxide) coating, but can be produced by welding in a steam, alcohol, or hydrogen atmosphere; and that root cracks may be produced even when a lime base stainless type coating is used if the moisture content of coating is quite high.

Hydrogen, which may be picked up from atmospheric moisture in contact with hot steel, has been definitely connected with such defects as flakes, shatter cracks, and quench cracks in unwelded steels, and very extensive literature references are available on this subject (4). Zapffe and Sims (5) have presented a very excellent discussion

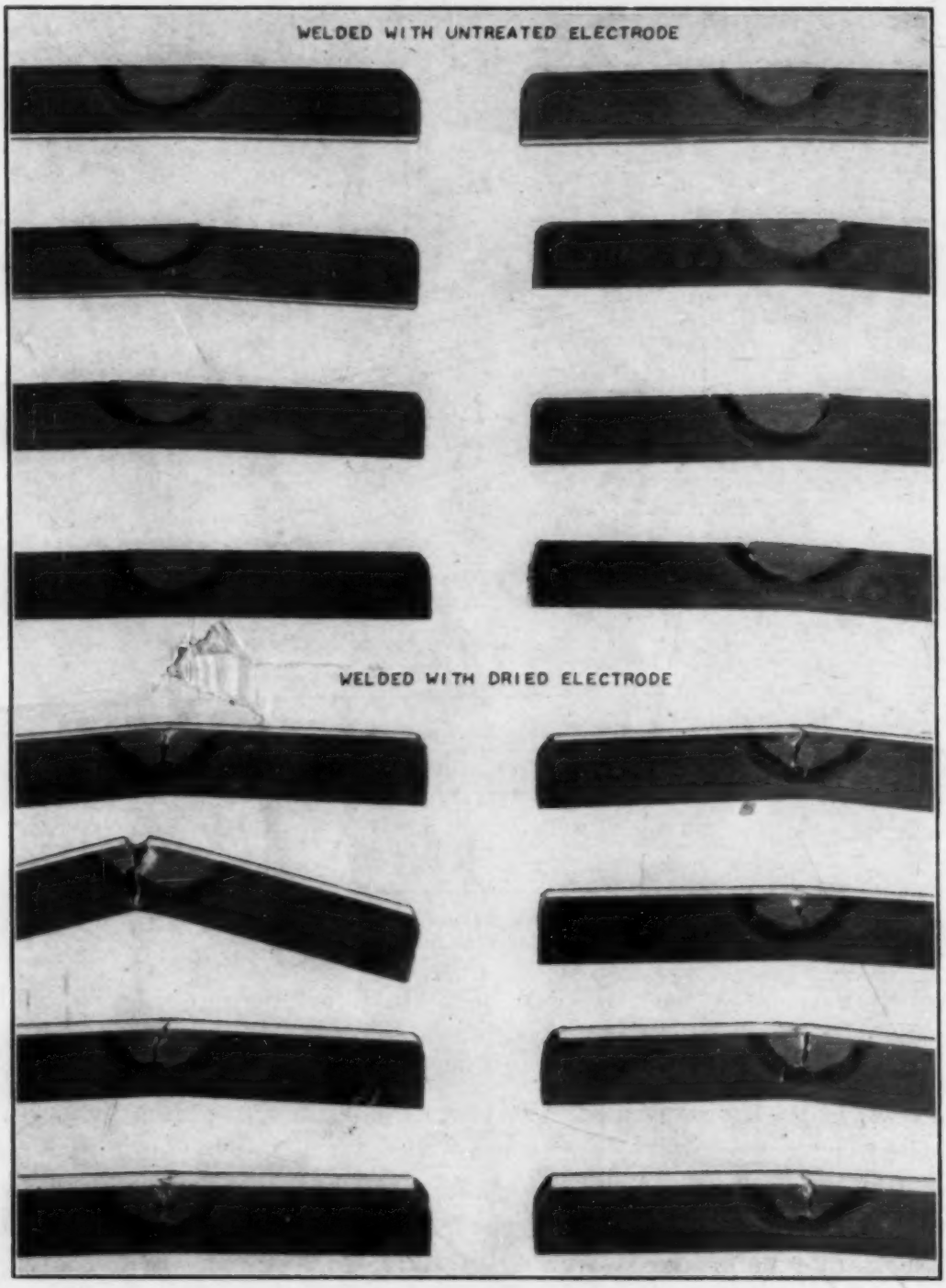

Fig. 8A—Groove-Bend Tests Showing Effect of Heating Electrode at 800 Degrees Fahr. for 1 Hour Prior to Welding. Two Passes with $\frac{5}{32}$-Inch Diameter SW-76 Ferritic Electrode on 1½-Inch Thick Quenched and Tempered Blocks—Initial Plate Temperature 60-70 Degrees Fahr. (Specimens at Left, WD4340. Specimens at Right, WD6150.)

of the fundamental aspects of hydrogen in steel and demonstrated experimentally that hydrogen (as absorbed by the weld metal from

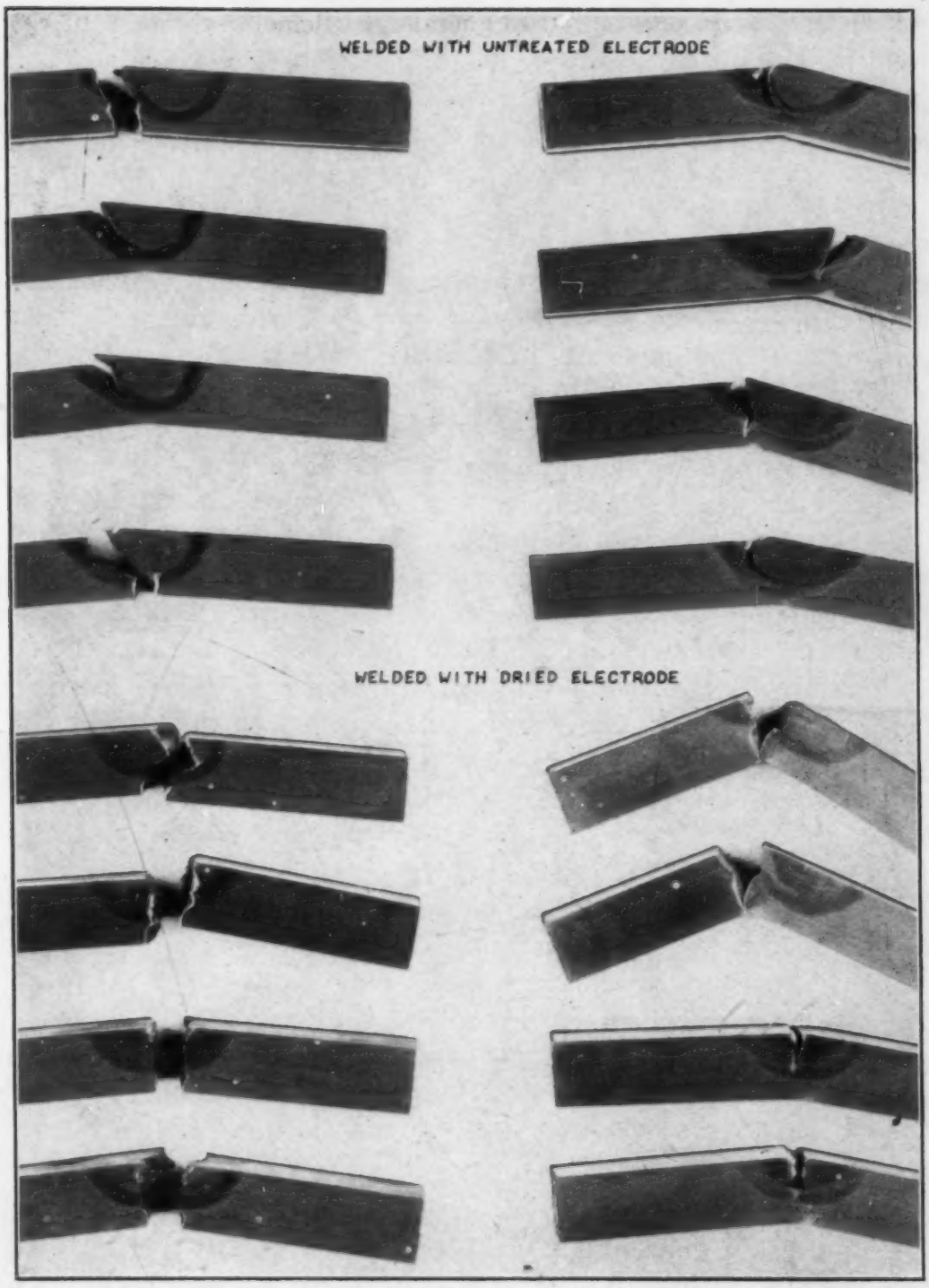

Fig. 8B—Groove-Bend Tests Showing Effect of Heating Electrode at 1000 Degrees Fahr. for 1 Hour Prior to Welding. Two Passes with $\frac{3}{16}$-Inch Diameter Shield Arc 100 Ferritic Electrode on 1½-Inch Thick Blocks—Initial Plate Temperature 60-70 Degrees Fahr. (Specimens at Left, WD4140. Specimens at Right, WD2340.)

organic compounds of the electrode coating and from moisture in the electrode coating and the atmosphere) is related to weld metal

defects such as fisheyes, fissures, and to general embrittlement of the weld metal with attendant low ductility in transverse tensile bars.

The literature regarding the possible effects of hydrogen on base metal cracking is very confused, and no experiments of the type herein reported are known to the author. The Welding Handbook for 1942 (6) disposes of hydrogen in the following two sentences in the Chapter on Weldability: "Little information is available on the effect of hydrogen in the base metal and this is conflicting. In welding, the chief sources are the gases in oxyacetylene and atomic hydrogen welding and moisture in electrodes and atmosphere in arc welding."

Spraragen and Claussen have reviewed the literature on the effect of hydrogen on the welding of steel (7) and found the results inconclusive. Zapffe (8) presents an interesting hypothesis which might be applied to base metal cracking in much the same way that it was later applied to weld metal cracking (5). Bordenheuer and Bottenberg (9) have investigated the effect of hydrogen content of base metal on cracking (at high temperatures) of thin aircraft sheet during oxyacetylene welding and found hydrogen to be an important factor. However, Spraragen and Claussen (7) state that differences in hydrogen content of these steels were hardly large enough to be convincing in view of differences among these steels in other respects. Much conflicting evidence is present in the accounts of cracking during welding of aircraft steels (10).

The probable role of hydrogen in hard cracking of steel may be summarized briefly, as follows:

1. If moisture or reducing gases containing hydrogen are present during welding, atomic hydrogen will be dissolved by the molten weld metal to the limit of its solubility under the conditions of temperature, pressure, and available time during the welding process. The amount of hydrogen dissolved by the weld metal is believed to be many hundred times that which can be held in solution by the solidified weld metal.

2. The base metal adjacent to the fusion line is heated to temperatures approaching the melting temperature and hydrogen will diffuse into this metal to the limit of its solubility under the conditions of the welding cycle. The amount of hydrogen dissolved by the base metal near the fusion zone may also be many hundred times that which can be held in solution at room temperature.

3. On cooling, the weld and base metals become supersaturated

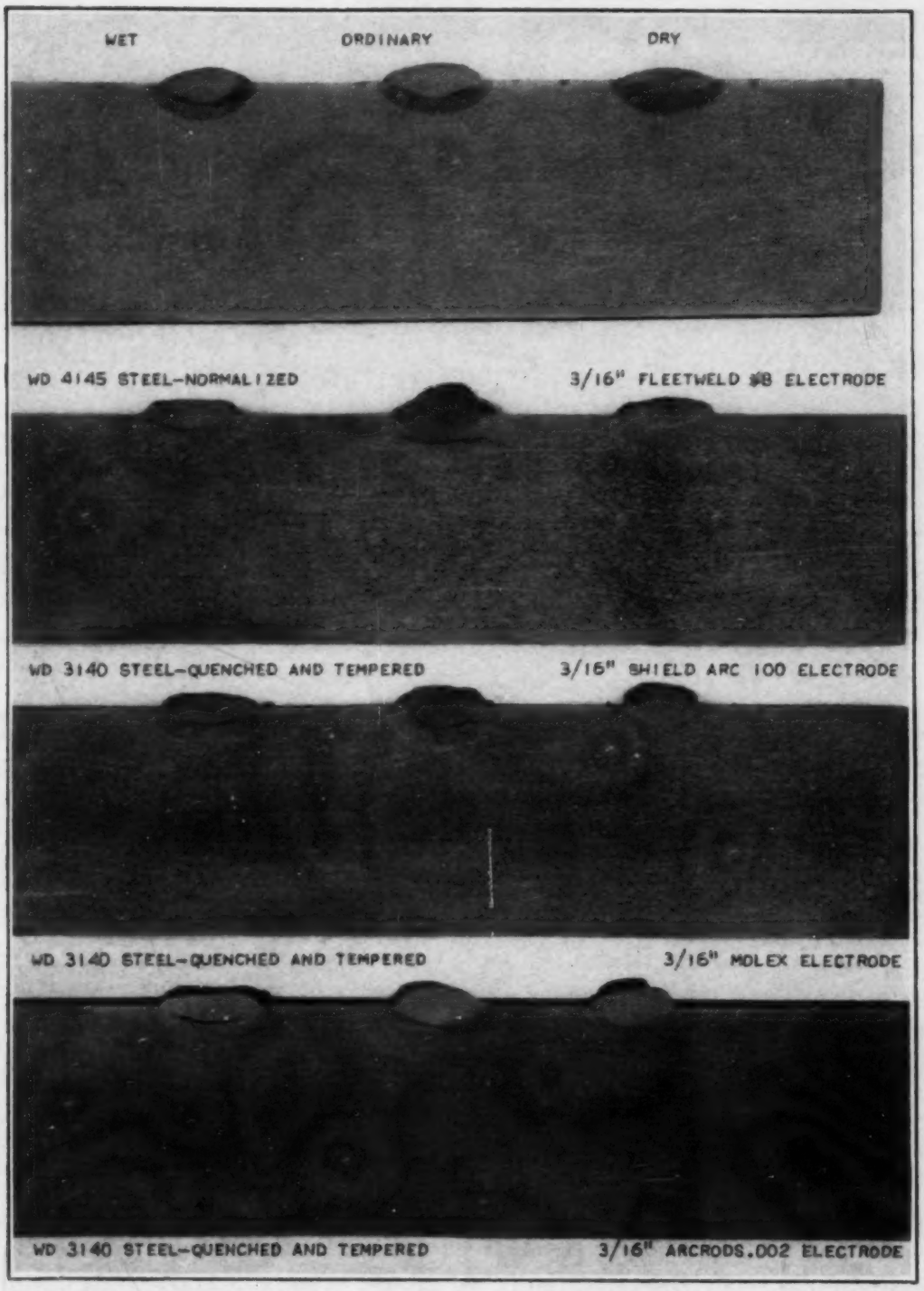

Fig. 9A—Macro-Etched Transverse Sections Through Single Weld Beads Deposited with Various Wet, Ordinary, and Dry Ferritic Electrodes on Structural Steel.

with atomic hydrogen. Hydrogen must then precipitate at all discontinuities (blowholes, inclusions, grain boundaries, or submicroscopic rifts in the metal) as insoluble molecules of hydrogen or other

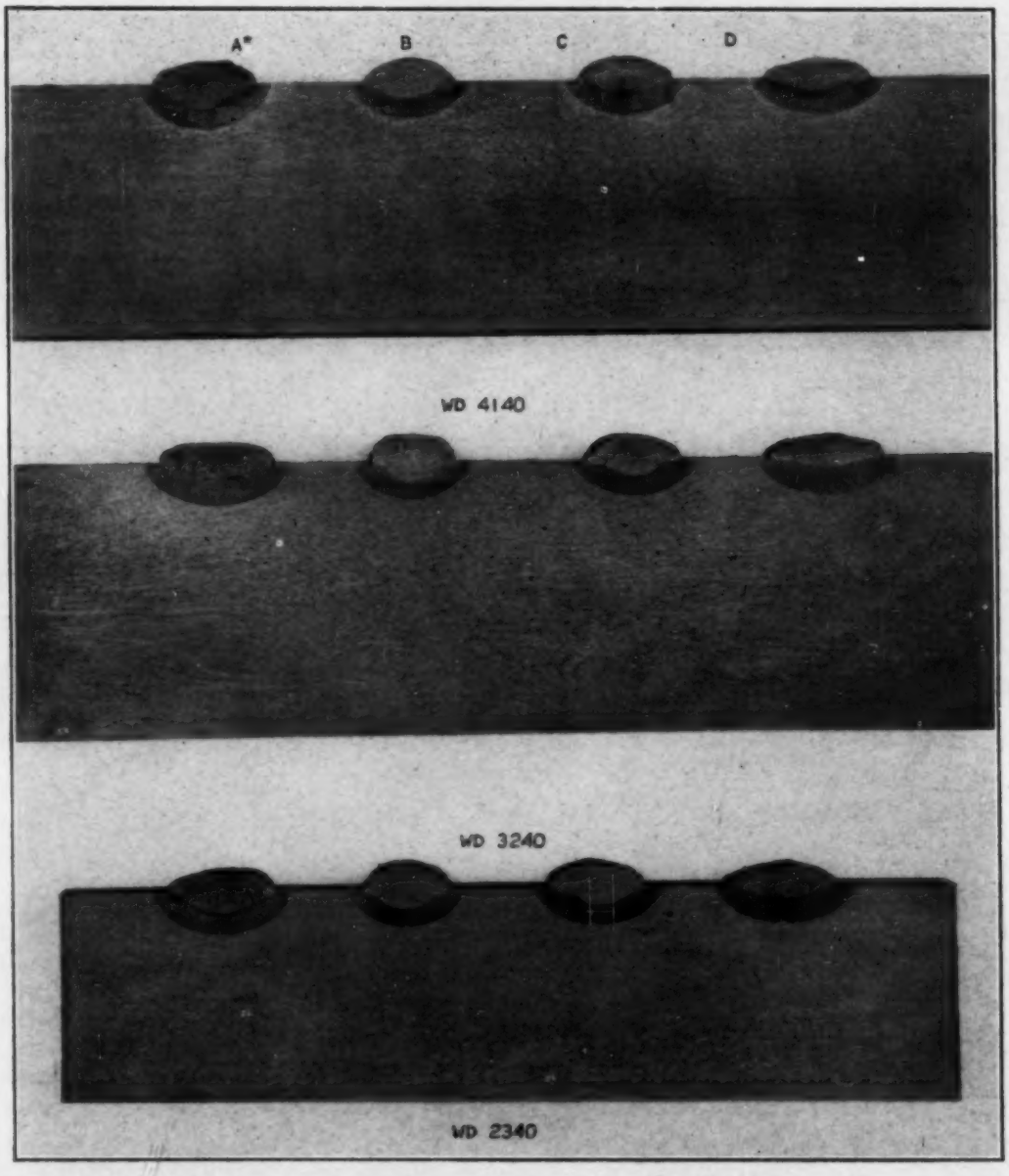

Fig. 9B—Macro-Etched Transverse Sections Through Single Weld Beads Deposited with $\frac{5}{32}$-Inch Diameter Shield Arc No. 100 on Structural Steel As-Rolled.

A—Deposited with Untreated Electrode. B—Deposited with Electrode Dried at 1000 Degrees Fahr. for 1 Hour Before Welding. C—Deposited with Electrode Dried at 600 Degrees Fahr. for 1 Hour Before Welding. D—Deposited with Electrode Dried at 400 Degrees Fahr. for 1 Hour Before Welding.

compounds of hydrogen such as methane. Pressures are thus built up causing stresses which may exceed the fracture stress of the metal.

4. In alloy steels fully hardened by the weld quenching cycle, the combination of hydrogen, thermal contraction, and martensitic transformation stresses may result in tensile deformation beyond the capacity of the metal causing failure by hard cracking.

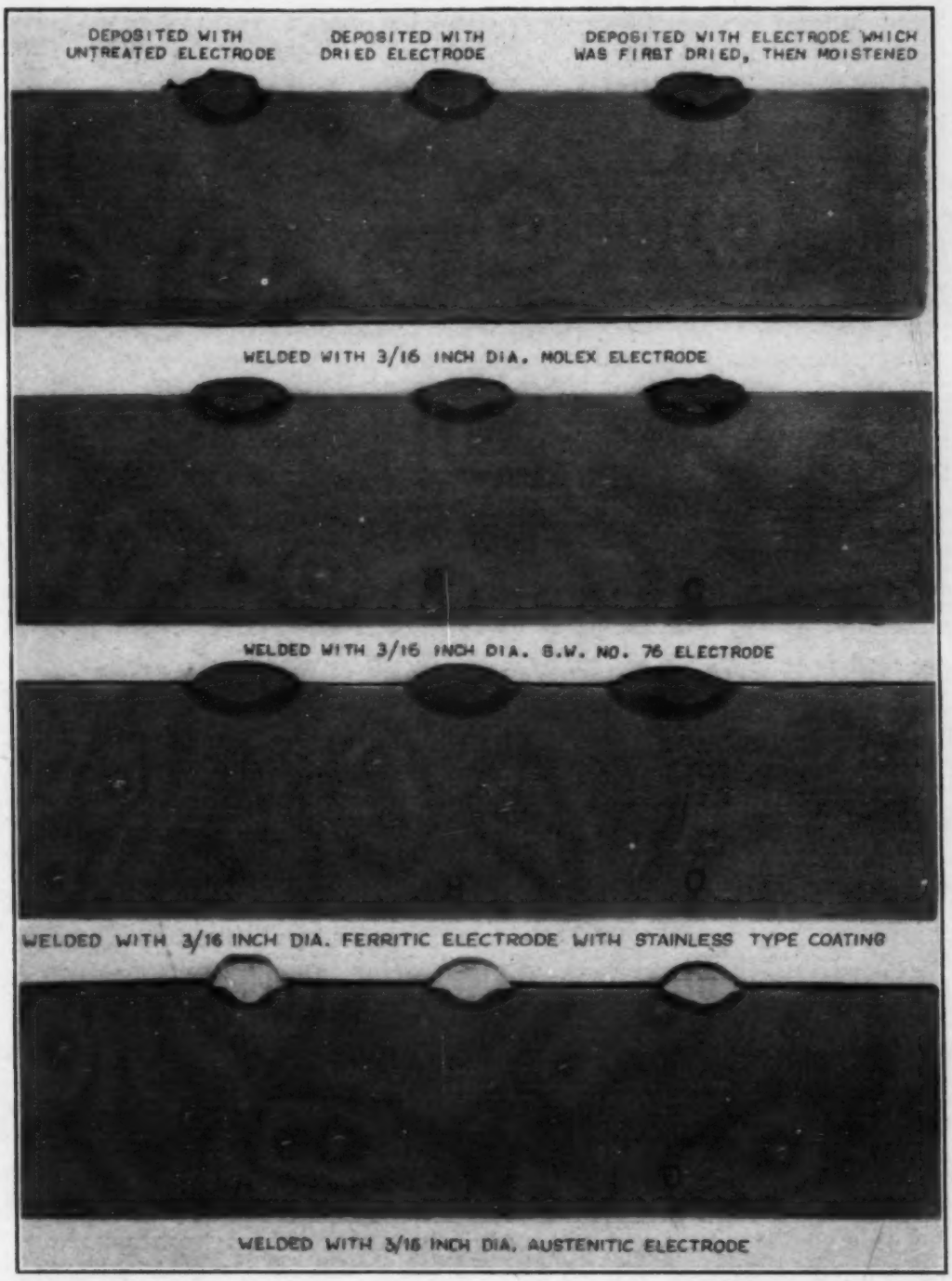
DEPOSITED WITH UNTREATED ELECTRODE
DEPOSITED WITH DRIED ELECTRODE
DEPOSITED WITH ELECTRODE WHICH WAS FIRST DRIED, THEN MOISTENED
WELDED WITH 3/16 INCH DIA. MOLEX ELECTRODE
WELDED WITH 3/16 INCH DIA. S.W. NO. 76 ELECTRODE
WELDED WITH 3/16 INCH DIA. FERRITIC ELECTRODE WITH STAINLESS TYPE COATING
WELDED WITH 3/16 INCH DIA. AUSTENITIC ELECTRODE

Fig. 9C—Macro-Etched Transverse Sections Through Single Weld Beads Deposited on Normalized WD6150 Steel.

5. The location of root cracks, and the fact that they are eliminated by drying the electrode coating, suggest that precipitated hydrogen is the principal cause of root cracking. High magnification photomicrographs (Fig. 10) showing the complex nature of hard

cracks indicate that high internal pressures may have been operative during crack formation.

The above mechanism is very helpful in accounting for all the hitherto unexplainable features of root cracking known to the author. The possibly very important part that oxygen may play in the action is not yet adequately known, hence the hypothesis may be subject to certain corrections and additions.

Toe and vertical cracks, the second and third types of hard cracks (Figs. 1B and 1C), appear to progress along paths to best relieve the overall thermal expansion and contraction stresses.

When heat input is relatively high and plate section is thin, the heat-affected zone cools most rapidly at the side of weld bead near the plate surface, and in some cases this area may be cooling and contracting at the same time that the bottom edge of plate is heating and expanding. The result is a high tensile stress at the top plate surface near junction with weld bead, which will tend to make the plate bow upwards at the ends of a transverse section. Such stresses are best relieved by a toe crack of the type shown in Fig. 1B.

When plate section is relatively heavy, the base metal under bead is restrained and may plastically deform on heating. Cooling is rapid and high tensile stress may be set up under bead parallel with fusion line. Such stresses are best relieved by a vertical crack of the type shown in Fig. 1C.

Either toe or vertical cracks, but particularly toe cracks, are apt to start as intergranular hot tears if tensile stresses exceeding the hot strength of base metal are developed during the welding cycle. Obviously, this tendency increases for base metals which are red-short and such steels should be avoided in welding. These cracks may continue to grow (sometimes at a very slow rate) as transgranular cracks, after the base metal has cooled, due to stress concentration at bottom of crack. Such growth will continue so long as tensile stress exceeds ability of base metal to plastically deform and relieve the stress. This condition may exist in highly hardenable base metals which have been hardened by the weld quenching cycle. When no hot tearing takes place, transcrystalline toe cracks may start at notch formed by slight undercutting at junction of weld bead and plate. Either toe or vertical cracks may start at nonmetallic inclusions or at root cracks. Vertical cracking appears to increase with moisture content of electrode coating, even with mineral coated, austenitic type electrodes. It is possible to have all three types of hard cracks, root, toe, and vertical, under the same weld bead.

Elimination of Hard Cracks

Hard cracks do not occur when a low hardenability base metal, which does not harden during the weld quenching cycle, is selected. Nor do hard cracks occur when sufficient preheat is used to develop an austempered (bainitic rather than martensitic) structure in the weld heat-affected zone. When neither of these measures is practical, the following should be considered:

1. Root cracks are prevented when a mineral coated electrode or an organic coated electrode which has been oven-heated to drive off absorbed and combined moisture and to break up cellulosic compounds is used, but the latter method sacrifices protective properties of coating and is no better than bare electrode welding.

2. Toe cracking may be prevented by reducing the ratio of heat input to plate section, by reducing the overall restraint on the joint, or by selecting a base metal which has higher strength at elevated temperatures.

3. Vertical cracks may be eliminated by reducing overall restraint, by reducing welding heat input, and possibly by eliminating moisture from electrode coating.

Cracks once formed cannot be healed by subsequent heat treatment, but thermal or mechanical stress-relieving treatments may limit growth of hard cracks. If care is exercised to avoid hard cracking when first, or root bead, is deposited in a multiple pass weld, a welding technique which tempers weld-hardened zone of first bead and maintains a suitable interpass temperature to provide preheat for subsequent beads, should result in superior service performance of welded joint.

All cracks and notches present in welded structures which are subject to impact, repeated high load, or fatigue stresses, are certain to accelerate failure. It is essential that weldments assembled from alloy structural steels be subject to inspection control tests that will disclose presence of hard cracks, that their importance be realized, and their causes studied and eliminated.

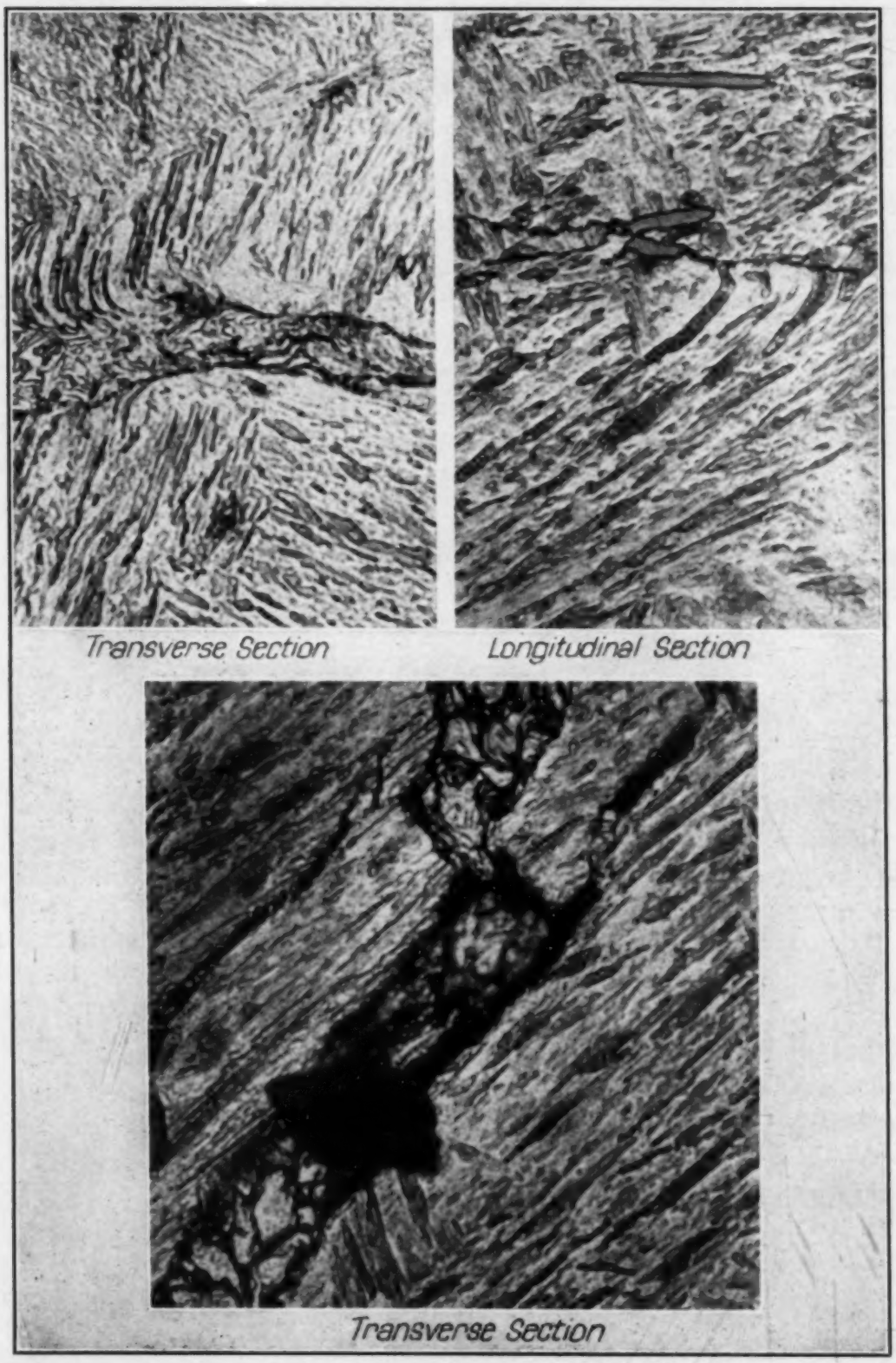

Fig. 10—Root Cracks Approximately 0.01 Inch Below Fusion Line in 0.26 to 0.30 Carbon Alloy Steels. Single Bead Weld Specimens Made with Ferritic Type Electrodes. Nital Etch. × 1000.

ACKNOWLEDGMENTS

The interest and helpful suggestions of Colonel H. H. Zornig and many members of the Watertown Arsenal Laboratory Staff are gratefully acknowledged. Assistance rendered by Miss A. M. Turkalo, Mr. R. M. Rodgers, and Mr. S. V. Arnold in conducting welding tests and preparing illustrations for this report is particularly appreciated.

Bibliography

1. W. Spraragen and G. E. Claussen, "Weldability—Base Metal Cracks," A review of the literature to July 1, 1939, *Welding Journal,* Research Supplement, May 19, 1941, Vol. 20, No. 5.
2. METALS HANDBOOK, 1939, p. 229. American Society for Metals, Cleveland, Ohio.
3. *Welding Handbook,* 1942, p. 110. American Welding Society, New York, N. Y.
4. C. A. Zapffe and C. E. Sims, "Hydrogen, Flakes, and Shatter Cracks," *Metals and Alloys,* May-August, 1941, Vol. 11, Nos. 5 and 6; Vol. 12, Nos. 1 and 2.
   "Hydrogen Embrittlement, Internal Stress and Defects in Steel," American Institute of Mining and Metallurgical Engineers Technical Publication No. 1307, *Metals Technology,* August, 1941, Vol. 8, No. 5.
5. C. A. Zapffe and C. E. Sims, "Defects in Weld Metal and Hydrogen in Steel," *Welding Journal,* Research Supplement, October, 1940, Vol. 19, No. 10.
6. *Welding Handbook,* 1942, p. 104. American Welding Society, New York. N. Y.
7. W. Spraragen and G. E. Claussen, "The Effect of Hydrogen, Arsenic, Titanium and Miscellaneous Elements on the Welding of Steel," *Welding Journal,* Research Supplement, January, 1940, Vol. 19, No. 1.
8. C. A. Zapffe, Private communication to W. Spraragen and G. E. Claussen. *Welding Journal,* Research Supplement, January, 1940, Vol. 19, No. 1.
9. P. Bordenheuer and W. Bottenberg, *"Arch. Eisenhüttenwesen,"* Vol. 11, 1938, p. 375-383.
10. W. Spraragen and G. E. Claussen, "Welding Chromium Steels," Welding Research Committee of the Engineering Foundation, July, 1938, Vol. 111, No. 7.

INDEX OF AUTHORS

VOLUME XXXIII

TRANSACTIONS OF AMERICAN SOCIETY FOR METALS

1944

A

Alexander, C. W. 42

B

Baldwin, Jr., William Marsh .. 88
Bishop, R. W. 455
Bowman, F. E..... 481
Brodie, Constance B. 126
Burgess, C. O..... 455
Burr, Arthur A..... 73

C

Cohen, Morris 411
Cole, P. S..... 396
Coleman, H. S..... 73
Comstock, George F..... 324

D

Davey, W. P. 73

E

Ebert, L. J..... 340
Elmendorf, H. J. 236

F

Fenstermacher, W. H. 19

G

Geil, G. W..... 514
Gordon, Paul 411

H

Harrington, R. H..... 494
Herres, S. A..... 535
Hollomon, J. H. 1, 163
Howald, Thomas S..... 88

L

Lansdale, P. T..... 42
Lehrer, Wm. 290
Lubahn, J. D. 340

M

McAdam, Jr., D. J..... 514
McGuire, Francis T..... 103

P

Parke, R. M..... 481
Parker, E. R..... 150
Payson, Peter 261
Post, C. B..... 19

R

Rose, Robert S. 411
Roth, R. A..... 396
Russell, John V..... 103

S

Sachs, G. 340, 396
Savage, Charles H..... 261
Spring, E. K..... 42

T

Townes, Charles H..... 281

Z

Zener, C. 1, 163

INDEX OF SUBJECTS AND AUTHORS OF PAPERS

VOLUME XXXIII

TRANSACTIONS OF AMERICAN SOCIETY FOR METALS

1944

A

Aircraft Tubes; Bright Gas Quenching of S.A.E. X-4130 and NE 8630 Welded—*By Wm. Lehrer* 290
Alloy Steel Bolts; Strength of Heat Treated—*By G. Sachs, P. S. Cole and R. A. Roth* 396
Alloy Steels; Arc Welding of—*By S. A. Herres*..... 535
Alloy Steels; Martensite Reactions in—*By Peter Payson and Charles H. Savage* 261
Aluminum; X-Ray Study of the Time-Rate of Precipitation from a Solid Solution of Copper in—*By Charles H. Townes*..... 281
Arc Welding of Alloy Steels—*By S. A. Herres*..... 535
Austenite in Manganese Steels; Metallographic Study of the Decomposition of—*By John V. Russell and Francis T. McGuire*..... 103
Austenite Remaining After Controlled Quenching; Effect of Varying Amounts of Martensite Upon the Isothermal Transformation of—*By H. J. Elmendorf*..... 236

B

Blocks and Cylinders; Rates of Cooling in—*By C. B. Post and W. H. Fenstermacher* 19
Bolts; Strength of Heat Treated Alloy Steel—*By G. Sachs, P. S. Cole and R. A. Roth*..... 396
Brasses Formed by the Interdiffusion of Copper and Zinc Deposited on Glass by Vaporization; X-Ray Study of—*By Arthur A. Burr, H. S. Coleman and W. P. Davey*..... 73
Bright Gas Quenching of S.A.E. X-4130 and NE 8630 Welded Aircraft Tubes—*By Wm. Lehrer* 290

C

Cast Irons Exposed to Elevated Temperatures; Optimum Silicon Range in Plain and 2.0 Per Cent Chromium—*By C. O. Burgess and R. W. Bishop* 455
Chromium (2.0 Per Cent) and Plain Cast Irons Exposed to Elevated Temperatures; Optimum Silicon Range in—*By C. O. Burgess and R. W. Bishop* 455
Cohesion of Metals; Intercrystalline—*By E. R. Parker*..... 150
Cooling in Blocks and Cylinders; Rates of—*By C. B. Post and W. H. Fenstermacher* 19
Copper and Zinc Deposited on Glass by Vaporization; X-Ray Study of Brasses Formed by the Interdiffusion of—*By Arthur A. Burr, H. S. Coleman and W. P. Davey*..... 73

Copper in Aluminum; X-Ray Study of the Time-Rate of Precipitation from a Solid Solution of—*By Charles H. Townes* 281
Cylinders; Quenching and Hardenability of Hollow—*By J. H. Hollomon and C. Zener* 1
Cylinders and Blocks; Rates of Cooling in—*By C. B. Post and W. H. Fenstermacher* 19

D

Decomposition of Austenite in Manganese Steels; Metallographic Study of the—*By John V. Russell and Francis T. McGuire* 103
Dimensional Changes Encountered in Tube Sinking—*By William Marsh Baldwin, Jr. and Thomas S. Howald* 88

E

Effect of Quenching-Bath Temperature on the Tempering of High Speed Steel—*By Paul Gordon, Morris Cohen and Robert S. Rose* 411
Effect of Varying Amounts of Martensite Upon the Isothermal Transformation of Austenite Remaining After Controlled Quenching—*By H. J. Elmendorf* 236
Effects of Heat Treatment on Low Alloy Titanium Steels—*By George F. Comstock* 324
Electrical Conductivity of Metals with Temperature; Variation of the Strength, Resistance to Oxidation and—*By D. J. McAdam, Jr. and G. W. Geil* 514
Evaluation of Quenching Oils—*By E. K. Spring, P. T. Lansdale and C. W. Alexander* 42

G

Gas Quenching of S.A.E. X-4130 and NE 8630 Welded Aircraft Tubes; Bright—*By Wm. Lehrer* 290

H

Hardenability and Quenching of Hollow Cylinders—*By J. H. Hollomon and C. Zener* 1
Heat Treated Alloy Steel Bolts; Strength of—*By G. Sachs, P. S. Cole and R. A. Roth* 396
Heat Treated Low Alloy Steels; Notched Bar Tensile Test Characteristics of—*By G. Sachs, J. D. Lubahn and L. J. Ebert* 340
Heat Treatment on Low Alloy Titanium Steels; Some Effects of—*By George F. Comstock* 324
High Speed Steel; Effect of Quenching-Bath Temperature on the Tempering of—*By Paul Gordon, Morris Cohen and Robert S. Rose* 411
Hollow Cylinders; Quenching and Hardenability of—*By J. H. Hollomon and C. Zener* 1

I

Intercrystalline Cohesion of Metals—*By E. R. Parker* 150
Interdiffusion of Copper and Zinc Deposited on Glass by Vaporization; X-Ray Study of Brasses Formed by the—*By Arthur A. Burr, H. S. Coleman and W. P. Davey* 73
Interrupted Quench and Isothermal Treatments of Precipitation Hardening Alloys: Introductory Notes—*By R. H. Harrington* 494

Iron-Carbon-Molybdenum Alloys at 1300 Degrees Fahr. and the Nature of the Carbides Formed; Partition of Molybdenum in—*By F. E. Bowman and R. M. Parke* 481
Isothermal Transformation of Austenite Remaining After Controlled Quenching; Effect of Varying Amounts of Martensite Upon the—*By H. J. Elmendorf* 236
Isothermal Treatments of Precipitation Hardening Alloys: Introductory Notes; Interrupted Quench and—*By R. H. Harrington* 494

L

Low Alloy Steels; Notched Bar Tensile Test Characteristics of Heat Treated—*By G. Sachs, J. D. Lubahn and L. J. Ebert* 340
Low Alloy Titanium Steels; Some Effects of Heat Treatment on—*By George F. Comstock* 324

M

Manganese Steels; Metallographic Study of the Decomposition of Austenite in—*By John V. Russell and Francis T. McGuire* 103
Martensite Reactions in Alloy Steels—*By Peter Payson and Charles H. Savage* 261
Martensite Upon the Isothermal Transformation of Austenite Remaining After Controlled Quenching; Effect of Varying Amounts of—*By H. J. Elmendorf* 236
Metallographic Study of the Decomposition of Austenite in Manganese Steels—*By John V. Russell and Francis T. McGuire* 103
Microhardness Tester as a Metallurgical Tool—*By Constance B. Brodie* 126
Molybdenum in Iron-Carbon-Molybdenum Alloys at 1300 Degrees Fahr. and the Nature of the Carbides Formed; Partition of—*By F. E. Bowman and R. M. Parke* 481

N

NE 8630 and S.A.E. X-4130 Welded Aircraft Tubes; Bright Gas Quenching of—*By Wm. Lehrer* 290
Notched Bar Tensile Test Characteristics of Heat Treated Low Alloy Steels—*By G. Sachs, J. D. Lubahn and L. J. Ebert* 340

O

Oils; Evaluation of Quenching—*By E. K. Spring, P. T. Lansdale and C. W. Alexander* 42
Optimum Silicon Range in Plain and 2.0 Per Cent Chromium Cast Irons Exposed to Elevated Temperatures—*By C. O. Burgess and R. W. Bishop* 455

P

Partition of Molybdenum in Iron-Carbon-Molybdenum Alloys at 1300 Degrees Fahr. and the Nature of the Carbides Formed—*By F. E. Bowman and R. M. Parke* 481
Plain and 2.0 Per Cent Chromium Cast Irons Exposed to Elevated Temperatures; Optimum Silicon Range in—*By C. O. Burgess and R. W. Bishop* 455
Plastic Flow and Rupture of Metals—*By C. Zener and J. H. Hollomon* 163

Precipitation from a Solid Solution of Copper in Aluminum; X-Ray Study of the Time-Rate of—*By Charles H. Townes*..... 281
Precipitation Hardening Alloys: Introductory Notes; Interrupted Quench and Isothermal Treatments of—*By R. H. Harrington*..... 494

Q

Quenching and Hardenability of Hollow Cylinders—*By J. H. Hollomon and C. Zener* 1
Quenching-Bath Temperature Effect on the Tempering of High Speed Steel—*By Paul Gordon, Morris Cohen and Robert S. Rose*..... 411
Quenching Oils; Evaluation of—*By E. K. Spring, P. T. Lansdale and C. W. Alexander* 42

R

Rates of Cooling in Blocks and Cylinders—*By C. B. Post and W. H. Fenstermacher* 19
Resistance to Oxidation, Strength, and Electrical Conductivity of Metals with Temperature; Variation of the—*By D. J. McAdam, Jr. and G. W. Geil* 514
Rupture of Metals and Plastic Flow—*By C. Zener and J. H. Hollomon* 163

S

S.A.E. X-4130 and NE 8630 Welded Aircraft Tubes; Bright Gas Quenching of—*By Wm. Lehrer*..... 290
Silicon Range in Plain and 2.0 Per Cent Chromium Cast Irons Exposed to Elevated Temperatures; Optimum—*By C. O. Burgess and R. W. Bishop* 455
Solid Solution of Copper in Aluminum; X-Ray Study of the Time-Rate of Precipitation from a—*By Charles H. Townes*..... 281
Some Effects of Heat Treatment on Low Alloy Titanium Steels—*By George F. Comstock*..... 324
Strength of Heat Treated Alloy Steel Bolts—*By G. Sachs, P. S. Cole and R. A. Roth*..... 396
Strength, Resistance to Oxidation and Electrical Conductivity of Metals with Temperature; Variation of the—*By D. J. McAdam, Jr. and G. W. Geil* 514

T

Tempering of High Speed Steel; Effect of Quenching-Bath Temperature on the—*By Paul Gordon, Morris Cohen and Robert S. Rose*..... 411
Tensile Test Characteristics of Heat Treated Low Alloy Steels; Notched Bar—*By G. Sachs, J. D. Lubahn and L. J. Ebert*..... 340
Tester (Microhardness) as a Metallurgical Tool—*By Constance B. Brodie* 126
Time-Rate of Precipitation from a Solid Solution of Copper in Aluminum; X-Ray Study of the—*By Charles H. Townes*..... 281
Titanium Steels; Some Effects of Heat Treatment on Low Alloy—*By George F. Comstock*..... 324
Tubes; Bright Gas Quenching of S.A.E. X-4130 and NE 8630 Welded Aircraft—*By Wm. Lehrer*..... 290
Tube Sinking; Dimensional Changes Encountered in—*By William Marsh Baldwin, Jr. and Thomas S. Howald*..... 88

V

Variation of the Strength, Resistance to Oxidation, and Electrical Conductivity of Metals with Temperature—*By D. J. McAdam, Jr. and G. W. Geil* 514

W

Welded Aircraft Tubes; Bright Gas Quenching of S.A.E. X-4130 and NE 8630—*By Wm. Lehrer* 290
Welding (Arc) of Alloy Steels—*By S. A. Herres* 535

X

X-Ray Study of Brasses Formed by the Interdiffusion of Copper and Zinc Deposited on Glass by Vaporization—*By Arthur A. Burr, H. S. Coleman and W. P. Davey* 73
X-Ray Study of the Time-Rate of Precipitation from a Solid Solution of Copper in Aluminum—*By Charles H. Townes* 281

Z

Zinc and Copper Deposited on Glass by Vaporization; X-Ray Study of Brasses Formed by the Interdiffusion of—*By Arthur A. Burr, H. S. Coleman and W. P. Davey* 73